Pau Farràs Costa

FUNCIONALITZACIÓ DE L'ANIÓ COBALTO·BIS(DICARBALLUR) PER A NOUS MATERIALS

Universitat Autònoma de Barcelona

TESI DOCTORAL

FUNCIONALITZACIÓ DE L'ANIÓ COBALTO-BIS(DICARBALLUR) PER A NOUS MATERIALS

AUTOR:

PAU FARRÀS COSTA

DIRECTOR:

PROF. FRANCESC TEIXIDOR BOMBARDÓ

PROGRAMA DE DOCTORAT EN QUÍMICA

DEPT. QUÍMICA. FACULTAT DE CIÈNCIES

2009

ICMAB

CSIC

Memòria presentada per aspirar al Grau de Doctor per Pau Farràs Costa

Vist i plau Prof. Francesc Teixidor Bombardó

Bellaterra 10-06-2009

Consejo Superior de Investigaciones Científicas
INSTITUT DE CIÈNCIA DE MATERIALS DE BARCELONA
Campus de la UAB. E-08193-Bellaterra. España
Tel. +34 93 580 18 53 Fax +34 93 580 57 29

En FRANCESC TEIXIDOR i BOMBARDÓ, Professor d'Investigació del *Consejo de Investigaciones Científicas* a l'*Institut de Ciència de Materials de Barcelona.*

CERTIFICA

Que en PAU FARRÀS COSTA, titulat en Enginyeria Química, ha realitzat sota la meva direcció la TESI DOCTORAL que porta per títol "**Funcionalització de l'anió cobalto-bis(dicarballur) per a nous materials**" i que recull aquesta memòria per optar al grau de Doctor en Química.

I, perquè consti i tingui els efectes corresponents, signo aquest certificat a Bellaterra, a 10 de Juny de 2009.

Prof. FRANCESC TEIXIDOR i BOMBARDÓ

Aquest treball d'investigació ha estat finançat per la *Comisión Interministerial de Ciencia y Tecnología*, CICYT, mitjançant els projectes MAT01-1575, MAT04-01108 i MAT06-05339, per la *Generalitat de Catalunya*, pels projectes 2001/SGR/00337 i 2005/SGR/00709, i per la *European Comission*, mitjançant el projecte FI6W-CT-2003-508 854; s'ha pogut realitzat gràcies a una beca de postgrau per a la formació i especialització en línies d'investigació d'interès pel sector industrial concedida pel *Consejo Superior de Investigaciones Científicas* avalada per ATIPIC S. L. i una beca predoctoral I3P concedida pel *Consejo Superior de Investigaciones Científicas.*

Aquest treball d'investigació, amb data de defensa del dia 27 de Juliol de 2009, té com a membres del tribunal a:

- Prof. Tomás Torres, catedràtic de Química Orgànica de la Universidad Autónoma de Madrid
- Prof. Alan J. Welch, full professor de Química de la Heriot-Watt University.
- Prof. Agustí Lledós, catedràtic de Química de la Universitat Autònoma de Barcelona

Com a membres suplents:

- Dra. Josefina Pons, professora titular de Química de la Universitat Autònoma de Barcelona
- Dra. Montse Rodríguez, professora associada de Química de la Universitat de Girona

Els avaluadors externs per optar a la Menció Europea del programa de Doctorat de la UAB són:

- Prof. Francesco Devillanova, catedràtic de Química Inorgànica de la Università degli Studi di Cagliari
- Prof. Zbigniew Jan Lésnikowski, full professor a la Polish Academy of Science.

AGRAÏMENTS

En primer lloc voldria expressar el meu agraïment més sincer al Prof. Francesc Teixidor, el meu director de Tesi, pels seus consells, per l'exemple que dóna amb la seva dedicació a la recerca i l'ajut permanent que m'ha brindat. Vull expressar la meva sincera gratitud també a la Prof. Clara Viñas. A ambdós vull agrair-los l'acollida al grup que dirigeixen i la seva gran aportació tant científica com personal. També voldria agrair-los la constant comunicació que hi ha hagut, donant-me la possibilitat d'aprendre diferents camps de la química que de ben segur em seran molt útils pel meu futur.

Agraeixo a la Dra. Rosario Núñez la seva preocupació i el suport que m'ha brindat sempre que l'he necessitat. També vull agrair al Dr. Pepe Giner la relació personal i professional que hem mantingut, tant al laboratori com fora d'ell.

Als quatre també els hi vull expressar la meva gratitud d'haver-me fet veure diferents punts de vista dins el món de la investigació, explicar-me les seves experiències i donar-me les seves opinions. Estic segur que totes les hores de conversa m'ajudaran a prendre les decisions més adequades en un futur.

Expressar igualment la meva gratitud al Prof. Josep Ros per haver acceptat la tutoria d'aquesta tesi doctoral dins el Pla de Doctorat en Química de la Universitat Autònoma de Barcelona.

Un agraïment molt especial també al Dr. Vicenç Branchadell per haver-me introduït en la química computacional, les bases que em va donar han estat fonamentals en una part d'aquest treball.

Dóno les gràcies al Prof. David Leigh de la Universitat d'Edinburgh per acceptar-me al seu grup, cosa que em va permetre adquirir coneixements d'un camp de la química molt interessant.

Vull agrair als Prof. Carles Miravitlles i Prof. Xavier Obradors, ex-Director i Director de l'Institut de Ciència de Materials de Barcelona (ICMAB-CSIC) respectivament, per l'acolliment al centre i a les seves instal·lacions. Amb ells, dedico un record molt cordial a tot el personal de l'Institut per la seva tasca, imprescindible pel bon funcionament del centre.

Al Prof. Reijo Sillanpää (Universitat de Jyväsklyä, Finlàndia), Dr. Raikko Kivekäs (Universitat de Helsinki, Finlàndia), Prof. Mike Hursthouse i Dr. Mark E. Light (Universitat de Southampton, Regne Unit) i Xavier Fontrodona (Universitat de Girona) els agraeixo la resolució de les estructures cristal·lines presentades en aquest treball.

Agraeixo semblantment, la tasca del personal de la Universitat Autònoma de Barcelona, especialment dels Serveis Científico-Tècnics, per la realització de les anàlisis elementals i l'espectrometria de masses.

Moltes gràcies, Jordi, per la teva constant dedicació al laboratori i a la gent que t'envolta, fent que la feina de tots i a tots, ens sigui més fàcil. Així mateix, la preocupació que sempre tens que tot estigui al seu lloc fa que la nostra feina sigui més agraïda.

Anna, t'haig d'agrair de tot cor el suport i l'ajuda incondicional esmerçat en tot moment, i la realització dels espectres de RMN i de MALDI-TOF. A més, des del primer moment has estat una bona amiga amb qui passar aquests anys.

M'agradaria tenir un record per totes aquelles persones que he conegut, encara que breument, durant aquests anys perquè cada una d'elles m'ha deixat la seva empremta. Moltes gràcies a l'Aysel, la Maren, la Janaina i la resta de gent del grup del Prof. Rainer Streubel per la seva acollida en la breu estada que vaig fer a Bonn.

També als companys de laboratori durant l'estada a Escòcia vull donar-los les gràcies per fer-me sentir acompanyat tot i estar lluny de casa. Moltes gràcies Romen, Luci, Amaya, Tim, Santi, Paul, l'estada no hagués sigut igual sense vosaltres. Un record també per l'Euan, Dan, Bryan, Christiane, Dominique, Satoshi i Aurilien per la paciència que van tenir durant els primers dies al grup.

Agraeixo a la gent de l'ICMAB, estudiants i no estudiants, els bons moments compartits amb ells. Sis anys són molts però gràcies a tots han passat volant.

Als meus companys de despatx i laboratori d'aquests anys, vull agrair-los tots els moments compartits. A la Isabel per haver-me transmès tot de coneixements i il·lusions mentre va estar al grup. Igualment als postdoctorands Iulia, Vasile, Alex, Dana, Cristian, Fred, Antonio i Iolanda per compartir la seva experiència, aconsellar-me i proporcionar-me

ajut en tot moment. Un apreci molt sentit als que han estat els meus veterans Anna, Arancha, Laia i Albert per la gran rebuda al grup que em van fer, i per la seva paciència en resoldre els meus dubtes. Igualment, als qui m'han tingut a mi de veterà Sasi, Mila, Emilio, Ariadna, Patrícia, Albert, David, Vincent, Ana C., Radu, Ana D., Eva, Ana M., Marius L., Jordi B., Víctor, Marius T., Greg i Mireia per les estones compartides i el recolzament que n'he rebut, fins i tot en les estones de lleure. No vull deixar de recordar l'Ana Virginia per l'ajut mutu compartit durant el nostre primer any en el grup. A uns i altres, moltes gràcies de nou per haver pogut gaudir de la vostra companyia. Una menció especial a les persones que han estat més que companys de laboratori, amb les qui he compartit bons i mals moments però que estic segur que l'amistat que ha nascut durant aquests anys junts romandrà per sempre.

Un agraïment molt especial a l'Andreu Ginestet, autor de la il·lustració de la portada, perquè ha sapigut posar en paper la idea que tenia al meu cap. Espero que sigui la primera però no l'última portada de tesi que facis.

Estic molt agraït a les persones del meu entorn, amics, amigues i família, per haver-me ajudat en tot moment, per la seva confiança i suport tant en els moments agradables com en els difícils. Voldria agrair molt especialment als meus pares el seu recolzament i la seva aportació per fer possible aquest treball. Al meu avi i a les meves germanes, moltes gràcies per la vostra companyia.

També li voldria dedicar especialment aquest treball a la meva àvia, que tot i no ser entre nosaltres, continua present en la vida de tota la família.

Maria, la teva paciència, suport i confiança han estat fonamentals perquè hagi arribat en aquest punt. Sense la teva insistència difícilment estaria a punt de convertir-me en Doctor. Gràcies per estar al meu costat.

ORGANITZACIÓ DEL MANUSCRIT

D'acord amb la normativa vigent, aquesta Memòria es presenta com a compendi d'articles. Això no obstant, a més d'incloure els articles publicats presentats a la comissió de Doctorat de la UAB al maig de 2009 (Capítol 4) i, amb l'interès de presentar una Memòria el més completa possible, també s'han inclòs en forma d'annex els treballs realitzats en el marc d'aquesta Tesi Doctoral que han estat acceptats després de la comissió de Doctorat o que estan en procés d'elaboració. Els treballs inclosos en aquesta memòria són:

Capítol 4: Articles publicats i presentats a la Comissió de Doctorat de la UAB al Maig de 2009:

1) A DISCRETE P···I-I···P ASSEMBLY: THE LARGE INFLUENCE OF WEAK INTERACTIONS ON THE ^{31}P-NMR SPECTRA OF PHOSPHANE-DIIODINE COMPLEXES. R. Núñez, P. Farràs, F. Teixidor, C. Viñas, R. Sillanpää, R. Kivekäs, *Angew. Chem. Int. Ed.* **2006**, *45*, 1270.

2) PREDICTION OF pK_a VALUES OF *NIDO*-CARBORANES BY DENSITY FUNCTIONAL THEORY METHODS. P. Farràs, F. Teixidor, V. Branchadell, *Inorg. Chem.* **2006**, *45*, 7947.

3) METALLACARBORANES AS BUILDING BLOCKS FOR POLYANIONIC POLYARMED ARYL-ETHER MATERIALS. P. Farràs, F. Teixidor, R. Kivekäs, R. Sillanpää, C. Viñas, B. Grüner, I. Cisarova, *Inorg. Chem.* **2008**, *47*, 9497.

Annex: Articles publicats o pendents de publicació posteriors a la Comissió de Doctorat de la UAB al Maig de 2009:

4) METALLACARBORANES AS BUILDING BLOCKS FOR POLYANIONIC POLYARMED ARYL-ETHER MATERIALS. P. Farràs, F. Teixidor, R. Kivekäs, R.

Sillanpää, C. Viñas, B. Grüner, I. Cisarova, *Inorg. Chem.* **2009**, *48*, 782. (vol 47, 9502, 2008)

5) SYNTHESES OF C-SUBSTITUTED ICOSAHEDRAL DICARBABORANES BEARING THE 8-DIOXANE-COBALT BISDICARBOLLIDE MOIETY. V. Šícha, P. Farràs, B. Štíbr, F. Teixidor, B. Grüner, C. Viñas, *J. Organomet. Chem.* **2009**, *694*, 1599.

6) TOWARDS THE SYNTHESIS OF HIGH BORON CONTENT POLYANIONIC MULTICLUSTER MACROMOLECULES. P. Farràs, A. Maria Cioran, V. Šícha, F. Teixidor, B. Štíbr, B. Grüner, C. Viñas, *Inorg. Chem.* **2009**, manuscrit acceptat.

7) Co•••P INTERACTION ON A NEW FAMILY OF BRIDGED COBALTACARBORANES. P. Farràs, I. Rojo, R. Kivekäs, R. Sillanpää, F. Teixidor, C. Viñas, manuscrit en preparació.

8) TO MULTICAGE POLYANIONIC THIOETHER DERIVATIVES OF METALLACARBORANES. P. Farràs, R. Kivekäs, R. Sillanpää, F. Teixidor, C. Viñas, manuscrit en preparació.

9) CHLORINATION OF CARBORANE ANIONS. AN EXPERIMENTAL AND THEORETICAL STUDY. P. Farràs, C. Viñas, R. Sillanpää, M. Rey, F. Teixidor, manuscrit en preparació.

10) ADDITIVE TUNING REDOX POTENTIAL IN METALLACARBORANES BY SEQUENTIAL HALOGEN SUBSTITUTION. P. González-Cardoso, A.-I. Stoica, P. Farràs, A. Pepiol, C. Viñas, F. Teixidor, manuscrit en preparació.

11) STARTING MATERIALS FOR π-CONJUGATED SYSTEMS IN METALLACARBORANE CHEMISTRY. P. Farràs, I. Rojo, F. Teixidor, C. Viñas, manuscrit en preparació.

12) UNPRECEDENTED B-H ACTIVATION THROUGH Pd-CATALYSED B-C BOND COUPLING ON BORANE SYSTEMS. P. Farràs, D. Olid, C. Viñas, F. Teixidor, manuscrit en preparació.

13) ALTERNATIVE COBALTABISDICARBOLLIDE REAGENTS. P. Farràs, P. González-Cardoso, R. Kivekäs, R. Sillanpää, F. Teixidor, C. Viñas, manuscrit en preparació.

14) BORON CLUSTERS' EFFECT IN ROTAXANE DYNAMICS. P. Farràs, P. McGonigal, E. R. Kay, C. Viñas, D. A. Leigh, F. Teixidor, manuscrit en preparació.

15) INVESTIGATIONS ON ANTIMICROBIAL EFFECT OF METALLACARBORANES AND THEIR INFLUENCE ON VIABILITY AND PROLIFERATION OF CULTURED TUMOR AND NONTUMOR CELLS. R. Alexandrova, P. Farràs, C. Viñas, R. Toshkova, T. Popova, F. Teixidor, G. Miloshev, R. Kalfin, manuscrit en preparació.

Annex II: Reconeixement científic:

a) Noticias Científicas Relevantes. Anales de la Real Sociedad Española de Química, **2006**, *102*, 75.

b) Article de portada de la revista *Journal of Organometallic Chemistry*, **2009**, *694*.

FIGURES

COBALTO-BIS(DICARBALLUR) SUBSTITUÏT ALS ÀTOMS DE CARBONI

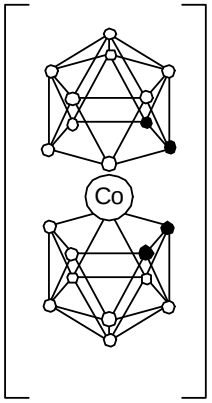

1

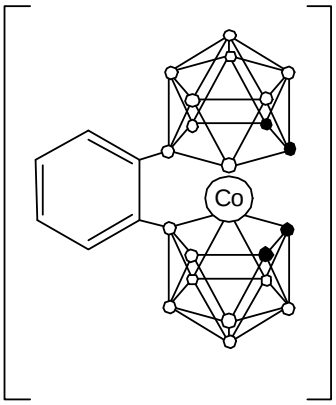

10

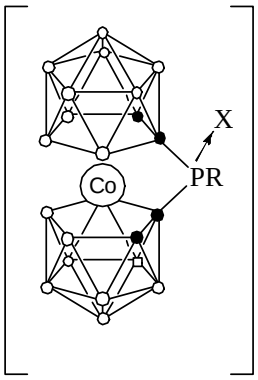

Compost	R	X
2	Ph	-
3	Ph	O
4	Ph	S
5	Ph	Se
6	^{t}Bu	-
7	^{t}Bu	O
8	^{t}Bu	S
9	^{t}Bu	Se

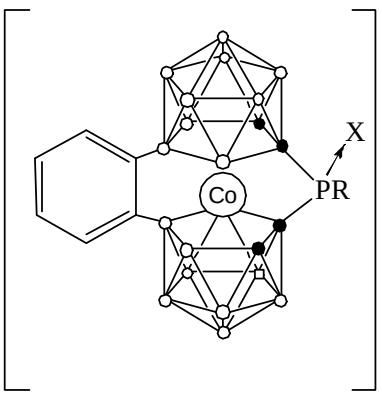

Compost	R	X
11	Ph	-
12	Ph	O
13	Ph	S
14	Ph	Se
15	^{t}Bu	-
16	^{t}Bu	O
17	^{t}Bu	S
18	^{t}Bu	Se

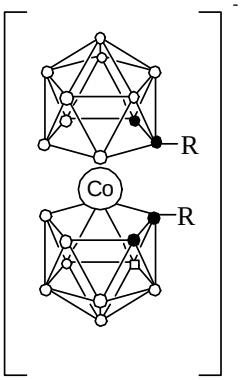

Compost	R
19	SPh
20	SCy
21	SEt
23	SMecarb
24	SPhcarb

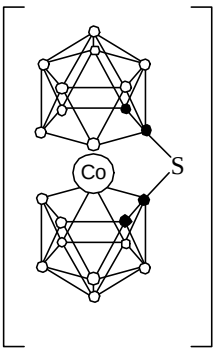

22

COBALTO-BIS(DICARBALLUR) SUBSTITUÏT ALS ÀTOMS DE BOR

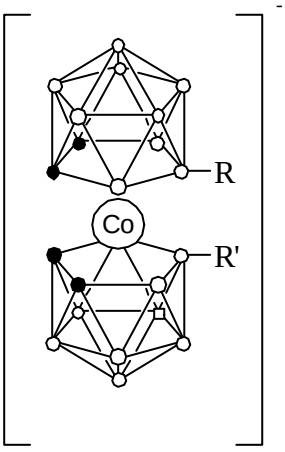

Compost	R	R'
25	I	H
26	4-PhCH=CH2	H
27	4-PhCHO	H
28	3-PhCHO	H
29	$(CH_2)_3CH=CH_2$	H
30	CH=CHPh	H
31	CH=CH-4-OH-Ph	H
32	CH=CH-4-NH_2-Ph	H
33	$CH=CH(CH_2)_3CH_3$	H
34	$CH=CH(CH_2)_7CH_3$	H
35	CH=CHCN	H
36	$CH=CHCH_2OH$	H
37	CH=CHPh	CH=CHPh
38	CH=CH-4-Me-Ph	CH=CH-4-Me-Ph
39	CH=CH-4-F-Ph	CH=CH-4-F-Ph
40	CH=CH-4-Cl-Ph	CH=CH-4-Cl-Ph
41	CH=CH-4-Br-Ph	CH=CH-4-Br-Ph
42	CH=CH-3-Br-Ph	CH=CH-3-Br-Ph
43	$O(CH_2CH_2)_20$	H

COBALTO-BIS(DICARBALLUR) SUBSTITUÏT ALS ÀTOMS DE BOR

R=

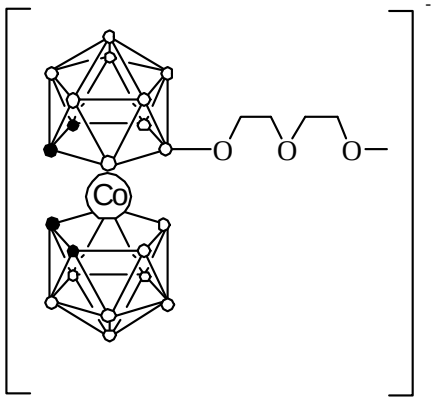

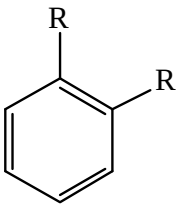

COMPOST 44

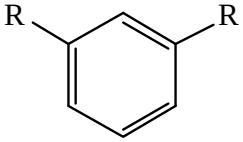

COMPOST 45

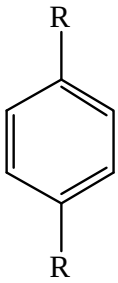

COMPOST 46

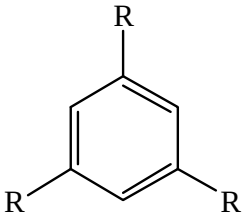

COMPOST 47

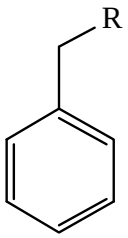

COMPOST 48

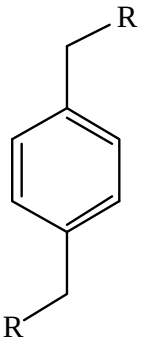

COMPOST 49

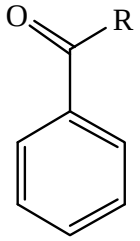

COMPOST 50

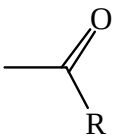

COMPOST 51

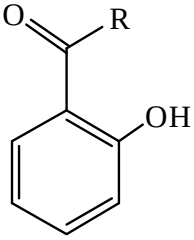

COMPOST 52

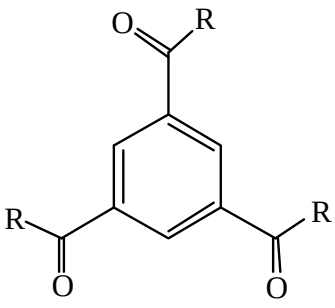

COMPOST 53

COBALTO-BIS(DICARBALLUR) SUBSTITUÏT ALS ÀTOMS DE BOR

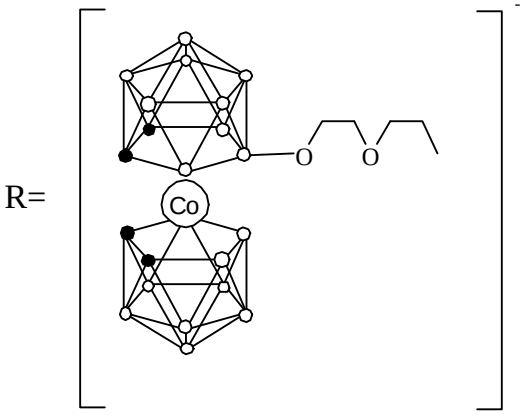

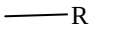

COMPOST 54

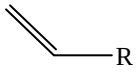

COMPOST 55

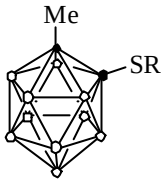

COMPOST 56

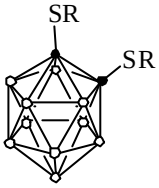

COMPOST 57

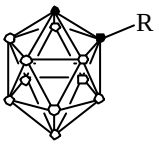

COMPOST 58

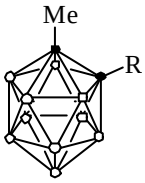

COMPOST 59

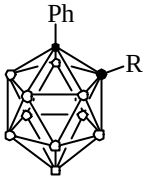

COMPOST 60

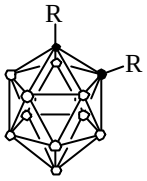

COMPOST 61

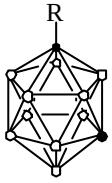

COMPOST 62

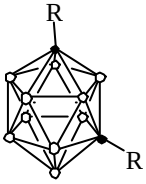

COMPOST 63

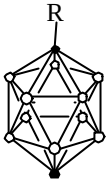

COMPOST 64

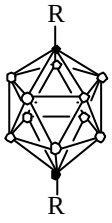

COMPOST 65

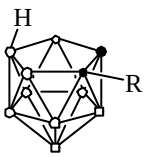

COMPOST 66

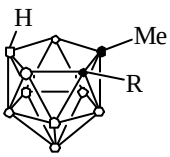

COMPOST 67

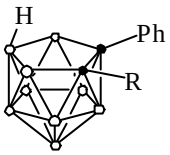

COMPOST 68

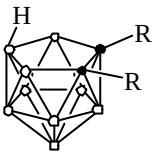

COMPOST 69

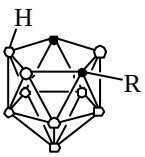

COMPOST 70

COBALTO-BIS(DICARBALLUR) SUBSTITUÏT ALS ÀTOMS DE BOR

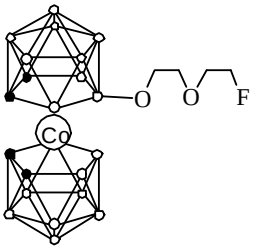

COMPOST 71

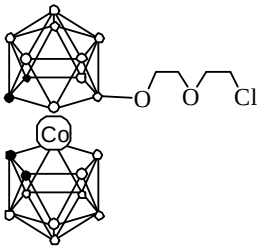

COMPOST 72

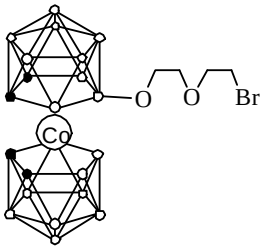

COMPOST 73

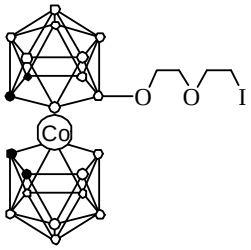

COMPOST 74

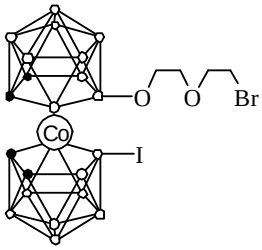

COMPOST 75

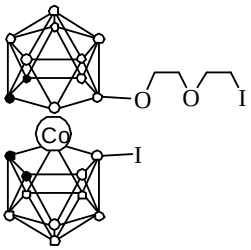

COMPOST 76

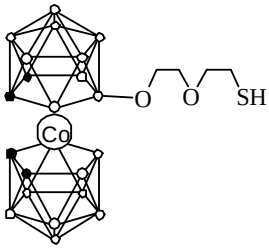

COMPOST 77

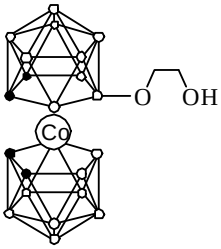

COMPOST 78

COBALTO-BIS(DICARBALLUR) FORMANT PART DE ROTAXANS

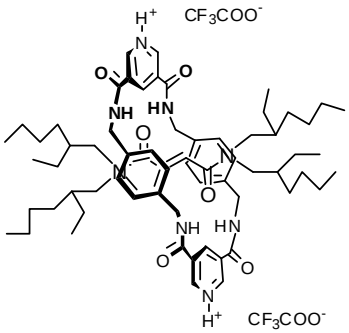

COMPOST 79

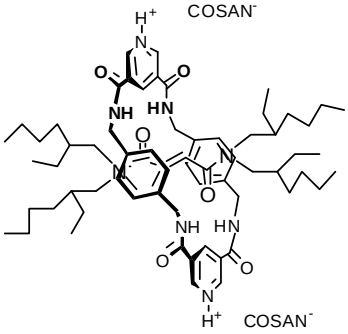

COMPOST 80

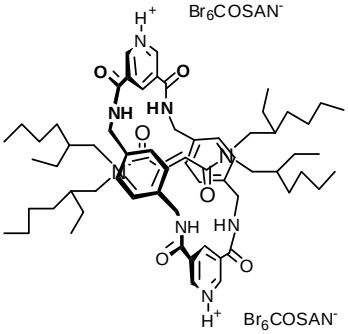

COMPOST 81

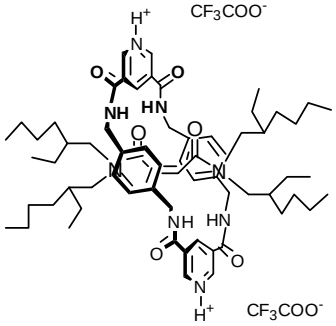

COMPOST 82

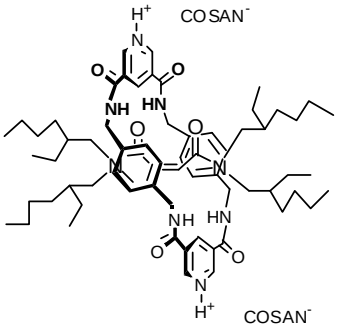

COMPOST 83

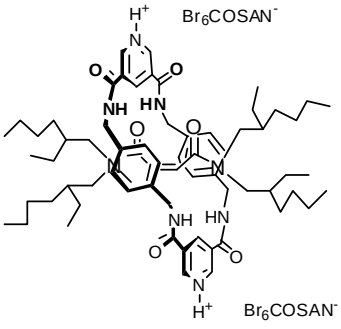

COMPOST 84

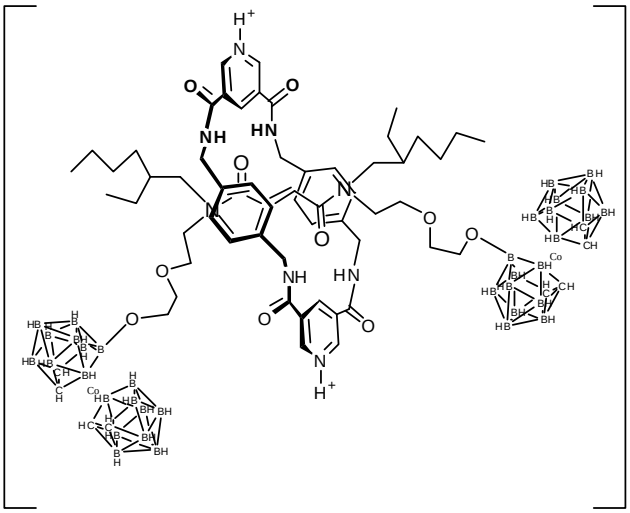

COMPOST 85

CARBORANS

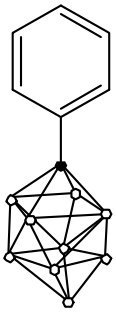

COMPOST 86

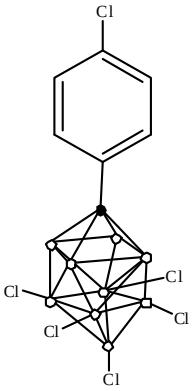

COMPOST 87

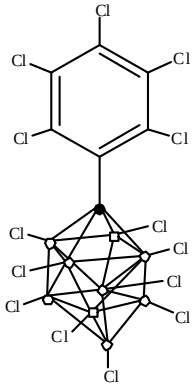

COMPOST 88

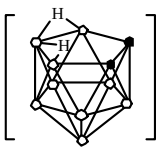

COMPOST 89

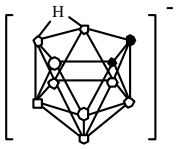

COMPOST 90

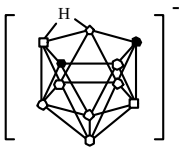

COMPOST 91

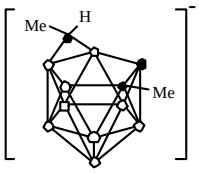

COMPOST 92

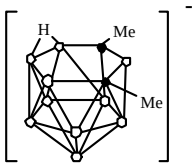

COMPOST 93

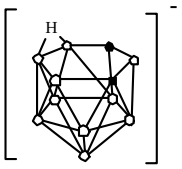

COMPOST 94

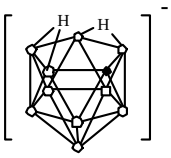

COMPOST 95

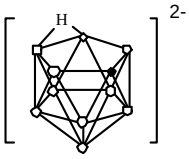

COMPOST 96

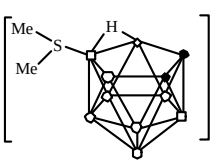

COMPOST 97

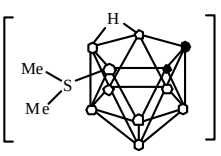

COMPOST 98

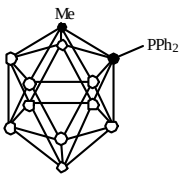

COMPOST 99

ABREUJAMENTS

C_c: àtom de carboni del clúster de carborà

H_{pontal}: àtom d'hidrogen unit *endo*-clúster a dos àtoms de bor de la cara oberta

$H_{terminal}$: àtom d'hidrogen unit a un àtom de bor

B(n): àtom de bor situat al vèrtex n del clúster

CSD: Cambridge Structural Database

o-carborà: *orto*-carborà

m-carborà: *meta*-carborà

p-carborà: *para*-carborà

^{t}Bu: grup *tert*-butil

Me: grup metil

Ph: grup fenil

n-BuLi: *n*-butilliti

EtOH: etanol

THF: tetrahidrofurà

DME: dimetoxietà

DMSO: dimetilsulfòxid

HOMO: Highest Occupied Molecular Orbital

LUMO: Lowest Unoccupied Molecular Orbital

En espectres de RMN:

δ (ppm): desplaçament químic en ppm

a: ampla

I: spin

s: singlet

d: doblet

t: triplet

m: multiplet

^{n}J(A,B): constant d'acoblament entre els nuclis A i B a n enllaços

TMS: tetrametilsilà

COSY: RMN bidimensional (COrrelation SpectroscopY)

EXSY: RMN bidimensional (EXchange SpectroscopY)

En espectres de IR:

I: intensa

mI: molt intensa

pI: poc intensa

ν: vibració de tensió

δ: vibració de deformació

γ: vibració esqueletal

ν_{as}: vibració de tensió assimètrica

SUMMARY OF THE THESIS

The work presented in this manuscript is the continuation and extension of the work done in the group of Inorganic Materials and Catalysis at the Institut de Ciència de Materials de Barcelona (CSIC) in the last years on the cobaltabisdicarbollide metallacarborane. To apply these molecules as components of molecular materials, the initial objectives were the synthesis and characterization of new derivatives of cobaltabisdicarbollide on the carbon and boron vertices of the cluster, as well as a theoretical study of some of these compounds that presented properties not previously observed. The second objective was the application of some of these compounds to different fields such as the treatment of nuclear waste, molecular synthetic motors and in biomedicine. Finally, work on carboranes has also been done as these are part of metallacarboranes. Theoretical calculations of pK_a values of *nido*-carboranes have been done. It has been studied both theoretically and experimentally the chlorination reaction of the anion $[Ph\text{-}CB_9H_9]^-$. Also, the intermolecular interaction between iodine molecules and phosphino-carboranes has been studied by computational methods.

Concerning the synthesis of carbon functionalized compounds, products substituted with phosphorus and sulphur have been obtained. Derivatization by phosphorus is the continuation of previous work done in this group while for sulphur the results are the first studies done on metallacarboranes. In the first case the phosphorus is bridging the two dicarbollide cages in a way similar to the already known ferrocene derivatives called ferrocenophanes. This structure confers them some unique properties as a consequence of an interaction between the cobalt and the phosphorus, the latter being anomalously deshielded. This interaction is maintained even if there is a change of the substituent on the phosphorus or if it is used a boron substituted cobaltabisdicarbollide as a starting material. Electron deficiency on phosphorus is clearly seen on ^{31}P-NMR since its signal moves downfield. Besides, we have done theoretical calculations that show a donor-acceptor interaction between the lone pair on phosphorus and the 4s orbital of cobalt. Conversely, when these compounds are oxidized, the signal moves upfield indicating an increase of the electronic density on phosphorus. These bridged phosphine metallacarboranes have been oxidized with oxygen, sulphur and selenium, and in all these oxidized cases theoretical calculations

show no interaction between phosphorus and cobalt. Moreover, if resonance peaks on ^{31}P-NRM between non-oxidized and oxidized species are compared, it can be observed that the signal corresponding to the non-oxidized phosphine is very similar to those oxidized with sulphur or selenium. This gives an estimation of the strength of the interaction between cobalt and phosphorus, being around 10 kcal/mol based on theoretical calculations.

Sulphur derivatives of cobaltabisdicarbollide have been obtained as disubstituted molecules with thioether groups coming from the appropriate organic disulfides. C,C bridging molecules in which one or two sulphur atoms bridge both dicarbollide cages have also been obtained. These are the first examples of direct substitution on cobaltabisdicarbollide anions with sulphur and the products have been obtained in good to high yields. In addition, we have been able to synthesize compounds combining cobaltabisdicarbollide and thiocarborane moieties, producing molecules with high boron content and with 2 or 3 negative charges. Some crystalline structures have been obtained that unambiguosly prove their existence, but it is important to highlight one of them. The crystal structure corresponds to compound **22** and represents the first example of sulphur bridging the two moieties of the metallacarborane. Theoretical calculations on this compound show an interaction between one of the lone pairs on sulphur and the 4s orbital of cobalt.

Boron substituted vertices have been studied in three different ways. The first concerns halogenation of the cobaltabisdicarbollide anion with chlorine, bromine and iodine atoms by using different methods, such as solution or solid state reactions. It has been studied more deeply the chlorination reaction because of the importance of these compounds on the extraction of radionuclides. The only pure chlorinated derivative is the disubstituted compound. All other compounds are obtained as mixtures with different degrees of chlorination. This prompted us to study a method to calculate the order of chlorination on the boron cluster or, alternatively, which are the most reactive vertices. This is important to learn on the relative stability of chlorinated derivatives to check on the possibility to obtain pure compounds. To do this we have calculated NPA charges on **1** and it has been found a very good correlation between the experimental chlorination sequence data and what we have called 2a-NPA charges, defined as the sum of boron or carbon and hydrogen NPA charges. We have done electrochemical

studies of different chlorinated mixtures observing a very interesting behaviour on their redox potential. There is a direct relationship between the reduction potential and the number of chlorine substituents in each molecule, so that each additional chlorine atom causes an anodic shift of 0.1V for the Co^{III}/Co^{II} pair. Then, it means that the total shift from compound **1** to its dodecachlorinated derivative $[Cl_{12}$-**1**$]^-$ is 1.2V. This additive shift behaviour on a single platform has no reference in the literature and the values of the redox potential reach the same level as this of the $C_{60}^{0/-I}$ pair, being the latter neutral whereas the cobaltabisdicarbollide is a monoanion. We hypothesize that the major difference is the greater enthalpy bond energy of B-Cl with respect to C-Cl. When a moderated potential is applied on an organic halide a rupture of the bond is found leading to the formation of a C-H bond, while this doesn't happen on boron cluster because the B-Cl bond is much more stable.

The second way studied concerning the derivatization of **1** refers to the formation of B-C bonds using the well established C-C coupling reaction conditions described in the Kumada or Heck reactions. In both cases the starting compound is the iodo-monosubstituted derivative **25**. Kumada reaction conditions have already been applied previously in our group but in this work we present derivatives with functional groups on the periphery, such as vinyl or aldehyde groups, that allow us to derivatize further these compounds with other reagents. It is interesting to observe the charge delocalization around the molecule since the aromatic groups help to dissipate the electrons out of the cluster. On the other hand, we have applied for the first time reaction conditions used in a Heck reaction in order to generate B-C bond on the cobaltabisdicarbollide anion. We have done experiments testing different reaction conditions, for example different catalysts, temperature, solvent, base, etc. As a result it has been found the optimum conditions for the reaction between **25** and styrene and these have been extended to other substrates with double bonds. It can be seen a rather large dispersity of the reaction yields depending on the substrate but, interestingly, the most important result has been the formation of disubstituted species instead of the expected monosubstituted. Moreover this can only be observed in the case of aromatic reagents, mainly these that have halogen atoms on the aromatic ring, increasing the reactivity of the double bond. The theoretical study of the reaction mechanism show that an intermediate species is generated between **25** and the palladium complex, in which the metal activates the B(8')-H bond of the unsubstituted dicarbollide cage rather

than the B(8)-Pd bond. This causes the substitution of the B(8') vertex to form B-C instead of the B(8) where the iodine atom was connected. This mechanism is different from the one described in the literature for the Heck reaction to couple C-C bonds. The new step of the mechanism results in the preservation of the B-Pd bond. Thus, while the B-C bond is formed, the B-Pd bond on the second cage is still active. This permits that another molecule having an activated C=C bond is getting closer to the B-Pd bond, leading to the formation of the disubstituted molecule.

The third way of cobaltabisdicarbollide derivatization has as the starting product the oxo-derivative of **1**, the zwitterion $[8\text{-}OC_4H_8O\text{-}1,2\text{-}(C_2B_9H_{11})_2]^-$ (**43**). This compound has an oxygen atom bonded to the B(8) vertex with a positive charge and this position is susceptible to the attack by nucleophiles. The reaction is known as ring-opening reaction of the dioxane ring. Using this methodology we have synthesized and characterized a wide range of compounds by using different nucleophiles such as alcohols, acids, Grignard reagents, thiols, carboranes and thiocarboranes. In this work we have used for the first time nucleophiles of carbon, sulphur and halogenated atoms on this platform. As a result we have obtained polyanionic compounds with a high boron content that makes them good candidates for the anticancer BNCT therapy. In addition, we have obtained compounds with free functional groups like thiols to assemble them on surfaces. Crystalline structures of the synthesized compounds as sodium salts show strong interactions between the cation and oxygen atoms of the polyether chain, as well as with B-H vertices of the unsubstituted dicarbollide cage. Remarkably, we have found that polyanionic species only appear on the mass spectra MALDI-TOF as monoanionic compounds. In order to have only one negative charge some of the molecules take a cation to compensate their charge, for example it is possible to observe the presence of Li^+ or even NMe_4^+ cations.

Some compounds synthesized during this work have been used in different applications. Chlorinated derivatives of cobaltabisdicarbollide have been tested as synergic agents in the selective extraction of radionuclides for nuclear waste treatment. Promising results have been obtained regarding the improvement of the selectivity when these compounds are used. Although it is true that compound **1** shows the best extraction results in moderate acidic media (HNO_3 1M), the problem is that it is easily degraded and thus it has no industrial usage. Therefore, it is mandatory the protection of

the most reactive vertices of the boron cluster by substitution of B-H for B-Cl groups. However, our results show that despite B-H groups tend to be altered, it is very important their presence. We have seen that experiments using mixtures with a higher degree of chlorination like $[Cl_7$-**1**$]^-$ result in worse extraction coefficients than in the case of using mixtures with a lower degree of chlorination such as $[Cl_4$-**1**$]^-$.

It has been tested the incorporation of metallacarborane cobaltabisdicarbollide in molecular machine structures, and more precisely in rotors like the organic rotaxanes. We have synthesized and characterized new rotaxanes specially designed to study intramolecular or intermolecular effects of the boron cluster in the dynamics of this kind of molecules. In addition, one of the produced molecules has the negative and positive charges completely separated, in other words they are connected through space without covalent bonds. The presence of C_c-H vertices on the cluster, that it is known to have a moderate tendency to form intermolecular interactions, causes a definitive but minor influence in the pirouetting motion of these molecules. For this reason we are studying the use of other boron clusters, less coordinative than cobaltabisdicarbollide and without C_c-H bonds for this application.

Moreover, some oxo-derivatives at the B(8) vertex of cobaltabisdicarbollide have been applied in the research of antimicrobial and antitumoral treatments. It has been seen that these compounds display a better activity against micro organisms than to a broad spectrum antibiotic used as control. In addition, it has been observed a good sensitivity against drug-resistant strains. The biological properties of **1** are modified with the substituents, it would be then interesting to correlate the biological properties of the boron clusters with their chemical modifications. Although the action mechanism of metallacarboranes is not known, the good results obtained *in* vitro show good expectations to start experiments *in vivo*.

Finally and although the aims of this work were centered on cobaltabisdicarbollide, some theoretical and experimental studies on carboranes have been done taking into account that these are part of the cobaltabisdicarbollide. Firstly we would like to improve the understanding of the chlorination reaction, extending the work done for **1** to other boron clusters. Anion $[Ph\text{-}CB_9H_9]^-$ (**86**) was selected because it has two very different reactivity points, aromatic C-H groups and B-H cluster vertices.

When we have used the methodology described for **1** to calculate the preferential substitution vertices, a good correlation between experimental data and 2a-NPA charges has been found for **86**. However, theoretical charges show that the first position to be chlorinated should be the B(10) vertex (antipodal to the carbon cluster atom) but experimentally it is known that the first chlorinated vertex is B(6). Therefore, we have calculated the mechanism of the chlorination reaction and have observed that the preference for the substitution on boron B(6) results from the first step of the reaction, the so called pre-reaction complex. At this stage the complex having B(6)-H···Cl is more stable than the isomer B(10)-H···Cl, and this may be the reason why the final product is isomer B(6)-Cl. In addition, by calculating the activation energy of the reaction we have found that the mechanism is better described as an attack of a radical chlorine $Cl^{\cdot}$. Until now it was thought that chlorination on boron clusters was an electrophilic substitution as a consequence of the attack of a Cl^{+} to the B-H group. Finally it has been checked experimentally the effect of adding a radical initiator or scavenger in the reaction and it can be observed that the radical scavenger diminishes notably the degree of chlorination of the mixtures. This confirms the theoretical results of a radical reaction.

On the other hand we have described a theoretical method to calculate the acidity of *nido*-carboranes by means of a fast, reliable and simple methodology. The pK_a of this type of compounds depends on the bridging hydrogen atom on the open face of a *nido*-carborane. This hydrogen atom has to be removed to obtain the dicarbollide dianion to do metal complexation. In this work we have described the step by step methodology to calculate pK_a values of *nido*-carboranes. We have also checked the validity of the method comparing experimental data with our calculated values observing a good correlation between them. Besides, this study has been useful to have more theoretical information of the studied compounds and also to confirm that theoretical ^{11}B-RMN values are comparable to experimental.

Finally, the last part of the manuscript describes a study on phosphino-carboranes, being my contribution to this work the computational interpretation of some experimental facts. This study was focused on interactions between phosphino-carboranes and iodine. With the help of theoretical calculations, it was possible to see that increasing quantities of iodine favour P···I interactions, but only until iodine begins

to generate $[I_3]^-$ and other polyiodinated $[I_x]^-$ species. This can be seen in the ^{31}P-NMR spectra because up to a 2:1 ratio between I_2:R_3P, the phosphorus ressonance peak shifts upfield, but from that point it goes downfield. However, it is remarkable the behaviour of compound [1-Me-2-PPh_2-1,2-$C_2B_{10}H_{10}$] (**99**), where upon addition of iodine the decrease of the interaction can't be observed, in other words no polyiodinated species are generated and no downfield shift is observed in the ^{31}P-NMR spectrum. This behaviour can be explained by the formation of a P···I-I···P moiety, which can be observed in solid state by its x-ray crystal structure.

ÍNDEX

1.- INTRODUCCIÓ

1. INTRODUCCIÓ

1.1. ANTECEDENTS HISTÒRICS

La història del bor es remunta força mil·lenis enrere, encara que la seva química continua sent molt desconeguda.[1] Fa prop de 6000 anys que els compostos de bor es coneixen i sembla que el bòrax va ésser un dels primers minerals a ser intercanviat en el món antic. Des dels babilònis i passant per egipcis, xinesos, tibetans, romans i àrabs, els compostos de bor s'han usat en soldadures d'or, materials per la momificació i sobretot, en la fabricació de vidres durs (borosilicats). Les primeres investigacions químiques documentades relacionades amb el bor daten de l'any 1702 quan W. Homberg va obtenir àcid bòric a partir de bòrax i sulfat ferrós. Tanmateix, no fou fins l'any 1808 quan H. Davy,[2] J. L. Gay-Lussac i L. J. Thénard van aïllar per primera vegada el bor amb un 50% de puresa per la reducció d'òxid de bor i potassi. El 1824 J. J. Berzelius va identificar aquella substància que s'havia obtingut com a un element. Finalment, el 1909 el químic americà W. Weintraub va sintetitzar per primera vegada bor amb un 100% de puresa.

El 1912 A. Stock[3] va preparar els primers compostos que contenien només bor i hidrogen, anomenats borans,[4] iniciant així una nova àrea de la química: la química del bor. El desenvolupament de la química dels borans va comportar dos grans reptes pels químics. Va ser necessari l'ús de noves tècniques de laboratori que permetessin una manipulació segura d'aquests compostos tan reactius; d'altra banda, les estructures d'aquests compostos no es regien per les lleis establertes fins aquell moment de l'enllaç químic i, per tant, seria necessària la formulació de noves teories. Tot i així, fins el final de la Segona Guerra Mundial aquesta química va ser purament acadèmica. La situació va canviar quan al 1946, tant els Estats Units com l'antiga URSS van invertir enormes quantitats de diners en la síntesi de diversos borans per la seva aplicació com a combustible d'aeronaus. Malgrat que no es van aconseguir els resultats esperats, les investigacions van servir per establir unes bases sòlides de la nova química. Els grans reptes de principi de segle es van començar a resoldre amb la utilització de les primeres línies de buit, més conegudes com a tècnica Schlenk i sobretot, amb l'obtenció l'any 1976 per part de W. N. Lipscomb del Premi Nobel de Química pels seus estudis sobre l'estructura dels borans.[5] Posteriorment, el 1979 H. C. Brown també va rebre el

Premi Nobel, compartit amb G. W. Wittig, pel desenvolupament de reactius importants de bor en síntesi orgànica.[6]

Tot i la gran quantitat d'informació, la química de bor no està, ni de bon tros, tan desenvolupada com la química orgànica. El coneixement dels compostos deficients en electrons és insuficient, i la recerca actual s'interessa tant per les propietats d'aquests compostos com pels principis que determinen el seu comportament. A més a més, la gran dificultat d'aquesta química és el preu relativament alt de la matèria primera, bàsicament en forma d'òxids de bor, degut tant a la dificultat per tractar aquesta matèria de partida com a la manca de la mateixa, centralitzada principalment en dipòsits de bòrax a Turquía i Estats Units.

1.2. GENERALITATS SOBRE BORANS I CARBORANS

La química dels compostos de bor forma actualment un pont entre la química orgànica, la inorgànica i la organometàl·lica. Estén la seva influència també en àrees com la química teòrica, els polímers o la medicina. Els borans són clústers de bor formats per poliedres de cares triangulars, que contenen una unitat B-H en cadascun dels vèrtexs. La incorporació d'heteroàtoms[7] en alguns vèrtexs genera la família dels heteroborans, i són els carborans (o carbaborans) els més estudiats. En aquests compostos s'han substituït un o més àtoms de bor per àtoms de carboni. La fórmula empírica d'aquests compostos és:

$$[C_nB_mH_{n+m+p}]^{x-} = [(CH)_n(BH)_mH_p]^{x-} \qquad \text{essent}$$

n: nombre d'àtoms de carboni en els vèrtexs del clúster.
m: nombre d'àtoms de bor en els vèrtexs del clúster.
p: nombre d'àtoms d'hidrogen pontal.

Els clústers de borans i carborans segueixen uns requisits electrònics, que han estat estudiats per Wade, Rudolph, Mingos i Williams, i són més coneguts com les **regles de Wade**.[8,9,10] Així, a partir del nombre de vèrtexs ocupats, el nombre d'electrons disponibles per a formar l'esquelet del clúster fixa una determinada estructura. Si el nombre d'electrons que manté cohesionat el clúster és 2n+2 (essent n el nombre de vèrtexs del políedre) el

compost té estructura *closo*; si és 2n+4 es tracta d'un compost *nido,* i si el nombre d'electrons és 2n+6 l'espècie és *arachno* (figura 1.1). L'any 1976 Rudolph hi va introduir una altra espècie que no apareix a la figura 1.1 anomenada *hypho*, que té 2n+8 electrons.[8] Un vèrtex constituït per una unitat B-H aporta dos electrons al clúster, provinents de l'àtom de bor. Si el vèrtex està format per la unitat C-H o C-R participa amb tres electrons, provinents de l'àtom de carboni. Finalment, cada H_{pontal} participa amb un electró a l'esquelet de la caixa.

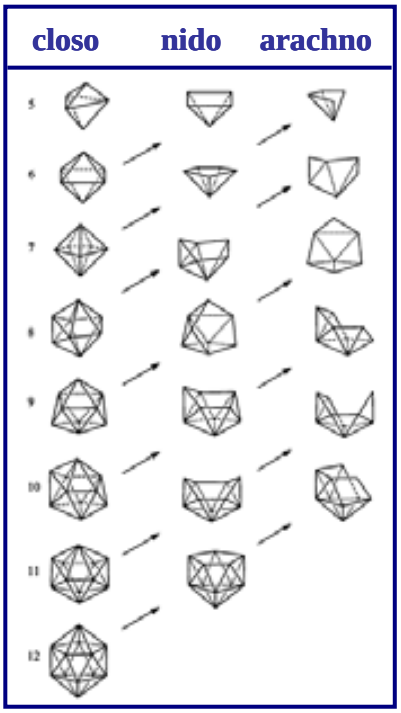

Figura 1.1. Principals xarxes de borans i heteroborans.

Una característica comuna a tots els carborans és l'elevat nombre de coordinació (generalment cinc o sis) dels àtoms de bor i carboni de les caixes. En conseqüència, l'enllaç no pot descriure's satisfactòriament en termes d'enllaç covalent localitzat bicèntric per un parell electrònic, sinó que en aquests compostos la manera més adequada és descriure'l com a dos electrons deslocalitzats entre tres centres (3c2e). D'aquí que aquests compostos foren coneguts durant molts anys com a "deficients en electrons".

La síntesi dels clústers de bor que s'utilitza actualment a la indústria té diverses etapes, en la majoria de les quals s'obtenen productes molt reactius i, per tant, calen unes mesures de seguretat i infrastructura inusualment altes. Com s'ha esmentat anteriorment, la matèria primera de tots els compostos de bor són els minerals que provenen majoritariament de Turquía i Estats Units i que estan formats per òxids de bor. El primer pas consisteix en la

conversió d'òxid a halur de bor mitjançant àcid fluorhídric preparat *in situ* per la reacció de CaF_2 (Fluorita) amb àcid sulfúric, obtenint BF_3 com a producte en baix rendiment. El segon pas consisteix en passar de l'halur a l'hidrur de bor per la reducció amb hidrur de sodi, obtenint ara diborà (B_2H_6) que torna a ser un gas molt reactiu i irritant, amb un 30% de conversió. Finalment, es fa la piròlisi al buit d'aquest per obtenir una mescla de clústers de bor de diversos tamanys, d'entre els quals el pentaborà (B_5H_9) i el decaborà ($B_{10}H_{14}$) s'obtenen preferencialment. Aquest últim és el material de partida de la major part de clústers de bor.

D'entre tots els carborans, els més coneguts són els clústers icosaèdrics que contenen dos àtoms de carboni, anomenats **dicarba-closo-dodecaborans**, i que responen a la fórmula empírica $C_2B_{10}H_{12}$. La síntesi de l'*o*-carborà es fa a partir de decaborà ($B_{10}H_{14}$) i acetilè en presència d'una base de Lewis (CH_3CN, Et_2S, Et_3N).[11] La senzillesa de la reacció dóna lloc a centenars de derivats d'aquest tipus de compostos amb un amplíssim ventall de propietats i reactivitats. Per aquest sistema *closo*, existeixen tres isòmers de posició depenent de la ubicació dels àtoms de carboni en el clúster (figura 1.2): 1,2-dicarba-*closo*-dodecaborà o *orto*-carborà (a); 1,7-dicarba-*closo*-dodecaborà o *meta*-carborà (b); i 1,12-dicarba-*closo*-dodecaborà o *para*-carborà (c). Tots tres isòmers i els seus derivats presenten una elevada estabilitat tèrmica, versatilitat química, resistència a l'atac d'àcids i inactivitat davant sistemes biològics.[12] Malgrat la seva estabilitat tèrmica, entre 460 i 500 ºC es produeix la isomerització a *m*-carbora[13], i entre 600 i 700ºC es forma l'isomer *p*-carborà, el termodinàmicament més estable.[7]

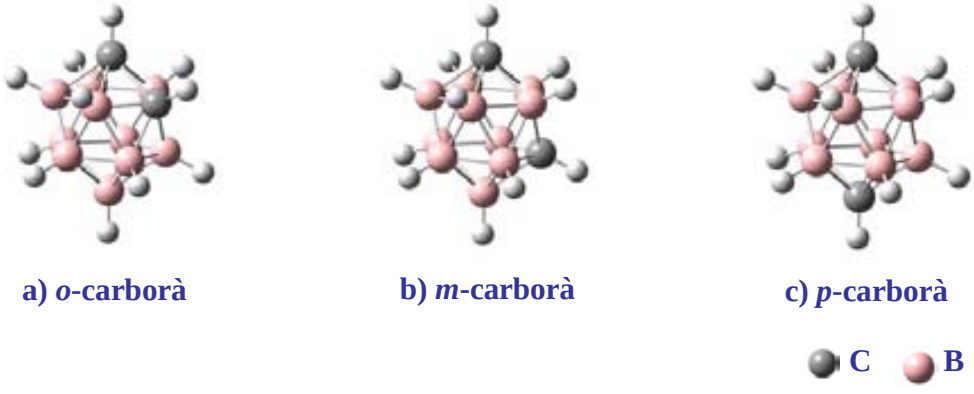

1.2. Estructura dels isòmers del dicarba-*closo*-dodecaborà.

La **reactivitat química** dels isòmers del $C_2B_{10}H_{12}$ ha estat extensament investigada des del seu descobriment a mitjans de la dècada dels cinquanta. Les reaccions bàsiques més importants en els *closo*-carborans són:

1) La desprotonació dels vèrtexs C-H i posterior substitució per grups funcionals:

Els àtoms d'hidrogen del C-H del clúster són més àcids que els que estan units a bor degut a la major electronegativitat del carboni respecte del bor (2.5 i 2.0 respectivament, segons l'escala de Pauling). A més, se sap que en els sistemes icosaèdrics del carborà, l'acidesa dels àtoms d'hidrogen units a carboni disminueix en els tres isòmers en l'ordre: 1,2 > 1,7 > 1,12.[14] Aquest caràcter relativament àcid permet substituir-los fàcilment per metalls alcalins emprant bases molt fortes com el *n*-Butilliti, l'hidrur sòdic o reactius de Grignard entre d'altres. A partir dels compostos metal·lats, i mitjançant els mètodes sintètics habituals en química orgànica, poden obtenir-se derivats del *o*-carborà amb una gran varietat d'elements com el C, P,[15] S,[16] Se,[17] Ge,[18] Au,[19] Si,[20] entre d'altres.

2) Reactivitat en els vèrtexs de bor:

Els àtoms d'$H_{terminals}$ units a bor poden ser l'objectiu de substitució electròfila,[7a,21] alquilació,[7a] sulfidrilació[22] i metal·lació[22a,23] segons la reactivitat de cada àtom de bor dins el clúster. No és tant comú com la substitució en els àtoms de carboni donada la no acidesa dels hidrògens units a ells. Les posicions més allunyades dels àtoms de carboni són les més reactives i per tant, més susceptibles a l'atac electrofílic.

3) Degradació parcial del clúster per eliminació:

El 1964 Hawthorne i col·laboradors van mostrar que l'*o*-carborà podia ser degradat parcialment utilitzant bases com l'ió etòxid o el metòxid,[24] entre d'altres. L'eliminació d'un àtom de bor es produeix com a conseqüència de l'atac nucleofílic d'una base de Lewis a l'àtom de bor amb menys densitat electrònica. La major electronegativitat dels àtoms de carboni respecte els àtoms de bor fa que els àtoms de bor units a carboni del clúster s'empobreixin electrònicament. Per tant, els àtoms de bor, B(3) i B(6), que estan enllaçats alhora als dos carbonis, seran els més susceptibles a l'atac, obtenint-se el 7,8-dicarba-*nido*-undecaborat (1-) (figura 1.3). Aquesta espècie només ha perdut formalment un fragment B^+ respecte de la inicial, fent que encara quedi el seu hidrogen. Estudis de difracció de raigs X mostren en estat sòlid com aquest H_{pontal} està més unit al B(10) que als B(9) o B(11), i que es manté a una distància equidistant d'aquests.[25] Aquest àtom d'hidrogen és prou àcid com per ser extret amb una base forta, formant-se el dianió dicarballur, $[7,8\text{-}C_2B_9H_{11}]^{2-}$.[24a,26]

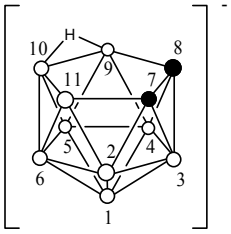

Figura 1.3. L'anió 7,8-dicarba-*nido*-undecaborat (1-)

En el dianió dicarballur els àtoms que formen la cara pentagonal oberta tenen orbitals híbrids sp^3. La combinació linial d'aquests cinc orbitals atòmics, un de cada atom, dóna lloc a cinc orbitals moleculars, tres d'ells enllaçants i dos antienllaçants. Els tres orbitals enllaçants estan ocupats per sis electrons deslocalitzats en el pla de la cara pentagonal, i donen lloc a una situació comparable a la de l'anió ciclopentadienur (figura 1.4). Aquesta semblança tant estructural com electrònica d'ambdós anions va portar al descobriment dels metal·locarborans tipus sandvitx. L'anió dicarballur pot aportar sis electrons a un metall de transició acceptor, els mateixos que l'anió ciclopentadienur $[\eta^5\text{-}C_5H_5]^-$, però el dicarballur contribueix amb una càrrega negativa de més que el ciclopentadienur.[27]

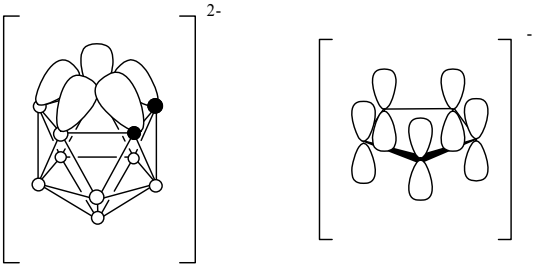

Figura 1.4. Representació esquemàtica del dicarballur, comparable a l'anió ciclopentadienur.

4) Reordenaments polièdrics

Com s'ha esmentat abans, un fet característic dels *closo*-carborans i d'altres clústers de bor polièdrics és la seva **isomerització tèrmica** que involucra reordenaments intramoleculars en l'esquelet de la caixa. La finalitat d'aquests processos és aconseguir la màxima separació entre els àtoms de carboni a fi de disminuir-ne la repulsió electrostàtica. Per això, la tendència és afavorir aquells isòmers on els àtoms de carboni estan el més allunyats possible.

5) Reacció de reducció

La reacció de reducció dels *closo*-carborans, publicada per primer cop l'any 1963,[28] consisteix en l'obertura del clúster per l'addició de dos electrons provocant el trencament de l'enllaç C_c-C_c. L'espècie formada és un clúster *nido* on es mantenen tots els vèrtexs inicials.

Els agents reductors que s'han utilitzat són el Na, K o el Mg, essent aquest últim el que facilita més la reacció.[29] Aquest tipus de reacció ha despertat un gran interès dins de la química del bor ja que obre la porta a l'expansió del clúster per succesives reduccions-insercions, obtenint-se compostos de 13 i 14 vèrtexs.[30,31]

1.3. METAL·LACARBORANS

L'any 1965 Hawthorne i col·laboradors van sintetitzar el primer metal·lacarborà, estructura composta per àtoms de bor, carboni i un metall. El primer exemple contenia ferro com a metall entre dos anions dicarballur: $[Fe^{III}(\eta^5\text{-}C_2B_9H_{11})_2]^-$.[32] Poc després, els mateixos autors van publicar un complex anàleg amb cobalt, que en l'argot de la química dels carborans sovint s'anomena *cosà*.[33] Aquests complexos tipus sandvitx són anàlegs als metal·locens i s'anomenen bis(dicarballurs) en contenir dues unitats de dicarballur. També s'han sintetitzat metal·lacarborans mixtes, amb un lligand dicarballur i un ciclopentadienur, amb ferro o cobalt com a metalls (figura 1.5).[34] L'estudi de l'estructura de raigs X del compost amb ferro va confirmar la localització de l'àtom de ferro al centre de la cara pentagonal de l'anió dicarballur i en la cara enllaçant de l'ió ciclopentadienur, completant així l'icosaedre.[35]

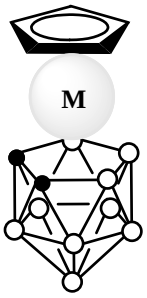

Figura 1.5. $[M(C_2B_9H_{11})(C_5H_5)]$ (M=Fe, Co)

L'anió dicarballur pot comparar-se amb l'anió ciclopentadienur per la seva capacitat de formar complexos estables amb metalls de transició tot i que, en general, els metal·lacarborans són molt menys reactius, més estables que els corresponents metal·locens. Això permet a l'anió dicarballur estabilitzar metalls en estat d'oxidació elevats, com és el cas de complexos com $[Cu^{II}(C_2B_9H_{11})_2]^{2-}$ i $[Cu^{III}(C_2B_9H_{11})_2]^-$, mentre que els anàlegs amb el $[C_5H_5]^-$ no s'han aïllat.[36]

1.4. COBALTO-BIS(DICARBALLUR)

En aquesta investigació ens centrarem en la química del metal·lacarborà cosà: [3,3'-Co(1,2-$C_2B_9H_{11})_2$]$^-$. L'estructura d'aquest compost *closo* consisteix en un àtom de cobalt central en estat d'oxidació +3 unit mitjançant enllaços π a dos lligands dicarballur que contribueixen amb dues càrregues negatives cadascun. La càrrega negativa total resultant es deslocalitza per tot el volum del compost i és per aquesta raó que és un anió de baixa densitat de càrrega. La figura 1.6 representa l'anió [3,3'-Co(1,2- $C_2B_9H_{11})_2$]$^-$ i indica la numeració dels vèrtexs.

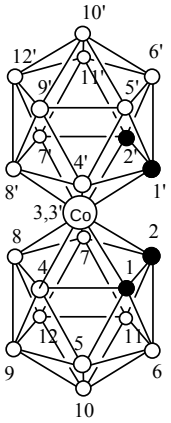

Figura 1.6. L'anió [3,3'-Co(1,2- $C_2B_9H_{11})_2$]$^-$

La preparació d'aquest compost implica: a) la degradació parcial de l'*o*-carborà a *nido*-[7,8-$C_2B_9H_{12}$]$^-$ amb una base, b) seguida de la desprotonació al dianió [7,8-$C_2B_9H_{11}$]$^{2-}$ i c) la reacció amb $CoCl_2$, com s'observa a la figura 1.7.[33]

Aquest anió presenta dos punts diferents de reactivitat: els vèrtexs C-H i els vèrtexs B-H. Tant uns com els altres no han estat estudiats amb detall tot i que a la literatura se'n troben exemples aïllats. Les substitucions en els àtoms de bor[37] són més difícils perquè hi ha molts àtoms de bor, no tots els vèrtexs B-H són iguals però alguns tampoc són tan diferents, per la qual cosa és difícil tenir una adequada regioselectivitat. Els més reactius són aquells que tenen una densitat electrònica més alta, essent els àtoms de bor 8, 9 i 12. Es coneixen així els derivats halogenats del *cosà* en les posicions 8-, 8,8'- i 8,8',9,9',12,12'.[38] No obstant això els més substituïts acostumen a ser una barreja de compostos amb diferents graus d'halogenació. Si bé aquests compostos halogenats van ser considerats inerts a reaccions de substitució, s'ha pogut demostrar que a partir dels derivats iodats és possible obtenir diferents substitucions.[39]

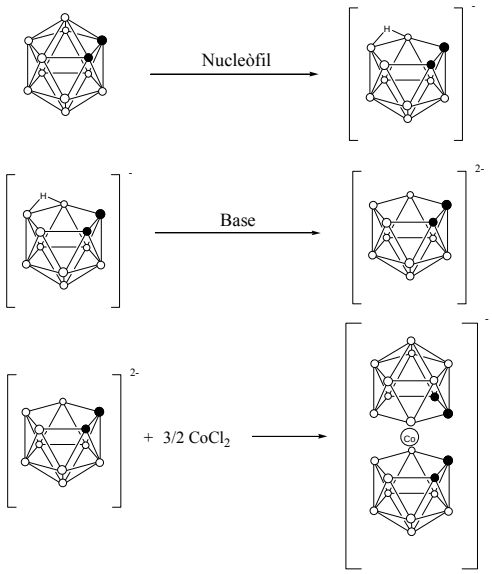

Figura 1.7. Esquema de la síntesi del cobalto-bis(dicarballur) [3,3'-Co(1,2- $C_2B_9H_{11})_2]^-$

A fi de sintetitzar derivats de [3,3'-Co(1,2- $C_2B_9H_{11})_2]^-$ (**1**) cal disposar de productes de partida que tinguin un procés sintètic amb bon rendiment. Per aquesta raó s'ha buscat un compost que es pugui sintetizar en grans quantitats i que serveixi com a punt de partida per a altres derivats en els àtoms de bor. Aquest és el compost monoiodat [8-I-3,3'-Co(1,2-$C_2B_9H_{10})$(1',2'- $C_2B_9H_{11})]^-$, el qual es sintetitza amb un 95% de rendiment per un mètode molt senzill i desenvolupat en el nostre grup (figura 1.8).[39b]

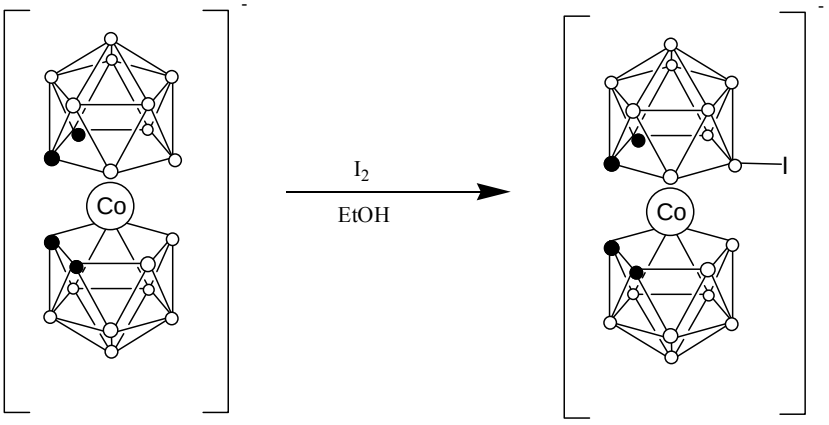

Figura 1.8. Esquema de la síntesi del compost [8-I-3,3'-Co(1,2- $C_2B_9H_{10})$(1',2'- $C_2B_9H_{11})]^-$

Una altra via de funcionalització de [3,3'-Co(1,2- $C_2B_9H_{11})_2]^-$ (**1**) en els vèrtexs de bor es basa en la formació del derivat zwitteriònic [8-{$O(CH_2CH_2)_2O$}-3,3'-Co(1,2-$C_2B_9H_{10})$(1',2'- $C_2B_9H_{11})]^-$[40] i posterior obertura de l'anell de dioxà amb una base de Lewis,[41] com es pot observar a la figura 1.9. Com en el cas anterior, la síntesi és senzilla i amb un alt rendiment.

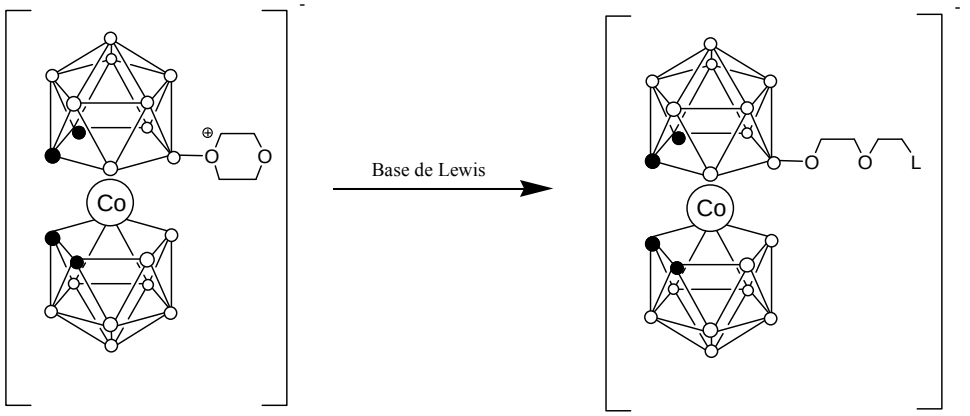

Figura 1.9. Esquema de la funcionalització del vèrtex B8 per l'obertura de l'anell de dioxà amb una base de Lewis (L)

El mètode més emprat per la síntesi de derivats de [3,3'-Co(1,2- $C_2B_9H_{11})_2]^-$ (**1**) en els vèrtexs de carboni consisteix en l'ensamblatge dels components adequadament funcionalitzats, és a dir, la preparació de l'*o*-carborà substituït, la seva degradació a clúster *nido* seguit de la desprotonació per formar el dicarballur i, per finalitzar, la reacció de complexació amb $CoCl_2$.[42] El problema és que requereix molts passos provocant un rendiment final molt baix. A més a més, aquest mètode només permet produir derivats del cobalto-bis(dicarballur) amb els mateixos substituents a cada una de les caixes de carborà. Un altre problema és que no es poden introduir grups funcionals que no suportin les condicions bàsiques que s'utilitzen en la síntesi del metal·lacarborà. Per aquestes raons es va buscar un nou mètode de síntesi que permetés dur a terme la reacció d'una manera més fàcil. Així, el 1997 Chamberlin i col·laboradors[43] van utilitzar *n*-BuLi per desprotonar els C_c-H del [3,3'-Co(1,2- $C_2B_9H_{11})_2]^-$ (**1**), i posterior reacció de substitució nucleofílica amb halurs d'alquil. Això no obstant, els resultats d'aquesta publicació són molt difícils de reproduir i no es pot considerar encara un mètode per produir enllaços C_c-C, almenys segons les nostres dades experimentals. S'ha obtingut més èxit amb la substitució per altres àtoms a part del carboni, com el fòsfor[44] o el silici (figura 1.10).[45]

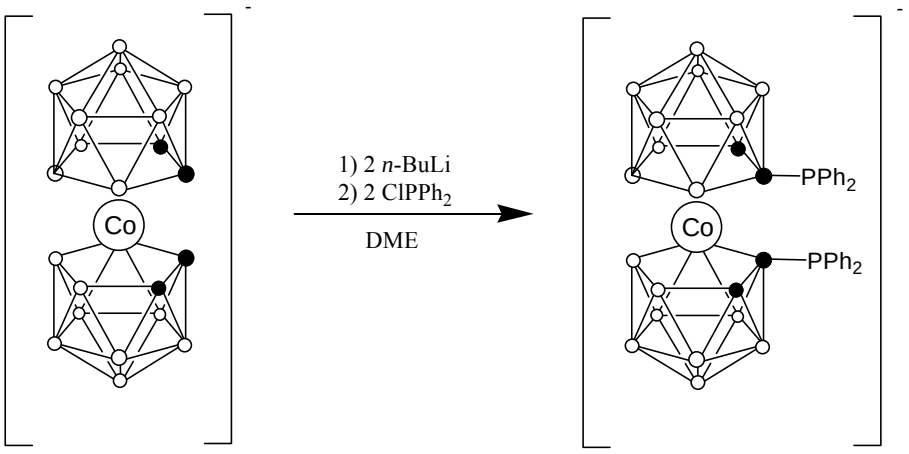

Figura 1.10. Mètode de síntesi de cobalto-bis(dicarballur) C-substituïts

1.5. APLICACIONS

En paral·lel als recents avenços en la química dels metal·lacarborans, s'estan fent esforços també per a potenciar-ne les actuals aplicacions ja que resulten cars per la dificultat en preparar-los, i només troben aplicació pràctica en aquelles àrees on no existeix cap altra alternativa. Tot i això, s'han obtingut resultats molt satisfactoris en un gran nombre d'aplicacions,[46] la majoria de les quals van lligades a les propietats úniques dels clústers de bor, com són la gran hidrofobicitat dels anions, la gran estabilitat de les espècies polièdriques degut a la seva "aromaticitat", la gran capacitat dels clústers oberts per formar complexes metàl·lics tipus sandvitx o a la necessitat de tenir àtoms de bor. D'entre les possibles aplicacions, es farà més èmfasi en aquelles que s'han estudiat en aquest treball.

1.5.1. Extracció de radionúclids

Una de les principals aplicacions de l'anió cobalto-bis(dicarballur) i derivats rau en l'extracció de radionúclids.[42,47] El funcionament i desmantellament de les centrals nuclears produeix residus líquids de baixa, mitja i alta activitat. La majoria dels nuclis d'aquests residus radioactius són de vida mitja, principalment emissors β/γ com els isòtops radioactius de Cs, Se, Tc, I, Zr, etc. o de vida llarga, principalment emissors α com els elements transurànics: Np, Pu, Am, Cm, etc.[48] Els residus d'alta activitat, procedents del reprocés de combustible gastat (procés PUREX), s'incorporen a blocs de vidre per a ser emmagatzemats en formacions geològiques profundes, i aïllar-los de les persones i del medi ambient, i és actualment el mètode considerat més segur.[49] Els residus de baixa i mitja activitat són tractats

per evaporació o per alguna altra tècnica convencional com la precipitació química o el bescanvi iònic, a fi de concentrar la seva radioactivitat en el volum més petit possible,[50] envasar-los en contenidors d'acer i emmagatzemar-los.

El procés PUREX s'utilitza principalment per recuperar la major part de l'urani i el plutoni procedents del combustible nuclear. El volum de residu emmagatzemat a gran profunditat que prové del procés PUREX pot ser reduït dràsticament si es separen els actínids minoritaris dels productes de fissió de vida llarga. Aquests radionúclids separats es poden transformar en nuclis de vida més curta en reactors nuclears avançats amb una tecnologia anomenada Partitioning & Transmutation.[51] A més, alguns metalls poden ser reciclats, com és el cas del ^{137}Cs, i ser reusats en radioteràpia i com a font de radiació γ per esterilitzar aliments i material mèdic.[52]

Fins ara s'han proposat una gran varietat de mètodes de separació basats predominantment en processos hidrometal·lúrgics i el mètode més emprat és l'extracció líquid-líquid, la qual requereix d'agents extractants selectius. La major part dels segrestants específics emprats són espècies orgàniques neutres com poden ser els èters corona, les malonamides, els calixarens,[53] les carbamoilfosfines (CMPO),[54] etc.[55] i pràcticament per a cada un hi ha un mètode de separació diferent com el TRUEX, DIAMEX, SANEX o UNEX. Aquests compostos actuen com a lligands neutres capaços de complexar fortament el radionúclid de la fase aquosa i facilitar-ne així el seu transport a una fase orgànica immiscible. A la figura 1.11 es mostra l'esquema de l'extracció líquid-líquid. En aquest cas, un adequat nombre de contraions aniònics, principalment el nitrat, ha de seguir al catió a la fase orgànica.[56]

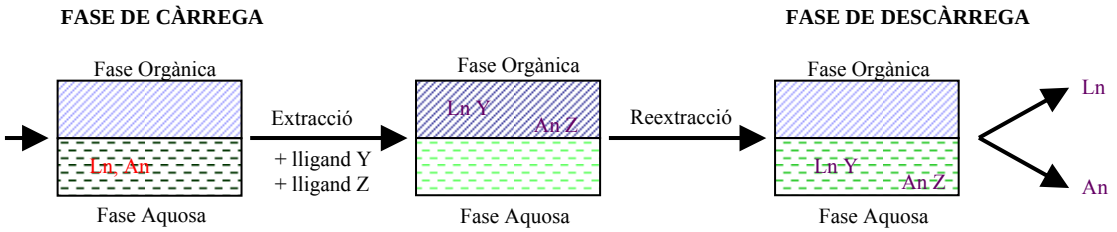

Figura 1.11. Diagrama d'extracció dels radionúclids

Així, aquesta separació **selectiva** és un punt clau en el tractament dels residus nuclears. L'anió cobalto-bis(dicarballur) va ser utilitzat per investigadors txecs com a agent

extractant selectiu de ^{137}Cs i ^{90}Sr, i així poder recuperar els radionúclids d'una fase aquosa 3M en HNO_3 a una fase orgànica.[57] Fou amb aquesta troballa com va començar l'estudi d'aquest anió i els seus derivats com a agents extractants. Així, des de principis dels anys 90 l'hexacloro derivat del cobalto-bis(dicarballur) s'està emprant a Rússia a escala industrial per la separació del $^{137}Cs^+$ i $^{90}Sr^+$ en el procés UNEX, i es continua estudiant per tal de separar altres radionúclids de manera selectiva.

Tot i això, cada vegada queda més clar que el paper dels anions cobalto-bis(dicarballur) en l'extracció selectiva és més de transportador que no pas d'extractor pròpiament. Per tant, poden ser implementats en membranes líquides suportades a fi de transportar els cations de la solució aquosa (o fase de càrrega) que ha de ser descontaminada, a una altra fase aquosa (o fase de descàrrega) a través d'una fase orgànica on l'anió té major solubilitat.

1.5.2. En medicina i farmacologia

L'aplicació mèdica dels clústers de bor on existeixen més publicacions és en el tractament anticancerigen amb la teràpia de captura de neutrons BNCT (boron neutron capture therapy), desenvolupada per Locher el 1936.[58] Actualment està en fase d'assaigs clínics als Estats Units, Japó i més recentment, Europa.[59] Es basa en la capacitat de l'isòtop ^{10}B d'absorbir neutrons lents d'una font externa i alliberar partícules α. Per tant, s'escull una molècula rica en ^{10}B i es funcionalitza perquè s'acumuli preferentment en el tumor. La concentració terapèutica és de 20-35 μg ^{10}B/gram de tumor.[60] Llavors, s'irradia la zona amb un raig de neutrons lents i, quan l'àtom de ^{10}B captura els neutrons, es forma un nucli excitat de $^{11}B^*$. Aquest es fissiona segons la reacció de la figura 1.12, i fa que les partícules α alliberades destrueixin les cèl·lules cancerígenes, mantenint intactes les cèl·lules sanes, ja que la trajectòria dels ions és aproximadament d'un diàmetre cel·lular (10μ).[60b]

Una altra aplicació semblant a la BNCT és la teràpia contra l'artritis reumàtica. Aquesta també es tracta d'una malaltia amb el teixit localitzat i afecta a més de l'1% de la població adulta. La malaltia no té cura, és dolorosa i el tractament normal en molts casos no és efectiu, com a última opció hi ha la cirurgia. L'aplicació de la captura de neutrons en aquest camp és prometedora ja que seria més barata que la cirurgia i requeriria de mínima hospitalització. El tractament de l'artritis BNCS (Boron Neutron Capture Synovectomy) també està en fase d'assaigs clínics.[61]

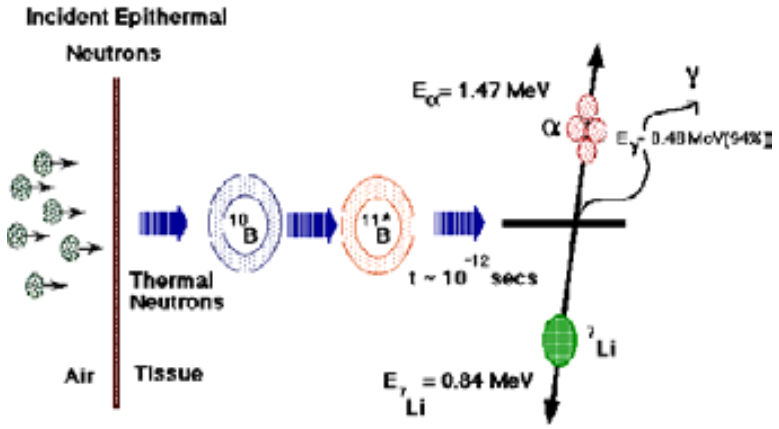

Figura 1.12. Esquema del procés de captura d'un neutró per part d'un nucli de ^{10}B

En el camp de la radiologia moderna s'aprofita l'opacitat dels àtoms de iode als raigs X per usar-los com a agents radioopacs.[62] Actualment s'està utilitzant compostos orgànics iodats derivats d'anells benzènics,[63] tot i que es creu que els clústers de bor iodats podrien arribar a substituir-los gràcies a la major estabilitat dels enllaços B-I respecte els enllaços C-I,[64] que en condicions fisiològiques es trenquen. Una altra avantatge és la possibilitat d'incrementar el percentatge de iode molecular, en el cas del carborà periodat arribant a un 90% del pes total en iode.

Finalment també es podria esmentar el recent interès en la utilització de derivats de l'anió cobalto-bis(dicarballur) com inhibidor de proteïnes, sobretot en el cas de la proteassa de l'VIH, amb resultats sorprenents.[65]

1.5.3. En màquines moleculars

Aquest tema ha despertat en les últimes dècades un enorme interès dins la comunitat científica amb nombroses publicacions a revistes de prestigi en diversos àmbits de la ciència.[66] En canvi, la introducció de clústers de bor en aquest tipus de mecanismes és molt més recent i, per aquesta mateixa raó, molt poc explorat. La primera publicació on s'esmenta la incorporació de carborans en estructures que es poden considerar màquines moleculars data de l'any 2001 on Vicente i col·laboradors estudiaven l'energia d'activació del moviment de rotació d'una porfirina.[67] Tot i així, no va ser fins l'any 2005 quan Hawthorne i col·laboradors van publicar el possible ús del metal·lacarborà níquel-bis(dicarballur) com a rotor molecular mitjançant un control redox del compost.[68] Finalment, l'aplicació on ha donat més fruits la

incorporació de clústers de bor (el *p*-carborà en aquest cas) és en nanocotxes o nanocucs, on s'utilitza el clúster com a roda de la màquina, tal com es mostra a la figura 1.13.[69]

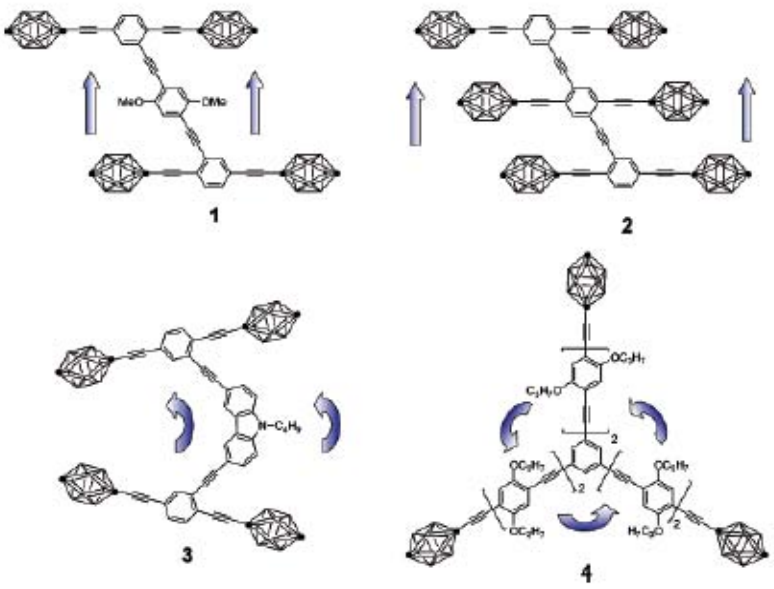

Figura 1.13. Ús del *p*-carborà com a roda en màquines moleculars

1.5.4. En catàlisi homogènia

S'ha trobat que alguns roda- i rutenacarborans presenten excel·lents activitats catalítiques en reaccions d'hidrogenació,[70] hidrosililació,[71] ciclopropanació[72] i reacció de Kharasch.[73] A més, metal·lacarborans amb metalls de transició del grup IV (Ti, Zr, Hf) són actius en la catàlisi de polimerització d'olefines.[74]

1.5.5. Polímers conductors orgànics

Els clústers de bor es poden emprar com agents dopants en polímers orgànics conductors ja que, pel fet de tenir una baixa densitat de càrrega, fa que se'n millori l'estabilitat d'aquests, especialment la seva resistència a la sobreoxidació.[75] L'anió cobalto-bis(dicarballur) s'utilitza com a dopant de membranes de polipirrole amb bons resultats.[76]

1.5.6. Sensors

També s'ha provat la seva utilitat com a sensors d'intercanvi selectiu d'ions[77] i ISFETs.[78]

1.5.7. Altres aplicacions

En el desenvolupament de nous materials, l'aplicació de clústers de bor també ha estat estudiada en materials com òptics no-linials,[79] cristalls líquids,[80] polímers de flama retardant,[81] polímers híbrids de tipus siloxà i precursors preceràmics[82] i en la modificació de nanopartícules i monocapes d'or.[83]

1.6. OBJECTIUS I JUSTIFICACIÓ DEL TREBALL

Amb la finalitat de la seva aplicació com a components de materials moleculars, calia com a objectiu inicial la síntesi i caracterització de nous derivats en els àtoms de carboni i de bor del clúster, així com l'estudi teòric d'alguns d'aquests compostos que presentaven propietats que no s'havien observat fins el moment. Per a funcionalitzar els àtoms de carboni s'utilitzarà el mètode directe ja utilitzat en el nostre grup. La funcionalització en els àtoms de bor es durà a terme a partir de l'anió cobalto-bis(dicarballur) però també a partir dels derivats monoiodat o del zwitterió amb un anell de dioxà enllaçat a un vèrtex de bor. A partir d'aquests compostos es volen buscar aplicacions en els camps del tractament de residus nuclears, motors sintètics moleculars i en el camp de la biomedicina. Finalment i per ampliar el coneixement en el camp dels carborans, s'han fet estudis teòrics del pK_a de *nido*-carborans, s'ha estudiat tant teòricament com experimental la reacció de cloració de l'anió $[Ph\text{-}CB_9H_9]^-$ i s'ha participat en l'elaboració d'un treball d'interaccions intermoleculars entre molècules de iode i fosfino-carborans

1.7. BIBLIOGRAFIA

[1] J. W. Mellor, *A Comprehensive Treatise on Inorganic and Theoretical Chemistry*, London, Longmans Green and Co., **1924**, *5*.

[2] H. Davy, *Philosophical Transactions of the Royal Society of London*, **1809**, *99*, 39.

[3] A. Stock, C. Massanez, *Chem. Ber.*, **1912**, *45*, 3539.

[4] N. N. Greenwood, A. Earnshaw, *Chemistry of Elements*, Butterworth-Heinemann, Oxford. **1997**, 139-215.

[5] a) J. Bicerano, D. S. Marynick, W. N. Lipscomb, *Inorg. Chem.,* **1978**, *17*, 3443; b) W. N. Lipscomb, *Science*, **1977**, *196*, 1047; c) W. N. Lipscomb, *Boron Hydrides,* Benjamin, New York, **1963**.

[6] H. C. Brown, *Organic Syntheses via Boranes,* John Wiley & Sons, Inc. New York. **1975**.

[7] a) R. N. Grimes, *Carbaboranes*, Academic Press New York, **1971**; b) S. Papetti, T. L. Heying, *J. Am. Chem. Soc.,* **1964**, *86*, 2295.

[8] R. W. Rudolph, *Acc. Chem. Res.,* **1976**, *9*, 446.

[9] R. E. Williams, *Inorg. Chem.,* **1971**, *10*, 210.

[10] a) K. Wade, *Adv. Inorg. Chem. Radiochem.,* **1976**, *18*, 1; b) D. M. P. Mingos, *Nature (Phy. Science).,* **1972**, *236*, 99; c) R. W. Rudolph, W. R. Pretzer, *Inorg. Chem.,* **1972**, *11*, 1974; d) K. Wade, *Chem. Commun.,* **1971**, 792.

[11] a) T.L. Heying, J.W. Ager, S.L. Clark, D.J. Mangold, H.L. Goldstein, M. Hillman, R.J. Polak, J.W. Szymanski, *Inorg. Chem.*, **1963**, 2, 1089; b) M.M. Fein, J. Bobinski, N. Mayes, N. Schwartz, M.S. Cohen, *Inorg. Chem*, **1963**, 2, 1111; c) L.I. Zakharkin, V.I. Stanko, V.A. Brattsev, Yu.A. Chapovsky, Yu.T. Struchlkov, *Izv. Akad. Nauk. SSSR, Ser.Khim*., **1963**, 2069; d) L.I. Zakharkin, V.I. Stanko, V.A. Brattsev, Yu.A. Chapowski, O.Yu. Ohlobystin, *IzvAkad. Nauk. SSSR. Ser. Khim.,* **1963**, 2238.

[12] a) R. B. King, *Chem. Rev.*, **2001**, *101*, 1119; b) B. M. Gimarc, M. Zhao, *Inorg. Chem.*, **1996**, *35*, 4, 825; c) V. I. Bregadze, *Chem. Rev.*, **1992**, *92*, 177; d) G. A. Olah, G. K. S. Prasah, R. E. Williams, L. E. Fidd, K. Wade, *Hypercarbon Chemistry*, Ed. Wiley; New York, **1987**.

[13] D. Grafstein, J. Dvork, *Inorg. Chem.*, **1963**, 2, 1128.

[14] K. Hermansson, M. Wójcik, S. Sjöberg, *Inorg. Chem.,* **1999**, 38, 6039.

[15] a) R. Núñez, P. Farràs, F. Teixidor, C. Viñas, R. Sillanpää, R. Kivekäs, *Angew. Chem. Int. Ed.*, **2006**, *45*, 1270; b) Y-J. Lee, J-D. Lee, S-J. Kim, S. Keum, J. Ko, I-H. Suh, M. Cheong, S. O. Kang, *Organometallics*, **2004**, *23*, 203; c) H. Wang, H-W. Li, Z. Xie, *Organometallics*, **2004**, *23*, 875; d) F. Teixidor, R. Núñez, C. Viñas, R. Sillanpää, R. Kivekäs, *Inorg. Chem.*, **2001**, *40*, 2587; e) F. Teixidor, R. Núñez, C. Viñas, R. Sillanpää, R. Kivekäs, *Angew. Chem. Int. Ed.*, **2000**, *39*, 4290; *Angew. Chem.*, **2000**, *112*, 4460.

[16] a) A. Laromaine, F. Teixidor, R. Kivekäs, R. Sillanpää, C. Viñas, R. Vespalec, H. Horakova, *Dalton Trans.*, **2008**, 345; b) F. Teixidor, A. Laromaine, R. Kivekäs, R. Sillanpää, R. Benakki, B. Grüner, C. Viñas, *Dalton Trans.*, **2005**, 1785; c) A. S. Batsanov, M. A. Fox, T. G. Hibbert, J. A. K. Howard, R. Kivekäs, A. Laromaine, R. Sillanpää, C. Viñas, K. Wade, *Dalton Trans.*, **2004**, 3822; d) F. Teixidor, C. Viñas, R. Benakki, R. Kivekäs, R. Sillanpää, *Inorg. Chem.*, **1997**, *36*, 1719; e) C. Viñas, R. Benakki, F. Teixidor, J. Casabó, *Inorg. Chem.*, **1995**, *34*, 3844; f) F. Teixidor, C. Viñas, R. Kivekäs, R. Sillanpää, J. Casabó, *Inorg. Chem.*, **1994**, *33*, 2645.

[17] a) B. Wrackmeyer, Z. G. Hernandez, R. Kempe, M. Herberhold, *Z. Anorg. Allg. Chem.*, **2007**, *633*, 851; b) A. Laromaine, F. Teixidor, R. Kivekäs, R. Sillanpää, M. Arca, V. Lippolis, E. Crespo, C. Viñas, *Dalton Trans.*, **2006**, 5240; c) S. Canales, O. Crespo, M. C. Gimeno, P. G. Jones, A. Laguna, P. Romero, *Dalton Trans.*, **2003**, 4525; d) M. Herberhold, H. Yan, W. Milius, B. Wrackmeyer, *Z. Anorg. Allg. Chem.*, **2000**, *626*, 1627.

[18] A. A. Korlyukov, K. A. Lyssenko, M. Y. Antipin, N. V. Alekseev, S. P. Kniasev, E. A. Chernyshev, *J. Mol. Struct.*, **2003**, *655*, 215.

[19] B. D. Reid, A. J. Welch, *J. Organomet. Chem.*, **1992**, *438*, 371.

[20] a) Y-M. Wang, N-Y. Fu, S-H. Chang, H-K. Lee, H. N. C. Wong, *Tetrahedron*, **2007**, *63*, 8586; b) Y-J. Lee, J-D. Lee, S-J. Kim, B. W. Yoo, J. Ko, I-H. Suh, M. Cheong, S. O. Kang, *Organometallics*, **2004**, *23*, 490; c) S. O. Kang, J. Lee, J. Ko, *Coord. Chem. Rev.*, **2002**, *231*, 47; d) Y. Wang, H. Wang, H-W. Li, Z. Xie, *Organometallics*, **2002**, *21*, 3311; e) R. Kivekäs, A. Romerosa, C. Viñas, *Acta. Crystallogr. Sect. C-Cryst. Struct. Commun.*, **1994**, C50, 638.

[21] a) G. Barberà, A. Vaca, F. Teixidor, R. Kivekäs, R. Sillanpää, C. Viñas, *Inorg. Chem.*, **2008**, *47*, 7309; b) F. Teixidor, G. Barberà, C. Viñas, R. Kivekäs, R. Sillanpää, *Inorg. Chem.*, **2006**, *45*, 3496; b) F. Teixidor, G. Barberà, A. Vaca, R. Kivekäs, R. Sillanpää, J. Oliva, C. Viñas, *J. Am. Chem. Soc.*, **2005**, *127*, 10158.

[22] a) S. Hermánek, *Chem. Rev.*, **1992**, *92*, 175; b) S. J. Plešek, S. Hermánek, *Chem. Ind.,* **1977**, 360.

[23] V. I. Bregadze, V. Ts. Kampel, N. N. Godovikov, *J. Organomet. Chem.,* **1976**, 112, 249.

[24] a) M. F. Hawthorne, D. C. Young, P. M. Garret, D. A. Owen, S. G. Schwerin, F. N. Tebbe, P. A. Wegner, *J. Am. Chem. Soc.,* **1968**, 90:4, 862; b) R. A. Wiesboeck, M. F. Hawthorne, *J. Am. Chem. Soc.,* **1964**, 86, 1642.

[25] a) J. Buchanan, E. M. J. Hamilton, D. Reed, A. J. Welch, *J. Chem. Soc., Dalton Trans.,* **1990**, 677; b) X. L. R. Fontaine, N. N. Greenwood, J. D. Kennedy, K. Nestor, M. Thornton-Pett, S. Hermánek, T. Jelinek, B. Stibr, *J. Chem. Soc., Dalton Trans.,* **1990**, 681.

[26] C. Viñas, J. Pedrajas, J. Bertran, F. Teixidor, R. Kivekäs, R. Sillanpää, *Inorg. Chem.*, **1997**, *36*, 2482.

[27] a) R. Núñez, O. Tutusaus, F. Teixidor, C. Viñas, R. Sillanpää, R. Kivekäs, *Chem. Eur. J.*, **2005**, *11*, 5637; b) J.G. Planas, C. Viñas, F. Teixidor, M.E. Light, M.B. Hursthouse, H.R. Ogilvie, *Eur. J. Inorg. Chem.*, **2005**, 4193; c) J.G. Planas, C. Viñas, F. Teixidor, A. Comas-Vives, G. Ujaque, A. Lledós, M.E. Light, M.B. Hursthouse, *J. Am. Chem. Soc.*, **2005**, *127*, 15976; d) F. Teixidor, C. Viñas, "Product Subclass 40: Carboranes and Metallacarborane", in *Science of Synthesis*, Eds.; D.S. Kaufmann, D.S. Matteson, Georg Thieme, Stuttgart, **2005**, 6, p. 1235; e) S. Tomlinson, C. Zheng, N.S. Hosmane, J. Yang, Y. Wang, H. Zhang, T.G. Gray, T. Demissie, J.A. Maguire, F. Baumann, A. Klein, B. Sarkar, W. Kaim, W.N. Lipscomb, *Organometallics*, **2005**, *24*, 2177; f) O. Tutusaus, R. Núñez, C. Viñas, F. Teixidor, I. Mata, E. Molins, *Inorg. Chem.*, **2004**, *43*, 6067; g) I. Rojo, F. Teixidor, C. Viñas, R. Kivekäs, R. Sillanpä, *Chem. Eur. J.*, **2004**, *10*, 5376; h) M. Hata, J.A. Kautz, X.L. Lu, T.D. McGrath, F.G.A. Stone, *Organometallics*¸ **2004**, *23*, 3590.

[28] M. M. Fein, J. Bobinski, N. Mayes, N. N. Schawartz, M. S. Cohen, *Inorg. Chem.*, **1963**, *2*, 1111.

[29] a) A. Laromaine, F. Teixidor, C. Viñas, *Angew. Chem. Int. Ed.*, **2005**, *44*, 2220; b) C. Viñas, G. Barberà, F. Teixidor, *J. Organomet. Chem.*, **2002**, *642*, 16.

[30] a) R. D. McIntosh, D. Ellis, G. M. Rosair, A. J. Welch, *Angew. Chem.*, **2006**, *118*, 4419; *Angew. Chem. Int. Ed.*, **2006**, *45*, 4313; b) L. Deng, J. Zhang, H.-S. Chan, Z. Xie, *Angew. Chem.*, **2006**, *118*, 4415; *Angew. Chem. Int. Ed.*, **2006**, *45*, 4309.

[31] L. Deng, H.-S. Chan, Z. Xie, *Angew. Chem. Int. Ed.*, **2005**, *44*, 2.

[32] M. F. Hawthorne, D. C. Young, P. A. Wegner, *J. Am. Chem. Soc.,* **1965**, *87*, 1818.

[33] M. F. Hawthorne, T. D. Andrews, *J. Chem. Soc., Chem. Comm.,* **1965**, 443.

[34] a) M. F. Hawthorne, R. L. Pilling, *J. Am. Chem. Soc.,* **1965**, *87*, 3987; b) D. Grafstein, J. Dvork, *Inorg. Chem.*, **1963**, *2*, 1128.

[35] A. Zalkin, D. H. Templeton, T. E. Hopkins, *J. Am. Chem. Soc.,* **1965**, *87*, 3988.

[36] a) R. M. Wing, *J. Am. Chem. Soc.,* **1968**, *90*, 4828; b) R. M. Wing, *J. Am. Chem. Soc.,* **1967**, *89*, 5599.

[37] a) I. B. Sivaev, V. I. Bregadze, *Collect. Czech. Chem. Commun.*, **1999**, *64*, 783; b) A. Franken, J. Plešek, C. Nachtigal, *Collect. Czech. Chem. Commun.*, **1997**, *62*, 746; c) J. Plešek, S. Heřmánek, *Collect. Czech. Chem. Commun.*, **1995**, *60*, 1297; d) M. R. Churchill, K. Gold, J. N. Francis, M. F. Hawthorne, *J. Amer. Chem. Soc.,* **1969**, *91*, 1222.

[38] a) A. N. Gashti, J. C. Huffman, A. Edwards, G. Szekeley, A. R. Siedle, J. A. Karty, J. P. Reilly, L. J. Todd, *J. Organomet. Chem.*, **2000**, *614*, 120; b) P. K. Hurlburt, R. L. Miller, K. D. Abney, T. D. Foreman, R. J. Butcher,

S. A. Kinkead, *Inorg. Chem.*, **1995**, *34*, 5215; c) L. Matel, F. Macásek, P. Rajec, S. Harmanek, J. Plešek, *Polyhedron,* **1982**, *1*, 511.

[39] a) I. P. Beletskaya, V. I. Bregadze, V. A. Ivushkin, P. V. Petrovskii, I. B. Sivaev, G. G. Zhigareva, *J. Organomet. Chem.*, **2004**, *689*, 2920; b) I. Rojo, F. Teixidor, C. Viñas, R. Kivekäs, R. Sillanpaä, *Chem. Eur. J.,* **2003**, *9*, 4311; c) I. Rojo, F. Teixidor, R. Kivekäs, R. Sillanpaä, C. Viñas, *J. Am. Chem. Soc.,* **2003**, *125*, 14720; d) I. Rojo, F. Teixidor, R. Kivekäs, R. Sillanpaä, C. Viñas, *Organometallics,* **2003**, *22*, 4642; e) M. D. Mortimer, C. B. Knobler, M. F. Hawthorne, *Inorg. Chem.,* **1996**, *35*, 5750.

[40] J. Plešek, S. Hermánek, A. Franken, I. Cisarova, C. Nachtigal, *Collect. Czech. Chem. Commun.,* **1997**, 62, 47.

[41] a) I. Rojo, J. Pedrajas, F. Teixidor, C. Viñas, R. Kivekas, R. Sillanpaä, I. Sivaev, V. Bregadze, S. Sjöberg. *Organometallics,* **2003**, 22, 3414; b) I. B. Sivaev, Z. A. Starikova, S. Sjöberg, V. I. Bregadze, *J. Organomet. Chem.*, **2002**, *649*, 1; c) J. Plešek, B. Grüner, S. Heřmánek, J. Báča, V. Mareček, J. Jänchenová, A. Lhotský, K. Holub, S. Selucký, J. Rais, I. Císařová, J. Čáslavský, *Polyhedron*, **2002**, *21*, 975; d) B. Grüner, J. Plešek, J. Báča, I. Císařová, J. F. Dozol, H. Rouquette, C. Viñas, P. Selucký, J. Rais, *New J. Chem.*, **2002**, *26*, 1519; e) P. Selucký, J. Plešek, J. Rais, M. Kyrs, L. Kadlecova, *J. Radioanal. Nucl. Chem.*, **1991**, *149*, 131.

[42] a) C. Viñas, S. Gómez, J. Bertran, F. Teixidor, J. Barron, R. Sillanpää, R. Kivekäs, J. F. Dozol, H. Rouquette, *J. Organomet. Chem.*, **1999**, *581*, 188; b) C. Viñas, S. Gómez, J. Bertran, F. Teixidor, J. F. Dozol, H. Rouquette, *Chem. Comm.*, **1998**, 191; c) C. Viñas, S. Gómez, J. Bertran, F. Teixidor, J. F. Dozol, H. Rouquette, *Inorg. Chem.*, **1998**, *43*, 3640; d) C. Viñas, J. Bertran, S. Gómez, F. Teixidor, R. Sillanpää, R. Kivekäs, J. F. Dozol, H. Rouquette, *J. Chem. Soc., Dalton Trans.*, **1998**, *17*, 2849.

[43] R. M. Chamberlin, B. L. Scott, M. M. Melo, K. D. Abney, *Inorg. Chem.*, **1997**, *36*, 809.

[44] I. Rojo, F. Teixidor, C. Viñas, R. Kivekäs, R. Sillanpaä, *Chem Eur. J.,* **2004**, *10*, 5376.

[45] E. J. Juarez, C. Viñas, A. Gonzalez-Campo, F. Teixidor, R. Sillanpaä, R. Kivekäs, R. Nunez, *Chem Eur. J.,* **2008**, *14*, 4924.

[46] a) R. N. Grimes, *J. Chem. Educ.*, **2004**, *81*, 657; b) F. Teixidor, C. Viñas, A.Demonceau, R. Nunez, *Pure Appl. Chem.*, **2003**, *75*, 1305; c) R. N. Grimes, *Coord. Chem. Rev.*, **2000**, *200*, 773; d) J. Plešek, *Chem. Rev.*, **1992**, *92*, 269.

[47] K. H. Pannel, B. L. Kalsotra, C. Parkanyi, *J. Heterocyclic Chem.*, **1978**, *15*, 1057.

[48] J. Lefevre, *Techniques de l'Ingénieurs-Mécanique et Chauleur* B8 II, **1990**, B 36600-1 à 3361-10.

[49] *Revue Générale Nucléaire*, **1992**, 5 September-October.

[50] P. Chauvet, T. Dippel, *Radioactive Waste Management,* **1979**, 1.

[51] A. Takibayev, M. Saito, V. Artisyuk, H. Sagara, *Progress in nuclear energy*, **2005**, *47*, 354.

[52] S. D. Reilly, C. F. V. Mason, P. H. Smith, *Cobalt(III) Dicarbollide: a potencial ^{137}Cs and ^{90}Sr waste extraction agent*, Report LA-11695, Los Alamos National Laboratory, Los Alamos, NM **1990**.

[53] B. Grüner, L. Mikulasek, I. Cisarova, V. Böhmer, C. Danila, M. M. Reinoso-Garcia, W. Verboom, D. N. Reinhoudt, A. Casnati, R. Ungaro. *Eur. J. Org. Chem.,* **2005**, 10, 2022.

[54] B. Grüner, J. Plêsek, J. Baca, I. Cisarova, J. F. Dozol, H. Rouquette, C. Viñas, P. Selucky, J. Rais. *New J. Chem.,* **2002**, 26, 1519.

[55] a) C. Hill, J. F. Dozol, H. Rouquette, S. Eymard, B. Tournois, *J. Membrane Sci.*, **1996**, *114*, 73; b) J. F. Dozol, F. López Calahorra, A. Mckervey, V. Böhmer, R. Ungaro, M. J. Schwing, F. Arnaud, D. Reinhoudt, G. Wipff, *Fourth Conference of the European Commission on the Management and Disposal of Radioactive Waste*,

European Commission, Book of Abstracts, **1996**, 23; c) Z. Asfari, M. Nierlich, P. Thuéry, V. Lamare, J. F. Dozol, M. Leroy, J. Vicens, *An. Quím.*, **1996**, *92*, 260; d) R. Ungaro, A. Casnati, F. Ugozzoli, A. Pochini, J. F. Dozol, C. Hill, H. Rouquette, *Angew. Chem. Int. Ed. Engl.*, **1994**, *33*, 1506.

[56] a) J. D. Kaw, K. N. Brewer, R. S. Herbst, T. A. Todd, D. J. Wood, *Waste Manage*, **1999**, 19, 27; b) E. P. Horwitz, D. G. Kalina, H. Diamond, G. Vandergrift, W. W. Schultz, *Solvent Extr. Ion Exch.*, **1985**, *3*, 75.

[57] a) P. K. Hurlburt, R. L. Miller, K. D. Abney, T. M. Foreman, R. J. Butcher, S. A. Kinkead, *Inorg. Chem.*, **1995**, *34*, 5215; b) J. Rais, P. Selucký, *Nucleon*, **1992**, *1*, 17; c) P. Selucký, K. Base, J. Plešek, S. Heřmánek, J. Rais, *Czech. Patent 215 282*, **1986**: *Chem. Abstr.*, **1986**, *104*, 186637.

[58] G. L. Locher, *Am. J. Roentgenol, Radium. Ther.*, **1936**, 36, 1.

[59] a) M. F. Hawthorne, M.W. Lee, *J. Neuro-Oncol.*, **2003**, *62*, 33; b) A. H. Soloway, J. C. Zhuo, F. G. Rong, A. J. Lunato, D. H. Ives, R. F. Barth, A.K. M. Anisuzzaman, C. D. Barth, B. A. Barnum, *J. Organometal. Chem.*, **1999**, *581*, 150; c) M. F. Hawthorne, A. Maderna, *Chem. Rev.*, **1999**, *99*, 3421; d) M. F. Hawthorne, *Mol. Med. Today*, **1998**, *4*, 174.

[60] a) A. H. Soloway, W. Tjarks, B. A. Barnum, F. G. Rong, R. F. Barth, I. M. Codogni, J. G. Wilson, *Chem. Rev.*, **1998**, *98*, 1515; b) M. F. Hawthorne, *Angew. Chem. Int. Ed. Engl.*, **1993**, *32*, 950.

[61] a) X. Zhu, R. Clackdoyle, S. Shortkroff, J. Yanch, *Phys. Med. Biol.*, **2008**, *53*, 2715; b) J. F. Valliant, K. J. Guenther, A. S. King, P. Morel, P. Schaffer, O. O. Sogbein, K. A. Stephenson, *Coord. Chem. Rev.*, **2002**, *232*, 173; c) J. C. Yanch, S. Shortkroff, R. E. Shefer, S. Johnson, E. Binello, D. Gierga, A. G. Jones, G. Young, C. Vivieros, A. Davison, C. Sledge, *Med. Phys.*, **1999**, *26*, 364.

[62] G. Barberà, F. Teixidor, C. Viñas, R. Sillanpää, R. Kivekäs, *Eur. J. Inorg. Chem.*, **2003**, 1511.

[63] H. Shalem, S. Shatzmiller, B. Feit, *J. Chem. Soc., Perkin Trans.*, **2000**, *1*, 2831.

[64] R. Srivastava, D. Hamlin, S. Wilbur, *J. Org. Chem.*, **1996**, *61*, 9041.

[65] a) M. Kožíšek, P. Cígler, M. Lepšík, J. Fanfrlík, P. Řezáčová, J. Brynda, J. Pokorná, J. Plešek, B. Grüner, J. Grantz-Šašková, J. Prejdová, V. Král, J. Konvalinka, *J. Med. Chem.*, **2008**, *51*, 4839; b) P. Cígler, M. Kožíšek, P. Řezáčová, J. Brynda, Z. Otwinowski, J. Pokorná, J. Plešek, B. Grüner, L. Dolecková-Maresová, M. Másа, J. Sedlácek, J. Bodem, H. G. Kräusslich, V. Král, J. Konvalinka, *Proc. Nat. Acad. Sci.*, **2005**, *102*, 15395.

[66] a) V. Serreli, C. F. Lee, E.R. Kay, D. A. Leigh, *Nature*, **2007**, *445*, 523; b) R. Eelkema, M. M. Pollard, J. Vicario, N. Katsonis, B. S. Ramon, C. W. M. Bastiaansen, D. J. Broer, B. L. Feringa, *Nature*, **2006**, *440*, 163; c) S. P. Fletcher, F. Dumur, M. M. Pollard,, B. L. Feringa, *Science*, **2005**, *310*, 80; d) R. Ballardini, V.Balzani, A. Credi, M. T. Gandolfi, M. Venturi, *Acc. Chem. Res.*, **2001**, *34*, 445.

[67] A. G. H. Vicente, D. J. Nurco, S. J. Shetty, C. J. Medforth, K. M. Smith, *Chem. Commun.*, **2001**, 483.

[68] M. F. Hawthorne, J. I. Zink, J. M. Skelton, M. J. Bayer, C. Liu, E. Livshits, R. Baer, D. Neuhauser *Science,* **2004**, *303*, 1849.

[69] a) J. F. Morin, T. Sasaki, Y. Shirai, J. M. Guerrero, J. M. Tour *J. Org. Chem.,* **2007**, *72*, 9481; b) T. Sasaki, J. M. Tour *Tetrahedron Lett.,* **2007**, *48*, 5821-5824; c) T. Sasaki, J. –F. Morin, M. Lu, J. M. Tour *Tetrahedron Lett.,* **2007**, *48*, 5817; d) Y. Shirai, A. J. Osgood, Y. Zhao, Y. Yao, L. Saudan, H. Yang, C. Yu-Hung, T. Sasaki, J. –F. Morin, J. M. Guerrero, K. F. Kelly, J. M. Tour *J. Am. Chem. Soc.,* **2006**, *128*, 4854; e) Y. Shirai, A. J. Osgood, Y. Zhao, K. F. Kelly, J. M. Tour *Nano Lett.,* **2005**, *5*, 2330.

[70] a) F. Teixidor, M. A. Flores, C. Viñas, R. Kivekäs, R. Sillanpää, *J. Am. Chem. Soc.*, **2000**, *122*, 1963; b) C. Viñas, M. A. Flores, R. Nuñez, F. Teixidor, R. Kivekäs, R. Sillanpää, *Organometallics,* **1998**, *17*, 2278; c) F. Teixidor, M. A. Flores, C. Viñas, R. Kivekäs, R. Sillanpää, *Angew. Chem., Int. Ed*., **1996**, *35*, 2251.

[71] M.F. Hawthorne, *Advances on Boron and the Boranes,* eds. J.F. Liebman, A. Greenberg, R.E. Williams, VCH Pubishers, New York, **1988**, Capítol 10, p. 225.

[72] a) O. Tutusaus, S. Delfosse, A. Demonceau, A.F. Noels, R. Nuñez, C. Viñas, F. Teixidor, *Tetrahedron Lett.*, **2002**, *43*, 983; b) A. Demonceau, F. Simal, A.F. Noels, C. Viñas, R. Nuñez, F. Teixidor, *Tetrahedron Lett.*, **1997**, *38*, 7879.

[73] a) O. Tutusaus, C. Viñas, R. Nuñez, F. Teixidor, A.. Demonceau, S. Delfosse, A.F. Noels, I. Mata, E. Molins, *J. Am. Chem. Soc.,* **2003**, *125*, 11830; b) F. Simal, S. Sebile, A. Demonceau, A.F. Noels, R. Nuñez, M. Abad, F. Teixidor, C. Viñas, *Tetrahedron Lett.*, **2000**, 41, 5347.

[74] O. Tutusaus, S. Delfosse, F. Simal, A. Demonceau, A.F. Noels, R. Nuñez, C. Viñas, F. Teixidor, *Inorg. Chem. Commun.,* **2002**, *5*, 941.

[75] a) C. Masalles, S. Borrós, C. Viñas, F. Teixidor, *Adv. Mater.*, **2000**, *16*, 1199; b) C. Masalles, J. Llop, C. Viñas, F. Teixidor, *Adv. Mater.*, **2002**, *14*, 826

[76] E. Crespo, *Tesi Doctoral*, Universitat Autònoma de Barcelona, Bellaterra, **2007**.

[77] a) A. I. Stoica, C. Viñas, F. Teixidor, *Chem. Commun.*, **2008**, 6492; b) Y. Quin, E. Bakker, *Anal. Chem.*, **2003**, *75*, 6002.

[78] a) N. Zine, J. Bausells, F. Teixidor, C. Viñas, C. Masalles, J. Smitier, A. Errachid, *Mater., Sci. Eng., C*, **2006**, *26*, 399; b) N. Zine, J. Bausells, E. Ivorra, J. Aguiló, M. Zabala, F. Teixidor, C. Viñas, A. Errachid, *Sensors and Actuators B*, **2003**, *91*, 76.

[79] a) R. Hamasaki, M. Ito, M. Lamrani, M. Mitsuishi, T. Miyashita, Y. Yamamoto, *J. Mater. Chem.*, **2003**, *13*, 21; b) J.T. Taylor, J. Carusso, A. Newlon, U. Englich, K. Ruhlandt-Sende, J.T. Spencer, *Inorg. Chem.*, **2001**, *40*, 3381; c) M. Lamrani, R. Hamasaki, M. Mitsuishi, T. Miyashita, Y. Yamamoto, *Chem. Commun.*, **2000**, 1595.

[80] a) K. Ohta, A. Januszko, P. Kaszynski, T. Nagamine, G. Sasnouski, Y. Endo, *Liq. Cryst.*, **2004**, *31*, 671; b) W. Piecek, J.M. Kaufman, P. Kaszynsky, *Liq. Cryst.*, **2003**, *30*, 39; c) P. Kaszynski, S. Pakhomov, K.F. Tesh, *Inorg. Chem.*, **2001**, *40*, 6622; c) P. Kasynsky, *Collect. Czech. Chem. Commun.*, **1999**, *64*, 895; d) A.G. Douglass, K. Czuprynski, M. Mierzwa, P. Kaszynski, *Chem. Mater.*, **1998**, *10*, 2399.

[81] S-Y. Lu, I. Hamerton, *Prog. Polym. Sci.*, **2002**, *27*, 1661.

[82] a) M.K. Kolel-Veetil, T. Keller, *J. Polym. Sci., Part A*, **2006**, *44*, 147; b) M.K. Kolel-Veetil, H.W. Beckham, T.M. Séller, *Chem. Mater.*, **2004**, *16*, 3162; c) H. Kimura, K. Okita, M. Ichitani, T. Sugimoto, S. Kuroki, I. Ando, *Chem. Mater.*, **2003**, *15*, 355; d) M.K. Kolel-Veetil, T.M. Keller, *J. Mater. Chem.*, **2003**, *13*, 1652; e) T.M. Keller, *Carbon*, **2002**, 225; f) M. Ichitani, K. Yonezawa, K. Okada, T. Sugimoto, *Polym. J.*, **1999**, *31*, 908; g) E.J. Houser, T.M. Keller, *Macromolecules*, **1998**, *31*, 4038.

[83] a) M. Ito, T.X. Wei, P-L. Chen, H. Akiyama, M. Matsumoto, K. Tamada, Y. Yamamoto, *J. Mater. Chem.*, **2005**, *15*, 478; b) T. Baše, Z. Bastl, Z. Plzák, T. Grygar, J. Plešek, M.J. Carr, V. Malina, J. Šubrt, J. Bohácek, E. Vecerníková, O. Kriz, *Langmuir*, **2005**, *21*, 7776.

2.- RESUM GLOBAL

2. RESUM GLOBAL

2.1 COBALTO-BIS(DICARBALLUR) SUBSTITUÏT EN ELS ÀTOMS DE CARBONI

El suggeriment l'any 1997[1] d'un mètode sintètic per obtenir de manera directa derivats de l'anió cobalto-bis(dicarballur) en els àtoms de carboni va despertar l'interès per aquest tipus de compostos. Tot i així, a la bibliografia s'han trobat pocs exemples on s'utilitzi aquesta metodologia, la majoria dels quals són fets al nostre grup.[2] A més, si es mira la base de dades de Cambridge d'estructures cristal·lines, només existeixen 20 estructures de C-derivats del compost **1**, i menys de la meitat s'han sintetitzat per aquest camí directe. Això ens va encoratjar a estudiar la reactivitat d'aquestes posicions i veure les propietats que oferien els compostos sintetitzats.

2.1.1 Substitució amb fòsfor en els àtoms de carboni.

La síntesi de derivats amb fòsfor ja s'havia dut a terme anteriorment al nostre grup.[2b] La dificultat d'obtenir la monosubstitució en els àtoms de carboni del compost **1** va portar a forçar les condicions de reacció a fi de desplaçar l'equilibri entre les espècies no-, mono- i di-substituïdes, tal com es mostra a la figura 2.1.1.

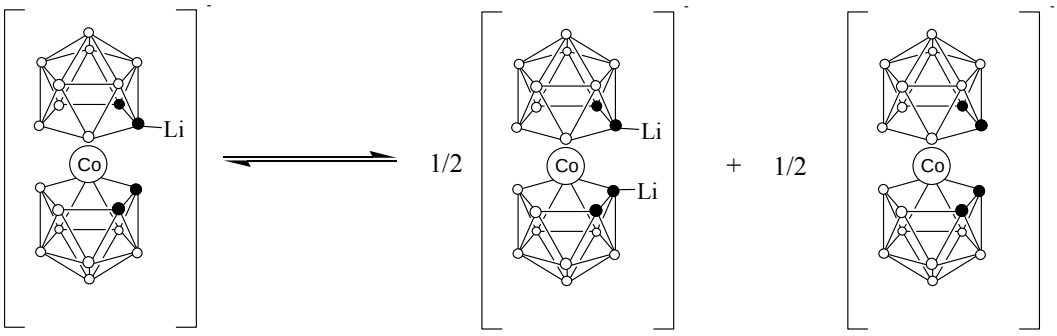

Figura 2.1.1. Equilibri entre les espècies mono i dilitiada

Així, les condicions de reacció òptimes per afavorir la disubstitució són una estequiometria 1:2:2 entre **1**:*n*-BuLi:halur de fosfina, el 1,2-dimetoxietà (DME) com a dissolvent, i una temperatura de -40ºC. D'aquesta manera, es van sintetitzar un conjunt de derivats disubstituïts amb àtoms de fòsfor amb unes propietats complexants molt interessants.

Si es fa una comparació entre els fòsfor-derivats del ferrocè i del cobalto-bis(dicarballur) es pot observar com les propietats complexants d'ambdós tipus de compostos són força diferents. Així com els derivats dels ferrocè es coordinen amb facilitat amb tot tipus de metalls, els derivats del cobalto-bis(dicarballur) coordinen només amb alguns metalls. A més, dels derivats del ferrocè se'n coneix també la seva activitat catalítica. En canvi, no hi havia possibilitat de comparació en el cas de derivats pinçats. Es coneix pel ferrocè que el pinçament dels dos anells de ciclopentadienur provoca un canvi de reactivitat important, de manera que en resulten compostos molt interessants en les reaccions d'obertura d'anell, en reaccions de metàtesi i en polimeritzacions. Aquests compostos s'anomenen ferrocenofans.

La geometria dels ferrocenofans s'ha estudiat en profunditat i s'ha trobat que hi ha una relació directa entre la reactivitat i fins i tot propietats òptiques i alguns paràmetres geomètrics que es mostren a la figura 2.1.2. Per aquesta raó, si es volen compostos més reactius davant de les reaccions d'obertura d'anell es busca que l'angle α sigui més gran, o sigui que la distorció dels plans entre els anells sigui major.

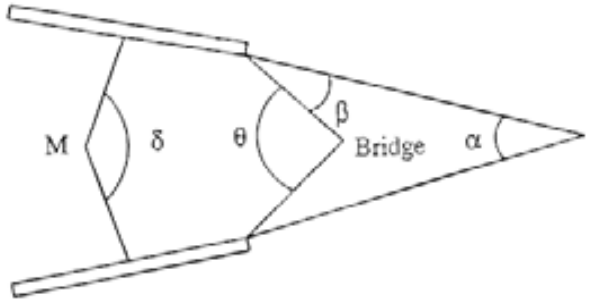

Figura 2.1.2. Esquema dels paràmetres geomètrics a estudiar en els ferrocenofans.

Amb aquestes consideracions es va començar a estudiar la possibilitat de sintetizar derivats amb fòsfor pinçats del compost **1**. La síntesi està esquematitzada a la figura 2.1.3 i com es pot observar s'ha intentat obtenir compostos diferents per comprovar l'efecte de cada variació en les propietats finals. Així, partint del compost **2** on es té el grup P-Ph, s'ha canviat l'anell aromàtic pel grup P-^{t}Bu per veure l'efecte del substituent a la fosfina. A més, s'ha partit del compost **10** (B-Ph-B), on ja hi ha un pinçament de les caixes de carborà pels àtoms de bor, i s'ha fet la mateixa reacció per obtenir tant el derivat P-Ph (compost **11**) com el derivat P-^{t}Bu (compost **15**), i comprovar així l'efecte d'un doble pinçament del clúster. Els rendiments dels productes són de moderats a alts i en tots els casos la purificació s'ha dut a terme per cromatografia de columna amb una mescla diclormetà/acetonitril. Tots els compostos s'han obtingut com a sals de NMe_4^+.

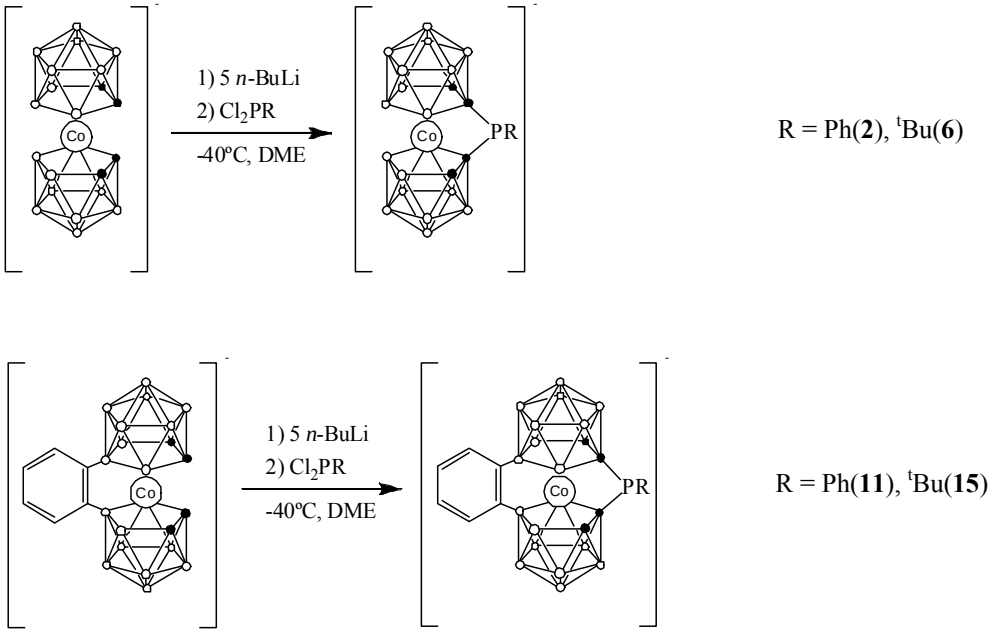

Figura 2.1.3. Síntesi dels derivats pinçats amb fòsfor.

Un cop sintetitzats aquests compostos s'ha dut a terme la caracterització. Aquesta s'ha fet utilitzant els mètodes convencionals utilitzats al llarg del treball. El resultat més sorprenent ha estat el desplaçament en l'espectre de ^{31}P-RMN en tots els compostos. Els valors es troben entre 70 i 96 ppm, molt lluny dels valors obtinguts en el cas de les fosfines disubstituïdes, al voltant de 25 ppm. Per aquesta raó s'ha volgut estudiar què passava en aquests compostos i quina o quines eren les causes d'aquest desplaçament anormal. La primera hipòtesi ve donada pel fet que un desplaçament a camp baix indica que l'àtom de fòsfor està més desapampolat, és a dir que la densitat electrònica al seu entorn més immediat és més baixa. Per tant, la densitat electrònica que s'hauria esperat prop del fòsfor s'ha afeblit en benefici d'una altra part de la molècula.

A fi d'esbrinar les raons d'aquest comportament s'ha realitzat càlculs teòrics als compostos **2** i **11**, que ens han servit a mode d'exemple. Es coneix en el cas del ferrocenofans que en uns pocs exemples hi ha indicis d'haver-hi una interacció entre l'àtom que està pinçant els dos anells de ciclopentadienur i el metall, en aquest cas el ferro.[3] Aquesta interacció pot fer que una part de la càrrega sobre el fòsfor se'n vagi cap al ferro que té capacitat acceptora. Això podria ser el que passa en el nostre cas i per confirmar la hipòtesi s'ha optimitzat la geometria del compost **2** i s'ha fet una anàlisi NBO (Natural Bond Orbitals). Els orbitals NBO es defineixen com orbitals localitzats en pocs centres (1, 2 o en alguns casos més) que descriuen la distribució d'enllaços moleculars tipus Lewis dels parells d'electrons en la forma

més compacta. Aquesta anàlisi permet trobar interaccions donador-acceptor entre aquests orbitals i, per tant, ens pot ser molt útil en l'estudi del nostre cas. El nivell de càlcul utilitzat ha estat B3LYP/6-31(d) a l'optimitzar l'estructura i B3LYP/6-311+G(d,p) per calcular les energies i l'anàlisi NBO. La geometria obtinguda s'ha pogut comparar amb dades experimentals ja que pel compost **11** s'ha obtingut l'estructura cristal·lina, com es mostra a la figura 2.1.4. Així doncs, comparant la geometria experimental i la calculada teòricament s'ha vist que la correlació era bona i que, per tant, el nivell de càlcul és suficient en aquest tipus de compostos.

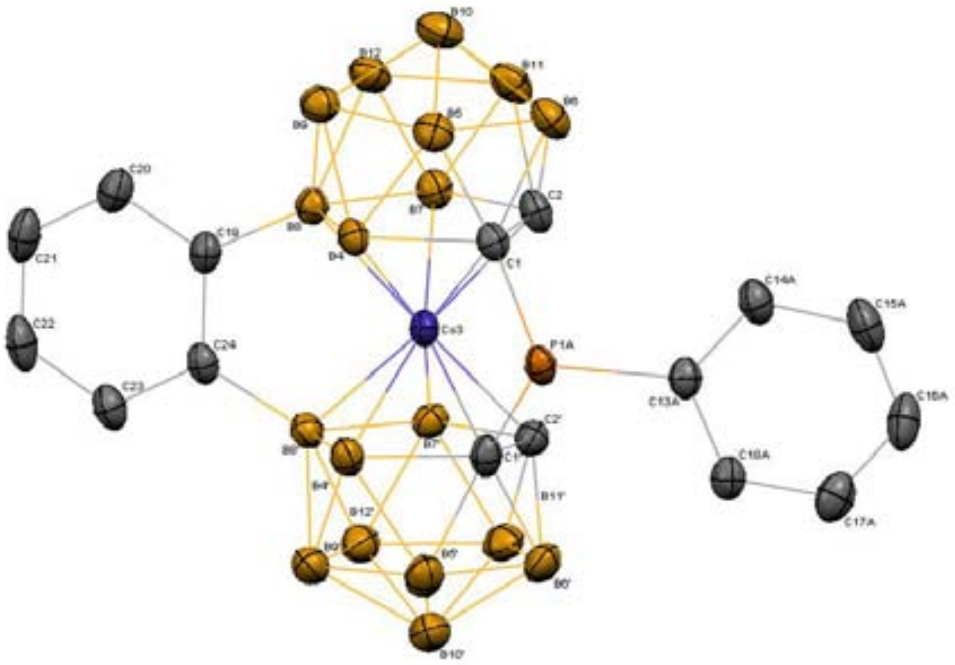

Figura 2.1.4. Estructura cristal·lina del compost **11**, amb grup espacial P21/c.

El resultat, com es pot veure de forma esquemàtica a la figura 2.1.5a, mostra interaccions de prop de 20 kcal/mol entre els enllaços C_c-P i el Co, però també una interacció més dèbil de 10 kcal/mol entre el fòsfor i el cobalt. Aquesta interacció es dóna més específicament entre el parell lliure d'electrons del fòsfor que actua com a donador, i l'orbital 4s buit del cobalt que actua com a acceptor. Tot i que aquesta interacció no és molt forta respecte a l'energia d'un enllaç covalent típic, sí que ho és respecte a un enllaç d'hidrogen i cal tenir-la en compte si es compara amb l'energia de l'enllaç Co-P que està entre 70-75 kcal/mol.[4] A la figura 2.1.5b es pot observar també la representació gràfica d'aquesta interacció. Es veu com l'orbital buit del cobalt es deforma totalment cap a la posició del fòsfor per tal de poder fer aquesta interacció.

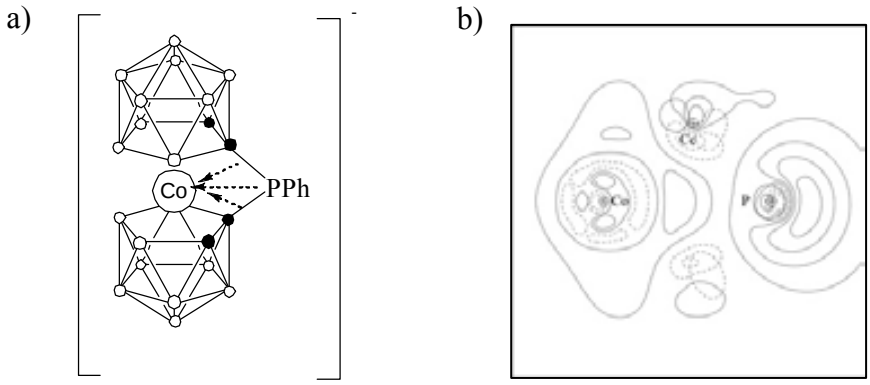

Figura 2.1.5. a) Esquema de les interaccions donador-acceptor entre fósfor i cobalt. b) Representació en 2D de la interacció P-Co.

L'efecte del substituent no és ni de bon tros tan gran com aquesta interacció si es té en compte la diferència en l'espectre de ^{31}P-RMN entre el senyal del compost disubstituït a 25 ppm i el senyal del compost pinçat a 70 ppm. Si es compara el desplaçament de ^{31}P-RMN entre els derivats P-Ph i P-^{t}Bu hi ha una diferència de només 7-8 ppm, essent el derivat amb el grup alifàtic el desplaçat a camp baix. En canvi, hi ha una diferència més gran en comparar els desplaçaments dels compostos **2** i **11**, o sigui en presència o absència de l'anell aromàtic pinçant els àtoms de bor B(8) i B(8'). En aquest cas la diferència és de 18 ppm, i és el compost **11** el que té el desplaçament de ^{31}P-RMN a camp més baix. Això pot ser degut a la naturalesa acceptora de l'anell aromàtic, que ajuda a desapampolar l'àtom de fòsfor. L'anàlisi NBO del compost **11** ens revela les mateixes interaccions entre l'àtom de cobalt i el fòsfor, però també hi ha interaccions addicionals entre els enllaços B(8)-C_{Ph} i B(8')-C_{Ph} i el cobalt. Aquestes transferències de càrrega donador-acceptor tenen una energia d'unes 7 kcal/mol. El fet de tenir l'anell aromàtic pinçant en els àtoms de bor ajuda la dissipació de la càrrega dins el clúster i, per tant, permet a aquest desapampolar més l'àtom de fòsfor.

Per tal de trencar la interacció fòsfor-cobalt, s'han oxidat aquestes fosfines de partida amb oxigen, sofre i seleni. D'aquesta manera el parell d'electrons lliure del fòsfor, responsable de la interacció, formarà enllaç amb aquests elements. La síntesi de les fosfines oxidades amb oxigen s'ha realitzat en acetona a 0ºC, afegint lentament una dissolució 0.1M de H_2O_2. Posteriorment s'addiciona una dissolució aquosa de clorur de tetrametilamoni per tal de precipitar els sòlids. D'aquesta manera els compostos oxidats **3**, **7**, **12**, **16** s'obtenen amb uns rendiments de 89, 89, 95 i 94 % respectivament. En el cas de l'oxidació amb sofre, la síntesi s'ha fet en acetona, amb 4 equivalents de sofre en pols i deixant la mescla 30h a reflux.

Un cop a temperatura ambient, el sofre s'ha filtrat i l'evaporació del dissolvent ha donat els compostos **4**, **8**, **13** i **17** amb uns rendiments de 94, 95, 86 i 86% respectivament. Finalment, l'oxidació amb seleni s'ha fet d'una manera semblant, però posant només un equivalent de seleni en pols. Amb l'evaporació de l'acetona s'obtenen els compostos **5**, **9**, **14** i **18** amb uns rendiments de 96, 86, 97 i 88% respectivament.

Un cop sintetitzats els compostos han estat caracteritzats per espectroscòpia d'infraroig, espectroscòpia de ressonància magnètica nuclear de ^{1}H, ^{11}B, ^{31}P i ^{13}C, anàlisi elemental, espectrometria de masses i difracció de raigs X. Ara bé, les dades que ens interessen més són els desplaçaments químics de ^{31}P-RMN perquè són els primers indicadors de l'existència o absència de la interacció trobada en les fosfines no-oxidades. Així, a la taula 2.1.1 es poden observar de forma resumida els desplaçaments químics de fòsfor de tots els compostos. La posició de l'àtom de fòsfor en les espècies oxidades amb oxigen es desplaça a camp alt, indicant-ne un apampolament d'aquest. Aquest comportament és del tot anormal en les fosfines ja que en ser oxidades se'n van a camp baix degut a la densitat electrònica que l'àtom d'oxigen treu al fòsfor. Per tant, podem dir que la interacció Co-P present en l'espècie no oxidada distorsiona més la densitat electrònica al voltant del fòsfor que no pas l'enllaç P-O. Per contra les espècies oxidades amb sofre i seleni presenten els seus desplaçaments de ^{31}P-RMN molt similars als dels compostos no oxidats corresponents. Per tant, en aquest cas els enllaços P-S i P-Se tenen un comportament semblant, pel que fa al desplaçament del fòsfor, que a la interacció descrita abans.

Compost	^{31}P-RMN	^{31}P-RMN (Oxigen)	^{31}P-RMN (Sofre)	^{31}P-RMN (Seleni)
2	70.4	34.6	71.7	68.8
6	77.3	35.6	68.4	62.7
11	88.3	52.7	95.3	99.6
15	96.7	55.5	95.6	97.5

Taula 2.1.1. Resum dels desplaçaments de ^{31}P-RMN pels compostos **2**, **6**, **11**, **15** i les seves espècies oxidades.

Per tal de corroborar la hipòtesi que en oxidar les fosfines es trenca la interacció P-Co, s'ha fet l'anàlisi NBO dels compostos **3**, **4** i **5**. En tots els casos aquesta interacció desapareix al no tenir l'àtom de fòsfor el parell d'electrons lliure. En canvi, continuen existint les interaccions febles entre els enllaços C_c-P i el Co. També s'ha fet una comparació dels orbitals HOMO dels compostos **2** i **3**. L'orbital HOMO és on es troben els electrons de valència, per tant els més fàcils de treure. Si hi ha la interacció en **2** entre el P i el Co, i si és

aquest darrer on es concentra la major part dels electrons de valència, en el cas que l'àtom de fòsfor hi contribueixi, voldrà dir que hi ha comunicació amb el cobalt. En cas contrari, i com s'hauria de veure en **3**, l'àtom de P no participaria a l'orbital HOMO. El resultat, que es pot veure a la figura 2.1.6, mostra clarament la diferència entre ambdós compostos. La contribució de l'àtom de fòsfor en l'HOMO de **2** és important i en **3** és inexistent.

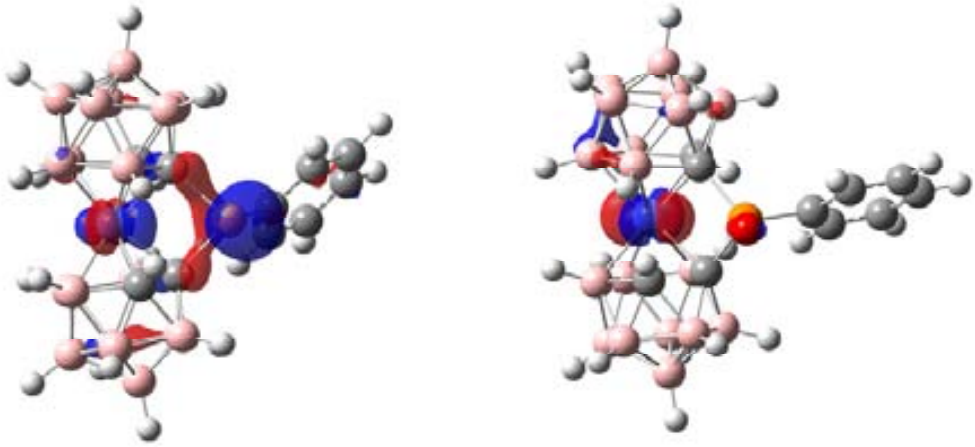

Figura 2.1.6. Orbital HOMO dels compostos **2** (esquerre) i **3** (dreta).

Per tenir una última dada experimental de la interacció P-Co s'ha fet la voltamperometria cíclica de **1**, del derivat disubstituït $[1,1'\text{-}(PPh_2)_2\text{-}3,3'\text{-}Co\text{-}(1,2\text{-}C_2B_9H_{10})_2]^-$ (diPhCOSAN) i de **2**. Aquests valors es mostren a la taula 2.1.2. S'ha observat que el valor del potencial mig $E_{1/2}$ d'aquests compostos varia de manera que és més positiu i, per tant, més fàcil de reduir, a mesura que passem de **1**, al compost disubstituït i acabem al **2**. Aquests valors demostren que hi ha una comunicació creixent amb el P, desde **1** on no n'hi hauria, a **2** on és clara tal com es veu a la figura 2.1.6.

Compost	**$E_{1/2}$ [V]**
1	-1.83
diPhCOSAN	-1.65
2	-1.62

Taula 2.1.2. Valors del potencial de reducció mig dels compostos **1**, diPhCOSAN i **2**.

Per acabar, cal destacar la importància de la geometria d'aquests compostos en relació amb els ferrocenofans. Abans s'havia dit que els ferrocenofans són compostos molt reactius degut a la deformació que presenten els anells de ciclopentadienur respecte el ferrocè lliure, i això es pot calcular mitjançant l'angle α. S'ha calculat aquest paràmetre geomètric pels

derivats del cobalto-bis(dicarballur) i el valor és molt més petit, de prop de 30º pel cas dels fosfino-ferrocenofans fins a 5º o 10º (depenent de si hi ha el pinçament en els àtoms de bor amb l'anell aromàtic) en el nostre cas. Aquesta diferència tan gran fa que els derivats que hem obtingut no siguin tan reactius i, per tant, no seran útils en reaccions d'obertura d'anell, però pel contrari els derivats del metal·lacarborà són més estables i ofereixen unes prestacions molt importants en el camp de nous materials.

2.1.2 Substitució amb sofre en els àtoms de carboni.

Després de veure l'interès que pot tenir la substitució amb àtoms de fòsfor i, especialment, el pinçament de les dues unitats dicarballur, s'ha estudiat sintetitzar compostos anàlegs amb sofre. La complexació de les difosfines en l'anió cobalto-bis(dicarballur) sintetitzades prèviament[2b] ha donat lloc a complexes amb diferents metalls de transició, tot i que encara no s'ha provat la seva activitat catalítica. El nostre grup té una àmplia experiència en la síntesi de catalitzadors derivats de l'*o*-carborà tant amb fòsfor com amb sofre.[5] Els resultats mostren com els tioèter derivats tenen una activitat més alta que les fosfines.[6] Per aquesta raó, s'ha cregut convenient sintetitzar tioèter derivats del compost **1**.

D'altra banda, a l'apartat anterior s'ha vist la importància que pot tenir el pinçament de les dues unitats de dicarballur a través dels àtoms de carboni del clúster. Si es torna a comparar amb el ferrocè, els derivats del darrer pinçats amb sofre estan més deformats que no amb els altres elements del tercer període de la taula periòdica. Els angles α (veure figura 2.1.2) van des de 21º pel silici fins als 31º en el cas del sofre.[7] Això provoca un canvi en les propietats òptiques observable a simple vista pel canvi de color d'aquests compostos. Tot i així, no hi ha un camí sintètic clar per obtenir el ferrocè pinçat amb sofre ja que el rendiment de la reacció és menor de 20% i, per tant, no s'han pogut estudiar en profunditat les propietats d'aquest.[8]

El problema que vam trobar al principi era que no hi havia cap mètode sintètic que ens permetés obtenir directament l'enllaç C_c-S en l'anió cobalto-bis(dicarballur). En el cas descrit abans amb fòsfor o el recentment publicat amb silici,[2a] s'utilitzava halurs d'aquests elements a fi d'obtenir el compost desitjat. El problema és que comercialment hi ha pocs halurs de sofre i els que hi ha són tòxics i perillosos. Per tant, hem vist necessari l'ús d'una nova via de síntesi de derivats amb sofre partint directament del compost **1**. Aquesta està basada en el mètode

descrit per Smith et al.,[9] i ha estat aplicada en el nostre grup en la introducció de grups tioèter en l'*o*-carborà.[10]

Tenint en compte que el mètode directe d'obtenir derivats en els àtoms de carboni es basa en la desprotonació dels grups C_c-H amb *n*-BuLi, s'han buscat reactius de sofre que puguin atacar aquesta posició desprotonada. Així, doncs, s'han utilitzat disulfurs com a reactius de partida i s'ha vist que el compost **1** desprotonat és prou nucleòfil per trencar l'enllaç RS-SR i formar l'enllaç C_c-SR. Això es pot veure esquematitzat a la figura 2.1.7. A més, la part que no ha reaccionat del disulfur, RS-, es pot oxidar i recuperar el RS-SR corresponent per tal de ser reutilitzat.

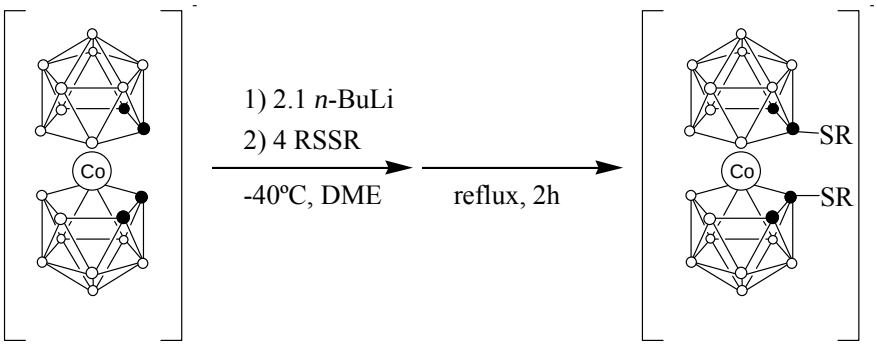

Figura 2.1.7. Esquema de la síntesis dels tioèter derivats de **1**.

La síntesi d'aquests compostos es basa, doncs, en la desprotonació a baixa temperatura del compost **1** on s'obté una dissolució lila del compost dilitiat i l'addició del disulfur corresponent que provoca un canvi instantani de color a vermell. Un cop addicionat es deixa la mescla de reacció 2h a temperatura ambient i 2h a reflux. Després de filtrar residus i evaporar el dissolvent es precipiten els compostos **19**, **20**, **21**, **23** i **24** com a sals de NMe_4^+, amb uns rendiments alts o molt alts. Amb el mateix procediment però deixant la reacció 24h a reflux s'ha pogut obtenir el compost **22**. En aquest s'utilitza sofre elemental o S_8 per formar l'enllaç C_c-S. La reacció no evoluciona de la mateixa manera que per l'*o*-carborà ja que no s'obté el tiol tot i afegir-hi excés d'àcid per protonar el sofre sinó que s'obté el pinçament de les caixes de dicarballur.

Cal destacar el cas dels dos derivats amb carborà, compostos **23** i **24**, ja que en el procés de precipitar-los com a sals de tetrametilamoni en etanol, aquest és capaç de degradar parcialment una de les dues unitats de carborà, obtenint-se espècies dianiòniques. Normalment per fer la degradació del carborà calen unes condicions bàsiques fortes com la

mescla KOH/EtOH però en aquest cas amb un nucleòfil dèbil com és l'etanol n'hi ha hagut prou. La degradació parcial amb etanol ja s'havia observat en el cas de complexar derivats tioéter de l'*o*-carborà amb sals de metalls de transició. L'exaltació de l'electrofília del B(3) queda indicada a la figura 2.1.8. En els compostos **23** i **24** s'estableix una competència entre els tres clústers pels electrons de valència disponibles. Amb les dades de que disposem fins al moment era difícil preveure quin esdevindria amb més densitat electrònica i quin amb menys. Pel que s'observa experimentalment es pot concloure que el metal·lacarborà atrau més densitat electrònica que el carborà, fent que les posicions adjacents als àtoms de carboni (B(3) i B(6)) esdevinguin més deficitàries en electrons i, per tant, més susceptibles a l'atac per un nucleòfil com pot ser l'etanol. Això provoca la degradació parcial d'aquest clúster i és llavors quan la molècula ja es troba en un estat electrònicament més equilibriat. Tot i això, la diferència en els substituents dels dos compostos (Me en **23** o Ph en **24**) fa que aquest equilibri no sigui igual en ambdós casos. Seguint el mateix procediment per obtenir la sal de NMe_4^+, el compost **23** es degrada totalment en presència d'etanol, mentre que el compost **24** es degrada molt poc. No se li ha pogut trobar encara una explicació tot i que l'obtenció d'ambdós compostos degradats s'està estudiant.

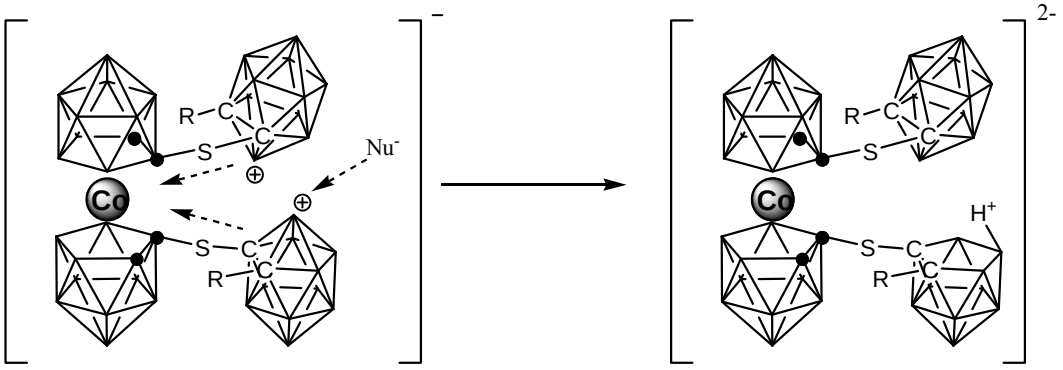

Figura 2.1.8. Esquema de degradació dels compostos **23** i **24** en presència d'un nucleòfil

La caracterització d'aquests compostos s'ha fet amb les tècniques habituals utilitzades en aquest treball. Cal destacar els següents aspectes:

- Els espectres de $^{11}B\{^1H\}$-RMN mostren 9 senyals diferents amb una disposició 2:2:6(2+2+2):2:2:2:2. En el cas del compost **19** es poden identificar els 9 senyals sense solapament. Pel compost **22**, el pinçament de les dues caixes també dóna 9 senyals amb una disposició 2:4(2+2):2:2:2:2:2:2.

En canvi, els espectres dels compostos **23** i **24** són més complicats en haver-hi el solapament dels senyals dels tres clústers, els dos fragments d'o-carborà i el metal·lacarborà. Tot i el solapament, l'espectre de $^{11}B\{^{1}H\}$-RMN ha resultat clau per veure la degradació d'una de les caixes de carborà tal com s'observa a la figura 2.1.9. Els senyals a -33 i -36 ppm, que apareixen a una zona de l'espectre on no hi ha altres ressonàncies, indiquen la degradació a *nido* de les caixes d'*o*-carborà i la integral d'aquests senyals respecte la resta, amb una relació 2:35, ens diu que només un dels clústers s'ha degradat. Una altra indicació de la formació del clúster *nido* es pot veure en l'espectre acoblat ^{11}B-RMN, on un d'aquests dos senyals a camp alt es desdobla com a conseqüència del seu enllaç amb un àtom d'hidrogen pontal, provinent de l'àtom de bor que s'ha perdut en el procés de degradació.

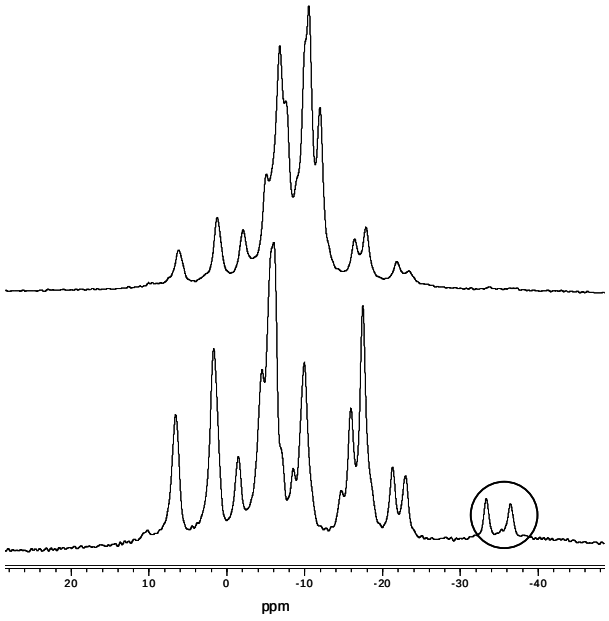

Figura 2.1.9. Espectres de ^{11}B-RMN del compost **23**. Dalt: producte no degradat. Baix: producte degradat amb un dels clústers *nido*.

L'espectre de ^{1}H-RMN ha estat útil per confirmar la puresa dels compostos obtinguts però també ens ha estat de gran ajuda a l'hora d'identificar el compost **22**. Aquest compost pinçat amb sofre pels àtoms de carboni té un senyal dels àtoms d'hidrogen dels grups C_c-H a camp molt baix, al voltant de 6 ppm. Això vol dir que aquests àtoms d'hidrogen són molt àcids, segurament degut a la naturalesa d'aquest compost, on hi ha una gran transferència electrònica entre l'àtom de sofre i el cobalt, com es veurà més endavant. L'acidesa d'aquests àtoms d'hidrogen també es pot observar en l'espectre d'infraroig on s'observa un desplaçament del senyal correponen a aquests grups C_c-H respecte l'anió **1**, de 3042 cm^{-1} en **1** a 3008 cm^{-1} en **22**.

Per altra banda, novament pel compost **23** s'ha pogut fer un espectre heterocosy $^{1}H/^{11}B\{^{1}H\}$-RMN per identificar el senyal de l'hidrogen pontal (veure figura 2.1.10).

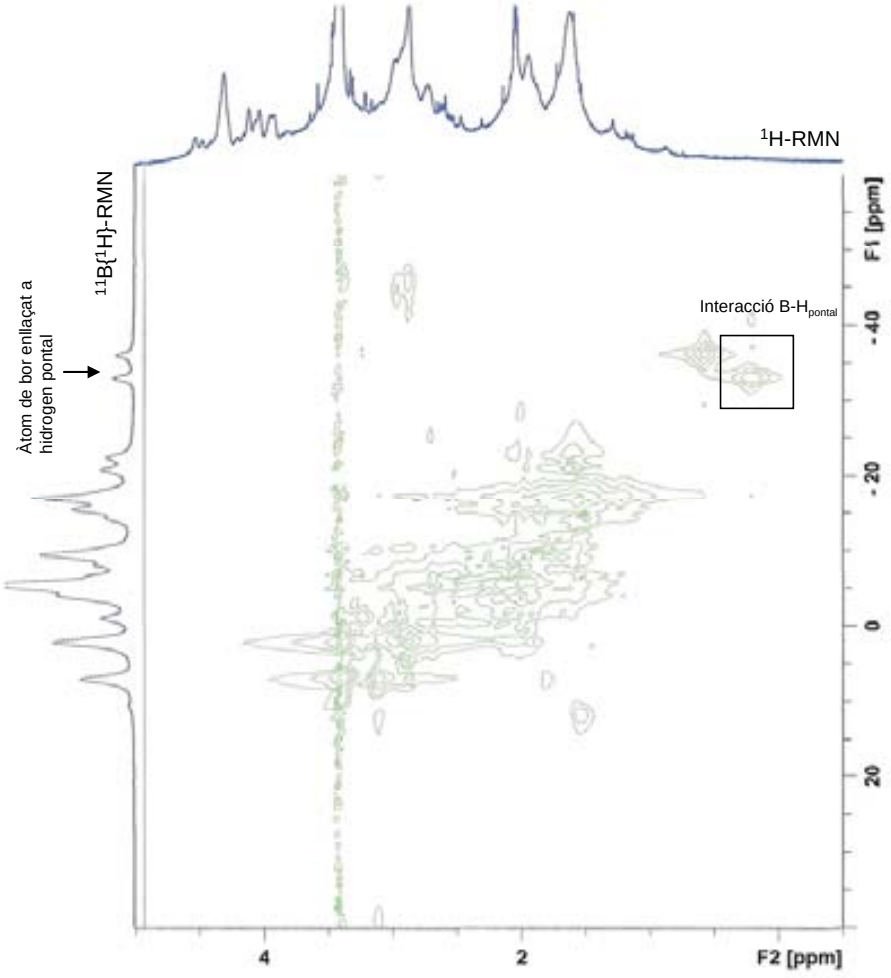

Figura 2.1.10. Espectre hetercosy $^{1}H/^{11}B\{^{1}H\}$-RMN del compost **23**.

- S'ha pogut obtenir l'estructura cristal·lina dels compostos **19**, **20** i **22**. El compost **19** s'ha obtingut a partir de l'evaporació lenta d'una solució de diclormetà. Aquest té una estructura racèmica i en l'estructura de raigs X s'observen unes interaccions intramoleculars fortes (Van der Waals -0.2Å) entre l'àtom de sofre d'una caixa de dicarballur i àtoms d'hidrogen dels grups C_c-H i B-H de l'altra caixa de dicarballur. A més a més, el conjunt d'interaccions tant inter com intramoleculars de la molècula li confereix un empaquetament per capes molt interessant com es mostra a la figura 2.1.11. Es pot veure com hi ha consecutivament capes de cobalto-bis(dicarballur) envoltades en un cantó per una capa de dissolvent i catió, i per l'altre dels anells aromàtics del substituent.

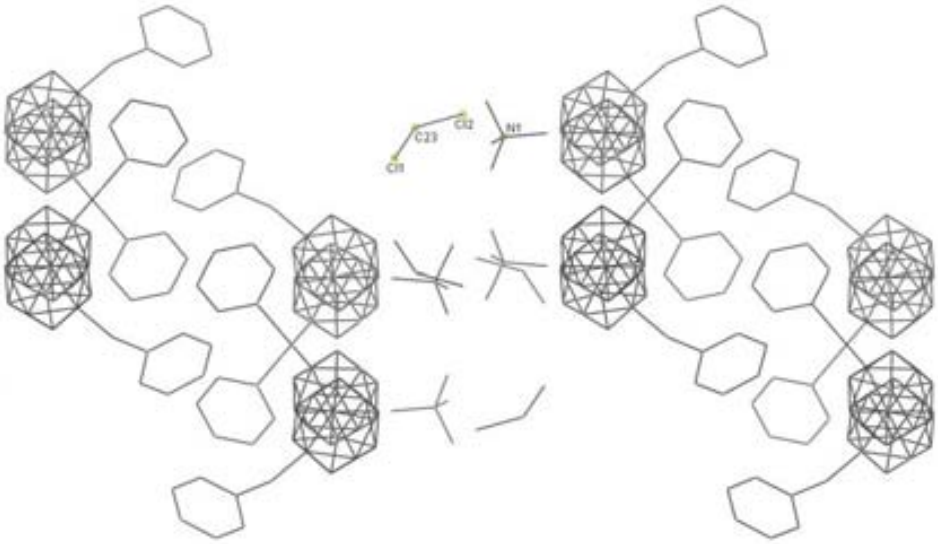

Figura 2.1.11. Estructura en capes del compost **23** vista des de l'eix b.

Tornant al compost **22** i a fi d'estudiar-lo en més detall s'han fet càlculs teòrics. En l'apartat anterior dels derivats amb fosfines s'ha vist com hi ha una interacció entre l'àtom de fòsfor i el de cobalt que provoca una transferència de càrrega entre ambdós. El fòsfor té un parell d'electrons lliure que és el que provoca en gran mesura aquesta interacció. Com que el sofre té dos parells d'electrons lliures la interacció s'hauria de veure intensificada per aquest compost. Per fer els càlculs s'ha partit de l'estructura obtinguda de raigs X i s'ha fet l'optimització amb el nivell de càlcul B3LYP/6-31G*. Una vegada obtinguda la geometria s'ha dut a terme l'anàlisi NBO. Aquesta mostra una interacció donador-acceptor de 10.57 kcal/mol entre dos orbitals NBO, essent el primer un dels parells d'electrons lliures del sofre i el segon l'orbital 4s buit del cobalt. En canvi, l'altre parell d'electrons no té cap interacció significativa amb el cobalt, però si amb els enllaços C_c-C_c d'ambdós dicarballurs, de 5.80 kcal/mol. L'entalpia de l'enllaç Co-S segons la literatura és de 79 kcal/mol,[11] per tant, l'energia d'aquesta interacció torna a ser significativa. Aquestes dues interaccions es mostren a la figura 2.1.12 com a mapes de densitat electrònica. A la figura 2.1.12a es pot veure el mapa de densitat electrònica en el pla entre l'àtom de cobalt i el sofre. S'hi pot veure clarament com hi ha un solapament d'ambdós orbitals donant lloc a aquesta interacció. A la part b s'ha agafat el pla entre els àtoms de carboni d'una caixa de dicarballur i l'àtom de sofre. Es pot observar com la geometria del segon parell d'electrons lliures del sofre fa impossible una interacció amb el cobalt, ja que pràcticament coincideix amb l'orbital p del sofre, i fa impossible el solapament amb cap dels orbitals del cobalt, ara bé, encaixa perfectament amb l'orbital antienllaçant de l'enllaç C_c-C_c, com s'observa a la representació.

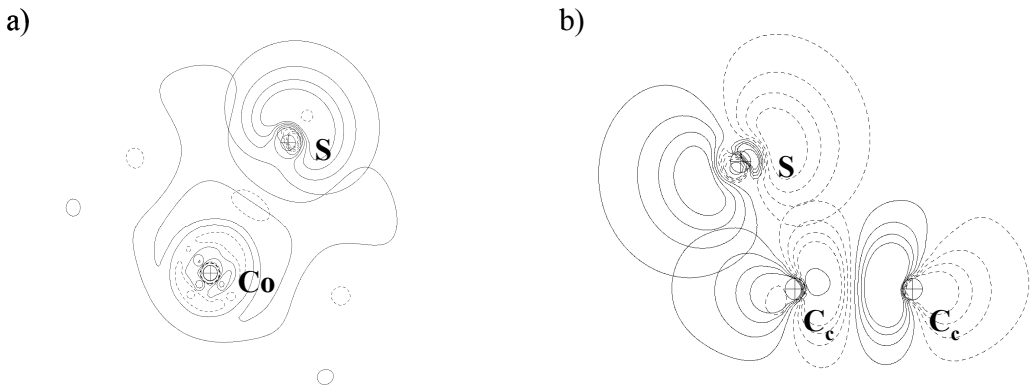

Figura 2.1.12. Mapes de densitat electrònica dels orbitals NBO corresponents a a) interacció Co-S; b) interacció S-C_c.

A continuació s'han calculat els orbitals HOMO i LUMO de la molècula. Com s'ha dit en el punt anterior amb les fosfines, el corrent electrònic entre l'àtom de cobalt i el sofre provoca que aquest últim també participi en els electrons de l'última capa. En canvi, l'orbital LUMO està distribuït entre l'àtom de cobalt i els àtoms de carboni i bor del clúster, però no sobre l'àtom de sofre. Això es pot observar a la figura 2.1.13. Es veu com l'orbital HOMO té majoritàriament contribució d'un orbital d del cobalt i un orbital p del sofre.

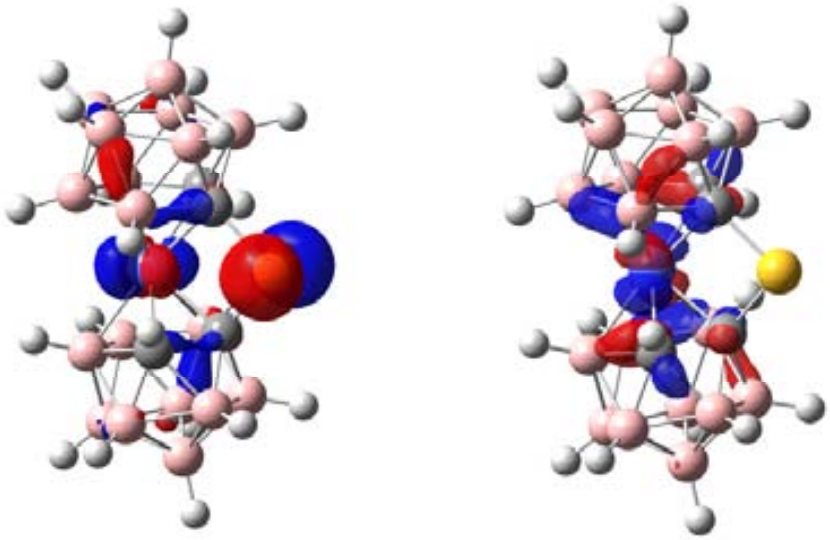

Figura 2.1.13. Orbitals HOMO i LUMO del compost **22**.

La disposició dels orbitals en l'HOMO (veure esquema a la figura 2.1.14) ens ha semblat molt interessant. Els pols estan posats de tal manera que el solapament és complet, el

pol positiu de l'orbital p del sofre està davant el positiu del d del cobalt i viceversa. Aquesta disposició ens va portar a pensar si aquesta molècula podia ser útil per l'emmagatzament d'hidrogen, ja que la molècula d'hidrogen tindria exactament la mateixa disposició d'orbitals.

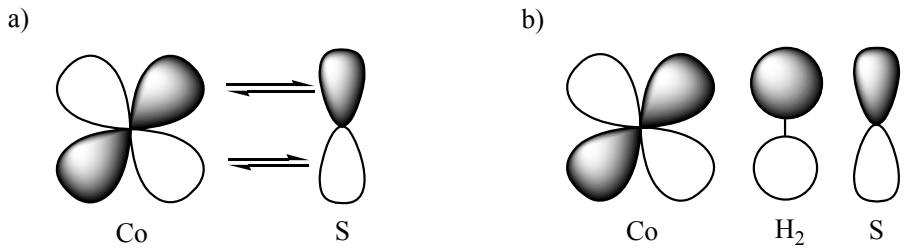

Figura 2.1.14. a) esquema del solapament d'orbitals en l'HOMO del compost **22**; b) esquema del possible emmagatzament d'hidrogen.

Això no obstant, no sembla ésser així i, partint d'una geometria inicial posant una molècula d'hidrogen enmig dels àtoms de cobalt i sofre, no s'obté un mínim energètic que mantingui l'hidrogen en aquella posició. Tal com es veu a la figura 2.1.15 la molècula d'hidrogen es trenca per formar el derivat monotiol del cobalto-bis(dicarballur). Si això fos possible experimentalment seria una bona manera d'obtenir aquest compost, que d'altra banda seria molt interessant per les complexacions amb diferents metalls. La hidrogenació del compost **22** amb H_2 per obtenir el derivat monotiol és un dels punts que queden pendents per acabar aquest treball.

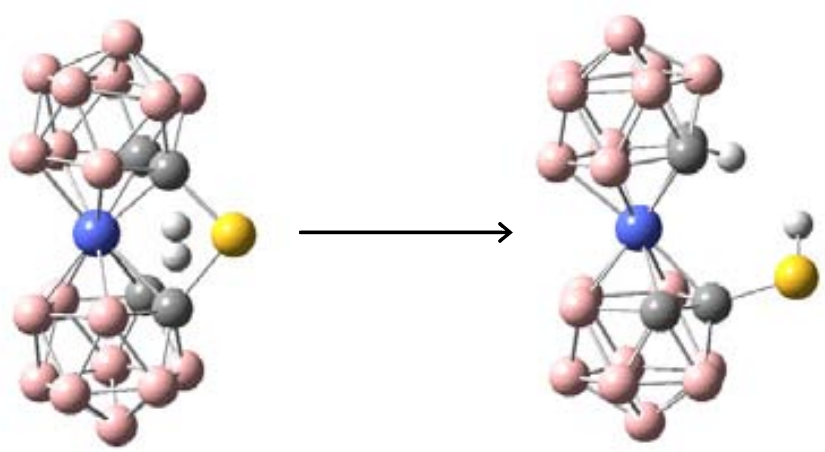

Figura 2.1.15. Optimització de la molècula que conté el compost **22** i hidrogen calculat amb B3LYP/6-31G*.

Finalment, s'ha dut a terme la voltamperometria cíclica del compost **22** per confirmar que segueix la mateixa tendència que els derivats amb fosfines. Tal com es veu a la taula 2.1.3, el valor del potencial de reducció mig de **22** es desplaça a valors positius, indicant una major facilitat de reduir el compost respecte **1**. Aquesta tendència també es pot observar si es comparen els valors de la càrrega total dins el clúster (CTC) i fins i tot la diferència d'energia entre els orbitals HOMO i LUMO. Així, si la càrrega CTC té un valor més positiu voldrà dir que hi ha menys densitat electrònica dins el clúster i per tant, serà més fàcil d'afegir un electró, és a dir de reduir. De la mateixa manera, si la diferència entre els orbitals HOMO i LUMO és més petita voldrà dir que serà més fàcil de posar un electró més perquè l'orbital LUMO estarà més a prop.

Compost	**$E_{1/2}$ [V]**	**CTC**	**E_{HOMO} [eV]**	**E_{LUMO} [eV]**	**$\Delta E_{HOMO-LUMO}$**
1	-1.83	-3.48	-3.96	0.55	-4.51
22	-1.51	-2.88	-4.04	0.27	-4.30

Taula 2.1.3. Valors de potencial de reducció mig, càrrega total del clúster (CTC), energies dels orbitals HOMO i LUMO i diferència entre elles dels compostos **1** i **22**.

2.2 COBALTO-BIS(DICARBALLUR) SUBSTITUÏT EN ELS ÀTOMS DE BOR

Les substitucions en els àtoms de bor es fan per dos objectius principals. El primer és la protecció de les posicions més reactives de l'anió cobalto-bis(dicarballur) mitjançant halògens, i augmenta la resistència d'aquest anió pel seu ús en condicions més extremes de temperatura, acidesa, radioactivitat, etc. El segon objectiu és poder derivatitzar el cobalto-bis(dicarballur) per tal d'obtenir compostos amb diferents propietats respecte l'inicial. Aquesta derivatització es fa, d'entrada, inspirant-se en reaccions orgàniques ja conegudes. En base a aquests dos objectius, aquest treball s'ha centrat en la síntesi i estudi de nous derivats halogenats, intentant aconseguir el màxim grau d'halogenació possible i mitjançant diversos camins sintètics. A més, i a partir de dos derivats del cobalto-bis(dicarballur), s'ha fet la derivatització mitjançant cadenes orgàniques.

2.2.1 Halogenació de l'anió cobalto-bis(dicarballur)

Fins ara s'han estudiat els derivats halogenats de l'anió **1** per diverses raons.[12,13] La reacció de substitució d'un hidrogen per un halur és la més fàcil en els àtoms de bor; per això és un punt de partida per a la derivatització del clúster en aquestes posicions emprant, d'entrada, reaccions del tipus Kumada, Suzuki, Heck, etc. Hem de tenir en compte, però, que aquestes reaccions estan fetes per acoblaments C-C, que en la major part de casos no tenen res a veure amb l'acoblament C-B. Els anions halogenats tenen un escàs poder coordinant, són poc nucleòfils, resistents tèrmicament i inerts davant gran quantitat de reactius, propietats que els fa ser dèbilment coordinants i, per tant, interessants en la generació de líquids iònics o en l'estabilització de cations altament reactius.

La reacció d'halogenació electrofílica de carborans s'ha estudiat en dissolució emprant diferents reactius, la majoria dels quals de perillositat elevada, cosa que dificulta l'obtenció de nous productes. A la bibliografia s'han trobat dos exemples on es fa una substitució electrofílica en els àtoms de bor de l'*o*-carborà, amb una reacció en estat sòlid,[14] un d'ells produït en aquest grup. Això ens va donar la idea de provar la reacció de diferents compostos halogenats amb l'anió **1**, en estat sòlid. Així, s'han fet proves de reacció amb I_2 i Br_2 amb bons resultats. Per una relació **1**:I_2 de 1:25 a 220 ºC i durant 24 hores l'espectre de MALDI-TOF-MS mostra la mescla de productes iodats que es forma en la reacció, fins a un màxim de

13 iodes, tal com s'observa a la figura 2.2.1. Aquest és el grau més elevat de iodació trobat a la bibliografia per l'anió **1**. En usar iode el problema detectat és la gran dispersió de productes que s'obtenen, ja que l'únic que s'ha pogut obtenir pur directament per substitució de l'anió cobalto-bis(dicarballur) és el derivat hexaiodat.

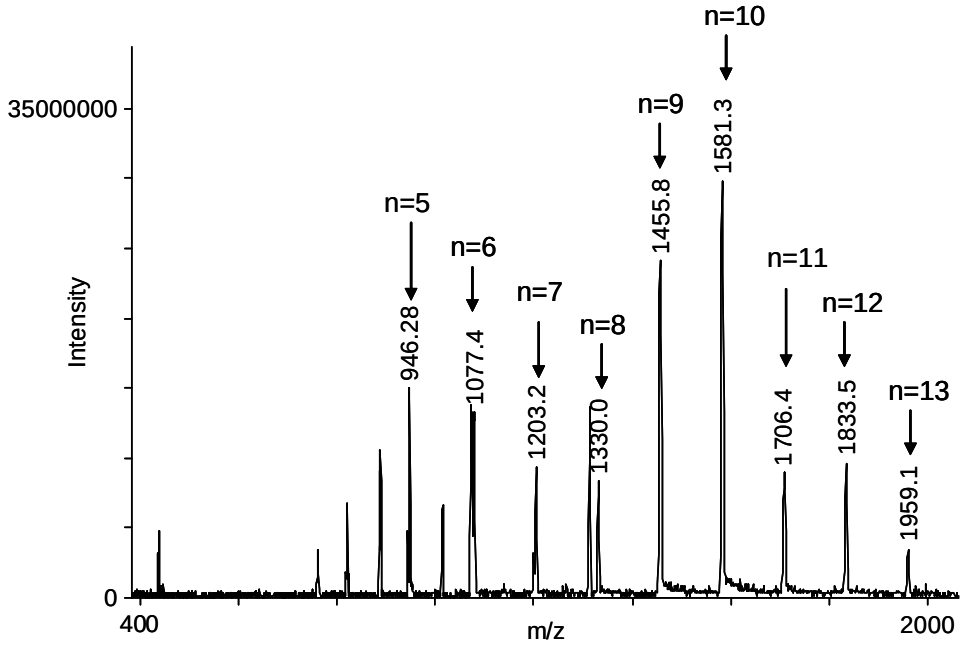

Figura 2.2.1. Espectre de MALDI-TOF que presenta masses moleculars $[M+H]^-$ de la sèrie d'anions $[I_n\text{-}3,3'\text{-}Co(1,2\text{-}C_2B_9H_{11\text{-}(n/2)})(1',2'\text{-}C_2B_9H_{11\text{-}(n/2)})]^-$, amb n= 5-13

En solució, la màxima iodació assolida és de n=6, la síntesi de la qual s'obté mitjançant la reacció de ICl (altament tòxic) i **1** en CH_2Cl_2 durant 22 hores a reflux i, després, cal encara fer el tractament de purificació.[12] Això fa llarg aquest camí sintètic. La reacció en estat sòlid es dóna a 150 ºC durant 3 hores i és totalment neta ja que el subproducte que es forma, àcid iodhídric, és un gas que no impurifica el producte, i l'únic pas de purificació que s'hi ha de fer és reduir l'excés de I_2 per sublimació o amb sulfit sòdic. Tot i així, el fet que es produeixi HI no fa fàcilment escalable la reacció ja que, a més producte, tenim més pressió dins el tub de reacció, amb el perill que exploti el recipient de vidre.

Pel que fa a les reaccions amb Br_2 , s'ha aconseguit un màxim de 11 Br, tot i que els productes amb 9 i 10 Br són els majoritaris en dues condicions diferents de reacció, 1:10 de **1**:Br_2 durant 3 hores a 150 ºC i 1:25 de **1**:Br_2 durant 60 hores a 300 ºC (figura 2.2.2). La reacció, en aquest cas, no s'ha optimitzat per obtenir un producte pur, ja que només es volia saber el nombre màxim de Br que entren al clúster. Les propietats d'aquest element fan més difícil la seva manipulació ja que té un punt d'ebullició molt baix i s'evapora molt

ràpidament, a més d'ésser un element altament tòxic. És per això que va deixar-se de banda el reactiu brom. En solució, com en el cas del I_2, s'ha aconseguit també com a màxim la hexabromació. Per tant, es demostra novament que la reacció en estat sòlid permet una halogenació major del clúster.

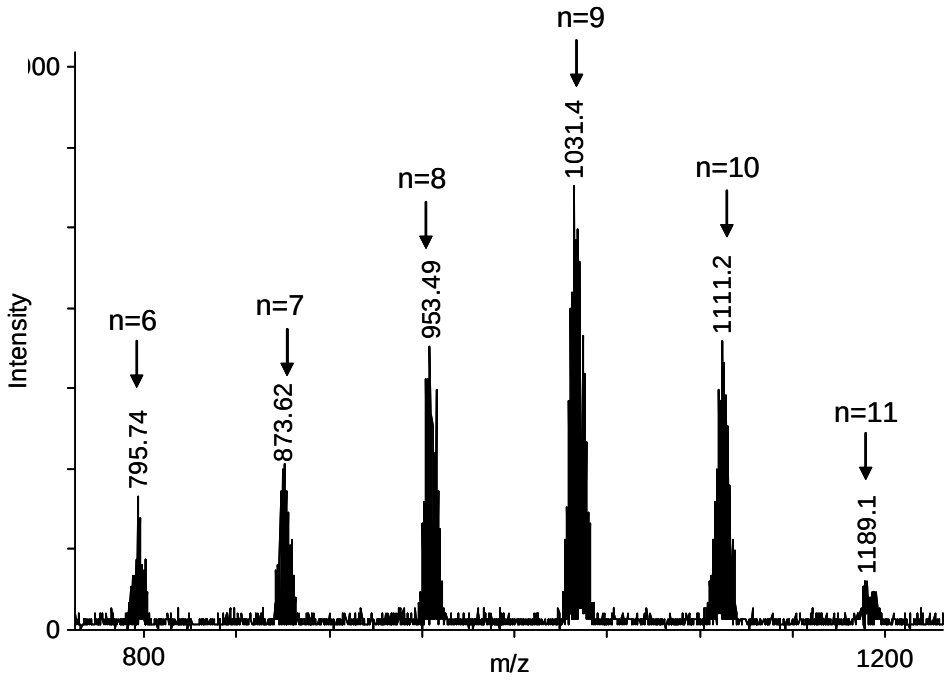

Figura 2.2.2. Espectre de MALDI-TOF que presenta masses moleculars $[M+H]^-$ de la sèrie d'anions $Cs[Br_n\text{-}3,3'\text{-}Co(1,2\text{-}C_2B_9H_{11\text{-}(n/2)})(1',2'\text{-}C_2B_9H_{11\text{-}(n/2)})]^-$, amb n= 6-11

A part d'intentar les reaccions en estat sòlid també s'han fet proves preliminars de reacció en microones. Aquestes s'han centrat únicament en la reacció de **1** amb I_2 utilitzant diferents dissolvents, temps de reacció i estequiometries. Entre els resultats obtinguts cal destacar que amb el màxim de temps utilitzat, 7 minuts, el grau més alt de iodació ha estat 4 I. Per altra banda, s'ha aconseguit obtenir el derivat diiodat pur usant 1:7 de **1**:I_2 amb CH_2Cl_2 com a dissolvent i 1' de temps de reacció. Tenint en compte que la reacció en dissolució necessita 10h de reacció, queda clar que l'ús del microones pot donar una empenta important en l'ús dels cobalto-bis(dicarballur) halogenats.

Per aquest motiu s'ha volgut estudiar de forma més exhaustiva la reacció d'halogenació. S'ha volgut utilitzar un altre tipus de reactiu per intentar controlar millor el nombre d'hidrògens que es substitueixen, i també per evitar els productes secundaris de les reaccions anteriors (àcids iodhídric i bromhídric). Per conseguir-ho, s'han utilitzat els derivats halogenats de la N-halosuccinimida, ja que l'únic subproducte que s'obté és la N-succinimida

que és molt fàcil de separar en ser insoluble en els dissolvents orgànics usuals en el tractament d'aquests clústers.

El primer pas ha estat intentar la cloració del compost **1** per reacció amb N-clorosuccinimida. S'han fet un seguit de reaccions amb estequiometries entre **1**:NCS de 1 a 20 equivalents i, després de 2 hores al forn a 190±10 ºC, s'han obtingut espectres de MALDI-TOF de les mostres confirmant l'existència de tots els compostos clorats fins a un màxim de 11 Cl (taula 2.2.1). Com s'esperava, no s'ha pogut obtenir el control de la reacció desitjat i no s'ha aconseguit cap producte pur. Tot i la gran barreja de productes, es pot observar com hi ha compostos més estables que d'altres, o sigui que persisteixen com a preferents tot i l'increment de reactiu. Aquest fet ens permet suggerir un mecanisme de la reacció de cloració i el per què i quins són els compostos més estables que es poden obtenir.

$\mathbf{r}_y$	y	$\mathbf{r}_y$	y
1	0, <u>1</u>, 2	11	7, <u>8</u>, 9
2	0, 1, <u>2</u>, 3, 4	12	7, <u>8</u>, 9, 10
3	2, <u>3</u>, 4	13	7, <u>8</u>, 9, 10
4	2, 3, 4, <u>5</u>, 6	14	7, <u>8</u>, 9, 10
5	4, 5, <u>6</u>, 7	15	7, <u>8</u>, 9, 10
6	5, <u>6</u>, 7	16	8, <u>9</u>, 10
7	5, 6, <u>7</u>, 8	17	8, <u>9</u>, 10
8	6, <u>7</u>, 8	18	8, <u>9</u>, 10
9	7, <u>8</u>, 9	19	8, <u>9</u>, 10, 11
10	7, <u>8</u>, 9	20	8, <u>9</u>, 10, 11

Taula 2.2.1. Composició treta del MALDI-TOF-MS després de la reacció entre **1**:NCS. r_y representa la fracció molar inicial de **1**:NCS des de 1:1 a 1:20. A la columna indicada com a y, les espècies observades per MALDI-TOF-MS estan indicades segons el número d'àtoms de clor insertats. L'espècie subratllada és la majoritaria en cada barreja.

Les fraccions molars dels compostos es poden treure de la integració dels espectres de MALDI-TOF-MS ja que s'ha comprovat que aquesta tècnica és quantitativa en els cas de compostos molt semblants com en aquest cas. Així doncs, per estequiometries de $\mathbf{r}_1$ a $\mathbf{r}_6$ el producte dominant concorda amb l'$\mathbf{r}_y$, és a dir que per exemple en la barreja de $\mathbf{r}_3$, el producte dominant conté tres àtoms de clor. Això es dóna excepte en el cas de $\mathbf{r}_4$ i $\mathbf{r}_5$ on el producte dominant ja és el que conté cinc o sis àtoms de clor. Així doncs, es pot dir que a partir de sis àtoms de clor la correlació s'acaba i es comença a trobar productes que persisteixen. Així, el

producte amb sis àtoms de clor és majoritari de $\mathbf{r}_5$ a $\mathbf{r}_6$, el de set entre $\mathbf{r}_7$ i $\mathbf{r}_8$, i el de vuit àtoms de clor de $\mathbf{r}_9$ fins a $\mathbf{r}_{15}$. La persistència d'aquestes espècies només es pot explicar coneixent la seqüència de cloració en el clúster i la velocitat de substitució de cada vèrtex. Tenint en compte que experimentalment es coneixen les espècies mono, di i hexasubstituïdes dels derivats halogenats, les posicions corresponents fins a sis substitucions queden establertes. D'aquesta manera, l'ordre de substitució tenint en compte la simetria del clúster seria primer l'atac sobre els vèrtex B(8) i després sobre els vèrtex B(9) i B(12). En aquests últims, al ser equivalents, no es pot saber quin és el primer en ser substituït i de fet, el derivat tetrasubstituït no s'obté per substitució directe de **1**. A partir d'aquest punt no es tenen resultats experimentals i la continuació de la seqüència de cloració és desconeguda.

Per tal d'explicar aquest mecanisme de cloració s'han realitzat càlculs *ab initio*, començant per calcular la termodinàmica de la reacció i observar si hi ha alguns derivats més estables que d'altres pel que fa a energia. Tenint en compte les energies dels enllaços B-H i B-Cl, 81 i 128 kcal/mol respectivament, s'haurien de poder substituir tots els B-H per B-Cl i no és el cas. Això es pot observar calculant les energies de reacció de l'addició consecutiva d'àtoms de clor al clúster segons l'equació 1.

$$[3,3'\text{-Co}(1,1',2,2'\text{-}C_4B_{18}Cl_yH_{22-y})]^- + Cl_2 \xrightarrow{\Delta H} [3,3'\text{-Co}(1,1',2,2'\text{-}C_4B_{18}Cl_{y+1}H_{21-y})]^- + HCl$$

Equació 1

El resultat es pot observar a la figura 2.2.3 en la representació de ΔH de la reacció en funció del número d'àtoms de clor. Com que el número de possibles isomers per cada derivat és força gran, s'ha calculat per cada derivat clorat els isomers més raonables i s'ha utilitzat el més estable per confeccionar la gràfica de la figura 2.2.3. Per exemple, els tres isomers possibles pel derivat nonaclorat, on el nou àtom de clor entra a les posicions B(4), B(5) o B(6), tenen uns valors molt semblants de l'entalpia de la reacció, de manera que confirma la independència de l'energia del compost depenent del vèrtex substituït. Es pot observar com no hi ha preferència respecte cap derivat i la pendent de la gràfica és comparable al valor esperat per la substitució de B-H per B-Cl (-47 kcal/mol), essent -53 kcal/mol. Per tant, amb aquests valors es podria arribar a pensar que no hi ha cap mena de regioselectivitat en el clúster i, amb les condicions adequades, no hi hauria problema per la percloració del clúster. Això es contradiu amb els resultats experimentals, i per tant podem assegurar que el mecanisme de cloració no té un origen termodinàmic, sinó cinètic.

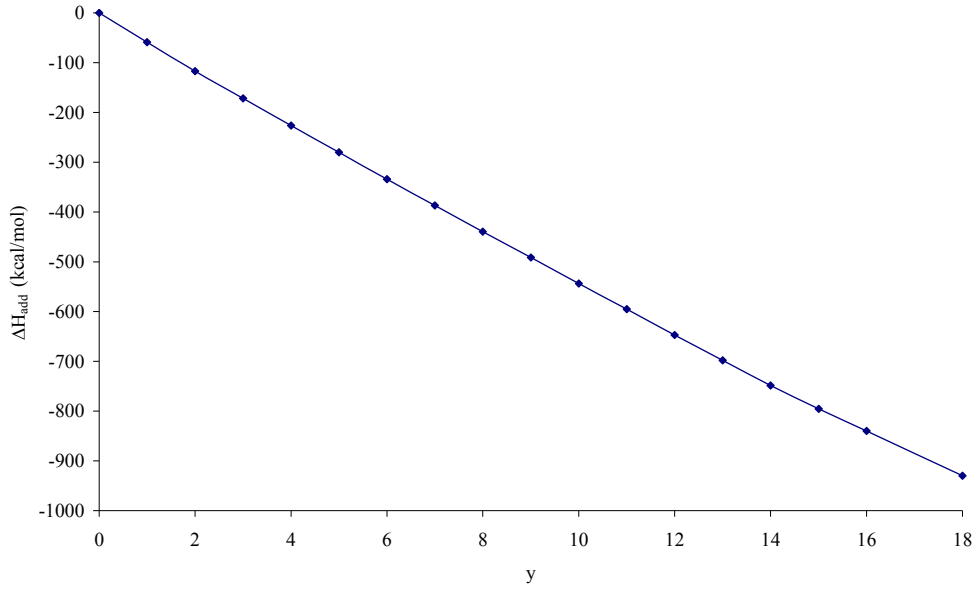

Figura 2.2.3. Representació gràfica de ΔH_{add} (addició acumulativa de l'energia de B-Cl en kcal/mol) pel compost [3,3'-Co(1,2-$C_2B_9Cl_nH_{11-n}$)(1,2-$C_2B_9Cl_zH_{11-z}$)]$^-$ (n+z = y) (per y=0-18), *vs* número d'àtoms de clor (y).

Per tal de conèixer la cinètica de la reacció s'ha pensat en estudiar la distribució de les càrregues de la molècula. En les substitucions en anells aromàtics, la distribució de càrregues dóna una idea força aproximada de l'ordre d'atac en l'anell, i aquests resultats estan relacionats amb la cinètica de la reacció de substitució. És per aquest motiu que vàrem pensar amb les càrregues. Per tant, si es calculen les càrregues sobre **1** es podria obtenir una primera idea de les posicions més susceptibles a ser atacades. Els resultats es mostren a la figura 2.2.4 juntament amb la numeració de clúster per una millor comprensió. Si es tenen en compte els valors obtinguts per les càrregues sobre els vèrtex de bor, l'ordre de les substitucions seria B(8)>B(9)≈B(12)>B(10)>B(4)≈B(5)≈B(7)≈B(11)>B(6). Així doncs, tindria sentit que els derivats més susceptibles a obtenir-se purs són els disubstituït i l'octasubstituït.

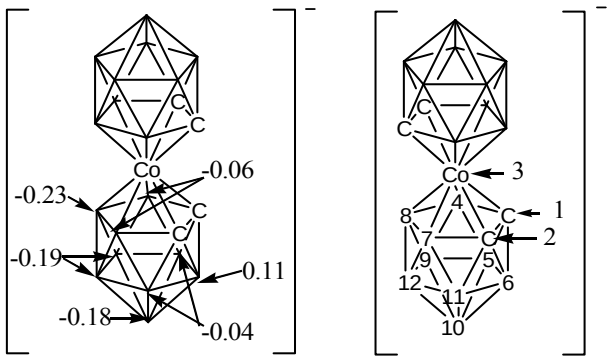

Figura 2.2.4. Càrregues NPA en els àtoms de bor de **1**, amb la numeració dels seus vèrtexs.

Tot i això, l'atac sobre el vèrtex de bor no representa bé el mecanisme descrit a la literatura,[15] on se suposa que la substitució electròfila es dóna sobre l'enllaç B-H i no només sobre l'àtom de bor. A partir d'això, s'han calculat les càrregues que hem anomenat 2a-NPA (Two Atom Natural Population analysis charge), sumant la càrrega de l'àtom de bor i la de l'àtom d'hidrogen. Els resultats es poden observar a la figura 2.2.5a i es veu com les posicions amb la càrrega més negativa segueixen el mateix ordre de substitució obtingut amb les càrregues només sobre els àtoms de bor. A més a més, s'ha volgut comprovar la influència en el cas de partir de derivats ja clorats en l'ordre de subsitució. S'han calculat les càrregues 2a-NPA pel compost parcialment clorat Cl_6-**1**, figura 2.2.5b, i es pot veure com l'ordre segueix sent el mateix que el predit pel compost inicial sense clorar. Per tant, podem dir que l'ordre calculat pel compost de partida es manté fins la percloració.

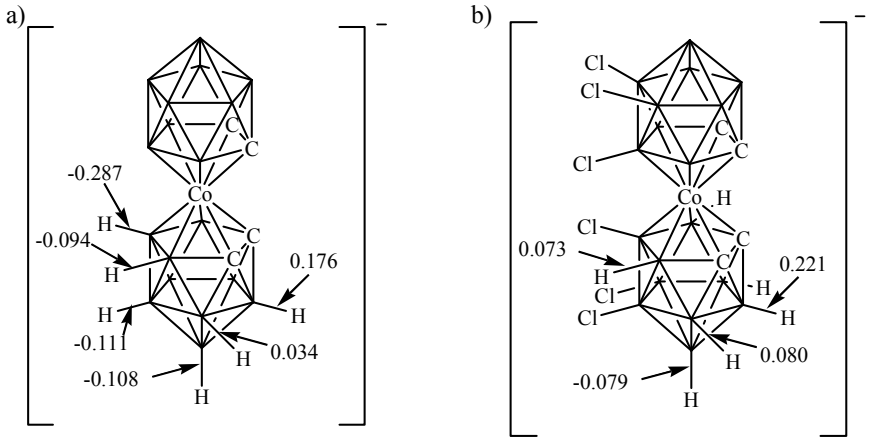

Figura 2.2.5. a) Càrregues 2a-NPA en els vèrtex B-H de **1**. b) Càrregues 2a-NPA en els vèrtex B-H de Cl_6-**1**.

Per tant, es pot concloure que l'ordre de substitució en la reacció de cloració de **1** es pot calcular acuradament mitjançant el càlcul de les càrregues en els vèrtexs del clúster. Això vol dir que la reacció està controlada cinèticament i que l'ordre a partir de sis àtoms de clor seria la substitució dels vèrtexs B(10) i B(10'). A més, tenint en compte la proximitat entre els valors de les càrregues entre els vèrtexs B(9)≈B(12)≈B(10), ens donaria una explicació de per què és tan difícil obtenir el derivat hexaclorat pur. Per acabar, els valors de les càrregues mostren que seria possible obtenir teòricament els compostos octaclorat Cl_8-**1** i dodecaclorat Cl_{12}-**1** bastant purs, ja que la diferència de valor amb els altres vèrtexs és significant. En l'apartat 2.4.1 es tracta el mecanisme en més detall utilitzant el clúster $[Ph\text{-}CB_9H_9]^-$ com a model, però ara per ara podem avançar que els resultats obtinguts mostren que el mecanisme de reacció és de caire radicalari.

Després d'estudiar la reacció de cloració en clústers de bor monoaniònics, s'ha volgut fer un estudi més profund de les propietats d'aquests compostos. En col·laboració amb les companyes de grup Dra. Anca-Iulia Stoica i Patrícia González s'ha estudiat el comportament electroquímic d'algunes de les mescles de derivats clorats que s'han obtingut dels experiments i els resultats han sigut sorprenents. El problema és que la tècnica convencional d'electroquímica, la voltamperometria cíclica (CV), no ens ha estat de gran ajuda, ja que al tenir mescles de compostos no es podia distingir bé els pics corresponents a cada compost. En canvi, utilitzant la tècnica anomenada voltamperometria d'ona quadrada (SWV) s'ha pogut diferenciar clarament els pics de potencial mig $E_{1/2}$ per cadascun dels compostos clorats. Això es pot observar a la figura 2.2.6.

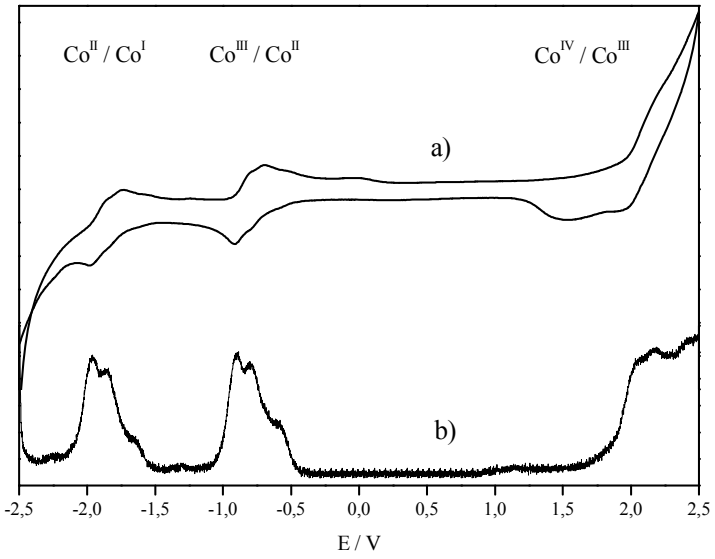

Figura 2.2.6. Voltamperograma cíclic (a) i voltamperograma d'ona quadrada (b) amb electrode de carbó en MeCN per Cl_x-**1** (x = 2-6).

Les mescles que s'han provat ens han donat la possibilitat de calcular el potencial mig pels compostos clorats Cl_x-**1** (x = 2-12), i és el derivat dodecaclorat el que s'ha aconseguit amb més atoms de clor. Com s'ha esmentat abans, la tècnica que ens ha funcionat millor per caracteritzar aquestes mescles ha estat el MALDI-TOF-MS, donant-nos la certesa de la massa per cada compost, així com la fracció molar de cada un d'ells per comparació d'alçades del pic màxim en l'espectre. Fins al moment, no s'havia utilitzat aquesta tècnica quantitativament, perquè les fragmentacions dels productes impossibilita la tasca. En canvi, pels derivats clorats no hi ha fragmentació visible i, com que són compostos molt semblants, permeten quantificar aquestes proporcions. Això s'ha demostrat comparant, per la mateixa

mescla de productes, els espectres de MALDI-TOF-MS amb els de SWV, ja que aquesta segona tècnica sí que se sap que és quantitativa.

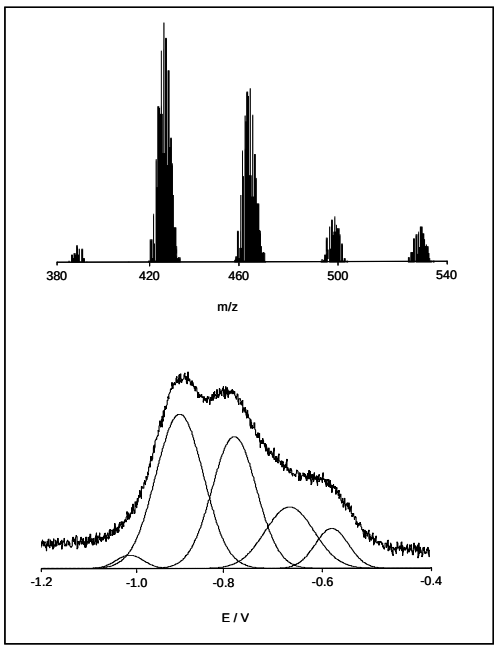

Figura 2.2.7. MALDI-TOF-MS de la mescla Cl_x-**1** amb x = 2-6 (dalt) i deconvolució en gaussianes del SWV de Co^{III}/Co^{II} (baix).

La comparació d'espectres s'ha fet de nou amb la mescla Cl_x-**1** (x = 2-6), i els resultats es poden observar a la figura 2.2.7. Es veu com la similitud és total, tant en la distribució periòdica dels pics amb la mateixa separació, com en l'intensitat de cada un d'ells. Així, en l'espectre de masses la separació és de 35 unitats de massa corresponents a compostos amb un àtom de clor menys, mentre que en la voltamperometria la separació és de 0.10V, també resultat d'un àtom de clor menys en el compost estudiat. També s'ha comprovat si la presència d'altres compostos altera el valor de $E_{1/2}$ respecte el producte pur. Això només s'ha pogut comprovar de manera directa amb el derivat Cl_2-**1** ja que és l'únic que es pot obtenir ben pur. Així, tant pel compost pur com per la mescla, el $E_{1/2}$ és de -1.00V. Per tant, es pot deduir que l'addició d'un àtom de clor no afecta l'estructura del compost, i el nou valor de $E_{1/2}$ és additiu al previ. A més, es podria predir el valor de derivats més clorats simplement afegint els 0.10V de desplaçament que provoca cada àtom de clor. Així, el valor esperat pel derivat Cl_{12}-**1** seria de -0.11V, i realment el valor que s'obté és de -0.11V. A la taula 2.2.2 es poden observar els valors experimentals per cada compost. Es pot veure com el compost Cl_9-**1** no compleix la tendència, tot i que això es pot atribuir a la poca quantitat d'aquest producte que es forma en les mescles, fent que els resultats obtinguts no siguin del tot correctes. Fins i

tot, en els casos que un mateix derivat clorat apareixen en més d'una mescla, els valors que s'han obtingut pel mateix són del tot comparables.

Compost	$E_{1/2}$ / [V]	$-E_{HOMO}$ / [eV]	$-E_{LUMO}$ / [eV]	CTC
1	-1.31	3.963	-0.546	-3.48
Cl_1-**1**	-	4.0607	-0.379	-3.25
Cl_2-**1**	-1.01	4.163	-0.153	-3.10
Cl_3-**1**	-0.89	4.261	0.019	-2.94
Cl_4-**1**	-0.78	4.409	0.195	-2.79
Cl_5-**1**	-0.68	4.492	0.344	-2.65
Cl_6-**1**	-0.57	4.609	0.496	-2.51
Cl_7-**1**	-0.47	4.698	0.596	-2.37
Cl_8-**1**	-0.36	4.784	0.698	-2.24
Cl_9-**1**	-0.32	4.838	0.819	-2.13
Cl_{10}-**1**	-	4.984	0.925	-2.01
Cl_{11}-**1**	-0.19	5.017	1.026	-1.90
Cl_{12}-**1**	-0.11	5.149	1.130	-1.78

Taula 2.2.2. Valors calculats de l'energia dels orbitals HOMO i LUMO de Cl_x-**1** comparats amb els valors corresponents de $E_{1/2}$ pel procés Co^{III}/Co^{II} (vs $Ag/AgCl/KCl_{sat}$). CTC correspon a la càrrega total del clúster, és a dir, la suma de les càrregues de tots els àtoms.

A més, s'han fet càlculs teòrics per trobar una explicació de l'additivitat en el potencial mig d'aquests derivats clorats. Així, a la taula 2.2.2 també es mostren les energies calculades pels orbitals HOMO i LUMO. D'aquests valors podem veure dues tendències molt similars. La primera correlació es pot trobar entre els valors de $E_{1/2}$ i $-E_{LUMO}$ segons el número de substituents de clor en **1**. La segona es troba entre $E_{1/2}$ i $-E_{HOMO}$. L'explicació d'aquesta bona correlació entre aquests valors es pot deduir si es té en compte que el valor de E_{LUMO} es relaciona amb la reducció de Co^{III} a Co^{II}, mentre que el valor de E_{HOMO} es relaciona amb la oxidació de Co^{III} a Co^{IV}. El derivat Cl_x-**1** més fàcil d'oxidar és el que té x=0, que alhora és el que té el valor més positiu de l'HOMO, tal com prediu el teorema de Koopman. D'altra manera, el de Cl_x-**1** més fàcil de reduir és el x=12, que és el que té un orbital LUMO més estable. A més, també s'ha calculat la càrrega CTC (càrrega total del clúster) ja que també ens pot donar una idea de la facilitat de reducció del mateix. Així, tal com es veu a la taula 2.2.2, a mesura que el grau de cloració augmenta, tant els valors del potencial de reducció com la càrrega CTC es tornen més positius. Si el valor de CTC és més positiu vol dir que hi ha menys electrons al clúster i per tant, serà més fàcil de reduir.

Així doncs, es pot concloure que mitjançant una successió de cloracions en l'anió **1** es pot arribar a modular el potencial redox, de manera que per cada àtom de clor addicional $E_{1/2}$ es mou 0.10V. Per tant, el valor pot arribar a variar de -1.31V per **1** fins a -0.11V en el cas de la parella Co^{III}/Co^{II}, i de -2.26V a -1.06V per $E_{1/2}(Co^{II}/Co^{I})$, al tenir el derivat Cl_{12}-**1**. Cal tenir en compte que aquests valors són comparables als dos primers valors de potencial de reducció del C_{60}, -0.30 per $[C_{60}]^{0/-I}$ i -0.95 V per $[C_{60}]^{-I/-II}$ *vs* SCE, essent aquest un compost neutre i el compost **1** un monoanió.

2.2.2 Formació de l'enllaç B-C en l'anió cobalto-bis(dicarballur)

Els derivats clorats, bromats i iodats de l'anió cobalto-bis(dicarballur) com els descrits en l'apartat anterior, s'han estudiat poc i es deu al fet que només s'ha pogut obtenir el derivat disubstituït del clor, el di i hexasubstituït del brom i el mono, di i hexasubstituïts del iode. A més, hi ha pocs exemples on hagin estat considerats com a possibles materials de partida per a produir nous derivats de l'anió **1**.[16] Continuant el treball d'una tesi anterior, s'ha utilitzat el compost monoiodat $[8\text{-I-}3,3'\text{-Co}(1,2\text{-}C_2B_9H_{10})(1',2'\text{-}C_2B_9H_{11})]^-$ (**25**) per generar regioselectivament derivats monoarílics en la posició B(8) a través d'una reacció d'acoblament B-C. Per fer l'acoblament B-C ens hem inspirat en les condicions de reacció emprades habitualment en reaccions de Kumada i de Heck per generar enllaços C-C (veure figura 2.2.8).

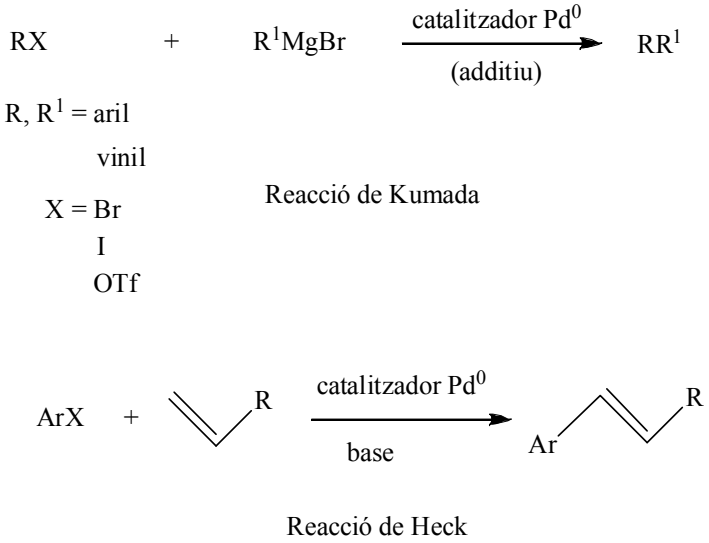

Figura 2.2.8. Esquema de les reaccions d'acoblament C-C de Kumada i Heck.

En el cas de les reaccions inspirades en les condicions de Kumada, s'ha volgut partir de compostos amb grups funcionals que permetessin posteriors reaccions dels derivats obtinguts (figura 2.2.9).

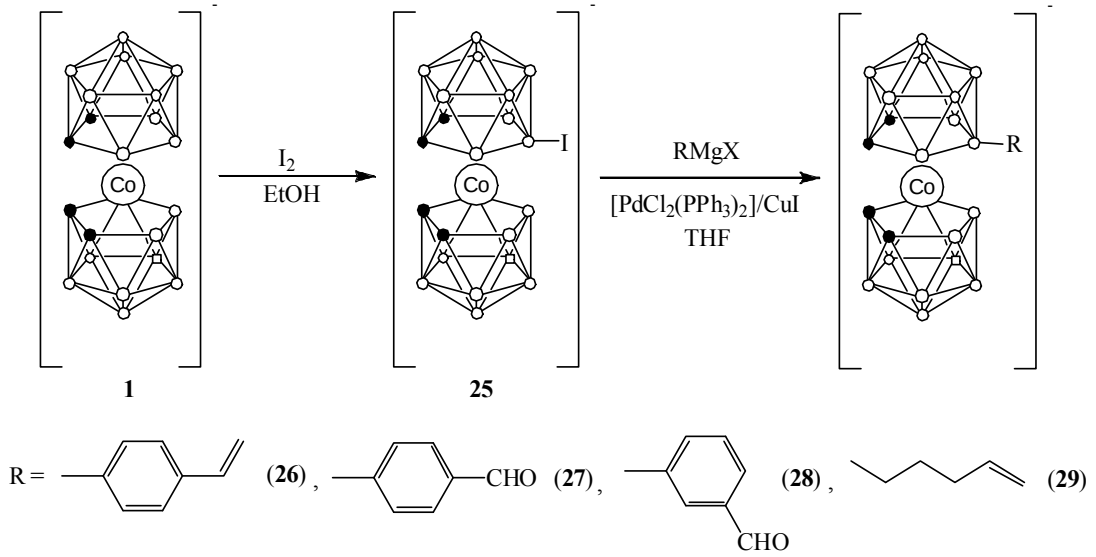

Figura 2.2.9. Esquema d'obtenció de derivats monosubstituïts en el bor B8 utilitzant les condicions inspirades en la reacció de Kumada.

En el cas de les reaccions tipus Heck s'han buscat les millors condicions de reacció pel compost **30**, i aquestes s'han aplicat a la síntesi dels compostos **31**-**42** donant com a resultat la majoria dels productes desitjats amb rendiments acceptables o alts (figura 2.2.10).

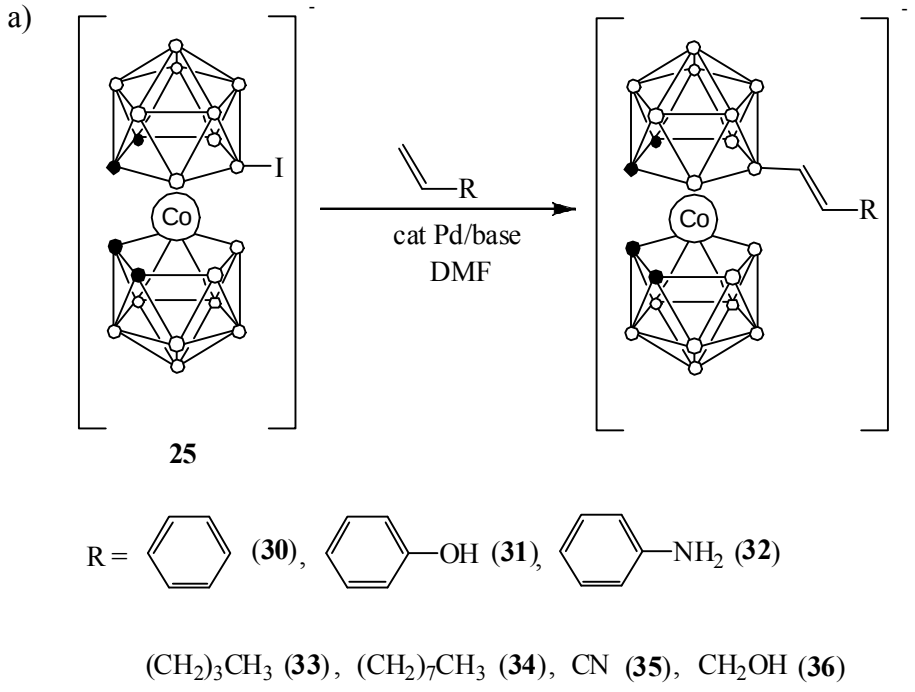

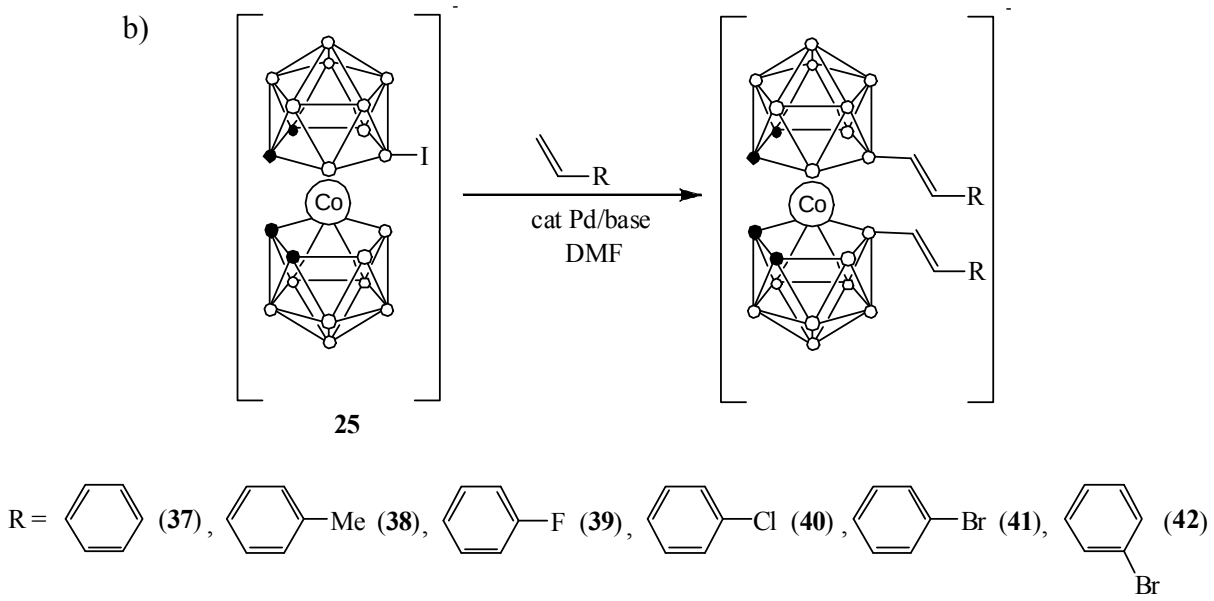

Figura 2.2.10. Esquema d'obtenció de derivats monosubstituïts en el bor B8 amb les condicions de reacció inspirades en la reacció de Heck. a) Obtenció dels derivats monosubstituïts. b) Obtenció dels derivats disubstituïts.

Derivats obtinguts amb les condicions inspirades per la reacció de Kumada.

Com s'ha esmentat abans, la reactivitat del compost monoiodat **25** envers alguns reactius de Grignard ja s'havia estudiat al nostre grup, tot i que encara no s'havien obtingut productes amb grups reactius. En el cas dels compostos **27** i **28** -on el grup aldehid pot reaccionar posteriorment mitjançant reaccions descrites a la bibliografia doncs ja se li suposa un comportament orgànic a aquesta distància del clúster- la reacció inspirada en Kumada es fa en presència d'un catalitzador de pal·ladi,[17] i el reactiu de Grignard se sintetitza amb el procediment descrit per Gilman i Kirby:[18] es renta el Mg amb THF i hexà i s'asseca al buit durant dues hores. Després s'afegeix una punta de I_2 per activar el Mg i, de mica en mica, es va addicionant el dissolvent (THF) i el bromur orgànic precursor de l'aldehid, escalfant el baló al principi per ajudar a iniciar la reacció. Un cop acabada l'addició, es deixa aproximadament una hora en agitació. Per a la reacció d'acoblament, el procediment consisteix en assecar bé el compost de partida **25**, afegir-hi el dissolvent i la solució de magnesià (4 equiv.) i finalment, el catalitzador de pal·ladi $[PdCl_2(PPh_3)_2]$ (4% equiv.) i el CuI (4% equiv.); el CuI actua de cocatalitzador i, segons Hawthorne et al.,[19] aquest agent fa augmentar en molts casos el rendiment de la reacció. La mescla es reflueix durant tota una nit i l'excés de magnesià es destrueix amb l'addició d'aigua. Les sals de Cs, tant de **27** com de **28**, s'obtenen, respectivament, amb un 82% i 70% de rendiment. Aquests compostos se

sintetitzen a partir d'un grup acetal (protector) que es desprotegeix cap a aldehid quan es fa el tractament amb aigua àcida.

En el cas dels compostos **26** i **29**, on tenim un grup alquè terminal, el procediment sintètic varia a l'hora de fer el reactiu de Grignard. La formació del magnesià d'halurs orgànics amb grups vinil canvia considerablement respecte els compostos emprats abans i no es pot utilitzar el mateix mètode. Per això, seguim el procediment descrit per Pearson,[20] on el reactiu de Grignard es forma durant una nit. De mica en mica, s'afegeix una solució de dibromoetà com activador del Mg sobre la solució del bromur d'estirè (en el compost **26**) amb Mg assecat tres hores al buit. La reacció es duu a terme a una temperatura d'uns 35 ºC que es manté durant tota l'addició. Cal mesurar, a més a més, la concentració de magnesià obtinguda perquè és un punt crític en la posterior reacció d'acoblament. Així, s'ha observat que el rang vàlid de concentració en la reacció final és de 0.2-0.25M. A menys concentració, la reacció no es duu a terme, mentre que a més concentració s'obté el trencament de l'anió cobalto-bis(dicarballur).

La purificació dels quatre compostos és molt semblant. Consisteix en la destrucció de l'excés de magnesià, filtració del precipitat, evaporació del dissolvent, extracció amb aigua àcida i precipitació del producte com a sal de NMe_4^+ o Cs^+. La diferència radica en l'extracció amb aigua àcida, ja que el grup alquè es polimeritza fàcilment en presència d'àcid i impurifica o destrueix el producte desitjat. S'ha solucionat fent una dissolució diluïda d'àcid (0.5M HCl) i fent l'extracció en fred (posant gel a l'embut d'extracció).

El compost **29** no s'ha pogut obtenir pur. El problema no sembla ser en la formació del magnesià, que es fa igual que amb el compost **26**, sinó en la reacció d'acoblament, molt més lenta en aquest cas i que s'atribueix al fet de tenir una cadena alquílica en comptes de l'anell de benzè. En tenir una cadena amb enllaços simples, fa que sigui més mòbil i que el doble enllaç pugui interaccionar amb el clúster i formi productes secundaris que impurifiquen el compost.

Aquests compostos han estat caracteritzats per les tècniques emprades al llarg del treball. Trets característics són:

- L'espectre de ^{1}H-RMN mostra les ressonàncies corresponents als àtoms d'hidrogen dels grups C_c-H. Al ser compostos monosubstituïts, es tenen dos senyals diferents pels 4 C_c-H. Un dels senyals correspon als dos àtoms d'hidrogen que es troben a la caixa substituïda i l'altre als de la no-substituïda, com es pot observar a la figura 2.2.11. La substitució de l'enllaç B-I per un B-C provoca un desplaçament en l'espectre de ^{1}H a camp alt dels dos hidròdens dels C_c-H d'aquella caixa de 4.2 a 3.8 ppm, mantenint pràcticament intacte el senyal dels hidròdens que resten a la part no substituïda a 4.5 ppm, on l'efecte del substituent és nul degut a la distància que hi ha.

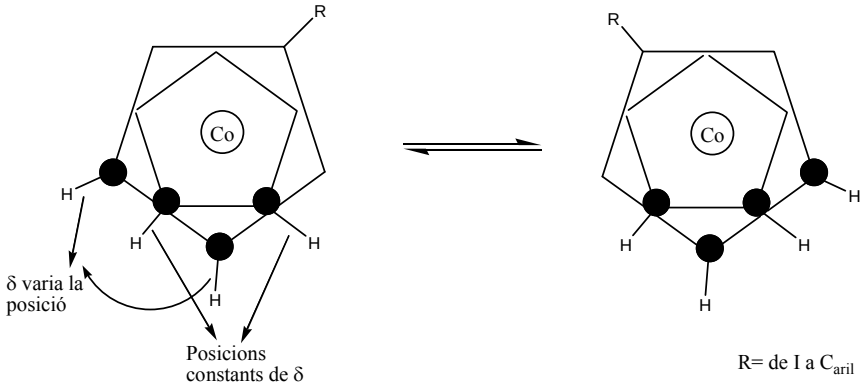

Figura 2.2.11 Posicions constants i variables de δ per ^{1}H i ^{13}C en passar de I a C_{aril}

- En l'espectre de ^{11}B-RMN és on s'observa el canvi més clar de que es forma el producte desitjat. El senyal corresponent a l'àtom de bor enllaçat a iode o carboni canvia totalment de posició. Així, a la taula 2.2.3 es mostren els desplaçaments de bor dels compostos **25-29**, i es pot observar que el senyal del B canvia de 6.5 ppm a l'estar enllaçat a iode a prop de 13 ppm a l'estar enllaçat a carboni aromàtic. En el cas del compost **29** el senyal només es mou fins a 7 ppm ja que tenim un carboni al·lifàtic i no aromàtic.

COMPOST	SUBSTITUENT AL B(8)	δ(^{11}B{^{1}H}) (ppm)
25	I	6.54 (1B), 3.51 (1B), 1.28 (1B), -1.73 (2B), -4.78 (5B), -5.38 (2B), -16.02 (2B), -17.45 (2B), -20.92 (1B), -23.06 (1B)
26	*p*-PhCH=CH$_2$	13.19 (1B), 6.07 (1B), 2.44 (2B), -2.86 (2B), -4.50 (4B), -5.90 (2B), -16.46 (2B), -17.70 (2B), -21.10 (1B), -22.23 (1B)
27	*p*-PhCHO	14.55 (1B), 9.15 (1B), 3.96 (2B), -1.53 (2B), -2.59 (2B), -4.08 (4B), -14.73 (2B), -15.99 (2B), -19.92 (1B), -20.87 (1B)
28	*m*-PhCHO	13.39 (1B), 7.69 (1B), 2.26 (2B), -3.34 (2B), -3.99 (4B), -5.74 (2B), -16.41 (2B), -17.65 (2B), -21.65 (1B), -22.61 (1B)
29	(CH$_2$)$_3$CH=CH$_2$	7.19 (1B), 1.53 (1B), 1.17 (1B), -4.82 (4B), -5.45 (5B), -16.74 (4B), -22.11 (2B).

Taula 2.2.3 Desplaçament químic dels àtoms de bor en l'espectre de ^{11}B-RMN

- Per una millor caracterització dels compostos presentats, es pot emprar la tècnica d'espectrometria de masses MALDI-TOF, que aporta informació sobre el pes molecular de l'anió generat, així com dels fragments formats pel trencament d'aquesta espècie aniònica. Aquesta tècnica és especialment útil degut als dos isòtops que té l'àtom de bor i a la seva abundància natural. Així, el ^{10}B té un pes atòmic de 10.013 i una abundància del 19.9%; i el ^{11}B té un pes atòmic de 11.009 i una abundància del 80.1%. Podem saber amb aquestes dades el nombre d'àtoms de bor que hi ha en cada distribució isotòpica ja que donarà una envolvent del pic característica. El senyal màxim està desplaçat a més massa molecular respecte el centre, degut a la major abundància de l'isòtop ^{11}B.

- El compost **26** va cristal·litzar en diclorometà obtenint-se monocristalls en forma d'agulla adequats per la resolució de la seva estructura cristal·lina mitjançant la difracció de raigs X (figura 2.2.12). El compost, de fórmula $C_{16}H_{40}B_{18}CoN$, cristal·litza en una cel·la amb dues unitats asimètriques del compost i en el grup espacial monoclínic *P*21/*n*. Entre les dues unitats es troba una interacció forta (distància de Van der Waals menys 0.3Å). Aquesta es dóna entre els àtoms C(2) i C(3) d'una unitat asimètrica amb l'àtom d'hidrogen del grup H-C_c(10') de l'altre unitat. També es troba una interacció entre el B(19) d'una unitat i el grup H-C_c(11') de l'altre. En ambdós casos els C_c-H pertanyen a la caixa amb el substituent i, per tant, amb més densitat electrònica com s'ha esmentat en l'apartat del ^{1}H-RMN.

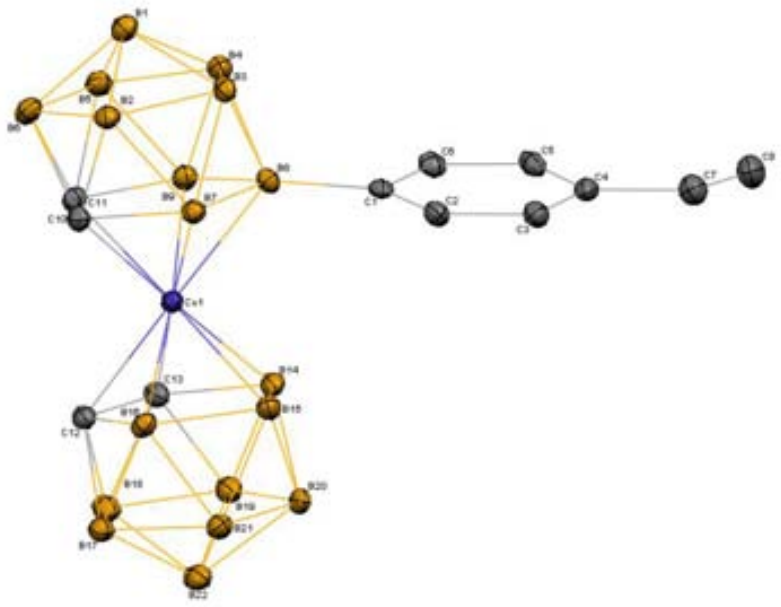

Figura 2.2.12 Representació ORTEP d'una de les dues unitats asimètriques de l'estructura cristal·lina del compost **26**.

Derivats obtinguts amb les condicions inspirades per la reacció de Heck.

La formació de l'enllaç B-C en l'anió cobalto-bis(dicarballur) mitjançant condicions de reacció basades en la reacció de Heck s'ha fet per primer cop en aquest treball en col·laboració amb el company de grup David Olid. Tot i això hi havia un exemple a la bibliografia de la reacció sobre carborans.[21] L'interés dels compostos que es poden obtenir radica en què hi hauria una conjugació total d'enllaços π a la molècula, de manera que pràcticament és l'única reacció on es pot obtenir l'enllaç B-C=C sense que els àtoms de carboni formin part d'un anell aromàtic. A més a més, hi ha la possibilitat d'utilitzar productes de partida amb grups funcionals, com en l'apartat anterior, per tal de sintetitzar derivats que siguin els reactius de noves reaccions.

Les condicions de reacció s'han provat sobre el compost **25** per generar el derivat amb estirè. Així, s'han fet proves variant el catalitzador de pal·ladi, l'estequiometria entre els reactius, la base i el dissolvent utiltizats i la temperatura. A la taula 2.2.4 es poden observar els resultats obtinguts i es veu com les millors condicions s'obtenen utilitzant un 5% del catalitzador $PdCl_2(PPh_3)_2$/CuI en DMF anhidre, amb 5 equivalents d'estirè, 3 equivalents de 2,6-Lutidina com a base i una temperatura de 140ºC (entrada 7).

entrada	equiv. d'estirè	catalitzador	base (equiv)	dissolvent	temps de reacció (h)	rendiment (%)[b]	T (ºC)
1[a]	2.5	8%$PdCl_2(PPh_3)_2$ 8%CuI	NEt_3 anhidre(2.5)	DMF anhidre	24	80	120
2	2.5	8%$PdCl_2(PPh_3)_2$ 8%CuI	NEt_3 (2.5)	THF	48	0	90
3	2.5	8%$PdCl_2(PPh_3)_2$ 8%CuI	$Ag_3(PO_4)$ (2.5)	DMF	24	60	120
4	1.5	8%$PdCl_2(PPh_3)_2$ 8%CuI	NEt_3 (2.5)	DMF	16	45	120
5	1.2	1% Pd Hermman's	$Ag_3(PO_4)$ (1.5)	DMF	6	45	120
6	5	5%$PdCl_2(PPh_3)_2$ 5%CuI	2,6-Lutidina (3)	DMF anhidre	16	45	140
7	5	5%$PdCl_2(PPh_3)_2$ 5%CuI	2,6-Lutidine anhidre(3)	DMF anhidre	24	90	140
8	2.5	5%$Pd(PPh_3)_4$	2,6-Lutidina (3)	DMF anhidre	16	45	130
9	5	5%$PdCl_2(PPh_3)_2$ 5%CuI	2,6-Lutidina (3)	DMF anhidre	24	55	130

[a] Afegint 15% del complex $Pd(ac)_2$; [b] Calculat a partir de ^{1}H-RMN

Taula 2.2.4 Resum de les diferents condicions de reacció provades entre **25** i estirè.

També s'ha notat com una petita quantitat d'aigua, bàsicament provinent del dissolvent, fa baixar el rendiment de la reacció. En canvi, l'increment de la temperatura accelera la reacció. Pel que fa a la base utilitzada es veu que el rendiment és menor en utilitzar la trietilamina, ja que al tenir un punt d'ebullició baix s'evapora amb facilitat a la temperatura de reacció. En canvi, l'ús d'una base no nucleòfila i amb un alt punt d'ebullició (170ºC aprox.) dóna lloc a rendiments més alts de reacció. Finalment, s'han provat també les condicions de reacció proposades a la bibliografia,[21] però el rendiment disminueix força degut a la formació de sub-productes que no s'han estudiat.

A continuació, amb les condicions optimitzades s'ha provat la reacció amb diferents substrats per tal d'aconseguir els productes **30**-**42**. El resultat de les reaccions ha estat especialment inesperat en el cas dels productes **37**-**42** on s'ha obtingut la disubstitució de l'anió cobalto-bis(dicarballur) tot i tenir només un àtom de iode. Com es pot observar a la taula 2.2.5, hi ha hagut compostos que no han reaccionat o ho han fet en un rendiment molt baix amb les condicions utilitzades com és el cas de **32**, **36** i **42**. A més a més, també s'ha provat la reacció utilitzant alquens terminals que no tinguessin un àtom d'hidrogen en la posició β, com en el compost α-metil-estirè, obtenint un rendiment de 0%. Per tant, s'ha deduït que és necessària la presència d'aquest àtom d'hidrogen i se suposa que ho és en el pas de l'addició oxidant de l'alquè al catalitzador de pal·ladi.

compost	rendiment (%)[a]	compost	rendiment (%)[a]
30	90	**37**	-
31	57	**38**	77
32	0	**39**	84
33	48	**40**	55
34	40	**41**	25
35	63	**42**	15
36	10		

[a] Calculat a partir de ^{1}H-RMN

Taula 2.2.5 Rendiment de les reaccions d'obtenció dels productes **30**-**42**.

La purificació d'aquests compostos ha estat difícil. Tot i fer extraccions per treure el catalitzador i excés de substrat, i precipitar el producte com a sal de NMe_4^+, al final s'acaba obtenint en el millor dels casos una mescla de producte final i compost de partida **25**. Tot i

que sembla que les diferències tant estructurals com electròniques entre **25** i els compostos **30**-**42** han de ser molt grans, s'ha trobat que la separació per cromatografia era molt complicada ja que no se separen prou els dos productes. Per aquesta raó, només s'han pogut obtenir de forma pura els compostos **30**, **34**, **39** i **42**. En el cas de **34** i **42**, tot i tenir uns rendiments de reacció baixos, sembla que les propietats entre aquests i **25** siguin prou diferents perquè es pugui dur a terme la separació per cromatografia i obtenir el producte pur. També és cert que augmentant el temps de reacció el rendiment també augmenta, per exemple en el cas del compost **34** on es passa del 40% en 24h a un 80% en 120h. Per tant, per evitar aquestes separacions tant feixugues es pot augmentar el temps de reacció i consumir pràcticament tot el reactiu **25**, encara que el temps dependrà de cada producte que es vulgui sintetitzar.

Aquests compostos han estat caracteritzats per espectroscòpia de ressonància magnètica nuclear de ^{1}H, ^{11}B i ^{13}C, espectrometria de masses i difracció de raigs X per **30**. A l'obtenir en la majoria dels casos mescla de productes només s'ha pogut fer una bona caracterització dels quatre productes purs que s'han obtingut. Trets característics són:

- Com en l'apartat anterior, els espectres de ^{1}H-RMN ens donen una informació molt important de la substitució de l'enllaç B-I per B-C. Així, els senyals corresponents als àtoms d'hidrogen dels grups C_c-H que en el compost **25** surten a prop de 4.5 i 4.3 ppm, en els derivats monosubstituïts **30**-**36** apareixen a 4.5 i 3.8 ppm, essent aquest segon senyal el corresponent a la caixa substituïda. En canvi, en els derivats disubstituïts **37**-**42** només apareix un sol senyal a prop de 4.3 ppm corresponent als quatre àtoms d'hidrogen dels C_c-H. Això va ser la primera indicació de què en aquests casos s'obtenia majoritàriament la di i no la monosubstitució. També és important indicar el desplaçament que pateixen els àtoms d'hidrogen del doble enllaç més propers a l'anió cobalto-bis(dicarballur), ja que per exemple en el compost **30** es desplacen de 6.8 a 7.1 ppm.

- Els espectres de ^{11}B-RMN també han estat de gran ajuda a l'hora d'analitzar els productes obtinguts de les reaccions. El senyal corresponent a l'àtom de bor enllaçat a carboni apareix cap a 12-13 ppm i, com que és una zona on el reactiu de partida **25** no té cap senyal, permet utilitzar l'espectre de bor per calcular el rendiment de la reacció. Com en el cas dels espectres de ^{1}H-RMN, l'espectre de bor ens ha donat indicació de la formació dels derivats disubstituïts, ja que la distribució dels senyals en aquests compostos no corresponia a la d'un

monoderivat. Així, tant en el reactiu de partida monoiodo **25** com en els monoderivats **30**-**36**, hi ha 10 senyals diferents amb una distribució 1:1:1:2:7:2:2:1:1 o 1:1:2:2:4:2:2:2:1:1 depenent del compost. En canvi, els derivats **37**-**42** mostren una distribució semblant a l'anió cobalto-bis(dicarballur) **1** amb 5 senyals i una distribució 2:2:8:4:2, fet que confirma la simetria d'aquests compostos.

- Els espectres de masses MALDI-TOF ens han confirmat l'existència de les espècies pures i ens han ajudat a determinar la composició de les mescles de reacció. És de destacar l'observació de derivats fins a la hexasubstitució, com per exemple en el cas del compost **42**. A la figura 2.2.13 es mostra l'espectre de MALDI-TOF de la mescla de reacció per donar el compost **42**. S'observen els senyals corresponents tant al reactiu de partida **25** com al compost **42**, però alhora també s'observa la presència de senyals corresponents a l'addició sucessiva de 3-bromoestirè fins arribar a la hexasubstitució del clúster. Això només pot ser fruit d'un mecanisme diferent al de la reacció de Heck convencional i s'ha fet un estudi teòric en profunditat per tal d'esbrinar la raó de la formació dels derivats di i fins a hexasubstituïts.

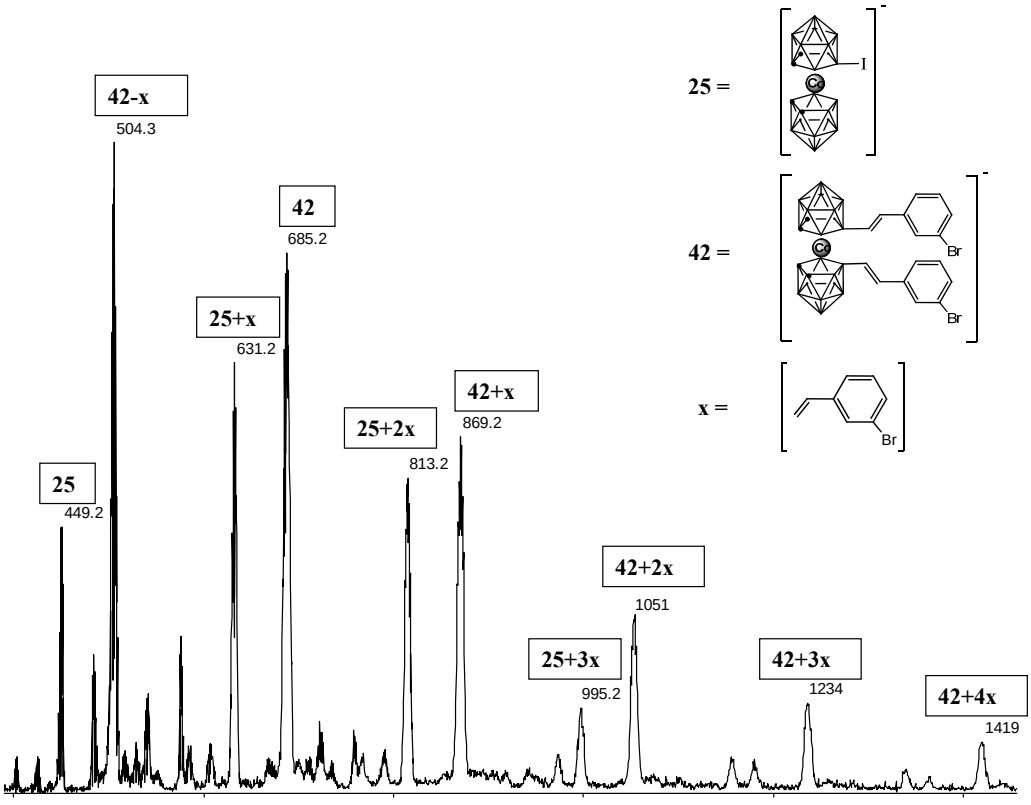

Figura 2.2.13. Espectre de MALDI-TOF-MS del compost **42**.

- Finalment s'ha pogut obtenir l'estructura cristal·lina del compost **30** en forma d'agulles. El compost, de fórmula $C_{16}H_{40}B_{18}CoN$, cristal·litza en el grup espacial monoclínic *P*21. Com es pot observar a la figura 2.2.14 hi ha una forta interacció entre els àtoms d'hidrogen del doble enllaç i la caixa de carborà, però també amb l'anell aromàtic.

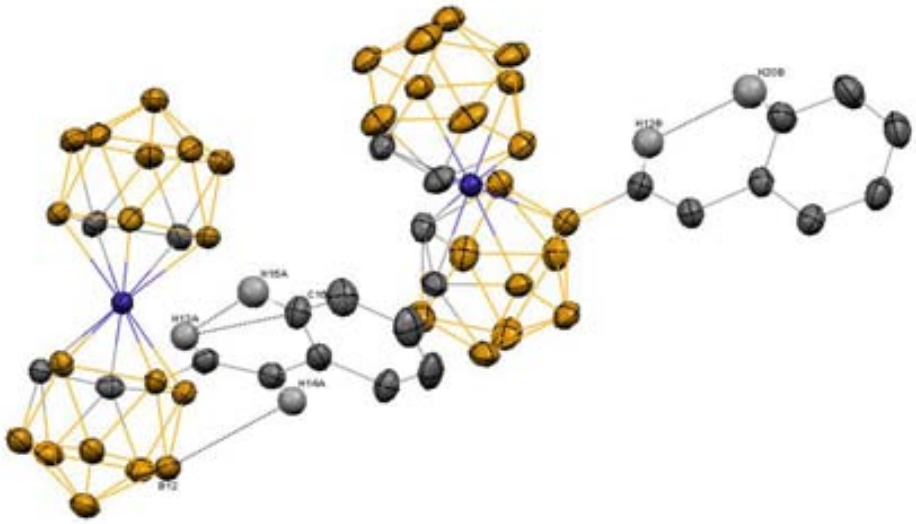

Figura 2.2.14. Estructura cristal·lina del compost **30**. S'indiquen en ratlles discontinues interaccions fortes corresponents a distàncies de radi de Van der Waals-0.2Å.

Per tal d'estudiar el mecanisme de la reacció de Heck modificada s'han fet els càlculs teòrics de les estructures que hi participen. S'ha partit d'un mecanisme descrit a la bibliografia d'una reacció de Heck, on ja s'havia estudiat d'entre tots els possibles camins quin era el més estable energèticament (figura 2.2.15).[22] Els càlculs s'han fet amb el programa Gaussian 03 utilitzant PBEPBE/lanl2dz. També s'ha comprovat pel càlcul de freqüències que els mínims no tinguessin cap freqüència imaginaria, i que els estats de transició en tinguessin una.

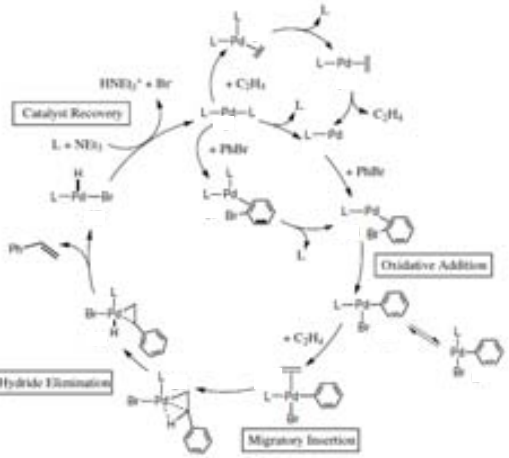

Figura 2.2.15. Mecanisme de la reacció de Heck amb catalitzadors de pal·ladi.[22]

El primer pas de la reacció és la inserció de l'espècie activa del catalitzador en el reactiu de partida **25**. Les reaccions de Heck utilitzen com a catalitzador el Pd^0; aquest es troba com a L-Pd-L (on L = lligand) tot i que segons la bibliografia l'espècie activa ha perdut un lligand, o sigui és Pd-L. Per tal de simplicar els càlculs s'ha utilitzat com a lligand el PH_3. El resultat es pot observar a la figura 2.2.16. Aquest primer pas és energèticament molt favorable amb una diferència d'energia de 41.5 kcal/mol. És interessant veure en l'espècie min_1 com l'àtom de pal·ladi s'acosta al compost **25** per dalt, interaccionant amb els àtoms de bor adjacents al B-I. En aquest primer estat de transició ts_1 es forma un anell tricèntric B-I-Pd, provocant un allargament de l'enllaç B-I. Això facilita la inserció del Pd per tal de formar l'enllaç B-Pd. Finalment, aquest primer pas s'acaba amb la formació de l'espècie intermitja min_2 que conté tant l'àtom de iode com el catalitzador de pal·ladi. Es veu com n'és d'important que l'àtom de pal·ladi vulgui interaccionar amb els grups B-H més reactius de l'anió cobalto-bis(dicarballur), que fa que l'àtom de fòsfor estigui en posició *trans* respecte al B enllaçat a pal·ladi. Aquesta disposició, que es pot observar a la bibliografia per un carborà complexat amb pal·ladi,[23] s'interpreta de manera que la càrrega del clúster es dissipa millor pels vèrtex B-H, i això provoca que l'halogen prefereixi estar en *trans* a aquests vèrtex que no al B-Pd. Aquest fet condiciona el següent pas, que és l'addició de l'alquè en aquesta espècie.

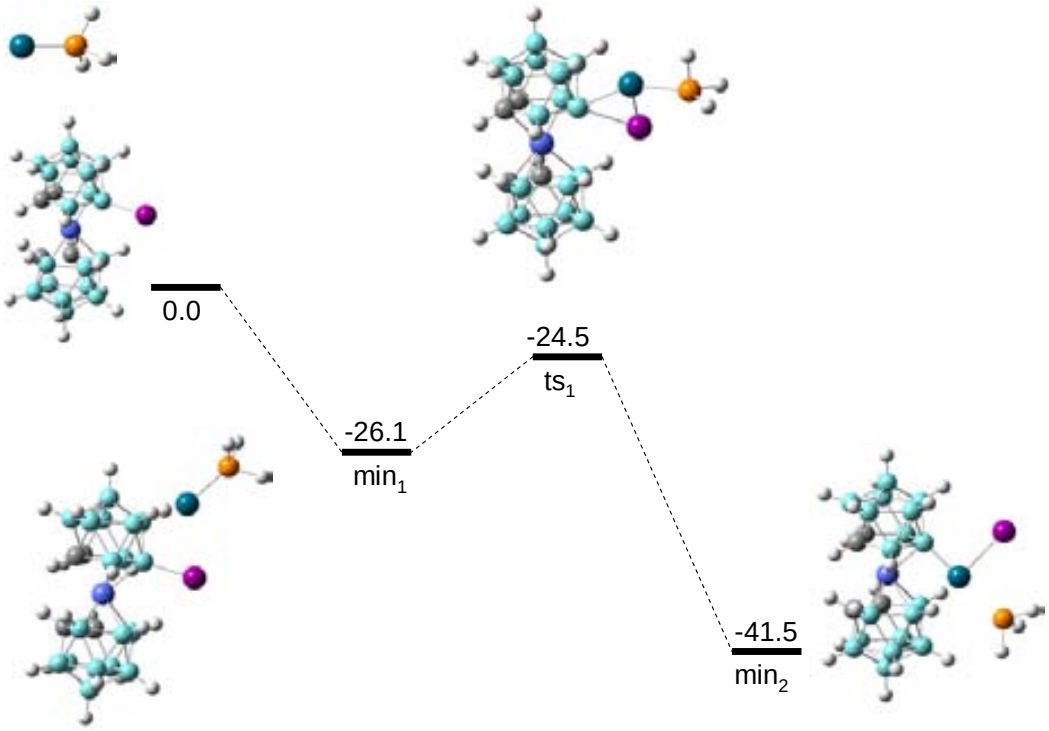

Figura 2.2.16. Mecanisme de reacció de la inserció del catalitzador de pal·ladi al compost **25**.

L'addició de l'alqué es pot donar per diferents camins, però geomètricament només hi pot haver tres possibilitats: 1) que l'alquè entri bissectant el fragment B-Pd-I (min'$_3$) o bé, 2) per l'altra banda bissectant el fragment B(H)-Pd-P (min$_3$) o bé, 3) bissectant el fragment I-Pd-P, descartant-se aquest darrer per motius energètics. A més a més, s'ha vist que el punt més reactiu del complex es troba en el grup B(H)-Pd i, energèticament, queda demostrat que és l'estructura més estable (min$_3$) com es mostra a la figura 2.2.17. Això provoca una reordenació del complex, tenint ara el iode en posició *trans* respecte l'enllaç B-Pd. Això es pot explicar per la desaparició de la interacció B-H··Pd en aquest intermig, fent que la transferència electrònica del clúster vagi a través del B-Pd. A més, aquest fet provoca que la distància entre l'alquè i el B-H de la caixa no substituïda sigui molt petita i, sense cap mena de dubte, dóna lloc a la substitució B-C en aquest àtom de bor i no del que està enllaçat a pal·ladi, com es dóna en la reacció de Heck tradicional. L'estat de transició ts$_2$ manté la geometria de l'intermig min$_3$ en el que el doble enllaç C=C de l'alquè cedeix densitat electrònica al pal·ladi. Això acaba de col·locar l'alquè en la posició correcta per fer la substitució B-C que s'observa en el min$_4$. En aquest últim intermig cal destacar que l'àtom d'hidrogen del carboni β del doble enllaç és el que es mou per fer l'enllaç B-H on abans hi havia B-Pd. També es pot tornar a veure la influència *trans* del clúster, ja que l'àtom de iode es col·loca *trans* a la part que està enllaçada al clúster, mentre que el grup PH$_3$ està *trans* a l'enllaç B-H.

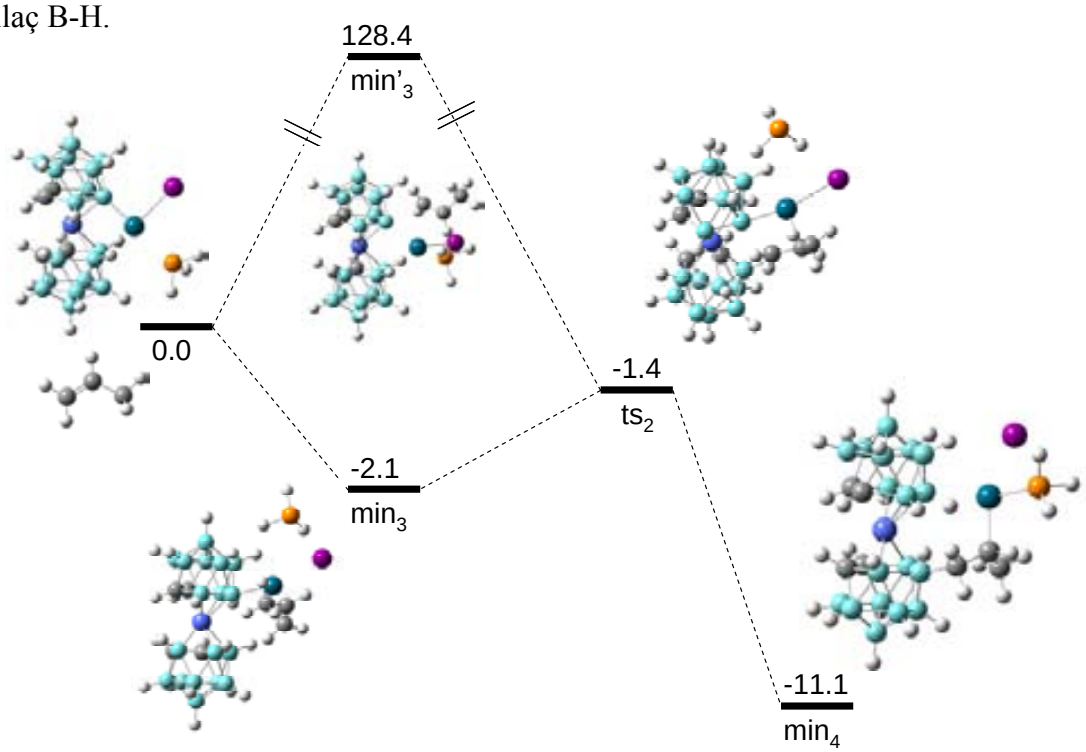

Figura 2.2.17. Mecanisme de reacció de l'addició oxidant de l'alquè en l'intermig entre el compost **25** i el catalitzador de Pd.

Per acabar, es pot concloure que aquest tipus de reacció d'acoblament B-C és una reacció d'alt interès sintètic per l'aplicació de l'anió cobalto-bis(dicarballur) ja que obre la porta a nous materials π-conjugats. Tot i que les condicions optimitzades per la reacció amb estirè han donat resultats satisfactoris en alguns casos, en d'altres el rendiment és de moderat a baix, tot i que s'ha demostrat que es pot augmentar amb més temps de reacció. D'especial interès ha estat la síntesi dels derivats disubstituïts en lloc dels monosubstituïts quan hi ha àtoms halogenats en l'anell aromàtic, fet que augmenta força la reactivitat del doble enllaç. El mecanisme teòric calculat demostra com la formació de l'enllaç B-C no es dóna al vèrtex B-I sinó en el B-H de la caixa no-substituïda, fet únic i diferencial respecte la reacció de Heck C-C on es forma en el mateix C-X.

2.2.3 Reactivitat front l'atac nucleofílic sobre el B(8) del derivat [3,3'-Co(8-$C_4H_8O_2$-1,2-$C_2B_9H_{10}$)(1',2'-$C_2B_9H_{11}$)].

El descobriment l'any 1976[24] de les reaccions d'obertura d'anells oxoni per atac nucleofílic en borans, carborans i metallacarborans va donar pas a la font més important de substitucions als àtoms de bor existent fins a l'actualitat. Un review recent resumeix la major part d'agents nucleòfils que s'han utilitzat.[25] L'atac nucleofílic al zwitterió [3,3'-Co(8-$C_4H_8O_2$-1,2-$C_2B_9H_{10}$)(1',2'-$C_2B_9H_{11}$)] (**43**) dóna lloc a la formació d'espècies aniòniques. Aquest atac es dóna sobre l'àtom d'oxigen carregat positivament enllaçat a l'àtom de bor B(8), resultant-ne l'obertura de l'anell de dioxà *exo*-clúster.

En aquesta tesi s'ha investigat l'obertura de l'anell de dioxà amb una gran varietat de nucleòfils, molts dels quals no havien estat estudiats fins el moment. A la figura 2.2.18 es troben de manera resumida els nucleòfils que s'han utilitzat i els compostos que n'han resultat. Cal destacar la importància dels compostos sintetitzats ja que s'han obtingut productes polianiònics i amb un alt contingut en bor, de manera que són uns bons candidats per la teràpia del BNCT (Boron Neutron Capture Therapy)[26] on precisament es busquen compostos amb un alt percentatge en bor i que siguin solubles en aigua, per tal de poder utilitzar-los en el cos humà. A més, alguns d'aquests compostos tenen grups funcionals lliures a fi d'utilitzar-los com a reactius de partida per fer nous materials, com és el cas del compost **55** amb un doble enllaç, els derivats halogenats **71**-**76** i el producte **77** amb un grup tiol. A més a més, per alguns dels productes obtinguts amb l'obertura de l'anell de dioxà amb *closo*-carborans (compostos **58**-**65**), s'ha obtingut el corresponent producte degradat a *nido*-carborà

per reacció amb una base forta (compostos **66-70**). Aquest darrer estudi s'ha dut a terme en col·laboració amb la companya de grup Ana Cioran i el grup del Prof. Grüner de la República Txeca.

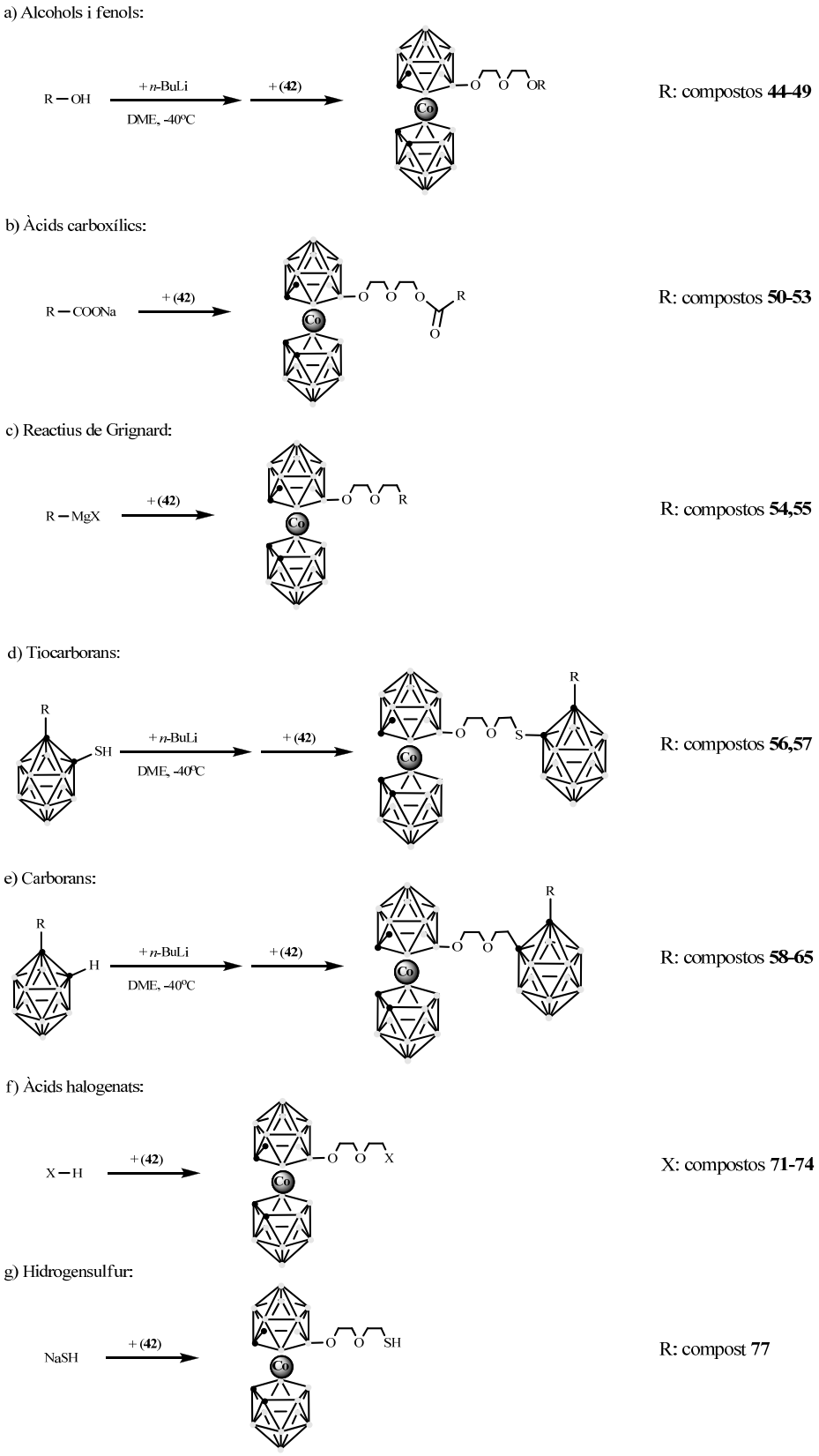

Figura 2.2.18. Resum dels nucleòfils utilitzats i els productes que n'han sortit.

La síntesi d'aquests productes varia segons la naturalesa del nucleòfil. En el cas d'alcohols, fenols, tiocarborans i carborans s'ha utilitzat una base forta com l'*n*-BuLi per incrementar el caràcter nucleofílic d'aquests i facilitar-ne la reacció. L'addició de la base s'ha dut a terme en DME a baixa temperatura durant 1h i posterior addició del compost **43**. Les salts sòdiques dels àcids carboxílics, els reactius de Grignard, els àcids halogenats i l'hidrogensulfur de sodi s'han utilitzat directament fent l'addició sobre una dissolució en DME del compost **43**, tot i que en el cas dels reactius de Grignard i els àcids halogenats l'addició s'ha fet a baixa temperatura i lentament per evitar la formació de subproductes. En tots els casos, la mescla s'ha deixat una nit en agitació i després d'evaporar el dissolvent s'ha aïllat el producte final com a salt de NMe_4^+, Cs^+, Li^+ o Na^+.

Cal destacar que la formació dels productes **75**, **76** i **78** ha estat inesperada i com a conseqüència de l'intent de fer magnesians dels compostos halogenats **72-74**. En presència de iode, l'anió cobalto-bis(dicarballur) té tendència a formar l'enllaç B-I en les seves posicions més reactives. Al tenir protegida la posició B(8) amb la cadena polieterada però desprotegida la B(8'), aquesta és molt susceptible a ser atacada pel iode del medi. Això explicaria la facilitat de la formació dels compostos **75** i **76** en una dissolució de THF en presència de iode, i s'ha descartat totalment la possibilitat que el magnesi present al medi fes algun efecte, ja que en la seva abscència la reacció també ha tingut lloc. El cas del compost **77** ve de l'intent de fer el reactiu de Grignard amb magnesi i activant-lo no amb iode com abans, sinó amb dibromoetà. S'ha comprovat que aquestes condicions provoquen el trencament de la cadena polieterada amb la pèrdua d'un fragment CH_2-CH_2X (figura 2.2.19).

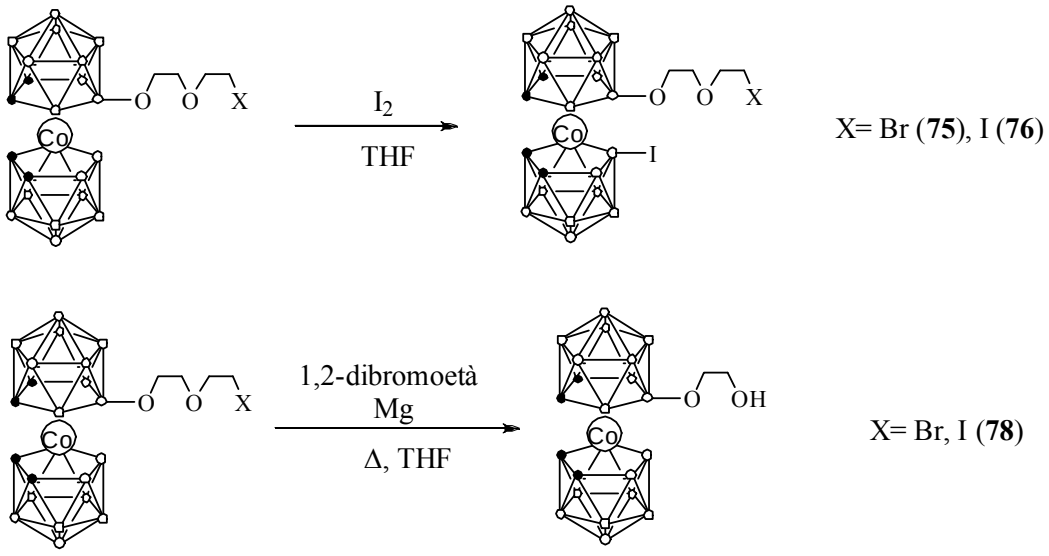

Figura 2.2.19. Esquema de la formació dels compostos **75**, **76** i **78**.

Aquests compostos han estat caracteritzats per les tècniques habituals utilitzades al llarg del treball. D'entre tota la caracterització cal destacar-ne els punts següents:

- Els espectres de ^{1}H-RMN d'aquestes espècies són molt dependents del dissolvent. En molts d'aquests compostos, utilitzant acetona com a dissolvent hi ha un solapament de les dues senyals corresponents als quatre àtoms d'hidrogen dels grups C_c-H (al ser compostos monosubstituïts al B(8)) amb una disposició 2:2. En canvi, al canviar d'acetona a diclorometà, la separació entre els senyals 2:2 és de 0.2 ppm. També és interessant l'espectre de baixa temperatura dels compostos que tenen Na^+ com a catió. Aquest fa interaccions del tipus B-H···Na tal com s'ha descrit a la bibliografia,[27] i el senyal corresponent a aquest grup B-H que interacciona es desplaça a camp baix a mesura que es disminueix la temperatura.

- Els espectres de ^{11}B-RMN són pràcticament iguals en tots els compostos, excepte aquells derivats on també hi ha unitats de carborà i hi ha els pics extres correponents. Tenen una disposició dels senyals del tipus 1:1:1:2:2:(2+2):2:2:1:1 que reflecteix la simetria C_s de les molècules. El senyal corresponent al B(8)-O apareix clarament diferenciat cap a 25 ppm. També és interessant destacar que per aquests compostos es poden diferenciar clarament els senyals de les dues meitats del clúster o, en el cas dels derivats amb l'anió cobalto-bis(dicarballur) i carborans, també es poden separar bé els senyals dels dos fragments d'entre l'espectre sencer. A la figura 2.2.20 es poden observar els dos fragments a estudiar pel compost **59**, mentre que a la figura 2.2.21 es pot observar el tractament matemàtic fet amb el programa DM2008[28] pel mateix, on es descomposa cada senyal amb una gaussiana. A la figura 2.2.21b hi ha l'espectre experimental corresponent a un compost amb l'anell de dioxà obert com el fragment I de la figura 2.2.20. Si s'eliminen aquests senyals del fragment I de l'espectre de **59** queda un espectre teòric pel fragment II com el que es mostra a l'apartat c. Si aquest es compara amb l'espectre experimental del compost [1-Me-2-$CH_3OC_2H_4$-*closo*-$C_2B_{10}H_{10}$], molt similar al fragment II, es veu que l'espectre és idèntic amb una disposició dels senyals del tipus 1:1:2:2:4.

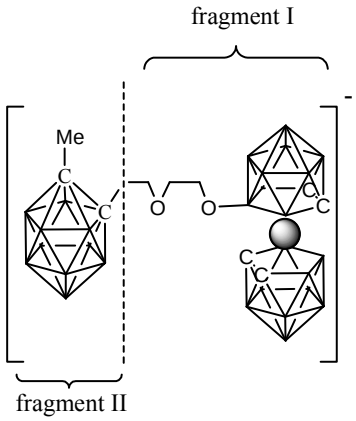

Figura 2.2.20. Fragmentació del compost **59**.

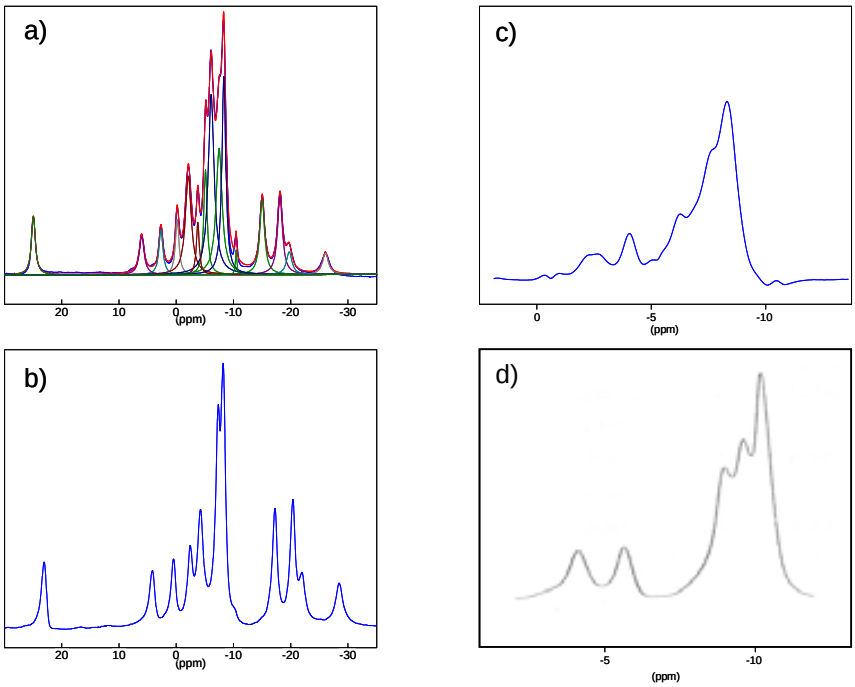

Figura 2.2.21. Estudi matemàtic de l'espectre experimental de $^{11}B\{^{1}H\}$-RMN de **59**.

- Els espectres de MALDI-TOF-MS d'aquests compostos mostren el pic corresponent al compost però també la fragmentació que experimenta en l'aparell. A més els compostos polianiònics agafen el que tenen a l'abast per tal de convertir-se en monoaniònics com per exemple cations Na^+, Li^+ o fins i tot NMe_4^+, com es pot observar a la figura 2.2.22.

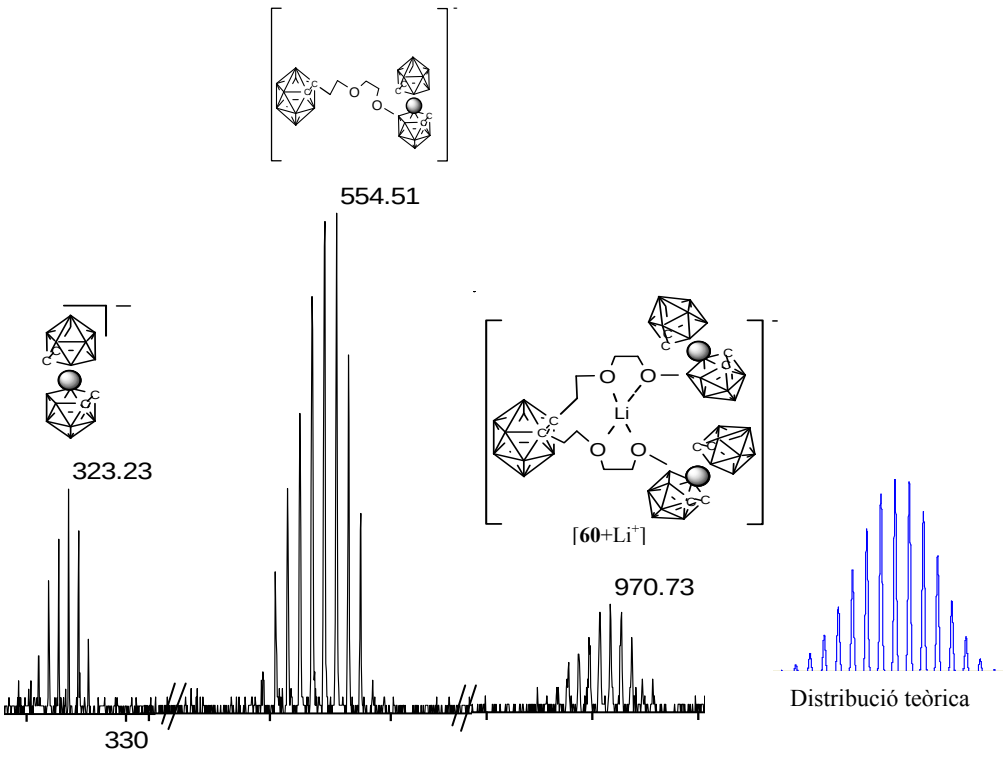

Figura 2.2.22. Espectre de MALDITOF-MS del compost **61** amb la fragmentació que experimenta dins l'aparell.

- D'entre aquests compostos, s'ha pogut obtenir monocristalls aptes per la resolució de la seva estructura cristal·lina de **47**, **50**, **51**, **73**, **74** i **78**. Cal destacar l'estructura del compost **47** que es mostra a la figura 2.2.23. Aquest compost és un trianió que queda compensat per tres cations sodi. Cada Na^+ presenta sis interaccions: tres interaccions Na···O que provenen dels àtoms d'oxigen de la cadena *exo*-clúster $–O(CH_2CH_2O)_2$- i tres interaccions Na···H-B que provenen de tres hidrògens terminals de la caixa de carborà no substituïda. A més a més, en aquesta estructura es pot observar una interacció extra de dos dels cations sodi, un d'ells amb una molècula d'aigua i l'altre amb una molècula d'etanol, provinent del dissolvent.

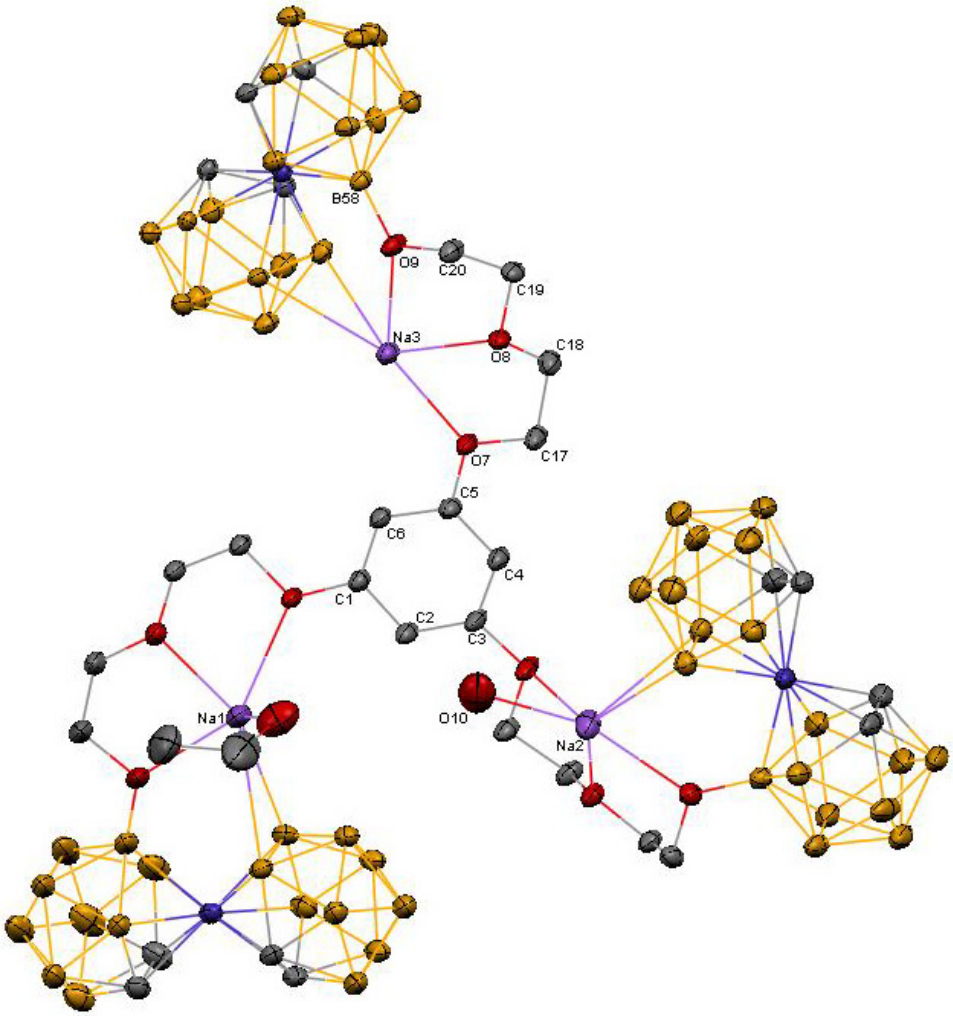

Figura 2.2.23. Estructura cristal·lina del compost **47** que evidencia la presència d'interaccions B-H···Na.

2.3 APLICACIONS DEL COBALTO-BIS(DICARBALLUR)

2.3.1 Aplicació en l'extracció de radionúclids.

Com s'ha comentat a l'introducció d'aquesta tesi, l'hexacloroderivat de l'anió cobalto-bis(dicarballur) Cl_6-**1** s'està utilitzant actualment a escala industrial com a extractant de ^{137}Cs i ^{90}Sr procedents dels residus de centrals nuclears. Aquest compost permet extreure selectivament el ^{137}Cs d'aigües residuals molt àcides (habitualment de HNO_3 3M) però no s'ha trobat cap agent extractant que separi els làntanids i actínids. Al començament de la tesi doctoral vaig participar en un projecte europeu del nostre grup anomenat EUROPART que buscava solucions a aquest problema mitjançant diferents estratègies. Les que implicaven l'ús de clústers de bor se separaven en dos blocs. En el primer cas es volia utilitzar derivats de l'anió cobalto-bis(dicarballur) que separessin selectivament lantànids i actínids; aquests incorporaven en la mateixa molècula el cobalto-bis(dicarballur) com a fragment i altres agents extractants com el CMPO o els calixarens també com a fragments. En el segon cas, el compost **1** o els seus derivats halogenats Cl_x-**1** s'utilitzaven com a agents sinèrgics juntament amb altres molècules, no havent-hi doncs enllaç covalent entre ells. En aquest segon cas és on s'han centrat els esforços del nostre grup i aquesta és la raó de l'estudi exhaustiu que s'ha fet dels derivats halogenats de **1**.

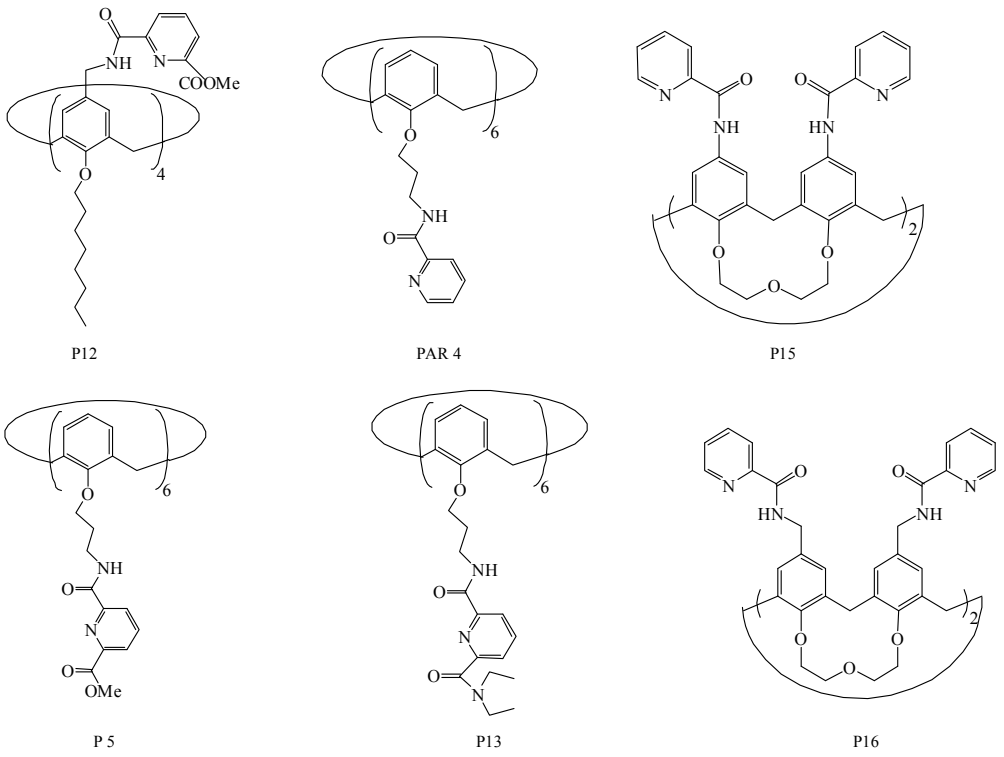

Figura 2.3.1. Calixarens preparats per a proves d'extracció com agents sinèrgics

Entre aquests esudis, hi va haver els que es varen fer en col·laboració amb el Politecnico di Milano on s'hi varen enviar una sèrie de mescles de Cl_x-**1** per fer proves d'extracció juntament amb un conjunt de calixarens preparats del grup del Prof. Casnati a Parma. Aquests es mostren a la figura 2.3.1. Els resultats es reflecteixen a la taula 2.3.1 amb els diferents lligands i les mescles de derivats clorats de **1** utilitzats. A la taula, el derivat clorat que s'especifica és el producte majoritari present en aquella mescla.

[lligand] (M)		**[agent sinèrgic] (M)**		**$[H^+]$ (M)**	**D-Am**	**D-Eu**	**SF**	
P12	0.001	**1**	0.0018	0.1	2496	777	3.08	
		Cl_2-**1**			311	88.8	3.56	
		Cl_4-**1**			544	188	2.89	
					1278	389	3.29	
					1878	572	3.31	
		Cl_7-**1**			181	50.3	3.59	
					3.08	0.93	3.32	(+ $NaNO_3$ 0.8 M)
		1		1	12.58	4.09	3.07	
		Cl_2-**1**			4.95	1.6	3.09	
		Cl_4-**1**			6.11	1.91	3.2	
		Cl_7-**1**			1.13	0.36	3.17	
P16	1.001	**1**	0.0018	0.1	1.12	0.23	5.42	
		Cl_2-**1**			0.5	0.044	11.5	
		Cl_4-**1**			1.31	0.184	7.42	
		Cl_7-**1**			2.2	0.88	2.55	
P16	0.001	**1**	0.0018	0.1	2.18	0.342	6.37	
		Cl_2-**1**			2.69	0.462	5.86	
		Cl_4-**1**			2.12	0.318	6.67	
		Cl_7-**1**			4.49	1.94	2.44	
PAR4	0.001	**1**	0.0018	0.01	n.a.	n.a.	n.a.	
		Cl_2-**1**			2.45	0.24	10.28	
		Cl_4-**1**			4.94	0.51	9.84	
		Cl_7-**1**			1.01	0.13	7.47	
P5	0.001	**1**	0.0015	1	n.a.	n.a.	n.a.	
		Cl_2-**1**			80.3	23.5	3.42	
		Cl_4-**1**			88.8	26.0	3.41	
		Cl_7-**1**			3.70	1.12	3.29	
P13	0.001	**1**	0.001	1	737	602	1.22	
		Cl_2-**1**			20.6	16.5	1.25	
		Cl_4-**1**			104	86.2	1.21	
		Cl_7-**1**			3.54	2.76	1.28	

Taula 2.3.1. Resultats dels tests d'extracció utilitzant diferents mescles de calixarens i derivats de l'anió cobalto-bis(dicarballur).

L'objectiu d'una separació a escala industrial és que el coeficient de separació SF sigui superior a 3. Com es pot observar hi ha molts casos on es supera aquest valor si bé és cert que la concentració d'àcid utilitzada és molt inferior al HNO_3 3M utilitzat industrialment, i l'augment de l'acidesa provoca una baixada dràstica del coeficient de separació. La mescla

sinèrgica que funciona millor és la constituïda pel calixarè P12 i la mescla de Cl_4-**1**. Es pot veure que en una concentració 0.1M d'àcid nítric els coeficients de distribució són de l'ordre de 1500 i 500 respectivament donant un valor de SF al voltant de 3. Augmentant la concentració d'àcid a 1M aquest valor de SF es manté a 3 tot i que els coeficients de distribució d'americi i europi disminueixen a 6 i 2 respectivament. Tot i això, aquests valors són suficientment bons per a la seva aplicació industrial si es mantinguessin en les condicions d'acidesa.

Cal destacar que en la majoria dels casos l'augment del grau de cloració millora l'extracció, però només fins un punt, ja que per la mescla amb Cl_7-**1** com a anió majoritari els valors disminueixen fins un ordre de magnitud com es veu pel calixarè P13. Tot i això, excepte pel calixarè P16 on el grau de cloració del cobalto-bis(dicarballur) no sembla influir en el resultat, en els altres casos el que extreu millor és l'anió **1**. L'explicació es troba en la tasca que fa el clúster de bor en l'extracció. Aquest actua a l'interfase entre les dues solucions fent de transportador dels cations i això està relacionat amb la influència que té sobre la tensió superficial d'aquest compost. Estudis teòrics demostren com la presència del cobalto-bis(dicarballur) augmenta aquest transport en l'interfase fent augmentar el coeficient de distribució.[29] Estudis en el nostre grup donen a entendre que la tensió superficial de **1** ve donada per interaccions febles C_c-H···H-B fent una mena d'agregats. A l'augmentar el nombre d'àtoms de clor al clúster, disminueix el número de vèrtexs B-H reactius disminuint les interaccions. Per aquesta raó suposem que hi ha un límit de substituents de clor que fan que a partir de llavors, l'anió no faci correctament el transport del catió radioactiu. Tot i que el compost **1** és el que dóna millor extracció, el seu ús és més limitat ja que es degrada gradualment en presència del medi àcid HNO_3 3M que s'usa en el procés. Per aquesta raó, industrialment ja s'usen derivats clorats tot i que aquest estudi pot ajudar a esbrinar quin és el grau de cloració òptim per fer l'extracció utilitzant el compost que aguanti més en medi àcid.

2.3.2 Aplicació en màquines moleculars.

El camp de les màquines moleculars està sent estudiat en profunditat a l'actualitat amb publicacions a les revistes de més alt nivell científic. Cal dir que s'han publicat més de 100 articles només en aquest any 2009.[30] Una màquina molecular es pot definir com un nombre discret de components moleculars que s'ha dissenyat per realitzar moviments mecànics com a resposta d'un estímul extern. Més concretament ens hem centrat en el camp dels motors

moleculars que estan basats en un moviment de rotació unidireccional. Els estímuls externs poden ser de moltes classes diferents: des de canvi de temperatura, de pH a canvis en les característiques redox de la molècula o fins i tot l'estímul pot ser la llum.

L'interés existent ens ha portat a intentar utilitzar metal·lacarborans com un dels components d'un motor molecular. L'estada feta pel candidat al grup del Prof. Leigh a Edinburgh va donar lloc a una col·laboració que tenia com a objectiu veure la influència dels clústers de bor en estructures utilitzades com a motors moleculars. Els compostos utilitzats han estat el compost **1**, el derivat hexabromat [8,8',9,9',12,12'-Br_6-3,3'-Co-(1,2-$C_2B_9H_8)_2$]$^-$ i uns rotaxans. Aquests presenten una arquitectura feta de peces mecànicament interrelacionades compostes per una molècula en forma de pesa amb grups voluminosos a cada punta anomenada component linial, i un macrocicle que està enfilat en la barra d'aquesta pesa, tal com es veu de forma esquemàtica a la figura 2.3.2.

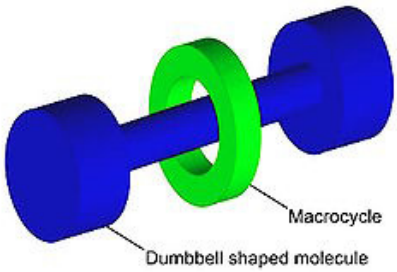

Figura 2.3.2. Representació esquemàtica de les parts d'un rotaxà.

L'aplicació de clústers de bor en màquines moleculars queda reduïda a les aportacions del grup del Prof. Tour on utilitza el *p*-carborà com a rodes de nanocotxes o nanocucs[31] i el possible ús del metal·lacarborà níquel-bis(dicarballur) com a rotor molecular a través de la oxidació-reducció de l'àtom de níquel descrit pel Prof. Hawthorne.[32] Per tant, aquest és un camp nou pel cobalto-bis(dicarballur) i com a objectiu s'ha estudiat com varia la dinàmica d'un rotaxà que conté un cobalto-bis(dicarballur) de manera que es veurà la influència de les interaccions intermoleculars i intramoleculars entre aquests anions i la part orgànica de la molècula. Per mesurar la dinàmica s'utilitzarà la tècnica de ressonància magnètica nuclear bidimensional 2D-EXSY,[33] que ens permetrà saber la velocitat de rotació del macrocicle .

Els compostos a estudiar s'han fet de dues maneres diferents. Per l'estudi de les interaccions intermoleculars s'han preparat rotaxans que tinguessin punts susceptibles a ser protonats de manera que es pogués utilitzat el cobalto-bis(dicarballur) com a anió. En canvi,

per les interaccions intramoleculars es necessitava que el clúster de bor estigués directament enllaçat al rotaxà, i això s'ha aconseguit utilitzant la metodologia descrita en el capítol anterior d'obertura de l'anell de dioxà del compost **43** per un nucleòfil.

Així doncs, la síntesi dels compostos s'ha fet com es mostra a la figura 2.3.3. El primer pas és sintetitzar el component linial fent reaccionar una amina amb un clorur d'àcid. L'amina tindrà substituents voluminosos que evitin la sortida del macrocicle mentre que el clorur d'àcid farà la feina d'estació i ajudarà a la formació del rotaxà mitjançant interaccions d'hidrogen. Aquest primer pas de la reacció es fa a 0ºC i en diclormetà. El segon és la formació del rotaxà mitjançant la unió de les peces, és a dir unint el component linial amb les dues parts que formen el macrocicle . Les interaccions d'hidrogen existents entre el grup N-H del macrocicle i el grup C=O del component linial fan que les unitats del macrocicle es tanquin sobre elles mateixes formant el dímer.[34] Per aquesta raó la reacció s'ha de fer en molt baixa dilució, per afavorir reaccions intramoleculars i no intermoleculars, i això s'aconsegueix amb l'addició molt lenta de les solucions que contenen les dues unitats del macrocicle. Abans d'obtenir el rotaxà precursor dels compostos **79-81**, s'ha sintetitzat un altre precursor amb grups fenil voluminosos però s'ha hagut de desestimar el seu ús per la seva baixa solubilitat en els dissolvents addients per fer els experiments de ressonància magnètica nuclear. En canvi, amb aquestes cadenes alquíliques la solubilitat dels compostos és bona en una mescla de cloroform+acetonitril 50%, que és el que s'utilitzarà per fer les mesures de RMN.

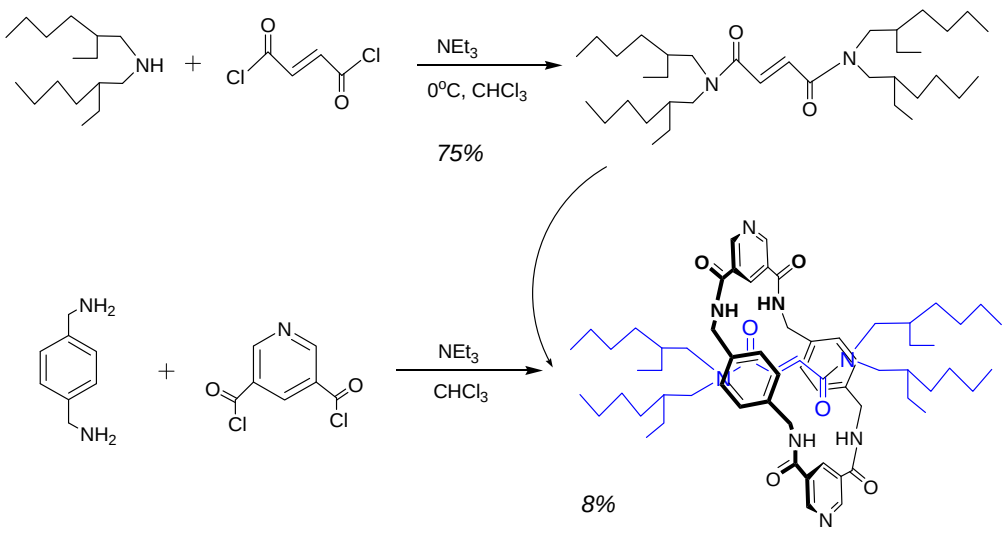

Figura 2.3.3. Síntesi del rotaxà precursor de les sals **79-81**.

Un cop tenim aquest rotaxà la protonació dels dos grups piridina es fa amb els àcids trifluoroacètic per obtenir la sal **79**, cobalto-bis(dicarballur) per la sal **80** o hexabromo-cobalto-bis(dicarballur) per la sal **81**.

D'altra banda, per estudiar les interaccions intramoleculars s'ha sintetizat l'anió **85** que conté dues unitats del cobalto-bis(dicarballur) en el component linial que actuen com a grup voluminós. La síntesi s'ha fet en tres passos com es mostra a la figura 2.3.4: un primer pas per obtenir el component linial amb un grup NH per ser funcionalitzat. El segon pas és la desprotonació de l'NH amb una base com l'hidrur de sodi i la reacció amb el compost **43**, el nitrogen desprotonat és prou nucleòfil per obrir l'anell de dioxà i així s'obté el component linial amb els clústers de bor enllaçats. Per últim, el tercer pas és la formació del rotaxà de la mateixa manera que abans, amb una addició lenta i molt baixa dilució. La presència dels clústers de bor fa que hi hagi menys plegament de les cadenes alquíliques i per aquesta raó el rendiment és major que el rotaxà anterior, 18% per 8% respectivament. En la formació d'ambdós rotaxans s'ha hagut de fer separació per cromatografia de columna que ens ha permès recuperar tota la resta de component linial no reaccionat.

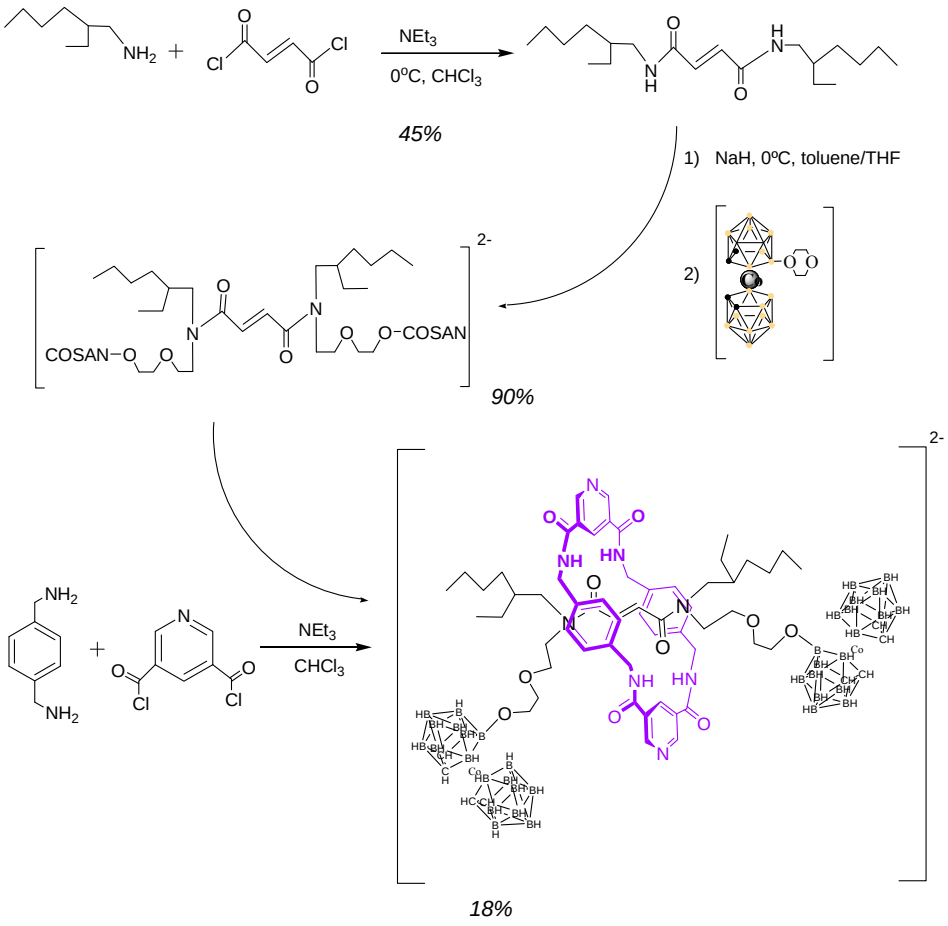

Figura 2.3.4. Síntesi del compost **85**.

El compost **85** s'ha protonat per obtenir un exemple únic de zwitterió, on la separació de càrregues és total ja que la càrrega negativa es troba al component linial i la positiva al macrocicle.

S'ha escollit el grup fumaril com a estació (CO-C=C-CO) perquè dóna la possibilitat de variar la isomeria dels compostos finals. Amb l'aplicació de llum es passa de l'isomer *trans* a l'isomer *cis*. Aquest canvi d'isomeria provoca un canvi radical en la dinàmica del rotaxà de manera que la velocitat de rotació pot variar fins a sis ordres de magnitud segons l'estudi publicat per Leigh i col·laboradors.[35] Això és degut a la desaparició de la meitat de les interaccions d'hidrogen com es pot veure a la figura 2.3.5. La reacció fotoquímica es dóna a 312 nm i durant 15' arribant a un 30% de conversió. La separació dels dos isomers es fa per cromatografia de columna utilitzant una mescla de cloroform i metanol.

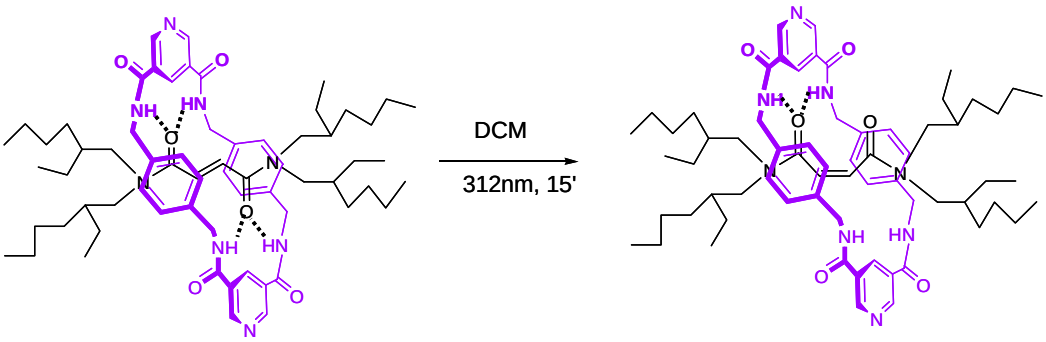

Figura 2.3.5. Fotoisomerització del rotaxà, precursor dels compostos **82-84**.

En el nostre cas també s'ha fet la isomerització del compost **85** amb les mateixes condicions, arribant-se fins a un 50% de conversió, aproximadament. Malauradament no s'han pogut separar els dos isomers amb les condicions de separació provades fins al moment.

Tal com s'havia dit al principi, l'objectiu d'aquest treball era estudiar la dinàmica del rotaxà, i per fer això es fan experiments bidimensionals EXSY per determinar la velocitat de rotació del macrocicle. Aquests experiments es basen en la velocitat d'intercanvi de posicions d'uns àtoms d'hidrogen per uns altres de manera que si la velocitat és molt alta es veuran equivalents. En els compostos estudiats els àtoms d'hidrogen que ens interessen són els grups $–CH_2-$ del macrocicle adjacents als –NH-, ja que a velocitat lenta els àtoms d'hidrogen axial i equatorial apareixeran a posicions diferents en l'espectre de ^{1}H-RMN. Aquest canvi és visible en els espectres de ^{1}H-RMN dels isomers *trans* i *cis* que es mostren a la figura 2.3.6. Com es pot observar hi ha un canvi de posicions d'alguns àtoms d'hidrogen però el més interessant és

la coalescència dels dos senyals corresponents als $–CH_2-$ de l'isomer *trans*, que apareixen a 3.8 i 5.1 ppm aproximadament, en un sol senyal a 4.5 ppm en l'isomer *cis*.

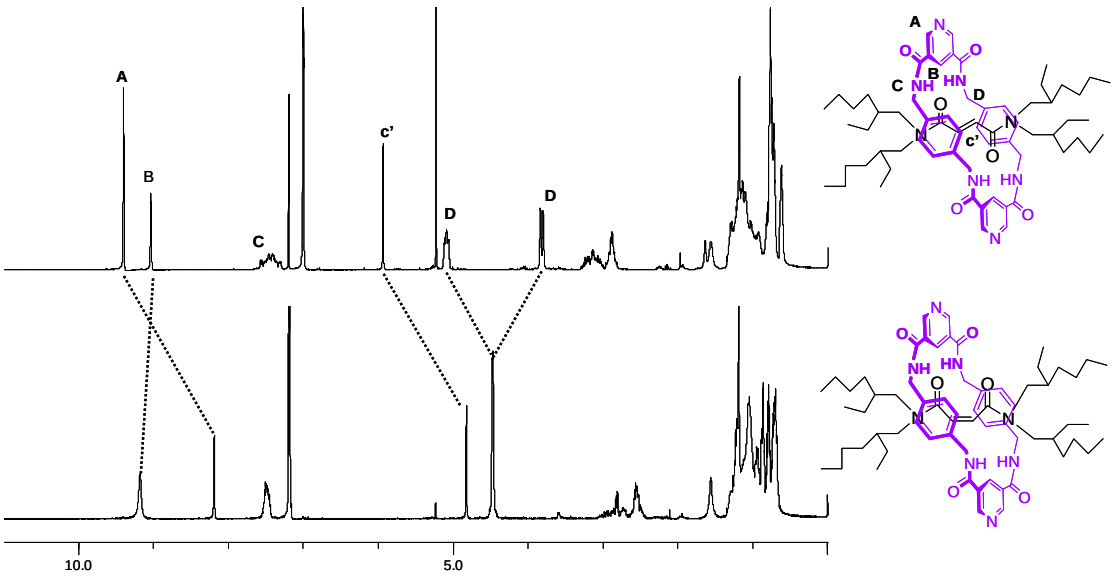

Figura 2.3.6. Comparació dels espectes de ^{1}H-RMN dels rotaxans *trans* i *cis* no protonats.

En l'espectre de ^{1}H-RMN dels compostos **79-84** es poden assignar tots els senyals corresponents als àtoms d'hidrogen de les molècules, i a tall d'exemple es mostra a la figura 2.3.7 l'espectre assignat de l'isomer *trans* no protonat, precursor dels compostos **79-81**.

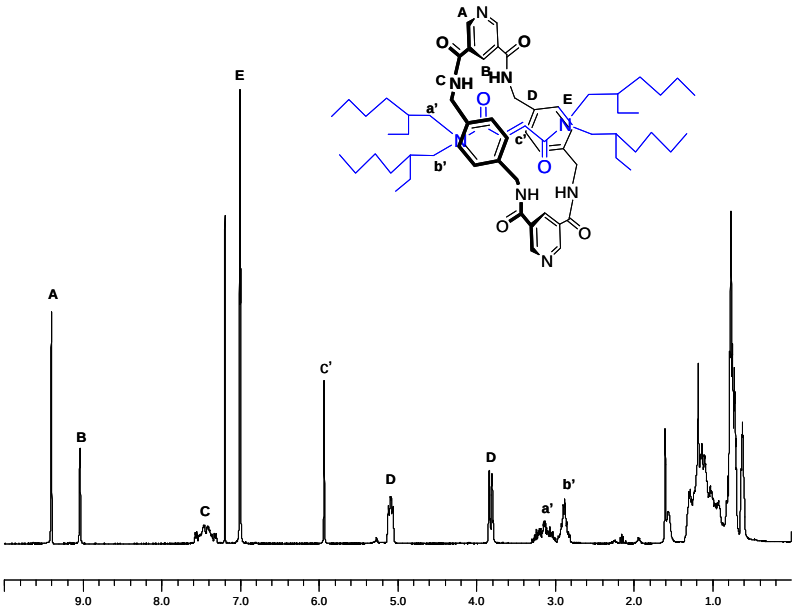

Figura 2.3.7. Espèctre de ^{1}H-RMN del rotaxà *trans* no protonat precursor dels compostos **79-81** (400 MHz, $CDCl_3$).

Una vegada se sap quins són els hidrògens que fan l'intercanvi (D) s'han fet els experiments 2D-EXSY per determinar la velocitat de rotació dels compostos **79-85**. Aquest mètode es basa en mesurar la integral dels pics fora la diagonal dels àtoms d'hidrogen que s'intercanvien, comparar els valors amb la integral dels senyals de la diagonal i mitjançant la fórmula matemàtica que es mostra a continuació es calcula la freqüència de rotació.

$$k = \frac{1}{t_m} \ln \frac{r+1}{r-1}$$

on t_m: temps de mescla

$r = (I_{AA}+I_{BB}) / (I_{AB}+I_{BA})$ essent les intensitats de la diagonal i fora la diagonal

Un cop tenim la freqüència es pot calcular la barrera energètica que hi ha entre els dos estats amb l'equació:

$$\Delta G = \left[R \cdot T \cdot \ln\left(\frac{k \cdot h}{k_B \cdot T}\right) \right] \Big/ 1000$$

on R: constant dels gasos ideals; T: temperatura de l'experiment; k: freqüència calculada amb l'equació anterior; h: constant de Planck; k_B: constant de Boltzmann.

El temps de mescla es varia per a cada experiment de manera que s'obtinguin uns valors de les integrals lluny de la saturació per obtenir uns valors de k que siguin constants independentment del temps de mescla. D'aquesta manera, pels compostos **79-81** i **85** s'han obtingut els valors que es mostren a la taula 2.3.2. En el cas dels compostos **82-84**, els isomers *cis*, ha estat impossible calcular la velocitat de rotació. Aquesta era massa alta i no s'ha aconseguit la separació dels dos senyals dels àtoms d'hidrogen axial i equatorial tot i baixar la temperatura a 210ºK. Al no tenir la separació dels senyals no s'ha pogut calcular la integral de cada un d'ells. A més a més, si tenim en compte el valor publicat de velocitat de rotació d'un isomer *cis* semblant, aquest és de l'ordre de 10^6 s^{-1},[35] i el rang d'aplicació de la tècnica 2D-EXSY per mesurar velocitats no supera els 10^3 s^{-1}.[36] Aquesta velocitat de rotació de la bibliografia tan alta s'ha calculat utilitzant el mètode de line shape analysis.

Compost	k (s^{-1})	ΔG (kJ/mol)
79	19.75	65.59
80	40.33	63.82
81	45.59	63.52
85	24.25	65.08

Taula 2.3.2. Valors de k i ΔG dels compostos **79-81** i **85** calculats per 2D-EXSY.

Si es compara els compostos **79-81** es pot observar com els dos compostos que contenen els clúster de bor (**80** i **81**) tenen unes velocitats de rotació lleugerament més altes. Aquest és l'efecte que s'esperava des del principi ja que els clústers de bor són anions poc coordinants i per tant s'enllacen més dèbilment al protó que un anió com el trifluoroacètic. D'altra banda es pot observar com el compost **85** té una velocitat semblant al **79** i per tant les interaccions intramoleculars entre el clúster de bor i el protons dels macrocicle són força importants. Ara bé, aquests canvis de velocitat provocats pels anions són mínims comparats amb els canvis provocats per la isomeria. Això ens ha portat a pensar quines poden ser les causes d'aquest efecte tant mínim que té l'anió en la dinàmica del rotaxà. Tot i que encara no s'ha pogut provar definitivament, la hipòtesi que es contempla és que els metal·lacarborans, tot i ser dèbilment coordinants, encara poden interaccionar bé a través dels enllaços C_c-H.[37] Especialment en el cas dels compost **80** es pot observar en l'espectre de ^{1}H-RMN com no hi ha l'equivalència esperada en els 8 àtoms d'hidrogen dels grups C_c-H, ja que apareixen tres senyals amb intensitats 1:1:6 (veure figura 2.3.8). Això vol dir que hi ha 1 àtom d'hidrogen de cada unitat cobalto-bis(dicarballur) que interacciona amb algun punt del rotaxà de manera que fa alentir la velocitat de rotació. Ens cal dedicar-hi més esforç i per això es vol sintetitzar un nou rotaxà que tingui com a contraanió un clúster de bor amb el màxim de posicions C_c-H i B-H protegides per tal de veure si es redueixen al mínim les interaccions.

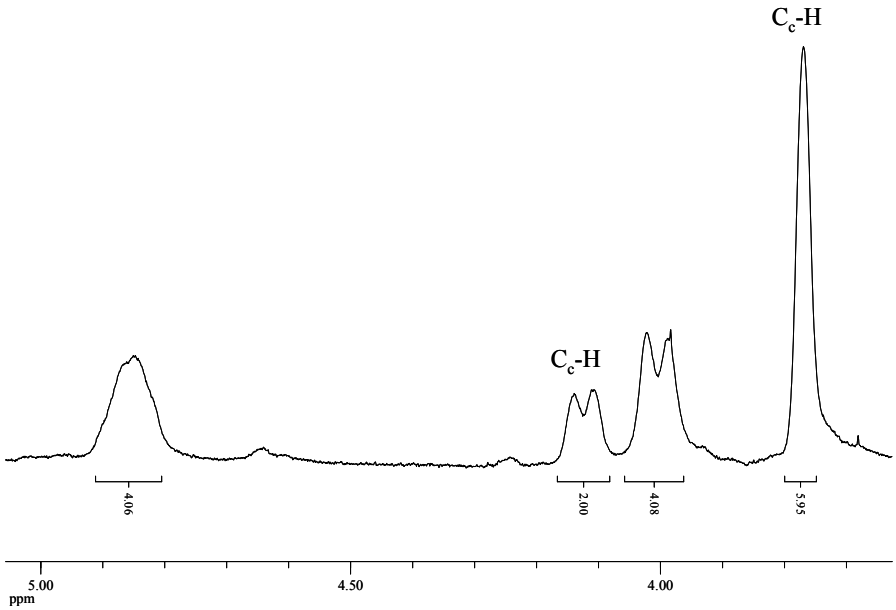

Figura 2.3.8. Espectre de ^{1}H-RMN de la zona entre 3-5 ppm del compost **80**.

Amb els resultats de què disposem fins ara es pot dir que l'efecte del contraanió en la dinàmica dels rotaxans estudiats no ha estat l'esperada. El canvi en les velocitats de rotació

segueix la tendència esperada de **79**<**80**<**81** sent el compost **81** el més ràpid a rotar ja que és el més dèbilment coordinant dels tres. Tot i això la diferència és menor que un ordre de magnitud i per tant, molt petita en comparació amb el canvi de sis ordres de magnitud que s'obté a l'aplicar llum en els compostos per passar dels isomers *trans* a *cis*. El problema que creiem que hi ha és que en aquest tipus de molècules, els clústers de bor utilitzats no semblen tan dèbilment coordinants com esperavem i és per aquesta raó que es comporten de manera semblant a l'anió trifluoroacetat. Per altra banda, el compost **85** presenta una velocitat intermitja entre el compost **79** i **80**, indicant que la interacció intramolecular entre els anions cobalto-bis(dicarballur) i els anells de piridina protonada és significativa. A més, aquest compost és un exemple únic de zwitterió amb les càrregues totalment separades i es continuarà estudiant les seves propietats, sobretot electroquímiques, que poden permetre utilitzar les propietats redox de l'anió com un estímul addicional a l'hora de controlar la dinàmica del compost.

2.3.3 Aplicació en biomedicina.

L'ús de compostos que contenen bor en el camp de la biomedicina neix amb el descobriment de la terapia contra el cancer BNCT. Des de llavors la investigació en aquest camp va anar creixent lentament fins arribar a l'última decada on, gràcies al desenvolupament de noves vies de síntesi que permeten l'obtenció de compostos a preus més baixos, hi ha hagut un increment espectacular en aplicacions biomèdiques més enllà de la teràpia antitumoral.[26a,38] L'ús de compostos de bor com a antibiòtics s'està tenint molt en compte degut a l'increment de la resistència dels bacteris a les medicines actuals. El fet que el bor estigui al costat del carboni a la taula periòdica fa que tingui semblances amb ell, però alhora també té moltes diferències com la capacitat de generar estructures tridimensionals més complexes que el carboni. La combinació d'aquestes semblances i diferències pot donar lloc a noves medicines ja que les diferències amb el carboni poden fer que als bacteris els costi més desenvolupar resistència front aquestes. A més, la terapia del BNCT continua necessitant de compostos amb un alt contingut en bor i solubles en aigua per augmentar-ne la quantitat en les cèl·lules tumorals.

Per aquesta raó es va iniciar una col·laboració amb el grup de la Prof. Alexandrova a Sofia per provar l'ús de compostos sintetitzats en el nostre grup en tractaments antimicrobians i antitumorals. Els compostos estudiats han estat l'**1**, **51**, **52**, **53** i els compostos prèviament

sintetitzats al nostre grup [8-$C_5H_{11}O_3$-3,3'-Co-(1,2-$C_2B_9H_{10}$)(1',2'-$C_2B_9H_{11}$)]$^-$ (**MeDiox**), [8-$C_6H_{13}O_3$-3,3'-Co-(1,2-$C_2B_9H_{10}$)(1',2'-$C_2B_9H_{11}$)]$^-$ (**EtDiox**), [1,1'-(PPh_2)$_2$-3,3'-Co-(1,2-$C_2B_9H_{10}$)$_2$]$^-$ (**DiPCosan**) (figura 2.3.9).[2b,27] L'activitat antimicrobiana d'aquests compostos s'ha provat amb els bacteris *Staphylococcus aureus*, *Streptococcus pyogenes*, *Escherichia coli* i *Pseudomonas aeruginosa*, així com soques pures dels fongs *Candida albicans* i *Candida tropicalis*. Totes les soques mostren *in vitro* una alta resistència a medicines com l'estreptomicina, penicilina, oxacilina, ampicilina, i alguns d'ells també a l'amoxicilina. Pel que fa als cultius de cèl·lules usats en l'estudi de l'activitat anticancerígena, a la taula 2.3.3 es mostren els sistemes model que s'han utilitzat en aquest treball, tant d'humans com animals i tumorals o no tumorals.

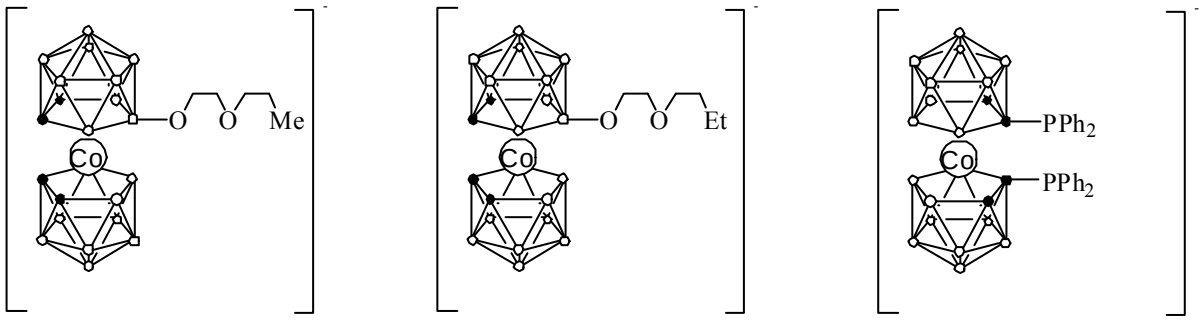

Figura 2.3.9. Esquema dels compostos utilitzats sintetitzats prèviament en el nostre grup

Origen	Tumoral	No-tumoral
Humà	**8 MG BA –** Glioblastoma multiforme **MCF-7** – Adenocarcinoma del pit **HEp-2** – Carcinoma de la laringe; **K 562** – Eritroleucèmia	-
Rata	**LSR-SF(SR)** – Sarcoma transplantable a la rata induït pel virus *Rous sarcoma*	-
Hamster	Tumor transplantable al mieloide induït pel virus *murine leukaemia Graffi*	**Cèl·lules de la medul·la òssia**
Ratolí	**P3U1 –** mieloma	**Limfòcits de la melsa, macròfags peritoneals** **Cèl·lules de la medul·la òssia**
Pollastre	**LSCC-SF(Mc29)** – Hepatoma transplantable induït pel virus *myelocytomatosis* Mc29	-

Taula 2.3.3. Sistemes model de cultius cel·lulars que s'han utilitzat en aquest treball

Pel que fa a l'estudi de l'activitat antimicrobiana, les propietats com a antibiòtics s'han mesurat amb el mètode de difusió del gel àgar.[39] En aquest es mesura el diametre d'inhibició

provocat pel compost a estudiar en una placa inoculada amb el microorganisme corresponent. A partir d'aquests valors es calculen les concentracions d'inhibició mínimes (MICs) que dónen una idea de l'efecte antimicrobià del compost per aquell bacteri o fong. A la taula 2.3.4 es mostren els MIC_{50} dels compostos més actius juntament amb el d'un antibiòtic conegut que s'utilitza de control, el tiamfenicol. El MIC_{50} es calcula matemàticament a partir del nombre de colònies inhibides del medi amb el compost o antibiòtic corresponent comparat amb el nombre de colònies en la mostra de control sense medicament.

Micro-organismes	Nombre de soques	MIC_{50}				
		$[EtDiox]^-$	$[DiPCosan]^-$	$[52]^-$	$[53]^-$	Tiam-fenicol
S. aureus	**4**	**12.8** ±7.3	**36** ±10.1	**10.1** ±7.3	**48** ±9.2	**21.3** ±6.2
S. pyogenes	**4**	**3.1** ±1.6	**26** ±6.0	**2.5** ±0.6	**48** ±9.2	**20** ±9.9
E. coli	**4**	**7** ±1.0	**26** ±6.0	**4** ±0.1	**22** ±6.0	**12** ±2.3
P. aeruginosa	**4**	**18** ±5.0	**22** ± 6.0	**8** ±2.8	**17** ±5.7	**20.5** ±3.8
Candida spp	**4**	**1.4** ±0.2	**28** ±4.0	**2.3** ±0.4	**32** ±0.1	**14** ±2.0

Taula 2.3.4. MIC_{50} dels compostos més actius comparats amb l'antibiòtic tiamfenicol.

Es pot observar com els compostos **EtDiox** i **52** són els més actius ja que necessiten d'una concentració menor per fer el mateix efecte que els altres. A més a més són més actius en tots els tipus de microorganismes utilitzats fent que es puguin considerar d'ample espectre, a l'atacar tant els gram-positiu com els gram-negatiu. Des d'un punt de vista pràctic té especial interès que la soca resistent a la meticilina, *S. Aureus,* i les soques de *P. aeruginosa* siguin sensibles a aquestes substàncies. El bacteri resistent *Staphylococcus aureus* és una de les causes freqüents d'infeccions en hospitals i és molt díficil de tractar, amb una moderada mortalitat. Si bé és cert que certs compostos de bor han estat documentats amb una bona activitat antimicrobiana,[40] fins ara no hi havia exemples de metal·lacarborans. També és important de comentar que el compost **52**, essent un dels més actius front els microorganismes, mostra comparativament una baixa citotoxicitat en cultius de cèl·lules tumorals i no-tumorals. Finalment, comparant els resultats dels derivats de l'anió cobalto-bis(dicarballur) amb **1**, queda clar que aquest presenta activitats menors i per tant la funcionalització d'aquest anió millora les seves propietats com a nous antibiòtics.

D'altra banda, l'estudi de les propietats antitumorals dels compostos utilitzats s'ha dut a terme amb l'assaig MTT. Aquest assaig és un mètode colorimètric que es basa en la mesura de l'activitat enzimàtica de les cèl·lules vives en la reducció del compost MTT (3-(4,5-Dimethylthiazol-2-yl)-2,5-diphenyltetrazolium bromide) que és groc, a formazan que és de color lila. Això serveix per mesurar la viabilitat o proliferació de les cèl·lules en un medi determinat. La viabilitat cel·lular es defineix com la probabilitat que té un organisme de prosperar o sobreviure. En l'assaig MTT, la intensitat del senyal mesurat amb un espectrofotòmetre ve donada per la quantitat de cèl·lules vives existents. Utilitzant diferents concentracions dels metal·lacarborans s'obtenen unes curves de resposta front la dosi. Quan es comparen les dades experimentals dels metal·lacarborans amb els valors experimentals de control s'obtenen els valors de CC_{50}. Aquests es mostren a la taula 2.3.5 pels diferents compostos utilitzats en aquest treball.

Cultiu cel·lular	**[51]$^-$**		**[52]$^-$**		**[53]$^-$**		**[EtDiox]$^-$**		**[MeDiox]$^-$**		**[1]$^-$**	
	24 h	48 h	24 h	48 h	24 h	48 h	24 h	48 h	24 h	48 h	24 h	48 h
LSCC-SF(Mc29)	62	29	65	15	-	48.5	11	6	26	15	41	19
LSR-SF-SR	42	23	45	28.2	-	-	24	16	30	20	54	27
P3U1	40.5	28.3	54.1	47.9	-	-	37.4	26.1	45.8	30.4	58.6	40.8
HEP-2	-	40	-	30	-	-	28	19	63	19	n.d.	n.d.
MCF-7	71.5	42	93.6	71.5	n.d.	n.d.	62.5	35	48	17.5	84.5	74
8 MG BA	76	25	86	47.2	n.d.	n.d.	60	28.5	66.5	43	n.d.	n.d.

n.d.: experiment no mesurat; (-): sense valor perquè la viabilitat cel·lular és major al 50%.

Taula 2.3.5. Valors de CC_{50} (μg/ml) dels metal·lacarborans amb els diferents cultius utilitzats.

Aquests experiments mostren en tots els casos com la viabilitat de les cèl·lules és proporcional al temps d'exposició. Cada cultiu té una resposta específica davant dels metal·lacarborans, de manera que varien en la citotoxicitat i la proliferació cel·lular. Cal destacar que el compost **EtDiox** és el que presenta la més alta citotoxicitat en tots els experiments realitzats, seguit pel compost **MeDiox**. En canvi, el menys efectiu ha estat el compost **53** on no s'ha pogut obtenir cap valor de CC_{50} perquè la viabilitat cel·lular era encara major al 50%. D'entre els diferents cultius, el de cèl·lules de pollastre LSCC-SF(Mc29) és el més sensible a la mort cel·lular per la majoria dels compostos.

A continuació s'ha comparat la viabilitat dels diferents compostos amb cèl·lules tumorals (figura 2.3.10) o no-tumorals (figura 2.3.11), a dues concentracions diferents de metal·lacarborà. Els resultats mostren com en les cèl·lules tumorals la concentració no influeix massa en la viabilitat de les cèl·lules i el valor és similar al control. En canvi, en usar cultius de cèl·lules no tumorals la viabilitat disminueix notablement fins a reduir-se a la meitat en els compostos **51**, **MeDiox** i **EtDiox**.

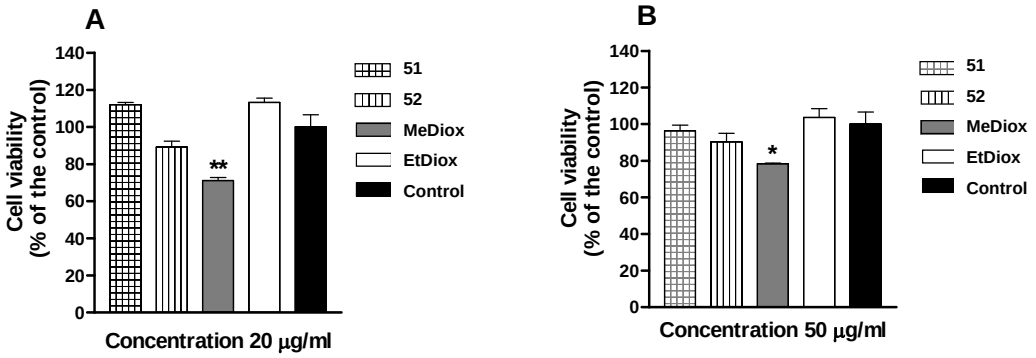

Figura 2.3.10. Viabilitat a dues concentracions diferents dels compostos estudiats d'un cultiu de cèl·lules de tumor Graffi provinents de hàmster.

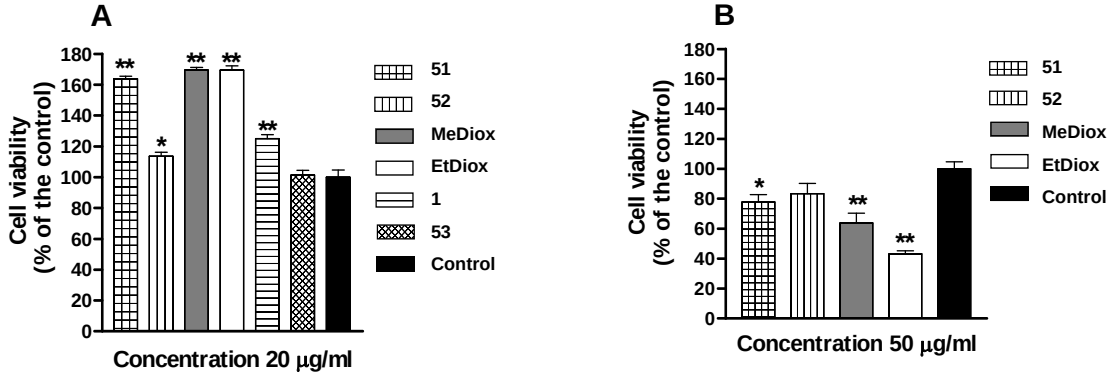

Figura 2.3.11. Viabilitat a dues concentracions diferents dels compostos estudiats d'un cultiu de cèl·lules de la medul·la òssia provinents de hàmster.

Finalment, també s'ha volgut comprovar la viabilitat de cèl·lules extretes directament de ratolins sans, com els macròfags peritoneals, limfòcits de la melsa i cèl·lules de la medul·la òssia. Es coneix que els macròfags tenen un paper clau en la defensa del cos front els antibiòtics i la fagocitosi d'aquests és un procés molt important en la funció immune. Els resultats pels compostos **1**, **52** i **53** (taula 2.3.6) mostren com la concentració d'aquests afecta

a la viabilitat d'aquestes cèl·lules sent aquests compostos els que presentaven una menor citotoxicitat en els assaigs anteriors.

Compost/ concentració, μg/ml		Limfòcits de la melsa	Macròfags peritoneals	Cèl·lules de la medul·la òssia
1	10	144.83 ± 2.60	161.70 ± 1.61	130.43 ± 0.52
	20	134.48 ± 1.59	136.17 ± 2.58	110.43 ± 0.82
	50	113.79 ± 3.28	102.13 ± 2.82	70.87 ± 2.75
52	10	165.52 ± 5.05	197.87 ± 3.77	118.26 ± 0.42
	20	165.52 ± 2.02	191.49 ± 2.60	100.00 ± 2.05
	50	131.03 ± 4.26	131.91 ± 1.62	63.47 ± 0.05
53	10	110.34 ± 6.04	151.06 ± 2.06	92.17 ± 1.28
	20	96.55 ± 3.84	108.51 ± 1.61	99.13 ± 2.28
	50	137.93 ± 5.79	100.00 ± 1.96	94.78 ± 2.98

Taula 2.3.6. Viabilitat de cèl·lules provinents de ratolins sans depenent de la concentració del compost.

Finalment, s'han fet experiments per veure l'efecte dels metal·lacarborans en l'habilitat de les cèl·lules tumorals de formar colònies. Els resultats es poden observar a la taula 2.3.7. Es pot veure com se segueix la mateixa tendència que pels cultius anteriors on els compostos més citotòxics són el **MeDiox** i l'**EtDiox**. D'entre els diferents cultius, el LSCC-SC(Mc29) de cèl·lules de pollastre continua sent el més sensible.

	LSCC-SF(Mc29)	LSR-SF(SR)	P3U1	Hep-2	K562	8 MG BA	MCF-7
[51]$^-$	≥ 50*	≥ 50	≥ 75	≥ 75	≥ 75	≥ 50	≥ 75
[52]$^-$	≥ 75	≥ 75	≥ 100	≥ 100	≥ 100	≥ 200	≥ 200
[53]$^-$	≥ 100	n.i.	≥ 200	n.i.	n.i.	≥ 200	≥ 150
[MeDiox]$^-$	≥ 25	≥ 50	≥ 50	≥ 50	≥ 50	≥ 50	≥ 50
[EtDiox]$^-$	≥ 10	≥ 25	≥ 50	≥ 50	≥ 50	≥ 50	≥ 50
[1]$^-$	≥ 50	≥ 75	≥ 100	≥ 100	≥ 75	n.i.	≥ 150

n.i.: no s'observa inhibició en totes les concentracions utilitzades

Taula 2.3.7. Concentració (μg/ml) on el compost inhibeix l'habilitat de les cèl·lules tumorals de formar colònies.

Els metal·lacarborans que s'han estudiat presenten una estructura química força semblant però en canvi tenen diferents propietats biològiques (citotòxiques, antimicrobials, antiproliferatives). Això no és sorprenent i hi ha altres exemples a la bibliografia amb altres tipus de compostos, on canviant només un substituent de l'estructura les propietats canviaven significativament.[41] Per tant, per concloure, es pot assegurar que els metal·lacarborans mostren propietats antiproliferatives i eficàcia antimicrobiana, essent el compost **EtDiox** el millor candidat. Tanmateix s'ha de seguir estudiant els mecanismes d'acció i mesurar la seguretat biològica d'aquests compostos pel seu ús en estudis *in vivo*. A més, també seria interessant esbrinar la relació entre les propietats química i física dels metal·lacarborans i la seva activitat biològica a fi de facilitar el disseny de nous fàrmacs i millors propietats antimicrobianes i anticancerígenes.

2.4 CARBORANS

Aquest capítol tractarà d'aspectes fonamentals dels carborans, aspectes importants per a conèixer la seva reactivitat posterior. El dividim en tres apartats. En primer lloc s'ha volgut ampliar l'estudi de cloració fet a l'anió **1** descrit a l'apartat 2.2.1 sobre un altre clúster de bor. L'anió $[Ph\text{-}CB_9H_9]^-$ (**86**) mostra l'interès de tenir dos punts de reactivitat molt diferent, els vèrtexs aromàtics C-H i els del clúster B-H. En el segon apartat es tractarà l'acidesa de *nido*-carborans ja que s'ha cregut necessari crear una metodologia teòrica per calcular el pK_a de *nido*-carborans derivats del $[C_2B_9H_{12}]^-$, el valor experimental dels quals és molt difícil d'aconseguir. Finalment, en el tercer punt s'estudiaran les carboranil-fosfines. Aquestes fan unes interaccions dèbils amb el iode i s'ha comparat el comportament d'aquestes amb fosfines convencionals, tant experimentalment com teòrica.

2.4.1 Estudi teòric i experimental de l'halogenació de l'anió $[Ph\text{-}CB_9H_9]^-$

L'estudi de cloració sobre l'anió $[Ph\text{-}CB_9H_9]^-$ (**86**) s'ha fet en col·laboració amb una antiga estudiant del grup, Na Milagros Rey. Com s'ha dit abans, aquest clúster dóna la possibilitat d'estudiar alhora la cloració en dos posicions ben diferents com són els àtoms de carboni aromàtics i els àtoms de bor del clúster. A més, la part teòrica d'aquest estudi s'ha pogut fer amb més detall ja que el consum de temps de càlcul d'aquest clúster més petit és molt menor al de l'anió **1**. Això ens ha permés calcular el mecanisme de reacció teòric més estable i esbrinar el camí més possible. Conjuntament amb els resultats teòrics també s'han dut a terme reaccions addicionals per obtenir dades experimentals que recolzin el mecanisme teòric. Així doncs, la reacció de **86**:NCS amb estequiometria de 1 a 20 equivalents a 194±6ºC durant 2 hores ha donat els resultats que es resumeixen a la taula 2.4.1.

Els resultats segueixen la mateixa tendència que per **1**, on es veu que hi ha compostos amb més tendència a generar-se que d'altres. Les fraccions molars dels compostos es poden treure de la integració dels espectres de MALDI-TOF-MS. Així doncs, per estequiometries de $\mathbf{r}_1$ a $\mathbf{r}_6$ el producte dominant concorda amb l'$\mathbf{r}_y$, és a dir que per exemple en la barreja de $\mathbf{r}_3$, el producte dominant conté tres àtoms de clor. A partir de sis àtoms de clor la correlació s'acaba i es comença a trobar productes que persisteixen. Així, el producte amb sis àtoms de clor encara és majoritari per $\mathbf{r}_7$ i $\mathbf{r}_8$, el de set entre $\mathbf{r}_9$ i $\mathbf{r}_{11}$, i el de vuit àtoms de clor de $\mathbf{r}_{12}$ fins $\mathbf{r}_{20}$.

r_y	y	r_y	y
1	0, **1**, 2	11	6, **7**, 8, 9, 10
2	0, 1, **2**, 3, 4	12	6, 7, **8**, 9, 10
3	2, **3**, 4, 5	13	6, 7, **8**, 9, 10
4	3, **4**, 5, 6	14	6, 7, **8**, 9, 10
5	3, 4, **5**, 6	15	6, 7, **8**, 9, 10, 11
6	**6**, 7	16	6, 7, **8**, 9, 10, 11, 12
7	**6**, 7	17	6, 7, **8**, 9, 10, 11, 12
8	5, **6**, 7, 8, 9	18	6, 7, **8**, 9, 10, 11, 12, 13
9	6, **7**, 8, 9	19	6, 7, **8**, 9, 10, 11, 12, 13, 14
10	6, **7**, 8, 9	20	7, **8**, 9, 10, 11, 12, 13, 14

Taula 2.4.1. Reacció entre **86**:NCS. r_y representa la fracció molar inicial des de 1:1 a 1:20. A la columna indicada com a y, les espècies observades per MALDI-TOF-MS estan indicades segons el número d'àtoms de clor insertats. L'espècie en negreta és la majoritària en cada barreja.

El producte amb sis àtoms de clor [1-(4'-Cl-C_6H_4)-6,7,8,9,10-Cl_5-1-CB_9H_4]$^-$ (**86**) només es pot explicar si la distribució dels sis àtoms de clor es fa d'acord amb conjunts de grups d'àtoms equivalents, en aquest cas 1(B) + 4(B)+1(C), grups que es poden intuir a la figura 2.4.1. Aquesta distribució es pot observar ja en l'estructura del derivat bromat [1-(4'-Br-C_6H_4)-6,7,8,9,10-Br_5-1-CB_9H_4]$^-$ present a la bibliografia.[42] A més a més, en aquest treball també s'ha pogut sintetitzar el derivat hexaclorat i se n'ha obtingut l'estructura de raigs X com es pot observar a la figura 2.4.2.

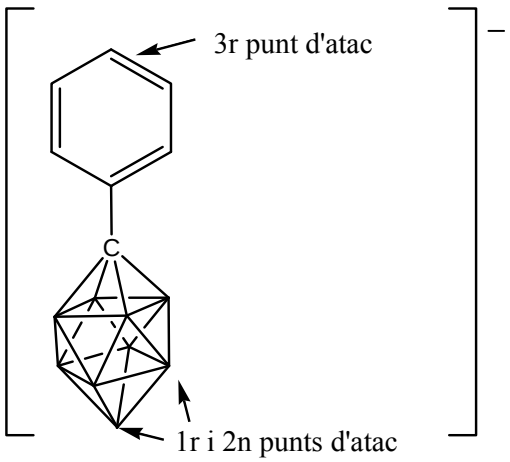

Figura 2.4.1. Evidència experimental per la substitució de [1-C_6H_5-1-CB_9H_9]$^-$.

A partir d'aquest resultat, es pot deduir que els següents punts d'atac serien les posicions *meta* de l'anell aromàtic, cosa que explica la persistència del derivat octaclorat en els experiments realitzats. Tot i així, un grau més alt de cloració també és possible ja que en

els espectres de masses s'ha arribat a observar fins la percloració, el compost [1-(2',3',4',5',6'-Cl-C_6)-2,3,4,5,6,7,8,9,10-Cl_9-1-CB_9]$^-$ (**88**). Els compostos entremig, o sigui entre 9 i 13 àtoms de clor, seran molt difícils d'aconseguir purs pels diferents possibles isomers, tal com passa amb els tri i tetraclorats.

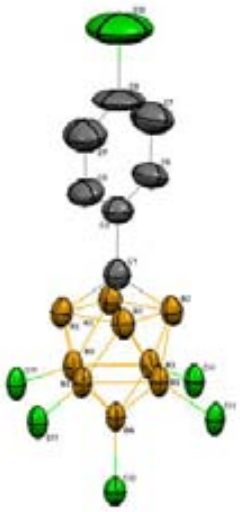

Figura 2.4.2. Estructura cristal·lina del compost **87**.

Per tal d'explicar aquest mecanisme de cloració s'han realitzat càlculs *ab initio*, començant per calcular la termodinàmica de la reacció i observar si hi ha alguns derivats més estables que d'altres pel que fa a l'energia. Tenint en compte les energies dels enllaços C-H, C-Cl, B-H i B-Cl, 81, 95, 81 i 128 kcal/mol respectivament, s'haurien de substituir primer tots els B-H per B-Cl i no és el cas. Això es pot observar calculant les energies de reacció de l'addició consecutiva d'àtoms de clor al clúster segons l'equació 1.

$$[Cl_yH_{14-y}\text{-}1\text{-}C_6\text{-}1\text{-}CB_9]^- + Cl_2 \xrightarrow{\Delta H} [Cl_{y+1}H_{13-y}\text{-}1\text{-}C_6\text{-}1\text{-}CB_9]^- + HCl$$

Equació 1

El resultat es pot observar a la figura 2.4.3 en la representació de ΔH de la reacció en funció del número d'àtoms de clor. Es veu com no hi ha preferència respecte cap derivat i la pendent del primer sector de la gràfica és comparable al valor esperat per la substitució de B-H per B-Cl (-47 kcal/mol). Tanmateix, el segon sector de la gràfica té una pendent de -26 kcal/mol corresponent a la substitució de C-H per C-Cl (valor esperat de -21 kcal/mol). Per tant, amb aquests valors es podria arribar a pensar que no hi ha cap mena de regioselectivitat en el clúster i, amb les condicions adequades, no hi hauria problema per la percloració del

clúster. Aquests resultats estan d'acord amb els obtinguts a l'apartat 2.2.1 per **1**, per tant podem assegurar que el mecanisme de cloració té un origen cinètic.

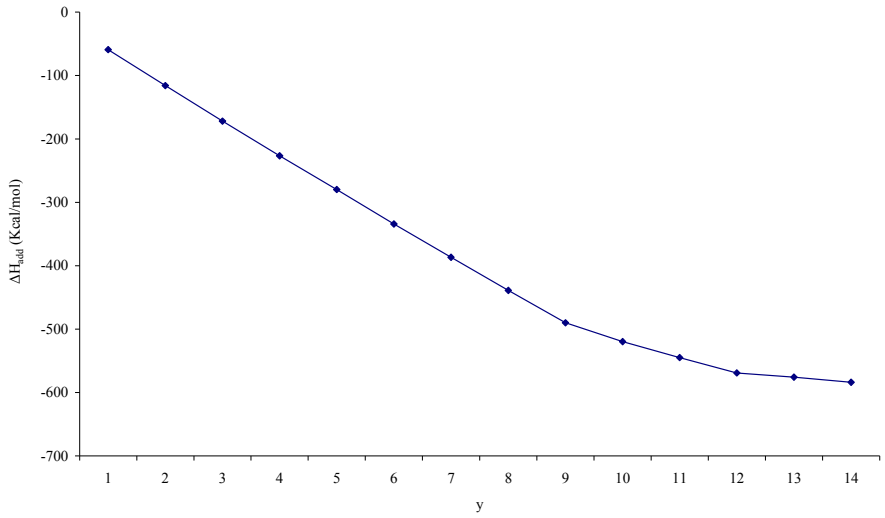

Figura 2.4.3. Representació gràfica de ΔH_{add} (addició acumulativa de l'energia de B-Cl en kcal/mol) pel compost $[Cl_yH_{14-y}\text{-}1\text{-}C_6\text{-}1\text{-}CB_9]^-$ (per y=0-14), *vs* número d'àtoms de clor (y).

Com s'ha vist pel compost **1**, la distribució de les càrregues en el clúster dóna una idea força bona de l'ordre d'atac. Tot i això, en el cas de **86** el problema és que si es calculen les càrregues NPA als vèrtexs del clúster, les posicions on la càrrega és més negativa són als àtoms de carboni de l'anell aromàtic, i això se sap que no és el que passa experimentalment, veure figura 2.4.4c. En canvi, com es pot veure a la figura 2.4.4a les càrregues 2a-NPA sí que segueixen l'ordre conegut experimentalment. A més, s'han calculat les càrregues per un compost parcialment clorat, figura 2.4.4b, per observar si hi ha algun canvi en l'ordre següent de cloració, i es veu com no influeix el fet que ja estigui substituït, l'ordre calculat pel compost de partida es manté fins la percloració.

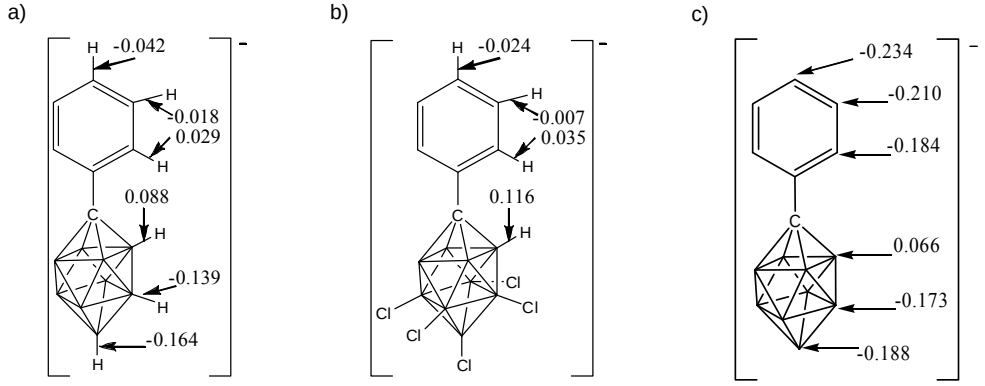

Figura 2.4.4. a) Càrregues 2a-NPA en els enllaços B-H i C-H per **86**. b) Càrregues 2a-NPA per $[1\text{-}C_6H_5\text{-}6,7,8,9,10\text{-}Cl_5\text{-}1\text{-}CB_9H_4]^-$ utilitzant B3LYP/6-31+G*. c) Càrregues NPA en els vèrtexs dels àtoms de bor i carboni.

Tot i que es pot deduir la regioselectivitat del clúster només per les càrregues 2a-NPA, la primera posició de cloració que es coneix experimental no és la que té una càrrega més negativa, sinó una de la capa inferior d'àtoms de bor (amb una càrrega de -0.139). Possiblement, això és degut a d'altres components cinètiques que no es tenen en compte a l'hora de calcular les càrregues NPA, que com ja s'ha esmentat abans és una manera ràpida de trobar la cinètica de la reacció. Per tant, s'ha fet un estudi més exhaustiu d'aquest primer pas de reacció. La diferència d'energia entre els isomers $[6\text{-Cl-1-}C_6H_5\text{-1-}CB_9H_8]^-$ i $[10\text{-Cl-1-}C_6H_5\text{-1-}CB_9H_8]^-$ és de 1.4 kcal/mol, sent l'isòmer 10-Cl el més estable. El càlcul del camí de reacció i, més concretament, de l'estat de transició ens pot donar una idea més clara del mecanisme. Si se suposa una geometria inicial de l'estat de transició amb un catió de clor, Cl^+, enmig dels enllaços B(10)-H i B(6)-H i es deixa relaxar l'estructura, el mínim energètic correspon a la formació de l'enllaç B(6)-Cl i l'H(6) es mou cap al centre d'una cara triangular del clúster. El problema rau en què l'energia d'activació per aquest estat de transició amb Cl^+ (equivalent a un atac electrofílic sobre el clúster) és exagerat, del voltant de 280 kcal/mol. Per tant, aquest valor ens obliga a pensar en un mecanisme alternatiu ja que aquest no té cap sentit físic. A la bibliografia s'havia insinuat una vegada que la reacció podria ésser radicalària.[43] Amb aquesta idea en ment s'han utilitzat uns indicadors anomenats índex de Fukui que s'utilitzen per tenir una idea de la susceptibilitat d'una posició de ser atacada per un electròfil, un nucleòfil o un radical. Si es calculen aquests índex de Fukui pel compost **86** s'obté que els índexs més positius es troben a les posicions B(6) i B(8), equivalents per la simetria del compost, i és l'índex calculat per un atac radicalari el que té un valor més positiu, 0.05 més que per l'atac d'un electròfil.

Aleshores, s'ha recalculat l'estat de transició posant un àtom de clor en lloc del clor catió. Per aquests càlculs s'ha emprat un clúster més adequat i en comptes d'utilitzar el compost **86** com a partida, s'ha canviat l'anell aromàtic per un hidrogen per simplificar els càlculs. D'aquesta manera i partint de la mateixa geometria inicial, l'estat de transició trobat té l'enllaç B(6)-Cl i el H(6) es troba a una cara triangular com abans. En aquesta ocasió, però, l'energia d'activació té un valor de 6.21 kcal/mol, energia força més acceptable que els 280 kcal/mol d'abans. A més a més, la diferència d'energia entre reactius i productes és de 2.7 kcal/mol cap a la formació de l'isòmer 6-Cl. Amb aquests valors d'energia d'activació queda demostrat que el mecanisme ha de ser radicalari i l'última cosa que queda per observar és la preferència de l'isòmer 6-Cl respecte el 10-Cl. Tot i que pel producte final la diferència és de 1.4 kcal/mol com s'ha esmentat, el primer pas del mecanisme demostra com la formació del

complex de l'isòmer 6-Cl és més favorable per 1.7 kcal/mol, i tot i que en els següents passos l'energia d'aquest isòmer sigui superior, la diferència en aquest complex de pre-reacció és suficient perquè es formi majoritàriament l'isòmer 6-Cl. El mecanisme es pot veure a la figura 2.4.5.

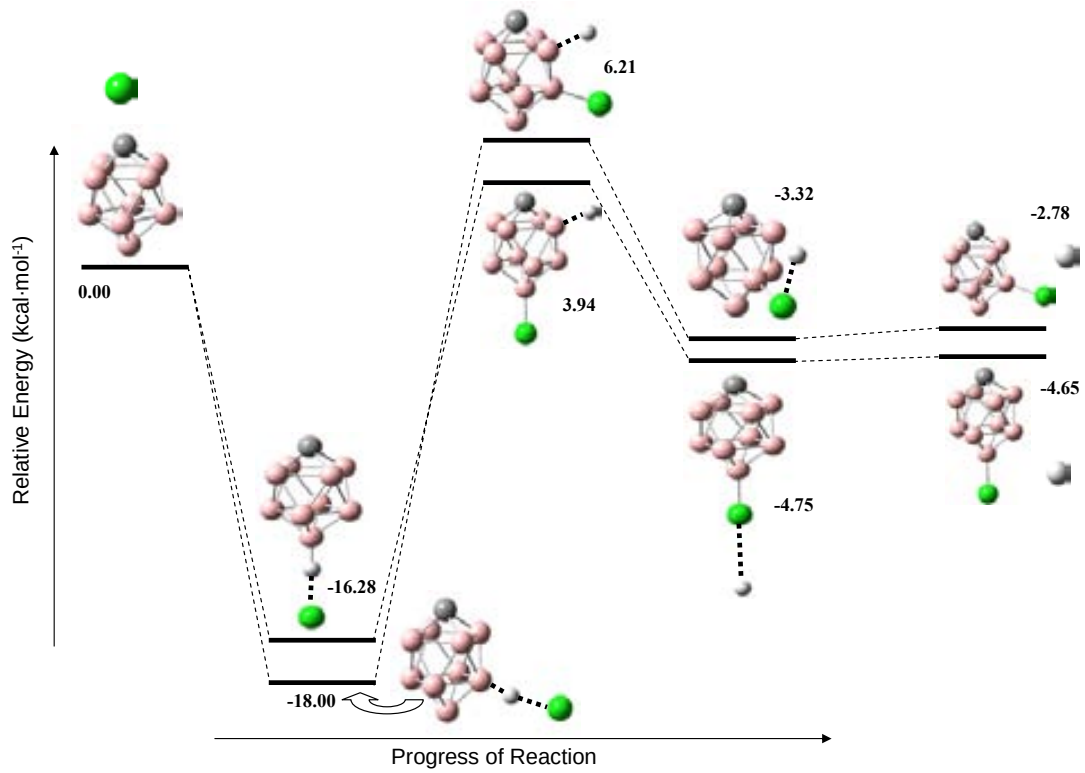

Figura 2.4.5. Mecanisme radicalari de cloració de $[1\text{-}CB_9H_{10}]^-$ utilitzant B3LYP/3-21G*. Només es mostren els àtoms d'hidrogen H(6) i H(10) per major claredat.

També s'ha calculat el mecanisme pel clúster parcialment clorat, $[6,10\text{-}Cl_2\text{-}1\text{-}CB_9H_8]^-$, amb la intenció de comprovar si era consistent amb l'atac radicalari. L'energia d'activació de l'estat de transició és de 8.4 kcal/mol, per tant es pot dir que las subseqüents cloracions continuen sent radicalàries.

Finalment, i per acabar de demostrar que la cloració del compost **86** té un mecanisme radicalari, s'ha fet un experiment comparant les mescles de reacció entre **86** i NCS amb i sense utilitzar tant un iniciador com un atrapador de radicals. D'aquesta manera, si la diferència en el grau de cloració de les mescles és gran, podrem assegurar que la reacció es dóna mitjançant radicals. S'ha utilitzat com a iniciador de radicals el compost VAZO®-88 i com a atrapador el TEMPO, ambdós comercialment disponibles sense problemes. Els resultats, que es poden observar a la taula 2.4.2, demostren com la diferencia entre utilitzar

l'iniciador o l'atrapador és de 4 àtoms de clor pel compost majoritari, amb les mateixes condicions de reacció. Així doncs, en aquest treball s'ha demostrat tant teòricament com experimental que el mecanisme de reacció de la cloració del compost **86** és de caràcter radicalari. A més a més, aquests resultats semblen indicar que aquest mecanisme es pot extendre a tots els clúster de bor monoaniònics ja que pel compost **1**, s'ha observat exactament la mateixa tendència.

$\mathbf{r_y}$	y
7	6, 7
7[a]	1, 2, 3, 4
7[b]	2, 3, 4, 5, 6, 7, 8, 9
14	6, 7, 8, 9, 10
14[a]	2, 3, 4, 5, 6
14[b]	3, 4, 5, 6, 7, 8, 9, 10

[a] 5 equiv de TEMPO; [b] 20 mg de VAZO®-88

Taula 2.4.2. r_y representa la fracció molar inicial. A la columna indicada com a y, les espècies observades per MALDI-TOF-MS estan indicades segons el número d'àtoms de clor insertats. L'espècie subratllada és la majoritària en cada barreja.

2.4.2 Estudi de pK_a de *nido*-carborans

Els derivats *nido* dels carborans són compostos clau en la coordinació dels clústers amb metalls per a formar complexos. Per fer aquesta complexació, cal fer una desprotonació del compost a fi de deixar un lloc vacant per coordinar-se al metall. Aquesta desprotonació depèn de cada compost, i es pot mesurar mitjançant el pK_a. A l'hora de mesurar aquest valor hi ha diferents mètodes experimentals, com les valoracions o les mesures espectroscòpiques de UV. Ara bé, la dificultat de mesurar aquests compostos *nido*, fa que hi hagi molt poca informació experimental dels valors de pK_a d'aquests carborans[44] i, per tant, s'ha optat per calcular aquests valors de forma teòrica. En la recerca bibliogràfica, hem trobat només un estudi d'acidesa de clústers de bor, però tracta només les molècules *closo* i tots els càlculs són en fase gas.[45] Tanmateix, per tenir un millor coneixement d'aquestes molècules, s'ha fet un estudi teòric de la seva estructura i del seu comportament en solució.

a) Optimització de les geometries

La primera part del treball és fer l'optimització de geometria dels diferents compostos *nido*. Per fer aquest càlcul s'ha utilitzat el mètode del funcional de la densitat B3LYP.[46,47] La base utilitzada ha estat la 6-31G(d). La raó d'utilitzar aquest funcional és que els mètodes híbrids, i més concretament el B3LYP (que és el més usat), donen, en general, molt bons resultats amb menor temps de càlcul i menys recursos de memòria que altres mètodes. La base ha estat triada després de fer unes proves preliminars, on s'ha comprovat que aquesta era la que ajustava millor les estructures a les dades que teníem de raigs X. S'ha fet el càlcul de freqüències i s'ha comprovat que totes elles eren positives, confirmant així que les estructures eren mínims energètics.

De tots els compostos estudiats, s'ha pogut comparar les estructures de set d'ells amb dades de raigs X. L'error en les distàncies dels enllaços de la cara oberta és com a màxim de 0.002Å, amb un factor de correlació de com a mínim 0.998. D'aquesta manera, queda clar que les optimitzacions fetes coincideixen amb les dades experimentals.

L'estudi de les geometries d'alguns dels compostos ja s'ha fet amb anterioritat, en línies generals es pot dir que tant les distàncies C-C com C-B disminueixen al passar de *closo* a *nido*. En canvi, l'enllaç B-B s'allarga com a conseqüència del corrent electrònic generat a la cara oberta.

b) Ressonància magnètica nuclear teòrica

La finalitat d'aquest treball és trobar l'acidesa d'aquests compostos en solució. Per aquesta raó, es vol saber si les estructures optimitzades en fase gas es poden considerar com a bones en solució. La millor manera de fer-ho és comparar els desplaçaments químics teòrics i els desplaçaments químics experimentals. D'aquesta manera, si coincideixen, podem assegurar que les estructures optimitzades en fase gas no varien en solució i, per tant, els càlculs posteriors es poden considerar com a bons. Atès que són compostos de bor i estan tots ben caracteritzats per l'espectroscòpia de ^{11}B-RMN, s'han escollit aquests valors per fer la comparació. El càlcul s'ha fet utilitzant el mètode GIAO/B3LYP[48] i els resultats obtinguts estan d'acord amb valors trobats a la bibliografia per alguns dels compostos que es presenten en el treball, però utilitzant altres nivells de càlcul.

Els resultats obtinguts es mostren a la taula 2.4.3 en forma de coeficients de correlació (R) entre els valors teòrics i experimentals de ^{11}B-RMN. S'observa com en els casos on la

posició de l'H_{pontal} pot donar simetria C_s (un pla de simetria, veure figura 2.4.6), en compostos com **90**, **93**, **94** i **97**, el coeficient de correlació és molt petit. Dèiem anteriorment que la posició d'aquests hidrògens afecta a l'estructura i, com queda demostrat ara, també afecta als $\delta(^{11}B)$. Així, aplicant l'operació de simetria als resultats obtinguts, es veu com, ara sí, els coeficients R milloren molt. L'explicació és que en solució, aquests àtoms d'hidrogen estan en constant moviment entre les dues posicions on hi ha un mínim energètic; per tant, la seva posició mitjana serà sobre l'àtom de bor central, i dóna la simetria C_s esmentada anteriorment.

	Coef. de correlació	
COMPOST	**Relació directe**	**Aplicant la simetria**
89	0,997	-
90	0,829	0,996
91	0,998	-
92	0,996	-
93	0,634	0,975
94	0,653	1,000
95	0,997	-
96	0,945	-
97	0,703	0,949
98	0,984	-

Taula 2.4.3. Coeficients de correlació entre ^{11}B-RMN teòric i experimental

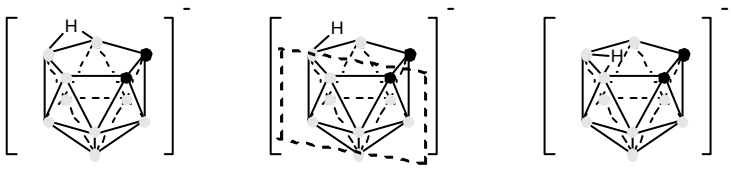

Figura 2.4.6. Compost **90** amb simetria C_s segons la posició de l'H_{pontal}

Aquests resultats confirmen la idea que les estructures que s'han optimitzat són iguals o molt properes a les existents en solució i, per tant, es pot continuar amb el càlcul de l'acidesa.

c) Càlcul de l'acidesa en fase gas

Abans de calcular l'acidesa en solució, cal veure si els resultats que s'obtenen en fase gas segueixen el mateix ordre que els valors experimentals de què es disposa, o si hi ha alguna diferència. Per tenir aquests valors, s'han calculat les entalpies de desprotonació dels compostos estudiats i efectivament, s'observa que l'ordre en fase gas és el mateix que l'ordre que tenim pels valors experimentals. I a més, si es comparen aquests valors obtinguts

teòricament amb valors experimentals trobats per àcids coneguts, ja es pot tenir una primera idea de l'acidesa de cada producte. Tot i així, l'efecte del dissolvent és diferent en cada cas i, per tant, no es pot agafar l'ordre obtingut en fase gas com el definitiu en solució.

Les entalpies s'han tret del resultat del càlcul de freqüències de cada compost. Amb el programa Gaussian, en calcular les freqüències d'una molècula també calcula les propietats termodinàmiques d'aquesta, com l'entalpia o l'energia lliure de Gibbs. S'ha calculat l'entalpia de desprotonació segons l`equació:

$$\Delta H_{(rx)} = H_{(A-)} + H_{(H+)} - H_{(AH)}$$

On: $\Delta H_{(rx)}$: Entalpia de la reacció
$H_{(A-)}$: Entalpia de la base conjugada
$H_{(H+)}$: Entalpia del protó
$H_{(AH)}$: Entalpia de l'àcid

Els resultats es poden veure a la figura 2.4.7 i es veu clarament com hi ha tres ordres diferents de magnitud. En el primer graó es troben els compostos amb una energia similar als àcids trifluoroacètic i benzoic, entre 330 i 350 kcal/mol. En el segon grup, amb una energia entre 380 i 450 kcal/mol hi trobem el metanol. Finalment i amb una energia de 556 kcal/mol, el compost **96** és el menys àcid de tots. Aquests tres ordres de magnitud es correlacionen perfectament amb la càrrega de les espècies calculades, ja que al primer grup hi ha els compostos neutres o zwiteriònics, en el segon els monoanònics i en el tercer el compost dianiònic. Per tant, només amb la càrrega ja es pot tenir una idea aproximada de l'acidesa que té el clúster de bor.

a)

Entalpies de desprotonació

COMPOST	ΔH (kcal/mol)	ΔH (kJ/mol)
89	309,81	1296,2
90	448,83	1877,9
91	448,26	1875,5
92	444,40	1859,4
93	436,39	1825,8
94	438,80	1835,9
95	440,75	1844,1
96	556,40	2328,0
97	339,23	1419,3
98	350,44	1466,2
Metanol*	381,45	1596
Àcid trifluoroacètic*	322,90	1351
Àcid benzoic*	340,11	1423

b)

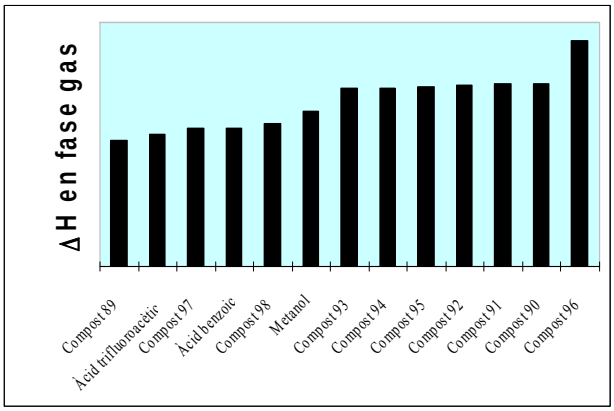

Figura 2.4.7. a) Entalpies de desprotonació teòriques dels compostos **89-98** i teòriques i experimentals(*) del metanol, àcid trifluoroacètic i àcid benzoic,[49] b) per ordre d'acidesa.

d) Càlcul de l'acidesa en dissolució

El càlcul en dissolució és el que ens permet arribar al valor de pK_a assimilable al pK_a experimental. A partir dels càlculs en fase gas, es pot obtenir l'energia de la molècula en solució calculant la seva energia de solvatació. La definició de pK_a és:

$$pK_a = -\log K_a$$

I com que:

$$\Delta G = -2.303RT \log K_a$$

$$pK_a = \Delta G / 2.303RT$$

Per tant, s'ha de calcular el valor de ΔG (energia lliure de Gibbs) de la reacció. A més, s'ha de calcular acuradament ja que un error de 1.36 kcal/mol en l'increment de G, provoca un error d'1 unitat en el pK_a.[50] A part de l'error degut al mètode de càlcul de les energies en fase gas i de solvatació, també hi ha l'error provocat pel cicle termodinàmic que s'usa per calcular el pK_a. A fi de fer una comparació dels resultats que s'obtenen segons el cicle, s'han utilitzat els cicles de les figures 2.4.8 i 2.4.9, on es poden calcular els pK_a que anomenarem absoluts o els pK_a relatius a una altra molècula amb un valor de pK_a conegut. El problema del pK_a absolut és com es descriu el H^+ en un entorn de dissolvent. Així, no es descriu com un H_3O^+ o un $H_9O_4^+$, que probablement és més realista, sinó un H^+ en un entorn físic de dissolvent; el resultat és un valor de $\Delta G_s(H^+)$ que difereix en 20 kcal/mol. Per això, aquest mètode no s'ha considerat correcte per a fer els càlculs, ja que depèn massa del valor escollit de $\Delta G_s(H^+)$.

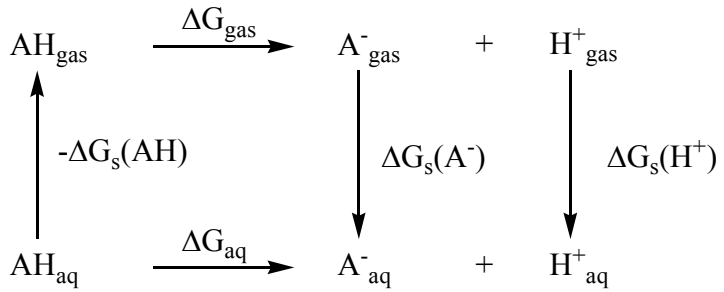

Figura 2.4.8. Cicle termodinàmic pel càlcul de pK_a absolut

El segon mètode no pateix el problema de la solvatació del protó, ja que aquest queda captat per una base i el que es calcula és la nova molècula protonada.

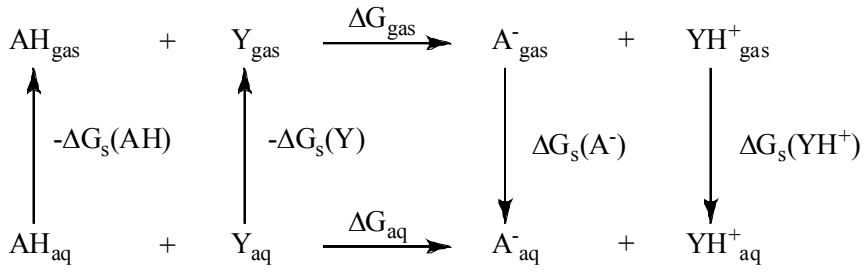

$$\Delta G_{aq}=\Delta G_{gas}-\Delta G_s(AH)-\Delta G_s(Y)+\Delta G_s(A^-)+\Delta G_s(YH^+)$$

Y= MeO^-, OH^-, H_2O, NH_3, **89**, **90**

Figura 2.4.9. Cicle termodinàmic pel càlcul de pK_a relatiu

Per aquest segon cas, el valor de pK_a vindrà donat per la fórmula següent:

$$pK_a= pK_a(YH^+)_{aq} + \Delta G_{aq} / 2.303RT$$

Com ja hem indicat, un altre punt important després de les energies de Gibbs és el càlcul de les energies de solvatació. Per fer aquests càlculs hi ha diferents mètodes i s'han comparat els resultats teòrics amb els dos valors experimentals disponibles per tal de trobar el millor mètode. S'han comparat els mètodes IPCM (Static Isodensity Surface Polarized Continuum Model)[51] i CPCM (Conductor Polarized Continuum Model).[52] A més, dins el model CPCM, el radi d'aquestes esferes també es pot modificar. En aquest treball s'ha fet una comparació entre els radis UAO (United Atom Topological Model) i els radis de Bondi (d'estructures de difracció de Raigs X). Tots els càlculs s'han fet tant en aigua com en dimetilsulfòxid (DMSO), ja que en aigua podem comparar els resultats obtinguts amb els valors experimentals de la bibliografia,[53] i en DMSO informa de l'acidesa d'aquests compostos en dissolvents orgànics, molt més útil per raons sintètiques. Una altra raó és que el càlcul de la solvatació en aigua és molt més complicat, i els resultats que dóna són bastant dolents.[54]

Per tal de millorar els resultats, s'ha volgut fer una regressió linial entre els valors de pK_a experimentals i les ΔG de la reacció de transferència del protó a l'anió MeO^- de diversos àcids coneguts, amb un rang de ΔG prou ampli per no haver d'extrapolar amb els compostos estudiats. La regressió s'ha calculat tant en aigua com en DMSO per poder obtenir els resultats de pK_a en els dos dissolvents. La gràfica corresponent a la regressió en aigua es mostra a la figura 2.4.10. D'aquesta manera, utilitzant la ΔG obtinguda en cada reacció, també es pot tenir el pK_a del compost, compensant els errors comesos pel mètode de càlcul.

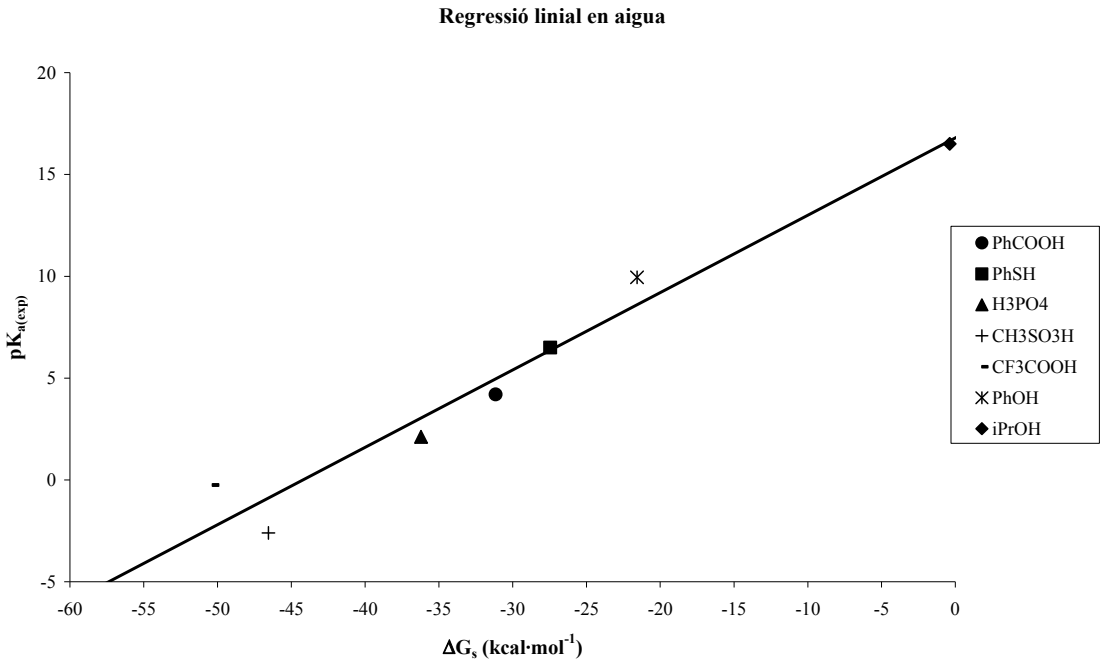

Figura 2.4.10. Recta de regressió linial entre $pK_{a(exp)}$ i ΔG_{aq}

Per tant, el mètode a seguir per tal de calcular el pK_a de *nido*-carborans és una combinació de dades experimentals i teòriques. Es pot resumir amb els punts següents:

1) Fer el càlcul d'optimització de geometria i freqüències dels compostos protonat i desprotonat, juntament amb l'anió MeO^- i el MeOH, amb la base de càlcul 6-31G*. Amb aquest càlcul s'aconsegueix tant l'entalpia com l'energia lliure de Gibbs en fase gas.

2) Calcular l'energia de solvatació en aigua o DMSO dels quatre compostos utilitzant el mètode B3LYP/6-311+G**. Amb aquesta energia calcular la ΔG en solució de la reacció.

3) Utilitzant la recta de regressió dels àcids coneguts, que es mostra a la figura 2.4.10 (7 àcids), calculada amb B3LYP/6-311**//B3LYP/6-31*, es troba el pK_a teòric del clúster de bor escollit (pK_a=0.3551ΔG + 15.844; R=0.98 per aigua; pK_a=0.5876ΔG + 29.082; R=0.99 per DMSO).

Amb aquesta metodologia, els pK_a dels compostos estudiats, tant en aigua com en DMSO, es mostren a la taula 2.4.4:

	pK_a calculat	
COMPOST	**AIGUA**	**DMSO**
89	-4,65	-4,9
90	13,49	25,5
91	12,77	24,3
92	13,80	26,0
93	11,49	22,2
94	10,89	21,2
95	9,58	21,1
96	23,68	45,8
97	5,16	11,3
98	6,67	15,4

Taula 2.4.4. pK_a calculats dels compostos estudiats

Finalment, es pot concloure que els mètodes on s'utilitza una sola referència experimental no han donat resultats satisfactoris. Tot i així, quan s'ha utilitzat un conjunt d'àcids coneguts com a referència, els valors de pK_a dels *nido*-carborans teòrics són comparables amb els valors experimentals trobats a la literatura i són consistents amb les estructures, el número de protons àcids i la càrrega de les espècies estudiades. Com a regla general també es pot dir que el zwiterions monopròtics tenen un pK_a semblant als àcids orgànics alquílics, els compostos neutres dipròtics a l'àcid trifluoroacètic, els monoanions monopròtics al pirrole, els monoanions dipròtics als fenols i per acabar, els dianions monopròtics a l'anilina o l'alcohol *tert*-butílic.

2.4.3 Interacció P···I en fosfino-carborans.

Tot i que compostos de l'estequiometria R_3PX_2 (R=substituent orgànic, X=halogen) fa més de 100 anys que es coneixen, la seva estructura està molt poc explorada. El descobriment l'any 1987 de l'estructura del $^tBuPI_2$[55] va fer augmentar considerablement l'interès en aquest camp ja que es va comprovar l'existència d'importants interaccions I-I i l'estructura tetracoordinada de la fosfina. Du Mont et al. van comparar les distàncies I-I de diverses iodo-fosfines i van arribar a la conclusió que es podia interpretar tant com a una sal de iodofosfoni com un complex de transferència de càrrega de iode. Més endavant i després de noves dades, va ser la segona interpretació la que va quedar com la més acceptada. Tot i així, la interpretació d'aquesta interacció és un punt de controvèrsia i s'ha arribat a considerar que, si la distància de van der Waals del I-I és 4.3 Å, qualsevol distància menor a aquesta ha de ser una interacció I-I.

Amb els anys, molts exemples de complexes de transferència de càrrega s'han sintetizat tant amb fosfines com amb tioèters. En el nostre grup es va sintetitzar per primera vegada un adducte de iode amb carboranilfosfina.[56] El complex (Mecarb)*i*Pr$_2$P (Mecarb = 1-(2-Me-1,2-$C_2B_{10}H_{10}$)) amb iode va donar la distància més petita I-I trobada per un adducte amb fosfines. Llavors, si amb el lligand s'havia aconseguit aquesta distància, i tenint en compte que com més feble és el coordinant la distància s'escurça, es va voler provar diferents substituents al fosfà, canviant els fragments isopropil per grups electroatraients com els fenils. D'aquesta manera s'ha sintetitzat el compost (Mecarb)Ph$_2$P (**99**). Amb l'evaporació lenta d'una solució 1:1 de **99**:I_2 en CH_2Cl_2 s'han obtingut cristalls amb els quals s'ha pogut estudiar l'estructura obtinguda.

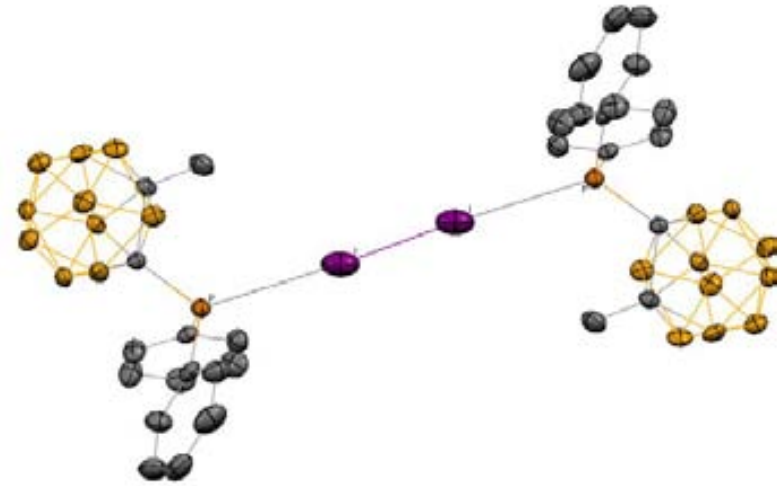

Figura 2.4.11. Estructura molecular de **99**·I_2. Els el·lipsoides tèrmics estan al 30%.

Com es pot observar a la figura 2.4.11 hi ha una disposició pràcticament linial dels P···I-I···P amb les distàncies per P···I i I-I de 3.3337 i 2.7753 Å, respectivament. La distància I-I és la més curta d'entre tots els adductes fosfina-I_2, i és poc més llarga que la que es troba en el I_2 sòlid a 110K (2.715 Å).[57] Fins i tot i tenint en compte que els tioèters són lligands molt menys coordinants que els fosfans, la distància es troba en l'ordre dels adductes $R_2S{\cdot}I_2{\cdot}SR_2$ (2.75-2.79 Å).

Per altra banda, cal observar si aquesta estructura es manté en solució o només s'observa en estat sòlid. Per aquest motiu, s'ha fet una valoració amb I_2 i s'ha seguit per $^{31}P\{^1H\}$-RMN. Es pot observar com hi ha un desplaçament continu cap a camp alt del fòsfor, des de δ = 11.5 (**99**:I_2 = 1:0), a -10.2 (1:1) i -12.4 ppm (1:2). A partir d'aquest punt l'addició de més iode no altera la posició del fòsfor. Aquest comportament és molt diferent de l'observat en altres fosfans, com és el cas del (Mecarb)*i*Pr$_2$P, on el fòsfor va a camp més alt

fins a una estequiometria de 1:1, i a partir d'aquest punt torna cap a camp més baix fins a recuperar pràcticament el desplaçament inicial. Aquest comportament s'explica per la formació de l'espècie $[R_3PI][I_3]$.[58] El fet que tingui lloc aquest canvi de tendència en la valoració de **99**, només pot explicar-se per la no formació de $[I_3]^-$. Per confirmar la hipòtesi s'han fet estudis de RMN a baixa temperatura, valoracions conductimètriques i espectroscopia de UV/Vis, i en tots els casos s'ha observat l'absència d'ions $[I_3]^-$.

La combinació de les dades experimentals amb la teoria del funcional de densitat (DFT) ens ha permès obtenir espectres teòrics de $^{31}P\{^1H\}$-RMN per $Ph_3P{\cdot}I_2$. Pel que fa a l'optimització de geometria, el fet de tenir iode a la molècula dificulta enormement els càlculs teòrics al ser un àtom amb tants electrons. Per tant, s'ha optat per utilitzar la geometria de raigs X com a punt de partida, i utilitzant el mètode GIAO (Gauge-including atomic orbitals) s'ha obtingut un desplaçament del fòsfor molt semblant a l'experimental, -26.3 per -23.4 ppm respectivament. També s'ha pogut observar que la posició relativa dels dos àtoms de iode P···I(1)···I(2) influeix molt en el desplaçament del fòsfor en l'espectre de $^{31}P\{^1H\}$-RMN. Quan es manté fixa la distància P···I(2) i es disminueix la distància P···I(1), l'apampolament en el fòsfor augmenta (figura 2.4.12a). En canvi, quan es manté P···I(1) i s'incrementa la distància P···I(2), disminueix l'apampolament (figura 2.4.12b). Per tant, la presència d'àtoms de iode en la proximitat del fòsfor provoca un desplaçament a camp alt. A més, els resultats concorden perfectament amb la tendència observada en la valoració de I_2 amb PPh_3. També s'ha calculat el $^{31}P\{^1H\}$-RMN de l'espècie $[Ph_3PI]^+$ a partir de l'estructura cristal·lina $[Ph_3PI][I_3]$, obtenint un valor de δ = -282 ppm, molt lluny del valor experimental δ = 44 ppm. Els resultats milloren clarissimament quan s'incorpora al càlcul l'espècie $[I_3]^-$ obtenint-ne un valor teòric de δ = 36 ppm. Amb aquests resultats es pot concloure que el desplaçament del fòsfor és molt dependent d'interaccions febles. A més, també demostra que l'única explicació del comportament de **99**·I_2, on després d'una relació 2:1 de I_2:**99** el desplaçament del fòsfor queda constant, és la formació de l'adducte **99**·I_2·**99**, aïllant els fòsfors de més interaccions amb altres molècules de iode.

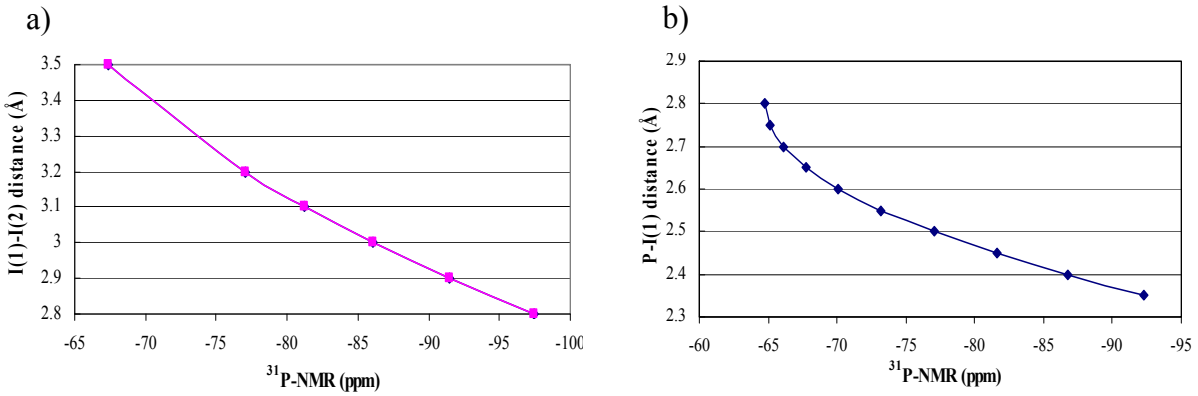

Figura 2.4.12. a) Influència de la distància P···I(1) en el ^{31}P-NMR mantenint P··I(2) constant. a) Influència de la distància P···I(2) en el ^{31}P-NMR mantenint P··I(1) constant

Finalment, també s'ha calculat les càrregues NPA del lligands PPh_3 i **99**. Com es pot observar a la figura 2.4.13, les càrregues en els fòsfors són molt similars. En canvi, el punt on hi ha més diferència és a les càrregues dels àtoms d'hidrogen dels grups fenil. Aquestes varien de 0.237-0.245 a 0.131-0.202 pel compost **99**. A més, també es pot observar que les interaccions entre ambdós són molt diferents. En el cas de **99**·I_2 es poden trobar interaccions intramoleculars entre I··H(Ph) mentre que per PPh_3·I_2 només veiem intermoleculars entre I(2)··H(Ph), sent l'hidrogen *para* el participant en aquest contacte. El diferent comportament dels hidrògens del fenil és crucial a l'hora d'entendre la formació de l'adducte, ja que l'àtom d'hidrogen en *orto* del grup fenil és el que té menys càrrega de tots i precisament és el que interacciona intramolecularment amb l'àtom de iode. Aquestes interaccions febles afavoreixen clarament l'adducte P···I-I···P.

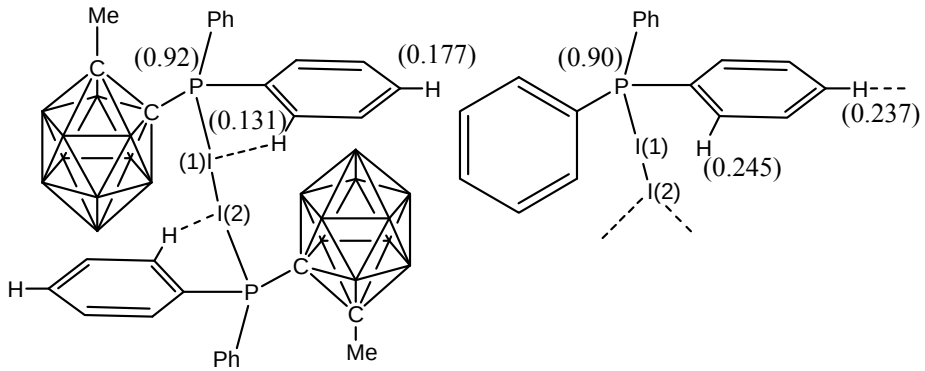

Figura 2.4.13. Representació esquemàtica de **99**·I_2·**99** i Ph_3P·I_2.

Per concloure, es pot veure que la incorporació del grup carboranil en adductes fosfano-I_2 dóna lloc a espècies molt interessants, sobretot pel que fa a les seves propietats estructurals. Si en l'anterior treball publicat al grup es va trobar la distància I-I més petita fins

aleshores per un complex $R_3P \cdot I_2$, en aquest s'ha disminuït encara més fins al punt de tenir pràcticament la mateixa distància que el I_2 en estat sòlid. L'estructura única d'aquest compost ha permès aïllar per primera vegada un complex de fosfà del tipus P···I-I···P i s'ha demostrat com també existeix en dissolució. Finalment, cal destacar la importància de les interaccions febles entre el fòsfor i espècies que continguin iode en el càlcul tant experimental com teòric dels espectres de ^{31}P-RMN.

2.5 BIBLIOGRAFIA

[1] R. M. Chamberlin, B. L. Scott, M. M. Melo, K. D. Abney, *Inorg. Chem.*, **1997**, *36*, 809.

[2] a) E. J. Juárez-Pérez, C.Viñas, A. González-Campo, F. Teixidor, R. Sillanpää, R. Kivekäs, R. Núñez, *Chem. Eur. J.*, **2008**, *14*, 4924; b) I. Rojo, F. Teixidor, C. Viñas, R. Kivekäs, R. Sillanpää, *Chem. Eur.J.*, **2004**, *10*, 5376; c) S. A. Fino, K. A. Benwitz, K. M. Sullivan, D. K. LaMar, K. M. Stroup, S. M. Giles, G. J. Balaich, *Inorg. Chem.*, **1997**, *36*, 4604.

[3] I. Manners, "Ring-Opening Polymerization of Metallocenophanes: A New Route to Transition Metal-Based Polymers", *Advances in Organometallic Chemistry*, Vol. 37, Academic Press, New York, **1995**.

[4] Y. R. Luo, "Comprehensive Handbook of Chemical Bond Energies", CRC Press, **2007**. Calculat fent la mitja de les energies d'enllaç Co-Co (30.4 kcal/mol) i P-P (116.9 kcal/mol).

[5] a) O. Tutusaus, S. Delfosse, A. Demonceau, A. F. Noels, C. Viñas, F. Teixidor, *Tetrahedron Lett.*, **2003**, *44*, 8421; b) F. Teixidor, R. Núñez, M. A. Flores, A. Demonceau, C. Viñas, *J. Organomet. Chem.*, **2000**, *614*, 48; c) F. Teixidor, M. A. Flores, C. Viñas, R. Sillanpää, R. Kivekäs, *J. Am. Chem. Soc.*, **2000**, *122*, 1963.

[6] a) C. Viñas, M. A. Flores, R. Núñez, F. Teixidor, R. Kivekäs, R. Sillanpää, *Organometallics*, **1998**, *17*, 2278; b) F. Teixidor, M. A. Flores, C. Viñas, R. Kivekäs, R. Sillanpää, *Angew. Chem., Int. Ed. Engl.*, **1996**, *35*, 2251.

[7] D. E. Herbert, U. F. J. Mayer, I. Manners, *Angew. Chem. Int. Ed.*, **2007**, *46*, 5060.

[8] J. K. Pudelski, D. P. Gates, R. Rulkens, A. J. Lough, I. Manners, *Angew. Chem.*, **1995**, *107*, 1633; *Angew. Chem. Int. Ed. Engl.*, **1995**, *34*, 1506.

[9] H. D. Smith, C. O. Obenland, S. Papetti, *Inorg. Chem.*, **1966**, *5*,1013.

[10] J. Llop, C. Viñas, J. M. Oliva, F. Teixidor, M. A. Flores, R. Kivekäs, R. Sillanpää, *J. Organomet. Chem.*, **2002**, *657*, 232.

[11] S. Smoes, *Bull. Soc. Chim. Belg.*, **1972**, *81*, 45. També es pot calcular de manera aproximada fent la mitja de l'energia dels enllaços Co-Co (30.4 kcal/mol) i S-S (101.65 kcal/mol), donant com a resultat 66 kcal/mol.

[12] J. Plešek, S. Heřmánek, A. Franken, I. Cisařová, C. Nachtigal, *Collect. Czech. Chem. Commun.*, **1997**, 62, 47.

[13] A. N. Gashti, J. C. Huffman, A. Edwards, G. Szekeley, A. R. Siedle, J. A. Karty, J. P. Reilly, L. J. Todd, *J. Organomet. Chem.*, **2000**, 614, 120.

[14] a) A. Vaca, F. Teixidor, R. Kivekäs, R. Sillanpää, C. Viñas, *Dalton Trans.*, **2006**, 4884; b) C. Tsang, Z. Xie, *Chem. Commun.*, **2000**, 1839.

[15] S. Heřmánek, *Chem. Rev.*, **1992**, *92*, 325.

[16] a) I. P. Beletskaya, V. I. Bregadze, V. A. Ivushkin, P. V. Petrovskii, I. B. Sivaev, G. G. Zhigareva, *J. Organomet. Chem.*, **2004**, *689*, 2920; b) I. Rojo, F. Teixidor, C. Viñas, R. Kivekäs, R. Sillanpaä, *Chem. Eur. J.*, **2003**, 9, 4311; c) M. D. Mortimer, C. B. Knobler, M. F. Hawthorne, *Inorg. Chem.*, **1996**, *35*, 5750.

[17] a) K. C. Nicolau, P. G. Bulger, D. Sarlah, *Angew. Chem. Int. Ed.*, **2005**, 44, 4442; b) A. F. Littke, G. C. Fu, *Angew. Chem. Int. Ed.*, **2002**, 41, 4176; c) J. Li, C. F. Logan, M. Jr. Jones, *Inorg. Chem.*, **1991**, 30, 4866; d) L. I. Zakharin, A. I. Kovredov, V. A. Ol'shevskaya, Zh. S. Shaugumbekova, *J. Organomet. Chem.*, **1982**, 226, 217.

[18] H. Gilman, R. H. Kirby, *Recl. Trav. Chim. Pays-Bas.*,, **1935**, 54, 577.

[19] a) Z. Zheng, W. Jiang, A. A. Zinn, C. B. Knobler, M. F. Hawthorne, *Inorg. Chem.*, **1995**, 34, 38; b) W. Jiang, C. B. Knobler, C. E. Curtis, M. D. Mortimer, M. F. Hawthorne, *Inorg. Chem.*, **1995**, 34, 3491.

[20] D.E. Pearson, D. Cowan, J.D. Beckler, *J. Org. Chem.*, **1959**, 24, 504.

[21] L. Eriksson, K. J. Winberg, R. Tascon-Claro, S. Sjöberg, *J. Org. Chem.*, **2003**, *68*, 3569.

[22] P. Surawatanawong, Y. Fan, M. B. Hall, *J. Organomet. Chem.*, **2008**, *693*, 1552.

[23] F. Teixidor, J. Casabo, A. M. Romerosa, C. Vinas, J. Rius, C. Miravitlles, *J. Am. Chem. Soc.*, **1991**, *113*, 9895.

[24] J. Plešek, S. Heřmánek, K. Baše, L. J. Todd, W. F. Wright, *Collect. Czech. Chem. Commun.*, **1976**, *41*, 3509.

[25] A. A. Semioshkin, I. B. Sivaev, V. I. Bregadze, *Dalton Trans.*, **2008**, 977.

[26] a) J. F. Valliant, K. J. Guenther, A. S. King, P. Morel, P. Schaffer, O. O. Sogbein, K. A. Stephenson, *Coord. Chem. Rev.*, **2002**, *232*, 173; b) I. B. Sivaev, V. I. Bregadze, S. Sjöberg, "Research and Development in Neutron Capture Therapy", ed. W. Sauerwein, R. Moss and A. Wittig, Monduzzi Editore S.p.A., Bologna, **2002**, pp. 19–23; c) A. H. Soloway, W. Tjarks, B. A. Barnum, F. G. Rong, R. F. Barth, I. M. Codogni, J. G. Wilson, *Chem. Rev.*, **1998**, *98*, 1515; d) M. F. Hawthorne, *Angew. Chem. Int. Ed.*, **1993**, *32*, 950.

[27] F. Teixidor, J. Pedrajas, I. Rojo, C. Viñas, R. Kivekäs, R. Sillanpää, I. B. Sivaev, V. I. Bregadze, S. Sjöberg, *Organometallics*, **2003**, *22*, 3414.

[28] D. Massiot, F. Fayon, M. Capron, I. King, S. Le Calvé, B. Alonso, J-O. Durand, B. Bujoli, Z. Gan, G. Hoatson, "Modelling one- and two-dimensional Solid State NMR spectra.", *Magnetic Resonance in Chemistry*, **2002**, *40*, 70-76.

[29] a) G. Chevrot, R. Schurhammer, G. Wipff, *Phys. Chem. Chem. Phys.*, **2007**, *9*, 5928; b) G. Chevrot, R. Schurhammer, G. Wipff, *Phys. Chem. Chem. Phys.*, **2007**, *9*, 1991.

[30] a) T. Omabegho, R. Sha, N. C. Seeman, *Science*, **2009**, *324*, 67; b) C. F. Lee, D. A. Leigh, R. G. Pritchard, D. Schultz, S. J. Teat, G. A. Timco, R. E. P. Winpenny, *Nature*, **2009**, *458*, 314; c) Z. Okten, M. Schliwa, *Nature*, **2007**, *450*, 625; d) V. Serreli, C. F. Lee, E. R. Kay, D. A. Leigh, *Nature*, **2009**, *445*, 523.

[31] a) J. F. Morin, T. Sasaki, Y. Shirai, J. M. Guerrero, J. M. Tour, *J. Org. Chem.*, **2007**, *72*, 9481; b) Y. Shirai, A. J. Osgood, Y. Zhao, Y. Yao, L. Saudan, H. Yang, C. Yu-Hung, T. Sasaki, J. F. Morin, J. M. Guerrero, K. F. Kelly, J. M. Tour, *J. Am. Chem. Soc.*, **2006**, *128*, 4854; c) Y. Shirai, A. J. Osgood, Y. Zhao, K. F. Kelly, J. M. Tour, *Nano Lett.*, **2005**, *5*, 2330.

[32] a) M. F. Hawthorne, B. M. Ramachandran, R. D. Kennedy, *Pure Appl. Chem.*, **2006**, *78*, 1299; b) M. F. Hawthorne, J. I. Zink, J. M. Skelton, M. J. Bayer, C. Liu, E. Livshits, R. Baer, D. Neuhauser, *Science*, **2004**, *303*, 1849.

[33] C. Wynants, G. Van Binst, C. Miigge, K. Jurkschat, A. Tzschach, H. Pepermans, M. Gielen, R. Willem, *Organometallics*, **1985**, *4*, 1906.

[34] A. G. Johnston, D. A. Leigh, L. Nezhat, J. P. Smart, M. D. Deegan, *Angew. Chem. Int. Ed. Eng.*, **1995**, *34*, 1212.

[35] F. G. Gatti, S. Leon, J. K. Y. Wong, G. Bottari, A. Altieri, M. A. Farran-Morales, S. J. Teat, C. Frochot, D. A. Leigh, A. M. Brouwer, F. Zerbetto, *Proc. Natl. Acad. Sci.*, **2003**, *100*, 10.

[36] C. L. Perrin, T. J. Dwyer, *Chem. Rev.*, **1990**, *90*, 935.

[37] J. G. Planas, C. Viñas, F. Teixidor, A. Comas-Vives, G. Ujaque, A. Lledós, M. E. Light, M. B. Hursthouse, *J. Am. Chem. Soc.*, **2005**, *127*, 15976.

[38] W. Yang, X. Gao, B. Wang, *Med. Res. Rev.*, **2003**, *23*, 346.

[39] A. W. Bauer, W. M. Kirby, J. C. Cherris, M. Truck, *Am. J. Clin. Pathol.*, **1966**, *45*, 493.

[40] a) A. A. Gorustovich, T. Steimetz, F. H. Nielsen, M. B. Guglielmotti, *Arch. Oral. Biol.*, **2008**, *53*, 677; b) Q. Luan, T. Desta, L. Chehab, V. J. Sanders, J. Plattner, D. T. Graves, *J. Dent. Res.*, **2008**, *87*, 148; c) S. J. Baker,

T. Akama, Y. K. Zhang, V. Sauro, C. Pandit, R. Singh, M. Kully, J. Khan, J. J. Plattner, S. J. Benkovic, V. Lee, K. R. Maples, *Bioorg. Med. Chem. Lett.*, **2006**, *16*, 5963; d) A. A. Alencar de Queroz, G. A. Abraham, M. A. Pires Camillo, O. Z. Higa, G. S. Silva, M. del Mar Fernandez, J. San Roman, *J. Biomater. Sci. Polym. Ed.*, **2006**, *17*, 689.

[41] R. Alexandrova, T. Varadinova, M. Velcheva, P. Genova, I. Sainova, *Exp. Pathol. Parasitol.*, **2000**, *4*, 8.

[42] A. Franken, C. A. Kilner, M. Thornton-Pett, J. D. Kennedy, *Collect. Czech. Chem. Commun.*, **2002**, *67*, 869.

[43] a) J. Holub, M. Bakardjiev, B. Štíbr, *Collect. Czech. Chem. Commun.*, **2002**, *67*, 783; b) K. E. Stockman, D. L. Garrett, R. N. Grimes, *Organometallics*, **1995**, *14*, 4661; c) G. E. Ryschkewitsch, V. R. Miller, *J. Am. Chem. Soc.*, **1973**, *95*, 2836.

[44] G.G. Hlatky, D.J. Crowther, *Inorg. Synth.*, **1998**, 32, 229.

[45] K. Hermansson, M. Wójcik, S. Sjöberg, *Inorg. Chem.*, **1999**, 38, 6039.

[46] a) A. D. Becke, *J. Chem. Phys.*, **1993**, *98*, 5648; b) C. Lee, W. Yang, R. G. Parr, *Phys. Rev. B*, **1988**, *37*, 785.

[47] a) R. Ditchfield, *Mol. Phys.*, **1974**, *27*, 789; b) F. London, *J. Phys. Radium*, **1937**, *8*, 397.

[48] P. Deplano, S. M. Godfrey, F. Isaia, C. A. McAuliffe, M. L. Mercuri, E. F. Trogu, *Chem. Ber. / Recueil*, **1977**, 130, 299.

[49] E.P. Hunter and S.G. Lias, "Proton Affinity Evaluation" en *NIST Chemistry WebBook*, NIST Standard Reference Database Number 69, Eds. P.J. Linstrom and W.G. Mallard, **2005**, National Institute of Standards and Technology, Gaithersburg MD, 20899 (http://webbook.nist.gov).

[50] M. D. Liptak, G. C. Shields, *J. Am. Chem. Soc.*, **2001**, 123, 7314.

[51] J. B. Foresman, T. A. Keith, K. B. Wiberg, J. Snoonian, M. J. Frisch, *J. Phys. Chem.*, **1996**, 100, 16098.

[52] V. Barone, M. Cossi, *J. Phys. Chem. A*, **1998**, 102, 1995.

[53] R. A. Wiesboeck, M. F. Hawthorne, *J. Am. Chem. Soc.*, **1964**, 86, 1642.

[54] D. M. Chipman, *J. Phys. Chem. A*, **2002**, 106, 7413.

[55] W. W. Du Mont, M. Batcher, S. Pohl, W. Saak, *Angew. Chem., Int. Ed. Engl.*, **1987**, *26*, 912

[56] F. Teixidor, R. Núñez, C. Viñas, R. Sillanpää, R. Kivekäs, *Angew. Chem.*, **2000**, *112*, 4460; *Angew. Chem. Int. Ed.*, **2000**, *39*, 4290.

[57] F. Bolhuis, P. B. van Koster, T. Migchelsen, *Acta Crystallogr.*, **1967**, *23*, 90.

[58] W. I. Cross, S. M. Godfrey, C. A. McAuliffe, R. G. Pritchard, J. M. Sheffield, G. M. Thompson, *J. Chem. Soc. Dalton Trans.*, **1999**, 2795, and references therein.

3.- CONCLUSIONS

3. CONCLUSIONS

C-SUBSTITUTED COBALTABISDICARBOLLIDE

1.- C-substituted phosphorus containing compounds were synthesized and characterized following the synthetic procedure developed in our group. Direct reaction of the dilithium salts of starting anions **1** and **10** with appropriate phosphine dihalides under controlled conditions lead to the first examples of C,C phosphorus-bridged cobaltabisdicarbollide derivatives.

2.- Synthesized anions **2**, **6**, **11** and **15** presented an unexpected downfield ^{31}P-NMR chemical shift if compared to similar non-bridged species. The expected electron density on phosphorus due to its lone pair has migrated to another part of the molecule. Density Functional Theory (DFT) and Natural Bond Order (NBO) analysis calculations indicated a donor-acceptor interaction between phosphorus lone pair and cobalt's empty 4s orbital.

3.- Oxidation of these molecules with oxygen, sulphur and selenium has been accomplished, obtaining the desired compounds in very high yields. Phosphine oxide anions **3**, **7**, **12** and **16** presented expected ^{31}P-NMR chemical shifts around 35 ppm. Neither an experimental nor a theoretical evidence has been found indicating a charge transfer between phosphorus and cobalt in all oxidized species.

4.- C-substituted sulphur containing compounds were synthesized by using appropriate organic or *closo*-carborane disulfide molecules or sulphur by direct reaction of the dilithium salts of starting anion **1**. Compounds **19**-**24** were obtained in high yields. The synthesis with sulphur allowed to obtain the first example of a C,C sulphur-bridged cobaltabisdicarbollide derivative. In addition, thioether carborane moieties were bonded to the cobaltabisdicarbollide fragment in compounds **23** and **24**.

5.- DFT and NBO analysis on compound **22** showed an interaction between one of the two lone pairs of sulphur and the empty 4s orbital of cobalt. The second lone pair interacts with both C_c-C_c bonds on the dicarbollide cages. HOMO orbital displays a clear overlap between cobalt and sulphur orbital contributions.

B-SUBSTITUTED COBALTABISDICARBOLLIDE

6.- Halogenation of cobaltabisdicarbollide has been studied for chlorine, bromine and iodine. In most cases, a mixture of compounds with different degree of halogenation is obtained. MALDI-TOF-MS technique has been very useful to study these mixtures and has proven quantitative, especially for chlorine derivatives.

7.- The chlorination reaction has been thoroughly studied from both an experimental and a theoretical point of view. We have proven that the mechanism is not of a thermodynamic but from a kinetic origin. Moreover, we have seen that preferential reaction sites are found on cobaltabisdicarbollide and these can be rationalized by the two atom natural population analysis (2a-NPA) charges on boron and carbon vertices, defined as the sum of boron or carbon and hydrogen NPA charges.

8.- Electrochemical studies on mixtures of chlorinated derivatives of cobaltabisdicarbollide have shown an additive behaviour in respect to their redox potential. In other words, each generated B-Cl bond causes an anodic shift of the cobaltabisdicarbollide framework of 0.1V. This fine tunning of redox potential on a single platform is unique and our hypothesis is that it is possible because of the high energy of the B-Cl bond. Organic compounds with C-Cl bonds decompose when a high redox potential is applied.

9.- The generation of B-C bonds has been studied. We have been able to obtain compounds by using reaction conditions inspired either by Kumada or Heck reactions. Firstly, we have coupled Grignard reagents bearing functional groups to be used in further reactions such as vinyl or aldehyde groups, to the monoiodo derivative of cobaltabisdicarbollide **25**.

10.- Generation of B-C bonds using Heck reaction conditions has been done by reacting **25** with styrene. After optimizing the reaction conditions, we have synthesized a broad range of compounds, see **30**-**42**, with some unexpected results. Compounds **37**-**42** have been obtained as disubstituted instead of monosubstituted molecules starting from the monoiodo derivative **25**.

11.- Based on DFT calculations on the Pd-catalysed reaction, a plausible mechanism for the preparation of disubstituted compounds can be given. An unprecedented B-H activation

through the palladium catalyst causes the substitution of this position instead of the expected B-I bond, as it happens on the Heck reaction mechanism.

12.- Polyanionic water-soluble molecules have been obtained by the ring-opening reaction of the zwitterionic compound **43**. This compound has a positively charged oxygen atom connected to the B(8) vertex of cobaltabisdicabollide which is susceptible to nucleophilic substitution. Nucleophiles with carbon, oxygen, sulphur and halogen atoms have been used, some of them for the first time.

APPLICATIONS

13.- Mixtures of chlorinated derivatives of **1** have been used as synergic agents with calixarenes in the radionuclide extraction process. Compound **1** show the best extraction results within all experiments although its resistance against acidic media is the lowest. Mixtures with an intermediate degree of chlorination have the best extraction:acid resistance ratio. Our hypothesis is that the presence of some B-H groups is needed for good extraction coefficients.

14.- Cobaltabisdicarbollides have been used for the first time as components of rotaxanes. A study of the intermolecular and intramolecular effect of this cluster to the dynamics of rotaxanes has been done calculating the pirouetting rate of the macrocycle. Rotaxanes having cobaltabisdicarbollide or trifluoroacetic acid as counteranions have been synthesized.

15.- A unique example of a zwitterionic rotaxane has been obtained having two positive charges on the pyridinium groups of the macrocycle and two negative charges on the cobaltabisdicarbollide fragments of the thread.

16.- Metallacarboranes synthesized in our group have been applied in antimicrobial tests. The results show that these compounds have better activiy against microorganisms compared to broad spectrum antibiotics.

17.- Compounds obtained by derivatization of **1** have proven efective to antitumoral tests with cultured and non-cultured cells. Experiments show good viability results with some tested metallacarboranes.

CARBORANES

18.- Chlorination reaction studies have also been done on carborane **86**. The experimental results show preferential sites as seen for **1**. The sequencial order of attack has been rationalized by 2a-NPA charges. To explain the first site of attack, DFT calculations on the reaction pathway have been done. Activation energies suggest that the reaction takes place by the attack of a chlorine radical $Cl^{\cdot}$ and not a Cl^{+}. Experimental tests using either a radical initiator or an scavenger confirm the hypothesis that chlorination on anionic boron clusters is of a radical origin.

19.- A theoretical method to calculate pK_a values of *nido*-carboranes has been published. This has been done taking compounds **89**-**98** as models of study. Theoretical values have been compared when possible with experimental data in order to confirm the feasability of the method. pK_a data is obtained combining theoretical calculations and experimental values obtained for a set of known acids.

20.- Phosphorus-iodine interactions have been studied for phosphino-carboranes. Phosphine-iodine adducts have a two step behaviour, increasing quantities of iodine favour P···I interactions, but only until a 2:1 ratio between iodine and phosphine. After that, the generation of $[I_3]^-$ and other polyiodinated species decrease the interaction. However, phosphino-carborane **99** does not present this behaviour as even after a 2:1 ratio, no decreasing in the interaction is observed in the ^{31}P-NMR spectrum. This can be explained by the formation of a P···I-I···P moiety in solution, which is also observed in the solid state.

4.- ARTICLES PUBLICATS

(Comissió de Doctorat de Maig de 2009)

Phosphane–Diiodine Complexes

DOI: 10.1002/anie.200503007

A Discrete P···I–I···P Assembly: The Large Influence of Weak Interactions on the ^{31}P NMR Spectra of Phosphane–Diiodine Complexes**

Rosario Núñez, Pau Farràs, Francesc Teixidor, Clara Viñas, Reijo Sillanpää, and Raikko Kivekäs*

Thioethers, except derivatives of $[7\text{-R-}7,8\text{-}C_2B_9H_{11}]^-$,[1] are more weakly coordinating ligands than phosphanes.[2] This difference is evidenced by the I–I distances in the spoke-shaped charge-transfer (CT) complexes $R_2S{\cdot}I_2$ and $R_3P{\cdot}I_2$ (Figure 1).[3] The I–I distance is sensitive to the strength of the interaction between the σ* LUMO orbital on I_2 and the HOMO orbital of the donor atom:[4] the stronger the donor, the longer the I–I distance. In these spoke CT complexes, the I–I distance varies from 3.2 ± 0.2 Å in $R_3P{\cdot}I_2$ adducts[5] to 2.80 ± 0.05 Å in $R_2S{\cdot}I_2$ adducts,[6] indicating the weaker donor character of the thioether group. Whereas extended I_2 arrays, spoke adducts of I_2, polyiodides, and other structural configurations involving I_2 molecules are well described,[7] examples of discrete assemblies incorporating an I_2 molecule bridging to two donor atoms are limited. The P···I–I···P assembly is unknown, and only a few examples of the S···I–I···S motif have been reported.[8] As thioethers are weaker donors than phosphanes, we predicted that $R_3P{\cdot}I_2{\cdot}PR_3$ adducts could be generated by using a very weakly coordinating phosphane ligand. By using the carboranyl phosphane (Mecarb)*i*Pr_2P (Mecarb = 1-(2-Me-1,2-$C_2B_{10}H_{10}$)), the complex (Mecarb)*i*$Pr_2P{\cdot}I_2$ containing the shortest I–I distance observed in a spoke adduct was produced.[9] A weaker donor ligand than (Mecarb)*i*Pr_2P can be obtained by replacing the isopropyl fragments by electron-withdrawing phenyl groups, as in (Mecarb)Ph_2P (**1**).[10]

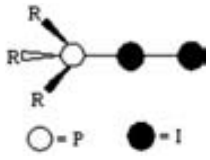

Figure 1. Spoke configuration of $R_3P{\cdot}I_2$ complexes.

Use of ligand **1** allowed the formation of the desired complex **1**·I_2·**1** (**2**), which was isolated as red-brown crystals from a solution of **1** and I_2 (1:1) in CH_2Cl_2 after 2 months at 4 °C. Single-crystal X-ray diffraction confirmed that the structure of **2** consists of one I_2 molecule bridging two molecules of **1** (Figure 2).[11] A nearly linear P···I–I···P arrangement is observed, in which the P···I and I–I distances

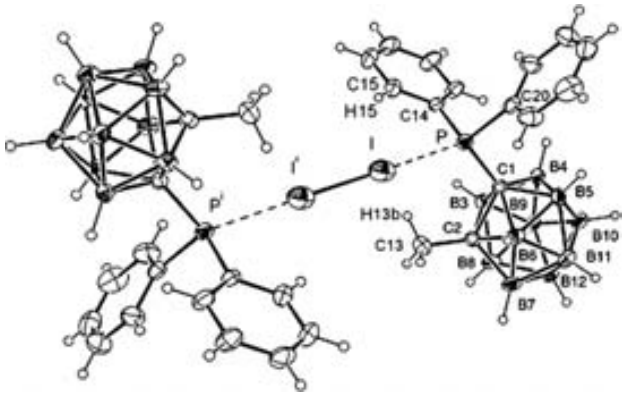

Figure 2. Molecular structure of **2**. The thermal ellipsoids are set at 30% probability. Selected interatomic distances [Å] and angles [°]: I–I^{i} 2.7753(14) (i = −*x*, −*y*, −*z*), P–C1 1.884(6), P–C14 1.831(6), P–C20 1.813(6), C1–C2 1.710(8), I···P 3.3337(18), I···H15 3.15, I···H13b 3.39; P-I-I^{i} 173.80(4), C1-P-C14 107.6(2), C1-P-C20 101.5(3), C14-P-C20 104.3(3).

are 3.3337(18) and 2.7753(14) Å, respectively. The I–I distance is the shortest found in a phosphane–I_2 adduct, and is only slightly longer than that in solid I_2 at 110 K (2.715(6) Å).[12] The I–I distance in **2** is similar to those in the $R_2S{\cdot}I_2{\cdot}SR_2$ adducts (2.75–2.79 Å).[8] Additionally, two weak I···H(Ph) contacts of 3.15 Å are observed in **2** (Figure 3).

Is the P···I–I···P structural motif observed in the solid state also stable in solution? Monitoring the titration of **1** with I_2 in dry $CDCl_3$ by $^{31}P\{^1H\}$ NMR spectroscopy revealed that increasing the ratio of I_2:**1** leads to a continuous upfield shift of the P-atom signal, from $\delta = 11.5$ (I_2:**1** = 0:1) to −10.2 (1:1) to −12.4 ppm (2:1). The same trend was observed for titrations in 1,2-dichloroethane and CH_2Cl_2. Ratios of I_2:**1** greater than 2:1 do not noticeably alter the chemical shift. These results do not parallel the behavior of other phosphanes, including (Mecarb)*i*Pr_2P,[9] for which an upfield shift of the P-atom resonance is observed when the ratio of I_2:R_3P is increased, up to a ratio of 2:1. Above this ratio, the signal shifts downfield, owing to the formation of $[R_3PI][I_3]$ species.[13] This difference in behavior implies that **1** does not induce the formation of the $[I_3]^-$ ion. To further confirm this point, temperature-dependent ^{31}P NMR spectroscopic studies of solutions of I_2:**1** in CD_2Cl_2 at ratios of 0.25:1, 0.5:1, 1:1, and 1.5:1 were carried out from 1–175 °C. In general, lower temperatures produced an upfield shift of the P-atom signal (see Supporting Information). Likewise, in conductometric titrations of solutions of I_2:**1** in CH_2Cl_2, very low conductance was observed, independent of the I_2:**1** ratio, which is inconsistent with the formation of ionic species. Finally, the I_2:**1** solutions were studied by UV/Vis spectros-

[*] Dr. R. Núñez, P. Farràs, Prof. F. Teixidor, Dr. C. Viñas
Institut de Ciència de Materials de Barcelona (CSIC)
Campus de la U.A.B., 08193 Bellaterra (Spain)
Fax: (+34) 935805729
E-mail: clara@icmab.es
Prof. R. Sillanpää
Department of Chemistry, University of Jyväskylä
FIN-40351 Jyväskylä (Finland)
Dr. R. Kivekäs
Department of Chemistry, PO Box 55
FIN-00014 University of Helsinki (Finland)

[**] This work was supported, in part, by MAT2004-01108 and the Generalitat de Catalunya, 2001/SGR/00337. P. Farràs is enrolled in the UAB PhD program.

Supporting information for this article is available on the WWW under http://www.angewandte.org or from the author.

copy, which confirmed the absence of $[I_3]^-$ ions.[5a,c] Therefore, in contrast to other phosphanes, **1** is incapable of sufficiently polarizing the I–I bond to allow the splitting required for the formation of $[I_3]^-$ ions, even in the presence of a large excess of I_2. But which species in solution, $\mathbf{1}\cdot I_2$ or $\mathbf{1}\cdot I_2\cdot\mathbf{1}$, best preserves the I–I fragment?

To learn more about the forces that bind phosphane–I_2 adducts, we combined experimental data with density functional theory (DFT) to calculate theoretical NMR spectra for $Ph_3P\cdot I_2$ (in spite of the difficulties encountered in the calculation of accurate NMR spectra for compounds containing P–I interactions using current computational methods[14]). Note that our attempts to reproduce the experimentally observed P···I–I arrangement in $Ph_3P\cdot I_2$ were unsuccessful; therefore, we decided to use geometric parameters from the crystal structure of $Ph_3P\cdot I_2$[5c] as input in our DFT calculations using gauge-including atomic orbitals (GIAO) (see Supporting Information). The calculated chemical shift of the donor P atom depends strongly on the positions of each of the two I atoms along the line defined by the other two atoms in the P···I(1)–I(2) assembly. When the P···I(2) distance is kept constant, moving the I(1) atom towards the P atom increases the shielding of the P nucleus. When the P···I(1) distance is fixed, moving the I(2) atom away from the P atom (and hence increasing the I(1)···I(2) distance) decreases the shielding at the P nucleus. Clearly, a larger number of I atoms in the near proximity of the P donor atom increase its shielding significantly. The results of the calculations are consistent with the upfield shift of the P-atom signal observed when the ratio of I_2:Ph_3P is increased in the titration of Ph_3P with I_2.[13] The removal of I(2) from the Ph_3P···I(1)–I(2) molecule to give the $[Ph_3PI]^+$ ion (along with an $[I_3]^-$ ion) deshields the P nucleus. The $[Ph_3PI]^+$ ion was examined in a separate set of calculations based on geometric parameters from the crystal structure of $[Ph_3PI][I_3]$.[15] The computed chemical shift of the P atom of the naked cation is $\delta = -282$ ppm, far from the experimental value of $\delta = 44$ ppm.[5c] However, if the $[I_3]^-$ ion is incorporated into the calculation the computed chemical shift of the P atom is $\delta = 36$ ppm. Therefore, the chemical shift is very dependent on weak interactions. All of these results suggest that when **1** and I_2 are combined in solution the moiety formed is P···I–I···P, and that the continuous decrease in the chemical shift of the P atoms with either increasing ratios of I_2 or lower temperatures arises from an increase in the number or strength of weak interactions between the P atoms in **1** and I_2 molecules or other I-containing species.

The natural population analysis (NPA) charges on the P atoms in the free ligands Ph_3P and **1**, calculated at the B3LYP/6-311 + G(d,p) level of theory, are 0.90 and 0.92, respectively (Figure 3; see Supporting Information). These values suggest that, as expected, the P atoms in PPh_3 are slightly better donors than those in **1**, but do not explain why very dissimilar P···I–I and P···I–I···P motifs are formed (Figure 3). The stabilization of one arrangement over the other may arise from differences in the charges on the phenyl hydrogen atoms in PPh_3 and in **1**. Charges ranging from 0.237 to 0.245 are calculated for those in PPh_3, whereas lower charges of 0.131 to 0.202 are calculated for those in **1** (some of these data are shown in Figure 3). The X-ray crystal structures of $Ph_3P\cdot I_2$[5c] and **2** also demonstrate the importance of the phenyl hydrogen atoms in PPh_3 and **1** for the stabilization of the P···I–I···P arrangement. Intramolecular I···H(Ph) interactions are absent in $Ph_3P\cdot I_2$ but present in **2**. In $Ph_3P\cdot I_2$, I(2) participates in intermolecular interactions with hydrogen atoms in the *para* positions on phenyl groups from two different molecules (Figure 3).

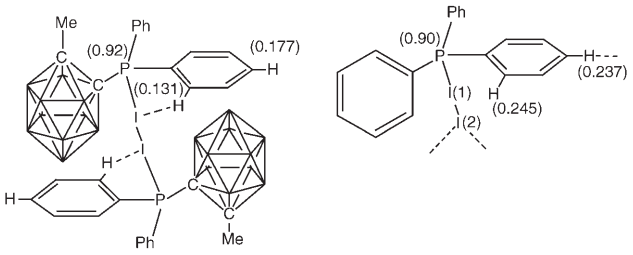

Figure 3. Schematic representation of $\mathbf{1}\cdot I_2\cdot\mathbf{1}$ (**2**) (left) and $Ph_3P\cdot I_2$ (right). Weak I···H contacts shorter than the sum of the van der Waals radii are indicated with dashed lines; those in $Ph_3P\cdot I_2$ are intermolecular contacts. The numbers in parentheses indicate the calculated NPA charges for the P atoms and selected H atoms of the free ligands **1** and PPh_3.

With regard to the influence of the carboranyl group in **1** on the formation of the P···I–I···P motif, it is noted that in addition to having a stronger electron-withdrawing character than a phenyl ring, the carboranyl group also redistributes the charges on the phenyl rings connected to the same P atom. The phenyl hydrogen atoms in **1** with the lowest charges are in the *ortho* positions, and are thus appropriately placed for a weak I···H(Ph) interaction involving a partial electron donation into the σ* orbital on the I_2 molecule in the adduct **2**. This is not the case for the phenyl rings in PPh_3, in which the hydrogen atoms with the lowest charges occupy the *para* positions. Some of these hydrogen atoms do participate in weak intermolecular interactions with I(2) in the crystal structure of the spoke adduct $Ph_3P\cdot I_2$.

The combination of experimental and computational techniques has shed some light on the P–I interactions in $R_3P\cdot I_2$ and $R_3P\cdot I_2\cdot PR_3$ complexes, and on the importance of weak interactions in the interpretation of their ^{31}P NMR spectra, but what can be said about the I–I interactions in these complexes? The I–I distances in $R_3P\cdot I_2\cdot PR_3$ (and $R_2S\cdot I_2\cdot SR_2$) are generally shorter than those in the spoke adducts $R_3P\cdot I_2$. This observation can be explained by considering the orbitals involved in the interaction between the donor P atoms and the I_2 molecule. The combination of the filled lone-pair sp^3 orbitals on each of the two P atoms leads to two filled orbitals, only one of which has the correct symmetry to interact with the σ* orbital on the I_2 molecule. Therefore, the number of electrons transferred from the donor atoms to the I_2 molecule is equal in $R_3P\cdot I_2\cdot PR_3$ and $R_3P\cdot I_2$. However, in $R_3P\cdot I_2$ the electrons in the sp^3 orbital on the donor atom are necessarily more polarizable, and therefore, produce a longer I–I bond. This explanation also accounts also for the similarity of the I–I bond lengths in the spoke $R_2S\cdot I_2$ (2.816(2) Å) and bridging $R_2S\cdot I_2\cdot SR_2$ (2.754(2) Å) adducts with equivalent thioethers in (1,4,7-trithiacyclononane)$_2(I_2)_4$.[3d] An alternative, but equivalent, explanation of

the bonding in $R_3P{\cdot}I_2{\cdot}PR_3$, based on the butadiene model, is given in the Supporting Information.

This research has substantiated the importance of ligands containing the carboranyl moiety in the formation of phosphane–I_2 adducts with novel structural motifs. Through the use of a carboranyl phosphane ligand, the P···I–I···P assembly was isolated for the first time. X-ray diffraction analysis of **2** demonstrated the presence of this structural motif in the solid state, and a variety of experimental techniques and computational methods suggest that it also exists when **2** is dissolved in halogenated solvents. Furthermore, we have shown that the ^{31}P NMR spectra of phosphane–I_2 adducts are greatly influenced by weak interactions between the adducts and I-containing species. This observation is of great relevance to the calculation of theoretical ^{31}P NMR spectra.

Received: August 23, 2005
Revised: November 22, 2005
Published online: January 20, 2006

Keywords: carboranes · iodine · noncovalent interactions · phosphanes · structure elucidation

[1] "Product Subclass 40: Carboranes and Metallacarboranes": F. Teixidor, C. Viñas in *Science of Synthesis, Vol. 6* (Eds.: D. S. Kaufmann, D. S. Matteson), Georg Thieme, Stuttgart, **2005**, pp. 1235 – 1275.

[2] W. Levason in *The Chemistry of Organophosphorus Compounds, Vol. 1* (Ed.: F. R. Hartley), Wiley, New York, **1990**, p. 567.

[3] a) P. Deplano, J. R. Ferraro, M. L. Mercuri, E. F. Trogu, *Coord. Chem. Rev.* **1999**, *188*, 71 – 95; b) M. C. Aragoni, M. Arca, F. A. Devillanova, A. Garau, F. Isaia, V. Lippolis, G. Verani, *Coord. Chem. Rev.* **1999**, *184*, 271 – 290; c) W.-W. du Mont, F, Ruthe, *Coord. Chem. Rev.* **1999**, *189*, 101 – 133; d) P. D. Boyle, S. M. Godfrey, *Coord. Chem. Rev.* **2001**, *223*, 265 – 299; e) S. M. Godfrey, C. A. McAuliffe in *Modern Coordination Chemistry. The Legacy of Joseph Chatt* (Eds.: G. J. Leigh, N. Winterton), The Royal Society of Chemistry, Cambridge, **2002**, pp. 79 – 89; f) S. Ito, H. Liang, M. Yoshifuji, *Chem. Commun.* **2003**, 398 – 399.

[4] K. F. Purcell, J. C. Kotz, *Inorganic Chemistry*, Saunders, Philadelphia, PA, **1977**, p. 209.

[5] a) W.-W. du Mont, M. Bätcher, S. Pohl, W. Saak, *Angew. Chem.* **1987**, *99*, 945 – 947; *Angew. Chem. Int. Ed. Engl.* **1987**, *26*, 912 – 913; b) F. Ruthe, P. G. Jones, W.-W. du Mont, P. Deplano, M. L. Mercuri, *Z. Anorg. Allg. Chem.* **2000**, *626*, 1105 – 1111; c) S. M. Godfrey, D. G. Kelly, A. G. Mackie, C. A. McAuliffe, R. G. Pritchard, S. M. Watson, *J. Chem. Soc. Chem. Commun.* **1991**, 1163 – 1164; d) N. Bricklebank, S. M. Godfrey, H. P. Lane, C. A. McAuliffe, R. G. Pritchard, M. M. Moreno, *J. Chem. Soc. Dalton Trans.* **1995**, 2421 – 2424.

[6] a) F. H. Herbstein, P. Ashkenazi, M. Kaftory, M. Kapon, G. M. Reisner, D. Ginsburg, *Acta Crystallogr. Sect. B* **1986**, *42*, 575 – 601; b) A. L. Tipton, M. C. Lonergan, C. L. Stern, D. F. Shriver, *Inorg. Chim. Acta* **1992**, *201*, 23 – 27; c) A. J. Blake, W.-S. Li, V. Lippolis, M. Schröder, *Acta Crystallogr. Sect. C* **1997**, *53*, 886 – 888, and references therein.

[7] a) V. Stenzel, J. Jeske, W.-W. du Mont, P. G. Jones, *Inorg. Chem.* **1997**, *36*, 443 – 448; b) A. J. Blake, F. A. Devillanova, R. O. Gould, W.-S. Li, V. Lippolis, S. Parson, C. Radek, M. Schröder, *Chem. Soc. Rev.* **1998**, *27*, 195 – 205; c) P. H. Svensson, L. Kloo, *Chem. Rev.* **2003**, *103*, 1649 – 1684.

[8] a) A. J. Blake, R. O. Gould, C. Radek, M. Schröder, *J. Chem. Soc. Chem. Commun.* **1993**, 1191 – 1193; b) A. J. Blake, F. Cristiani, F. A. Devillanova, A. Garau, L. M. Gilby, R. O. Gould, F. Isaia, S. Parsons, C. Radek, M. Schröder, *J. Chem. Soc. Dalton Trans.* **1997**, 1337 – 1346; c) A. J. Blake, F. A. Devillanova, A. Garau, L. M. Gilby, R. O. Gould, F. Isaia, V. Lippolis, S. Parsons, C. Radek, M. Schröder, *J. Chem. Soc. Dalton Trans.* **1998**, 2037 – 2046.

[9] F. Teixidor, R. Núñez, C. Viñas, R. Sillanpää, R. Kivekäs, *Angew. Chem.* **2000**, *112*, 4460 – 4462; *Angew. Chem. Int. Ed.* **2000**, *39*, 4290 – 4292; .

[10] R. Kivekäs, R. Sillanpää, F. Teixidor, C. Viñas, R. Núñez, *Acta Crystallogr. Sect. C* **1994**, *50*, 2027 – 2030.

[11] CCDC-186442 (**2**) contains the supplementary crystallographic data for this paper. These data can be obtained free of charge from The Cambridge Crystallographic Data Centre via www.ccdc.cam.ac.uk/data_request/cif.

[12] F. Bolhuis, P. B. van Koster, T. Migchelsen, *Acta Crystallogr.* **1967**, *23*, 90 – 91.

[13] W. I. Cross, S. M. Godfrey, C. A. McAuliffe, R. G. Pritchard, J. M. Sheffield, G. M. Thompson, *J. Chem. Soc. Dalton Trans.* **1999**, 2795 – 2798, and references therein.

[14] a) S. Patchkovskii, T. Ziegler, *J. Phys. Chem. A* **2002**, *106*, 1088 – 1099; b) A. Dransfeld, P. V. Schleyer, *Magn. Reson. Chem.* **1998**, *36*, S29-S43; c) C. van Wüllen, *Phys. Chem. Chem. Phys.* **2000**, *2*, 2137 – 2144.

[15] F. A. Cotton, P. A. Kibala, *J. Am. Chem. Soc.* **1987**, *109*, 3308 – 3312.

Inorg. Chem. **2006**, *45*, 7947−7954

Prediction of pK_a Values of *nido*-Carboranes by Density Functional Theory Methods

Pau Farràs,[†,‡] Francesc Teixidor,*[,‡] and Vicenç Branchadell*[,§]

Institut de Ciència de Materials de Barcelona, CSIC, and Department de Química, Universitat Autònoma de Barcelona, E-08193 Bellaterra, Spain

Received May 24, 2006

A great parallel exists between metal complexes of cyclopentadienyl and arene ligands on one side and metal complexes of the nido derivatives of the icosahedral *o*-carborane clusters. With few exceptions, the metal complexation in the cluster can be viewed as the substitution of one or more bridging hydrogen atoms by the metal. Therefore, a necessary requirement for the complexation is the deprotonation of the nido cluster to generate a coordination site for that metal. The reaction to remove these protons, which most probably is one of the most commonly done processes in boron and metallaborane chemistry, is barely known, and no quantitative data are available on the magnitude of their pK_a values. With the purpose of determining the acidity of *nido*-carboranes, a procedure to calculate the pK_a values of nido boron clusters is presented in this paper for the first time. To this objective, some nido clusters have been selected and their geometry and NMR-spectroscopic properties have been studied, giving a good correlation between the theoretical and experimental data in both geometry distances and ^{11}B NMR spectroscopy. Of notice is the result that proves that the singular carbon atom in the thermodynamic isomer of $[C_2B_{10}H_{13}]^-$ is definitely part of the cluster and that its connection with the C_2B_3 face would be better defined by adding additional interactions with the two boron atoms nearest to the second cluster carbon. The pK_a values of the nido species have been calculated by correlating experimental pK_a values and calculated reaction Gibbs energies ΔG_s. Some pK_a values of importance are −4.6 and +13.5 for 7,8-$[C_2B_9H_{13}]$ (**1**) and 7,8-$[C_2B_9H_{12}]^-$ (**2**), respectively.

1. Introduction

The characteristic feature of carboranes is a triangular-face polyhedral or polyhedral fragment framework of carbon and boron atoms. Prefix designations indicate the degree of "closed" or "open" deltahedral character, with "closo" being a closed deltahedra, "nido" a deltahedral fragment minus a vertex, and "arachno" a deltahedral fragment minus two vertexes. Carboranes follow electron counting rules developed by Mingos,[1] Wade,[2,3] Williams,[4,5] and Rudolph[6,7] that provide an empirical way for predicting the structure of cluster molecules. The polyhedron numbering is illustrated in Figure 1 for the three kinds of boron clusters studied in this work. The boron and carbon atoms are located at the polyhedron vertexes. A terminal hydrogen atom or *exo*-hydrogen is bonded to the cluster's vertex via a classical two-center, two-electron bond. Hydrogen atoms bound intimately to the cluster and whose projection to the cluster's open face falls within its limits are termed *endo*-hydrogen atoms. Also belonging to this type are the hydrogen atoms placed in the surface spanned by the cluster atoms.

nido-Carborane derivatives are key compounds for the coordination of boron clusters with metal ions in the formation of complexes.[8−11] With few exceptions,[12,13] the metal complexation or metal insertion in the cluster can be viewed

* To whom correspondence should be addressed. E-mail: teixidor@icmab.es (F.T.), vicenc.branchadell@uab.es (V.B.).
† P.F. is enrolled in the Ph.D. program at Universitat Autònoma de Barcelona.
‡ Institut de Ciència de Materials de Barcelona, CSIC.
§ Department de Química.

(1) Mingos, D. M. P. *Nature (London), Phys. Sci.* **1972**, *236*, 99.
(2) Wade, K. *J. Chem. Soc. D* **1971**, 792.
(3) Wade, K. *Adv. Inorg. Chem. Radiochem.* **1976**, *18*, 1.
(4) Williams, R. E. *Inorg. Chem.* **1971**, *10*, 210.
(5) Williams, R. E. *Adv. Inorg. Chem. Radiochen.* **1976**, *18*, 67.
(6) Rudolph, R. W.; Pretzer, W. R. *Inorg. Chem.* **1972**, *11*, 1974.
(7) Rudolph, R. W. *Acc. Chem. Res.* **1976**, *9*, 446.
(8) Hawthorne, M. F.; Young, D. C.; Wegner, P. A. *J. Am. Chem. Soc.* **1965**, *87*, 1818.
(9) Zalkin, A.; Templeton, D. H.; Hawthorne, M. F. *J. Am. Chem. Soc.* **1965**, *87*, 3988.
(10) Llop, J.; Viñas, C.; Teixidor, F.; Sillanpää, R.; Kivekäs, R. *Chem.—Eur. J.* **2005**, *11*, 1939.

10.1021/ic060908b CCC: $33.50
Published on Web 08/25/2006

Figure 1. Numbering scheme for nido deltahedral cluster fragments.

as the substitution of one or more bridging hydrogen atoms by the metal. Therefore, a necessary requirement for the complexation is the deprotonation of the nido cluster to generate a coordination site for that metal. The ease of deprotonation is different for each molecule and can be measured by its pK_a value. Experimentally, this can be done by titration or UV spectroscopic measurements. There is, however, little experimental information about the pK_a values of boron clusters[14] because of the difficulty to run on them the methods mentioned above. Therefore, finding a theoretical model to calculate or estimate the pK_a of nido boron clusters will bring relevant information to predicting their behavior. To this objective, some nido clusters have been selected in order to create a procedure that can be used for other *nido*-boranes/carboranes. The studied *nido*-carboranes are shown in Figure 2, also including **2*** for deprotonated **2**.

The binding behavior of the capping hydrogen atoms is shown by studying the geometry and NMR-spectroscopic properties of these molecules. The structure's energy minima found in the gas phase contain the *endo*-hydrogen atoms always bridging two boron atoms. However, there are some molecules in which the bridging hydrogen bounces between two degenerate energy-minimum positions. In these cases, an apparent C_s symmetry is observed in solution by ^{11}B NMR spectroscopy. By analysis of the charge distribution of these compounds, it is demonstrated that the carbon atom on the open face in compound **4**, the thermodynamic $[C_2B_{10}H_{13}]^-$ derivative, is part of the cluster. This had already been discussed, but no proof had been provided. It has also been observed that a clear trend between acidity and molecular charge exists. Thus, neutral compounds are the most acidic, and dianions are the least acidic. This can be proven through the simple model elaborated in this paper to calculate pK_a values of *nido*-carboranes. The procedure is based on a combination of theoretical results and experimental data. Although the matching for **1** with the given experimental value is less than expected, the error for **2** has only been about 0.75 pK_a units.

2. Computational Details

All computations here were carried out with the *Gaussian 98* and *Gaussian 03* packages.[15,16] All geometries were optimized at the B3LYP/6-31G* level[17−21] with no symmetry constraints. Frequency calculations were computed on these geometries at the same level of calculation to verify that they are energy minima. To obtain accurate energies, single-point calculations on the optimized geometries have been performed at the B3LYP/6-311+G** level of theory. Natural population analysis (NPA)[22] charges were also calculated at the B3LYP/6-311+G** level of theory.

^{11}B NMR chemical shifts were calculated at the gauge invariant atomic orbital (GIAO)−B3LYP/6-311+G** level. They have been referenced to B_2H_6 (16.6 ppm)[23] and converted to the usual $BF_3{\cdot}OEt_2$ scale; $\delta(^{11}B) = 100.68 - \sigma(^{11}B)$.

The solvation free energy was calculated with either the IPCM (static isodensity polarized continuum model)[24] or the CPCM (conductor polarized continuum model).[25] Dielectric constant values of 78.39 for water and 46.45 for dimethyl sulfoxide (DMSO) were used. In the CPCM model, both UA0 and Bondi radii[26] were used. The Gibbs reaction energies in solution have been computed at 1 mol·L^{-1} and 298.15 K.

3. Results and Discussion

Cluster Geometries and Relative Stabilities of Selected Compounds. Geometry optimizations of the targeted compounds are the first calculations that have to be done in order to get the structure with the minimal energy. This is the starting point from which most of the properties of the molecule can be calculated. A comparison between the X-ray experimental data and theoretical interatomic distances of selected bonds is shown in Table 1.

(11) Núñez, R.; Tutusaus, O.; Teixidor, F.; Viñas, C.; Sillanpää, R.; Kivekäs, R. *Chem.—Eur. J.* **2005**, *11*, 5637.
(12) Tutusaus, O.; Viñas, C.; Kivekäs, R.; Sillanpää, R.; Teixidor, F. *Chem. Commun.* **2003**, *19*, 2458.
(13) Teixidor, F.; Flores, M. A.; Viñas, C.; Sillanpää, R.; Kivekäs, R. *J. Am. Chem. Soc.* **2000**, *122*, 1963.
(14) Hlatky, G. G.; Crowther, D. J. *Inorg. Synth.* **1998**, *32*, 229.
(15) Frisch, M. J.; Trucks, G. W.; Schlegel, H. B.; Scuseria, G. E.; Robb, M. A.; Cheeseman, J. R.; Zakrzewski, V. G.; Montgomery, J. A.; Stratmann, R. E.; Burant, J. C.; Dapprich, S.; Millam, J. M.; Daniels, A. D.; Kudin, K. N.; Strain, M. C.; Farkas, O.; Tomasi, J.; Barone, V.; Cossi, M.; Cammi, R.; Mennucci, B.; Pomelli, C.; Adamo, C.; Clifford, S.; Ochterski, J.; Petersson, G. A.; Ayala, P. Y.; Cui, Q.; Morokuma, K.; Malick, D. K.; Rabuck, A. D.; Raghavachari, K.; Foresman, J. B.; Cioslowski, J.; Ortiz, J. V.; Stefanov, B. B.; Liu, G.; Liashenko, A.; Piskorz, P.; Komaromi, I.; Gomperts, R.; Martin, R. L.; Fox, D. J.; Keith, T.; Al-Laham, M. A.; Peng, C. Y.; Nanayakkara, A.; Gonzalez, C.; Challacombe, M.; Gill, P. M. W.; Johnson, B. G.; Chen, W.; Wong, M. W.; Andres, J. L.; Head-Gordon, M.; Replogle, E. S.; Pople, J. A. *Gaussian 98*, revision A.11.3; Gaussian, Inc.: Pittsburgh, PA, 2002.
(16) Frisch, M. J.; Trucks, G. W.; Schlegel, H. B.; Scuseria, G. E.; Robb, M. A.; Cheeseman, J. R.; Montgomery, J. A., Jr.; Vreven, T.; Kudin, K. N.; Burant, J. C.; Millam, J. M.; Iyengar, S. S.; Tomasi, J.; Barone, V.; Mennucci, B.; Cossi, M.; Scalmani, G.; Rega, N.; Petersson, G. A.; Nakatsuji, H.; Hada, M.; Ehara, M.; Toyota, K.; Fukuda, R.; Hasegawa, J.; Ishida, M.; Nakajima, T.; Honda, Y.; Kitao, O.; Nakai, H.; Klene, M.; Li, X.; Knox, J. E.; Hratchian, H. P.; Cross, J. B.; Bakken, V.; Adamo, C.; Jaramillo, J.; Gomperts, R.; Stratmann, R. E.; Yazyev, O.; Austin, A. J.; Cammi, R.; Pomelli, C.; Ochterski, J. W.; Ayala, P. Y.; Morokuma, K.; Voth, G. A.; Salvador, P.; Dannenberg, J. J.; Zakrzewski, V. G.; Dapprich, S.; Daniels, A. D.; Strain, M. C.; Farkas, O.; Malick, D. K.; Rabuck, A. D.; Raghavachari, K.; Foresman, J. B.; Ortiz, J. V.; Cui, Q.; Baboul, A. G.; Clifford, S.; Cioslowski, J.; Stefanov, B. B.; Liu, G.; Liashenko, A.; Piskorz, P.; Komaromi, I.; Martin, R. L.; Fox, D. J.; Keith, T.; Al-Laham, M. A.; Peng, C. Y.; Nanayakkara, A.; Challacombe, M.; Gill, P. M. W.; Johnson, B.; Chen, W.; Wong, M. W.; Gonzalez, C.; Pople, J. A. *Gaussian 03*, revision C.02; Gaussian, Inc.: Wallingford, CT, 2004.
(17) Hariharan, P. A.; Pople, J. A. *Theor. Chim. Acta* **1973**, *28*, 213.
(18) Becke, A. D. *J. Chem. Phys.* **1993**, *98*, 5648.
(19) Lee, C.; Yang, W.; Parr, R. G. *Phys. Rev. B* **1988**, *37*, 785.
(20) Ditchfield, R. *Mol. Phys.* **1974**, *27*, 789.
(21) London, F. *J. Phys. Radium* **1937**, *8*, 397.
(22) Reed, A. E.; Curtiss, L. A.; Weinhold, F. *Chem. Rev.* **1988**, *88*, 899.
(23) Onak, T. P.; Landesman, H. L.; Williams, R. E. *J. Phys. Chem.* **1959**, *63*, 1533.
(24) Foresman, J. B.; Keith, T. A.; Wiberg, K. B.; Snoonian, J.; Frisch, M. J. *J. Phys. Chem.* **1996**, *100*, 16098.
(25) Cossi, M.; Rega, N.; Scalmani, G.; Barone, V. *J. Comput. Chem.* **2003**, *24*, 669.
(26) Bondi, A. *J. Phys. Chem.* **1964**, *68*, 441.

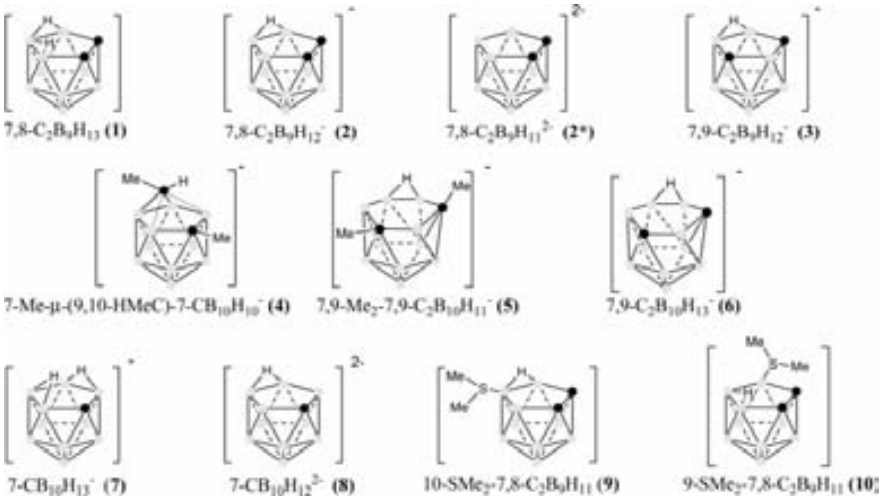

Figure 2. Skeletal structure of studied nido boron clusters. Boron and carbon atoms are shown as light gray and black dots, respectively. *exo*-Hydrogen atoms are not shown.

Table 1. Comparison between the Atom Distances on the Open-Face C_xB_y (Error by the Root-Mean-Square Method)

	2[a]		**3**[b]	
	theor (Å)	exp (Å)	theor (Å)	exp (Å)
C(7)−C(8)	1.557	1.555	1.623	1.625
C(7)−B(11)	1.624	1.607	1.651	1.646
B(11)−B(10)	1.861	1.831	1.851	1.845
B(10)−B(9)	1.882	1.856	1.651	1.641
B(9)−C(8)	1.607	1.614	1.623	1.626
	$R = 0.998$	error = 0.0019	$R = 0.999$	error = 0.0002
	4[c]		**7**[d]	
	theor (Å)	exp (Å)	theor (Å)	exp (Å)
C(7)−B(8)	1.634	1.624	1.648	1.635
C(7)−B(11)	1.634	1.625	1.649	1.640
B(11)−B(10)	1.875	1.867	1.871	1.860
B(10)−C(9)	1.870	1.843	1.905	1.870
B(9)−C(8)	1.875	1.864	1.871	1.851
	$R = 0.998$	error = 0.0011	$R = 0.999$	error = 0.0003
	9[e]		**10**[f]	
	theor (Å)	exp (Å)	theor (Å)	exp (Å)
C(7)−B(8)	1.559	1.547	1.542	1.525
C(7)−B(11)	1.619	1.613	1.601	1.571
B(11)−B(10)	1.852	1.852	1.769	1.775
B(10)−C(9)	1.780	1.792	1.868	1.844
B(9)−C(8)	1.610	1.597	1.646	1.622
	$R = 0.998$	error = 0.002	$R = 0.999$	error = 0.0005

	5[g]	
	theor (Å)	exp (Å)
C(7)−B(8)	1.521	1.506
C(7)−B(12)	1.512	1.513
B(12)−B(11)	1.886	1.885
B(11)−B(10)	1.851	1.846
B(10)−C(9)	1.653	1.648
C(9)−B(8)	1.644	1.638
	$R = 0.999$	error = 0.0003

[a] Experimental data from ref 54. [b] Reference 28. [c] Reference 55. [d] Reference 56. [e] Reference 57. [f] Reference 58. [g] Reference 59.

The relaxed molecular structures of the *nido*-carboranes display considerable deviation from those of the *closo*-carboranes, in which the C−C bond length in *o*-carborane is 1.61 Å, the C−B bonds lie in the range 1.70−1.72 Å, and the B−B bonds lie in the range 1.77−1.79 Å.[38] These parameters are considerably different in the nido species. Therefore, it is clear that removal of the boron atom adjacent to both carbon atoms in *o*-carborane causes a large distortion in the geometry. For example, the two *nido*-carboranes originating from *o*-carborane after formal abstraction of one boron atom, [7,8-$C_2B_9H_{13}$] and [7,8-$C_2B_9H_{12}]^-$, display a C−C bond length in the range 1.53−1.55 Å, a C−B bond length of 1.60−1.66 Å, and B−B bonds in the range 1.76−1.89 Å. These changes may be a consequence of a ring current generated in the open face of the nido cluster.

Some of the molecules studied here have already been structurally presented by different authors. This is not the case for compounds **9** and **10**, which had not previously been studied theoretically. The presence of the sulfonium group leads to zwitterionic species. It could be hypothesized that the cluster structural parameters would vary with the sulfonium group. This is not the case, however, because the B−B bond length on the open face is altered only for those bonds incorporating the boron atom bonded to the sulfonium group, producing a bond shortening from 1.88 Å to 1.78 Å in **9** and from 1.86 Å to 1.77 Å in **10**. Moreover, the bond lengths within the cluster are basically equal for both isomers, except those that involve the boron−sulfonium moiety. A comparison between the calculated cage geometries and experimental data shows a good agreement, as seen in Table 2. Experimental C−C distances from X-ray crystallographic investigations for **9** and **10** lie in the range 1.52−1.54 Å, C−B distances in the range 1.57−1.71 Å, and B−B distances in the range 1.72−1.85 Å.

Theoretical structural parameters from this study are as follows: for C−C, 1.54−1.56 Å; for C−B, 1.60−1.74 Å; for B−B, 1.74−1.85 Å. When the *endo*-hydrogen may adopt a bridging or an endo terminal disposition, the bridging disposition is preferred. When compound **9** is symmetrized to C_s symmetry, the energy increases by 15.7 kcal·mol^{-1}, clearly indicating that an nonbridging *endo*-hydrogen is less stable than a bridging hydrogen. The difference in energy

Table 2. Resulting NPA Charges for the Targeted Compounds

	1	2	2*	3	4	5
C(7)	−0.503	−0.577	−0.58	−0.805	−0.728	−0.637
C(8)	−0.503	−0.543	−0.58			
C(9)				−0.805		−0.701
C(12)					−0.501	
B(1)	−0.208	−0.213	−0.243	−0.213	−0.159	−0.203
B(2)	0.039	−0.01	−0.053	−0.022	0.007	0.085
B(3)	0.141	0.127	0.099	−0.022	0.007	0.017
B(4)	0.039	−0.044	−0.053	0.039	−0.231	0.026
B(5)	−0.13	−0.159	−0.184	−0.209	−0.117	−0.214
B(6)	−0.13	−0.184	−0.184	0.039	−0.231	−0.214
B(8)				0.202	0.255	0.325
B(9)	−0.104	−0.018	−0.086		−0.064	
B(10)	−0.125	−0.298	−0.343	−0.035	−0.064	0.08
B(11)	−0.104	−0.01	−0.086	−0.035	0.255	−0.224
B(12)						0.137
H on C	0.274	0.240−0.242	0.21	0.248	0.22	
H on B	0.050−0.202	0.003−0.200	−0.034 to +0.013	−0.007 to +0.156	−0.012 to +0.049	−0.024 to +0.181

	6	7	8	9	10
C(7)	−0.803	−0.801	−0.786	−0.551	−0.562
C(8)				−0.561	−0.529
C(9)	−0.842				
C(12)					
B(1)	−0.207	−0.183	−0.219	−0.197	−0.2
B(2)	0.073	0.014	−0.031	−0.051	0.003
B(3)	0.013	0.014	−0.031	−0.155	0.14
B(4)	0.011	−0.208	−0.19	−0.169	−0.027
B(5)	−0.217	−0.178	−0.183	0.011	−0.144
B(6)	−0.213	−0.208	−0.19	0.142	−0.196
B(8)	0.322	0.019	−0.076		
B(9)		−0.194	−0.285	0.014	−0.037
B(10)	0.064	−0.194	−0.284	−0.282	−0.255
B(11)	−0.223	0.019	−0.077	−0.019	−0.009
B(12)	0.118				
H on C	0.229−0.259	0.25	0.217	0.266	0.264
H on B	−0.030 to +0.180	0.019−0.156	−0.030 to +0.200	0.040−0.195	0.027−0.198

between positional isomers **9** and **10** is 9.1 kcal·mol^{-1}, with **9** being the most stable one.

Concerning **1**−**8** already studied by other authors, our results are in good agreement with theirs.[27−31] Compounds **1**−**3** have been studied using either MP2 or B3LYP methods. If carbon positional isomers **2** and **3** are compared, it is observed that **3** is the most stable by 16.8 kcal·mol^{-1}, similar to the 16.3 kcal·mol^{-1} found in the literature.[27]

For the 12-vertex clusters, two common isomers are known: thermodynamic and kinetic. The former is numbered **4** in this work, whereas the kinetic ones are represented by **5** and **6**. The thermodynamic **4** (with a five-membered face) is the most stable by 3.89 kcal·mol^{-1}, in good agreement with the value found by McKee et al.[32]

Fox et al.[33] have also studied geometrical aspects for the monocarboranes **7** and **8**. As described above, the bridging hydrogen is the most stable of the possible orientations of a capping hydrogen atom and this motif finds its most favorable situation in monocarboranes **7** and **8** for which C_s symmetry instead of C_1 symmetry is possible.

Atomic Charges. This section focuses on the electron distribution in the selected nido compounds. We have analyzed the charge distribution using charges derived from the natural atomic orbital scheme (NPA) because it is known that Mulliken charges are strongly basis set dependent. Calculated NPA charges are shown in Table 2. Trends caused by the difference in electronegativity between carbon and boron atoms, 2.6 and 2.0, respectively, are observed in all compounds. Boron atoms with no carbon neighbors have charges in the range −0.12 to −0.30, those with only one carbon neighbor are in the range +0.14 to −0.11, and those with two carbon neighboring lie between 0.12 and 0.32. The carbon atoms induce an electron flow inside the cluster, causing the boron atoms furthest away from them to be more electron-rich than the other boron atoms. Deprotonation of a *nido*-carborane also changes the electronic distribution in the molecule, especially for the boron atoms that lose the proton and for those occupying their antipodal positions. For example, if Table 2 is inspected, NPA charges on boron atoms B(9,10) and B(2,3) in **2** vary an average of 0.05 units compared with **2*** (**2** deprotonated) as a consequence of losing the bridging hydrogen atom.

Data details in Table 3 indicate that some values are out of the normal range of charges discussed above, and this

(27) Fox, M. A.; Hughes, A. K.; Johnson, A. L.; Paterson, M. A. J. *J. Chem. Soc., Dalton Trans.* **2002**, 2009.
(28) Fox, M. A.; Goeta, A. E.; Hughes, A. K.; Johnson, A. L. *J. Chem. Soc., Dalton Trans.* **2002**, 2132.
(29) Fox, M. A.; Hughes, A. K.; Malget, J. M. *J. Chem. Soc., Dalton Trans.* **2002**, 3505.
(30) Lee, H.; Onak, T.; Jaballas, J.; Tran, U.; Truong, T. U.; To, H. T. *Inorg. Chim. Acta* **1999**, *289*, 11.
(31) Kiani, F. A.; Hofmann, M. *Inorg. Chem.* **2004**, *43*, 8561.
(32) McKee, M. L.; Bühl, M.; Schleyer, P. v. R. *Inorg. Chem.* **1993**, *32*, 1712.
(33) Batsanov, A. S.; Fox, M. A.; Goeta, A. E.; Howard, J. A. K.; Hughes, A. K.; Malget, J. M. *J. Chem. Soc., Dalton Trans.* **2002**, 2624.

Table 3. Summary of Calculated ^{11}B NMR Shifts

compd	formula	calcd ^{11}B NMR chemical shifts (ppm)
1	7,8-$C_2B_9H_{13}$	3.7 (2,4), −3.4 (5,6), −17.3 (3), −20.6 (10), −30.4 (9,11), −31.0 (1)
2	7,8-$C_2B_9H_{12}^-$	−14.6 (9,11), −18.0 (5,6), −20.5 (3), −24.6 (2,4), −35.1 (10), −41.1 (1)
3	7,9-$C_2B_9H_{12}^-$	−6.3 (2,5), −8.3 (8), −23.7 (3,4), −26.8 (10,11), −37.8 (1), −38.3 (6)
4	7-Me-μ-(9,10-HMeC)-7-$CB_{10}H_{10}^-$	16.9 (8,11), 8.4 (5), −1.0 (1), −6.9 (2,3), −14.7 (9,10), −21.6 (4,6)
5	7,9-Me_2−7,9-$C_2B_{10}H_{11}^-$	8.8 (8), 0.8 (10,12), −2.6 (3), −10.9 (5,6), −17.8 (2,4), −21.6 (1), −22.3 (11)
6	7,9-$C_2B_{10}H_{13}^-$	8.7 (8), −0.2 (10,12), −7.1 (3), −9.8 (5,6), −19.6 (1), −21.8 (11), −23.7 (2,4)
7	7-$CB_{10}H_{13}^-$	−1.3 (5), −13.5 (2,3), −15.2 (8,11), −26.2 (9,10), −29.0 (1), −33.6 (4,6)
8	7-$CB_{10}H_{12}^{2-}$	−17.7 (8,11), −18.9 (4,6), −25.7 (2,3), −29.1 (5), −31.8 (9,10), −46.1 (1)
9	10-SMe_2−7,8-$C_2B_9H_{11}$	−15.5 (5,6), −17.3 (9,11), −18.9 (3), −20.6 (2,4), −25.9 (10), −39.5 (1)
10	9-SMe_2−7,8-$C_2B_9H_{11}$	−4.5 (5), −6.3 (9), −12.7 (2), −16.9 (11), −18.6 (3), −23.5 (4), −26.6 (6), −30.3 (10), −37.1 (1)

Table 4. Correlation Coefficients between Theoretical and Experimental ^{11}B NMR Chemical Shifts

	correlation coefficient	
	no symmetry	with apparent symmetry
1[a]	0.997	
2[b]	0.829	0.996
3[c]	0.998	
4[c]	0.996	
5[d]	0.634	0.975
6[c]	0.653	1.000
7[c]	0.997	
8[e,g]	0.945	
9[f]	0.703	0.949
10[c]	0.984	

[a] Experimental data from ref 14. [b] Reference 60. [c] Reference 61. [d] Unpublished results. [e] Reference 33. [f] Reference 62. [g] Not known experimentally. Data from a zwitterionic-based molecule: $[Me_3NCB_{10}H_{11}]^-$.

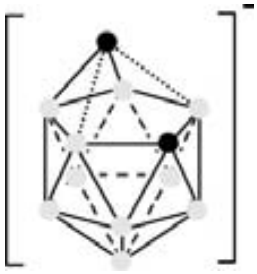

Figure 3. Scheme of B−C interactions in **4**.

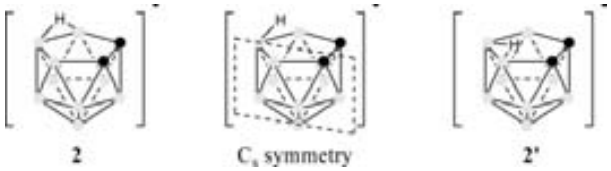

Figure 4. C_s symmetry caused by the fluxional hydrogen atom.

could imply relevant structural information. In this context, NPA charges on B(8,11) in **4** are 0.255, much higher than would be expected for boron atoms bonded to only one carbon. In the common structural representation, these boron atoms are linked to one carbon atom, but their charge is out of the margin of NPA charges expected for a boron atom connected to a carbon and is closer to the value of a boron atom attached to two carbon atoms. Indeed, **4** originates from a *closo*-carborane (*o*-carborane) in which C(12) is attached to both C(7) and B(8,11). Thus, in *o*-carborane, these two boron atoms are bonded to two carbon atoms, and the introduction of two electrons (reduction of the cluster) moves C(12) away from C(7), diminishing the bond order with C(7) and B(8,11) but not to the point of reducing it to zero. We understand that Figure 3 represents more precisely the bonding interaction in **4**.

Using the natural atomic orbitals obtained from the NPA calculation, Wiberg bond orders[34] have been calculated for compound **4**. The Wiberg bond order of the B−C bonds indicated by the dotted lines in Figure 3 is 0.1694, which represents 24.4% of the average value of the remaining B−C bonds in **4** (0.695). This is the first confirmation that the previously known $C_{exo\ cluster}$ [C(12)] is, indeed, part of the cluster because there is additional interaction as shown before with the two remaining boron atoms of the open face.

NMR Calculations. The ultimate goal of this work is to calculate the acidity of the targeted compounds in solution. Thus, it was first necessary to verify if the optimized structures in the gas phase are consistent with the experimental data in solution. NMR gives information on the nature of each nucleus in a liquid environment (a solution). Therefore, if a good correlation between the theoretical and experimental chemical shifts is achieved, then the optimized geometry may be considered a good representation of its molecular structure in solution.[35−38] Because all molecules are boron cages and they are well characterized by ^{11}B NMR spectroscopy, we can use the experimental values obtained with this technique and compare them with the calculated ones. It has already been proven that the GIAO/B3LYP method is suitable for these molecules, and our calculations on compounds **1**−**3** and **6**−**8** are in agreement with previously reported values in the literature at various computational levels.[27−33] A summary of our results is shown in Table 3.

These values can be compared with experimental data. Table 4 shows the corresponding correlation coefficients (*R*). It can be observed that in cases where the position of the fluxional proton can produce C_s symmetry the correlation is very bad. However, if it is considered that apparent C_s symmetry is achieved by a fast interchange of the bridging proton between the two extreme positions shown in Figure 4, then *R* becomes very good indeed. The reason is that these protons have a rapid movement between two positions that corre-

(34) Wiberg, K. B. *Tetrahedron* **1968**, *24*, 1083.
(35) Bühl, M.; Schleyer, P. v. R. *J. Am. Chem. Soc.* **1993**, *114*, 477.
(36) Bühl, M.; Gauss, J.; Hofmann, M.; Schleyer, P. v. R. *J. Am. Chem. Soc.* **1993**, *115*, 12385.
(37) Schleyer, P. v. R.; Gauss, J.; Bühl, M.; Greatrex, R.; Fox, M. A. *J. Chem. Soc., Chem. Commun.* **1993**, 1766.
(38) Fox, M. A.; Greatrex, R.; Hofmann, M.; Schleyer, P. v. R. *J. Organomet. Chem.* **2000**, *614*−*615*, 262.

Table 5. Theoretical Gas-Phase Deprotonation Enthalpies for Carboranes **1**−**10**, Methanol, Trifluoroacetic Acid, and Benzoic Acid[53]

compound	ΔH (kcal·mol^{-1})	compound	ΔH (kcal·mol^{-1})[a]
1	305.32	**8**	534.79
2	438.44	**9**	333.82
3	437.71	**10**	347.95
4	434.35	methanol	384.1 (381.5)
5	427.22	trifluoroacetic acid	321.4 (322.9)
6	429.72	benzoic acid	343.5 (340.1)
7	433.99		

[a] The experimental values in parentheses were taken from ref 53.

sponds to degenerate energy minima, giving as an average a central position with the corresponding C_s symmetry.

The worst correlation coefficient (R) is 0.945 for **8**. This is due to the lack of a experimental structure, this for $[7\text{-}CB_{10}H_{12}]^{2-}$, from which the NMR data could be taken to be compared with the computed structure. The compared NMR data are from $[7\text{-}Me_3N\text{-}7\text{-}CB_{10}H_{11}]^-$ (exp) and $[7\text{-}CB_{10}H_{12}]^{2-}$ (computed). In the case for **9**, the fitting $R =$ 0.949 is not too good either. This may be interpreted as if the proton bouncing process and the restricted sulfonium group rotation have dissimilar rates. This results in the fact that the simple apparent C_s symmetry procedure described above does not describe accurately the molecular structure in solution. Besides these two cases, there is a good agreement between the calculated and experimental chemical shifts. Therefore, the assumption that the optimized geometry is representative of the geometry in solution is reasonable.

Gas-Phase Acidity. Because of substantial experimental and theoretical difficulties, well-defined pK_a values of carborane molecules are not available in almost any case. Measurements and calculations on *closo*-carborane isomers have been reported, although their calculation method was at most qualitative.[39] More recently and because of new experimental results, the interest for carborane acidity has grown and gas-phase acidity calculations have been done for *closo*-$CB_{11}H_{12}^-$ and its derivatives showing its strongly acidic properties.[40−45]

Gas-phase deprotonation enthalpies provide valuable information about the inherent solvent-independent properties of acids AH. They correspond to the reaction enthalpy of the gas-phase process

$$AH \rightarrow A^- + H^+$$

The computed deprotonation enthalpies of carboranes **1**−**10** are presented in Table 5 and Figure 5 along with those computed for three organic acids for which experimental values are known.

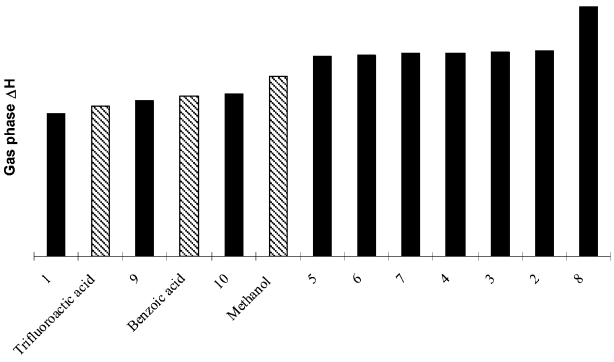

Figure 5. Theoretical gas-phase deprotonation enthalpies (kcal·mol^{-1}) by acidity order.

From Figure 5, three different orders of magnitude of acidity can be observed. Compounds **9** and **10** have a deprotonation energy between 330 and 350 kcal·mol^{-1}, which is in the range of trifluoroacetic acid and benzoic acid. Compound **1** can also be included in this group although its deprotonation energy is lower, 305 kcal·mol^{-1}; thus, it is the strongest acid. Compounds **2**−**7** have $\Delta H = 433 \pm 5$ kcal·mol^{-1} and can be set in a second group. Although these values are higher than that of methanol, 384 kcal·mol^{-1}, we have taken this as a reference and it would be the strongest acid within this group. Within another range of acidity, we encounter compound **8** with $\Delta H = 535$ kcal·mol^{-1}.

A parallel between the deprotonation energy and charge properties of the studied compounds can be found. The most acidic ones are neutral (**1**) or zwitterionic (**9** and **10**); compounds in the second range are monoanions, and the least acidic (**8**) is a dianion. In summary, it is possible to have a first qualitative approximation to the acidity of a nido-targeted compound from its charge.

Solution-Phase Acidity. The pK_a of an acid AH can be computed[46−50] from the reaction Gibbs energy associated with direct deprotonation in solution

$$AH(solv) \rightarrow A^-(solv) + H^+(solv) \qquad (1)$$

or with proton transfer to the conjugate base of a reference acid (BH).

$$AH(solv) + B^-(solv) \rightarrow A^-(solv) + BH(solv) \qquad (2)$$

$$pK_a(AH) = \Delta G_s/2.30RT + pK_a(BH)$$

where ΔG_s = reaction Gibbs energy in solution

This second approach avoids the difficult problem of computing the Gibbs solvation energy of the proton and is the one that we have chosen, using methanol as the reference acid.

(39) Hermansson, K.; Wójcik, M.; Sjöberg, S. *Inorg. Chem.* **1999**, *38*, 6039.
(40) Koppel, I. A.; Burk, P.; Koppel, I.; Leito, I.; Sonoda, T.; Mishima, M. *J. Am. Chem. Soc.* **2000**, *122*, 5114.
(41) Juhasz, M.; Hoffmann, S.; Stoyanov, E. S.; Kim, K.; Reed, C. A. *Angew. Chem., Int. Ed.* **2004**, *43*, 5352.
(42) Reed, C. A. *Chem. Commun.* **2005**, 1669.
(43) Stoyanov, E. S.; Kim, K.; Reed, C. A. *J. Am. Chem. Soc.* **2006**, *128*, 1948.
(44) Stoyanov, E. S.; Hoffmann, S. P.; Juhasz, M.; Reed, C. A. *J. Am. Chem. Soc.* **2006**, *128*, 3160.
(45) Balanarayan, P.; Gadre, S. R. *Inorg. Chem.* **2005**, *44*, 9613.
(46) Klamt, A.; Eckert, F.; Diedenhofen, M. *J. Phys. Chem. A* **2003**, *107*, 9380.
(47) Almerindo, G. I.; Tondo, D. W.; Piego, J. R., Jr. *J. Phys. Chem. A* **2004**, *108*, 166.
(48) Liptak, M. D.; Shields, G. C. *J. Am. Chem. Soc.* **2001**, *123*, 7314.
(49) Magill, A. M.; Cavell, K. J.; Yates, B. F. *J. Am. Chem. Soc.* **2004**, *126*, 8717.
(50) Martin, D.; Illa, O.; Baceiredo, A.; Bertrand, G.; Ortuño, R. M.; Branchadell, V. *J. Org. Chem.* **2005**, *70*, 5671.

Table 6. Comparison of Calculated pK_a Values in Water Using Different Methods According to Equation $pK_a = pK_a(exp,MeOH) + \Delta G_s/2.303RT$

	IPCM[a,b]	CPCM(UA0)[a,b]	CPCM(Bondi)[a,b]	exp
1	−26.8	−23.5	−17.9	2.98
2	10.7	5.6	9.5	14.25

	CPCM/6-311+G(2d,2p)[a,c]	CPCM/CPCM[b,d]
1	−24.2	−20.1
2	7.4	10.9

[a] Geometries optimized in the gas phase at the B3LYP/6-31G* level. [b] Solvation energies computed at the B3LYP/6-311+G** level. [c] Solvation energies computed at the B3LYP/6-311+G(2d,2p) level using UA0 radii. [d] Geometries optimized in solution at the B3LYP/6-31G* level using UA0 radii.

Our initial goal was to compute pK_a values in water; however, the preliminary inconsistent results led us to use DMSO in preference, although studies in water have also been done. The problem with water is that polarizable continuum models for solvation are less accurate in this solvent than in others.[51] Moreover, most of the reactions of *nido*-carboranes are done in organic solvents so data in an organic solvent such as DMSO should be useful for synthetic purposes.

Calculation of the solvation energies for all molecules participating in the reaction can be done by different available continuum methods such as IPCM or CPCM. Both have been used to find the best model that parallels the computed values and the experimental data found in the literature.[14] To choose a suitable method for our compounds, a comparison of the results obtained by the different methods is shown in Table 6 for **1** and **2**. It is clear that the results for **1** are very bad in all cases, whereas for **2**, the best result is obtained by using IPCM. We have also studied the benefits that would generate a more accurate calculation using either a larger basis set to calculate solvation energies of the molecules or the optimization of the molecules in solution. Although results have been improved by optimizing geometries in solution, the calculated value for **2** is still very similar to the one obtained by IPCM. To our understanding, the computational time used by each molecule is so high (4 times more in the optimization) that it does not make the larger cost in computing time worthy. Therefore, IPCM has been selected as the best method available for our calculation. For further information, see the Supporting Information.

To improve the values obtained before, a combination between the experimental and theoretical data is used. The reaction Gibbs energy in solution ΔG_s has been computed for the proton transfer indicated in eq 2 from seven organic acids to MeO^-, and these values have been correlated with the experimental pK_a values. The linear regression leads to the following equations:

$$pK_a = 0.3551\Delta G_s + 15.844 \ (r = 0.98) \qquad \text{for water} \qquad (3)$$

$$pK_a = 0.5876\Delta G_s + 29.082 \ (r = 0.99) \qquad \text{for DMSO} \qquad (4)$$

(51) Chipman, D. M. *J. Phys. Chem. A* **2002**, *106*, 7413.

Table 7. Calculated ΔG_s (kcal·mol^{-1}) for the Proton Transfer to MeO^- and pK_a Values of Studied Compounds in Water and DMSO

	water		DMSO	
	ΔG_s	pK_a	ΔG_s	pK_a
1	−57.7	−4.6	−57.9	−4.9
2	−6.6	13.5	−6.1	25.5
3	−8.7	12.8	−8.1	24.3
4	−5.8	13.8	−5.2	26.0
5	−12.3	11.5	−11.7	22.2
6	−14.0	10.9	−13.4	21.2
7	−17.6	9.6	−13.6	21.1
8	22.1	23.7	28.5	45.8
9	−30.1	5.2	−30.3	11.3
10	−25.8	6.7	−23.3	15.4

These equations have been used to compute the pK_a values of the targeted molecules from the computed ΔG_s. The results obtained in both water and DMSO are shown in Table 7.

The critical point in calculating pK_a values is the solvation energies of the participating molecules. If for organic molecules good accuracy is difficult to obtain, in *nido*-carboranes, the accuracy would be even worse because of the size of these molecules. The results obtained in water for **1** and **2** can be compared with the experimental values, 2.98 and 14.25, respectively, found in the literature.[14] The discrepancy in **1** is considerable, although it is well-known that experimental pK_a calculation of very acidic compounds is still very difficult, and perhaps the −4.6 value may not be so far from reality. On the contrary, the error for **2** is only 0.75 units of pK_a. Thus, we can consider that the results obtained for the other compounds are good enough and that this procedure may be worth quantitatively calculating pK_a values of *nido*-carboranes, taking the values for very acidic compounds with caution. Therefore, we feel that this procedure provides sufficient accuracy, reliability, and easiness to make it valuable for the calculation of pK_a values of *nido*-carborane anions.

4. Conclusions

Theoretical methods incorporating solvation energy protocols based only on one experimental reference have proven to be unsuccessful in calculating pK_a values of *nido*-carboranes because the computed values are very far from the few experimental data available. More realistic and useful pK_a data have been obtained through the use of a set of acids with well-defined pK_a values, which have made it possible to describe a linear equation relating the pK_a with the reaction Gibbs energy in solution, ΔG_s, in both water and DMSO. From ΔG_s for the studied nido species, it is then possible to calculate the pK_a values. The results obtained compare well with the experimental data available and are consistent with the structures, number of acidic protons, and charges of the species studied. From these, it is then possible to draw some pK_a conclusions: the monoprotic zwitterionic species represented by the sulfonium derivatives **9** and **10** have pK_a values comparable to those of alkyl organic acids; the diprotic neutral species [7,8-$C_2B_9H_{13}$] may be comparable to a trifluoroacetic acid, the monoprotic monoanionic species to pyrrole, and monoanionic diprotic species to phenols. Finally,

the least acidic are the dianionic monoprotic species that compare with *tert*-butyl alcohol/aniline.

In addition to the charge structure/pK_a correlation described here, these studies also suggest that the problem associated with the pK_a calculation derives from the solvation energy. Taking this into account, the extremely good correlation between the calculated and experimental ^{11}B NMR data is remarkable. It is even more so if we consider that energy optimization of the boron clusters is done in the gas phase. This leads to the conclusion that there is, in general, little interaction of these nido species with solvent molecules, in contrast with phosphorus-containing species, which seem to interact strongly.[52]

Acknowledgment. This work was supported, in part, by CICYT (Project MAT2004-01108), Generalitat de Catalunya (Grant 2005/SGR/00709), and CSIC (Grant I3P for P.F.). Access to the computational facilities of Centre de Supercomputació de Catalunya and the CSIC computing center is also gratefully acknowledged.

Supporting Information Available: Table containing computed total energies and Cartesian coordinates for compounds **1**−**10**, tables for computed ΔG_s and pK_a for compounds **1**−**10** and selected acids using different available continuum methods, figures for the linear regressions between theoretical ΔG_s and experimental pK_a using ICPM and CPCM to calculate solvation energies. This material is available free of charge via the Internet at http://pubs.acs.org.

IC060908B

(52) Nuñez, R.; Farras, P.; Teixidor, F.; Viñas, C.; Sillanpää, R.; Kivekäs, R. *Angew. Chem., Int. Ed.* **2006**, *45*, 1270.
(53) Hunter, E. P.; Lias, S. G. In *Proton Affinity Evaluation*; Linstrom, P. J., Mallard, W. G., Eds.; NIST Chemistry WebBook, NIST Standard Reference Database Number 69; National Institute of Standards and Technology: Gaithersburg, MD, June 2005 (http://webbook.nist.gov).
(54) Davidson, M. G.; Fox, M. A.; Hibbert, T. G.; Howard, J. A. K.; Mackinnon, A.; Neretin, I. S.; Wade, K. *Chem. Commun.* **1999**, 1649.
(55) Churchill, M. R.; DeBoer, B. G. *Inorg. Chem.* **1973**, *12*, 2674.
(56) Whitaker, C. R.; Romerosa, A.; Teixidor, F.; Rius, J. *Acta Crystallogr.* **1995**, *C51*, 188.
(57) Tutusaus, O.; Teixixor, F.; Nuñez, R.; Viñas, C.; Sillanpää, R.; Kivekäs, R. *J. Organomet. Chem.* **2002**, *657*, 247.
(58) Cowie, J.; Hamilton, E. J. M.; Laurie, J. C. V.; Welch, A. J. *Acta Crystallogr.* **1988**, *C44*, 1648.
(59) Getman, T. D.; Knobler, C. B.; Hawthorne, M. F. *Inorg. Chem.* **1990**, *29*, 158.
(60) Fontaine, X. L. R.; Greenwood, N. N.; Kennedy, J. D.; Nestor, K.; Thornton-Pett, M.; Hernanek, S.; Jelinek, T.; Stibr, B. *J. Chem. Soc., Dalton Trans.* **1990**, 681.
(61) Plesek, J.; Stibr, B.; Fontaine, X. L. R.; Kennedy, J. D.; Hermanek, S.; Jelinek, T. *Collect. Czech. Chem. Commun.* **1991**, *56*, 1618.
(62) Plesek, J.; Jelinek, T.; Mares, F.; Hermanek, S. *Collect. Czech. Chem. Commun.* **1993**, *58*, 1534.

Inorg. Chem. **2008**, *47*, 9497−9508

Metallacarboranes as Building Blocks for Polyanionic Polyarmed Aryl-Ether Materials

Pau Farràs,[†,#] Francesc Teixidor,[†] Raikko Kivekäs,[‡] Reijo Sillanpää,[§] Clara Viñas,*[,†] Bohumir Grüner,[||] and Ivana Cisarova[⊥]

Institut de Ciència de Materials de Barcelona (CSIC), Campus de la U.A.B., E-08193 Bellaterra, Spain, Department of Chemistry, University of Helsinki, P.O. Box 55, FIN-00014, Finland, Department of Chemistry, University of Jyväskylä, FIN-40351, Finland, Institute of Inorganic Chemistry, Academy of Sciences of the Czech Republic, 250 68 Řez, Czech Republic, and Faculty of Natural Sciences of Charles University, Hlavova 2030, 128 42 Prague 2, Czech Republic

Received June 19, 2008

Polyanionic species have been obtained in high yield by a new route in the ring-opening reaction of cyclic oxonium [3,3′-Co(8-$C_4H_8O_2$-1,2-$C_2B_9H_{10}$)(1′,2′-$C_2B_9H_{11}$)] (**2**) by using carboxylic acids, Grignard reagents, and thiocarboranes as nucleophiles. The crystal structures of $Na_3(H_2O)(C_2H_5OH)$[1″,3″,5″-{3,3′-Co(8-O(CH_2CH_2O)$_2$-1,2-$C_2B_9H_{10}$)(1′,2′-$C_2B_9H_{11}$)}$_3$-C_6H_3] and $Na(H_2O)$[3,3′-Co(8-O(CH_2CH_2O)$_2$C(O)CH_3-1,2-$C_2B_9H_{10}$)(1′,2′-$C_2B_9H_{11}$)] show that the chain contributes three or two oxygen atoms for coordination to Na^+, and interestingly, the [3,3′-Co(1,2-$C_2B_9H_{11}$)$_2$]$^-$ moiety provides extra B−H coordination sites. These B−H···Na interactions in the solid state have also been confirmed by dynamic NMR studies in solution. These new polyanionic compounds that contain multiple carborane or metallacarborane clusters at their periphery may prove useful as new classes of boron neutron capture therapy compounds with enhanced water solubility and as a core to make a new class of dendrimers.

Introduction

The derivative chemistry of the most intensively studied anionic borate cluster, the cobaltabisdicarbollide [3,3′-Co(1,2-$C_2B_9H_{11}$)$_2$]$^-$, **1**, remains very much unexplored.[1] The fundamental reason is the synthetic strategy leading to these derivatives. Two basic substitutions may occur on [3,3′-Co(1,2-$C_2B_9H_{11}$)$_2$]$^-$, either on carbon or on boron. With few exceptions,[2] substitutions on carbon have been achieved only at an early stage of the synthetic process, that is, on the starting *o*-carborane,[3] but not by direct reaction at the [3,3′-Co(1,2-$C_2B_9H_{11}$)$_2$]$^-$ cage. Substitution at boron has been achieved under Friedel−Crafts conditions[4] or with strong alkylating agents.[5] Consequently, regioselective substitutions were not possible, and specific derivatives could be obtained only after careful separations of complex mixtures. The high yield synthesis and easy preparation of the zwitterionic 8-dioxanate [3,3′-Co(8-$C_4H_8O_2$-1,2-$C_2B_9H_{10}$)(1′,2′-$C_2B_9H_{11}$)], **2**, derivative has been reported.[6,7] Compound **2** has been proven to be susceptible to nucleophilic attack on the positively charged oxygen atom, for example, by pyrrolyl,[8] imide, cyanide or amines,[9] phenolate, dialkyl or diarylphosphite,[10] N-alkylcarbamoyldiphenylphosphine oxides,[3d] alkox-

* Author to whom correspondence should be addressed. Telefax: Int. Code +34 93 5805729. E-mail: clara@icmab.es.
† Institut de Ciència de Materials de Barcelona (CSIC).
‡ University of Helsinki.
§ University of Jyväskylä.
|| Academy of Sciences of the Czech Republic.
⊥ Faculty of Natural Sciences of Charles University.
Pau Farras is enrolled in the PhD program of the UAB.

(1) Sivaev, I. B.; Bregadze, V. I. *Collect. Czech. Chem. Commun.* **1999**, *64*, 783.
(2) (a) R, M; Chamberlin, B. L.; Scott, M. M; Melo, K. D. A. *Inorg. Chem.* **1997**, *36*, 809. (b) Rojo, I.; Teixidor, F.; Viñas, C.; Kivekäs, R.; Sillanpää, R. *Chem.—Eur. J.* **2004**, *10*, 5376.
(3) (a) Viñas, C.; Pedrajas, J.; Bertran, J.; Teixidor, F.; Kivekäs, R.; Sillanpää, R. *Inorg. Chem.* **1997**, *36*, 2482. (b) Viñas, C.; Gomez, S.; Bertran, J.; Teixidor, F.; Dozol, J. F.; Rouquette, H. *Chem. Commun.* **1998**, 191. (c) Viñas, C.; Gomez, S.; Bertran, J.; Teixidor, F.; Dozol, J. F.; Rouquette, H. *Inorg. Chem.* **1998**, *37*, 3640. (d) Viñas, C.; Bertran, J.; Gomez, S; Teixidor, F.; Dozol, J. F.; Rouquette, H.; Kivekäs, R.; Sillanpää, R. *J. Chem. Soc., Dalton Trans.* **1998**, 2849. (e) Viñas, C.; Pedrajas, J.; Teixidor, F.; Kivekäs, R.; Sillanpää, R.; Welch, A. J. *Inorg. Chem.* **1997**, *36*, 2988.
(4) Francis, J. N.; Hawthorne, M. F. *Inorg. Chem.* **1971**, *10*, 594.
(5) (a) Plesek, J.; Hermánek, S.; Base, K.; Todd, L. J.; Wright, W. F. *Collect. Czech. Chem. Commun.* **1976**, *41*, 3509. (b) Janousek, Z.; Plesek, J.; Hermánek, S.; Base, K.; Todd, L. J.; Wright, W. F. *Collect. Czech. Chem. Commun.* **1981**, *46*, 2818. (c) Rojo, I.; Teixidor, F.; Viñas, C.; Kivekäs, R.; Sillanpää, R. *Chem.—Eur. J.* **2003**, *9*, 4311.

10.1021/ic801139x CCC: $40.75
Published on Web 09/20/2008

ides,[7,11] and nucleosides,[12] resulting in one anionic species formed by the opening of the dioxane ring. A recent review[13] covers the known scope of reactions of different oxonium derivatives of polyhedral boron hydrides. The ring-opening reactions of cyclic oxonium derivatives of polyhedral boron hydrides with sulfur nucleophiles are rare and include the ring-opening reactions of cyclic oxonium derivatives of the *closo*-dodecaborate[14] and *closo*-decaborate anions with dihydrosulfide.[15] The tetramethylene oxonium *closo*-dodecaborate anion reacts with lithium derivatives of carboranes, giving the dianionic $[C_2B_{11}]-[B_{12}]$ double-cage boron compounds.[16]

Cobaltabisdicarbollide **1** has been proposed in a wide range of applications, such as the extraction of radionuclides,[3b−d,17] in conducting organic polymers,[18] or a use in medicine.[19] Recently, the construction of high-boron-content molecules has received considerable interest.[20] At the same time, the introduction of carboranes into different types of dendrimeric structures, at the inner region or at the surface of the molecules, is also being explored.[21] The design of water-soluble boron-rich dendritic or macromolecular systems is of interest for boron neutron capture therapy (BNCT) or for drug delivery systems. The *closo*-carboranes have been tested for boron delivery into tumors; however, their extreme lipophilicity often produces water-insoluble structures with limited bioavailability, precluding thus effective application of such compounds in BNCT. One solution to the problem of the water solubility of BNCT agents could be to replace a neutral carborane with an anionic metallacarborane.

Following our studies on metallacarboranes' direct substitution, we report herein on the high-yield synthesis of polyanionic species as novel high-boron-content molecules with enhanced water solubility. The synthetic ways were based on the use of carboxylic acid, Grignard reagents, and thiocarboranes as nucleophiles in the ring-opening reaction of cyclic oxonium $[3,3'\text{-}Co(8\text{-}C_4H_8O_2\text{-}1,2\text{-}C_2B_9H_{10})(1',2'\text{-}C_2B_9H_{11})]$ (**2**). The crystal structures of $Na_3(H_2O)(C_2H_5OH)[1'',3'',5''\text{-}\{3,3'\text{-}Co(8\text{-}O(CH_2CH_2O)_2\text{-}1,2\text{-}C_2B_9H_{10})(1',2'\text{-}C_2B_9H_{11})\}_3\text{-}C_6H_3]$, $[N(CH_3)_4][3,3'\text{-}Co(8\text{-}O(CH_2CH_2O)_2C(O)C_6H_5\text{-}1,2\text{-}C_2B_9H_{10})(1',2'\text{-}C_2B_9H_{11})]$, and $Na(H_2O)[3,3'\text{-}Co(8\text{-}O(CH_2CH_2O)_2C(O)CH_3\text{-}1,2\text{-}C_2B_9H_{10})(1',2'\text{-}C_2B_9H_{11})]$ are also reported.

Results and Discussion

Synthesis and Characterization of Monosubstituted Cobaltabisdicarbollide Derivatives Incorporating Three or Four Ether Groups in the *exo*-Cluster Chain. We were interested in exploring the possibility of using both known and new types of nucleophiles to get high-boron-content compounds. Although a large range of nucleophiles has already been investigated in boron clusters, we aimed to use other compounds to compare their nucleophilicity. To learn about the nucleophilic character of carboxylic acids, Grignard reagents, and thiocarboranes in the ring-opening reaction of cyclic oxonium $[3,3'\text{-}Co(8\text{-}C_4H_8O_2\text{-}1,2\text{-}C_2B_9H_{10})(1',2'\text{-}C_2B_9H_{11})]$, **2**, we have synthesized ligands incorporating both the $(OCH_2CH_2)_2R$ chain and the $[3,3'\text{-}Co(1,2\text{-}C_2B_9H_{11})_2]^-$ moiety. Chart 1 shows the anionic species synthesized from the zwitterionic **2** according to Scheme 1.

(6) (a) Plesek, J.; Hermánek, S.; Franken, A.; Cisarova, I.; Nachtigal, C. *Collect. Czech. Chem. Commun.* **1997**, *62*, 47. (b) Selucky, P.; Plesek, J.; Rais, J.; Kyrs, M.; Kadlecova, L. *J. Radioanal. Nucl. Chem.* **1991**, *149*, 131.

(7) Teixidor, F.; Pedrajas, J.; Rojo, I.; Viñas, C.; Kivekäs, R.; Sillanpää, R.; Sivaev, I.; Bregadze, V.; Sjöberg, S. *Organometallics* **2003**, *22*, 3414.

(8) Llop, J.; Masalles, C.; Viñas, C.; Teixidor, F.; Sillanpää, R.; Kivekäs, R. *Dalton Trans.* **2003**, 556.

(9) (a) Sivaev, I. B.; Starikova, Z. A.; Sjöberg, S.; Bregadze, V. I. *J. Organomet. Chem.* **2002**, *649*, 1. (b) Sivaev, I. B.; SjöbergS.; Bregadze, V. I. *International Conference Organometallic Compounds - Materials of the Next Century*, Nizhny, Novgorod, Russia, May 29−June 2, 2000.

(10) Plešek, J.; Grüner, B.; Heřmánek, S.; Báča, J.; Mareček, V.; Jänchenová, J.; Lhotský, A.; Holub, K.; Selucký, P.; Rais, J.; Císařová, I.; Čáslavský, J. *Polyhedron* **2002**, *21*, 975.

(11) (a) Grüner, B.; Mikulšek, L.; Bača, J.; Cisařova, I.; Böhmer, V.; Danila, C.; Reinoso-Garcia, M. M.; Verboom, W.; Reinhoudt, D. N.; Casnati, A.; Ungaro, R. *Eur. J. Org. Chem.* **2005**, 2022. (b) Mikulašek, L.; Grüner, B.; Danila, C.; Böhmer, V.; Časlavsky, J.; Selucky, P. *Chem. Commun.* **2006**, 4001.

(12) (a) Olejniczak, A. B.; Pleek, J.; Kříž, O.; Lesnikowski, Z. J. *Angew. Chem., Int. Ed.* **2003**, *42*, 5740. (b) Lesnikowski, Z. J.; Paradowska, E.; Olejniczak, A. B.; Studzinska, M.; Seekamp, P.; Schüβler, U.; Gabel, D.; Schinazi, R. F.; Plešek, J. *Bioorg. Med. Chem.* **2005**, *13*, 4168. (c) Olejniczak, A. B.; Plešek, J.; Lesnikowski, Z. J. *Chem.—Eur. J.* **2007**, *13*, 311.

(13) Semioshkin, A. A.; Sivaev, I. B.; Bregadze, V. I. *Dalton Trans.* **2008**, 977.

(14) Crossley, E. L.; Rendina, L. M. *RACI Inorganic Conference*, Hobart, Tasmania, February 2007.

(15) (a) Voloshin, Ya. Z.; Varzatskii, O. A.; Zhizhin, K. Yu; Kuznetsov, N. T. *XXIII Chugaev International Conference on Coordination Chemistry*, Odessa, Ukraine, September 2007. (b) Voloshin, Ya. Z.; Varsatskii, O. A.; Bubnov, Yu. N. *Russ. Chem. Bull.* **2007**, *56*, 577.

(16) Sivaev, I. B.; Sjöberg, S.; Bregadze, V. I. *J. Organomet. Chem.* **2003**, *680*, 106.

(17) (a) Grüner, B.; Plešek, J.; Báča, J.; Císařová, I.; Dozol, J.-F.; Rouquette, H.; Viňas, C.; Selucký, P.; Rais, J. *New J. Chem.* **2002**, *26*, 1519. (b) Rais, J.; Grüner, B. In *Ion Exchange and Solvent Extraction*; Marcus, Y., Sengupra, A. K.; CRC Press: Boston, 2004; Vol. *17*, p 243. (c) Mikulasek, L.; Grüner, B.; Crenguta, D.; Rudzevich, V.; Boehmer, V.; Haddaoui, J.; Hubscher-Bruder, V.; Arnaud-Nue, F.; Caslavsky, J.; Selucký, P. *Eur. J. Org. Chem.* **2007**, 4772.

(18) (a) Masalles, C.; Borros, S.; Viñas, C.; Teixidor, F. *Adv. Mater.* **2000**, *12*, 1199. (b) Masalles, C.; Llop, J.; Viñas, C.; Teixidor, F. *Adv. Mater.* **2002**, *14*, 826. (c) Masalles, C.; Borrós, S.; Viñas, C.; Teixidor, F. *Adv. Mater.* **2002**, *14*, 449. (d) Svorcik, V.; Gardasova, R.; Rybka, V.; Hnatowicz, V.; Cervena, J.; Plešek, J. *J. Appl. Polym. Sci.* **2004**, *91*, 40.

(19) (a) Hao, E.; Vicente, M. G. H. *Chem. Commun.* **2005**, 1306. (b) Barth, R. F.; Coderre, J. A.; Vicente, M. G. H.; Blue, T. E. *Clin. Cancer Res.* **2005**, *11*, 3987. (c) Gottumukkala, V.; Ongayi, O.; Baker, D. G.; Lomax, L. G.; Vicente, M. G. H. *Bioorg. Med. Chem.* **2006**, *14*, 1871. (d) Wang, J.-Q.; Ren, C.-X.; Weng, L.-H.; Jin, G.-X. *Chem. Commun.* **2006**, 162. (e) Bregadze, V. I.; Sivaev, I. B.; Glazun, S. A. *Anti-Cancer Agents Med. Chem.* **2006**, *6*, 75. (f) Cigler, P.; Kožišek, M.; Řezačova, P.; Brynda, J.; Otwinowski, Z.; Pokorna, J.; Plešek, J.; Gruner, B.; Doleˇckova-Marešova, L.; Maša, M.; Sedlaˇcek, J.; Bodem, J.; Kräusslich, H.; Kral, V.; Konvalinka, J. *PNAS* **2005**, *102*, 15394.

(20) (a) Thomas, J.; Hawthorne, M. F. *Chem Commun.* **2001**, 1884. (b) Azev, Y.; Slepukhina, I.; Gabel, D. *Appl. Radiat. Isot.* **2004**, *61*, 1107. (c) Ma, L.; Hamdi, J.; Wong, F.; Hawthorne, M. F. *Inorg. Chem.* **2006**, *45*, 278. (d) Genady, A. R.; El-Zaria, M. E.; Gabel, D. *J. Organomet. Chem.* **2004**, *689*, 3242. (e) Luguya, R.; Fronczek, F. R.; Smith, K. M.; Vicente, M. G. H. *Appl. Radiat. Isot.* **2004**, *61*, 1117. (f) Clark, J. C.; Fronczek, F. R.; Vicente, M. G. H. *Tetrahedron Lett.* **2005**, *46*, 2365.

(21) (a) Newkome, G. R.; Moorefield, C. N.; Keith, J. M.; Baker, G. R.; Escamilla, G. H. *Angew. Chem., Int. Ed. Engl.* **1994**, *33*, 666. (b) Barth, R. F.; Adamns, D. M.; Solovay, A. H.; Alam, F.; Darby, M. V. *Bioconjugate Chem.* **1994**, *5*, 58. (c) Armspach, D.; Cattalini, M.; Constable, E. C.; Housecroft, C. E.; Phillips, D. *Chem. Commun.* **1996**, 1823. (d) Qualman, B.; Kessels, M. M.; Musiol, H.-J.; Sierralta, W. D.; Jungblut, P. W.; Moroder, L. *Angew. Chem., Int. Ed. Engl.* **1996**, *35*, 909. (e) Parrott, M. C.; Marchington, E. B.; Valliant, J. F.; Adronov, A. *J. Am. Chem. Soc.* **2005**, *127*, 12081. (f) Nuñez, R.; González, A.; Viñas, C.; Teixidor, F.; Sillanpää, R.; Kivekäs, R. *Org. Lett.* **2005**, *7*, 231. (g) Nuñez, R.; González, A.; Viñas, C.; Teixidor, F.; Sillanpää, R.; Kivekäs, R. *Organometallics* **2005**, *24*, 6351.

Chart 1. Monosubstituted **2**−**16** Anions

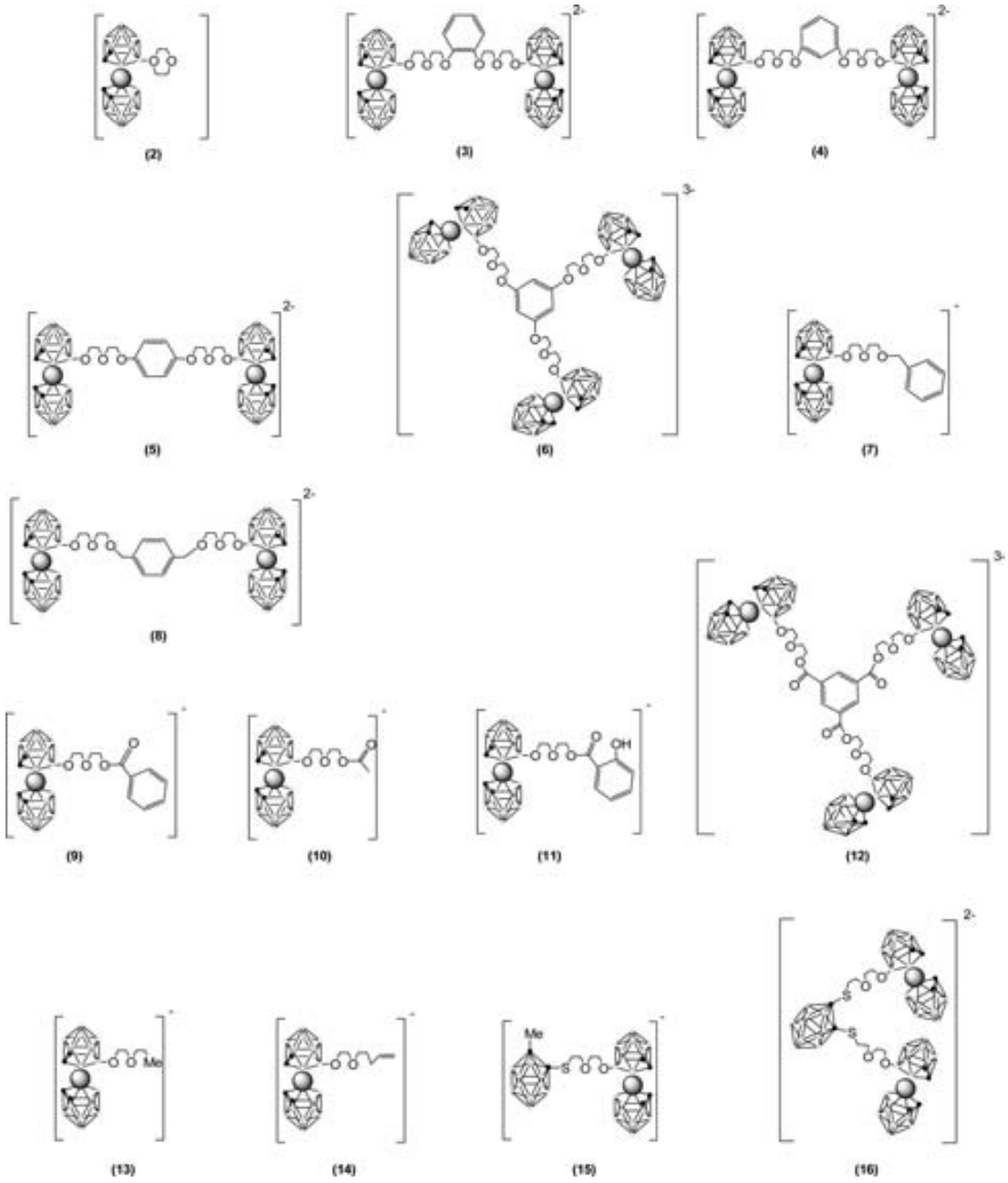

In order to enchance the nucleophilic character of the alcohols and thiocarboranes, we used *n*-BuLi to deprotonate the nucleophile. The addition of the base was done dropwise at low temperatures, and it was left stirring for 1 h. Afterward, the reaction was cooled down again to −40 °C, followed by the addition of **2**. After stirring overnight, the compounds (**3**−**8** and **15** and **16**) were isolated either by evaporation of the solvent or by a cationic metathesis to tetramethylammonium salts, getting in all cases orange solids as the final product. For the organic carboxylic acids, their salts were used as nucleophiles, whereas the Grignard reagents were used as obtained. For these cases, the reagents were mixed together, and after stirring overnight, the compounds (**9**−**14**) were isolated by evaporation of the solvent or by cationic exchange. As the reactivity of Grignard reagents is very high and to prevent the formation of undesired side products, their addition was done dropwise at low temperatures.

The nature of anions **3**−**16** with cations like $[N(CH_3)_4]^+$, Li^+, and Na^+ has been corroborated by elemental analysis, matrix-assisted laser desorption/ionization−time of flight mass spectrometry (MALDI-TOF-MS); IR; and ^1H, $^1H\{^{11}B\}$, $^{13}C\{^1H\}$, ^{11}B, and $^{11}B\{^1H\}$ NMR spectroscopies. For $Na_3[\mathbf{6}]\cdot H_2O\cdot C_2H_5OH$, $[N(CH_3)_4][\mathbf{9}]$ and $Na_2[\mathbf{10}]_2\cdot 2H_2O$, the solid-state X-ray crystal structures were also determined.

Scheme 1. Opening of the *exo*-Cluster Dioxanate Ring Reaction by Nucleophilic Attack[a]

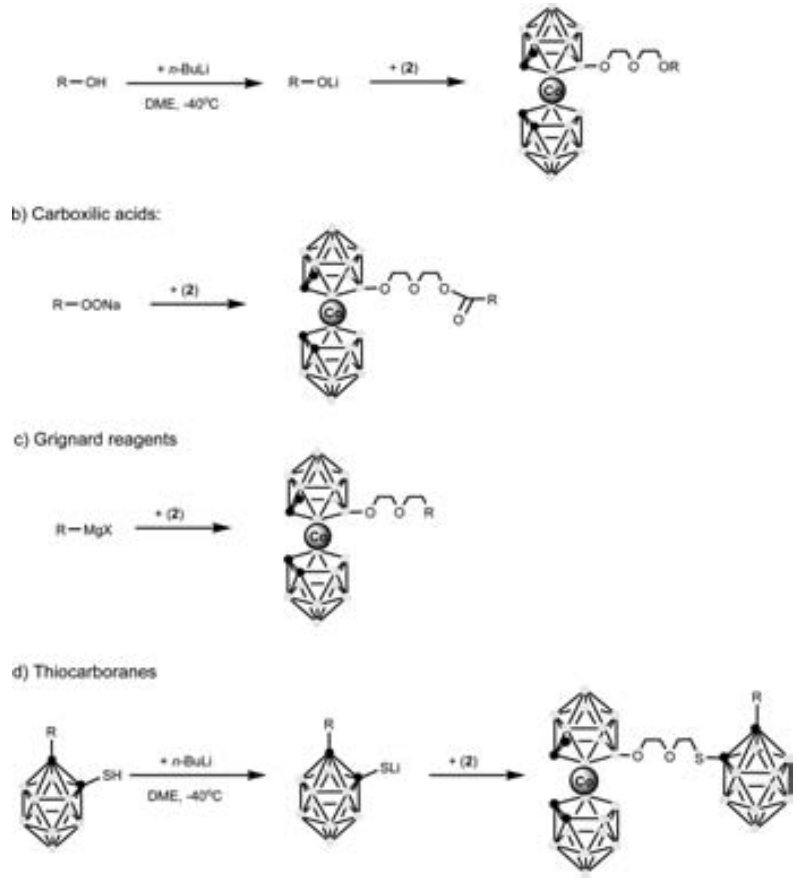

[a] Atoms in black are CH vertexes, the rest of the vertices in the clusters are BH.

Table 1. $^{11}B\{^1H\}$ NMR Spectra (all in ppm) of B(8) Monosubstituted Derivatives of $[3,3'\text{-}Co(1,2\text{-}C_2B_9H_{11})_2]^-$[a]

1	6.5B(8,8′)		1.4B(10,10′)		−6.0 B(4,4′,7,7′,9,9′,12,12′)			−17.2 B(5,5′,11,11′)		−22.7 B(6,6′)		<δ> −8.1
	24.6	8.4	4.9	−2.7	−4.1	−8.0	−9.3	−15.0	−18.5	−20.8	−26.5	
2	*B(8)*	B(8′)	B(10)	B(10′)	B(4′,7′)	B(4,7)	B(9,9′,12,12′)	B(5′,11′)	B(5,11)	B(6)	B(6′)	−7.8
3	*25.5*	6.4	2.8	−0.2	−2.0	−5.0	−5.9	−15.1	−18.2	−19.5	−26.3	−6.4
4	*25.3*	6.3	2.8	−0.1	−1.8	−5.1	−5.8	−14.9	−18.0	−19.5	−26.0	−6.3
5	*25.2*	6.2	2.8	−0.1	−1.7	−5.1	−5.8	−14.9	−18.0	−19.5	−26.0	−6.3
6	*25.3*	6.3	2.8	−0.1	−1.9	−5.1	−5.8	−14.9	−18.1	−19.6	−26.1	−6.4
7	*25.0*	5.9	2.7	−0.2	−1.9	−5.2	−6.0	−15.0	−18.2	−19.5	−26.2	−6.5
8	*25.2*	6.2	2.7	−0.2	−1.9	−5.1	−5.9	−15.0	−18.2	−19.5	−26.2	−6.8
9	*30.3*	11.3	7.9	5.0	3.3	0.0	−0.8	−9.8	−12.9	−14.4	−21.0	**-1.6**
10	*30.5*	11.5	7.9	5.1	3.3	−0.1	−0.7	−9.7	−12.8	−14.3	−20.9	**-1.2**
11	*25.3*	6.3	2.6	−0.2	−2.1	−5.2	−6.1	−15.1	−18.3	−19.8	−26.5	−6.6
12	*23.6*	4.7	1.1	−1.8	−3.5	−6.7	−7.5	−16.5	−19.7	−21.2	−27.6	**-8.0**
13	*25.2*	6.3	2.7	−0.2	−1.9	−5.1	−5.9	−14.9	−18.0	−19.5	−26.1	−6.4
14	*22.8*	3.7	−0.4	−2.5	−4.1	−7.5	−8.3	−17.3	−20.5	−21.9	−28.4	**-8.8**

[a] In each column, the number of boron atoms is preserved. In italics are represented the resonances due to B−O. <δ> is the mean value of the ^{11}B NMR spectrum for each compound.

NMR Spectral Considerations. The $^{11}B\{^1H\}$ NMR spectra of anions **3**−**16** featured an identical 1:1:1:1:2:2:4:2:2:1:1 pattern ranging from +31 to −28 ppm. The $^{11}B\{^1H\}$ NMR of **2** and monosubstituted **3**−**16** anions, except for the carborane-containing molecules, are shown in Table 1. The resonance at the lowest field remains as a singlet in the ^{11}B NMR spectrum, corresponding to the B(8) substituted boron atom. The mean value <δ> of the ^{11}B NMR spectrum of each compound is also presented in Table 1. This value represents the electronic effect of the B(8) substituent in the cluster. The <δ> of $[3,3'\text{-}Co(1,2\text{-}C_2B_9H_{11})_2]^-$, **1**, is −8.1, and the introduction of the dioxane moiety in the zwiterionic species **2** produces a deshielding of 0.3 ppm due to the withdrawing effect of the B−O bond. When the ring opening has taken place, a <δ> value in the range −6.3 to −6.8 is observed for most of the compounds except for **9**, **10**, **12**, and **14**.

The observed ^{11}B NMR pattern, 1:1:1:1:2:2:4:2:2:1:1, reflects the C_s symmetry of the molecules (12 different signals). The boron resonance with a relative intensity of 4 is due to a coincidental overlap of two resonances with a

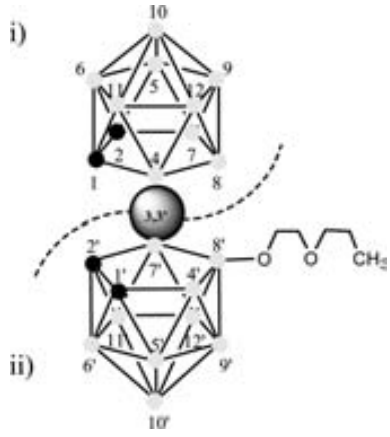

Figure 1. The $^{11}B\{^1H\}$ NMR spectrum of **13** is the result of the addition of the two individual halves: i + ii. Vertexes numbering for **13**.

2:2 relative intensity. The $^{11}B\{^1H\}$ NMR of [3,3′-Co(1,2-$C_2B_9H_{11})_2$]$^-$ displays five resonances in the range +6.5 to −22.7 ppm with a 2:2:8:4:2 pattern, in agreement with an averaged C_{2v} symmetry. The ^{11}B NMR chemical shifts' assignments of [3,3′-Co(1,2-$C_2B_9H_{11})_2$]$^-$ were determined by 2D $^{11}B\{^1H\}-^{11}B\{^1H\}$ COSY spectroscopy and correspond to B(8,8′), B(10,10′), B(4,4′,7,7′,9,9′,12,12′), B(5,5′,11,11′), and B(6,6′) from low to high field.[22] The incorporation of one substituent at position B(8) lowers the symmetry to C_s, maintaining only one symmetry plane and making the two dicarbollide moieties no longer equivalent. A stick representation of the chemical shifts and relative intensities in the $^{11}B\{^1H\}$ NMR spectra of [3,3′-Co(1,2-$C_2B_9H_{11})_2$]$^-$ and **13** are shown in Figure S.1 (Supporting Information).We have reported[7,11] that the ^{11}B NMR spectrum of monosubstituted derivatives of [3,3′-Co(1,2-$C_2B_9H_{11})_2$]$^-$ is the result of the plain addition of the two individual halves, as schematized in Figure 1. As an example, the $^{11}B\{^1H\}$ NMR of Cs[3,3′-Co(8-$(OCH_2CH_2)_2CH_3$-1,2-$C_2B_9H_{10}$)(1′,2′-$C_2B_9H_{11}$)] (**13**) is the addition of the $^{11}B\{^1H\}$ NMR of the parent Cs[3,3′-Co(1,2-$C_2B_9H_{11})_2$] plus the spectrum of [3,3′-Co((8,8′-$(OCH_2CH_2)_2CH_3)_2$-1,2-$C_2B_9H_{10})_2$]$^-$. The spectrum of Cs[3,3′-Co(1,2-$C_2B_9H_{11})_2$] displays resonances at 6.5(1), 1.4(1), −6.0(4), −17.2(2), and −22.7(1) ppm, and the spectrum of Cs[3,3′-Co(8-$(OCH_2CH_2)_2CH_3$-1,2-$C_2B_9H_{10}$)(1′,2′-$C_2B_9H_{11}$)] (**13**) displays resonances at 25.2(1), 6.3(1), 2.7(1), −0.2(1), −1.9(2), −5.1(2), −5.9(4), −14.9(2), −18.0(2), −19.5(1), and −26.1(1) ppm. If resonances attributable to the unsubstituted ligand, showing only minor shifts in respect to parent Cs[3,3′-Co(1,2-$C_2B_9H_{11})_2$], are removed, the resonances of the unknown disubstituted [3,3′-Co(8,8′-$(OCH_2CH_2)_2CH_3)_2$-1,2-$C_2B_9H_{10})$]$^-$ ligand could be clearly distinguished and assigned at 25.2(1), −0.2(1), −1.9(2), −5.1(2), −14.9(2), and −19.5(1) ppm. The 1:1:2:2:2:1 pattern is consistent with a C_s fragment symmetry, and the high chemical shift value at 25.2 strongly supports assignment to B(8)−O−.

Stuctures of the Salts in the Solid State. Red crystals, suitable for X-ray diffraction structure determination, were obtained from diffusion crystallization using a CH_2Cl_2/C_2H_5OH/*i*-octane system. Interesting features in the structure (Figure 2 and Table S.1, Supporting Information) consist of the coordination of three sodium atoms. This evidence, species **6** exists in solution and in the solid state as the true trivalent anion, points to no possible exchange of sodium for the proton having occurred even after aqueous treatment. This can be assumed to be a result of the relatively tight coordination of each sodium atom by all three oxygens (with the exception of Na2, where the distance Na2−O4 is unbonding) present in ethyleneglycol chains. Another coordination site is formed by B(8′)− and B(4′ or 7′)−H···Na bonding interactions. Along with a few univalent anion structures where B(8′)−H···M^+ (M = Na^+ or K^+) bonds were present,[7,10] this is the most convincing example of high hydrolytic stability of this kind of coordination. The coordination sphere of sodium atom Na1 is completed by a molecule of ethanol. One molecule of water is coordinated to the Na2 sodium atom, replacing coordination by the O4 oxygen from the trihydroxybenzene, which remains at a long unbonded distance (2.757 Å).

Crystallization by slow diffusion of a dichloromethane solution of [$N(CH_3)_4$][**9**] at room temperature afforded air- and moisture-insensitive red single crystals suitable for X-ray analysis, which confirmed the proposed structure of [$N(CH_3)_4$][**9**]. A drawing of the compound is shown in Figure 3, and selected bond lengths and angles are listed in Table S.2 (Supporting Information). The cation and the anion are held together by electrostatic forces. Weak H bonds (C2H2···O4^i and C2′H2′···O4^i, i = 1/2 + x, 1/2 − y, 1/2 + z) can be found. Other weak interactions are BH···C(phenyl) and BH···H and CH···H contacts.

Crystallization by the slow diffusion of a toluene solution of Na[**10**] at room temperature afforded air- and moisture-insensitive yellow needle-shaped single crystals suitable for X-ray analysis, which revealed that the polymeric structure with dinuclear [$Na_2(H_2O)_2$(**10**)$_2$] units had formed (the compound is named as Na_2[**10**]$_2$·$2H_2O$ in the text). A drawing of the dinuclear unit with the extra O4 and C17 atoms which are part of the molecules that link the dinuclear units to polymers is shown in Figure 4, and selected bond lengths and angles are listed in Table S.3 (Supporting Information). The ligand [**10**]$^-$ coordinates as a tetradentate ligand in the solid state. Also, two bridging water molecules bond to the sodium cation that has a distorted octahedral coordination sphere. The distortions in bonding are due to a rigid carborane polyether ligand. It is typical for Na^+ to use two bridged water molecules to fullfil its coordination sphere (88 hits in the Cambridge Structural Database, CSD, version 5.29, November 2007).

The Na−O1 and Na−O2 bonds are 2.393(3) Å and 2.362(3) Å, respectively. Due to the negative charge of the ligands, the sodium is bonded quite tightly to the ligand's oxygen atoms. For example, the shortest Na−O distances in the dinuclear [Na(L)]I compound are 2.375 and 2.395 Å, whereas there are several longer Na−O bonds (L = cyclic polyether).[23]

(22) Janousek, Z.; Plesek, J.; Hermanek, S.; Base, K; Todd, L. J.; Wright, W. F. *Collect. Czech. Chem. Commun.* **1981**, *46*, 2818.

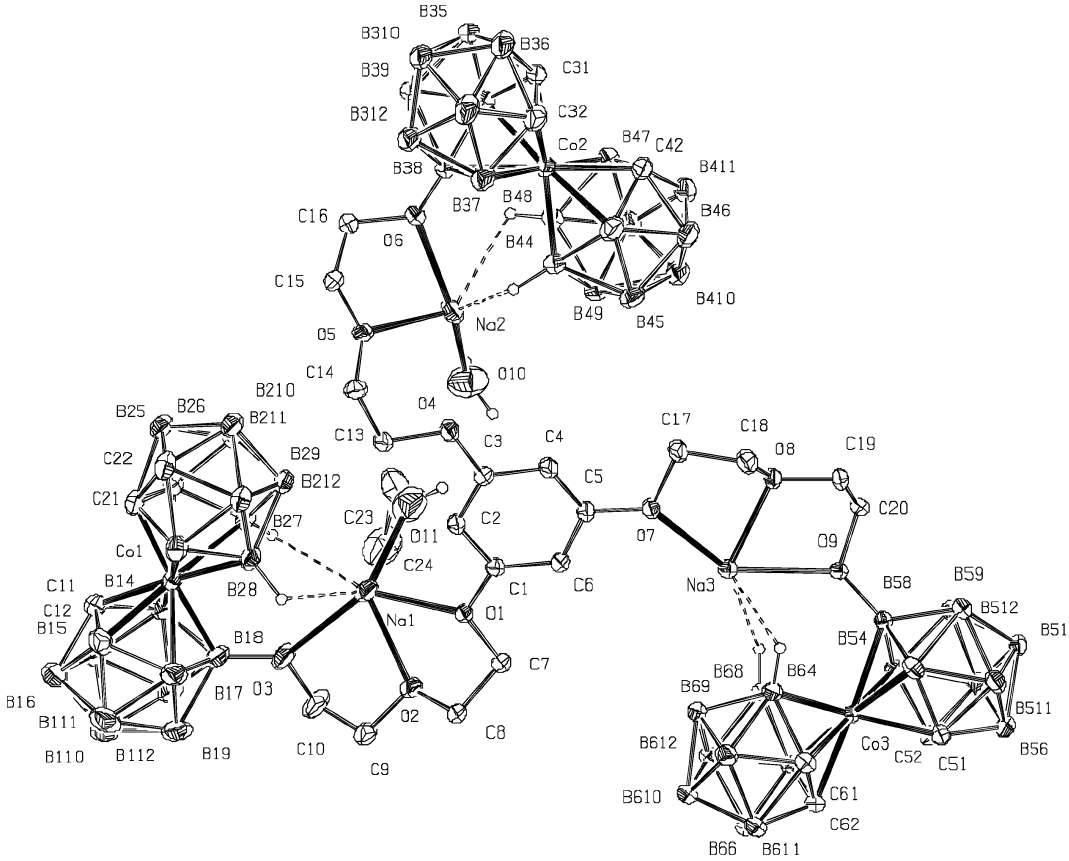

Figure 2. Overall view on the Na_3[**6**]·H_2O·C_2H_5OH salt. The displacement ellipsoids are drawn on the 30% probability level (PLATON).

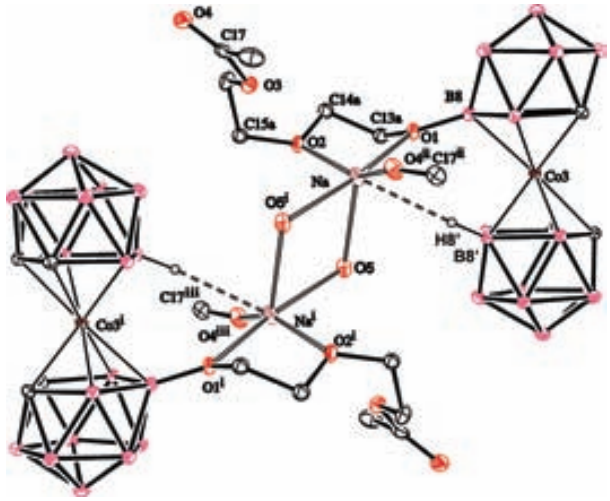

Figure 3. Solid-state structure of [$N(CH_3)_4$][**9**]. From the disordered alkyl chain, only the main conformer (74%) is depicted.

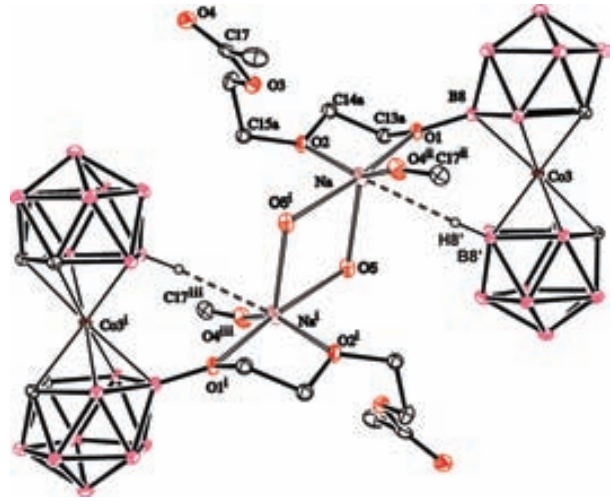

Figure 4. Dinuclear structural motif of Na_2[**10**]$_2$·$2H_2O$. Hydrogens are omitted for clarity (except H8′). From the disordered alkyl chain, only the main conformer (75%) is depicted. Half of the molecule has been generated by inversion ($i = -x, 1 - y, -z$). Also, a part of the coordinating ester group (O4 and C17) with symmetry operations $ii = -1/2 - x, -1/2 + y, z$ and $iii = 1/2 + x, 11/2 + y, -z$ is presented.

The packing in Na_2[**10**]$_2$·$2H_2O$ is dominated by the shortest Na−O4(ester carbonyl) bond, 2.327 Å (that causes polymerization), from the neighbor molecule and weak van der Waal's interactions.

Coordination in Solution. Although definitive evidence for B−H···Na^+ interactions in the solid state is given by the X-ray analysis of the sodium salt of **10**, no proof of its existence in solution has been found in the $^1H\{^{11}B\}$ NMR spectrum at room temperature. We have run low-temperature experiments with the aim of freezing out the more stable rotamers and fixing specific B−H···Na^+ interactions. How-

(23) Rogers, R. D.; Bond, A. H.; Henry, R. F.; Rollins, A. N. *Supramol. Chem.* **1994**, *4*, 191.

ever, we have noticed that even at room temperature the compound is extremely dependent upon the solvent. Figure S.2 (Supporting Information) shows a comparison between $^1H\{^{11}B\}$ NMR spectra recorded in acetone and those in dichloromethane. Although peaks corresponding to B−H bonds do not change much, it can be observed that the broad signal corresponding to C_c−H in acetone has moved upfield, splitting into two singlets in dichloromethane. The shape of the ^1H NMR spectrum in dichloromethane resembles the corresponding spectrum of any B(8)−O monosubstituted ligand where the four C_c−H's should appear as a 2:2 pattern.

Variable-temperature $^1H\{^{11}B\}$ NMR spectra recorded in the range 295−204 K using dichloromethane as a solvent are shown in Figure S.3 (Supporting Information). As it can be seen, there is a high dependence of the chemical shift of one B−H signal on the temperature. This B−H resonance becomes broader and shifts to lower field as the temperature decreases. These spectroscopic data are in agreement with intramolecular B−H···Na^+ or Na^+···O interactions, most probably corresponding to those observed in the solid state (Figure 4). The NMR data above −70 °C could be explained either by the rapid exchange between the available geometric rotamers providing different B−H···Na^+ interactions or by a progressive increase in the number of molecules whose B−H···Na^+ interactions have been replaced by coordinating solvent molecules. There is also a significant change in the shift of the CH_2 at 4.34 ppm as the temperature decreases, due to the C−H···Na^+ interactions also observed in the X-ray analysis.

The Role of the Electron-Rich Atom (O) Directly Bonded to a Cluster Boron Atom. It has been proven that anionic monothioether- and monophosphine-*nido*-carborane clusters containing electron-rich *exo*-cluster substituents (S or P) dissipate electron density into the electron-rich element.[24] This element becomes a strong Lewis base and a very good coordinating ligand.[25] Most probably the oxygen atom in the B(8)−O bond in **3**−**16** can play the same role as S and P atoms, dissipating the negative charge and becoming a strong Lewis base. Thus, the anionic **3**−**16** species can coordinate to a Lewis acid through the oxygen atom at the B(8) position. The existence of a second oxygen atom that can also interact with the Lewis acid like sodium or lithium cations (M) forming a O···M···O interaction facilitates the coordination.

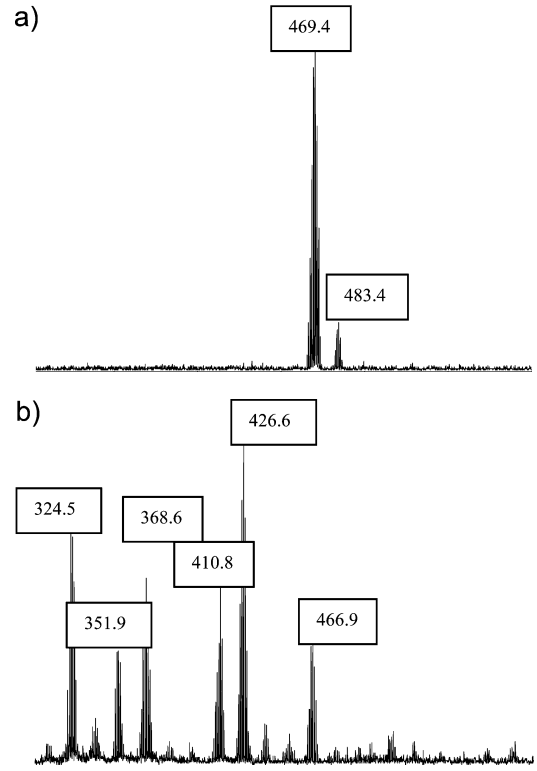

Figure 5. MALDI-TOF-MS spectra of compounds **3** (a) and **5** (b). See the Experimental Section for the fragmentation.

MALDI[26] supports, although does not confirm, the special nucleophilic character of the B−O unit. Compounds **3**−**16** were studied by the MALDI-MS technique at the negative ion mode without the use of matrices. The lack of matrices aids the interpretation of the primary and secondary mechanisms. We understand as a "primary" mechanism the separation of the anionic cobaltabisdicarbollide derivatives from the bonded cation. The "secondary" mechanism can give some clues about the nucleophilic character of the electron-rich oxygen atom directly bonded to the cluster B(8) boron atom. Figure 5 shows the MALDI-TOF-MS spectra of compounds **3** and **5** as a representative example. A peak with an ion mass higher than the molecular ion peak at 469.4 ((M + Li)/2) is observed at 483.4, although with less intensity, corresponding to (M + CH_2). This had been noted previously[7] and can be interpreted as an electrophilic reaction between like anions. Of more importance is the different behavior between isomers on the interaction between the polyether chain and the cation, O−M−O, and their own stability against the laser pulse. For compound **3**, the strong interaction with O−Li−O allows that the cation is ionized along with the molecule, and the peak corresponding to (M + Li) appears in the spectra. However, in compound **5**, this is not observed, probably due to the longer distance between the two polyether chains. Moreover, compound **3** stays almost intact upon applying the laser pulse with only two

(24) (a) Teixidor, F.; Casabó, J.; Viñas, C.; Sanchez, E.; Escriche, Ll.; Kivekäs, R. *Inorg. Chem.* **1991**, *30*, 3053–3058. (b) Teixidor, F.; Flores, M. A.; Viñas, C.; Kivekäs, R.; Sillanpää, R. *Angew. Chem.* **1996**, *108*, 2388. Teixidor, F.; Flores, M. A.; Viñas, C.; Kivekäs, R.; Sillanpää, R. *Angew. Chem., Int. Ed. Engl.* **1996**, *35*, 2251. (c) Teixidor, F.; Núñez, R.; Viñas, C.; Sillanpää, R.; Kivekäs, R. *Inorg. Chem.* **2001**, *40*, 2587.

(25) (a) Teixidor, F.; Flores, M. A.; Viñas, C.; Kivekäs, R.; Sillanpää, R. *J. Am. Chem. Soc.* **2000**, *122*, 1963. (b) Teixidor, F.; Romerosa, A; Viñas, C.; Rius, J.; Miravitlles, C.; Casabó, J. *J. Chem. Soc., Chem. Comm.* **1991**, 192. (c) Teixidor, F.; Ayllón, J. A.; Viñas, C.; Rius, J.; Miravitlles, C.; Casabó, J. *J. Chem. Soc., Chem. Comm.* **1992**, 1279. (d) Teixidor, F.; Casabó, J.; Romerosa, A. M.; Viñas, C.; Rius, J.; Miravitlles, C. *J. Am. Chem. Soc.* **1991**, 9895.

(26) (a) Karas, M.; Hillenkamp, F. *Anal. Chem.* **1988**, *60*, 2299. (b) Karas, M.; Bachmann, D.; Hillenkamp, F. *Anal. Chem.* **1985**, *57*, 2935. (c) Tanaka, K.; Waki, H.; Ido, Y.; Akita, S.; Yoshida, Y.; Yoshida, T. *Rapid Commun. Mass Spectrom.* **1988**, *2*, 151.

peaks in its MALDI-TOF spectrum. This can be explained again for the strong O−Li−O interaction present in the molecule. The decomposition in **5** is explained by breaking the molecule into smaller parts, and all the peaks in their MALDI-TOF spectra can be assigned thereby.

Conclusions

The present study has opened a new route in the ring-opening reaction of cyclic oxonium [3,3′-Co(8-$C_4H_8O_2$-1,2-$C_2B_9H_{10}$)(1′,2′-$C_2B_9H_{11}$)] (**2**) by using carboxylic acids, Grignard reagents, and thiocarboranes as nucleophiles. The crystal structures of $Na_3(H_2O)(C_2H_5OH)$[1″,3″,5″-{3,3′-Co-(8-$O(CH_2CH_2O)_2$-1,2-$C_2B_9H_{10}$)(1′,2′-$C_2B_9H_{11}$)}$_3$-C_6H_3] and $Na(H_2O)$[3,3′-Co(8-$O(CH_2CH_2O)_2C(O)CH_3$-1,2-$C_2B_9H_{10}$)(1′,2′-$C_2B_9H_{11}$)] show that the polyether chain contributes three oxygen atoms for coordination to Na^+, and interestingly, the [3,3′-Co(1,2-$C_2B_9H_{11})_2$]$^-$ moiety provides extra B−H coordination sites. The availability of B−H groups and their geometrical distribution offers an extraordinary possibility to satisfy metal's demand. These B−H−Na interactions in the solid state have also been confirmed by dynamic NMR studies in solution. We have shown that polyanionic species, as novel high-boron-content molecules, can be obtained in high-yield synthesis. Furthermore, compounds **13**−**16** can be used as cores to make a new class of dendrimers that contain multiple carborane or metallacarborane clusters at their periphery. Further work to synthesize potential new classes of BNCT water-soluble compounds is now underway.

Experimental Section

Instrumentation. Elemental analyses were performed using a Carlo Erba EA1108 microanalyzer. IR spectra were recorded from KBr pellets on a Shimadzu FTIR-8300 spectrophotometer. The ^{1}H NMR, ^{1}H{^{11}B} NMR (300.13 M), ^{11}B NMR (96.29 M), and ^{13}C{^{1}H} NMR (75.47 M) spectra were recorded with a Bruker ARX 300 instrument equipped with the appropriate decoupling accessories using deuterated acetone as the solvent. Chemical shift values for ^{11}B NMR spectra were referenced to external BF_3·OEt_2, and those for ^{1}H, ^{1}H{^{11}B}, and ^{13}C{^{1}H} NMR spectra were referenced to $Si(CH_3)_4$. Chemical shifts are reported in units of parts per million downfield from the reference, and all coupling constants are reported in hertz. The mass spectra were recorded in the negative ion mode using a Bruker Biflex MALDI-TOF-MS (N_2 laser; λ_{exc} 337 nm, 0.5 ns pulses; voltage ion source 20.00 kV (Uis1) and 17.50 kV (Uis2)) or in the negative ion mode using a Bruker Daltonics esquire3000 (N_2 laser; λ_{exc} 337 nm, 0.5 ns pulses; Skim1 voltage 37.5 V).

Materials. Experiments were carried out, except when noted, under a dry, oxygen-free dinitrogen atmosphere using standard Schlenk techniques, with some subsequent manipulation in the open laboratory. 1,2-Dimethoxyethane (DME) and tetrahydrofuran (THF) were distilled from sodium benzophenone before use. Other solvents were reagent grade. All organic and inorganic salts were Fluka or Aldrich analytical reagent grade and were used as received. [8-{3,3′-Co(8-$C_4H_8O_2$-1,2-$C_2B_9H_{10}$)(1′,2′-$C_2B_9H_{11}$)] (**2**), 1-SH-2-CH_3-*closo*-1,2-$C_2B_{10}H_{10}$, and 1,2-SH-*closo*-1,2-$C_2B_{10}H_{10}$ were prepared according to the literature.[27]

Synthesis of [Li_2(DME)][1″,2″-{3,3′-Co(8-$O(CH_2CH_2O)_2$-1,2-$C_2B_9H_{10}$)(1′,2′-$C_2B_9H_{11}$)}$_2$-C_6H_4] (3). Under an inert atmosphere, *n*-butyllithium (0.305 mL, 0.488 mmol; 1.6 M in hexanes) was added dropwise to a stirred solution of catechol (25.6 mg, 0.232 mmol) in 15 mL of anhydrous DME at −40 °C. The resulting solution was stirred for 1 h at a low temperature. Then, a solution of **2** (200 mg, 0.488 mmol) in 15 mL of anhydrous DME was added dropwise at a low temperature. After stirring overnight, a white precipitate appeared and was discarded. The solvent was removed, and acidic water (20 mL; 1 M HCl) was added to the orange residue. This was extracted with diethyl ether (3 × 20 mL). The solvent was removed; the product was redissolved in the minimum volume of ethanol, and an aqueous solution containing an excess of [$N(CH_3)_4$]Cl was added, resulting in the formation of an orange precipitate. This was filtered off, washed with water and petroleum ether, and dried in vacuo. Yield: 0.333 g (74%). Anal. calcd for $C_{26}H_{72}B_{36}Co_2Li_2O_8$: C, 30.21; H, 7.02. Found: C, 29.40; H, 6.62. IR: ν (cm^{-1}) 3043 (C_c−H), 2947, 2877, 2752 (C−H)$_{alkyl}$, 2607, 2597, 2561, 2478, 2357 (B−H), 1505, 1475 δ(CH_2), 1253 δ(CH), 1160 (C−O−C). ^{1}H NMR: δ 7.04−6.92 (m, 4H, C_6H_4), 4.24 (br s, 8H, C_c−H), 4.19 (t, ^3J(H,H) = 5, 4H, OCH_2CH_2), 3.85 (t, ^3J(H,H) = 5, 4H, OCH_2CH_2), 3.64 (t, ^3J(H,H) = 2, 8H, OCH_2CH_2), 3.45 (s, 4H, DME), 3.27 (s, 6H, DME), 2.92−1.47 (m, 34H, B−H). ^{1}H{^{11}B} NMR: δ 7.04−6.92 (m, 4H, C_6H_4), 4.24 (br s, 8H, C_c−H), 4.19 (t, ^3J(H,H) = 5, 4H, OCH_2CH_2), 3.85 (t, ^3J(H,H) = 5, 4H, OCH_2CH_2), 3.64 (t, ^3J(H,H) = 2, 8H, OCH_2CH_2), 3.45 (s, 4H, DME), 3.27 (s, 6H, DME), 2.92 (s, 8H, B−H), 2.75 (s, 4H, B−H), 2.71 (s, 2H, B−H), 2.52 (s, 2H, B−H), 2.01 (s, 4H, B−H), 1.79 (s, 4H, B−H), 1.66 (s, 4H, B−H), 1.56 (s, 4H, B−H), 1.47 (s, 2H, B−H). ^{13}C{^{1}H} NMR: δ 121.63 (s, C_6H_4), 114.86 (s, C_6H_4), 71.87 (s, OCH_2), 71.54 (s, OCH_2), 69.23 (s, OCH_2), 68.38 (s, OCH_2), 54.15 (s, C_c−H), 46.41 (s, C_c−H). ^{11}B NMR: δ 25.5 (s, 2B, B(8)), 6.4 (d, ^1J(B,H) = 135, 2B), 2.8 (d, ^1J(B,H) = 148, 2B), −0.2 (d, ^1J(B,H) = 158, 2B), −2.0 (d, ^1J(B,H) = 165, 4B), −5.0 (d, ^1J(B,H) = 84, 4B), −5.9 (d, ^1J(B,H) = 114, 8B), −15.1 (d, ^1J(B,H) = 150, 4B), −18.2 (d, ^1J(B,H) = 151, 4B), −19.5 (d, 2B), −26.3 (d, ^1J(B,H) = 132, 2B). MALDI-TOF-MS: (*m*/*z*) 469.38 ((M + Li)/2, 100%); 483.39 ((M + Li)2 + CH_2; 15%).

Synthesis of [$N(CH_3)_4$]$_2$[1″,3″-{3,3′-Co(8-$O(CH_2CH_2O)_2$-1,2-$C_2B_9H_{10}$)(1′,2′-$C_2B_9H_{11}$)}$_2$-C_6H_4] (4). This compound was prepared using the same procedure as for **3**, but using resorcinol (25.6 mg, 0.232 mmol) instead of catechol. Yield: 0.374 g (83%). Anal. calcd for $C_{30}H_{86}B_{36}Co_2N_2O_6$: C, 33.42; H, 8.04; N, 2.60. Found: C, 33.70; H, 7.95; N, 2.65. IR: ν(cm^{-1}) 3041 (C_c−H), 2918, 2864, 2825 (C−H)$_{alkyl}$, 2584, 2482, 2364, 2228 (B−H), 1483, 1462 δ(CH_2), 1286, 1255 δ(CH), 1184, 1124 (C−O−C), 941 (C−N). ^{1}H NMR: δ 7.15 (t, ^3J(H,H) = 8, 1H, C_6H_4), 6.54 (s, 1H, C_6H_4), 6.52 (d, ^3J(H,H) = 2, 2H, C_6H_4), 4.28 (br s, 8H, C_c−H), 4.10 (t, ^3J(H,H) = 5, 4H, OCH_2CH_2), 3.80 (t, ^3J(H,H) = 5, 4H, OCH_2CH_2), 3.59 (t, ^3J(H,H) = 3, 8H, OCH_2CH_2), 3.43 (s, 24H, $N(CH_3)_4$), 2.99−1.47 (m, 34H, B−H). ^{1}H{^{11}B} NMR: δ 7.15 (t, ^3J(H,H) = 8, 1H, C_6H_4), 6.54 (s, 1H, C_6H_4), 6.54 (d, ^3J(H,H) = 2, 2H, C_6H_4), 4.28 (br s, 8H, C_c−H), 4.10 (t, ^3J(H,H) = 5, 4H, OCH_2CH_2), 3.80 (t, ^3J(H,H) = 5, 4H, OCH_2CH_2), 3.59 (t, ^3J(H,H) = 3, 8H, OCH_2CH_2), 3.43 (s, 24H, $N(CH_3)_4$), 2.99 (s, 8H, B−H), 2.77 (s, 4H, B−H), 2.69 (s, 2H, B−H), 2.44 (s, 2H, B−H), 1.99 (s, 4H, B−H), 1.78 (s, 4H, B−H), 1.67 (s, 4H, B−H), 1.57 (s, 4H, B−H), 1.47 (s, 2H, B−H).

(27) (a) Smith, H. D.; Obenland, C. O.; Papetti, S. *Inorg. Chem.* **1966**, *5*, 1013. (b) Teixidor, F.; Viñas, C.; Casabó, C.; Romerosa, A. M.; Rius, J.; Miravitlles, C. *Organometallics* **1994**, *13*, 914. (c) Zakharki, L. I.; Zhigareva, G. G. *Izv. Akad. Nauk SSSR, Ser. Khim.* **1967**, *6*, 1358.

$^{13}C\{^1H\}$ NMR: δ 160.34 (s, C_6H_4), 129.73 (s, C_6H_4), 106.83 (s, C_6H_4), 101.26 (s, C_6H_4), 71.96 (s, OCH_2), 69.37 (s, OCH_2), 68.34 (s, OCH_2), 67.44 (s, OCH_2), 55.16 (s, $N(CH_3)_4$), 54.56 (s, C_c−H), 46.36 (s, C_c−H). ^{11}B NMR: δ 25.3 (s, 2B, B(8)), 6.3 (d, ^1J(B,H) = 134, 2B), 2.8 (d, ^1J(B,H) = 152, 2B), −0.1 (d, ^1J(B,H) = 148, 2B), −1.8 (d, ^1J(B,H) = 160, 4B), −5.1 (d, ^1J(B,H) = 80, 4B), −5.8 (d, ^1J(B,H) = 121, 8B), −14.9 (d, ^1J(B,H) = 156, 4B), −18.0 (d, ^1J(B,H) = 150, 4B), −19.5 (d, 2B), −26.0 (d, ^1J(B,H) = 150, 2B). MALDI-TOF-MS: (*m*/*z*) 1003.8 (M + $N(CH_3)_4$).

Synthesis of $[N(CH_3)_4]_2[1'',4''$-{3,3′-Co(8-O($CH_2CH_2O)_2$-1,2-$C_2B_9H_{10}$)(1′,2′-$C_2B_9H_{11}$)}$_2$-C_6H_4] (5). This compound was prepared using the same procedure as for **3**, but using hydroquinone (25.6 mg, 0.2324 mmol) instead of cathecol. Work-up and purification ends without the cation exchange. Yield: 0.386 g (85%). Anal. calcd for $C_{30}H_{86}B_{36}Co_2N_2O_6$: C, 33.42; H, 8.04; N, 2.60. Found: C, 33.64; H, 8.00; N, 2.42. IR: ν(cm^{-1}) 3039 (C_c−H), 2920, 2864, 2831 (C−H)$_{alkyl}$, 2610, 2482, 2545, 2434, 2363, 2339 (B−H), 1504, 1481, 1454 δ(CH_2), 1284 δ(CH), 1232, 1178, 1126 (C−O−C), 943 (C−N). ^1H NMR: δ 6.88 (s, 4H, C_6H_4), 4.28 (br s, 8H, C_c−H), 4.06 (t, ^3J(H,H) = 5, 4H, OCH_2CH_2), 3.77 (t, ^3J(H,H) = 5, 4H, OCH_2CH_2), 3.57 (t, ^3J(H,H) = 3, 8H, OCH_2CH_2), 3.44 (s, 24H, $N(CH_3)_4$), 2.92−1.45 (m, 34H, B−H). $^1H\{^{11}B\}$ NMR: δ 6.88 (s, 4H, C_6H_4), 4.28 (br s, 8H, C_c−H), 4.06 (t, ^3J(H,H) = 5, 4H, OCH_2CH_2), 3.77 (t, ^3J(H,H) = 5, 4H, OCH_2CH_2), 3.57 (t, ^3J(H,H) = 3, 8H, OCH_2CH_2), 3.44 (s, 24H, $N(CH_3)_4$), 2.92 (s, 8H, B−H), 2.77 (s, 4H, B−H), 2.69 (s, 4H, B−H), 2.42 (s, 2H, B−H), 1.99 (s, 4H, B−H), 1.78 (s, 4H, B−H), 1.67 (s, 4H, B−H), 1.57 (s, 2H, B−H), 1.45 (s, 2H, B−H). $^{13}C\{^1H\}$ NMR: δ 115.39 (s, C_6H_4), 71.94 (s, OCH_2), 69.50 (s, OCH_2), 68.38 (s, OCH_2), 67.99 (s, OCH_2), 55.18 (s, $N(CH_3)_4$), 54.68 (s, C_c−H), 46.91 (s, C_c−H). ^{11}B NMR: δ 25.2 (s, 2B, B(8)), 6.2 (d, ^1J(B,H) = 141, 2B), 2.8 (d, ^1J(B,H) = 151, 2B), −0.1 (d, ^1J(B,H) = 141, 2B), −1.7 (d, ^1J(B,H) = 162, 4B), −5.1 (d, ^1J(B,H) = 90, 4B), −5.8 (d, ^1J(B,H) = 110, 8B), −14.9 (d, ^1J(B,H) = 153, 4B), −18.0 (d, ^1J(B,H) = 150, 4B), −19.5 (d, 2B), −26.0 (d, ^1J(B,H) = 140, 2B). MALDI-TOF-MS: (*m*/*z*) 466.91 (M/2, 38%), 426.5 (M − $C_{14}H_{33}B_{18}CoO_3$, 100%), 410.7 (M − $C_{14}H_{33}B_{18}CoO_4$, 55%), 368.5 (M − $C_{16}H_{37}B_{18}CoO_5$, 58%), 351.8 (M − $C_{17}H_{41}B_{18}CoO_5$, 35%), 324.3 (M − $C_{18}H_{41}B_{18}CoO_6$, 73%).

Synthesis of [Li(DME)]$_3$[1″,3″,5″-{3,3′-Co(8-O($CH_2CH_2O)_2$-1,2-$C_2B_9H_{10}$)(1′,2′-$C_2B_9H_{11}$)}$_3$-C_6H_3] [Li(DME)]$_3$[6]. This compound was prepared using the same procedure as for **3**, but using 1,3,5-trihydroxybenzene (26.4 mg, 0.163 mmol) instead of catechol. Work-up and purification were carried out without the cation exchange. Yield: 0.25 g (93%). Anal. calcd for $C_{42}H_{120}B_{54}Co_3Li_3O_{15}$: C, 30.63; H, 7.34. Found: C, 31.15; H, 6.85. IR: ν(cm^{-1}) 3041 (C_c−H), 2935, 2879 (C−H)$_{alkyl}$, 2608, 2570, 2524, 2492, 2358 (B−H), 1514, 1452 δ(CH_2), 1276, 1249 δ(CH), 1149, 1130, 1097 (C−O−C). ^1H NMR: δ 6.12 (s, 3H, C_6H_3), 4.25 (br s, 12H, C_c−H), 4.14 (t, ^3J(H,H) = 6, 6H, OCH_2CH_2), 3.81 (t, ^3J(H,H) = 5, 6H, OCH_2CH_2), 3.62 (t, ^3J(H,H) = 6, 12H, OCH_2CH_2), 3.45 (s, 12H, DME), 3.28 (s, 18H, DME), 2.94−1.47 (m, 51H, B−H). $^1H\{^{11}B\}$ NMR: δ 6.12 (s, 3H, C_6H_3), 4.25 (br s, 12H, C_c−H), 4.14 (t, ^3J(H,H) = 6, 6H, OCH_2CH_2), 3.81 (t, ^3J(H,H) = 5, 6H, OCH_2CH_2), 3.62 (t, ^3J(H,H) = 6, 12H, OCH_2CH_2), 3.45 (s, 12H, DME), 3.28 (s, 18H, DME), 2.94 (s, 12H, B−H), 2.76 (s, 6H, B−H), 2.70 (s, 3H, B−H), 2.47 (s, 3H, B−H), 2.00 (s, 6H, B−H), 1.79 (s, 6H, B−H), 1.67 (s, 6H, B−H), 1.57 (s, 6H, B−H), 1.47 (s, 3H, B−H). $^{13}C\{^1H\}$ NMR: δ 158.42 (s, C_6H_3), 92.55 (s, C_6H_3), 72.35−67.20 (m, OCH_2), 54.48 (s, C_c−H), 46.41 (s, C_c−H). ^{11}B NMR: δ 25.3 (s, 3B, B(8)), 6.3 (d, ^1J(B,H) = 130, 3B), 2.8 (d, ^1J(B,H) = 145, 3B), −0.1 (d, ^1J(B,H) = 147, 3B), −1.9 (d, ^1J(B,H) = 172, 6B), −5.1 (d, ^1J(B,H) = 85, 6B), −5.8 (d, ^1J(B,H) = 99, 12B), −14.9 (d, ^1J(B,H) = 150, 6B), −18.1 (d, ^1J(B,H) = 152, 6B), −19.6 (d, ^1J(B,H) = 144, 3B), −26.1 (d, ^1J(B,H) = 153, 3B). ESI-MS: (*m*/*z*) 1363.1 (M + Li, 10%), 951.7 (M − $C_8H_{29}B_{18}CoO_2$ + Na, 100%).

Trisodium Salt Na_3[6]. 1,3,5-Trihydroxybenzene (125 mg, 0.99 mmol) was reacted in toluene−DME (2:1, 25 mL) with NaH (solid 96%, 82 mg, 3.4 mmol), and then **2** (1.24 g, 3.02 mmol) was added in the same solvent (25 mL). The reaction mixture was stirred at 60 °C for 14 h. After cooling down, the reaction was quenched by the addition of CH_3OH (2 mL), water (10 mL), and a few drops of acetic acid (1 M). The organic solvents were vacuum-removed, water (15 mL) was added, and the crude product was extracted into toluene (3 × 15 mL). Combined toluene fractions were evaporated, dissolved in CH_2Cl_2−CH_3CN (1:4), injected on top of a silica gel column (2 × 25 cm), and chromatographed in the same solvent mixture, increasing the CH_3CN content to 1:3. Yield: 805 mg, 57%. The product was characterized with NMR and MS, showing only minor deviations given by the different cation. Compound Na_3[**6**] was dissolved for crystals grown in methylene chloride upon the addition of a drop of ethanol. This solution was layred by *i*-octane and left to crystallize for several days. Red barlike crystals were obtained. ^1H NMR: δ 6.16 (s, 3H, C_6H_3), 4.25 (br s, 12H, C_c−H), 4.11 (t, ^3J(H,H) = 4.8, 6H, OCH_2CH_2), 3.82 (t, ^3J(H,H) = 4.8, 6H, OCH_2CH_2), 3.66 (t, ^3J(H,H) = 4.8, 12H, OCH_2CH_2), 3.61 (t, ^3J(H,H) = 4.8, 12H, OCH_2CH_2), 2.94−1.47 (m, 51H, B−H). $^1H\{^{11}B_{selective}\}$ NMR: δ 2.93 (H10′), 2.75 (H4′,7′), 2.69 (H10), 2.58 (H8′), 2.91, 1.98, 1.80 (H 4, 7, 9, 12, 9′,12′), 1.66 (H5′, 11′), 1.66 (H6′), 1.56 (H5, 11), 1.45 (H6). $^{13}C\{^1H\}$ NMR: δ 158.5 (s, C_6O_3), 92.7 (s, C_6H_3), 72.6 (CH_2−O), 70.3 (CH_2−O), 68.2 (CH_2−O), 67.7 (CH_2−O), 54.6 (s, C_c−H), 47.4 (s, C_c−H). ^{11}B NMR: δ 23.2 (s, 3B, B8), 4.3 (d, ^1J(B,H) = 132, 3B, B8′), 0.45 (d, ^1J(B,H) = 138, 3B, B10′), −2.4 (d, ^1J(B,H) = 147, 3B, B10), −4.4 (d, ^1J(B,H) = 149, 6B, B4′, 7′), −7.3 (d), −8.0 (2d, overlap 12B, B9, 12, 9′, 12′), −17.2 (d, ^1J(B,H) = 146, 6B, B5′, 11′), −20.4 (d, ^1J(B,H) = 149, 6B, B5, 11), −22.3 (d, ^1J(B,H) = 158, 3B, B6′), −28.5 (d, ^1J(B,H) = 140, 3B, B6). ESI^- MS: (*m*/*z*) = 451.9 (30%), 455.3 (2%) $(M)^{3-}$ (4%); 689.9 (100%), 694.6 (M + Na)$^{2-}$ (4%), 1400.9 (20%), 1411.8 (2%) (M + Na)$^-$.

Synthesis of $[N(CH_3)_4][3,3'$-Co(8-O($CH_2CH_2O)_2CH_2C_6H_5$-1,2-$C_2B_9H_{10}$)(1′,2′-$C_2B_9H_{11}$)] (7). This compound was prepared using the same procedure as for **3**, but using benzyl alcohol (0.046 mL, 0.444 mmol) instead of catechol. Yield: 0.25 g (87%). Anal. calcd for $C_{19}H_{48}B_{18}CoNO_3$: C, 38.54; H, 8.17; N, 2.37. Found: C, 38.23; H, 7.98; N, 2.18. ^1H NMR: δ 7.35 (s, 5H, C_6H_5), 4.55 (s, 2H, CH_2), 4.29 (br s, 4H, C_c−H), 3.62 (m, 4H, OCH_2CH_2), 3.58 (t, ^3J(H,H) = 5, 2H, OCH_2CH_2), 3.51 (t, ^3J(H,H) = 5, 2H, OCH_2CH_2), 3.43 (s, 12H, $N(CH_3)_4$), 2.93−1.48 (m, 17H, B−H). $^1H\{^{11}B\}$ NMR: δ 7.35 (s, 4H, C_6H_4), 4.55 (s, 2H, CH_2), 4.29 (br s, 4H, C_c−H), 3.62 (m, 4H, OCH_2CH_2), 3.58 (t, ^3J(H,H) = 5, 2H, OCH_2CH_2), 3.51 (t, ^3J(H,H) = 5, 2H, OCH_2CH_2), 3.43 (s, 12H, $N(CH_3)_4$), 2.93 (s, 4H, B−H), 2.77 (s, 2H, B−H), 2.70 (s, 1H, B−H), 2.39 (s, 1H, B−H), 1.99 (s, 2H, B−H), 1.78 (s, 2H, B−H), 1.67 (s, 2H, B−H), 1.56 (s, 2H, B−H), 1.48 (s, 1H, B−H). $^{13}C\{^1H\}$ NMR: δ 139.04 (s, C_6H_4), 128.12 (s, C_6H_4), 127.49 (s, C_6H_4), 127.18 (s, C_6H_4), 72.57 (s, OCH_2), 71.87 (s, OCH_2), 70.29 (s, OCH_2), 69.63 (s, OCH_2), 68.39 (s, CH_2), 55.15 (s, $N(CH_3)_4$), 54.59 (s, C_c−H), 46.39 (s, C_c−H). ^{11}B NMR: δ 25.0 (s, 1B, B(8)), 5.9 (d, ^1J(B,H) = 135, 1B), 2.7 (d, ^1J(B,H) = 141, 1B), −0.2 (d, ^1J(B,H) = 155, 1B), −1.9 (d, ^1J(B,H) = 158, 2B), −5.2 (d, ^1J(B,H) = 80, 2B), −6.0 (d, ^1J(B,H) = 131, 4B), −15.0 (d, ^1J(B,H) = 154, 2B), −18.2 (d, ^1J(B,H) = 152, 2B), −19.5 (d, ^1J(B,H) = 141, 1B), −26.2 (d, ^1J(B,H) = 165, 1B). MALDI-TOF-MS: (*m*/*z*) 518.52 (M, 100%); 532.43 (M + CH_2, 15%).

Synthesis of [Li(DME)]$_2$[1″,4″-{3,3′-Co(8-O(CH$_2$CH$_2$O)$_2$CH$_2$-1,2-C$_2$B$_9$H$_{10}$)(1′,2′-C$_2$B$_9$H$_{11}$)}$_2$-C$_6$H$_4$] (8). This compound was prepared using the same procedure as for **3**, but using 1,4-benzene dimethanol (32.11 mg, 0.244 mmol) instead of catechol. Work-up and purification ends without the cation exchange. Yield: 0.40 g (86%). Anal. calcd for $C_{32}H_{86}B_{36}Co_2Li_2O_{10}$: C, 33.36; H, 7.52. Found: C, 33.08; H, 7.26. IR: ν(cm^{-1}) 3039 (C$_c$−H), 2931, 2877 (C−H)$_{alkyl}$, 2607, 2572, 2505, 2362 (B−H), 1454, 1426 δ(CH$_2$), 1245, 848 δ(CH), 1151, 1122 (C−O−C). ^{1}H NMR: δ 7.33 (s, 4H, C$_6$H$_4$), 4.54 (s, 4H, CH$_2$), 4.26 (br s, 8H, C$_c$−H), 3.63 (m, 8H, OCH$_2$CH$_2$), 3.59 (t, ^3J(H,H) = 5, 4H, OCH$_2$CH$_2$), 3.53 (t, ^3J(H,H) = 5, 4H, OCH$_2$CH$_2$), 3.45 (s, 8H, DME), 3.27 (s, 12H, DME), 2.92−1.47 (m, 34H, B−H). ^{1}H{^{11}B} NMR: δ 7.33 (s, 4H, C$_6$H$_4$), 4.54 (s, 4H, CH$_2$), 4.26 (br s, 8H, C$_c$−H), 3.63 (m, 8H, OCH$_2$CH$_2$), 3.59 (t, ^3J(H,H) = 5, 4H, OCH$_2$CH$_2$), 3.53 (t, ^3J(H,H) = 5, 4H, OCH$_2$CH$_2$), 3.45 (s, 8H, DME), 3.28 (s, 12H, DME), 2.92 (s, 8H, B−H), 2.76 (s, 4H, B−H), 2.69 (s, 2H, B−H), 2.45 (s, 2H, B−H), 1.99 (s, 4H, B−H), 1.79 (s, 4H, B−H), 1.66 (s, 4H, B−H), 1.56 (s, 4H, B−H), 1.47 (s, 2H, B−H). ^{13}C{^{1}H} NMR: δ 137.99 (s, C$_6$H$_4$), 127.49 (s, C$_6$H$_4$), 72.46 (s, OCH$_2$), 71.82 (s, OCH$_2$), 70.25 (s, OCH$_2$), 69.45 (s, OCH$_2$), 68.40 (s, CH$_2$), 54.48 (s, C$_c$−H), 46.43 (s, C$_c$−H). ^{11}B NMR: δ 25.2 (s, 2B, B(8)), 6.2 (d, ^1J(B,H) = 132, 2B), 2.7 (d, ^1J(B,H) = 141, 2B), −0.2 (d, ^1J(B,H) = 159, 2B), −1.9 (d, ^1J(B,H) = 161, 4B), −5.1 (d, ^1J(B,H) = 80, 4B), −5.9 (d, ^1J(B,H) = 124, 8B), −15.0 (d, ^1J(B,H) = 156, 4B), −18.2 (d, ^1J(B,H) = 152, 4B), −19.5 (d, ^1J(B,H) = 153, 2B), −26.2 (d, ^1J(B,H) = 151, 2B). MALDI-TOF-MS: (*m*/*z*) 964.91 (M + Li, 100%); 978.91 (M + Li + CH2, 18%), 547.47 (M − C$_8$H$_{29}$B$_{18}$CoO$_2$, 47%).

Synthesis of [N(CH$_3$)$_4$][3,3′-Co(8-O(CH$_2$CH$_2$O)$_2$C(O)C$_6$H$_5$-1,2-C$_2$B$_9$H$_{10}$)(1′,2′-C$_2$B$_9$H$_{11}$)] (9). Under an inert atmosphere, dried sodium benzoate (77.4 mg, 0.488 mmol) and **2** (200 mg, 0.488 mmol) were dissolved in 20 mL of anhydrous DME. After stirring overnight, the solvent was removed. The product was redissolved in the minimum volume of ethanol, and an aqueous solution containing an excess of [N(CH$_3$)$_4$]Cl was added, resulting in the formation of an orange precipitate. This was filtered off, washed with water and petroleum ether, and dried in vacuo. Yield: 0.237 g (88%). Anal. calcd for $C_{19}H_{46}B_{18}CoNO_4$: C, 37.65; H, 7.65; N, 2.31. Found: C, 36.83; H, 7.61; N, 2.31. IR: ν(cm^{-1}) 3033 (C$_c$−H), 2959, 2918, 2866 (C−H)$_{alkyl}$, 2602, 2584, 2543, 2496, 2362 (B−H), 1708 (C═O), 1483, 1450 δ(CH$_2$), 1280 δ(CH), 1178, 1116 (C−O−C), 945 (C−N). ^{1}H NMR: δ 8.04 (d, ^3J(H,H) = 8, 2H, C$_6$H$_5$), 7.62 (t, ^3J(H,H) = 8, 1H, C$_6$H$_5$), 7.51 (dd, ^3J(H,H) = 7, 2H, C$_6$H$_5$), 4.43 (t, ^3J(H,H) = 5, 2H, OCH$_2$CH$_2$), 4.29 (br s, 4H, C$_c$−H), 3.82 (t, ^3J(H,H) = 5, 2H, OCH$_2$CH$_2$), 3.59 (m, 4H, OCH$_2$CH$_2$), 3.46 (s, 12H, N(CH$_3$)$_4$), 2.93−1.49 (m, 17H, B−H). ^{1}H{^{11}B} NMR: δ 8.04 (d, ^3J(H,H) = 8, 2H, C$_6$H$_5$), 7.62 (t, ^3J(H,H) = 8, 1H, C$_6$H$_5$), 7.51 (dd, ^3J(H,H) = 7, 2H, C$_6$H$_5$), 4.43 (t, ^3J(H,H) = 5, 2H, OCH$_2$CH$_2$), 4.29 (br s, 4H, C$_c$−H), 3.82 (t, ^3J(H,H) = 5, 2H, OCH$_2$CH$_2$), 3.59 (m, 4H, OCH$_2$CH$_2$), 3.46 (s, 12H, N(CH$_3$)$_4$), 2.93 (s, 4H, B−H), 2.7 (s, 2H, B−H), 2.71 (s, 1H, B−H), 2.44 (s, 1H, B−H), 2.00 (s, 2H, B−H), 1.79 (s, 2H, B−H), 1.67 (s, 2H, B−H), 1.58 (s, 2H, B−H), 1.49 (s, 1H, B−H). ^{13}C{^{1}H} NMR: δ 165.87 (s, COO), 132.88 (s, C$_6$H$_5$), 129.39 (s, C$_6$H$_5$), 128.45 (s, C$_6$H$_5$), 71.89 (s, OCH$_2$), 68.78 (s, OCH$_2$), 68.49 (s, OCH$_2$), 64.30 (s, OCH$_2$), 54.48 (s, C$_c$−H), 46.38 (s, C$_c$−H). ^{11}B NMR: δ 30.3 (s, 1B, B(8)), 11.3 (d, ^1J(B,H) = 132, 1B), 7.9 (d, ^1J(B,H) = 138, 1B), 5.0 (d, ^1J(B,H) = 152, 1B), 3.3 (d, ^1J(B,H) = 158, 2B), 0.0 (d, ^1J(B,H) = 93, 2B), −0.8 (d, ^1J(B,H) = 128, 4B), −9.8 (d, ^1J(B,H) = 153, 2B), −12.9 (d, ^1J(B,H) = 151, 2B), −14.4 (d, ^1J(B,H) = 165, 1B), −21.0 (d, ^1J(B,H) = 177, 1B). MALDI-TOF-MS: (*m*/*z*) 532.44 (M, 100%); 546.45 (M + CH$_2$, 13%).

Synthesis of Na(H$_2$O)[3,3′-Co(8-O(CH$_2$CH$_2$O)$_2$C(O)CH$_3$-1,2-C$_2$B$_9$H$_{10}$)(1′,2′-C$_2$B$_9$H$_{11}$)]Na$_2$[10]$_2$·2H$_2$O. This compound was prepared using the same procedure as for **9**, but using sodium acetate (73.1 mg, 0.488 mmol) instead of sodium benzoate. Work-up and purification ends without the cation exchange. Yield: 0.233 g (96.8%). Anal. calcd for $C_{10}H_{32}B_{18}CoNaO_4$: C, 24.37; H, 6.54. Found: C, 24.54; H, 6.36. IR: ν(cm^{-1}) 3035 (C$_c$−H), 2937, 2875 (C−H)$_{alkyl}$, 2576, 2551, 2520, 2447 (B−H), 1716 (C═O), 1448, 1375 δ(CH$_2$), 1267, 1244 δ(CH$_3$), 1139, 1097 (C−O−C). ^{1}H NMR: δ 4.26 (br s, 4H, C$_c$−H), 4.14 (t, ^3J(H,H) = 5, 2H, OCH$_2$CH$_2$), 3.65 (t, ^3J(H,H) = 5, 2H, OCH$_2$CH$_2$), 3.58 (t, ^3J(H,H) = 5, 2H, OCH$_2$CH$_2$), 3.52 (t, ^3J(H,H) = 5, 2H, OCH$_2$CH$_2$), 2.91−1.48 (m, 17H, B−H), 2.00 (s, 3H, CH$_3$). ^{1}H{^{11}B} NMR: δ 4.26 (br s, 4H, C$_c$−H), 4.14 (t, ^3J(H,H) = 5, 2H, OCH$_2$CH$_2$), 3.65 (t, ^3J(H,H) = 5, 2H, OCH$_2$CH$_2$), 3.58 (t, ^3J(H,H) = 5, 2H, OCH$_2$CH$_2$), 3.52 (t, ^3J(H,H) = 5, 2H, OCH$_2$CH$_2$), 2.91 (s, 4H, B−H), 2.76 (s, 2H, B−H), 2.69 (s, 1H, B−H), 2.45 (s, 1H, B−H), 2.00 (s, 3H, CH$_3$), 1.99 (s, 2H, B−H), 1.78 (s, 2H, B−H), 1.65 (s, 2H, B−H), 1.56 (s, 2H, B−H), 1.48 (s, 1H, B−H). ^{13}C{^{1}H} NMR: δ 170.21 (s, COO), 71.52 (s, OCH$_2$), 68.75 (s, OCH$_2$), 68.36 (s, OCH$_2$), 63.45 (s, OCH$_2$), 54.37 (s, C$_c$−H), 46.41 (s, C$_c$−H), 19.85 (s, CH$_3$). ^{11}B NMR: δ 30.5 (s, 1B, B(8)), 11.5 (d, ^1J(B,H) = 136, 1B), 7.9 (d, ^1J(B,H) = 141, 1B), 5.1 (d, ^1J(B,H) = 158, 1B), 3.3 (d, ^1J(B,H) = 160, 2B), −0.1 (d, ^1J(B,H) = 108, 2B), −0.7 (d, ^1J(B,H) = 115, 4B), −9.7 (d, ^1J(B,H) = 153, 2B), −12.8 (d, ^1J(B,H) = 151, 2B), −14.3 (d, ^1J(B,H) = 149, 1B), −20.9 (d, ^1J(B,H) = 180, 1B). MALDI-TOF-MS: (*m*/*z*) 935.69 (M, 100%); 483.43 ((M + Na)/2, 90%).

Synthesis of Na[1″-{3,3′-Co(8-O(CH$_2$CH$_2$O)$_2$C(O)-1,2-C$_2$B$_9$H$_{10}$)(1′,2′-C$_2$B$_9$H$_{11}$)}-2″-OH-C$_6$H$_4$}] (11). This compound was prepared using the same procedure as for **9**, but using sodium salicylate (85.9 mg, 0.488 mmol) instead of sodium benzoate. Work-up and purification ends without the cation exchange. Yield: 0.248 g (89.3%.). Anal. calcd for $C_{15}H_{32}B_{18}CoNaO_4$: C, 31.55; H, 6.06. Found: C, 32.90; H, 5.66. IR: ν(cm^{-1}) 3629, 3558 (O−H), 3174 (C−H)$_{aryl}$, 3062 (C$_c$−H), 2908, 2873 (C−H)$_{alkyl}$, 2603, 2563, 2520, 2364 (B−H), 1664 (C═O), 1485, 1463 δ(CH$_2$), 1238, 1222 δ(CH), 1115, 1097 (C−O−C). ^{1}H NMR: δ 7.92 (m, 1H, C$_6$H$_4$), 7.52 (m, 1H, C$_6$H$_4$), 6.96 (m, 1H, C$_6$H$_4$), 6.73 (m, 1H, C$_6$H$_4$), 4.50 (t, ^3J(H,H) = 5, 2H, OCH$_2$CH$_2$), 4.26 (br s, 4H, C$_c$-H), 3.87 (t, ^3J(H,H) = 5, 2H, OCH$_2$CH$_2$), 3.61 (m, 4H, OCH$_2$CH$_2$), 2.93−1.48 (m, 17H, B−H). ^{1}H{^{11}B} NMR: δ 7.92 (m, 1H, C$_6$H$_4$), 7.52 (m, 1H, C$_6$H$_4$), 6.96 (m, 1H, C$_6$H$_4$), 6.73 (m, 1H, C$_6$H$_4$), 4.50 (t, ^3J(H,H) = 5, 2H, OCH$_2$CH$_2$), 4.26 (br s, 4H, C$_c$−H), 3.87 (t, ^3J(H,H) = 5, 2H, OCH$_2$CH$_2$), 3.61 (m, 4H, OCH$_2$CH$_2$), 2.93 (s, 4H, B−H), 2.77 (s, 2H, B−H), 2.70 (s, 1H, B−H), 2.48 (s, 1H, B−H), 2.00 (s, 2H, B−H), 1.79 (s, 2H, B−H), 1.66 (s, 2H, B−H), 1.57 (s, 2H, B−H), 1.48 (s, 1H, B−H). ^{13}C{^{1}H} NMR: δ 169.99 (s, COO), 135.78 (s, C$_6$H$_4$), 130.19 (s, C$_6$H$_4$), 119.31 (s, C$_6$H$_4$), 117.18 (s, C$_6$H$_4$), 71.91 (s, OCH$_2$), 71.50 (s, OCH$_2$), 68.51 (s, OCH$_2$), 64.91 (s, OCH$_2$), 54.32 (s, C$_c$−H), 46.40 (s, C$_c$−H). ^{11}B NMR: δ 25.3 (s, 1B, B(8)), 6.3 (d, ^1J(B,H) = 135, 1B), 2.6 (d, ^1J(B,H) = 140, 1B), −0.2 (d, ^1J(B,H) = 164, 1B), −2.1 (d, ^1J(B,H) = 159, 2B), −5.2 (d, ^1J(B,H) = 122, 2B), −6.1 (d, ^1J(B,H) = 102, 4B), −15.1 (d, ^1J(B,H) = 153, 2B), −18.3 (d, ^1J(B,H) = 159, 2B), −19.8 (d, ^1J(B,H) = 157, 1B), −26.5 (d, ^1J(B,H) = 164, 1B). MALDI-TOF-MS: (*m*/*z*) 548.43 (M, 43%); 450.63 (M − C$_6$H$_5$O, 38%); 428.38 (M − C$_7$H$_5$O$_2$, 100%).

Synthesis of Na$_3$[C$_{12}$H$_{24}$O$_6$][1″,3″,5″-{3,3′-Co(8-O(CH$_2$CH$_2$O)$_2$CO-1,2-C$_2$B$_9$H$_{10}$)(1′,2′-C$_2$B$_9$H$_{11}$)}$_3$-C$_6$H$_3$] (12). This compound was prepared using the same procedure as for **3**, but using sodium 1,3,5-benzenetricarboxylate (45 mg, 0.163 mmol) with 18-crown-6 ether (129 mg, 0.488 mmol) instead of hydroquinone and diethyl ether

instead of DME. Work-up and purification ends without the cation exchange. Yield: 0.168 g (61.2%). Anal. calcd for $C_{45}H_{114}B_{54}Co_3Na_3O_{12}$: C, 32.23; H, 6.85. Found: C, 33.21; H, 7.13. IR: ν(cm^{-1}) 3047 (C_c−H), 2951, 2912, 2873 (C−H)$_{alkyl}$, 2598, 2559, 2533 (B−H), 1722 (C═O), 1471, 1454 δ(CH_2), 1353, 1249 δ(CH), 1165, 1134, 1103 (C−O−C). ^{1}H NMR: δ 8.84 (s, 3H, C_6H_3), 4.53 (t, ^3J(H,H) = 5, 6H, OCH_2CH_2), 4.25 (br s, 12H, C_c−H), 3.88 (t, ^3J(H,H) = 6, 5H, OCH_2CH_2), 3.65 (s, 24H, crown ether), 3.61 (m, 12H, OCH_2CH_2), 2.90−1.47 (m, 51H, B−H). ^{1}H{^{11}B} NMR: δ 8.84 (s, 3H, C_6H_3), 4.53 (t, ^3J(H,H) = 5, 6H, OCH_2CH_2), 4.25 (br s, 12H, C_c−H), 3.88 (t, ^3J(H,H) = 6, 5H, OCH_2CH_2), 3.65 (s, 24H, crown ether), 3.61 (m, 12H, OCH_2CH_2), 2.90 (s, 9H, B−H), 2.74 (s, 6H, B−H), 2.68 (s, 3H, B−H), 2.44 (s, 3H, B−H), 1.99 (s, 6H, B−H), 1.80 (s, 3H, B−H), 1.78 (s, 6H, B−H), 1.63 (s, 6H, B−H), 1.55 (s, 6H, B−H), 1.47 (s, 3H, B−H). ^{13}C{^{1}H} NMR: δ 164.53 (s, COO), 135.09 (s, C_6H_3), 131.54 (s, C_6H_3), 71.87 (s, OCH_2CH_2), 69.44 (s, crown ether), 68.60 (s, OCH_2CH_2), 68.47 (s, OCH_2CH_2), 64.91 (s, OCH_2CH_2), 54.39 (s, C_c−H), 46.38 (s, C_c−H). ^{11}B NMR: δ 23.6 (s, 3B, B(8)), 4.7 (d, ^1J(B,H) = 129, 3B), 1.1 (d, ^1J(B,H) = 140, 3B), −1.8 (d, ^1J(B,H) = 152, 3B), −3.5 (d, ^1J(B,H) = 166, 6B), −6.7 (d, ^1J(B,H) = 94, 6B), −7.5 (d, ^1J(B,H) = 104, 12B), −16.5 (d, ^1J(B,H) = 150, 6B), −19.7 (d, ^1J(B,H) = 152, 6B), −21.2 (d, ^1J(B,H) = 125, 3B), −27.6 (d, ^1J(B,H) = 108, 3B). ESI-MS: (*m*/*z*) 480.71 (M/3, 100%); 484.9 ((M + CH_2)/3, 10%).

Synthesis of Cs[3,3′-Co(8-(OCH$_2$CH$_2$)$_2$CH$_3$-1,2-C$_2$B$_9$H$_{10}$)(1′,2′-C$_2$B$_9$H$_{11}$)] (13). Under an inert atmosphere, a diluted solution of methylmagnesium bromide (0.16 mL, 0.49 mmol) was added slowly to a solution of **2** (200 mg, 0.488 mmol) in 10 mL of anhydrous DME at 0 °C. After stirring overnight, the solvent was removed, the product was redissolved in the minimum volume of ethanol, and an aqueous solution containing an exces of CsCl was added, resulting in the formation of an orange precipitate. This was filtered off, washed with water and petroleum ether, and dried in vacuo. Yield: 0.232 g (85%). Anal. calcd for $C_9H_{32}B_{18}CoCsO_2$: C, 19.34; H, 5.77. Found: C, 20.68; H, 5.12. IR: ν(cm^{-1}) 3043 (C_c−H), 2926, 2922, 2868 (C−H)$_{alkyl}$, 2557, 2551, 2544, 2530 (B−H), 1456, 1423, 1358 δ(CH_2), 1229 δ(CH_3), 1161, 1134, 1097 (C−O−C). ^{1}H NMR: δ 4.26 (br s, 4H, C_c−H), 3.78 (t, ^3J(H,H) = 6, 2H, OCH_2CH_2), 3.55 (t, ^3J(H,H) = 5, 2H, OCH_2CH_2), 3.51 (t, ^3J(H,H) = 6, 2H, OCH_2CH_2), 1.59 (m, 2H, CH_2CH_3), 2.92−1.48 (m, 17H, B−H), 1.22 (s, 3H, CH_3). ^{1}H{^{11}B} NMR: δ 4.26 (br s, 4H, C_c−H), 3.78 (t, ^3J(H,H) = 6, 2H, OCH_2CH_2), 3.55 (t, ^3J(H,H) = 5, 2H, OCH_2CH_2), 3.51 (t, ^3J(H,H) = 6, 2H, OCH_2CH_2), 2.92 (s, 3H, B−H), 2.76 (s, 2H, B−H), 2.69 (s, 1H, B−H), 2.45 (s, 1H, B−H), 1.98 (s, 2H, B−H), 1.79 (s, 2H, B−H), 1.66 (s, 3H, B−H), 1.59 (m, 2H, CH_2CH_3), 1.57 (s, 2H, B−H), 1.48 (s, 1H, B−H), 1.22 (s, 3H, CH_3). ^{13}C{^{1}H} NMR: δ 71.69 (s, OCH_2), 70.88 (s, OCH_2), 68.42 (s, OCH_2), 54.39 (s, C_c−H), 46.40 (s, C_c−H), 31.03 (s, CH_2), 21.93 (s, CH_3). ^{11}B NMR: δ 25.2 (s, 1B, B(8)), 6.3 (d, ^1J(B,H) = 145, 1B), 2.7 (d, ^1J(B,H) = 141, 1B), −0.2 (d, ^1J(B,H) = 149, 1B), −1.9 (d, ^1J(B,H) = 169, 2B), −5.1 (d, ^1J(B,H) = 82, 2B), −5.9 (d, ^1J(B,H) = 117, 4B), −14.9 (d, ^1J(B,H) = 151, 2B), −18.0 (d, ^1J(B,H) = 153, 2B), −19.5 (d, ^1J(B,H) = 145, 1B), −26.1 (d, ^1J(B,H) = 146, 1B). MALDI-TOF-MS: (*m*/*z*) 461.25 (M + ClCs, 26%); 446.23 (M + ClCs − CH_3, 100%).

Synthesis of [NEt$_3$H$^+$] [3,3′-Co(8-(OCH$_2$CH$_2$)$_2$C$_3$H$_5$-1,2-C$_2$B$_9$H$_{10}$)(1′,2′-C$_2$B$_9$H$_{11}$)] (14). This compound was prepared using the same procedure as for **13** but using allylmagnesium chloride (0.18 mL, 0.24 mmol) instead of methylmagnesium bromide. Work-up and purification ends with the precipitation of the NEt_3H^+ salt. Yield: 0.16 g (79%). Anal. calcd for $C_{17}H_{50}B_{18}Co_1N_1O_2$: C, 36.85; H, 9.10; N, 2.53. Found: C, 37.05; H, 9.51; N, 2.38. IR: ν(cm^{-1}) 3041 (C_c−H), 2954, 2925, 2870 (C−H)$_{alkyl}$, 2600, 2565, 2539 (B−H), 1709 (C═C), 1454, 1433, 1421, 1359 δ(CH_2), 1298, 1230 δ(CH_3), 1151, 1134, 1122, 1097 (C−O−C). ^{1}H NMR: δ 5.83 (ddt, ^3J(H_c,H_a) = 17, ^3J(H_c,H_b) = 10, ^3J(H_c,H_d) = 7, 1H, $CH_{2d}C\mathbf{H_c}$═CH_aH_b), 5.00 (dd, ^3J(H_a,H_c) = 17, ^3J(H_a,H_b) = 2, 1H, $CH_{2d}CH_c$═C$\mathbf{H_a}H_b$), 4.91 (dd, ^3J(H_b,H_a) = 2, ^3J(H_b,H_c) = 10, 1H, $CH_{2d}CH_c$═$CH_a\mathbf{H_b}$), 4.29 (br s, 2H, C_c−H), 4.25 (br s, 2H, C_c−H), 3.65 (m, 2H, C$\mathbf{H_{2d}}CH_c$═CH_aH_b), 3.55 (t, ^3J(H,H) = 4, 2H, OCH_2CH_2), 3.49 (q, ^3J(H,H) = 7, 6H, NEt_3H^+), 3.41 (t, ^3J(H,H) = 6, 2H, OCH_2CH_2), 2.10 (t, ^3J(H,H) = 7, 2H, OCH_2CH_2), 1.63 (q, ^3J(H,H) = 8, 2H, C$\mathbf{H_2}CH_{2d}$), 2.90−1.46 (m, 17H, B−H), 1.42 (t, ^3J(H,H) = 7, 9H, NEt_3H^+). ^{1}H{^{11}B} NMR: δ 5.83 (ddt, ^3J(H_c,H_a) = 17, ^3J(H_c,H_b) = 10, ^3J(H_c,H_d) = 7, 1H, $CH_{2d}C\mathbf{H_c}$═CH_aH_b), 5.00 (dd, ^3J(H_a,H_c) = 17, ^3J(H_a,H_b) = 2, 1H, $CH_{2d}CH_c$═C$\mathbf{H_a}H_b$), 4.91 (dd, ^3J(H_b,H_a) = 2, ^3J(H_b,H_c) = 10, 1H, $CH_{2d}CH_c$═$CH_a\mathbf{H_b}$), 4.29 (br s, 2H, C_c−H), 4.25 (br s, 2H, C_c−H), 3.65 (m, 2H, C$\mathbf{H_{2d}}CH_c$═CH_aH_b), 3.55 (t, ^3J(H,H) = 4, 2H, OCH_2CH_2), 3.49 (q, ^3J(H,H) = 7, 6H, NEt_3H^+), 3.41 (t, ^3J(H,H) = 6, 2H, OCH_2CH_2), 2.90 (s, 2H, B−H), 2.75 (s, 2H, B−H), 2.68 (s, 1H, B−H), 2.42 (s, 1H, B−H), 2.33 (s, 1H, B−H), 2.10 (t, ^3J(H,H) = 7, 2H, OCH_2CH_2), 1.96 (s, 2H, B−H), 1.76 (s, 2H, B−H), 1.69 (s, 1H, B−H), 1.63 (q, ^3J(H,H) = 8, 2H, C$\mathbf{H_2}CH_{2d}$), 1.63 (s, 2H, B−H), 1.54 (s, 2H, B−H), 1.46 (s, 1H, B−H), 1.42 (t, ^3J(H,H) = 7, 9H, NEt_3H^+). ^{13}C{^{1}H} NMR: δ 138.96 (s, **C**HCH_aH_b), 113.74 (s, $CH\mathbf{C}H_aH_b$), 71.78 (s, OCH_2), 70.19 (s, OCH_2), 68.70 (s, OCH_2), 54.44 (s, C_c−H), 46.34 (s, C_c−H), 44.87 (s, NEt_3H^+), 33.12 (s, $CH_2\mathbf{C}H_{2d}$), 26.18 (s, **C**H_2CH_{2d}), 13.41 (s, NEt_3H^+). ^{11}B NMR: δ 22.8 (s, 1B, B(8)), 3.7 (d, ^1J(B,H) = 128, 1B), −0.4 (d, ^1J(B,H) = 141, 1B), −2.5 (d, ^1J(B,H) = 151, 1B), −4.1 (d, ^1J(B,H) = 161, 2B), −7.5 (d, ^1J(B,H) = 82, 2B), −8.3 (d, ^1J(B,H) = 124, 4B), −17.3 (d, ^1J(B,H) = 154, 2B), −20.5 (d, ^1J(B,H) = 152, 2B), −21.9 (d, ^1J(B,H) = 147, 1B), −28.4 (d, ^1J(B,H) = 162, 1B). MALDI-TOF-MS: (*m*/*z*) 466.32 (M + CH3, 7%); 452.29 (M, 100%); 426.24 (M, 10%); 411.25 (M, 37%).

Synthesis of [Li(THF)$_2$][1″-{3,3′-Co(8-(OCH$_2$CH$_2$)$_2$S-1,2-C$_2$B$_9$H$_{10}$)(1′,2′-C$_2$B$_9$H$_{11}$)}−2″-CH$_3$-1″,2″-C$_2$B$_{10}$H$_{10}$)] (15). This compound was prepared using the same procedure as for **3**, but using 1-SH-2-CH_3-1,2-*closo*-$C_2B_{10}H_{10}$ (92.7 mg, 0.488 mmol) instead of catechol and THF instead of DME. Work-up and purification ends without the cation exchange. Yield: 0.315 g (86%). Anal. calcd for $C_{19}H_{58}B_{28}CoLiO_4S$: C, 30.37; H, 7.78; S, 4.27. Found: C, 29.84; H, 7.92; S, 4.03. IR: ν(cm^{-1}) 3049, 3039 (C_c−H), 2981, 2937, 2879 (C−H)$_{alkyl}$, 2593, 2565, 2531, 2490, 2360, 2343 (B−H), 1473, 1458 δ(CH_2), 1380, 1352, 1280 δ(CH), 1143, 1132, 1087, 1041 (C−O−C), 748, 723 (C−S). ^{1}H NMR: δ 4.26 (br s, 4H, C_c−H), 3.73 (t, ^3J(H,H) = 6, 2H, OCH_2CH_2), 3.63 (m, 8H, THF), 3.56 (t, ^3J(H,H) = 6, 2H, OCH_2CH_2), 3.51 (t, ^3J(H,H) = 6, 2H, OCH_2CH_2), 3.19 (t, ^3J(H,H) = 6, 2H, CH_2), 2.19 (s, 3H, CH_3), 1.79 (m, 8H, THF), 2.94−1.46 (m, 27H, B−H). ^{1}H{^{11}B} NMR: δ 4.26 (br s, 4H, C_c−H), 3.73 (t, ^3J(H,H) = 6, 2H, OCH_2CH_2), 3.63 (m, 8H, THF), 3.56 (t, ^3J(H,H) = 6, 2H, OCH_2CH_2), 3.51 (t, ^3J(H,H) = 6, 2H, OCH_2CH_2), 3.19 (t, ^3J(H,H) = 6, 2H, CH_2), 2.94 (s, 1H, B−H), 2.90 (s, 2H, B−H), 2.76 (s, 2H, B−H), 2.69 (s, 1H, B−H), 2.47 (s, 4H, B−H), 2.30 (s, 3H, B−H), 2.21 (s, 4H, B−H), 2.19 (s, 3H, CH_3), 2.09 (s, 2H, B−H), 1.98 (s, 2H, B−H), 1.79 (m, 8H, THF), 1.66 (s, 2H, B−H), 1.58 (s, 3H, B−H), 1.46 (s, 1H, B−H). ^{13}C{^{1}H} NMR: δ 85.86 (s, C_c−S), 81.82 (s, C_c−CH_3), 72.72 (s, OCH_2), 71.09 (s, OCH_2), 69.39 (s, OCH_2), 68.06 (s, THF), 55.31 (s, C_c−H), 47.28 (s, C_c−H), 38.47 (s, CH_2S), 26.15 (s, THF), 23.47 (s, CH_3). ^{11}B NMR: δ 25.1 (s, 1B, B(8)), 6.3 (d, ^1J(B,H) = 139, 1B), 2.7 (d, ^1J(B,H) = 137, 1B), −0.2 (d, ^1J(B,H) = 140, 1B), −1.9 (d, ^1J(B,H) = 157, 2B), −2.9 (d, ^1J(B,H) = 135, 2B), −5.1 (d, ^1J(B,H) = 93, 2B), −6.1 (d, ^1J(B,H) = 125, 6B), −7.6 (d, ^1J(B,H) = 162, 6B), −14.9 (d, ^1J(B,H) = 141, 2B), −18.1 (d,

^1J(B,H) = 156, 2B), −19.6 (d, ^1J(B,H) = 141, 1B), −26.1 (d, ^1J(B,H) = 177, 1B). MALDI-TOF-MS: (*m*/*z*) 601.42 (M, 100%) 615.41 (M + CH_2, 18%).

Synthesis of [N(CH$_3$)$_4$]$_2$[1″,2″-{3,3′-Co(8-(OCH$_2$CH$_2$)$_2$S-1,2-C$_2$B$_9$H$_{10}$)(1′,2′-C$_2$B$_9$H$_{11}$)}$_2$-1″,2″-C$_2$B$_{10}$H$_{10}$)] (16). This compound was prepared using the same procedure as for **3**, but using 1,2-$(SH)_2$-1,2-*closo*-$C_2B_{10}H_{10}$ (50.7 mg, 0.244 mmol) instead of catechol and THF instead of DME. Work-up and purification ends with the precipitation of the $N(CH_3)_4$ salt. Yield: 0.288 g (57%). Anal. calcd for $C_{26}H_{92}B_{46}Co_2N_2O_4S_2$: C, 26.55; H, 7.88; S, 5.45. Found: C, 26.78; H, 7.09; S, 5.25. IR: ν(cm^{-1}) 3037, 3020 (C_c−H), 2920, 2860 (C−H)$_{alkyl}$, 2597, 2555, 2516, 2360, 2343 (B−H), 1481 $\delta(CH_2)$, 1284 δ(CH), 1170, 1119, 1097 (C−O−C), 748, 723 (C−S). ^{1}H NMR: δ 4.27 (br s, 8H, C_c−H), 3.76 (t, ^3J(H,H) = 6, 4H, OCH_2CH_2), 3.58 (t, ^3J(H,H) = 6, 4H, OCH_2CH_2), 3.55 (t, ^3J(H,H) = 6, 4H, OCH_2CH_2), 3.45 (s, 24H, $N(CH_3)_4$), 3.18 (t, ^3J(H,H) = 6, 4H, CH_2), 2.91−1.48 (m, 44H, B−H). ^{1}H{^{11}B} NMR: δ 4.27 (br s, 8H, C_c−H), 3.76 (t, ^3J(H,H) = 6, 4H, OCH_2CH_2), 3.58 (t, ^3J(H,H) = 6, 4H, OCH_2CH_2), 3.55 (t, ^3J(H,H) = 6, 4H, OCH_2CH_2), 3.45 (s, 24H, $N(CH_3)_4$), 3.18 (t, ^3J(H,H) = 6, 4H, CH_2), 2.91 (s, 2H, B−H), 2.77 (s, 4H, B−H), 2.69 (s, 4H, B−H), 2.53 (s, 4H, B−H), 2.42 (s, 4H, B−H), 2.34 (s, 4H, B−H), 2.25 (s, 2H, B−H), 2.10 (s, 2H, B−H), 1.98 (s, 4H, B−H), 1.78 (s, 4H, B−H), 1.68 (s, 4H, B−H), 1.56 (s, 4H, B−H), 1.48 (s, 2H, B−H). ^{13}C{^{1}H} NMR: δ 94.50 (s, C_c−S), 71.76 (s, OCH_2), 68.56 (s, OCH_2), 67.22 (s, OCH_2), 55.13 (s, $N(CH_3)_4$), 54.50 (s, C_c−H), 48.56 (s, C_c−H), 37.61 (s, CH_2S). ^{11}B NMR: δ 25.0 (s, 2B, B(8)), 6.1 (d, ^1J(B,H) = 138, 2B), 2.7 (d, ^1J(B,H) = 144, 2B), −0.2 (d, ^1J(B,H) = 148, 2B), −1.8 (d, ^1J(B,H) = 152, 4B), −5.2 (d, ^1J(B,H) = 99, 8B), −6.0 (d, ^1J(B,H) = 116, 8B), −7.8 (d, ^1J(B,H) = 183, 4B), −10.9 (d, ^1J(B,H) = 155, 2B), −14.9 (d, ^1J(B,H) = 148, 4B), −18.1 (d, ^1J(B,H) = 152, 4B), −19.5 (d, ^1J(B,H) = 130, 2B), −26.2 (d, ^1J(B,H) = 144, 2B). MALDI-TOF-MS: (*m*/*z*) 1049.5 (M + Li + CH_2, 15%); 1035.5 (M + Li, 100%); 586.35 (M − $C_8H_{29}B_{18}CoO_2S$, 67%).

X-Ray Structure Determinations of Na$_3$[6]·H$_2$O·C$_2$H$_5$OH, [N(CH$_3$)$_4$][9], and Na$_2$[10]$_2$·2H$_2$O. A red crystal of dimensions 0.4 × 0.2 × 0.18 mm of Na_3[**6**]·H_2O·C_2H_5OH was mounted into a Lindemann capillary and measured on a Nonius KappaCCD diffractometer by monochromatized Mo Kα radiation (λ = 0.71073 Å) at 150(2) K. An absorption was neglected (μ = 0.73 mm^{-1}); a total of 137 134 reflections were measured in the ranges h = −17 to +17, k = −26 to +26, and l = −35 to +35 (θ_{max}= 27.5°), from which 16 892 were unique (R_{int} = 0.050) and 12 266 were observed according to the $I > 2\sigma(I)$ criterion. Cell parameters were from 17 287 reflections (θ = 1−27.5°). The structure was solved by direct methods (SIR92)[28] and refined by full-matrix least-squares based on F^2 (SHELXL97).[30] The hydrogen atoms were fixed into idealized positions (riding model) and assigned temperature factors of either $H_{iso}(H) = 1.2U_{eq}$ (pivot atom) or $H_{iso}(H) = 1.5U_{eq}$ (pivot atom) for the methyl moiety. The refinement converged (Δ/σ_{max} = 0.001) to R = 0.050 for observed reflections and $wR(F^2)$ = 0.145 and GOF = 1.02 for 929 parameters and all 16892 reflections. The final difference map displayed no peaks of chemical significance ($\Delta\rho_{max}$ = 0.81, $\Delta\rho_{min}$ −0.64 e Å^{-3}). The results are presented in a condensed form in Figure 2 and Table 2.

Table 2. Crystallographic Data and Refinement Parameters of Na$_3$[**6**]·H$_2$O·C$_2$H$_5$OH, [NMe$_4$][**9**], and Na$_2$[**10**]$_2$·2H$_2$O

	Na$_3$[**6**]·H$_2$O·C$_2$H$_5$OH	[NMe$_4$][**9**]	Na$_2$[**10**]$_2$·2H$_2$O
empirical formula	$C_{32}H_{98}B_{54}Co_3Na_3O_{11}$	$C_{19}H_{46}B_{18}CoNO_4$	$C_{20}H_{68}B_{36}Co_2Na_2O_{10}$
fw	1488.60	606.08	1021.74
cryst syst	monoclinic	monoclinic	orthorhombic
cryst habit, color	bar, red	plate, red	needle, yellow
space group	$P2_1/n$	$P2_1/n$ (no. 14)	*Pbca* (no. 61)
a (Å)	13.38900 (10)	16.9749(5)	14.6132(4)
b (Å)	20.1590 (2)	12.0269(3)	11.4205(2)
c (Å)	27.5480 (2)	17.0544(4)	29.7296(8)
β (deg)	97.5690 (5)	113.182(2)	90
V (V^3)	7370.66 (11)	3200.63(14)	4961.6(2)
Z	4	4	4
T (°C)	−123	−100	−100
λ (Å)	0.71073	0.71073	0.71073
ρ (g cm^{-3})	1.341	1.258	1.368
μ (mm^{-1})	0.73	0.566	0.733
data/restraints/params	6892/-/929	7755/4/389	6095/13/321
goodness-of-fit[a] on F^2	1.020	1.026	1.048
$R1$[b] [$I > 2\sigma(I)$]	0.050	0.0681	0.0530
$wR2$[c] [$I > 2\sigma(I)$]	0.145	0.1225	0.1213

[a] $S = [\sum(w(F_o^2 - F_c^2)^2]/(n-p)^{1/2}$. [b] $R1 = \sum||F_o| - |F_c||/\sum|F_o|$. [c] $wR2 = [\sum w(|F_o^2| - |F_c^2|)^2/\sum w|F_o^2|^2]^{1/2}$.

Single-crystal data collections for [N(CH$_3$)$_4$][**9**] and Na$_2$[**10**]$_2$·2H$_2$O were performed at −100° with an Enraf Nonius KappaCCD diffractometer using graphite monochromatized Mo Kα radiation. The structures were solved by direct methods and refined on F^2 by the SHELXL97 program.[29] The structure of [N(CH$_3$)$_4$][**9**] is partially disordered with the atoms O2, C14, C15, and C16 each occupying two positions. An asymmetric unit of the structure of Na$_2$[**10**]$_2$·2H$_2$O consists of half of the dimeric unit, and in the asymmetric unit, the atoms C13, C14, and C15 are disordered, each occupying two positions. DFIX restraints were utilized to obtain reasonable bond parameters for the atoms at the disordered parts of the molecules. For both compounds, the disordered non-hydrogen atoms were refined with isotropic thermal displacement parameters and the rest of the non-hydrogen atoms with anisotropic displacement parameters. The hydrogen atoms were treated as riding atoms using the SHELX97 default parameters, except positional parameters of the hydrogen atoms connected to the water molecule in Na$_2$[**10**]$_2$·2H$_2$O, which were refined. Crystallographic parameters for [NMe$_4$][**9**] and Na$_2$[**10**]$_2$·2H$_2$O are gathered in Table 2.

Acknowledgment. This work was supported by MEC (MAT2006-05339), CSIC (I3P grant to P.F.), and the Generalitat de Catalunya 2005/SGR/00709 and in part by Research Plan AV0Z40320502 and Project LC 523 awarded by the AS CR and Ministry of Education of the Czech Republic.

Supporting Information Available: Crystallographic data (CIF) for Na$_3$[**6**]·H$_2$O·C$_2$H$_5$OH, [NMe$_4$][**9**], and Na$_2$[**10**]$_2$·2H$_2$O; Figures S.1, S.2, and S.3 and Tables S.1, S.2, and S.3. This material is available free of charge via the Internet at http://pubs.acs.org.

IC801139X

(28) Altomare, A.; Cascarano, G.; Giacovazzo, C.; Guagliardi, A.; Burla, M. C.; Polidori, G.; Camalli, M. *J. Appl. Crystallogr.* **1994**, *27*, 435.
(29) Sheldrick, G. M. *SHELX97*; University of Göttingen: Göttingen, Germany, 1997.
(30) Spek, A. L. *PLATON*; Utrecht University: Utrecht, The Netherlands, 2001.

ANNEX

(Manuscrits posteriors a la Comissió de Doctorat de Maig de 2009)

Inorg. Chem. **2009**, *48*, 782

Inorganic Chemistry
Additions and Corrections

2008, Volume 47

Pau Farràs, Francesc Teixidor, Raikko Kivekäs, Reijo Sillanpää, Clara Viñas,* Bohumir Grüner, and Ivana Cisarova: Metallacarboranes as Building Blocks for Polyanionic Polyarmed Aryl-Ether Materials

Page 9502. In the Results and Discussion section, the correct Figure 3 is as follows:

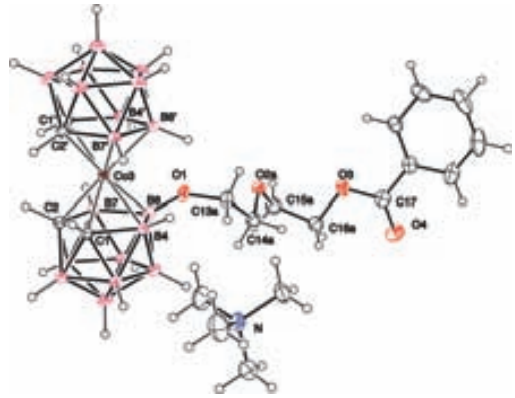

Figure 3. Solid-state structure of $[N(CH_3)_4][\mathbf{9}]$. From the disordered alkyl chain, only the main conformer (74%) is depicted.

IC8022997

10.1021/ic8022997
Published on Web 12/17/2008

Journal of Organometallic Chemistry 694 (2009) 1599–1601

Contents lists available at ScienceDirect

Journal of Organometallic Chemistry

journal homepage: www.elsevier.com/locate/jorganchem

Syntheses of C-substituted icosahedral dicarbaboranes bearing the 8-dioxane-cobalt bisdicarbollide moiety

Václav Šícha [a], Pau Farràs [b,1], Bohumil Štíbr [a], Francesc Teixidor [b], Bohumír Grüner [a,*], Clara Viñas [b,*]

[a] Institute of Inorganic Chemistry, Academy of Sciences of the Czech Republic, 250 68 Řez, Czech Republic
[b] Institut de Ciència de Materials de Barcelona (CSIC), Campus de la U.A.B., E-08193 Bellaterra, Spain

ARTICLE INFO

Article history:
Received 29 August 2008
Received in revised form 30 October 2008
Accepted 31 October 2008
Available online 20 November 2008

Keywords:
Carborane
Metallacarborane
Ring-opening
BNCT
Polyanion

ABSTRACT

The treatment of 1,2-, 1,7- and 1,12-carbaborane lithiated isomers with [3,3′-Co-8-$(CH_2CH_2O)_2$-(1,2-$C_2B_9H_{10}$)-(1′,2′-$C_2B_9H_{11}$)] (**1**) at molar ratios 1:1 or 1:2 at room temperature in THF leads generally to the formation of a series of orange double-cluster mono and dianions. These were characterized by NMR and MS methods as [1″-X-1″,2″-*closo*-$C_2B_{10}H_{11}]^-$, $[\mathbf{2}]^-$; [1″-X-1″,7″-*closo*-$C_2B_{10}H_{11}]^-$, $[\mathbf{3}]^-$ and [1″-X-1″,12″-*closo*-$C_2B_{10}H_{11}$], $[\mathbf{4}]^-$ for the monoanions, whereas [1″,2″-X_2-1″,2″-*closo*-$C_2B_{10}H_{10}]^{2-}$, $[\mathbf{2}]^{2-}$; [1″,7″-X_2-1″,7″-*closo*-$C_2B_{10}H_{10}]^{2-}$, $[\mathbf{3}]^{2-}$; and [1″,12″-X_2-1″,12″-*closo*-$C_2B_{10}H_{10}]^{2-}$, $[\mathbf{4}]^{2-}$ for the dianions (where X = 3,3′-Co-8-$(CH_2CH_2O)_2$-(1,2-$C_2B_9H_{10}$)-1′,2′-($C_2B_9H_{11}$)). Moreover, these borane-cage subunits can be easily modified *via* attaching variable substituents onto cage carbon and boron vertices, which makes these compounds structurally flexible potential candidates for BNCT of cancer and HIV-PR inhibition.

1. Introduction

Since the discovery of nucleophilic oxonium ring-opening (ORO) reactions in the carborane and metallacarborane series by Plešek et al. [1–3], has elapsed more than 30 years. These reactions represent an important feature of substitution boron chemistry and many examples can be found in the literature of these last years [4–10]. Moreover, a recent exhaustive review by Semioshkin et al. [11] has been published on this field. Relevant for this communication is that five years ago Sivaev et al. [12] demonstrated that the THF ring of the $B_{12}H_{11}\cdot THF^-$ anion can be opened by all three isomers (1,2-, 1,7- and 1,12-) of $LiC_2B_{10}H_{11}$ to obtain dianions of general constitution $[1\text{-}B_{12}H_{11}O(CH_2)_4\text{-}1,2\text{-}C_2B_{10}H_{11}]^{2-}$, $[1\text{-}B_{12}H_{11}O(CH_2)_4\text{-}1,7\text{-}C_2B_{10}H_{11}]^{2-}$, and $[1\text{-}B_{12}H_{11}O(CH_2)_4\text{-}1,12\text{-}C_2B_{10}H_{11}]^{2-}$ containing two different boron clusters. In this paper, we would like to extend this viable structural feature by our results on the isolation of mono and dianions of structures combining both the [3,3′-Co(1,2-$C_2B_9H_{11})_2]^-$ and $C_2B_{10}H_{12}$ structural motifs.

2. Results and discussion

Scheme 1 shows that treatment of $LiC_2B_{10}H_{11}$ (1,2-, 1,7- and 1,12-isomers) with [3,3′-Co-8-$(CH_2CH_2O)_2$-(1,2-$C_2B_9H_{10}$)-(1′,2′-$C_2B_9H_{11}$)] (**1**) (molar ratio 1:1) at room temperature in THF leads generally to the formation of a series of orange double-cluster monoanions, which were identified by NMR and MS methods as [1″-X-1″,2″-*closo*-$C_2B_{10}H_{11}]^-$, $[\mathbf{2}]^-$), [1″-X-1″,7″-*closo*-$C_2B_{10}H_{11}]^-$, $[\mathbf{3}]^-$, [1″-X-1″,12″-*closo*-$C_2B_{10}H_{11}]^-$, $[\mathbf{4}]^-$ (where X = 3,3′-Co-8-$(CH_2CH_2O)_2$-(1,2-$C_2B_9H_{10}$)-1′,2′-($C_2B_9H_{11}$)). It should be noted that the reaction of 1-Li-1,12-$C_2B_{10}H_{11}$ is accompanied by the formation of a doubly substituted tricluster dianion [1″,12″-(8-$CH_2CH_2OCH_2$-CH_2O-1,2-$C_2B_9H_{10}$-3,3′-Co-1′,2′-$C_2B_9H_{11})_2$-1″,12″-$C_2B_{10}H_{10}]^-$, $[4]^{2-}$, arising from the ring-opening reaction involving the contaminant $[1,12\text{-}C_2B_{10}H_{10}]^{2-}$ anion with two molecules of compound **1**. The anions were isolated as either Cs^+ or $[N(CH_3)_4]^+$ salts and can be converted into other salts *via* metathesis with suitable counter-cations. It is evident that the formation of these anions is a consequence of the attack of the nucleophilic $[C_2B_{10}H_{11}]^-$ or [R-$C_2B_{10}H_{10}]^-$ anions at one of the dioxane carbon atoms adjacent to the oxonium O atom in structure **1**, followed by the ring opening under the formation of carborane-substituted 1,4-dioxahexane chain.

Application of the same synthetic procedure to the Li[1-R-1,2-$C_2B_{10}H_{10}]^-$ anions (where R = Me and Ph) led to a straightforward isolation of the methylated and phenylated analogues which analyze as [1″-X-2″-Me-1″,2″-*closo*-$C_2B_{10}H_{10}]^-$, [Me-**2**]$^-$ and [1″-X-2″-Ph-1″,2″-*closo*-$C_2B_{10}H_{10}]^-$, [Ph-**2**]$^-$.

As anticipated, an analogous treatment of the corresponding dilithia carboranes $Li_2C_2B_{10}H_{10}$ (1,2-, 1,7- and 1,12-isomers) with dioxanate **1** (molar ratio 1:2) at room temperature in THF leads generally to the formation of a series of orange triple-cluster dianions formulated as [1″,2″-X_2-1″,2″-*closo*-$C_2B_{10}H_{10}]^{2-}$, $[\mathbf{2}]^{2-}$, [1″,7″-X_2-1″,7″-*closo*-$C_2B_{10}H_{10}]^{2-}$, $[\mathbf{3}]^{2-}$ and [1″,12″-X_2-1″,12″-

* Corresponding authors. Tel./fax: +42 02 20941502 (B. Grüner), tel./fax: +34 93 5805729 (C. Viñas).
E-mail addresses: gruner@iic.cas.cz (B. Grüner), clara@icmab.es (C. Viñas).
[1] Pau Farras is enrolled in the Ph.D. program of the UAB.

0022-328X/$ - see front matter © 2008 Published by Elsevier B.V.
doi:10.1016/j.jorganchem.2008.10.059

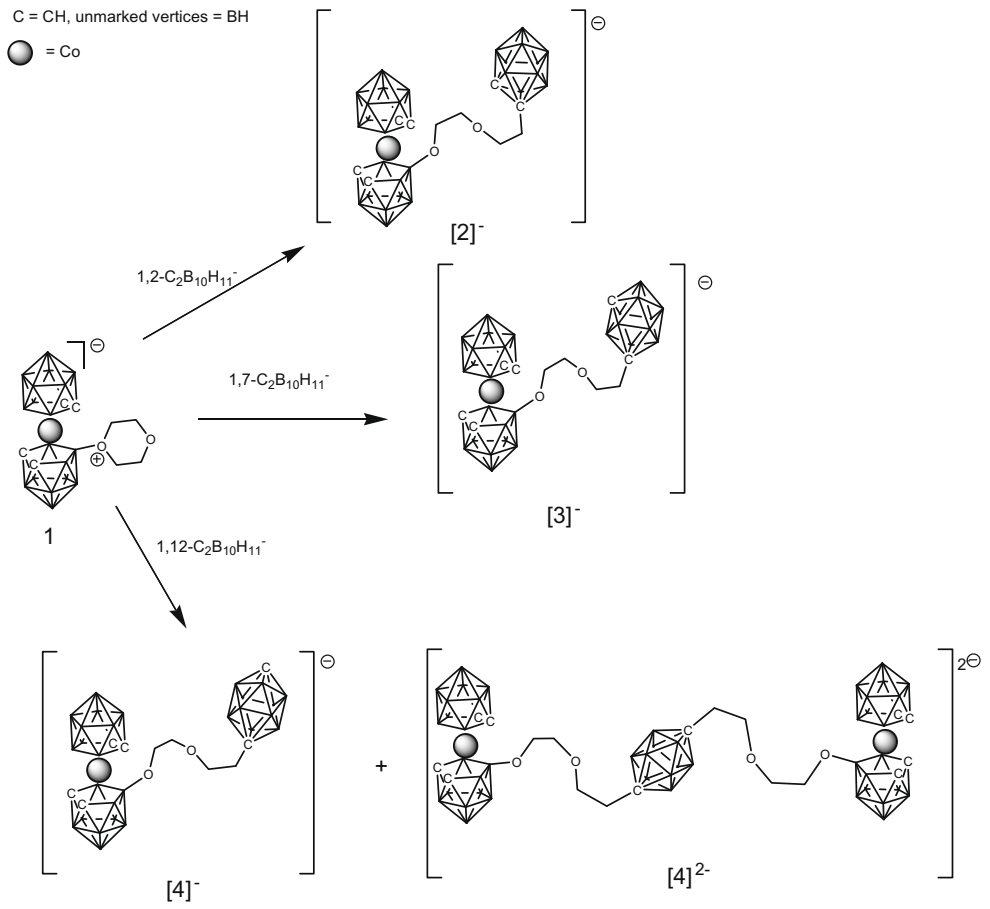

Scheme 1. Treatment of $LiC_2B_{10}H_{11}$ (1,2-, 1,7- and 1,12-isomers) with [3,3′-Co-8-$(CH_2CH_2O)_2$-(1,2-$C_2B_9H_{10}$)-(1′,2′-$C_2B_9H_{11}$)] (**1**).

closo-$C_2B_{10}H_{10}]^{2-}$, $[\mathbf{4}]^{2-}$. A full account on the Me and Ph derivatives and the dianionic compounds will be given in a full paper together with more detailed structural data.

The structure of all compounds isolated in this study has so far been suggested on the basis NMR and MS methods [13]. The ^{11}B NMR spectra of the cobaltabisdicarbollide part of all monoanionic and dianion compounds isolated bear distinct similarities to that of the dioxanate **1**, consisting of a downfield B8 singlet and eleven doublets of approximate areas 1:1:1:2:2:2:2:2:2:1:1, some of which being coincidentally overlapped. This section of the spectrum, however, coincides with that of the carboranyl $C_2B_{10}H_{11}$ substituent, the shape of which is dictated by the symmetry of the corresponding monosubstituted carborane cage, i.e. C_2 for anions $[\mathbf{2}]^-$ and $[\mathbf{3}]^-$ and C_{5v} for anion $[\mathbf{4}]^-$. The most diagnostic feature of the ^1H NMR spectra of monoanions $[\mathbf{2}]^-$, $[\mathbf{3}]^-$ and $[\mathbf{4}]^-$ is the presence of cage $C_{cluster}$–H signals of integral intensity 4 along with one carborane $C_{cluster}$–H resonance of relative area 1 in the case of unsubstituted carborane $[\mathbf{4}]^-$ species. The $C_{cluster}$–H signals of the $BOCH_2$, CH_2OCH_2 and CH_2-carborane units of the interconnecting 1,4-dioxahexane chain usually occur within the range of *δ 3.7–1.9* ppm.

3. Conclusions

It should be concluded that reactions between lithiated 12-vertex carboranes and the dioxanate **1** lead generally to monoanionic and dianionic compounds that contain both metallabisdicarbaborane and carborane structural motifs in one molecule. Moreover, these borane-cage subunits can be easily modified *via* attaching variable substituents onto cage carbon and boron vertices, which makes these compounds structurally flexible potential candidates for BNCT [14,15] of cancer and HIV-PR inhibition. One of the most important reasons for the growing interest in the use of metallacarboranes in biological systems is the suspected high lipophilicity of metallacarborane derivatives, which is a bottleneck for their application in human body. Consequently, these compounds were primarily designed to help to elucidate the effect of steric and hydrophobic interactions on the efficiency of the HIV-PR inhibition in the region of enzyme flaps and the effect of overall charge on the mechanism of the inhibition as well. Corresponding HIV-PR inhibition tests on compounds discussed in this study are being in high progress in our laboratories.

4. Experimental

For the purpose of this paper, the experimental procedure is demonstrated by the isolation of $[\mathbf{4}]^-$ and $[\mathbf{4}]^{2-}$, but is generally valid for the synthesis of all compounds mentioned above: In a typical experiment, a solution of 1,12-$C_2B_{10}H_{12}$ (200 mg, 1.39 mmol) in THF (5 ml) was treated with 2.5 M *n*-BuLi in THF (0.6 ml, 1.5 mmol) at ca. −33 °C. The solution of 1-Li-1,12-$C_2B_{10}H_{11}$ thus obtained was stirred for 1 h at ambient temperature and then treated with a solution of **1** (600 mg, 1.46 mmol) in THF (20 ml). After stirring for additional 4 h, the mixture was then decomposed by adding EtOH (1 ml) and 3 M HCl (0.25 ml) and the organic volatiles were removed by vacuum evaporation. The viscous orange residue was digested with Et_2O (15 ml) and 3 M HCl (7 ml) under shaking. The Et_2O layer was separated, treated with water (2 × 10 ml) and

evaporated. After adding CH_3OH until dissolution of the solid residue and filtration, the filtrate was precipitated with an excess of aqueous CsCl. The orange Cs salts were isolated by filtration. Crystallizations from hot aqueous ethanol and additional crystallization of the solids from CH_2Cl_2-hexane gave the main bulk of Cs[**4**] (300 mg, 20.8%) The salts obtained by evaporation of the mother liquors from the first crystallization in ethanol were subjected to LC on silica gel, using CH_2Cl_2–CH_3CN (from 4:1 to 3:1) as the mobile phase to obtain additional Cs[**4**] (300 mg, total yield 20.8%, R_f 0.27) and the second orange fraction of R_f 0.13 contained $[Cs]_2$[**4**] (450 mg, 17.5 %).

Acknowledgements

Support from the Ministry of Education of the Czech Republic (Project LC523), Research Plan AV0Z40320502 from AS CR, MEC (Grant MAT2006-05339), CSIC (I3P grant to P.F.) and the Generalitat de Catalunya 2005/SGR/00709 is appreciated. We also thank Dr. M. Kvíčalová for MS measurements.

References

[1] J. Plešek, S. Heřmánek, K. Baše, L.J. Todd, W.F. Wright, Collect. Czech. Chem. Commun. 41 (1976) 3509.
[2] A. Petřina, V. Petříček, K. Malý, V. Šubrtová, A. Línek, L. Hummel, Z. Kristallogr. 154 (1981) 217.
[3] V. Šubrtová, V. Petříček, L. Hummel, Acta Crystallogr., Sect. C 45 (1989) 1964.
[4] J. Plešek, S. Heřmánek, A. Franken, I. Císařová, C. Nachtigal, Collect. Czech. Chem. Commun. 62 (1997) 47.
[5] F. Teixidor, J. Pedrajas, I. Rojo, C. Vinas, R. Kivekäs, R. Sillanpää, I. Sivaev, V. Bregadze, S. Sjöberg, Organometallics 22 (2003) 3414.
[6] P. Farràs, F. Teixidor, R. Kivekäs, R. Sillanpää, C. Viñas, B. Grüner, I. Cisarova, Inorg. Chem. 47 (2008) 9497.
[7] J. Llop, C. Viñas, F. Teixidor, Ll. Victori, J. Chem. Soc., Dalton Trans. 8 (2002) 1559.
[8] B. Grüner, L. Mikulášek, J. Báča, I. Císařová, V. Böhmer, C. Danila, M.M. Resinoso-García, W. Verboom, D.N. Reihoudt, A. Casnati, R. Ungaro, Eur. J. Org. Chem. (2005) 2022–2039;
L. Mikulášek, B. Grüner, C. Danila, V. Bõhmer, J. Čáslavský, P. Selucký, Chem. Commun. (2006) 4001–4003;
L. Mikulášek, B. Grűner, C. Dordea, V. Rudzevich, V. Bőhmer, J. Haddaoui, V. Hubscher, F. Arnaud-Neu, J. Čáslavský, P. Selucký, Eur. J. Org. Chem. (28) (2007) 4772–4783.
[9] P. Selucký, J. Rais, M. Lučaníková, B. Grüner, M. Kvíčalová, K. Fejfarová, I. Císařová, Radiochim. Acta 96 (4–5) (2008) 273–284. and the references therein.
[10] P. Cígler, M. Kožíšek, P. Řezáčová, J. Brynda, Z. Otwinowski, J. Pokorná, J. Plešek, B. Grüner, L. Dolečková-Marešová, M. Máša, J. Sedláček, J. Bodem, H.G. Kräusslich, V. Král, J. Konvalinka, PNAS 102 (2005) 15394.
[11] A.A. Semioshkin, I.B. Sivaev, V.I. Bregadze, Dalton Trans. (2008) 977.
[12] I.B. Sivaev, S. Sjöberg, V.I. Bregadze, J. Organomet. Chem. 680 (2003) 106.
[13] Selected structural data: Data for **2**$^-$: Yield 76.8 %; R_f (CH_2Cl_2:CH_3CN 3:1) 0.27; HPLC k′ 5.75; ^{1}B NMR (128.3 MHz, acetone-d_6, 293K): δ = 23.2 (s, 1B, B8), 4.5 (d, J = 141, 1B, B8′), 0.4 (d, J = 139, 1B, B10′), −2.7, −2.8 (d, 2B, B10, 9″), −4.5 (d, 2B, B4′,7′), −5.9 (d, 1B, B12″), −7.3, (d, 2B, B4,7), −7,9 (d, 4B, B9,9′12,12), −9.9 (d, 2B, B8″,10″), −10.7 (d, J = 152, 2B, B4″,5″), −11.9 (d, 2B, 3″,6″), −12.7 (d, 2B, 7″,11″), −17.3 (d, J = 155, 2B, B5′,11′), −20.4 (d, J = 159, 2B, B5,11), −22.1 (d, J = 165, 2B, B6′), −28.4 (d, J = 165, 1B, B6); ^{1}H NMR (400 MHz, acetone-d_6, 293K): δ = 4.80 (s, 1H, H2″-carborane CH), 4.23, 4.20 (2s, H, H1,2,1′,2′cage CH), 3.60 (t, ^3J(H,H) = 5.6 Hz, 4H, OCH_2), 3.46 (t, ^3J(H,H) = 4.8 Hz, 2H,OCH_2), 2.61 (t, ^3J(H,H) = 5.6 Hz, 2H,CH_2); MS (ESI^-): m/z (%) 554.60 (100), 558.50 (5) $[M]^-$ (calcd. 558.50). Anal. Calc. for $C_{10}H_{40}B_{28}CoCs$ (686.94): C, 17.48; H, 5.86. Found: C, 17.62; H, 5.71%. Data for **3**$^-$: Yield 568 mg, (23.7%), R_f (CH_2Cl_2:CH_3CN 3:1) 0.27; HPLC k′ 5.83; ^{11}B NMR (128.3 MHz, acetone-d_6, 293 K): δ = 22.7 (s, 1B, B8), 3.7 (d, J = 134, 1B, B8′), 0.5 (d, J = 136, 1B, B10′), −2.4 (d, 1B, B10), −4.1 (2d, 3B, B4′,7′,5″), −7.4 (d, 2B, B4,7), −8.2 (d, 2B, 9′,12′), −9.2 (d, 1B,12″), −10.9 (d, 4B, 9, 12, 9″,10″), −13.5, −14.9 (d, 4B, B4″, 6″, 8″,11″), −16.6 (d, J = 180, 2B, B2″,3″), −17.3 (d, J = 159, 2B, B5′,11′), −20.4 (d, J = 159, 2B, B5,11), −21.8 (d, J = 160, 1B, B6′), −28.3 (d, J = 164, 1B, B6); ^{1}H NMR (400 MHz, acetone-d_6, 293 K): δ = 4.26 (s, 4H, H1,2, 1′,2′ cage CH), 3.62 (s, 1H, H7″-carborane CH), 3.52 (t, ^3J(H,H) = 5.8 Hz, 2H, $BOCH_2$), 3.41 (2t, ^3J(H,H) = 6.8 Hz, 4H, OCH_2), 2.20 (t, ^3J(H,H) = 6.8 Hz, 2H, CCH_2); MS (ESI^-): m/z (%) 554.60 (100), 558.50 (5) $[M]^-$ (calcd. 558.50). Anal. Calc. for $C_{10}H_{40}B_{28}CoCs$ (686.94): C, 17.48; H, 5.86. Found: C, 17.78; H, 5.93%. Data for **4**$^-$: Yield 300 mg, (20.8%), R_f (CH_2Cl_2:CH_3CN 3:1) 0.28; HPLC k′ 6.18; ^{11}B NMR (128.3 MHz, acetone-d_6, 293 K): δ = 22.5 (s, 1B, B8), 3.5 (d, J = 130, 1B, B8′), 0.5 (d, J = 136, 1B, B10′), −2.4 (d, J = 140, 1B, B10), −4.1 (d, J = 156, 2B, B4′,7′), −7.5 (d, 2B, B4,7), −8.3 (d, 4B, B9,9′,12,12′), −12.4 (d, J = 162, 5B, B2″–B6″), −15.1 (d, J = 165, 5B, B7″–11″), −17.3 (d, J = 156, 2B, B5′,11′), −20.5 (d, J = 155, 2B, B5,11), −21.8 (d, J = 170, 1B, B6′), −28.4 (d, J = 171, 1B, B6). ^{1}H {^{11}B} NMR (400 MHz, acetone-d_6), ^{1}H NMR (400 MHz, acetone-d_6, 293K): δ = 4.29 (s, 4H, H1,2,1′,2′cage CH), 3.50 (s, 1H, H12″, carborane CH), 3.22 (br. t, 2H, OCH_2), 3.04 (br. t, 4H, OCH_2), 1.92 (br. t, 2H, CCH_2). MS (ESI^-): m/z (%) 555.62 (100), 558.54 (5) $[M]^-$ (calcd. 558.50). Anal. Calc. for $C_{10}H_{40}B_{28}CoCs$ (686.94): C, 17.48; H, 5.86. Found: C, 17.81; H, 5.54%. Data for **4**$^{2-}$: Yield 450 mg, (17.5%), R_f (CH_2Cl_2:CH_3CN 3:1) 0.13; HPLC k′ 2.60; ^{11}B NMR (128.3 MHz, acetone-d_6, 293 K): δ = 23.5 (s, 1B, B8), 3.5 (d, J = 140, 1B, B8′), 0.4 (d, J = 144, 1B, B10′), −2.4 (d, J = 140, 1B, B10), −4.1 (d, J = 159, 2B, B4′,7′), −7.5 (d, 2B, B4,7), −8.3 (d, 4B, B9,9′,12,12′), −12.7 (d, J = 162, 10B, B2′−B11″), −17.3 (d, J = 152, 2B, B5′,11′), −20.5 (d, J = 155, 2B, B5,11), −22.0 (d, J = 170, 1B, B6′), −28.4 (d, J = 170, 1B, B6). ^{1}H NMR (400 MHz, acetone-d_6, 293 K): δ = 4.28 (s, 8H, H1,2,1′,2′cage CH), 3.50 (t, 4H, ^3J(H,H) = 5.8 Hz, OCH_2), 3.21 (t, 8H, ^3J(H,H) = 7, 8 Hz, OCH_2), 1.92 (t, ^3J(H,H) = 7, 2 Hz, 4H, CCH_2); MS (ESI^-): m/z (%) 482.33 (100), 486.58 (8) $[M]^{2-}$ (calcd. 486.40); 962.75 (12), 969.75 (1) $[M+H]^-$ (calcd. 969.81); 1096.75 (11), 1102.75 (1) $[M+Cs]^-$ (calcd. 1102.71).
[14] M.F. Hawthorne, Angew. Chem., Int. Ed. Engl. 32 (1993) 950.
[15] A.H. Soloway, W. Tjarks, B.A. Barnum, F.-G. Rong, R.F. Barth, I.M. Codogni, J.G. Wilson, Chem. Rev. 98 (2002) 1515. 1998.

Towards the synthesis of high boron content polyanionic multicluster macromolecules.

Pau Farras,[a,1] Ana Maria Cioran, [a,1] Václav Šícha,[b] Francesc Teixidor,[a] Bohumil Štíbr,[b] Bohumír Grüner[b,*] and Clara Viñas[a,*]

[a] Institut de Ciència de Materials de Barcelona (CSIC), Campus de la U.A.B., E-08193 Bellaterra, Spain. Telefax: Int. Code + 34 93 5805729. E-mail: clara@icmab.es.

[b] Institute of Inorganic Chemistry, Academy of Sciences of the Czech Republic, 250 68 Řez, Czech Republic.

[1] P.F. and A.C. are enrolled in the PhD program of the UAB.

Abstract

Reported are further consequences of the dioxane ring-opening in [3,3'-Co(8-$(CH_2CH_2O)_2$-1,2-$C_2B_9H_{10}$)(1',2'-$C_2B_9H_{11}$)] [**1**] with twelve-vertex carborane mono- and dianions. The removal of one BH vertex from the *o*-carborane part of the double-cluster monoanions of type [1''-X-2''-R-*closo*-1'',2''-$C_2B_{10}H_{11}]^-$ $[\mathbf{2}]^-$ (where X = [3,3'-Co(8-$(CH_2CH_2O)_2$-1,2-$C_2B_9H_{10}$)(1',2'-$C_2B_9H_{11}$)]$^-$ and R = H $[\mathbf{2}]^-$, CH_3 $[\mathbf{8}]^-$ and C_6H_5 $[\mathbf{9}]^-$) via heating with ethanolic KOH or CsF led to the isolation of a series of orange dianions having as general formula [7''-X-8''-R-7'',8''-*nido* -$C_2B_9H_{11}]^{2-}$ (R = H, $[\mathbf{11}]^{2-}$; CH_3, $[\mathbf{12}]^{2-}$ and C_6H_5, $[\mathbf{13}]^{2-}$) cluster constitution. The same procedure applied to the dianionic triple-cluster compound [1'',2''-X_2-1'',2''-*closo*-$C_2B_{10}H_{10}]^{2-}$ $[\mathbf{5}]^{2-}$ yielded the trianionic species [7'',8''-X_2-7'',8''-*nido* -$C_2B_9H_{10}]^{3-}$ $[\mathbf{14}]^{3-}$. Boron degradation of the related *m*-carborane anion [1''-X-1'',7''-*closo*-$C_2B_{10}H_{11}]^-$ $[\mathbf{3}]^-$ was achieved upon heating with CsF in ethylene glycol to generate the [7''-X-7'',9''-*nido*-$C_2B_9H_{11}]^{2-}$ $[\mathbf{15}]^{2-}$ dianion. However, the degradation of the corresponding [1'',7''-X_2-1'',7''-*closo*-$C_2B_{10}H_{10}]^{2-}$ $[\mathbf{6}]^{2-}$ dianion under the same conditions led only to the cleavage of the ether chain with no possible isolation the expected [7'',9''-X_2-7'',9''-*nido*-$C_2B_9H_{10}]^{3-}$ trianion. The study has been complemented by experimental procedures leading to the still not fully reported starting monoanionic compounds $[\mathbf{2}]^-$, $[\mathbf{8}]^-$, $[\mathbf{9}]^-$ and $[\mathbf{3}]^-$ and to the starting dianions $[\mathbf{5}]^{2-}$ and $[\mathbf{6}]^{2-}$. The anions containing the eleven-vertex moiety can be isolated as either Cs^+ or $[N(CH_3)_4]^+$ salts and can be converted into other salts *via* metathesis with suitable counter-cations. The structure of all compounds isolated in this study has been suggested on the basis of NMR and MS methods. The disarticulation of complex ^{11}B NMR spectra has been successfully achieved in this work and has been proven to be a powerful tool for the characterization of multicluster boron containing molecules.

Introduction

The synthetic strategy based on the attack of oxonium derivatives of borane[1] and metallacarborane[2] anions in the presence of nucleophilic agents was firstly reported in 1976.[3] The discovery of the nucleophilic ring-opening reaction in boranes[4] and metallacarboranes[5] has been one of the most important features in boron chemistry over the last several years. A review on this field has been published recently, summarizing some of the nucleophiles that have been used so far.[6]

The derivatization of boranes and metallacarboranes may open the way for new possible applications of these anions. The use of a variaty of ring-opening nucleophiles on [3,3'-Co(8-$(CH_2CH_2O)_2$-1,2-$C_2B_9H_{10}$)(1',2'-$C_2B_9H_{11}$)] [1] has led to the synthesis of compounds of promising practical uses in various fields, including the treatment of nuclear wastes,[7] conducting polymers in materials science,[8] solid electrolytes, strong non-oxidizing acids,[9] weakly coordinating anions,[10] ionic liquids,[11] and enzyme inhibitors.[12] Applications associated with the properties of boron as element within deltahedral species primarily exploit the ^{10}B isotope for neutron capture which led to the development of the Boron Neutron Capture Therapy (BNCT)[13] of cancer tumors.

Compound [1] has been shown to be susceptible to nucleophilic attack at the dioxane carbon adjacent to the positively charged oxygen atom by a variety of nucleophile agents containing oxygen,[14,15] nitrogen,[5a,8b,12,16,17] phosphorus[5c,18] and carbon.[5e,15d,19]

Sivaev et al.[19] demonstrated that the THF ring in the $[B_{12}H_{11}{\cdot}THF]^-$ anion can be opened by all three isomers (1,2-, 1,7- and 1,12-) of Li$[C_2B_{10}H_{11}]$. Additionally, in a preliminary communication[20] we have briefly outlined the synthesis and isolation of mono and dianion species combining the [3,3'-Co$(1,2\text{-}C_2B_9H_{11})_2]^-$ and $[C_2B_{10}H_{12}]$ structural motifs.

In this paper, we extend this viable concept of multicage boron chemistry by giving full experimental details and complete structural data. Moreover, the deboronation of the *closo*-carborane moieties allowed the preparation of a novel type of polyanionic water-soluble high boron content macromolecules that could be good candidates for BNCT techniques' efficiency.

Results and discussion

Synthesis and characterization of *closo*-C_2B_{10} or *nido*-$[C_2B_9]^-$ frameworks incorporating monosubstituted Cobaltabisdicarbollide derivatives.

Following our studies on cobaltabisdicarbollides' direct substitution[15d] to obtain novel high boron content polyanionic species with enhanced water solubility we have recently explored the possibility of using lithiated boron clusters as nucleophiles to produce a new family of high boron content polyanionic macromolecules.[15d,20] This has been, in part, stimulated by the high water solubility of the cobaltabisdicarbollide salts of potassium, sodium or lithium.[21] With these two points in mind, we studied the nucleophilic behaviour of *o*-, *m*- and *p*-Li$[C_2B_{10}H_{11}]$ isomers

and their nucleophilic behaviour towards [3,3'-Co(8-$(CH_2CH_2O)_2$-1,2-$C_2B_9H_{10}$)(1',2'-$C_2B_9H_{11}$)] [**1**] Scheme 1 shows that treatment of Li[$C_2B_{10}H_{11}$] (1,2-, 1,7- and 1,12-isomers) with [**1**] (molar ratio 1:1) produces Li[1''-X-1'',2''-*closo*-$C_2B_{10}H_{11}$]$^-$, Li[**2**], Li[1''-X-1'',7''-*closo*-$C_2B_{10}H_{11}$]$^-$, Li[**3**] and Li_2[1''-X-1'',12''-*closo*-$C_2B_{10}H_{11}$], Li_2[**4**] (where X = [3,3'-Co(8-$(CH_2CH_2O)_2$-1,2-$C_2B_9H_{10}$)(1',2'-$C_2B_9H_{11}$)]$^-$), results already published in a previous communication.[20] In order to establish substituent effects in this series, we have applied the same synthetic procedure to the C-anions Li[1-R-1,2-$C_2B_{10}H_{10}$]$^-$ (where R = CH_3 and C_6H_5), which led as expected to the isolation of the C-methylated and phenylated analogues, the structure of which was in agreement with the constitution of the monoanionic salts Li[1''-X-2''-CH_3-1'',2''-*closo*-$C_2B_{10}H_{10}$], Li[**8**] and Li[1''-X-2''-C_6H_5-1'',2''-*closo*-$C_2B_{10}H_{10}$], Li[**9**]. The anions were isolated for their full characterization either as Cs^+ or $[N(CH_3)_4]^+$ salts and can be converted into other salts *via* metathesis with suitable counter-cations. As anticipated and shown in Scheme 1, an analogous treatment of the corresponding dilithium carboranes Li_2[$C_2B_{10}H_{10}$] (1,2-, 1,7- and 1,12-isomers) with [**1**] (molar ratio 1:2) at room temperature in THF leads generally to the formation of a series of orange triple-cluster dianionic salts formulated as Li_2[1'',2''-X_2-1'',2''-*closo*-$C_2B_{10}H_{10}$], Li_2[**5**], Li_2[1'',7''-X_2-1'',7''-*closo*-$C_2B_{10}H_{10}$], Li_2[**6**]$^{2-}$, and Li_2[1'',12''-X_2-1'',12''-*closo*-$C_2B_{10}H_{10}$], Li_2[**7**]. The Li_2[**7**] compound was also isolated as a side product in the preparation of the monoanionic salt Li[**4**].

Even if the *closo* carborane clusters are structures showing high stability with respect to strong acids they do however react with Lewis bases yielding more opened structures, known as *nido*, by a partial deboronation process that implies the loss of a clusters' vertex. Several nucleophiles such as alkoxides,[22] amines,[23] fluorides,[24] phosphanes[25] have been used. The nucleophilic attack takes place at the boron atoms directly bounded to both carbon atoms, the B(3) or its equivalent B(6), since they both present electronic deficiency. Scheme 2 shows that regioselective removal of one BH vertex from the *o*-carborane cluster of the double-cluster monoanion of type [1''-X-2''-R-1'',2''-*closo* -$C_2B_{10}H_{10}$]$^-$ [**2**]$^-$ species (R = H, [**2**]$^-$; CH_3, [**8**]$^-$ and C_6H_5, [**9**]$^-$) takes place *via* heating with ethanolic KOH or CsF. This reaction led to a good yield isolation (68, 55 and 70%, respectively) of a series of orange dianions with the general formula [7''-X-8''-R -7'',8''-*nido*-$C_2B_9H_{10}$]$^{2-}$ (R = H, [**11**]$^{2-}$; CH_3, [**12**]$^{2-}$ and C_6H_5, [**13**]$^{2-}$).

As expected, the same degradation procedure applied to the dianionic triple-cluster compound [1'',2''-X_2-1'',2''-*closo*-$C_2B_{10}H_{10}$]$^{2-}$ [**5**]$^{2-}$ gave rise to the trianionic species [7'',8''-X_2- 7'',8''-*nido*-$C_2B_9H_{10}$]$^{3-}$ [**14**]$^{3-}$, which is substituted at both carbon atoms of the eleven-vertex dicarborane cluster. For their full characterization these anionic species can be isolated as either Cs^+ or $[N(CH_3)_4]^+$ salts and converted into other salts *via* metathesis with suitable counter-cations.

Boron degradation of the cage isomeric *m*-carborane anion [1''-X-*closo*-1'',7''-$C_2B_{10}H_{11}$]$^-$ [**3**]$^-$ requires more severe reaction conditions - the loss of one boron vertex was achieved upon heating with CsF in ethylene glycol to generate the [7''-X -7'',9''-*nido*-$C_2B_9H_{11}$]$^{2-}$ [**15**]$^{2-}$ dianion. Nevertheless, application of a similar procedure to the disubstituted dianion [1'',7''-X_2-1'',7''-*closo*-$C_2B_{10}H_{10}$]$^{2-}$ [**6**]$^{2-}$ did not lead to the expected [7'',9''-X_2-7'',9''-*nido*-$C_2B_9H_{10}$]$^{3-}$ trianion. Moreover, the prolonged treatment (2 days) with large excess of CsF (10 molar) led to a cleavage of ether chains. It should also be noted that no degradation of the *p*-carborane cluster of anions [**4**]$^-$ and [**7**]$^{2-}$ was observed with CsF under comparable conditions.

NMR studies.

In the absence of suitable crystals for X-ray diffraction studies, the structure of all compounds isolated has been solved by multinuclear NMR spectroscopy and mass spectrometry.

a) *closo* species. One of our groups reported[15d] that the ^{11}B NMR spectrum of monosubstituted derivatives of [3,3'-Co(1,2-$C_2B_9H_{11}$)$_2$]$^-$ is the result of plain addition of the spectra of the two individual halves. In a similar manner, as exemplified in Figure 1, the ^{11}B NMR spectrum of [**8**]$^-$ can be interpreted as a sum of the spectra of two fragments. The spectrum of fragment I is approximated this of the anion [3,3'-Co(8-$(CH_2CH_2O)_2$-1,2-$C_2B_9H_{10}$)(1',2'-$C_2B_9H_{11}$)]$^-$ and the one of fragment II by the spectrum of 1-CH_3-1,2-*closo*-$C_2B_{10}H_{11}$ or more precisely by the one of the model compound 1-CH_3-2-$CH_3OCH_2CH_2$-*closo*-$C_2B_{10}H_{10}$, **10**. Compound **10** has been synthesized only for this purpose.

In order to understand the spectrum and assign the peaks corresponding to each fragment we have used the DM2008 program.[26] The latter has been used almost exclusively for modelling solid-state NMR spectra of non-cluster compounds and in this paper we report for the first time on the computational disarticulation of the ^{11}B NMR spectra in solution to analyse the multicluster compounds isolated. These species contain either 28 or 46 boron atoms of different degrees of symmetry. Table 1 and Figure 2a

exemplify the disarticulation of the ^{11}B NMR spectrum of the methylated anion [**8**]$^-$, for which it is possible to find 14 different Gaussian-type curves fitting to experimental spectra.

Figure 2b represents the typical 1:1:1:1:2:2:(2+2):2:2:1:1 ^{11}B NMR spectrum of a fragment I [3,3'-Co(8-$(CH_2CH_2O)_2$-1,2-$C_2B_9H_{10}$)(1',2'-$C_2B_9H_{11}$)]$^-$ anion with a C_s-symmetry (12 different signals, two overlapped). This leaves only 2 signals corresponding to fragment II (heterosubstituted methyl-carborane) although there should be others overlapped with the peaks of fragment I. To get the spectrum of fragment II it is possible to subtract the already known spectrum of the fragment I from the full spectrum of [**8**]$^-$.

The result is shown in Figure 2c where 5 different signals can be seen. Moreover, it is possible to get the pattern of this fragment II by subtracting the integrals of fragment I from the full spectrum. As it is shown in Table 1, it is possible to get a 1:1:2:2:4 pattern for the fragment II. To compare this theoretical spectrum we have also synthesized [1-$CH_3OCH_2CH_2$-2-CH_3-1,2-*closo*-$C_2B_{10}H_{10}$] [**10**]**,** which is very similar to fragment II. As seen in Figure 2c, the theoretical spectrum of [**10**] is in excellent agreement with experimental data obtained for [**10**] with 1:1:2:2:4 resonances at -4.28, -5.82, -9.25, -9.90 and -10.54 (see Figure 2d).

The most diagnostic feature of the ^1H NMR spectra of monoanions [**2**]$^-$, [**3**]$^-$, [**4**]$^-$ is the presence of C_c-H signals corresponding to the [3,3'-Co(8-$(CH_2CH_2O)_2$-1,2-$C_2B_9H_{10}$)(1',2'-$C_2B_9H_{11}$)]$^-$ unit (integral intensity 2+2 or 4) along with one carborane CH resonance of relative area 1, corresponding to 1,2-*closo*-$C_2B_9H_{11}$ which is missing in the spectra of [**8**]$^-$, [**9**]$^-$, and dianionic compounds [**5**]$^{2-}$, [**6**] $^{2-}$ and [**7**]$^{2-}$. The signals of the $BOCH_2$-, -CH_2OCH_2- and -CH_2-carborane units of the interconnecting 1,4-dioxahexane chain usually occur within the range of $\delta \approx 3.7$-1.9 ppm.

b) *nido* species

Similar considerations were used for analyzing the spectra of the corresponding *nido*-[C_2B_9]$^-$ counterparts. The typical differences between the spectra of *closo*-compounds and their eleven-vertex *nido* counterparts are exemplified for the methylated species [**8**]$^-$ and [**12**]$^{2-}$ in Figure 3.

The NMR analysis used for the characterization of all the above presented compounds gives valuable information regarding the differences between the *closo* and the *nido* species. As presented in Figure 3, additional peaks for the *nido* compounds with respect to the corresponding *closo* species appear in the experimental $^{11}B\{^1H\}$ NMR spectra at the range $\delta \approx$ -34/-36 ppm that clearly confirms the deboronation of the neutral *closo* [C_2B_{10}] cluster to the anionic *nido* [C_2B_9]$^-$ one. As shown in Figure 1b, the methylated *nido* dianion [**12**]$^{2-}$ could be considered as the sum of the fragment I and fragment III. As exemplified in Figure 4, the schematic representation of the $^{11}B\{^1H\}$ NMR spectrum of the methylated *nido* dianion [**12**]$^{2-}$ consists of 12 resonances from the fragment I plus 9 resonances of the fragment III. Its experimental $^{11}B\{^1H\}$ NMR spectrum (Figure 4b)) confirms it.

MALDI-TOF-MS characterization.

Another method used for the characterization of these newly synthesized high Boron content anionic compounds was Matrix-assisted Laser Desorption/Ionization (MALDI)[27] spectroscopy. The MALDI-TOF-MS spectra of compound [**5**]$^{2-}$ is taken as a representative example of the divalent *closo* family of ions with the properly isotopic distribution showing a peak at 970.80, that corresponds to [M+Li^+]$^-$, and the fragmentation peaks at 553.55 and 323.24 respectively (Figure 5). The capability of ESI mass spectrometry for studying weak, non-covalent interactions between metal cations and organic ligands was recognized almost immediately after the introduction of this technique[28] but there is no reported example by using MALDI-TOF-MS. The MALDI-TOF-MS spectrum of compound [**12**]$^{2-}$, taken as a representative example of the divalent *nido* family of ions, displays a signal group centred at *m*/*z* 556.57 corresponding to the molecular peak [M+H^+]$^-$ and peaks at 408.38 and 146.06, similar with fragments I and III, respectively. As shown in Figures 5 and 6, the experimental isotopic pattern was in a good agreement with the calculated isotopic plot (Molecular Weight Calculator for Windows 9x/NT/00/ME/XP is Version 6.38). In agreement with MALDI-TOF-MS spectra we have encountered that the polyanionic species appear as monovalent compounds, by adding either sodium, lithium, potassium or hydrogen cations.

The capability of ESI mass spectrometry for studying weak, non-covalent interactions between metal cations and organic ligands was recognized almost immediately after the introduction of this technique[29] but there is no reported example up to this work of having observed such interactions with Boron hydrides by using MALDI-TOF-MS.

Conclusions

It should be concluded that the reactions shown in Schemes 1 and 2 lead to monoanionic, dianionic and trianionic compounds containing both metal cobaltabisdicarbollide and carborane

structural motifs within the same molecule. The presence of carborane subclusters may add new properties to boron clusters and, in fact, give rise to new species which can be used potentially in various fields of chemistry, biology and medicine. Moreover, the deboronation of the *closo*-carborane moieties allowed for the obtaining of a novel type of high boron content (almost 50%) polyanionic macromolecules. Likewise, the fact that these compounds are polyanionic makes them more soluble in water, which therefore increases their potential for biological uses. Furthermore, the carborane subunits can be easily modified by attaching variable substituents onto the carbon and boron vertex, making out of these structurally flexible compounds potential candidates for BNCT[13] of cancer and HIV-Protease inhibition. In this last respect, these compounds were primarily designed to help elucidate the effect of steric and hydrophobic interactions on the efficiency of the HIV-Protease inhibition in the region of enzyme flaps as well as the effect of overall charge on the mechanism of inhibition. Corresponding HIV-Protease inhibition tests on compounds studied in this research are being in progress in our laboratories. The disarticulation of complex ^{11}B NMR spectra has been successfully achieved in this work and has been proven to be a powerful tool for the characterization of multicluster boron containing molecules.

4. Experimental Section

Elemental analyses were performed using a Carlo Erba EA1108 microanalyzer. IR spectra were recorded from KBr pellets on a Shimadzu FTIR-8300 spectrophotometer. The ^{1}H NMR, $^{1}H\{^{11}B\}$ NMR (300.13 MHz), ^{11}B NMR (96.29 MHz), and $^{13}C\{^{1}H\}$ NMR (75.47 MHz) spectra were recorded with a Bruker ARX 300 instrument equipped with the appropriate decoupling accessories and on a Varian Mercury Plus 400 MHz spectrometer at 295K in acetone-d_6 (frequencies 399.893 MHz for ^{1}H, 128.329 MHz for ^{11}B and 100.55 MHz for ^{13}C). Chemical shift values for ^{11}B NMR spectra were referenced to external $BF_3{\cdot}OEt_2$, and those for ^{1}H, $^{1}H\{^{11}B\}$, and $^{13}C\{^{1}H\}$ NMR spectra were referenced to $Si(CH_3)_4$. Chemical shifts, δ, are reported in ppm and coupling constants in Hz. The mass spectra were recorded in the negative ion mode using either a Bruker Biflex MALDI-TOF-MS (N_2 laser; λ_{exc} 337 nm, 0.5 ns pulses); voltage ion source 20.00 kV (Uis1) and 17.50 kV (Uis2)), in the negative ion mode using a Bruker Daltonics esquire3000 (N_2 laser; λ_{exc} 337 nm, 0.5 ns pulses); Skim1 voltage 37.5V, or on a LCQ-Fleet Ion Trap (Thermo-Finnigan) spectrometer using Electrospray Ionization (ESI). Negative ions were detected in all cases. Full scans and zoom scans in the range of 100 DA around the molecular ions were measured with a resolution of two decimal digits. Samples dissolved in acetonitrile (concentrations 1 mg·μL-1) were introduced to ion source by a syringe pump, flow rate 5 μL·min-1, drying temperature was 180°C, nebula gas flow 12 L·min-1. Analytical HPLC was used to check the purity A Merck-Hitachi HPLC system LaChrom 7000 series equipped with DAD 7450 detector and an intelligent injector L7250 was used. Chromatographic procedure: An Ion-Pair RP chromatographic method with an isocratic elution was based on the methods reported previously for the separation of hydrophobic borate anions. Column: RP Separon™ SGX C8, 7μm (silica with chemically bonded octyl groups) Tessek Prague, Czech Rep. Chromatographic conditions: Solvent 3 mmol L^{-1} hexylamine acetate in 65% aqueous acetonitrile, detection DAD, fixed wavelengths 254, 225, 290 and 312 nm; sensitivity range 0.2 A.U.F.S; samples of concentration approx. 0.5 mg·mL^{-1} in the mobile phase or CH_3CN were injected (3 μL); the method allowed the resolution of most of the compounds from the real reaction mixtures and for the purity assay. Purity of all the compounds was better then 97%. Capacity factors k'= $(t_R-t_0)/t_0$ (where t_R is retention time *and* t_0 is the void retention time of an non retained peak) are given for individual compounds.

All reactions were performed with the use of standard vacuum or inert-atmosphere techniques as described by Shriver,[30] although some operations, such as flash chromatography and crystallization, were carried out in air.

Materials

$Cs[3,3'\text{-}Co(1,2\text{-}C_2B_9H_{11})_2]$, 1-R-1,2-*closo*-$C_2B_{10}H_{11}$, (R= H, CH_3, C_6H_5); 1,7-*closo*-$C_2B_{10}H_{12}$ and 1,12-*closo*-$C_2B_{10}H_{12}$ carboranes were purchased from Katchem Ltd., Czech Republic. [3,3'-Co(8-$(CH_2CH_2O)_2$-1,2-$C_2B_9H_{10}$)(1',2'-$C_2B_9H_{11}$)] [**1**] was prepared according to described procedure[14] and was dried in vacuum for 8-12 h over P_2O_5, at 60ºC prior to use. [1''-X-1'',2''-*closo*-$C_2B_{10}H_{11}]^-$ [**2**]$^-$, [1''-X-1'',7''-*closo*-$C_2B_{10}H_{11}]^-$ [**3**]$^-$, [1''-X-1'',12''-*closo*-$C_2B_{10}H_{11}$] [**4**]$^-$ and [1'',12''-X_2-1'',12''-*closo*-$C_2B_{10}H_{10}]^{2-}$ [**7**]$^{2-}$ (where X = [3,3'-Co(8-$(CH_2CH_2O)_2$-1,2-$C_2B_9H_{10}$)(1',2'-$C_2B_9H_{11}$)]$^-$) were prepared according to the literature.[20]

1,2-dimethoxyethane (DME), diethyl ether and tetrahydrofuran (THF) were dried with sodium/benzophenone. N-butyllithium (1.6 M in hexane) and other chemicals were purchased from Aldrich; the solvents were acquired from Aldrich and Penta Ltd. Czech Republic, respectively, and used without purification. Analytical TLC was carried out on Silufol® (silica gel on aluminium foil, starch as the binder, Kavalier, Czech Republic). Unless otherwise specified, column chromatography was performed on a high purity silica gel (Merck Grade, Type 7754, 70-230 mesh, 60 Å), using acetonitrile/dichloromethane 1:3 as the mobile phase.

a) Monoanions:

Synthesis of $[N(CH_3)_4][1''\text{-}\{3,3'\text{-}Co(8\text{-}(CH_2CH_2O)_2\text{-}1,2\text{-}C_2B_9H_{10})(1',2'\text{-}C_2B_9H_{11})\}\text{-}2''\text{-}CH_3$-*closo*-1'',2''-$C_2B_{10}H_{10}]$, $[N(CH_3)_4]$[8].

Under inert atmosphere, *n*-butyllithium (0.305 mL, 0.488 mmol) (1.6 M in hexane) was added dropwise to a stirred solution of 1''-CH_3-1'',2''-*closo*-$C_2B_{10}H_{11}$ (76.92 mg, 0.488 mmol) in 15 mL of anhydrous DME at 0 ºC. The resulting solution was stirred for 1 h at low temperature. Then a solution of **1** (200 mg, 0.488 mmol) in 15 mL of anhydrous

DME was added dropwise at low temperature. After stirring overnight a white precipitate appeared, which was discarded. The solvent was removed and acidic water (20 mL, 1M HCl) was added to the orange residue. The organic phase was extracted with diethyl ether (3x20 mL). The solvent was evaporated and the solid dissolved in the minimum volume of ethanol and an aqueous solution containing an excess of $[N(CH_3)_4]Cl$ was added, resulting in the formation of an orange precipitate. This was filtered off, washed with water and petroleum ether, and dried in vacuum. Yield: 280 mg (89%). Anal. Calcd for $C_{15}H_{54}B_{28}CoNO_2$: C: 28.05, H: 8.47, N: 2.18. Found: C: 28.02, H: 8.56, N: 2.23. IR: ν(cm^{-1})= 3051, 3037 (C_c-H), 2943, 2916, 2894, 2864 (C-H)$_{alkyl}$, 2598, 2561, 2511 (B-H), 1481, 1448, 1415 δ(CH_2), 1359, 1284, 1247 δ(CH), 1174, 1120, 1110 (C-O-C), 945 (C-N). ^{11}B RMN: δ= 25.0 (s, 1B, B(8)), 5.9 (d, ^{1}J(B,H) = 132, 1B), 2.7 (d, ^{1}J(B,H) = 140, 1B), -0.1 (d, ^{1}J(B,H) = 150, 1B), -2.0 (d, ^{1}J(B,H) = 185, 2B), -3.7 (d, ^{1}J(B,H) = 151, 1B), -5.2 (d, ^{1}J(B,H) = 108, 2B), -6.1 (d, ^{1}J(B,H) = 111, 4B), -7.6 (d, ^{1}J(B,H) = 167, 4B), -8.2 (d, ^{1}J(B,H) = 157, 4B), -10.4 (d, 1B), -15.0 (d, ^{1}J(B,H) = 147, 2B), -18.1 (d, ^{1}J(B,H) = 157, 2B), -19.6 (d, ^{1}J(B,H) = 165, 1B), -26.2 (d, ^{1}J(B,H) = 135, 1B). ^{1}H {^{11}B} NMR: δ= 4.28 (br s, 4H, C_c-H), 3.62 (t, ^{3}J(H,H)= 6, 2H, OCH_2CH_2), 3.53 (t, ^{3}J(H,H)= 6, 2H, OCH_2CH_2), 3.47 (t, ^{3}J(H,H)= 6, 2H, OCH_2CH_2), 3.45 (s, 12H, $N(CH_3)_4$), 2.61 (t, ^{3}J(H,H)= 6, 2H, CH_2), 2.94 (br s, 1H, BH), 2.90 (br s, 2H, BH), 2.81 (br s, 2H, BH), 2.78 (br s, 2H, BH), 2.70 (br s, 1H, BH), 2.40 (br s, 2H, BH), 2.28 (br s, 6H, BH), 2.18 (s, 3H, CH_3), 2.08 (br s, 2H, BH), 1.97 (br s, 2H, BH), 1.79 (br s, 2H, BH), 1.68 (br s, 2H, BH), 1.57 (br s, 2H, BH), 1.48 (br s, 1H, BH). ^{13}C{^{1}H} RMN: δ= 72.3 (s, C_c), 71.8 (s, OCH_2), 68.8 (s, OCH_2), 68.2 (s, OCH_2), 55.2 (s, $N(CH_3)_4$), 54.6 (s, C_c-H), 46.4 (s, C_c-H), 35.2 (s, CH_2), 22.8 (s, CH_3). MALDI-TOF-MS *m/z*: 567.41 (M, 100%).

Synthesis of $[N(CH_3)_4][1''$-{3,3'-Co(8-$(CH_2CH_2O)_2$-1,2-$C_2B_9H_{10}$)(1',2'-$C_2B_9H_{11}$)}-2''-C_6H_5-*closo*-1",2"-$C_2B_{10}H_{10}]$, $[N(CH_3)_4][9]$

The compound was prepared using the same procedure as for $[N(CH_3)_4][$**8**] but using 1-C_6H_5-1,2-*closo*-$C_2B_{10}H_{11}$. Yield: 290 mg (85%); Anal. Calcd for $C_{20}H_{56}B_{28}CoNO_2$: C: 34.11, H: 8.01, N: 1.99. Found: C: 35.10, H: 8.10, N: 2.03. IR: ν(cm^{-1})= 3053, 3041 (C_c-H), 2953, 2914, 2894, 2862 (C-H)$_{alkyl}$, 2604, 2565 (B-H), 1481, 1446, 1415 δ(CH_2), 1359, 1284, 1249 δ(CH), 1174, 1121, 1097 (C-O-C), 945 (C-N). ^{11}B RMN: δ= 24.9 (s, 1B, B(8)), 5.9 (d, J = 137, 1B), 2.6 (d, ^{1}J(B,H) = 144, 1B), -0.4 (d, ^{1}J(B,H) = 125, 1B), -1.7 (d, ^{1}J(B,H) = 137, 3B), -5.2 (d, 2B), -6.1 (d, ^{1}J(B,H) = 140, 4B), -8.3 (d, ^{1}J(B,H) = 146, 8B), -10.5 (d, 1B), -15.1 (d, ^{1}J(B,H) = 152, 2B), -18.2 (d, ^{1}J(B,H) = 156, 2B), -19.7 (d, ^{1}J(B,H) = 146, 1B), -26.3 (d, ^{1}J(B,H) = 159, 1B). ^{1}H{^{11}B} NMR: δ= 7.78-7.50 (m, 5H, C_6H_5), 4.26 (br s, 2H, C_c-H), 4.22 (br s, 2H, C_c-H), 3.46 (t, ^{3}J(H,H)= 5, 2H, OCH_2CH_2), 3.45 (s, 12H, $N(CH_3)_4$), 3.44 (t, ^{3}J(H,H)= 5, 2H, OCH_2CH_2), 3.33 (t, ^{3}J(H,H)= 5, 2H, OCH_2CH_2), 2.94 (br s, 1H, BH), 2.87 (br s, 2H, BH), 2.79 (br s, 1H, BH), 2.74 (br s, 2H, BH), 2.69 (br s, 2H, BH), 2.55 (br s, 1H, BH), 2.50 (br s, 1H, BH), 2.39 (br s, 3H, BH), 2.35 (br s, 3H, BH), 2.22 (br s, 2H, BH), 2.12 (t, ^{3}J(H,H)= 6, 2H, CH_2), 1.95 (br s, 2H, BH), 1.78 (br s, 2H, BH), 1.62 (br s, 2H, BH), 1.56 (br s, 2H, BH), 1.48 (br s, 1H, BH). ^{13}C{^{1}H} RMN: δ= 131.3 (s, C_6H_5), 131.0 (s, C_6H_5), 129.2 (s, C_6H_5), 127.4 (s, C_6H_5), 84.0 (s, C_c), 80.6 (s, C_c), 71.6 (s, OCH_2), 68.5 (s, OCH_2), 68.2 (s, OCH_2), 55.1 (s, $N(CH_3)_4$), 54.6 (s, C_c-H), 46.3 (s, C_c-H), 34.6 (s, CH_2). MALDI-TOF-MS *m/z*: 644.48 (M+CH_2, 15%), 630.49 (M, 100%), 384.19 (M-$C_{10}B_{10}H_{29}$, 10%)

b) Dianions.

Synthesis of $[NMe_4]Li[1''$,2''-{3,3'-Co(8-$(CH_2CH_2O)_2$-1,2-$C_2B_9H_{10}$)(1',2'-$C_2B_9H_{11}$)}$_2$-1'',2''-*closo*-$C_2B_{10}H_{10}]$, $[NMe_4]$Li[**5**].

A solution of 1,2- *closo*-$C_2B_{10}H_{12}$ (35 mg, 0.24 mmol) in DME (10 mL) was treated with 1.6 M *n*-butyllithium in hexane (0.31 mL, 0.49 mmol) at 0 °C for 30 min and left under stirring at room temperature for additional 30 min. A solution of [**1**] (200 mg, 0.49 mmol) in DME (30 mL) was added to the dilithium salts $Li_2[C_2B_{10}H_{11}]$ and reflux for 30 min. The solvent was evaporated at vacuum and the orange solid dissolved in water. Treatment the solution containing $[$**5**$]^{2-}$ with aqueous solution of $[N(CH_3)_4]Cl$ gave the $[NMe_4]$Li [**5**] salt. Yield: 221 mg (87%); R_f (CH_2Cl_2: CH_3CN 3: 1) 0.10; HPLC k' 3.31; Anal. Calcd for $C_{22}H_{80}B_{46}Co_2LiNO_4$: C: 25.29, H: 7.72, N: 1.34. Found: C: 25.16, H: 7.58, N: 1.38. IR: ν(cm^{-1})= 3051, 3037 (C_c-H), 2920, 2901, 2866 (C-H)$_{alkyl}$, 2597, 2576, 2561, 2528 (B-H), 1481, 1446, 1418 δ(CH_2), 1359, 1284, 1249 δ(CH), 1174, 1120, 1107, 1099 (C-O-C), 947 (C-N). ^{11}B NMR: δ= 23.8 (s, 2B, B8), 3.8 (d, ^{1}J(B,H) = 137, 2B), 0.5 (d, ^{1}J(B,H) = 140, 2B), -2.4 (d, ^{1}J(B,H) = 161, 2B), -4.2 (d, ^{1}J(B,H) = 130, 4B), -4.9 (d, ^{1}J(B,H) = 120, 2B), -7.4 (d, ^{1}J(B,H) = 130, 6B), -8.3 (d, ^{1}J(B,H) = 130, 8B), -10.5 (d, ^{1}J(B,H) = 149, 2 B), -17.2 (d, ^{1}J(B,H) = 155, 4B), -20.4 (d, ^{1}J(B,H) = 156, 4B), -22.0 (d, ^{1}J(B,H) = 175, 2B), -28.4 (d, ^{1}J(B,H) = 175, 2B). ^{1}H {^{11}B} NMR: δ= 4.29 (br s, 8H, C_c-H), 3.65-3.47 (m, 12H, OCH_2CH_2), 3.45 (s, 12H, $N(CH_3)_4$) 2.66-2.58 (m, 4H, CH_2), 2.94-1.48 (m, 44H, B-H). ^{13}C{^{1}H} NMR: δ= 78.8 (s, C_c), 71.7 (s, O-CH_2), 68.9 (s, O-CH_2), 68.2 (s, O-CH_2), 55.2 (s, $N(CH_3)_4$), 54.7 (s, C_c), 54.1 (s, C_c), 46.4 (s, C_c), 34.9 (s, CH_2). MALDI-TOF-MS *m/z*: 970.8 (M+Li, 71%), 553.55 ($CoC_{10}B_{28}H_{40}O_2$, 100%), 323.24 (3,3'-$Co(C_2B_9H_{11})_2$, 26%).

Synthesis of $Na_2[1''$,2''-{3,3'-Co(8-$(CH_2CH_2O)_2$-1,2-$C_2B_9H_{10}$)(1',2'-$C_2B_9H_{11}$)}$_2$-1'',2''-*closo*-$C_2B_{10}H_{10}]$, Na_2[5**].**

A solution of 1,2- *closo*-$C_2B_{10}H_{12}$ (200 mg, 1.39 mmol) in THF (5 mL) was treated with 2.5 M *n*-butyllithium in THF (1.2 mL, 3.0 mmol) at ca. -33 °C for 1h and left under stirring for 2-3 h at ambient temperature . The solution of the corresponding dilithium salts $Li_2[C_2B_{10}H_{11}]$ was then treated with a solution of [**1**] (1200 mg, 2.92 mmol) in THF (30 mL) and stirred for additional 4 h. The mixture was then decomposed by adding CH_3OH (1 mL) and 3M HCl (0.25 mL) and the organic volatiles were removed by vacuum evaporation. The acidic aqueous solution was extracted with diethyl ether (3 x 10 mL), 3M HCl (10 mL) and 10% Na_2CO_3 (3 x 10 mL). The organic layer was dried over $MgSO_4$, filtered, evaporated in vacuum, and dried at room temperature. The residue (crude Na^+_2 salts) was dissolved in a minimum amount of CH_2Cl_2 and purified by LC chromatography on silica gel to collect the main orange bands of the dianions. IR, ^{11}B and ^{1}H{^{11}B} NMR spectra are the same as above.

$^{13}C\{^1H\}$ NMR: δ= 79.7 (s, C_c), 72.6 (s, O-CH_2), 69.8 (s, O-CH_2), 69.1 (s, O-CH_2), 55.5 (s, C_c), 47.3 (s, C_c), 35.7 (s, CH_2). MS (ESI) *m/z*: 482.25 (M/2; 100%), 986.83 (M + Na; 10%).

Synthesis of Cs_2[1'',7''-{3,3'-Co-(8-($CH_2CH_2O)_2$-1,2-$C_2B_9H_{10}$)(1',2'-$C_2B_9H_{11}$)}$_2$-1'',7''-*closo*-$C_2B_{10}H_{10}$], Cs_2[6].

The same procedure as for $[N(CH_3)_4]$Li [**5**] but using 1,7- *closo*-$C_2B_{10}H_{12}$. The treatment of the solution containing $[\mathbf{6}]^{2-}$ with aqueous solution of CsCl gives the corresponding dicesium salt which can be recrystallized from hot aqueous ethanol and additional crystallization of the solid from CH_2Cl_2-hexane.Yield: 585 mg (40%): R_f (CH_2Cl_2:CH_3CN, 3:1) 0.07; HPLC k' 3.31; Anal. Calcd for $C_{18}H_{68}B_{46}Co_2Cs_2O_4$: C: 17.58, H: 5.57. Found: C: 17.12, H: 5.65. IR: ν(cm^{-1})= 3041 (C_c-H), 2926, 2871, 2867 (C-H)$_{alkyl}$, 2565, 2538 (B-H), 1455 δ(CH_2), 1365, 1247, 1249 δ(CH), 1150, 1134, 1097 (C-O-C). ^{11}B NMR (in CD_2Cl_2): δ= 24.5 (s, 2B, B8), 5.2 (d, ^{1}J(B,H) = 141, 2B), 0.1 (d, ^{1}J(B,H) = 144, 2B), -3.1 (d, ^{1}J(B,H) = 118, 2B), -6.6 (d, ^{1}J(B,H) = 140, 4B), -7.5 (d, z^{1}J(B,H) = 137, 10B), -10.0 (d, 4B), -11.9 (d, ^{1}J(B,H) = 156, 4B), -14.5 (d, ^{1}J(B,H) = 160, 2B), -16.2 (d, ^{1}J(B,H) = 190, 2B), -18.1 (d, ^{1}J(B,H) = 165, 4B), -20.3 (d, ^{1}J(B,H) = 165, 4B), -21.5 (d, ^{1}J(B,H) = 175, 2B), -29.5 (d, ^{1}J(B,H) = 175, 2B). $^1H\{^{11}B\}$ NMR (CD_2Cl_2): δ= 3.83 (br s, 8H, C_c-H), 3.66-3.51 (m, 12H, OCH_2), 2.27-2.35 (m, 4H, CH_2), 3.85-1.58 (m, 44H, B-H). $^{13}C\{^1H\}$ NMR: δ= 74.5 (s, C_c), 72.4 (s, O-CH_2), 70.0 (s, O-CH_2), 69.1 (s, O-CH_2), 55.6 (s, C_c), 47.2 (s, C_c), 37.3 (s, CH_2)). MS (ESI) *m/z:* 987.92 (M + Na; 100%).

Synthesis of 1-$CH_3OCH_2CH_2$-2-CH_3-1,2-*closo*-$C_2B_{10}H_{10}$, 10.

1-CH_3-1,2-*closo*-$C_2B_{10}H_{11}$ (1g, 6.32 mmol) was dissolved in 70 mL diethyl ether under nitrogen. Then it was cooled down to 0 ºC for 30 min and *n*-butyllithium (5 mL, 6.32 mmol) was added dropwise. The reaction was left for 30 min at 0 ºC and 30 min at room temperature. It was then cooled again at 0 ºC and ethyl methyl ether chloride (0.7 mL, 3.88 mmol) was added slowly. After 30 min at low temperature, the solution was stirred for 5 h at 25 ºC. Finally it was treated with water; the organic layer was washed several times. The organic phase was dried over $MgSO_4$, filtered and evaporated to dryness. The final residue was treated with hot hexane to obtain transparent oil. Yield: 1.21 g (88.6%). Anal. Calcd for $C_6H_{20}B_{10}O$: C: 33.31, H: 9.32. Found: C: 33.35, H: 9.08. IR: ν(cm^{-1})= 2987, 2938, 2903, 2838, 2804 (C-H), 2587 (B-H), 1482, 1462, 1426, 1391 δ(C-H), 1201, 1124 (C-O). ^{11}B RMN: δ= -4.3 (d, ^{1}J(B,H) = 178, 1B), -5.8 (d, ^{1}J(B,H) = 167, 1B), -9.2 (d, 2B), -9.9 (d, 2B), -10.5 (d, ^{1}J(B,H) = 155, 4B). ^{1}H NMR: δ= 3.50 (t, ^{3}J(H,H)= 6, 2H, OCH_2), 3.31 (s, 3H, OCH_3), 2.46 (t, ^{3}J(H,H)= 6, 2H, CH_2-C_c), 2.03 (s, 3H, CH_3-C_c). $^{13}C\{^1H\}$ RMN: δ= 75.9 (s, C_c), 74.8 (s, C_c), 70.5 (s, OCH_2), 58.6 (s, OCH_3), 35.1 (s, CH_2-C_c), 23.3 (s, CH_3-C_c).

Synthesis of Cs_2[7"-{3,3'-Co-(8-(OCH_2CH_2)$_2$-1,2-$C_2B_9H_{10}$)(1',2'-$C_2B_9H_{11}$)}-7'',8''-*nido*-$C_2B_9H_{11}$)], Cs_2[11].

Cs[**2**] (100 mg, 1.45 mmol) was dissolved in 96% ethanol (5 mL) and solid CsF (67 mg, 4.35 mmol) was added. The resulting solution was refluxed for 20 h. After cooling down, the solvents were vacuum evaporated and the dried solid residue, dissolved in a mixture of methylene chloride:acetonitrile (3:1), was injected at the top of a silica gel column (1 cm x 15 cm); the product was eluted using the same solvent mixture as the mobile phase R_f (CH_2Cl_2: CH_3CN 3: 1)= 0.15. Yield 81 mg (68%). For characterization, this salt was dissolved in aqueous ethanol 60% and precipitated by excess of aqueous $[HN(CH_3)_3]$Cl; the precipitate was filtered and dried in vacuum at 60ºC. Anal. Calcd for $C_{10}H_{40}B_{27}CoCs_2O_2$: C: 14.84, H: 4.98. Found: C: 14.51, H: 5.04; IR: ν(cm^{-1})= 3040 (C_c-H), 2924, 2871, 2867 (C-H)$_{alkyl}$, 2563, 2531 (B-H), 1455 δ(CH_2), 1385, 1362, 1247, (CH), 1152, 1132, 1097 (C-O-C).^{11}B NMR (CD_3CN): δ= 23.1 (s, 1B), 3.8 (d, ^{1}J(B,H) = 117), -0.1 (d, ^{1}J(B,H) = 140, 1B), -2.7 (d, ^{1}J(B,H) = 133, 1B), -4.8 (d, ^{1}J(B,H) = ca. 146, 1B), -8.2 (d, ^{1}J(B,H) = ca. 130, 6B), -8.6 (d, 2B), -11.33 (d, 2B), -14.5 (d, 1B), -17.6 (d, ^{1}J(B,H) = 155, 4B), -18.7 (d, ^{1}J(B,H) = 155, 1B), -20.6 (d, ^{1}J(B,H) = 156, 2B), -22.4 (d, ^{1}J(B,H) = ca. 149, 2B), -28.5 (d, ^{1}J(B,H) = 175, 1B), -33.8 (d, ^{1}J(B,H) = 107, 1B), -37.8 (d, ^{1}J(B,H) = 135, 1B). $^1H\{^{11}B\}$ NMR: 7.05 (br. s, 1H, NH), 4.23 (s, 2H, C_c-H), 4.18 (s, 2H, C_c-H), 3.5 (br t, 2H, CH_2O), 3.4 (m, 2H, CH_2O), 3.36 (t, 2H, ^{3}J(H,H)= 6.0, CH_2O), 2.78 (s, 9H, $HN(CH_3)_3$), 2.15 (s, 1H, CH), 1.75 (m, 2H, C-CH_2), 2.64 (br s, 4B), 2.63 (br s, 1B), 2.44 (br s, 1B), 2.89, 1.94, 1.88 (br s, 5B), 1.65 (br s, 2B), 1.63, 1.12 (br s, 2B), 1.60 (br s, 1B), 1.57, 1.13 (br s, 4B), 1.47 (br s, 2B), 1.41 (br s, 1B), 1.02 (br s, 1B), 0.36 (br s, 1B), -0.55 (br s, 1B), -2.78 (br s, 1B, BHB). $^{13}C\{^1H\}$ RMN (CD_3CN): 72.7 (s, CH_2O), 69.2 (s, CH_2O), 55.0 (s, C_c-H), 45.8 (s, $HN(CH_3)_3$), 39.7 (s, CH_2). MS (ESI) *m/z*: 271.92 (M/2, 100%), 544.50 (M + 2H, 10%).

Synthesis of $[N(CH_3)_4]_2$[7"-{3,3'-Co-(8-(OCH_2CH_2)$_2$-1,2-$C_2B_9H_{10}$)(1',2'-$C_2B_9H_{11}$)}-8''-Me-7'',8''-*nido*-$C_2B_9H_{10}$)], $[N(CH_3)_4]_2$[12].

Under nitrogen atmosphere, KOH (461 mg, 8.22 mmol) was dissolved completely in ethanol (20 mL), followed by the addition of Li[8] (150 mg, 0.26 mmol). The reaction mixture was refluxed on an oil bath for 5 h at 100 ºC. The solvent was then evaporated and over the product obtained, a saturated solution of $[N(CH_3)_4]$Cl was added, leading to the formation of an yellow compound, $[N(CH_3)_4]_2$[12]. Yield: 100 mg (55%); Anal. Calcd for $C_{19}H_{66}B_{27}CoO_2N_2$: C: 32.36, H: 9.37, N: 3.97. Found: C: 32.29, H: 9.59, N: 3.95. IR (cm^{-1}): υ= 3035 (C_c-H), 2923 (C_{alkyl}-H), 2866 (N-H), 2527 (B-H), 1481 (N-C). ^{11}B NMR: δ = 22.3 (s, 1B), 3.1 (d, ^{1}J(B,H) = 132, 1B), 0.2 (d, ^{1}J(B,H) = 147, 1B), -2.7 (d, ^{1}J(B,H) = 149, 1B), -4.3 (d, ^{1}J(B,H) = 157, 2B), -7.9, -8.58, -10.9 (d, 12B), -13.6 (d, ^{1}J(B,H) = 155, 1B), -18.4 (d, ^{1}J(B,H) = 90, 2B), -20.8 (d, ^{1}J(B,H) = 154, 2B), -22.5 (d, ^{1}J(B,H) = 157, 2B), -28.7 (d, ^{1}J(B,H) = 152, 1B), -34.8 (d, ^{1}J(B,H) = 200, 1B), -37.2 (d, ^{1}J(B,H) = 143, 1B). $^1H\{^{11}B\}$ NMR: δ= 4.31 (s, 4H, C_c-H), 3.54 (m, 2H, OCH_2CH_2), 3.51 (m, 2H, OCH_2CH_2), 3.43 (s, 12H, $N(CH_3)_4$), 2.08, 1.96, 1.74, 1.66, 1.54, 1.44, 1.33, 1.18 (br s, B-H), 2.83 (s, 3H, C_c-CH_3), -2.65 (s, 1H, BHB). $^{13}C\{^1H\}$ NMR (300 MHz, acetone-d_6, 293K): δ= 71.9 (s, O-CH_2), 71.4 (s, O-CH_2), 68.3 (s, O-CH_2), 55.2 (s, $N(CH_3)_4$), 54.7(s, C_c), 46.3 (s, C_c), 35.1 (s, CH_2), 21.5 (s, CH_3). MALDI-TOF-MS *m/z*: 556.57 (M, 43%), 408.38 (fragment I, 45%), 146.06 (fragment III, 100 %).

Synthesis of $[N(CH_3)_4]_2$[7”-{3,3’-Co-(8-$(OCH_2CH_2)_2$-1,2-$C_2B_9H_{10}$)(1’,2’-$C_2B_9H_{11}$)}-8’’-C_6H_5-7’’,8’’-*nido*-$C_2B_9H_{10}$)], $[N(CH_3)_4]_2$[13].

Under nitrogen atmosphere, KOH (461 mg, 8.22 mmol) was dissolved completely in ethanol (20 mL), followed by the addition of Li[9] (150 mg, 0.23 mmol). The reaction mixture was refluxed on an oil bath for 5 h at 100 ^{0}C. The solvent was then evaporated and over the product obtained, a saturated solution of $[N(CH_3)_4]$Cl was added, leading to the obtaining of an orange solid, $[N(CH_3)_4]_2$[13]. Yield: 126 mg (70%). Anal. Calcd for $C_{24}H_{68}B_{27}CoO_2N_2$: C: 37.57, H: 8.87, N 3.65. Found: C: 36.82, H: 8.81, N: 4.17. IR (cm^{-1}): υ= 3039 (C_c-H), 2534 (B-H), 2924 (C_{alkyl}-H), 2739 (N-H), 1477 (N-C). ^{11}B NMR: δ= 23.7 (s, 1B), 4.6 (d, ^{1}J(B,H) = 134, 1B), 1.4 (d, ^{1}J(B,H) = 142, 1B), -1.6 (d, ^{1}J(B,H) = 141, 1B), -3.0 (d, ^{1}J(B,H) = 145, 2B), -6.6, -7.4, -9.4 (d, 12B), -12.6 (d, ^{1}J(B,H) = 139, 1B), -16.4 (d, ^{1}J(B,H) = 161, 2B), -19.5 (d, ^{1}J(B,H) = 150, 2B), -21.1 (d, ^{1}J(B,H) = 205, 1B), -27.5 (d, ^{1}J(B,H) = 152, 1B), -31.7 (d, ^{1}J(B,H) = 103, 1B), -34.8 (d, ^{1}J(B,H) = 147, 1B). ^{1}H NMR: δ= 7.75-7.05 (m, 5H, C_6H_5), 4.21 (br s, 2H, C_c-H), 4.16 (br s, 2H, C_c-H), 3.44 (s, 12 H, $N(CH_3)_4$), 3.36 (m, 4H, OCH_2CH_2), 2.91-1.74 (br s, B-H), 2.12 (t, 2H, CH_2), -2.2 (s, 1H, BHB). ^{13}C{^{1}H} NMR (300 MHz, acetone-d_6, 293K): δ= 131.8-124.2 (C_{C6H5}), 71.38 (s, O-CH_2), 71.0 (s, O-CH_2), 68.3 (s, O-CH_2), 55.2 (s, $N(CH_3)_4$), 54.4(s, C_c), 46.4 (s, C_c), 35.2 (s, CH_2).

Trianions

Synthesis of K_2Li**[7”,8”-{3,3’-Co-(8-$(OCH_2CH_2)_2$-1,2-$C_2B_9H_{10}$)(1’,2’-$C_2B_9H_{11}$)}$_2$-7’’,8’’-*nido*-$C_2B_9H_{10}$],** K_2Li**[14].**

KOH method: In a typical experiment, to a 25 mL round bottomed flask containing 12 mL deoxygenated ethanol, KOH (620 mg, 11.05 mmoles) was added and stirred until complete dissolution. Li_2[**5**] (300 mg, 0.307 mmoles) was added and the reaction mixture was refluxed for 21 h at ≈100 ^{0}C. The reaction mixture was then neutralized with gaseous CO_2; the resulted white precipitate was filtered and the liquid obtained evaporated, yielding an orange compound, K_2Li[**14**]. Yield: 272 mg (86%). Anal. Calcd for $C_{18}H_{68}B_{45}CoO_2K_2Li$: C: 22.18, H: 6.98. Found: C: 22.03, H: 6.77. IR (cm^{-1}): υ= 3036 (C_c-H), 2922 (C_{alkyl}-H), 2865 (N-H), 2526 (B-H), 1481 (N-C). ^{11}B NMR: δ= 23.8 (s, 2B), 4.6 (d, ^{1}J(B,H) = 128.7, 2B), 1.4 (d, ^{1}J(B,H) = 143, 2B), -1.5 (d, ^{1}J(B,H) = 155, 2B), -3.3 (d, ^{1}J(B,H) = 161, 4B), -6.5, -7.2 (d, 14B), -10.1 (d, ^{1}J(B,H) = 128, 2B), -13.3 (d, ^{1}J(B,H) = 119, 1B), -16.3 (d, ^{1}J(B,H) = 146, 4B), -17.8 (d, ^{1}J(B,H) = 161.5, 2B), -19.6 (d, ^{1}J(B,H) = 157, 4B), -21.0 (d, ^{1}J(B,H) = 126, 2B), -27.5 (d, ^{1}J(B,H) = 125, 2B), -32.6 (d, ^{1}J(B,H) = 86, 1B), -36.5 (d, ^{1}J(B,H) = 160, 1B). ^{1}H{^{11}B} NMR: δ= 4.26 (br s, 8H, C_c-H), 3.61-3.48 (m, 8H, CH_2CH_2), 2.92-1.56 (br s, B-H), -2.68 (s, 1H, BHB). ^{13}C{^{1}H} NMR: δ= 71.8 (s, O-CH_2), 71.3 (s, O-CH_2), 68.1 (s, O-CH_2), 54.1 (s, C_c), 46.3 (s, C_c), 33.9 (s, CH_2).

Synthesis of Cs_3**[7”,8”-{3,3’-Co-(8-$(OCH_2CH_2)_2$-1,2-$C_2B_9H_{10}$)(1’,2’-$C_2B_9H_{11}$)}$_2$-7’’,8’’-*nido*-$C_2B_9H_{10}$],** Cs_3**[14].**

CsF method: The Cs_2[5] (400 mg, 0.32 mmol) was dissolved in deoxygenated ethanol (15 mL) and CsF (500 mg, 3.27 mmol) was added. The reaction mixture was refluxed for 24 h. Then the ethanol was evaporated and water (20 mL) was added. The orange aqueous solution was extracted with diethyl ether (2x 10 mL) and then with ethylacetate (2 x 20 mL) to remove unreacted anion $[5]^{2-}$ and other impurities. The aqueous solution was evaporated to dryness, dried in vacuum and the resulting solids were extracted with acetone (2 x 5 mL); the solution was concentrated to ca 1 mL, yielding an orange compound. The product Cs_3[14] was recrystallized from hot water. Yield: 343 mg (78%). HPLC k' 3.03 (Separon SGX C8, 250x 4 mm I.D., 4.5 mM hexylamine acetate in 58% aqueous CH_3CN, pH 5.6), HPLC purity 98.5%, R_f (CH_2Cl_2:CH_3CN, 3:1= 0.02. Anal. Calcd for $C_{18}H_{68}B_{45}Co_2Cs_3O_4$, C: 15.99, H: 5.07. Found: C: 15.51, H: 5.18; IR: ν(cm^{-1})= 3042 (C_c-H), 2925, 2871, 2867 (C-H)$_{alkyl}$, 2560, 2531 (B-H), 1608, 1455 δ(CH_2), 1383, 1360, 1249 δ(CH), 1163, 1134, 1107, 1099 (C-O-C). ^{11}B NMR: δ= 23.6 (s, 2B, B8), 5.2 (d, ^{1}J(B,H) = 117, 2B), 0.5 (d, ^{1}J(B,H) = 140, 2B), -2.4 (d, ^{1}J(B,H) = 133, 2B), -4.6 (d, ^{1}J(B,H) = ca. 146, 2B), -7.1 (d, ^{1}J(B,H) = ca. 130, 8B), -8.6 (d, 2B), -10.1 (d, 2B), -12.1 (d, 1B), -17.1 (d, ^{1}J(B,H) = 155, 4B), -17.8 (d, ^{1}J(B,H) = 155, 2B), -19.1 (d, ^{1}J(B,H) = 155, 2B), -20.3 (d, ^{1}J(B,H) = 156, 4B), -22.0 (d, ^{1}J(B,H) = ca. 149, 2B), -28.3 (d, ^{1}J(B,H) = 175, 2B), -34.0 (d, ^{1}J(B,H) = 107, 1B), -37.0 (d, ^{1}J(B,H) = 135, 1B). ^{1}H{^{11}B} NMR: 4.18 (s, 4H, CH), 4.14 (s, 4H, CH), 3.65 (t, 4H, *J*(H,H)= 4.8, CH_2O), 3.65 (m, 8H, CH_2O), 2.93 (br s, 1BH), 2.900 (s, 2H, H_2O), 2.83 (br s, 1BH), 2.72 (br s, 1BH), -2.71 (br s, 2BH), 2.68 (br s, 1BH), 2.03, 1.97 (br s, 2BH), 1.915 (m, 4H, C-CH_2), 1.82 (br s, 6BH), 1.69 (br s, 4BH), 1.63 (br s, 2BH), 1.45 (br s, 3BH), 1.29 (br s, 1BH), 0.52 (br s, 1BH), 0.05 (br s, 1BH), -1.53 (br s, 1BH), -2.70 (br s, 1BH, BHB). ^{13}C{^{1}H} NMR: 72.8 (s, CH_2O), 72.6 (s, CH_2O), 69.3 (s, CH_2O), 58.5 (s, C_c-H), 53.9 (s, C_c-H), 47.4 (s, C_c-H), 34.9 (s, CH_2). MS (ESI) *m/z*: 318.40 (M/3 + H, 100 %), 319.68 (M/3 + 2H, 4 %).

Synthesis of Cs_2[7”-{3,3’-Co-(8-$(OCH_2CH_2)_2$-1,2-$C_2B_9H_{10}$)(1’,2’-$C_2B_9H_{11}$)}-7’’,9’’-*nido*-$C_2B_9H_{11}$)], Cs_2[15].

The Cs[**3**] (100 mg, 1.45 mmol) was dissolved in 1,2-ethanediol (5 mL) and solid CsF (67 mg, 4.35 mmol) was added. The resulting solution was refluxed for 16 h. After cooling down, water (2 mL) was added, the solvents were evaporated in vacuum and the solid residue dried under reduced pressure; afterwards it was dissolved in a mixture of methylene chloride-acetonitrile 9:1, injected at the top of a silica gel column (1 x 15 cm) and the product eluted using the same solvent mixture as the mobile phase. Yield 29 mg (24%). Anal. Calcd for $C_{10}H_{40}B_{27}CoCs_2O_2$: C: 14.84, H: 4.98. Found: C: 15.01, H: 5.03. IR: ν(cm^{-1})= 3043, 2958 (C_c-H), 2925, 2874, 2854 (C-H)$_{alkyl}$, 2565, 2537, (B-H), 1616, 1458, δ(CH_2), 1383, 1360, 1262 δ(CH), 1154, 1133, 1098 (C-O-C). ^{11}B NMR: δ= 23.9 (s, 1B, B8), 3.7 (d, ^{1}J(B,H) = 134, 1B), 0.5 (d, ^{1}J(B,H) = 140, 1B), -1.2 (d, ^{1}J(B,H) = 153, 1B), -2.4 (d, ^{1}J(B,H) = 149, 1B), -4.2 (d, ^{1}J(B,H) = ca. 177, 2B), -4.9 (d, ^{1}J(B,H) = 128, 1B), ca. 6.2 (d, 1B), -7.4 (d, ^{1}J(B,H) = ca. 123, 2B), -8.1 (d, ^{1}J(B,H) = 129, 4B), -17.2 (d, ^{1}J(B,H) = 143, 2B), -20.5 (d, ^{1}J(B,H) = 156, 2B), -21.6, (d, ^{1}J(B,H) = ca. 150, 2B), -22.6 (d, ^{1}J(B,H) = ca. 150, 2B), ca. -22.9 (d, 1B) -28.4 (d, ^{1}J(B,H) = 172, 1B), -34.5 (d, ^{1}J(B,H) = 134, 1B), -35.4 (d, ^{1}J(B,H) = 135 1B). ^{1}H{^{11}B} NMR: 4.29 (s,

4H, C_c-H), 3.61 (m, 4H, CH_2O), 3.48 (t, 2H, J(H,H)=4.8, CH_2O), 2.94 (br s, 1H), 2.88 (s, H_2O), 2.76 (br s, 1H), 2.75 (br s, 1H), 2.69 (br s, 1H), 2.40 (br s, 1H), 2.39 (br s, 1H), 2.095 (s, 1H, CH), 1.78 (br s, 2H), 1.65 (br s, 2H), 1.29 (m, 2H, C-CH_2), 3.08, 2.92, 1.97 (br s, 5H), 1.67, (br s, 2H), 1.63, 1.19 (br s, 3H), 1.55 (br s, 2H), 1.46 (br s, 1H), 0.72 (br s, 1H), 0.24 (br s, 1H), -2.18 (br s, 1H, BHB). $^{13}C\{^1H\}$ RMN ($[HN(CH_3)_3]^+$): 56.2 (s, CH_2O), 51.3 (s, CH), 47.28 (s, CH), 39.5 (s, CH_2C), 21.2 (s, CH). MS (ESI) *m/z*: 271.92 (M/2, 100%), 566.58 (M + Na, 28%).

Acknowledgements

Spanish Ministerio de Ciencia y Tecnología (MAT2006-05339 and FPU grant to A.C.), CSIC (I3P grant to P.F.) and the Generalitat de Catalunya 2005/SGR/00709 are appreciated. Support from the Ministry of Education of the Czech Republic (Project LC523 and Research Plan AV0Z40320502) and Grant Agency of the Academy of Sciences of Czech Republic (Project No. IAAX00320901). We also thank Dr. M. Kvíčalová for part of MS measurements. We also thank to Dipl. Ing. M. Kvíčalová, Dr. E. Vecernikova Mrs. M. Marikova for part of MS and IR measurements.

Scheme 1. Simplified structures and formation of the monoanionic and dianionic twelve-vertex dicarboranes modified by the 8-substituted [3,3'-Co(1,2-$C_2B_9H_{11})_2$]$^-$ function via a 1,4-dioxahexane interconnection chain

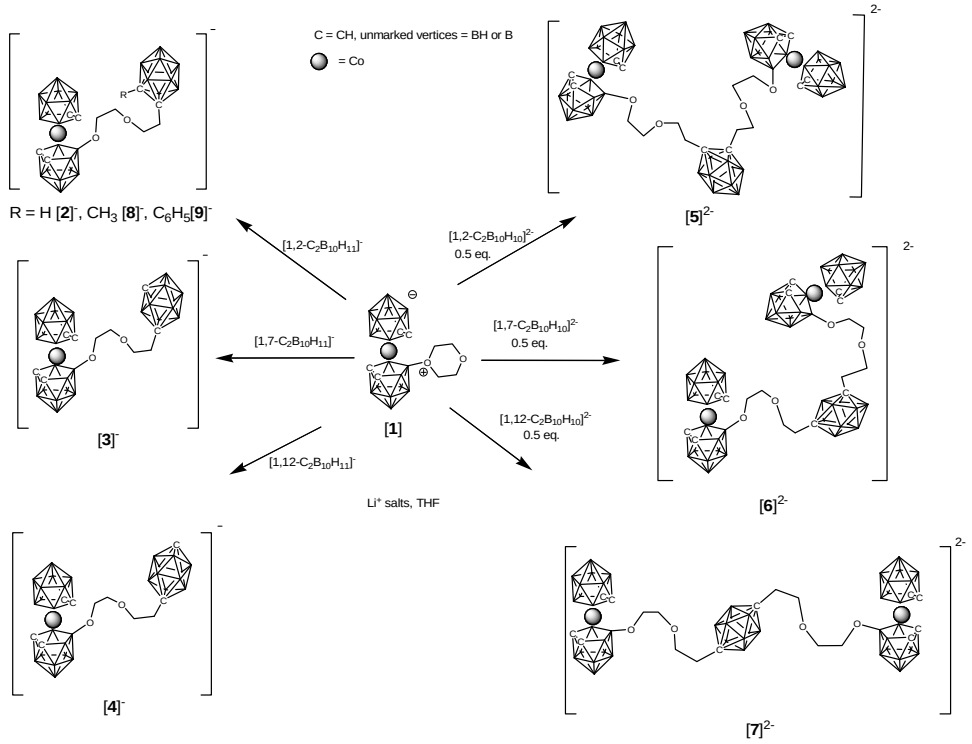

Scheme 2. Partial deboronation reaction of *closo* compounds yielding the corresponding di- and tri-anionic species.

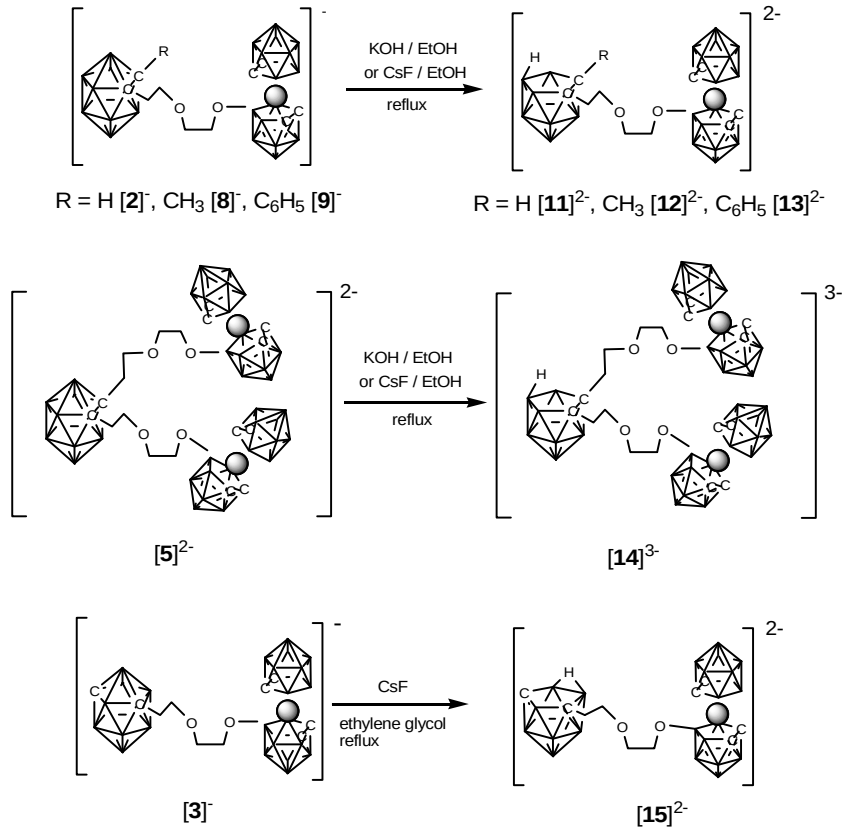

Figure 1. a) Notional fragmentation of the monoanionic methyl derivative $[8]^-$; b) fragmentation of the dianionic methyl derivative $[12]^{2-}$

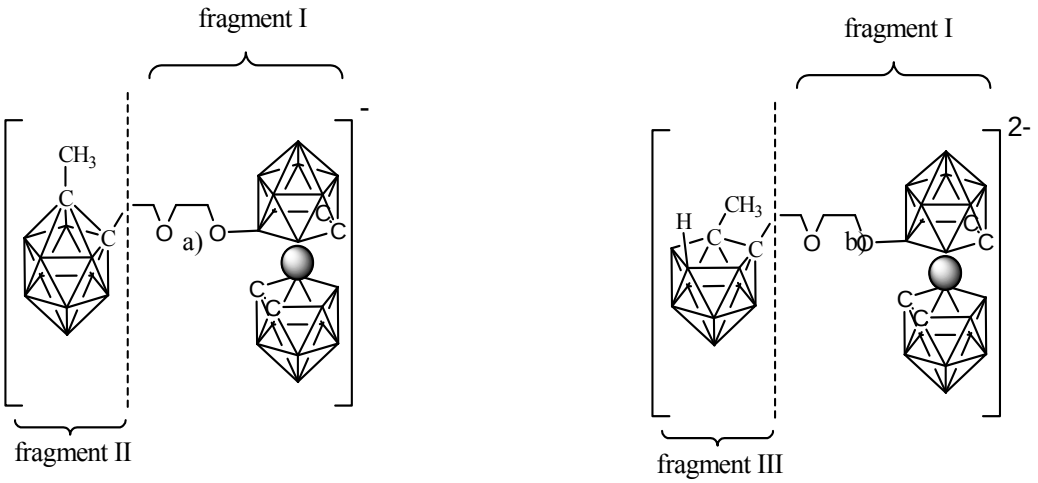

Figure 2. a) Disarticulation of the experimental ^{11}B NMR spectrum of [**8**]$^-$. b) ^{11}B NMR spectrum of [3,3'-Co-8-$(CH_2CH_2O)_2$-(1,2-$C_2B_9H_{10}$)-(1',2'-$C_2B_9H_{11}$)]$^-$. c) Theoretical spectrum of fragment II. d) Experiment ^{11}B NMR spectrum of [**10**].

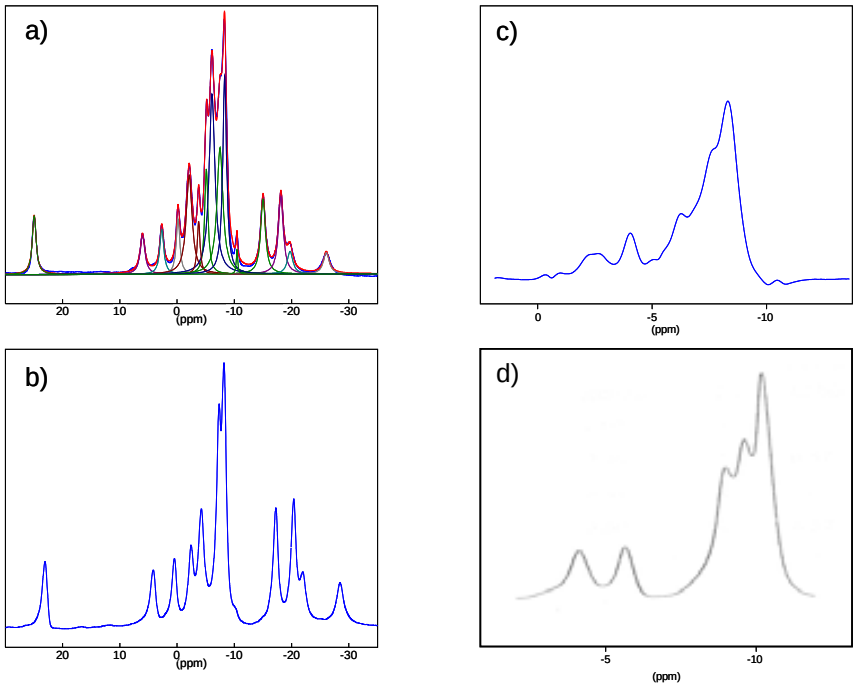

Figure 3. Comparison between $^{11}B\{^{1}H\}$ NMR spectra of the *closo* compound $[8]^-$ and its corresponding *nido* species $[12]^{2-}$.

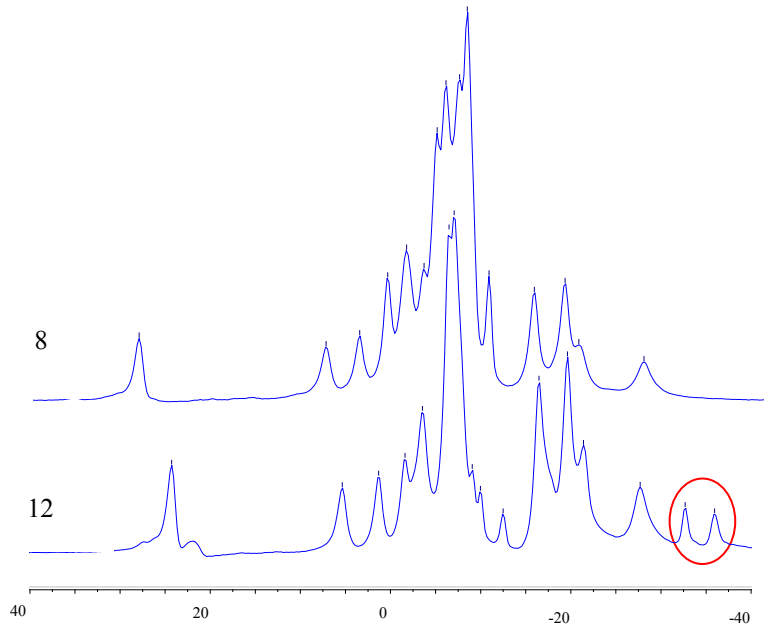

Figure 4. a) Schematic representation of $^{11}B\{^{1}H\}$ NMR spectrum of compound $[12]^{2-}$ as sum of fragment I and III and b) its experimental one.

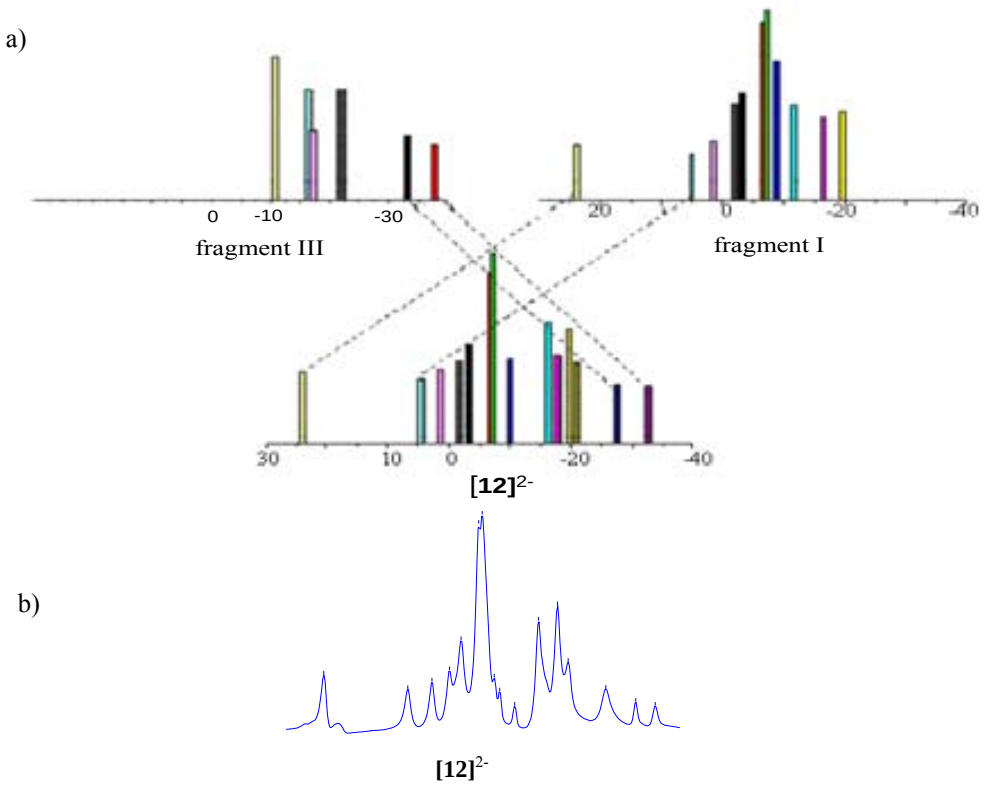

Figure 5. The experimental MALDI-TOF-MS spectrum of $[NMe_4]Li[\mathbf{5}]$.with its theoretical molecular peak MS spectrum.

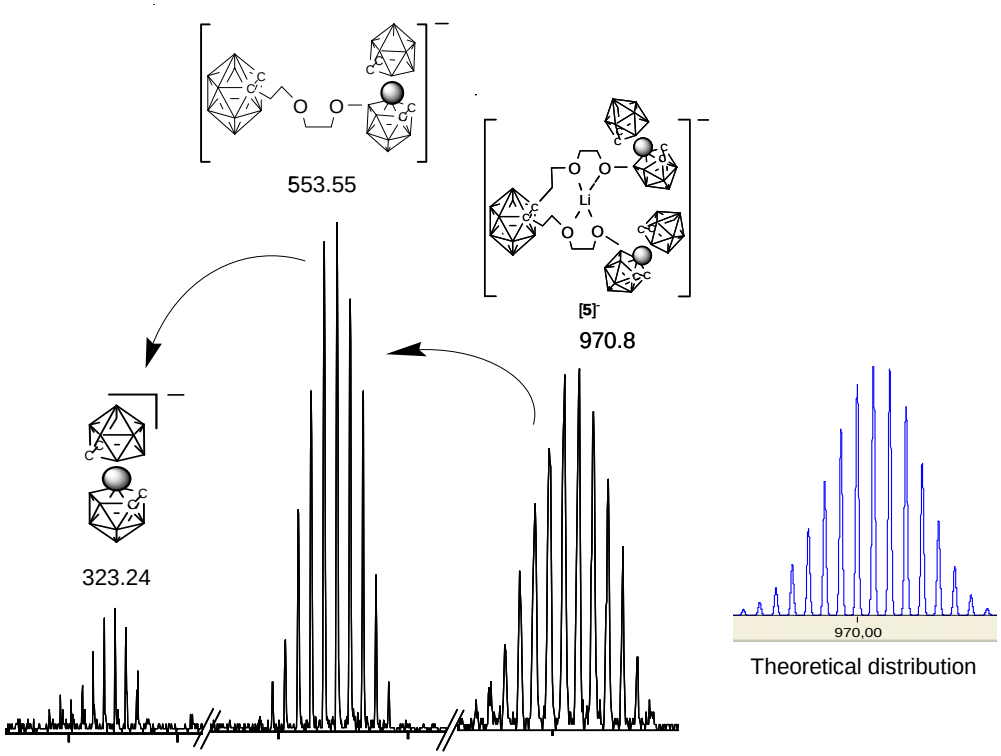

Figure 6. The MALDI-TOF-MS spectroscopy of compound $[NMe_4]_2[\mathbf{12}]$.

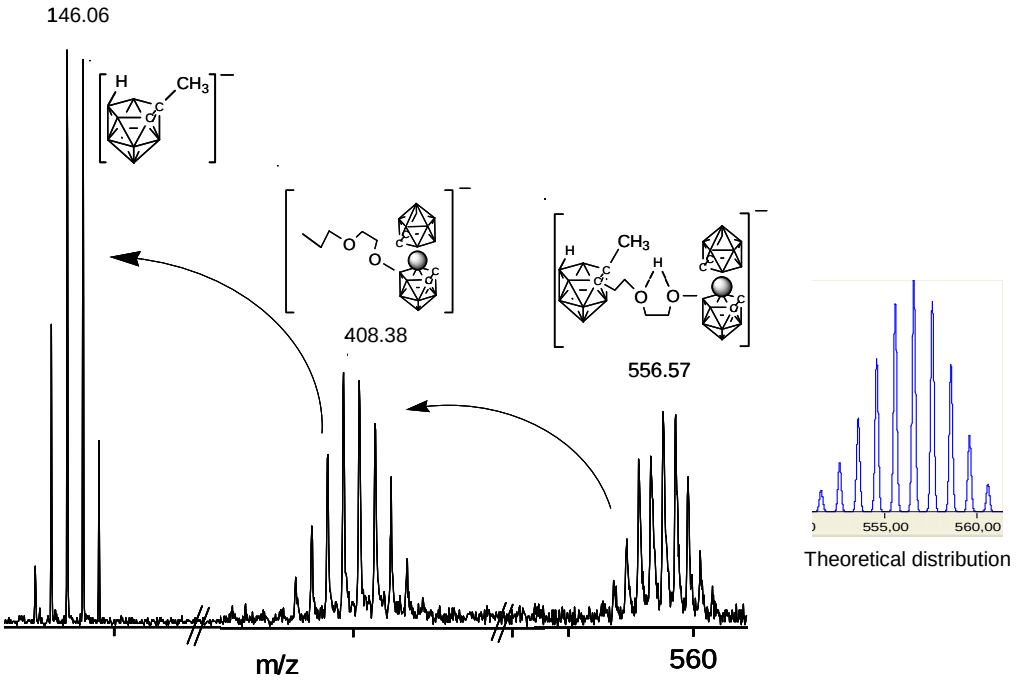

Table 1. Summary of disarticulation of the ^{11}B NMR signals for compound [8]$^-$ together with peak assignments

Gaussian nº	δ(ppm)	% integral	overall integration	Fragm. I	Fragm. II
1	24.95	4.19	1	1	
2	6.04	3.37	1	1	
3	2.67	3.28	1	1	
4	-0.16	3.61	1	1	
5	-2.11	10.68	3	2	1
6	-3.77	2.80	1		1
7	-5.11	6.47	2	2	
8	-6.1	19.15	6	4	2
9	-7.49	13.86	2		2
10	-8.31	13.96	4		4
11	-15.01	6.48	2	2	
12	-18.12	6.96	2	2	
13	-19.73	2.29	1	1	
14	-26.05	2.26	1	1	

References

[1] a) Bernard, R.; Cornu, D.; Perrin, M.; Schaff. J. P.; Miele, P. *J. Organomet. Chem.*, **2004**, *689*, 2581. b) Zhizhin, K. Y.; Mustyatsa, V. N.; Malinina, E. A.; Votinova, N. A.; Matveev, E. Y.; Goeva, L. V.; Polyakova, I. N.; Kuznetsov, N. T. *Russ. J. Inorg. Chem.*, **2005**, *50*, 203.

[2] a) Sivaev, I. B.; Starikova, Z. A.; Sjöberg S.; Bregadze, V. I. *J. Organomet. Chem.*, **2002**, *649*, 1-8. b) Plešek, J.; Grüner, B.; Heřmánek, S.; Báča, J.; Mareček, V.; Jänchenová, J.; Lhotský, A.; Holub, K.; Selucký, P.; Rais, J.; Císařová I.; Čáslavský, J. *Polyhedron* **2002**, *21*, 975-986. c) Plešek, J.; Hermanek, S.; Nöth H.; Franken, A. Preparations and Structures of New [(1,2-$C_2B_9H_{11})_2$-3-Co]$^-$ Derivatives, Ninth International Meeting on Boron Chemistry, Ruprech-Karls-Universität, Heidelberg, Germany, July 14-18, **1996**, Poster #82. d) Plešek, J.; Hermánek, S.; Franken, A.; Cisarova I.; Nachtigal, C. *Collect. Czech. Chem. Commun.*, **1997**, *62*, 47-56. e) Sivaev, I. B.; Semioshkin, A. A.; Brellochs, B.; Sjöberg, S.; Bregadze, V. I. *Polyhedron*, **2000**, *19*, 627.

[3] a) Plesek, J.; Hermánek, S.; Base, K.; Todd, L. J.; Wright, W. F. *Collect. Czech. Chem. Commun.*, **1976**, *41*, 3509. b) Petřina, A.; Petříček, V.; Malý, K.; Šubrtová, V.; Línek, A.; Hummel, L. *Z. Kristallogr.*, **1981**, *154*, 217. c) Selucký, P.; Plešek, J.; Rais, J.; Kyrš, M.; Kadlecová, L. *J. Radioanal. Nucl. Chem.*, **1991**, *149*, 131. d) Šubrtová, V.; Petříček, V.; Hummel, L. *Acta Crystallogr., Sect. C*, **1989**, *45*, 1964.

[4] a) Bernard, R.; Cornu, D.; Perrin, M.; Schaff. J. P.; Miele, P. *J. Organomet. Chem.*, **2004**, *689*, 2581. b) Zhizhin, K. Y.; Mustyatsa, V. N.; Malinina, E. A.; Votinova, N. A.; Matveev, E. Y.; Goeva, L. V.; Polyakova, I. N.; Kuznetsov, N. T. *Russ. J. Inorg. Chem.*, **2005**, *50*, 203.

[5] a) Sivaev, I. B.; Starikova, Z. A.; Sjöberg S.; Bregadze, V. I. *J. Organomet. Chem.*, **2002**, *649*, 1. b) Plešek, J.; Grüner, B.; Heřmánek, S.; Báča, J.; Mareček, V.; Jänchenová, J.; Lhotský, A.; Holub, K.; Selucký, P.; Rais, J.; Císařová I.; Čáslavský, J. *Polyhedron* **2002**, *21*, 975. c) Plešek, J.; Hermanek, S.; Nöth H.; Franken, A. Preparations and Structures of New [(1,2-$C_2B_9H_{11})_2$-3-Co]$^-$ Derivatives, Ninth International Meeting on Boron Chemistry, Ruprech-Karls-Universität, Heidelberg, Germany, July 14-18, **1996**, Poster #82. d) Plešek, J.; Hermánek, S.; Franken, A.; Cisarova I.; Nachtigal, C. *Collect. Czech. Chem. Commun.*, **1997**, *62*, 47. e) Sivaev, I. B.; Semioshkin, A. A.; Brellochs, B.; Sjöberg, S.; Bregadze, V. I. *Polyhedron*, **2000**, *19*, 627.

[6] Semioshkin, A. A.; Sivaev, I. B.; Bregadze, V. I. *Dalton Trans.*, **2008**, 977.

[7] a) Romanovskiy, V. N.; Smirnov, I. V.; Babain, V. A.; Todd, T. A.; Law, J. D.; Herbst, R. S.; Brewer, K. N. *Solvent Extr. Ion Exch.*, **2001**, *19*, 1. b) Dozol, J. F.; Dozol, M.; Macias, R. M. *J. Inclusion Phenom. Macrocyclic Chem.*, **2000**, *38*, 1. c) Rais, J.; Grüner, B. in *Ion Exchange and Solvent Extraction*, ed. Y. Marcus and A. K. Sengupra, CRC Press, Boston, **2004**, vol. *17*, pp. 243–334. d) Mikulasek, L.; Grüner, B.; Crenguta, D.; Rudzevich, V.; Boehmer, V.; Haddaoui, J.; Hubscher-Bruder, V.; Arnaud-Nue, F.; Caslavsky, J.; Selucký, P. *Eur. J. Org. Chem.*, **2007**, 4772.

[8] a) Masalles, C.; Llop, J.; Viñas, C.; Teixidor, F. *Adv. Mater.*, **2002**, *14*, 826. b) Llop, J.; Masalles, C.; Viñas, C.; Teixidor, F.; Sillanpää, R.; Kivekäs, R. *Dalton Trans.*, **2003**, 556. c) Svorcik, V.; Gardasova, R.; Rybka, V.; Hnatowicz, V.; Cervena, J.; Plešek, J. *J. Appl. Polym. Sci.*, **2004**, *91*, 40. d) Gentil, S.; Crespo, E.; Rojo, I.; Friang, A.; Viñas, C.; Teixidor, F.; Grüner, B.; Gabel, D. *Polymer*, **2005**, *46*, 12218. e) Mola, J.; Mas-Marza, E.; Sala, X.; Romero, I.; Rodríguez, M.; Viñas, C.; Parella, T.; Llobet, A. *Angew. Ch. Int. Ed.*, **2008**, *47*, 5830.

[9] Plesek, J. *Chem. Rev.*, **1992**, *92*, 269.

[10] a) Strauss, S. H. *Chem. Rev.*, **1993**, *93*, 927. b) Reed, C. A. *Acc. Chem. Res.*, **1998**, *31*, 133.

[11] Nieuwenhuyzen, M; Seddon, K. R.; Teixidor, F.; Puga, A. V.; Viñas, C. *Inorg. Chem.*, **2009**, *48*, 889.

[12] Cigler, P.; Kožišek, M.; Řezačova, P.; Brynda, J.; Otwinowski, Z.; Pokorna, J.; Plešek, J.; Gruner, B.; Dolečkova-Marešova, L.; Maša, M.; Sedlaček, J.; Bodem, J.; Kräusslich, H.; Kral, V.; Konvalinka, J. *PNAS*, **2005**, *102*, 15394.

[13] a) Hawthorne, M. F. *Angew. Chem. Int. Ed.*, **1993**, *32*, 950. b) Soloway, A.H.; Tjarks, W.; Barnum, B. A.; Rong, F.-G.; Barth, R. F.; Codogni, I.M.; Wilson, J. G. *Chem. Rev.*, **1998**, *98*, 1515. c) Valliant, J. F.; Guenther, K. J.; King, A. S.; Morel, P.; Schaffer, P.; Sogbein, O. O.; Stephenson, K. A. *Coord. Chem. Rev.*, **2002**, *232*, 173. d) Sivaev, I. B.; Bregadze, V.; Sjöberg, S. in *Research and Development in Neutron Capture Therapy*, ed. W. Sauerwein, R. Moss and A. Wittig, Monduzzi Editore S.p.A., Bologna, **2002**, pp. 19–23.

[14] Teixidor, F.; Pedrajas, J.; Rojo, I.; Viñas, C.; Kivekäs, R.; Sillanpää, R.; Sivaev, I. B.; Bregadze, V. I.; Sjöberg S. *Organometallics*, **2003**, *22*, 3414.

[15] a) Grüner, B.; Plešek, J.; Báča, J.; Císařová, I.; Dozol, J.-F.; Rouquette, H.; Viñas, C.; Selucký, P.; Rais, J. *New J. Chem.*, **2002**, *26*, 1519. b) Rojo, I.; Teixidor, F.; Kivekäs, R.; Sillanpää, R.; Viñas, C *Inorg. Chem.*, **2003**, *22*, 4642. c) Hao, E.; Sibrian-Vazquez, M.; Serem, W.; Garno, J. C.; Fronczek, F. R.; Vicente, M. G. H. *Chem. Eur. J.*, **2007**, *13*, 9035. d) Farràs, P.; Teixidor, F.; Kivekäs, R.; Sillanpää, R.; Viñas, C; Bohumir, G; Cisarova, I. *Inorg. Chem.*, **2008**, 47, 9497.

[16] a) Hao, E.; Vicente, M. G. H. *Chem. Commun.*, **2005**, 1306. b) Hao, E.; Jensen, T. J.; Courtney, B. H.; Vicente, M. G. H. *Bioconjugate Chem.*, **2005**, *16*, 1495.

[17] a) Olejniczak, A. B.; Plešek, J.; Křiž, O.; Lesnikowski, Z. J. *Angew. Chem. Int. Ed.*, **2003**, *42*, 5740. b) Lesnikowski, Z. J.; Paradowska, E.; Olejniczak, A. B.; Studzinska, M; Seekamp, P.; Schußler, U.; Gabel, D.; Schinazi, R. F.; Plešek, J. *Bioorg. Med. Chem.*, **2005**, *13*, 4168. c) Olejniczak, A. B.; Plešek, J.; Lesnikowski, Z. J. *Chem. Eur. J.*, **2007**, *13*, 318.

[18] Bernard, R.; Cornu, D.; Grüner, B.; Dozol, J. F.; Miele, P.; Bonnetot, B. *J. Organomet. Chem.*, **2002**, *657*, 83.

[19] Sivaev, I. B.; Sjöberg S.; Bregadze, V. *J. Organomet. Chem.*, **2003**, *680*, 106.

[20] Šícha, V.; Farràs, P.; Štíbr, B.; Teixidor, F.; Grüner, B.; Viñas, C. *J. Organomet. Chem.*, **2009**, *694*, 1599.

[21] Fanning, J.C. *Coord. Chem. Rev.* **1995**, *140*, 27.

[22] a) Wiesboeck, R. A.; Hawthorne, M. F. *J. Am. Chem. Soc*., **1964**, *86*, 1642. b) Garret, P. M.; Tebbe, F. N.; Hawthorne, M. F. *J. Am. Chem. Soc*., **1964**, *86*, 5016. c) Hawthorne, M. F.; Young, D. C.; Garret, P. M.; Owen, D. A.; Schwerin, S. G.; Tebbe, F. N.; Wegner, P. M. *J. Am. Chem. Soc.*, **1968**, *90*, 862.

[23] a) Zakharkin, L. I.; Kalinin, U. N. *Tetrah. Letters*, **1965**, 407. b) Zakharkin, L. I.; Kirillova, V. S. *Izv. Akad. Nauk SSSR, Ser. Khim*., **1975**, 2596. c) Taoda, Y.; Sawabe, T.; Endo, Y.; Yamaguchi, K.; Fujii, S.; Kagechika, H. *Chem. Commun.*, **2008**, 2049.

[24] a) Fox, M. A.; Gill, W. R.; Herbertson, P. L.; MacBride, J. A. H.; Wade, K. *Polyhedron*, **1996**, *16*, 565. b) Fox, M. A.; MacBride, J. A. H.; Wade, K. *Polyhedron*, **1997**, *16*, 2499. c) Fox, M.A.; Wade, K. *Polyhedron*, **1997**, *16*, 2517. d) Yoo, J.; Hwang, J. W.; Do, Y. *Inorg. Chem.*, **2001**, *40*, 568.

[25] Davidson, M. G.; Fox, M. A.; Hibbert, T.G.; Howard, J.A.K.; Mackinnon, A.; Neretin, I.S.; Wade, K. *Chem. Commun.*, **1999**, 1649.

[26] Massiot, D.; Fayon, F.; Capron, M.; King, I.; Le Calvé, S.; Alonso, B.; Durand, J-O.; Bujoli, B.; Gan, Z.; Hoatson, G. *Magn. Reson. Chem.*, **2002**, *40*, 70.

[27] a) Karas, M.; Hillenkamp, F. *Anal. Chem*., **1988**, *60*, 2299. b) Karas, M.; Bachmann, D.; Hillenkamp, F. *Anal. Chem.*, **1985**, *57*, 2935. c) Tanaka, K.; Waki, H.; Ido, Y.; Akita, S.; Yoshida, Y.; Yoshida, T. *Rapid Commun. Mass Spectrom*., **1988**, *2*, 151.

[28] a) Bienkowski, T.; Brodzik-bienkowska, A.; Danikiewicz, W. *J. Mass Spectrom.* **2002**; *37*: 617. b) Gatlin, C. L.; Turecek, F. In *Electrospray Ionization Mass Spectrometry: Fundamentals, Instrumentation and Applications*, Cole, R. B. (ed.). Wiley: New York, **1997**; chapt. 15.

[29] a) Henderson, W.; Scott McIndoe, J. S. In *Mass Spectroscopy of Inorganic, coordination and Organometallic Chemistry*, Wiley **2005**. b) Gatlin, C. L.; Turecek, F. In *Electrospray Ionization Mass Spectrometry: Fundamentals, Instrumentation and Applications*, Cole, R. B. (ed.). Wiley, **1997**.

[30] Shriver, D. F.; Drezdon, M. A. *Manipulation of Air Sensitive Compounds*, 2nd Ed., Wiley, New York, **1986**.

Co···P Interaction on a new family of bridged cobaltacarboranes.

(Preliminary version)

Pau Farràs,[a,±] Isabel Rojo,[a] Raikko Kivekäs,[b] Reijo Sillanpää,[c] Francesc Teixidor,[a] Clara Viñas,[a,*]

[a] Institut de Ciència de Materials de Barcelona (CSIC), Campus de la U.A.B., E-08193 Bellaterra, Spain. Telefax: Int. Code + 34 93 5805729. E-mail: clara@icmab.es.

[b] Department of Chemistry, P.O. Box 55, University of Helsinki, FIN-00014, Finland.

[c] Department of Chemistry, University of Jyväskylä, FIN-40351, Finland.

[±] Pau Farras is enrolled in the PhD program of the UAB.

Introduction

To be written later.

Computational details

Calculations were performed with the Gaussian 03 suite of programs.[1] All geometries were optimized at the B3LYP/6-31G* level of theory,[2] with no symmetry constraints. Frequency calculations were computed on these geometries at the same level of calculation to verify that they are energy minima. NBO (natural bond orbital) analysis,[3] including NPA charges of the compounds, were calculated at the B3LYP/6-311+G** level of theory along with their frontier orbitals. ^{31}P-NMR chemical shifts were calculated at the GIAO-B3LYP/6-311+G** level. They have not been referenced, only relative differences between the compounds were taken into consideration in order to compare them with experimental data.

Results and Discussion

1. Synthesis of non-oxidized anions 3, 7, 11 and 15. See Chart 1 for numbering of metallacarboranes.

The desired anionic bridged phosphine compounds may be conveniently prepared by metallation of Cs[3,3'-Co(1,2-$C_2B_9H_{11}$)$_2$] (**1**) or Cs[8,8'-C_6H_4-3,3'-Co(1,2-$C_2B_9H_{11}$)$_2$] (**2**) with *n*-BuLi, followed by simple reaction with the corresponding dichlorophosphine in 1,2-dimethoxyethane (DME) at low temperature, as shown in Scheme 1. The NMe_4 salts can be produced by metathesis dissolving Li^+ salts in ethanol and adding an aqueous solution of [NMe_4]Cl. Solids corresponding to NMe_4^+ salts separate well and can be collected by filtration. Column cromatography is needed to purify the compounds by using a dicloromethane/acetonitrile mixture 70:30. The formula of [**3**]$^-$, [**7**]$^-$, [**11**]$^-$ and [**15**]$^-$ were established from the mass spectrum obtained by the matrix-assisted laser desorption ionization (MALDI-TOF) technique in the negative-ion mode without the use of a matrix. Figure 1 shows the MALDI-TOF mass spectrum of the anion [**3**]$^-$. Peaks corresponding to masses higher and lower than the molecular ion peak at m/z 430.8 are observed at m/z 446.8 (M+O) and 323.6 (M-PPh). Full agreement between the experimental and calculated patterns was obtained for the molecular ion peak. The ^{11}B, ^{1}H, and ^{31}P-NMR spectra of the compounds were found to be in accord with the proposed structures shown in Chart 1. For example, the ^{11}B{^{1}H}-NMR spectrum of NMe_4[**7**] displays a 2:2:1:3:2:2:2:2:2 pattern in the range δ = +8.7 to -22.5 ppm, indicative of a *closo* species with all boron atoms in nonequivalent vertices in one dicarbollide unit. The resonance of relative intensity 3 may be attributed to the coincidental overlap of two absorptions one of intensity 2 and a second of intensity 1. The non-boron bridged anion [**3**]$^-$ and [**11**]$^-$ have even more asymmetry as most of boron atoms can be assigned in a 1:1:2:1:3:3:1:1:1:2:1:1 pattern, for example for [**3**]$^-$. This is due to the mixture of two diastereoisomers, the racemic mixture and the *meso* form. This pattern is consistent with single substitution at a cluster carbon in each dicarbollide moiety. In agreement with this, the ^{31}P{^{1}H}-NMR spectrum shows only one resonance at δ = 70.4 to 88.3 ppm for anions [**3**]$^-$ and [**11**]$^-$. However, for anions [**7**]$^-$ and [**15**]$^-$ two different resonances can be found attributed to the *meso* and *racemic* isomers. This is due to the less flexible structure caused by the aromatic bridged group on boron atoms. The ^{1}H-NMR spectrum displays a group of resonances between δ = 7.64 and 7.48 ppm corresponding to the aromatic protons, two resonances at δ = 5.3-5.0 ppm on anions [**3**]$^-$ and [**11**]$^-$ and at δ = 4.3-4.0 ppm on anions [**7**]$^-$ and [**15**]$^-$ corresponding to the C_c-H proton (C_c = cluster carbon atom), and one resonance at δ = 1.1 ppm corresponding to the *tert*-butyl groups. Finally, the ^{13}C{^{1}H}-NMR spectra show a group of ressonances at δ = 133 to 128 ppm corresponding to the aromatic protons with coupling constants with phosphorus from 6 to 34Hz depending on their relative position, a doublet centered at δ = 63-60 ppm with ^{2}J(C,P) = 21 Hz corresponding to C_c-P carbon, an a ressonance at δ = 53-50 ppm corresponding to C_c-H carbon. Interestingly, anions [**7**]$^-$ and [**15**]$^-$ where a mixture of *meso* and *racemic* isomers is observed, no signal corresponding to C_c-P carbon atoms can be seen due to the complicated couplings within the isomers. It has been not possible to separate them although an x-ray diffraction study of [NMe_4]**7** confirmed that one of the synthesized geometrical isomer was indeed the *meso* form.

2. Crystal structure of [NMe_4]7.

Crystals of [NMe_4]**7** suitable for an X-ray diffraction study were obtained by slow evaporation of the solvent from a solution of the compound in dichloromethane. The structure consists of well-separated [NMe_4]$^+$ ions and phenylphosphine cobaltabisdicarbollide [**7**]$^-$ ions. Figure 2 shows a drawing of the compound. As expected, the metal in [**7**]$^-$ is sandwiched by the pentagonal faces of the two dicarbollide units. The pentagonal faces have a mirror conformation, with the torsion angle C1-c-c'-C1' being 0.97º (c = centroid of

C1,C2,B7,B8,B4 face; c' = centroid of C1',C2',B7',B8',B4' face). Thus, the dicarbollide moieties have a *meso* disposition. The symmetry of [**7**]$^-$ is P21/c in the solid state. The distance Co-P is 2.768Å, which is lower the sum of van der Waals radii of these atoms.

3. Synthesis of the oxidized anions of 3, 7, 11 and 15 with oxygen, sulphur and selenium.

The moderate stability of these compounds under air have required to be oxidized to their corresponding cobaltabisdicarbollide phosphine oxides to use hydrogen peroxide in acetone. By using this strong oxidizing agent the reaction can be done at room temperature. However, in order to obtain the oxidized molecules with sulphur and selenium we have required to use 30h refux to a complete oxidation. After work-up procedures the compounds have been obtained in very high yields. Characterization has been done using the same techniques. For example, MALDI-TOF-MS spectra can be used in order to compare the relative stability of the molecules depending on the substituent on phosphorus. Mass spectra of anions [**5**]$^-$ and [**13**]$^-$ are shown in figure 3. Peaks corresponding to masses lower than the molecular ion peak at m/z 462.64 for [**5**]$^-$ are observed at m/z 429.63 (M-S); however, for [**13**]$^-$ fragmentation peaks corresponding to masses lower than the molecular ion peak at m/z 442.69 are observed at m/z 386.56 (M-^{t}Bu), 353.53 (M-^{t}Bu-S) and 323.53 (M-^{t}Bu-S-P). This difference in fragmentation is also observed in all other oxidized species. The ^{11}B, ^{1}H, and ^{31}P-NMR spectra of the compounds were found to be in agreement with the proposed structures shown in Chart 1. For example, it can be observed that in general ^{11}B{^{1}H}-NMR spectra of oxidized species have less ressonances in respect to the non-oxidized due a major incidental overlap. Remarkable are the ^{31}P-NMR spectra in comparison to the non-oxidized species which are discused below. In addition, it has been possible to obtain crystal structures of compounds [NMe$_4$]**4**, [NMe$_4$]**5** and [NMe$_4$]**6**.

4. Crystal structures of [NMe$_4$]4, [NMe$_4$]5 and [NMe$_4$]6.

Good quality crystals for x-ray diffraction studies were grown by slow evaporation of compounds [NMe$_4$]**4** and [NMe$_4$]**5** in dichloromethane solutions and by slow evaporation of [NMe$_4$]**6** in toluene. Figure 4, figure 5 and figure 6 show a drawing of each compound.

5. Comparison between ^{31}P-NMR spectra of non-oxidized and oxidized species.

In table 1 are shown the ressonances corresponding to all synthesized compounds. First of all, ressonance peaks of anions [**3**]$^-$, [**7**]$^-$, [**11**]$^-$ and [**15**]$^-$ appear in a very downfield chemical shift. Cobaltabisdicarbollide phosphine compounds already synthesized in our grup showed ressonances at 25 ppm[4] but these new bridged-phosphine compounds have ressonances between 70 and 96 ppm. This means that the electronic environment on phosphorus is totally different and that phosphorus atoms on bridged species are very deshielded. Moreover, electrons cannot disappear so instead they move away from phosphorus to another part of the molecule. Once oxidized, the species have resonances between 35 and 55 ppm indicating a shielding on phosphorus due to the presence of oxygen electron density. The oxidation with sulphur and selenium causes again a downfield shift to approximately the same ressonances as for the non-oxidized starting species. In fact, this behaviour is already seen in most of phosphine molecules and it is due to an electron retrodonation from phosphorus to sulphur or selenium, causing a decrease on the electron density on the first. Therefore, we can conclude that the electronic environment on phosphorus on the P-S and P-Se species is the same as for the non-oxidized compounds. But, what can it be?

6. Theoretical calculations on phosphorus-bridged compounds.

In the introduction we have compared the structures of bridged ferrocenophanes and bridged cobaltacarboranophanes. The first have distorted ciclopentadiene planes calculated by the geometrical parameter α. In contrast, cobaltacarboranophanes have less distorted dicarbollide planes and this is accentuated in boron phenyl-bridged anions [**7**]$^-$ and [**15**]$^-$ where the planes are almost parallel. However, the proximity of the phosphorus atom to the metal is greater in bridged cobaltacarboranophanes in comparison to ferrocenophanes, taking into consideration the relative van der Waals radii of cobalt and iron. Moreover, it is known that boron clusters are electron-withdrawing groups that can decrease the electron density on phosphous but in our previously synthesized disubstituted diphenylphoshine derivatives, the abnormal shifting on ^{31}P-NMR for the bridged compounds wasn't observed. Therefore, we have to assume that the metal is the responsible for the deshielding on phosphorus *via* a ligand-to-metal interaction. This was already hypothesized in

ferrocenophanes by doing Mössbauer spectroscopy.[5]

Geometry optimizations of the targeted compounds are the first calculations that have to be done in order to get the structure with the minimal energy. This is the starting point from which most of the properties of the molecule can be calculated. A comparison between the available X-ray experimental data and theoretical interatomic distances of selected bonds are done in order to check the validity of the optimitzed structures. Then, a calculation of theorical ^{31}P-NMR ressonances has been done because NMR gives information on the nature of each nucleus in solution. Thus, if a good correlation between the theoretical and experimental chemical shifts is achieved, then the optimized geometry may be considered a good representation of its molecular structure in solution. This would allow us to study the possible interactions seen in solution by using the calculated structures. In table 2 are shown the absolut chemical shifts calculated for anions [**3**]$^-$, [**4**]$^-$, [**5**]$^-$ and [**6**]$^-$. The relative differences between the non-oxidized and oxidized species are also shown from both theoretical and experimental data. It can be seen that differences of 20 ppm are found for [**4**]$^-$ and [**6**]$^-$ but in general the tendency is comparable between theoretical and experimental data, despite the complexity of the studied molecules.

To learn on the nature of intramolecular interactions, NBO analysis has been performed to anions [**3**]$^-$, [**4**]$^-$, [**5**]$^-$, [**6**]$^-$ and [**7**]$^-$. By using the second order perturbation theory analysis included in NBO it is possible to estimate donor-acceptor interactions between natural bond orbitals, along with their energy. For non-oxidized anions [**3**]$^-$ and [**7**]$^-$ three different interactions can be found between phosphorus and cobalt. Two of them with an energy of 20 kcal/mol correspond to the interaction between P-C_c bond and an empty 4s orbital of cobalt. The other interaction is found between the lone pair on phosphorus and the same empty 4s orbital as before, with an energy of 10 kcal/mol. The interactions are shown in figure 7 along with a representation of the interaction between phosphorus and cobalt.

On the other hand, for oxidized anions [**4**]$^-$, [**5**]$^-$ and [**6**]$^-$ there is no interaction between phosphorus and cobalt due to the abscence of the lone pair, which is bonded to the chalcogen atoms. The only interaction found in those compounds is between the P-C_c bond and the empty 4s orbital of cobalt with an energy of approximately 8 kcal/mol. This energy is independent of the chalcogen atom as in all compounds is very similar.

Finally, HOMO orbitals of molecules [**3**]$^-$ and [**4**]$^-$ have been compared as shown in figure 8. It can be seen that the contribution of phosphorus atom in the HOMO orbital of anion [**3**]$^-$ is very important, while for [**4**]$^-$ is inexistent. This is in accordance with the results obtained by the NBO analysis because the only way that phosphorus contributes to HOMO orbital is by a transfer of electrons to the metal. Moreover, it is also seen that there is a high contribution of the P-C_c bonds helping the electronic transfer from/to phosphorus and cobalt. For [**4**]$^-$ the lone pair of phosphorus is bonded to oxygen cancelling the contribution to the HOMO orbital, which is mostly formed by a d orbital of cobalt.

Conclusions

To be written latter.

Experimental Section

Instrumentation. Elemental analyses were performed in our laboratory using a Carlo Erba EA1108 microanalyzer. IR spectra (ν, cm^{-1}; KBr pellets) were obtained on a Shimadzu FTIR-8300 spectrophotometer. The ^{1}H- and ^{1}H{^{11}B}-NMR (300.13 MHz), ^{13}C{^{1}H}-NMR (75.47 MHz), ^{11}B- and ^{11}B{^{1}H}-NMR (96.29 MHz) and ^{31}P{^{1}H}-NMR (121.48 MHz) spectra were recorded on a Bruker ARX 300 instrument equipped with the appropriate decoupling accessories. All NMR spectra were performed in deuterated solvents at 22ºC. The ^{11}B- and ^{11}B{^{1}H}-NMR shifts were referenced to external $BF_3{\cdot}OEt_2$, while the ^{1}H, ^{1}H{^{11}B}, and ^{13}C{^{1}H}-NMR shifts were referenced to $SiMe_4$ and the ^{31}P{^{1}H}-NMR to external 85% H_3PO_4. Chemical shifts are reported in units of parts per million downfield from reference, and all coupling constants in Hz. The mass spectra were recorded in the negative ion mode using a Bruker Biflex MALDI-TOF-MS [N_2 laser; λ_{exc} 337 nm (0.5 ns pulses); voltage ion source 20.00 kV (Uis1) and 17.50 kV (Uis2)].

Materials. All manipulations were carried out under inert atmosphere. 1,2-dimethoxyethane (DME) was distilled from sodium benzophenone prior to use. Reagents were obtained commercially and used as purchased. Cs[3,3'-Co(1,2-$C_2B_9H_{11})_2$] **(1)** and Cs[8,8'-μ-(1'',2''-C_6H_4)-3,3'-Co(1,2-$C_2B_9H_{10})_2$] **(2)** were obtained from Katchem while dichlorophenylphosphine and dichlorotertbutylphosphine from Aldrich.

Synthesis of [N(CH$_3$)$_4$][1,1'-μ-PPh-3,3'-Co(1,2-$C_2B_9H_{10})_2$] (3). Under an inert atmosphere, *n*-butyllithium (1.6M in hexanes, 2.8 mL, 4.38 mmol) was added dropwise to a

stirred solution of **1** (1.0 g, 2.19 mmol) in anhydrous DME (30 mL) at -40ºC. The resulting purple solution was stirred for 60 min at low temperature. Then, dichlorophenylphosphine (0.3 mL, 2.19 mmol) was added, causing a rapid color change to red. After the mixture had been stirred all night at room temperature, a grey solid was filtered off and discarded. After removal of the solvent, the residue was dissolved in the minimum volume of EtOH and an aqueous solution containing an excess of $[Me_4N]Cl$ was added, resulting in the formation of a precipitate. This was filtered off, washed with water and petroleum ether, and dried in vacuo. The resulting orange solid was purified by column chromatography using CH_2Cl_2/CH_3CN (75/25) as the mobile phase (R_f=0.42). Yield: 0.96 g (87%). Elemental analysis calcd (%) for $C_{14}H_{37}B_{18}CoNP$: C=33.37, H=7.40, N=2.42; found: C=33.26, H=7.21, N=1.34. IR: ν = 3048 (C_c-H), 2957, 2927 (C_{aryl}-H), 2547 (B-H), 1480 δ(C-H)$_{alkyl}$, 946 (C-N), 1433, 1093, 741, 698. ^{1}H-NMR: δ = 7.64-7.49 (m, 5H, Ph), 5.31 (br s, 1H, C_c-H), 4.95 (br s, 1H, C_c-H), 3.44 (s, 12H, $N(CH_3)_4$), 4.68–0.97 (br m, 18H, B-H). ^{1}H{^{11}B}-NMR: δ = 7.64-7.49 (m, 5H, Ph), 5.31 (br s, 1H, C_c-H), 4.95 (br s, 1H, C_c-H), 3.44 (s, 12H, $N(CH_3)_4$), 4.68, 4.58, 3.97, 3.69, 3.00, 2.79, 2.07, 1.88, 1.64, 1.31, 0.97 (s, 18H, B-H). ^{13}C{^{1}H}-NMR: δ = 132.91 (d, ^{1}J(P,C) = 26 Hz, P-C), 131.97 (d, ^{2}(P,C) = 34 Hz, P-C_{ortho}), 131.45 (s, P-C_{para}), 128.48 (d, ^{3}(P,C) = 6 Hz, P-C_{meta}), 60.49 (d, ^{1}J(P,C) = 21 Hz, P-C_c), 59.40 (d, ^{1}(P,C) = 19 Hz, P-C_c), 54.98 (s, $N(CH_3)_4$), 53.66 (s, C_c-H), 50.85 (s, C_c-H). ^{11}B-NMR: δ = 8.29 (d, ^{1}J(B,H) = 160 Hz, 1B), 6.32 (d, ^{1}J(B,H) = 170 Hz, 1B), 2.21 (d, ^{1}J(B,H) = 142 Hz, 2B), -0.95 (d, ^{1}J(B,H) = 153 Hz, 1B), -2.45 (d, ^{1}J(B,H) = 123 Hz, 3B), -3.11 (d, ^{1}J(B,H) = 140 Hz, 3B), -4.60 (d, ^{1}J(B,H) = 149 Hz, 1B), -6.25 (d, ^{1}J(B,H) = 149 Hz, 1B), -14.62 (d, ^{1}J(B,H) = 158 Hz, 1B), -16.32 (d, ^{1}J(B,H) = 154 Hz, 2B), -20.40 (d, ^{1}J(B,H) = 184 Hz, 1B), -22.73 (d, ^{1}J(B,H) = 203 Hz, 1B). ^{31}P{^{1}H}-NMR: δ = 70.37 (s, $(C_c)_2$-PPh). MALDI-TOF MS: m/z (%): 430.73 (M), 446.75 (M+O).

Synthesis of $[N(CH_3)_4][1,1'$-μ-OPPh-3,3'-Co(1,2-$C_2B_9H_{10})_2]$ (4). To a round bottom flask (100 mL) containing **3** (1 g, 1.98 mmol) was added acetone (50 mL). The mixture was cooled (ice-water) during the drop wise addition of a 0.1 M solution of H_2O_2 (56 mL, 5.66 mmol). After stirring four hours a solution of $[N(CH_3)_4]Cl$ was added. The orange product was filtered, washed with water and cold petroleum ether. Yield: 0.92 g (89%). Elemental analysis calcd (%) for $C_{14}H_{37}B_{18}CoNOP$: C=32.34, H=7.17, N=2.69; found: C=32.03, H=7.01, N=2.73. IR: ν = 3065, 3055, 3034 (C_c-H), 2957, 2921 ($C_{aryl/alkyl}$-H), 2576, 2552, 2505 (B-H), 1485 δ(C_{alkyl}-H), 1212 (P=O), 945 (C-N), 1435, 1037, 742, 686, 490. ^{1}H-RMN: δ = 8.02, 7.95, 7.73, 7.62 (m, 5H, Ph), 4.95 (s, 1H, C_c-H), 4.41 (s, 1H, C_c-H), 3.44 (s, 12H, $N(CH_3)_4$), 4.42-1.22 (br m, 18H, B-H). ^{1}H{^{11}B}-RMN: δ = 8.02, 7.95, 7.73, 7.62 (m, 5H, Ph), 4.95 (s, 1H, C_c-H), 4.41 (s, 1H, C_c-H), 3.44 (s, 12H, $N(CH_3)_4$), 3.33, 3.29, 3.13, 3.03, 2.77, 2.61, 2.41, 2.29, 2.16, 1.88, 1.77, 1.66, 1.21, 0.89 (s, 18H, B-H). ^{13}C{^{1}H}-RMN: δ = 133.54 (s, Ph), 131.55 (d, ^{3}J(P,C)=10, Ph), 128.57 (d, ^{2}J(P,C)=12, Ph), 56.86 (s, C_c), 54.87 (s, $N(CH_3)_4$), 54.06 (s, C_c). ^{11}B-RMN: δ = 8.7 (d, ^{1}J(B,H)=141, 2B), 2.6 (d, ^{1}J(B,H)=142, 2B), -0.2 (d, ^{1}J(B,H)=114, 1B), -1.3 (d, ^{1}J(B,H)=138, 3B), -3.2 (d, ^{1}J(B,H)=181, 2B), -4.7 (d, ^{1}J(B,H)=132, 2B), -15.2 (d, ^{1}J(B,H)=160, 2B), -17.1 (d, ^{1}J(B,H)=164, 2B), -22.5 (d, ^{1}J(B,H)=142, 2B). ^{31}P{^{1}H}-RMN: δ = 34.6 (s, $(C_c)_2$-OPPh). MALDI-TOF MS: m/z (%): 446.76 (M), 324.59 (M-POPh).

Synthesis of $[N(CH_3)_4][1,1'$-μ-SPPh-3,3'-Co(1,2-$C_2B_9H_{10})_2]$ (5). To a round bottom flask (50 mL) containing **3** (50 mg, 0.099 mmol) was added acetone (10 mL) and sulphur powder (13.2 mg, 0.41 mmol). The mixture was refluxed for 30 hours and cooled to room temperature. The excess of sulphur was filtrated and evaporation of the solvent yielded an orange solid. Yield: 52.0 mg (94%). Elemental analysis calcd (%) for $C_{14}H_{37}B_{18}CoNSP$: C=31.37, H=6.96, N=2.61, S=5.98; found: C=31.46, H=7.02, N=2.18, S=4.51. IR: ν = 3049 (C_c-H), 2943, 2921, 2849 ($C_{aryl/alkyl}$-H), 2575, 2557, 2538, 2511 (B-H), 1480 δ(C_{alkyl}-H), 946 (C-N), 645 (P=S), 1435, 1099, 1033, 998, 721, 685, 664. ^{1}H-RMN: δ = 8.14, 8.09, 7.67, 7.59 (m, 5H, Ph), 5.09 (s, 1H, C_c-H), 4.36 (s, 1H, C_c-H), 3.43 (s, 12H, $N(CH_3)_4$), 3.72-1.23 (br m, 18H, B-H). ^{1}H{^{11}B}-RMN: δ = 8.14, 8.09, 7.67, 7.59 (m, 5H, Ph), 5.09 (s, 1H, C_c-H), 4.36 (s, 1H, C_c-H), 3.43 (s, 12H, $N(CH_3)_4$), 3.72, 3.29, 3.21, 3.12, 3.03, 2.75, 2.41, 2.25, 2.19, 1.90, 1.80, 1.58, 1.23 (s, 18H, B-H). ^{13}C{^{1}H}-RMN: δ = 132.21 (s, Ph), 132.26 (d, ^{3}J(P,C)=11, Ph), 128.46 (d, ^{2}J(P,C)=13, Ph), 58.25 (s, C_c), 55.25 (s, $N(CH_3)_4$), 54.19 (s, C_c). ^{11}B-RMN: δ = 8.2 (d, ^{1}J(B,H)=143, 2B), 2.1 (d, ^{1}J(B,H)=146, 2B), -0.4 (d, ^{1}J(B,H)=141, 1B), -1.7 (d, ^{1}J(B,H)=143, 3B), -3.2 (d, ^{1}J(B,H)=146, 2B), -4.8 (d, ^{1}J(B,H)=140, 2B), -15.6 (d, ^{1}J(B,H)=158, 2B), -17.5 (d, ^{1}J(B,H)=181, 2B), -22.7 (d, ^{1}J(B,H)=120, 2B). ^{31}P{^{1}H}-RMN: δ = 71.68 (s, $(C_c)_2$-SPPh). MALDI-TOF MS: m/z (%): 462.64 (M), 429.63 (M-S).

Synthesis of $[N(CH_3)_4][1,1'$-μ-SePPh-3,3'-Co(1,2-$C_2B_9H_{10})_2]$ (6). To a round bottom flask (50 mL) containing **3** (50 mg, 0.099 mmol) was added acetone (10 mL) and selenium powder (8.4 mg, 0.099 mmol). The mixture was refluxed for 30 hours and cooled to room temperature. Evaporation of the solvent yielded an orange solid. Yield: 54.6 mg (96%). Elemental analysis calcd (%) for $C_{14}H_{37}B_{18}CoNSeP$: C=28.85, H=6.40, N=2.40; found: C=30.45, H=6.75, N=2.30. IR: ν = 3050 (C_c-H), 2944, 2916 ($C_{aryl/alkyl}$-H), 2577, 2549, 2524 (B-H), 1479 δ(C_{alkyl}-H), 942 (C-N), 688 (P=Se), 1435, 1035, 997, 942, 744, 726. ^{1}H-RMN: δ = 8.16, 8.11, 7.63, 7.58 (m, 5H, Ph), 5.11 (s, 1H, C_c-H), 4.37 (s, 1H, C_c-H), 3.42 (s, 12H, $N(CH_3)_4$), 3.74-1.29 (br m, 18H, B-H). ^{1}H{^{11}B}-RMN: δ = 8.16, 8.11, 7.63, 7.58 (m, 5H, Ph), 5.11 (s, 1H, C_c-H), 4.37 (s, 1H, C_c-H), 3.42 (s, 12H, $N(CH_3)_4$), 3.74, 3.29, 3.19, 3.13, 2.99, 2.77, 2.39, 2.23, 2.18, 1.86, 1.79, 1.69, 1.63, 1.57, 1.29 (s, 18H, B-H). ^{13}C{^{1}H}-RMN: δ = 133.07 (s, Ph), 132.55 (d, ^{3}J(P,C)=19, Ph), 128.34 (d, ^{2}J(P,C)=22, Ph), 58.72 (s, C_c), 55.21 (s, $N(CH_3)_4$), 53.97 (s, C_c). ^{11}B-RMN: δ = 8.1 (d, ^{1}J(B,H)=142, 2B), 2.1 (d, ^{1}J(B,H)=145, 2B), -0.3 (d, ^{1}J(B,H)=151, 1B), -1.8 (d, ^{1}J(B,H)=146, 3B), -3.4 (d, ^{1}J(B,H)=145, 2B), -4.8 (d, ^{1}J(B,H)=137, 2B), -15.6 (d, ^{1}J(B,H)=154, 2B), -17.3 (d, ^{1}J(B,H)=160, 2B), -22.3 (d, ^{1}J(B,H)=154, 2B). ^{31}P{^{1}H}-RMN: δ = 69.76 (s, ^{1}J(P,Se)=833, $(C_c)_2$-SePPh). MALDI-TOF MS: m/z (%): 509.65 (M), 429.66 (M-Se).

Synthesis of $[N(CH_3)_4][8,8'$-μ-(1'',2''-C_6H_4)-1,1'-μ-PPh-3,3'-Co(1,2-$C_2B_9H_9)_2]$ (7). This compound was prepared using the same procedure as for **3**, but using a stirred solution of Cs[8,8'-μ-(1'',2''-C_6H_4)-3,3'-Co(1,2-$C_2B_9H_{10})_2$] (**2**) (300 mg, 0.56 mmol) instead of **1**. Work-up and purification ends by column chromatography using CH_2Cl_2/CH_3CN (80/20) as the mobile phase (R_f=0.58). Yield: 192 mg (59%). Eelemental analysis calcd (%) for $C_{20}H_{39}B_{18}CoNP$: C=41.56, H=2.42; found: C=41.70, H=2.40. IR: ν = 3031 (C_c-H), 2975, 2958, 2927, 2869 ($C_{aryl/alkyl}$-H), 2563 (B-H), 1479 δ(C_{alkyl}-H), 946 (C-N), 1431, 1085, 743, 691, 482. ^{1}H-NMR: δ = 7.69-7.48 (m, 5H, Ph), 6.80 (m, 4H, B_2(Ph)), 4.35 (br s, 1H, C_c-H), 4.08 (br s, 1H, C_c-H), 3.38 (s, 12H, $N(CH_3)_4$), 4.80–1.49 (br m, 16H, B-H). ^{1}H{^{11}B}-NMR: δ = 7.69-7.48 (m, 5H, Ph), 6.80 (m, 4H, B_2(Ph)), 4.35 (br s, 1H, C_c-H), 4.08 (br s, 1H, C_c-H), 3.38 (s, 12H, $N(CH_3)_4$), 3.72, 2.90, 2.22, 1.99, 1.75, 1.49 (s, 16H, B-H). ^{13}C{^{1}H}-NMR: δ = 131.43-128.08 (m, Ph), 128.67 (s, B_2(Ph)), 124.99 (s, B_2(Ph)), 55.09 (s, $N(CH_3)_4$), 50.48 (s, C_c-H). ^{11}B-NMR: δ = 26.32 (s, 1B, B(8,8')), 23.94 (s, 1B, B(8,8')), 1.88 (d, 1B), 0.17 (d, ^{1}J(B,H) = 140 Hz, 4B), -1.31 (d, 1B), -5.39 (d, ^{1}J(B,H) = 140 Hz, 3B), -6.99 (d, ^{1}J(B,H) = 153 Hz, 1B), -12.80 (d, ^{1}J(B,H) = 150 Hz, 1B), -13.81 (d, ^{1}J(B,H) = 125 Hz, 1B), -15.51 (d, ^{1}J(B,H) = 162 Hz, 1B), -26.32 (d, ^{1}J(B,H) = 169 Hz, 2B). ^{31}P{^{1}H}-NMR: δ = 77.26 (s, $(C_c)_2$-PPh), 73.24 (s, $(C_c)_2$-PPh). MALDI-TOF MS: m/z (%): 503.89 (M), 520.82 (M+O), 398.67 (M-PPh).

Synthesis of $[N(CH_3)_4][8,8'$-μ-(1'',2''-C_6H_4)-1,1'-μ-OPPh-3,3'-Co(1,2-$C_2B_9H_9)_2]$ (8). This compound was prepared using the same procedure as for **4**, but using compound $[N(CH_3)_4][8,8'$-μ-(1'',2''-C_6H_4)-1,1'-μ-PPh-3,3'-Co(1,2-$C_2B_9H_9)_2$] (500 mg, 0.86 mmol) (**7**) instead of **3**. Yield: 490 mg (95%). Elemental analysis calcd (%) for $C_{20}H_{39}B_{18}CoNOP$: C=40.44, H=6.61; found: C=40.75, H=6.40. IR: ν = 3030 (C_{aryl}-H), 2975, 2960, 2923 (C_{alkyl}-H), 2571 (B-H), 1481 δ(C_{alkyl}-H), 1205 (P=O), 945 (C-N), 1435, 1107, 743, 691, 505. ^{1}H-RMN: δ = 8.07, 7.88, 7.69, 7.58 (m, 5H, Ph), 6.84 (m, 4H, C_6H_4), 3.81 (s, 2H, C_c-H), 3.36 (s, 12H, $N(CH_3)_4$), 3.00-1.61 (br m, 16H, B-H). ^{1}H{^{11}B}-RMN: δ = 8.07, 7.88, 7.69, 7.58 (m, 5H, Ph), 6.84 (m, 4H, C_6H_4), 3.81 (s, 2H, C_c-H), 3.36 (s, 12H, $N(CH_3)_4$), 3.00, 2.39, 2.28, 2.15, 1.94, 1.72, 1.61 (s, 16H, B-H). ^{13}C{^{1}H}-RMN: δ = 133.29 (s, Ph), 133.12 (s, Ph), 131.38 (d, ^{1}J(P,C)=11, Ph), 130.88 (d, ^{1}J(P,C)=11, Ph), 128.86 (s, $B_2(C_6H_4)$), 128.56 (d, ^{1}J(P,C)=13, Ph), 128.21 (d, ^{1}J(P,C)=13, Ph), 125.11 (s, $B_2(C_6H_4)$), 54.80 (s, $N(CH_3)_4$), 50.94 (s, C_c), 50.63 (s, C_c). ^{11}B-RMN: δ = 26.7 (s, 2B, B(8,8')), 0.7 (d, ^{1}J(B,H)=137, 6B), -3.9 (d, ^{1}J(B,H)=152, 2B), -5.7 (d, ^{1}J(B,H)=157, 2B), -13.7 (d, ^{1}J(B,H)=110, 4B), -26.6 (d, ^{1}J(B,H)=115, 2B). ^{31}P{^{1}H}-RMN: δ = 35.4 (s, $(C_c)_2$-OPPh), 35.6 (s, $(C_c)_2$-OPPh). MALDI-TOF MS: m/z (%): 520.91 (M), 445.89 (M-C_6H_4), 324.56 (M-POPhC_6H_4).

Synthesis of $[N(CH_3)_4][8,8'$-μ-(1'',2''-C_6H_4)-1,1'-μ-SPPh-3,3'-Co(1,2-$C_2B_9H_9)_2]$ (9). This compound was prepared using the same procedure as for **5**, but using compound $[N(CH_3)_4][8,8'$-μ-(1'',2''-C_6H_4)-1,1'-μ-PPh-3,3'-Co(1,2-$C_2B_9H_9)_2$] (50 mg, 0.087 mmol) (**7**) instead of **3**. Yield: 42.9 mg (86%). Elemental analysis calcd (%) for $C_{20}H_{39}B_{18}CoNSP$: C=39.37, H=6.44, N=2.30, S=5.26; found: C=39.88, H=6.70, N=2.03, S=6.68. IR: ν = 3036 (C_c-H), 2953, 2921 ($C_{aryl/alkyl}$-H), 2574, 2540 (B-H), 1480 δ(C_{alkyl}-H), 946 (C-N), 670 (P=S), 1435, 1094, 1028, 996, 832, 740. ^{1}H-RMN: δ = 8.17, 7.92, 7.55 (m, 5H, Ph), 6.79 (m, 4H, C_6H_4), 3.96 (s, 2H, C_c-H), 3.82 (s, 2H, C_c-H), 3.35 (s, 12H, $N(CH_3)_4$), 4.47-1.60 (br m,

16H, B-H). $^{1}H\{^{11}B\}$-RMN: δ = 8.17, 7.92, 7.55 (m, 5H, Ph), 6.79 (m, 4H, C_6H_4), 3.96 (s, 2H, C_c-H, 3.82 (s, 2H, C_c-H), 3.35 (s, 12H, $N(CH_3)_4$), 4.47, 4.10, 3.67, 3.59, 2.96, 2.35, 2.29, 2.25, 1.97, 1.92, 1.79, 1.72, 1.60 (s, 16H, B-H). $^{13}C\{^{1}H\}$-RMN: δ = 131.42 (s, Ph), 130.89 (s, Ph), 130.34 (s, Ph), 129.77 (s, Ph), 128.54 (s, $B_2(C_6H_4)$), 127.58 (s, Ph), 127.10 (s, Ph), 123.85 (s, $B_2(C_6H_4)$), 54.71 (s, $N(CH_3)_4$), 50.86 (s, C_c), 49.23 (s, C_c). ^{11}B-RMN: δ = 26.2 (s, 2B), 0.2 (d, ^{1}J(B,H)=137, 6B), -4.4 (d, ^{1}J(B,H)=143, 2B), -5.9 (d, J(B,H)=141, 2B), -14.2 (d, ^{1}J(B,H)=130, 4B), -26.5 (d, ^{1}J(B,H)=149, 2B). $^{31}P\{^{1}H\}$-RMN: δ = 72.96, 68.36 (s, $(C_c)_2$-SPPh). MALDI-TOF MS: m/z (%): 536.74 (M).

Synthesis of $[N(CH_3)_4][8,8'$-μ-(1'',2''-C_6H_4)-1,1'-μ-SePPh-3,3'-Co(1,2-$C_2B_9H_9)_2$] (10). This compound was prepared using the same procedure as for **6**, but using compound $[N(CH_3)_4][8,8'$-μ-(1'',2''-C_6H_4)-1,1'-μ-PPh-3,3'-Co(1,2-$C_2B_9H_9)_2$] (50 mg, 0.087 mmol) (**7**) instead of **3**. Yield: 55.3 mg (97%). Elemental analysis calcd (%) for $C_{20}H_{39}B_{18}CoNSeP$: C=36.56, H=5.98, N=2.13; found: C=34.47, H=5.81, N=1.94. IR: ν = 3037 (C_c-H), 2975, 2953, 2919 ($C_{aryl/alkyl}$-H), 2576, 2539 (B-H), 1480 δ(C_{alkyl}-H), 946 (C-N), 690 (P=S), 1435, 1090, 995, 832, 739. ^{1}H-RMN: δ = 8.13, 7.95, 7.91, 7.55 (m, 5H, Ph), 6.81 (m, 4H, C_6H_4), 3.97 (s, 2H, C_c-H), 3.87 (s, 2H, C_c-H), 3.33 (s, 12H, $N(CH_3)_4$), 4.49-1.61 (br m, 16H, B-H). $^{1}H\{^{11}B\}$-RMN: δ = 8.13, 7.95, 7.91, 7.55 (m, 5H, Ph), 6.81 (m, 4H, C_6H_4), 3.97 (s, 2H, C_c-H), 3.87 (s, 2H, C_c-H), 3.33 (s, 12H, $N(CH_3)_4$), 4.49, 4.09, 3.79, 3.66, 3.57, 2.95, 2.42, 2.32, 1.95, 1.88, 1.85, 1.76, 1.61 (s, 16H, B-H). $^{13}C\{^{1}H\}$-RMN: δ = 132.26 (s, Ph), 131.41 (s, Ph), 129.07 (s, Ph), 128.45 (s, Ph), 125.33 (s, $B_2(C_6H_4$)), 55.17 (s, $N(CH_3)_4$), 53.07 (s, C_c), 50.16 (s, C_c). ^{11}B-RMN: δ = 26.3 (s, 2B), 0.2 (d, ^{1}J(B,H)=139, 6B), -4.4 (d, ^{1}J(B,H)=141, 2B), -5.9 (d, J(B,H)=140, 2B), -14.1 (d, ^{1}J(B,H)=129, 4B), -26.3 (d, ^{1}J(B,H)=151, 2B). $^{31}P\{^{1}H\}$-RMN: δ = 71.04, 62.73 (s, ^{1}J(P,Se)=848, $(C_c)_2$-SePPh). MALDI-TOF MS: m/z (%): 583.76 (M), 504.77 (M-Se).

Synthesis of $[N(CH_3)_4][1,1'$-μ-PC_4H_9-3,3'-Co(1,2-$C_2B_9H_{10})_2$] (11): Under an inert atmosphere, *n*-butyllithium (1.6M in hexanes, 1,6 mL, 2.41 mmol) was added dropwise to a stirred solution of **1** in anhydrous DME (25 mL) at -78ºC. The resulting purple solution was stirred for 60 min at low temperature. Then, dichlorotertbutylphosphine (180 mg, 1.21 mmol) was added, causing a rapid color change to red. After the mixture had been stirred all night at room temperature, a grey solid was filtered off and discarded. After removal of the solvent, the residue was dissolved in the minimum volume of EtOH and an aqueous solution containing an excess of $[Me_4N]Cl$ was added, resulting in the formation of a precipitate. This was filtered off, washed with water and petroleum ether, and dried in vacuo. The resulting light red solid was purified by column chromatography using CH_2Cl_2/CH_3CN (80/20) as the mobile phase (R_f=0.44). Yield: 290 mg (55%). Elemental analysis calcd (%) for $C_{12}H_{41}B_{18}CoNP$: C=29.78, H=8.54, N=2.89; found: C=33.26, H=7.21, N=1.34. IR: ν = 3036 (C_c-H), 2949, 2920, 2893, 2862 (C_{aryl}-H), 2567 (B-H), 1481 δ(C_{alkyl}-H), 1362 (P-C), 945 (C-N), 1392, 1173, 1103, 1038, 1015, 873, 802, 727, 601. ^{1}H-NMR: δ = 5.38 (br s, 1H, C_c-H), 5.09 (br s, 1H, C_c-H), 3.44 (s, 12H, $N(CH_3)_4$), 3.09–1.55 (br m, 18H, B-H), 1.18 (d, ^{3}J(H,H) = 14 Hz, 9H). $^{1}H\{^{11}B\}$-NMR: δ = 5.38 (br s, 1H, C_c-H), 5.09 (br s, 1H, C_c-H), 3.44 (s, 12H, $N(CH_3)_4$), 3.09, 3.02, 2.16, 2.12, 1.92, 1.86, 1.79, 1.75, 1.68, 1.61, 1.58, 1.52 (s, 18H, B-H), 1.18 (d, ^{3}J(H,H) = 14 Hz, 9H). $^{13}C\{^{1}H\}$-NMR: δ = 63.46 (d, ^{1}J(P,C) = 21 Hz, P-C_C), 57.03 (s, C_C), 55.18 (s, $N(CH_3)_4$), 37.16 (d, ^{1}J(P,C) = 29 Hz, P-C), 26.31 (d, ^{2}J(P,C) = 18 Hz, CH_3). ^{11}B-NMR: δ = 8.24 (d, ^{1}J(B,H) = 146 Hz, 1B), 5.23 (d, ^{1}J(B,H) = 142 Hz, 1B), 2.09 (d, ^{1}J(B,H) = 143 Hz, 2B), 0.51 (d, ^{1}J(B,H) = 152 Hz, 1B), -1.05 (d, ^{1}J(B,H) = 157 Hz, 1B), -2.63 (d, ^{1}J(B,H) = 135 Hz, 3B), -3.41 (d, ^{1}J(B,H) = 96 Hz, 1B), -5.06 (d, ^{1}J(B,H) = 147 Hz, 1B), -6.60 (d, ^{1}J(B,H) = 144 Hz, 1B), -14.75 (d, ^{1}J(B,H) = 168 Hz, 1B), -16.59 (d, ^{1}J(B,H) = 161 Hz, 1B), -20.75 (d, ^{1}J(B,H) = 182 Hz, 1B), -22.76 (d, ^{1}J(B,H) = 178 Hz, 1B). $^{31}P\{^{1}H\}$-NMR: δ = 88.32 (s, $(C_c)_2$-PC_4H_9). MALDI-TOF MS: m/z (%): 410.38 (M), 353.28 (M-C_4H_9), 324.30 (M-PC_4H_9).

Synthesis of $[N(CH_3)_4][1,1'$-μ-OPC_4H_9-3,3'-Co(1,2-$C_2B_9H_{10})_2$] (12). This compound was prepared using the same procedure as for **4**, but using compound $[N(CH_3)_4][1,1'$-μ-PC_4H_9-3,3'-Co(1,2-$C_2B_9H_{10})_2$] (30 mg, 0.06 mmol) (**11**) instead of **3**. Yield: 0.92 g (89%). Elemental analysis calcd (%) for $C_{12}H_{41}B_{18}CoNOP$: C=28.83, H=8.27, N=2.80; found: C=29.85, H=8.05, N=2.65. IR: ν = 3043 (C_c-H), 2968, 2931, 2904, 2871 (C_{aryl}-H), 2582, 2571 (B-H), 1614 (P=O), 1479, 1462 δ(C_{alkyl}-H), 1367 (P-C), 945 (C-N), 1396, 1174, 1101, 1037, 1001, 874, 806, 727. ^{1}H-RMN: δ = 4.89 (s, 1H, C_c-H), 4.70 (s, 1H, C_c-H), 3.44 (s, 12H, $N(CH_3)_4$), 3.29-1.59 (br m, 18H, B-H), 1.31 (d, ^{3}J(H,H) = 16 Hz, 9H). $^{1}H\{^{11}B\}$-RMN: δ =4.89 (s, 1H, C_c-H), 4.70 (s, 1H, C_c-H), 3.44 (s, 12H, $N(CH_3)_4$), 3.29, 3.21, 3.13, 2.71, 2.54, 2.34, 2.01, 1.86, 1.75, 1.71, 1.59 (s, 18H, B-H), 1.31 (d, ^{3}J(H,H) = 16 Hz, 9H). $^{13}C\{^{1}H\}$-RMN: δ = 58.04 (s, C_c), 55.56, 55.21 (s, $N(CH_3)_4$), 51.12 (d, ^{1}J(P,C)=50,

P-C_c), 41.12 (d, ^{1}J(P,C)=22, P-C), 26.41, 24.03 (s, CH_3). ^{11}B-RMN: δ = 8.6 (d, ^{1}J(B,H)=147, 1B), 2.6 (d, ^{1}J(B,H)=144, 1B), -1.2 (d, ^{1}J(B,H)=147, 2B), -3.1 (d, 1B), -5.5 (d, ^{1}J(B,H)=132, 6B), -15.5 (d, ^{1}J(B,H)=166, 2B), -16.6 (d, 1B), -17.5 (d, ^{1}J(B,H)=176, 2B), -22.2 (d, ^{1}J(B,H)=120, 2B). ^{31}P{^{1}H}-RMN: δ = 52.7 (s, $(C_c)_2$-OPC_4H_9). MALDI-TOF MS: m/z (%): 426.39 (M), 370.29 (M-C_4H_9), 324.30 (M-POC_4H_9).

Synthesis of [$N(CH_3)_4$][1,1'-μ-SPC_4H_9-3,3'-Co(1,2-$C_2B_9H_{10})_2$] (13). This compound was prepared using the same procedure as for **5**, but using compound [$N(CH_3)_4$][1,1'-μ-PC_4H_9-3,3'-Co(1,2-$C_2B_9H_{10})_2$] (50 mg, 0.10 mmol) (**11**) instead of **3**. Yield: 51.1 mg (95%). Elemental analysis calcd (%) for $C_{12}H_{41}B_{18}CoNSP$: C=27.93, H=8.01, N=2.71, S=6.21; found: C=28.74, H=8.34, N=2.66, S=3.49. IR: ν = 3044 (C_c-H), 2968, 2922, 2899 (C_{aryl}-H), 2565 (B-H), 1481 δ(C_{alkyl}-H), 1362 (P-C), 945 (C-N), 669 (P=S), 1265, 1175, 1098, 1035, 861, 800, 735. ^{1}H-RMN: δ = 5.05 (s, 1H, C_c-H), 4.92 (s, 1H, C_c-H), 3.43 (s, 12H, $N(CH_3)_4$), 3.67-1.68 (br m, 18H, B-H), 1.43 (d, ^{3}J(H,H) = 18 Hz, 9H). ^{1}H{^{11}B}-RMN: δ = 5.05 (s, 1H, C_c-H), 4.92 (s, 1H, C_c-H), 3.43 (s, 12H, $N(CH_3)_4$), 3.67, 3.18, 3.08, 2.79, 2.72, 2.28, 2.04, 1.99, 1.91, 1.74, 1.68 (s, 18H, B-H), 1.43 (d, ^{3}J(H,H) = 18 Hz, 9H). ^{13}C{^{1}H}-RMN: δ = 59.92 (s, C_c), 55.22 (s, $N(CH_3)_4$), 50.29 (d, ^{1}J(P,C)=30, P-C_c), 47.95 (s, P-C), 45.17 (d, ^{1}J(P,C)=35, P-C), 26.66, 26.15, 18.60 (s, CH_3). ^{11}B-RMN: δ = 8.5 (d, ^{1}J(B,H)=72, 2B), 2.5 (d, ^{1}J(B,H)=142, 2B), -1.5 (d, ^{1}J(B,H)=88, 6B), -5.5 (d, ^{1}J(B,H)=143, 2B), -15.6 (d, ^{1}J(B,H)=160, 3B), -17.7 (d, ^{1}J(B,H)=198, 1B), -22.5 (d, ^{1}J(B,H)=91, 2B). ^{31}P{^{1}H}-RMN: δ = 95.27 (s, $(C_c)_2$-SPC_4H_9). MALDI-TOF MS: m/z (%): 442.69 (M), 386.56 (M-C_4H_9), 353.53 (M-SC_4H_9), 323.53 (M-PSC_4H_9).

Synthesis of [$N(CH_3)_4$][1,1'-μ-$SePC_4H_9$-3,3'-Co(1,2-$C_2B_9H_{10})_2$] (14). This compound was prepared using the same procedure as for **6**, but using compound [$N(CH_3)_4$][1,1'-μ-PC_4H_9-3,3'-Co(1,2-$C_2B_9H_{10})_2$] (50 mg, 0.10 mmol) (**11**) instead of **3**. Yield: 50.0 mg (86%). Elemental analysis calcd (%) for $C_{12}H_{41}B_{18}CoNSeP$: C=25.60, H=7.34, N=2.49; found: C=25.28, H=7.46, N=2.09. IR: ν = 3034 (C_c-H), 2944, 2923, 2852 (C_{aryl}-H), 2565 (B-H), 1481, 1462 δ(C_{alkyl}-H), 1362 (P-C), 945 (C-N), 701 (P=Se), 1362, 1263, 1174, 1087, 1014, 736. ^{1}H-RMN: δ = 5.12 (s, 1H, C_c-H), 5.03 (s, 1H, C_c-H), 3.45 (s, 12H, $N(CH_3)_4$), 3.68-1.64 (br m, 18H, B-H), 1.49 (d, ^{3}J(H,H) = 16 Hz, 9H). ^{1}H{^{11}B}-RMN: δ = 5.12 (s, 1H, C_c-H), 5.03 (s, 1H, C_c-H), 3.45 (s, 12H, $N(CH_3)_4$), 3.68, 3.28, 3.12, 2.99, 2.73, 2.32, 2.28, 2.03, 1.95, 1.77, 1.64 (s, 18H, B-H), 1.49 (d, ^{3}J(H,H) = 16 Hz, 9H). ^{13}C{^{1}H}-RMN: δ = 60.95 (s, C_c), 55.21 (s, $N(CH_3)_4$), 51.05 (m, P-C_c), 46.00 (s, P-C), 45.73 (s, P-C), 26.45, 13.08 (s, CH_3). ^{11}B-RMN: δ = 7.4 (d, ^{1}J(B,H)=111, 1B), 2.1 (d, ^{1}J(B,H)=115, 2B), -1.6 (d, ^{1}J(B,H)=176, 3B), -5.7 (d, ^{1}J(B,H)=99, 4B), -6.5 (d, ^{1}J(B,H)=89, 2B), -15.8 (d, ^{1}J(B,H)=148, 2B), -17.7 (d, ^{1}J(B,H)=141, 2B), -22.4 (d, ^{1}J(B,H)=113, 2B). ^{31}P{^{1}H}-RMN: δ = 99.62 (s, ^{1}J(P,Se)=679, $(C_c)_2$-$SePC_4H_9$). MALDI-TOF MS: m/z (%): 489.72 (M), 433.60 (M-C_4H_9), 353.53 (M-SeC_4H_9), 324.56 (M-$PSeC_4H_9$).

Synthesis of [$N(CH_3)_4$][8,8'-μ-(1'',2''-C_6H_4)-1,1'-μ-PC_4H_9-3,3'-Co(1,2-$C_2B_9H_9)_2$] (15). This compound was prepared using the same procedure as for **11**, but using a stirred solution of Cs[8,8'-μ-(1'',2''-C_6H_4)-3,3'-Co(1,2-$C_2B_9H_{10})_2$] (**2**) (300 mg, 0.56 mmol) instead of **1**. Work-up and purification ends by column chromatography using CH_2Cl_2/CH_3CN (80/20) as the mobile phase (R_f=0.43). Yield: 215 mg (51%). Elemental analysis calcd (%) for $C_{18}H_{43}B_{18}CoNP$: C=38.74, H=7.77, N=2.51; found: C=40.03, H=7.71, N=3.63. IR: ν = 3032 (C_c-H), 2955, 2938, 2899, 2864 (C_{aryl}-H), 2598, 2584 (B-H), 1479, 1445, 1429, 1416 δ(C_{alkyl}-H), 1360 (P-C), 947 (C-N), 1391, 1203, 1163, 1089, 1030, 995, 833, 760, 744. ^{1}H-NMR: δ = 6.75 (m, 4H, C_6H_4), 4.19 (br s, 2H, C_c-H), 3.36 (s, 12H, $N(CH_3)_4$), 4.66–1.48 (br m, 16H, B-H), 1.15 (d, ^{3}J(H,H) = 15 Hz, 9H). ^{1}H{^{11}B}-NMR: δ = 6.75 (m, 4H, C_6H_4), 4.19 (br s, 2H, C_c-H), 3.36 (s, 12H, $N(CH_3)_4$), 4.66, 3.71, 3.57, 3.43, 2.90, 2.20, 1.96, 1.84, 1.74, 1.47 (s, 16H, B-H), 1.15 (d, ^{3}J(H,H) = 15 Hz, 9H). ^{13}C{^{1}H}-NMR: δ = 129.02 (s, C_6H_4), 124.86 (s, BC_6H_4), 55.15 (s, $N(CH_3)_4$), 52.79 (s, C_c-H), 44.55 (s, P-C_C), 37.28 (m, P-C), 26.55 (d, ^{2}J(P,C) = 19 Hz, CH_3). ^{11}B-NMR: δ = 26.09 (s, 1B, B(8,8')), 23.41 (s, 1B, B(8,8')), 3.56 (d, ^{1}J(B,H) = 159 Hz, 1B), 0.05 (d, ^{1}J(B,H) = 142 Hz, 3B), -2.37 (d, 1B), -3.52 (d, ^{1}J(B,H) = 161 Hz, 1B), -5.55 (d, ^{1}J(B,H) = 139 Hz, 4B), -12.97 (d, ^{1}J(B,H) = 150 Hz, 2B), -13.86 (d, 1B), -14.45 (d, 1B), -15.38 (d, ^{1}J(B,H) = 154 Hz, 1B), -26.71 (d, ^{1}J(B,H) = 146 Hz, 1B). ^{31}P{^{1}H}-NMR: δ = 96.71 (s, $(C_c)_2$-P^{t}Bu), 89.91 (s, $(C_c)_2$-P^{t}Bu). MALDI-TOF MS: m/z (%): 484.41 (M), 443.33 (M-$(CH_3)_3$), 427.32 (M-C_4H_9), 398.33 (M-PC_4H_9).

Synthesis of [$N(CH_3)_4$][8,8'-μ-(1'',2''-C_6H_4)-1,1'-μ-OPC_4H_9-3,3'-Co(1,2-$C_2B_9H_9)_2$] (16). This compound was prepared using the same procedure as for **4**, but using compound [$N(CH_3)_4$][8,8'-μ-(1'',2''-C_6H_4)-1,1'-μ-PC_4H_9-3,3'-Co(1,2-$C_2B_9H_9)_2$] (90 mg, 0.15 mmol) (**15**) instead of **3**. Yield: 87.4 mg (94%). Elemental

analysis calcd (%) for $C_{18}H_{43}B_{18}CoNOP$: C=37.66, H=7.55, N=2.44; found: C=38.45, H=7.36, N=2.36. IR: ν = 3038 (C_c-H), 2970, 2930 (C_{aryl}-H), 2571 (B-H), 1699 (P=O), 1481 δ(C_{alkyl}-H), 947 (C-N), 1252, 1203, 1169, 1085, 1030, 997, 877, 833, 808, 742. ^{1}H-NMR: δ = 6.80 (s, 4H, C_6H_4), 3.84 (br s, 1H, C_c-H), 3.63 (br s, 1H, C_c-H), 3.35 (s, 12H, $N(CH_3)_4$), 4.21–1.67 (br m, 16H, B-H), 1.30 (d, ^{3}J(H,H) = 17 Hz, 6H), 1.27 (d, ^{3}J(H,H) = 17 Hz, 3H). ^{1}H{^{11}B}-NMR: δ = 6.80 (s, 4H, C_6H_4), 3.84 (br s, 1H, C_c-H), 3.63 (br s, 1H, C_c-H), 3.35 (s, 12H, $N(CH_3)_4$), 4.21, 4.05, 3.75, 3.64, 3.03, 2.36, 2.24, 1.94, 1.87, 1.67 (s, 16H, B-H), 1.30 (d, ^{3}J(H,H) = 17 Hz, 6H), 1.27 (d, ^{3}J(H,H) = 17 Hz, 3H). ^{13}C{^{1}H}-NMR: δ = 129.04 (s, C_6H_4), 125.24 (s, BC_6H_4), 55.09 (s, $N(CH_3)_4$), 52.22 (s, C_c-H), 51.65 (s, P-C_C), 23.98 (d, ^{2}J(P,C) = 45 Hz, CH_3), 23.84 (d, ^{2}J(P,C) = 23 Hz, CH_3). ^{11}B-NMR: δ = 26.27 (s, 1B, B(8,8')), 23.70 (s, 1B, B(8,8')), 0.59 (d, ^{1}J(B,H) = 136 Hz, 4B), -2.30 (d, 2B), -4.13 (d, ^{1}J(B,H) = 156 Hz, 2B), -6.01 (d, ^{1}J(B,H) = 156 Hz, 2B), -14.35 (d, ^{1}J(B,H) = 102 Hz, 4B), -26.60 (d, ^{1}J(B,H) = 142 Hz, 2B). ^{31}P{^{1}H}-NMR: δ = 55.51 (s, $(C_c)_2$-P^{t}Bu), 52.21 (s, $(C_c)_2$-P^{t}Bu). MALDI-TOF MS: m/z (%): 500.39 (M), 398.33 (M-POC_4H_9).

Synthesis of [$N(CH_3)_4$][8,8'-μ-(1'',2''-C_6H_4)-1,1'-μ-SPC_4H_9-3,3'-Co(1,2-$C_2B_9H_9)_2$] (17). This compound was prepared using the same procedure as for **5**, but using compound [$N(CH_3)_4$][8,8'-μ-(1'',2''-C_6H_4)-1,1'-μ-PC_4H_9-3,3'-Co(1,2-$C_2B_9H_9)_2$] (50 mg, 0.09 mmol) (**15**) instead of **3**. Yield: 45.2 mg (86%). Elemental analysis calcd (%) for $C_{18}H_{43}B_{18}CoNSP$: C=36.64, H=7.04, N=2.37, S=5.43; found: C=38.28, H=7.63, N=2.06, S=4.53. IR: ν = 3034 (C_c-H), 2956, 2924, 2870 ($C_{aryl/alkyl}$-H), 2563, 2538 (B-H), 1480, 1459 δ(C_{alkyl}-H), 944 (C-N), 676 (P=S), 1361, 1177, 1086, 1032, 992, 831, 741. ^{1}H-NMR: δ = 6.80 (m, 4H, C_6H_4), 4.05 (br s, 2H, C_c-H), 3.28 (s, 12H, $N(CH_3)_4$), 4.43–1.79 (br m, 16H, B-H), 1.40 (d, ^{3}J(H,H) = 18 Hz, 9H). ^{1}H{^{11}B}-NMR: δ = 6.80 (m, 4H, C_6H_4), 4.05 (br s, 2H, C_c-H), 3.28 (s, 12H, $N(CH_3)_4$), 4.43, 3.74, 3.65, 2.99, 2.31, 2.23, 1.96, 1.88, 1.79 (s, 16H, B-H), 1.40 (d, ^{3}J(H,H) = 18 Hz, 9H). ^{13}C{^{1}H}-NMR: δ = 128.85 (s, C_6H_4), 125.18 (s, BC_6H_4), 54.80 (s, $N(CH_3)_4$), 51.58 (s, C_c-H), 48.29 (s, P-C_C), 44.84 (d, ^{1}J(P,C) = 37 Hz, P-C), 26.23 (s, CH_3). ^{11}B-NMR: δ = 25.99 (s, 1B, B(8,8')), 23.48 (s, 1B, B(8,8')), 0.36 (d, ^{1}J(B,H) = 141 Hz, 4B), -4.45 (d, ^{1}J(B,H) = 140 Hz, 2B), -5.94 (d, ^{1}J(B,H) = 138 Hz, 2B), -14.31 (d, ^{1}J(B,H) = 147 Hz, 4B), -26.23 (d, ^{1}J(B,H) = 133 Hz, 2B). ^{31}P{^{1}H}-RMN: δ = 95.56 (s, $(C_c)_2$-SP^{t}Bu). MALDI-TOF MS: m/z (%): 516.77 (M), 460.67 (M-^{t}Bu), 426.60 (M-S^{t}Bu), 398.61 (M-PS^{t}Bu).

Synthesis of [$N(CH_3)_4$][8,8'-μ-(1'',2''-C_6H_4)-1,1'-μ-$SePC_4H_9$-3,3'-Co(1,2-$C_2B_9H_9)_2$] (18). This compound was prepared using the same procedure as for **6**, but using compound [$N(CH_3)_4$][8,8'-μ-(1'',2''-C_6H_4)-1,1'-μ-PC_4H_9-3,3'-Co(1,2-$C_2B_9H_9)_2$] (50 mg, 0.09 mmol) (**15**) instead of **3**. Yield: 50.0 mg (88%). Elemental analysis calcd (%) for $C_{18}H_{43}B_{18}CoNSeP$: C=33.94, H=6.80, N=2.20; found: C=34.44, H=7.17, N=1.83. IR: ν = 3045, 3019 (C_c-H), 2971, 2923, 2864 ($C_{aryl/alkyl}$-H), 2595, 2537, 2508 (B-H), 1479 δ(C_{alkyl}-H), 943 (C-N), 693 (P=Se), 1360, 1203, 1162, 991, 830, 795, 756. ^{1}H-NMR: δ = 6.80 (m, 4H, C_6H_4), 4.16 (br s, 2H, C_c-H), 3.30 (s, 12H, $N(CH_3)_4$), 4.52–1.87 (br m, 16H, B-H), 1.47 (d, ^{3}J(H,H) = 15 Hz, 9H). ^{1}H{^{11}B}-NMR: δ = 6.80 (m, 4H, C_6H_4), 4.16 (br s, 2H, C_c-H), 3.30 (s, 12H, $N(CH_3)_4$), 4.52, 3.77, 3.61, 2.99, 2.31, 2.25, 2.19, 1.95, 1.87 (s, 16H, B-H), 1.47 (d, ^{3}J(H,H) = 15 Hz, 9H). ^{13}C{^{1}H}-NMR: δ = 129.07 (s, C_6H_4), 125.26 (s, BC_6H_4), 55.07 (s, $N(CH_3)_4$), 51.37 (s, C_c-H), 46.13 (d, ^{1}J(P,C) = 19 Hz, P-C_c), 45.36 (d, ^{1}J(P,C) = 14 Hz, P-C), 27.19 (s, CH_3). ^{11}B-NMR: δ = 25.65 (s, 1B, B(8,8')), 23.21 (s, 1B, B(8,8')), 0.15 (d, ^{1}J(B,H) = 125 Hz, 4B), -4.65 (d, ^{1}J(B,H) = 123 Hz, 2B), -5.99 (d, ^{1}J(B,H) = 111 Hz, 2B), -14.36 (d, ^{1}J(B,H) = 113 Hz, 4B), -26.34 (d, ^{1}J(B,H) = 82 Hz, 2B). ^{31}P{^{1}H}-RMN: δ = 97.47 (s, ^{1}J(P,Se) = 692), $(C_c)_2$-SeP^{t}Bu). MALDI-TOF MS: m/z (%): 562.89 (M), 506.68 (M-^{t}Bu), 427.66 (M-Se^{t}Bu), 398.65 (M-PSe^{t}Bu).

X-ray Structure Determinations of [NMe_4]4, [NMe_4]5, [NMe_4]6 and [NMe_4]7:

CCDC-??? contain the supplementary crystallographic data for this paper. These data can be obtained free of charge via www.ccdc.cam.ac.uk/conts/retrieving.html (or from the Cambridge Crystallographic Data Centre, 12 Union Road, Cambridge CB2 1EZ, U.K.; fax: (+44) 1223-336033; or e-mail: deposit@ccdc.cam.ac.uk).

Supporting material available:

Acknowledgement
This work was supported by MEC (Grant MAT2006-05339), CSIC (I3P grant to P.F.) and the Generalitat de Catalunya 2005/SGR/00709. Access to the computational facilities of Centre de Supercomputació de Catalunya and the CSIC computing center is also gratefully acknowledged.

Chart 1.- Monosubstituted **3-18** anions.

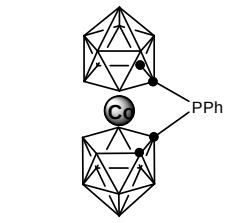

3

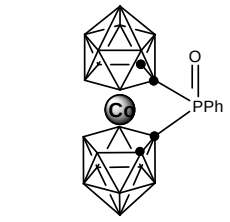

4

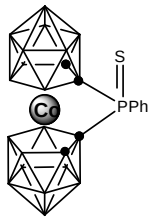

5

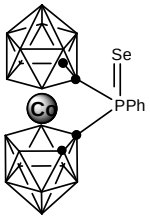

6

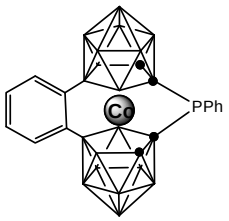

7

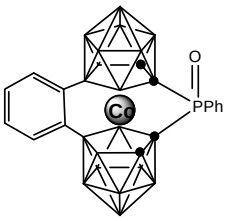

8

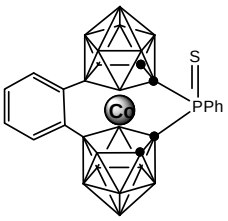

9

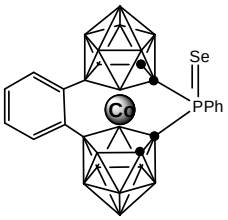

10

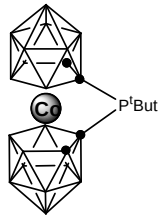

11

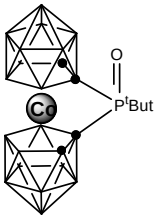

12

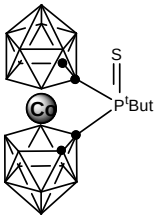

13

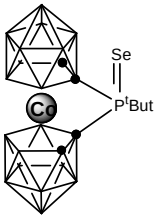

14

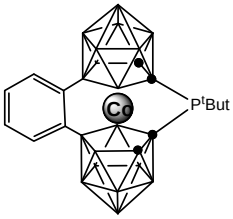

15

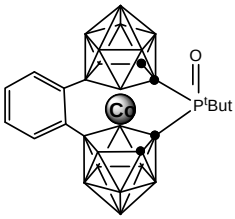

16

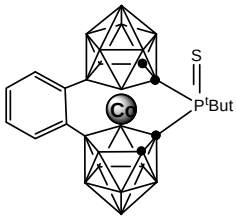

17

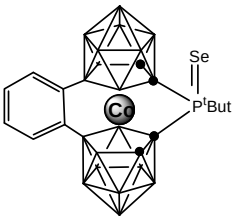

18

Scheme 1. Synthetic procedure for the preparation of bridged-phosphorus derivatives of **1** and **2**.

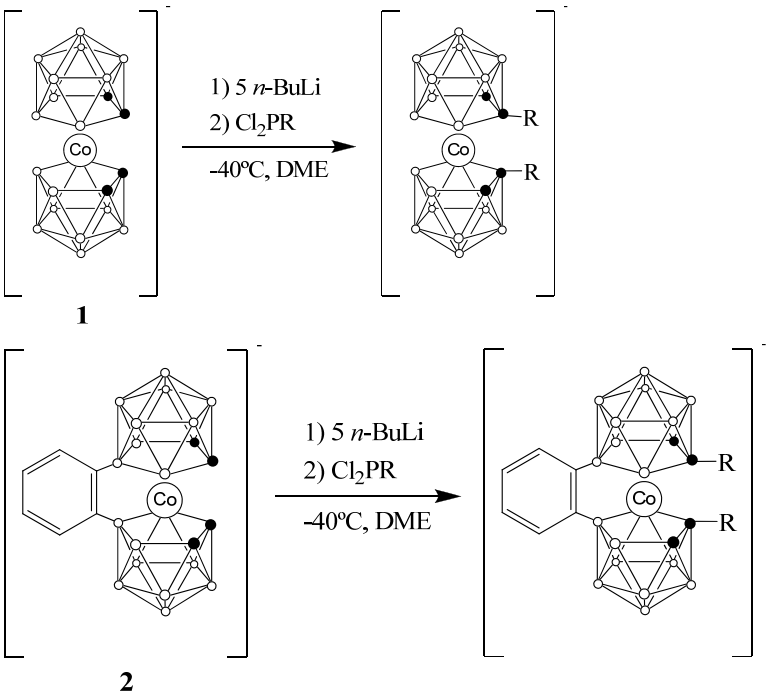

Figure 1. MALDI-TOF mass spectrum of compound [NMe_4]**3**.

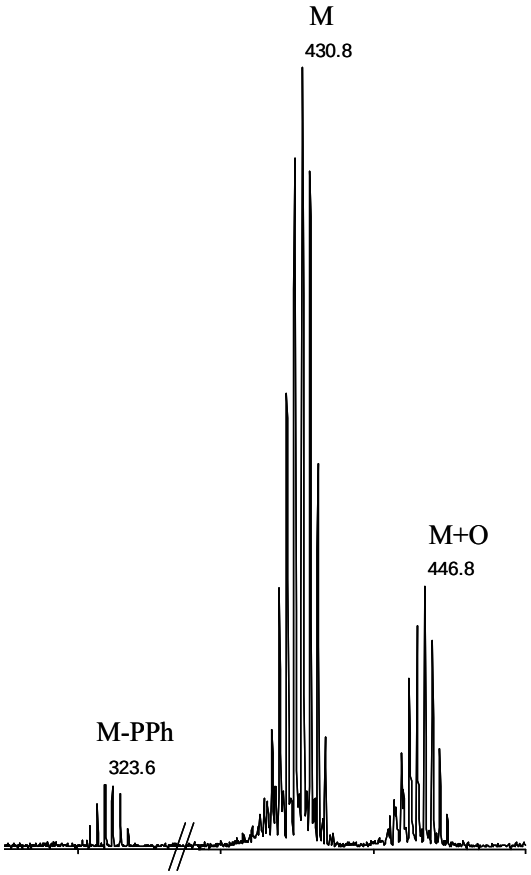

Figure 2. Molecular structure of $[NMe_4]$**7**·CH_2Cl_2. The thermal ellipsoids are set at 30% probability.

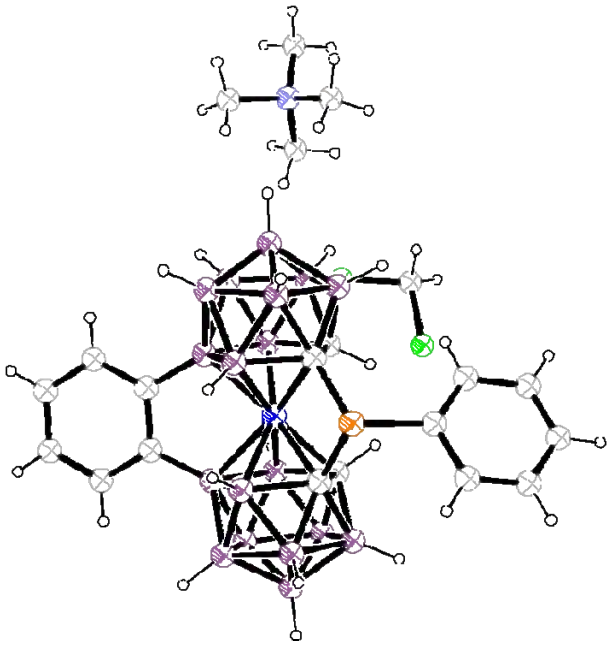

Figure 3. Comparison of MALDI-TOF mass spectra of compounds $[NMe_4]$**5** and $[NMe_4]$**13**.

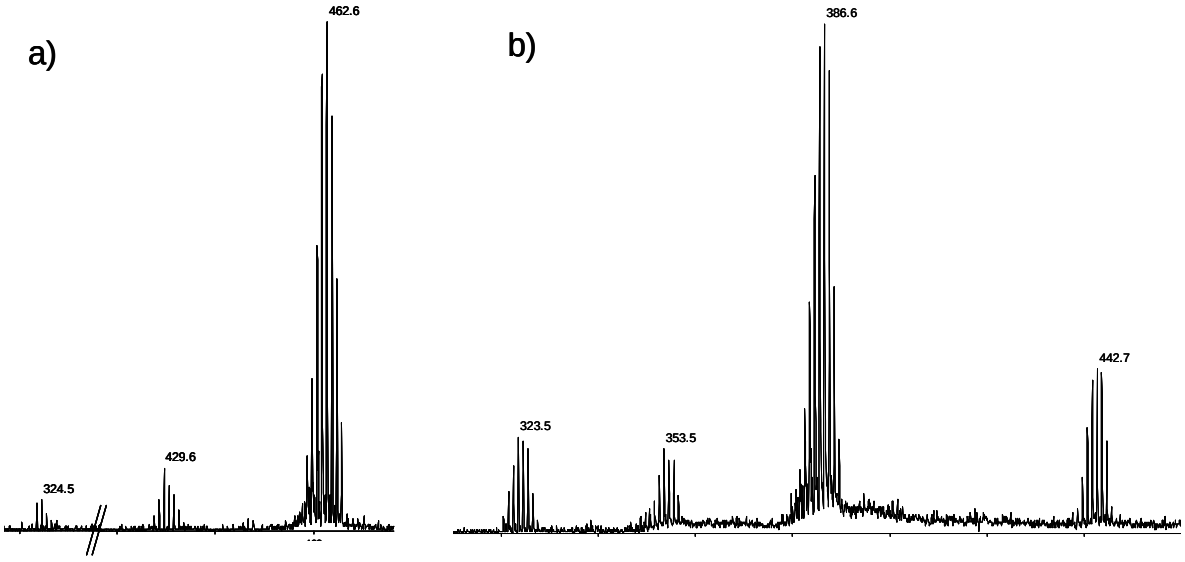

Figure 4. Molecular structure of [NMe_4]**4**. The thermal ellipsoids are set at 30% probability.

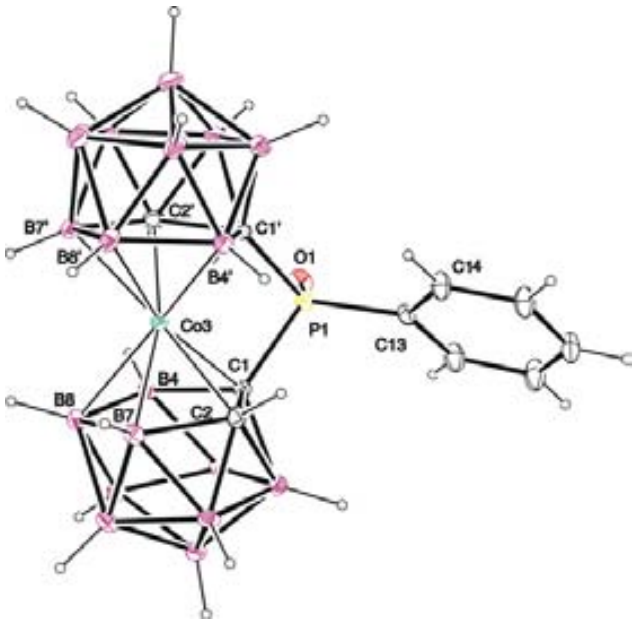

Figure 5. Molecular structure of [NMe_4]**5**. The thermal ellipsoids are set at 30% probability.

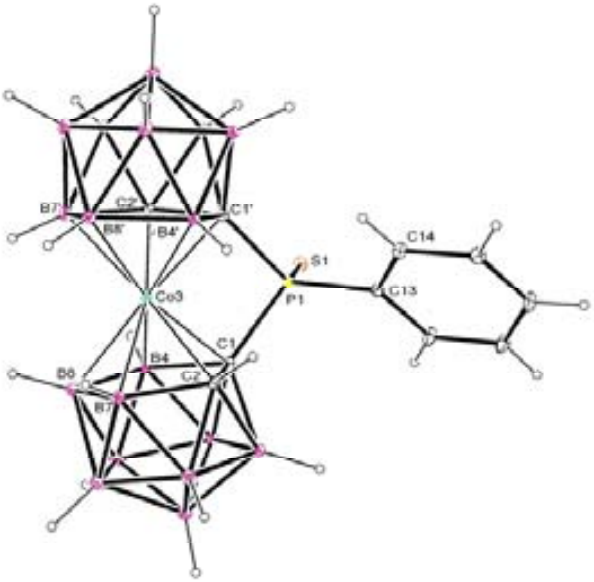

Figure 6. Molecular structure of [NMe_4]**6**. The thermal ellipsoids are set at 30% probability.

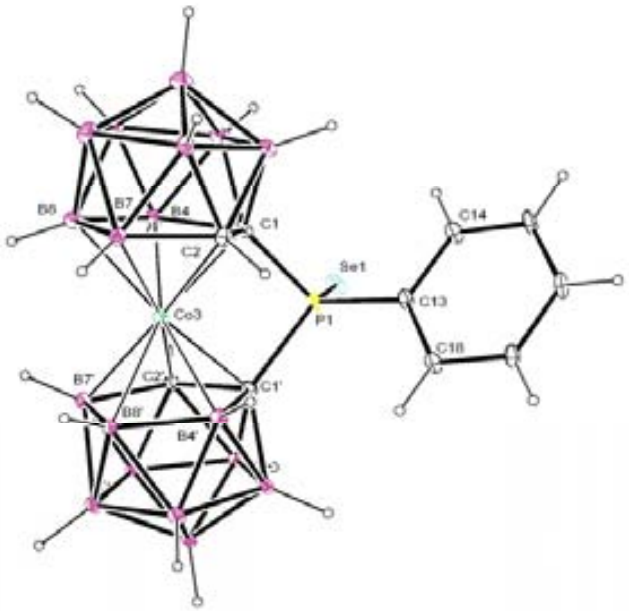

Figure 7. a) Graphical representation of the interactions found in anion [**3**]$^-$. b) 2D plot of the NBO orbitals corresponding to the interaction P-Co. The plane contains Co1-C2-P3 atoms.

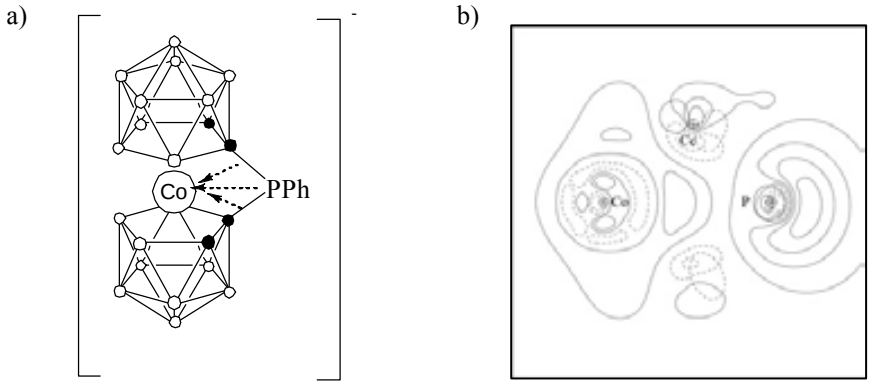

Figure 8. HOMO orbitals of anions [**3**]$^-$ (left) and [**4**]$^-$ (right).

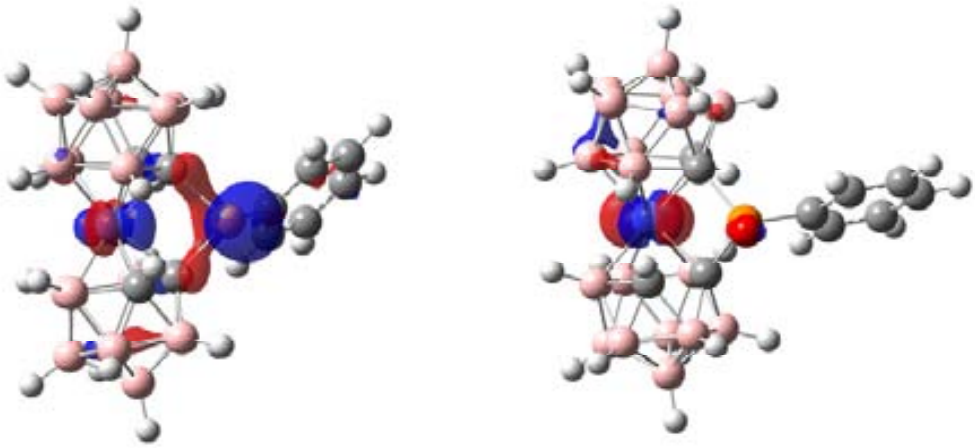

Table 1. Summary of ^{31}P-NMR ressonance peaks of anions [**3**]$^-$, [**7**]$^-$, [**11**]$^-$ and [**15**]$^-$ and their corresponding oxidized compounds.

Compound	^{31}P-RMN	^{31}P-RMN (Oxygen)	^{31}P-RMN (Sulphur)	^{31}P-RMN (Selenium)
[3]$^-$	70.4	34.6	71.7	68.8
[7]$^-$	77.3	35.6	68.4	62.7
[11]$^-$	88.3	52.7	95.3	99.6
[15]$^-$	96.7	55.5	95.6	97.5

Table 2. Comparison between experimental and theoretical data from ^{31}P-NMR spectra.

Compound	Theoretical absolut chemical shift (ppm)	Theoretical relative chemical shift (ppm)	Experimental relative chemical shift (ppm)
3	214.5	0.0	0.0
4	269.9	-55.3	-35.7
5	211.9	2.7	1.3
6	193.2	21.4	-0.6

References

[1] Frisch, M. J.; Trucks, G. W.; Schlegel, H. B.; Scuseria, G. E.; Robb, M. A.; Cheeseman, J. R.; Montgomery, Jr., J. A.; Vreven, T.; Kudin, K. N.; Burant, J. C.; Millam, J. M.; Iyengar, S. S.; Tomasi, J.; Barone, V.; Mennucci, B.; Cossi, M.; Scalmani, G.; Rega, N.; Petersson, G. A.; Nakatsuji, H.; Hada, M.; Ehara, M.; Toyota, K.; Fukuda, R.; Hasegawa, J.; Ishida, M.; Nakajima, T.; Honda, Y.; Kitao, O.; Nakai, H.; Klene, M.; Li, X.; Knox, J. E.; Hratchian, H. P.; Cross, J. B.; Bakken, V.; Adamo, C.; Jaramillo, J.; Gomperts, R.; Stratmann, R. E.; Yazyev, O.; Austin, A. J.; Cammi, R.; Pomelli, C.; Ochterski, J. W.; Ayala, P. Y.; Morokuma, K.; Voth, G. A.; Salvador, P.; Dannenberg, J. J.; Zakrzewski, V. G.; Dapprich, S.; Daniels, A. D.; Strain, M. C.; Farkas, O.; Malick, D. K.; Rabuck, A. D.; Raghavachari, K.; Foresman, J. B.; Ortiz, J. V.; Cui, Q.; Baboul, A. G.; Clifford, S.; Cioslowski, J.; Stefanov, B. B.; Liu, G.; Liashenko, A.; Piskorz, P.; Komaromi, I.; Martin, R. L.; Fox, D. J.; Keith, T.; Al-Laham, M. A.; Peng, C. Y.; Nanayakkara, A.; Challacombe, M.; Gill, P. M. W.; Johnson, B.; Chen, W.; Wong, M. W.; Gonzalez, C.; Pople, J. A. *Gaussian 03*, Revision C.02,; Gaussian, Inc.: Wallingford CT, **2004**.

[2] a) Hariharan, P. C.; Pople, J. A. *Theor. Chim. Acta* **1973**, *28*, 213. b) Becke, A. D. *J. Chem. Phys.* **1993**, *98*, 5648.

[3] Glendening, E. D.; Badenhoop, J, K.; Reed, A. E.; Carpenter, J. E.; Bohmann, J. A.; Morales, C. M.; Weinhold, F., *NBO 5.0*, Theoretical Chemistry Institute, University of Wisconsin, Madison, **2001**.

[4] Rojo, I.; Teixidor, F.; Viñas, C.; Kivekäs, R.; Sillanpää, R. *Chem. Eur. J.* **2004**, *10*, 5376.

[5] Manners, I. "Ring-Opening Polymerization of Metallocenophanes: A New Route to Transition Metal-Based Polymers", *Advances in Organometallic Chemistry*, Vol. 37, Academic Press, New York, **1995**.

To multicage polyanionic thioether derivatives of metallacarboranes.

(Preliminary version)

Pau Farràs,[a,±] Raikko Kivekäs,[b] Reijo Sillanpää,[c] Francesc Teixidor,[a] Clara Viñas,[a,*]

[a] Institut de Ciència de Materials de Barcelona (CSIC), Campus de la U.A.B., E-08193 Bellaterra, Spain. Telefax: Int. Code + 34 93 5805729. E-mail: clara@icmab.es.

[b] Department of Chemistry, P.O. Box 55, University of Helsinki, FIN-00014, Finland.

[c] Department of Chemistry, University of Jyväskylä, FIN-40351, Finland.

[±] Pau Farras is enrolled in the PhD program of the UAB.

Introduction

To be written later.

Computational details

Calculations were performed with the Gaussian 03 suite of programs.[1] All geometries were optimized at the B3LYP/6-31G* level of theory,[2] with no symmetry constraints. Frequency calculations were computed on these geometries at the same level of calculation to verify that they are energy minima. NBO (natural bond orbital) analysis,[3] including NPA charges of the compounds, were calculated at the B3LYP/6-311+G** level of theory along with their frontier orbitals.

Results and Discussion

1.- Synthesis of anions 2-8. See Chart 1 for numbering of metallacarboranes.

The desired anionic thioether compounds may be conveniently prepared following the reaction procedure described by Smith et al.[4] and later applied by our group in the synthesis of thioether derivatives of *o*-carborane.[5] The procedure consists on the metallation of $Cs[3,3'\text{-}Co(1,2\text{-}C_2B_9H_{11})_2]$ (**1**) with two equivalents of *n*-BuLi, followed by reaction with the corresponding disulfide derivative in 1,2-dimethoxyethane (DME) at low temperature, as shown in Scheme 1. The reaction mixture was then refluxed for several hours depending on the compound. In the case of the bridged-sulphur derivative, an overnight reflux is needed to obtain the desired compound. In this case the reagent is not a disulfide but S_8. The NMe_4 salts can be produced by metathesis dissolving Li^+ salts in ethanol and adding an aqueous solution of $[NMe_4]Cl$. Solids corresponding to NMe_4^+ salts separate well and can be collected by filtration.

It is remarkable the case of anions **6** and **8** These compounds have both metallacarborane and carborane moieties connected through the sulphur atom. In the work-up procedure after precipitating them as NMe_4^+ salts, a solubilization step with ethanol is used. This process leads to a partial degradation of one of the two units of carborane, producing dianionic species. Usually strong basic conditions such as KOH/EtOH mixtures are used to partially degrade *o*-carborane. Partial degradation with ethanol was already observed when thioether derivatives of *o*-carborane were complexed with transition metal salts.[6] B(3) electrophilic exaltation is indicated in figure 1. In **6** and **8** a competition between the three boron clusters for the available valence electrons occurs. Both type of clusters are electron withdrawing when connected through the carbon atoms. The experimental evidence indicates that the metallacarborane attracts more electron density than carborane, causing that the adjacent positions to the carbon atoms (B(3) and B(6)) become electron deficient, and therefore more susceptible to the attack of a nucleophile such as ethanol. This triggers the partial degradation of the boron cluster and then, the molecule finds its electronic equilibrium. It is important to observe the difference in behaviour between the two compounds regarding their substituents (Me in **6** or Ph in **8**). Following the same procedure to obtain the NMe_4^+ salt, **6** degrades to the dianionic species in the presence of ethanol, while **8** remains as a monoanionic compound with a minor amount of the dianionic compound. These mild conditions have lead selectively to dianionic species, and applying more harsh conditions it should be possible to get the trianionic multicluster.

Formulas **2-5** were established from the mass spectrum obtained by the matrix-assisted laser desorption ionization (MALDI-TOF) technique in the negative-ion mode without the use of a matrix. Full agreement between the experimental and calculated patterns was obtained for the molecular ion peak. The ^{11}B and ^{1}H spectra of the compounds were found to be in accord with the proposed structures shown in Chart 1. For example, the $^{11}B\{^{1}H\}$-NMR spectrum of NMe_4[**2**] displays a 2:2:4(2+2):2:2:2:2:2 pattern in the range δ = +7.9 to -19.8 ppm, indicative of a *closo* species with all boron atoms in nonequivalent vertices in one dicarbollide unit. The resonance of relative intensity 4 may be attributed to the coincidental overlap of two absorptions of intensity 2. Spectra of **6-8** are more complicated due to the overlap of the peaks corresponding to the three boron clusters, two *o*-caborane and one metallacarborane fragments. However, it has been very useful to see the partial degradation of one fragment of *o*-carborane. As it can be seen in figure 2, peaks at -33 and -36 ppm appear in the $^{11}B\{^{1}H\}$-NMR spectrum after using ethanol, indicative of the degradation to *nido* species of one *o*-carborane cage. Moreover, the integral of these peaks in respect to the rest of the spectrum is found to be 2:35, and this indicates that only one *o*-carborane fragment has been degraded. Another indication of the formation of the *nido* cluster can be seen in the coupled ^{11}B-NMR spectra, where the peak at -33 ppm appears as a double doublet as a consequence of the coupling with both the terminal and the bridging hydrogen atoms.

^{1}H-RMN spectra has been useful to confirm the purity of the synthesized compounds but also to identify **5**. This sulphur-bridged compound on the carbon atoms of dicarbollide cages has the peaks correponding to the hydrogen atoms of the C_c-H groups very downfield, at 6 ppm. This means that these hydrogen atoms are acidic. It can also be observed in its IR spectrum, where the resonance peak of the C_c-H groups shifts from 3042 cm^{-1} in **1** to 3008 cm^{-1} in **5**.

Crystal structures of **2**, **3** and **5** have been obtained. For example, compound **2** has been obtained by slow evaporation of a dichloromethane solution. This compound has a racemic structure and its x-ray structure show strong intramolecular interactions (Van der Waals radii -0.2Å) between the sulphur atom of one dicarbollide cage and the nearest hydrogen atoms of the C_c-H and B-H groups of the other dicarbollide fragment. In addition, all the inter and intramolecular interactions found in the molecule confers an interesting packing on display in figure 3. The packing consists of three consecutive layers repeated through space but in a a:b:b:a pattern. The first layer consists of solvent and cation units in a zig-zag disposition. Then, a layer of cobaltabisdicarbollide fragments and, finally, the third contains the aromatic rings of the substituent, which are facing the aromatic rings of the next set of layers.

2.- Theoretical study of anion 5.

Previous work done in our group has shown that phosphorus-bridged C,C-substituted cobaltabisdicarbollide produces an interaction between the lone pair on phosphorus and the 4s orbital of cobalt. We think that this interaction can also be found in compound **5** and may be stronger because sulphur has two available lone electron pairs instead of one as for phosphorus. Theoretical calculations have been done on this compound. First, the structure from the x-ray data of compound **5** has been optimitzed, followed by an NBO analysis. The analysis shows a donor-acceptor interaction of 10.57 kcal/mol between two NBO orbitals, the first being one of the lone electron pairs of sulphur and the second the empty 4s orbital of cobalt. The second lone pair on sulphur has no significant interaction with cobalt, but yields an interaction of 5.80 kcal/mol with the antibonding orbital placed between C_c-C_c bonds on both dicarbollide units. The bond enthalpy of Co-S found in the literature is of 79 kcal/mole,[7] therefore the energy of these interactions described here have to be taken into account. These two interactions are shown in figure 4 as electron density maps. Figure 4a shows the electron density map on the cobalt-sulphur plane. A good overlap between both orbitals can there be seen. The plane comprising carbon cluster atoms in one dicarbollide unit and the sulphur is shown in figure 4b. It can there be observed how the second lone electron pair of sulphur coincides with the p orbital of sulphur, preventing any possible overlap with any of the orbitals of cobalt. Notwithstanding so, there is a good interaction between the antibonding orbital in the C_c-C_c bond and this lone pair.

In addition, HOMO and LUMO orbitals have been calculated. The electronic communication between the cobalt and sulphur atoms causes that atomic orbitals of the latter take part on the HOMO orbital. This can be observed in figure 5 where the HOMO orbital is made mainly by the contribution of a d orbital on cobalt and a p orbital of sulphur. Instead, the LUMO orbital is distributed among the cobalt and the atoms of cluster carbon and boron atoms, but not on sulphur.

3.- Eletrochemical studies

Electrochemistry of **5** has been done to see if the electron communication from the sulphur to cobalt affect the redox potential on cobalt. If this electron transfer was the only one found in the molecule, this would imply a cathodic shift of the half-wave potential of **5** in respect to **1** indicating that **5** is more easily oxidized. However, this is not the case because the $E_{1/2}$ value of **5** is more positive. This can be explained comparing this molecule with other thiocarborane compounds found in the literature.[8] There, the C_c-SR group pulls electron density off the cage and this is in competition with the electron communication described above. If **5** resulted to be easily reduced than **1**, the effect of the sulphur pulling electrons off the cage is higher than that of its dative interaction with cobalt. This trend can be observe if a comparison between the cluster total charge (CTC: sum of the charge of all atoms in the cluster) and the energy difference between the HOMO and LUMO orbitals is done. If the CTC charge has a more positive value it means that has less electron density and therefore, it would be easier to add electrons or in other words to be reduced. In the same way, if the difference between HOMO and LUMO orbitals is smaller it means that it would be easier to add an electron because the LUMO orbital would be nearer. The values can be seen in table 1.

Conclusions

To be written later.

Experimental Section

Instrumentation. Elemental analyses were performed in our laboratory using a Carlo Erba EA1108 microanalyzer. IR spectra (ν, cm^{-1}; KBr pellets) were obtained on a Shimadzu FTIR-8300 spectrophotometer. The ^{1}H- and $^{1}H\{^{11}B\}$-NMR (300.13 MHz), $^{13}C\{^{1}H\}$-NMR (75.47 MHz), ^{11}B- and $^{11}B\{^{1}H\}$-NMR (96.29 MHz) spectra were recorded on a Bruker ARX 300 instrument equipped with the appropriate decoupling accessories. All NMR spectra were performed in deuterated solvents at 22ºC. The ^{11}B- and $^{11}B\{^{1}H\}$-NMR shifts were referenced to external $BF_3{\cdot}OEt_2$, while the ^{1}H, $^{1}H\{^{11}B\}$, and $^{13}C\{^{1}H\}$-NMR shifts were referenced to $SiMe_4$. Chemical shifts are reported in units of parts per million downfield from reference, and all coupling constants in Hz. The mass spectra were recorded in the negative ion mode using a Bruker Biflex MALDI-TOF-MS [N_2 laser; λ_{exc} 337 nm (0.5 ns pulses); voltage ion source 20.00 kV (Uis1) and 17.50 kV (Uis2)].

Materials. All manipulations were carried out under inert atmosphere. 1,2-dimethoxyethane (DME) was distilled from sodium benzophenone prior to use. Reagents were obtained commercially and used as purchased. $Cs[3,3'\text{-}Co(1,2\text{-}C_2B_9H_{10})_2]$ **(1)** was supplied by Katchem Ltd. (Prague) and was used as received. Reagents were obtained commercially and used as purchased in Aldrich.

Synthesis of $[N(CH_3)_4][1,1'\text{-}(SPh)_2\text{-}3,3'\text{-}Co(1,2\text{-}C_2B_9H_{10})_2]$ (2): Under an inert atmosphere, *n*-butyllithium (1.22M in hexanes, 1.98 mL, 2.42 mmol) was added dropwise to a stirred solution of $Cs[3,3'\text{-}Co(1,2\text{-}C_2B_9H_{11})_2]$ (0.5 g, 1.1 mmol) (**1**) in anhydrous 1,2-dimethoxyethane (25 mL) at -40ºC. The resulting purple solution was stirred for 60 min at low temperature. Then, phenyl disulfide (0.96 mg, 4.4 mmol) was added, causing a rapid color change to red. The mixture was stirred for 2 hours at room temperature and then was reflux for 2 hours. A grey solid was filtered off and discarded. After removal of the solvent, the residue was dissolved in the minimum volume of EtOH and an aqueous solution containing an excess of $[Me_4N]Cl$ was added, resulting in the formation of a precipitate. The resulting red solid was filtered off, washed with water and petroleum ether, and dried in vacuo. Yield: 0.57 g (85%). Elemental analysis calcd (%) for $C_{20}H_{42}B_{18}CoNS_2$: C=39.11, H=6.89, N=2.28, S=10.44; found: C=40.10, H=6.69, N=2.25, S=11.16. ^{1}H-NMR: δ = 7.64-7.24 (m, 10H, Ph), 4.29 (br s, 2H, C_c-H), 3.45 (s, 12H, $N(CH_3)_4$), 4.07–1.41 (br s, 18H; B-H). $^{13}C\{^{1}H\}$-NMR: δ = 137.67 (s, S-C), 129.29 (s, C_{ortho}), 128.76 (s, C_{metha}), 127.38 (s, C_{para}), 68.58 (s, C_c-S), 63.53 (s, C_c-H), 55.16 (s, $N(CH_3)_4$). ^{11}B-NMR: δ = 7.88 (d, $^{1}J(B,H)$ = 131 Hz, 2B), 0.69 (d, $^{1}J(B,H)$ = 140 Hz, 2B), -2.77 (d, $^{1}J(B,H)$ = 127 Hz, 4B), -3.66 (d, $^{1}J(B,H)$ = 118 Hz, 2B), -7.76 (d, $^{1}J(B,H)$ = 142 Hz, 2B), -12.88 (d, $^{1}J(B,H)$ = 156 Hz, 2B), -15.82 (d, $^{1}J(B,H)$ = 155 Hz, 2B), -19.82 (d, $^{1}J(B,H)$ = 113 Hz, 2B). MALDI-TOF MS: m/z (%): 539.35 (M, 100%), 430.31 (M-SC_6H_5, 17%), 323.32 (M-$S_2C_{12}H_{10}$, 6%).

Synthesis of $[Cs][1,1'\text{-}(SCy)_2\text{-}3,3'\text{-}Co(1,2\text{-}C_2B_9H_{10})_2]$ (3). This compound was prepared using the same procedure as for **2,** but using cyclohexyl disulfide (0.97 mL, 4.4 mmol) instead of phenyl disulfide. Work-up ends with the precipitation of the caesium salt. Yield: 0.63 g (92%). Elemental analysis calcd (%) for $C_{16}H_{42}B_{18}CoCsS_2$: C=28.05, H=6.18, S=9.36; found: C=26.10, H=5.74, S=7.30. ^{1}H-NMR: δ = 3.93 (br s, 2H, C_c-H), 3.11 (m, 2H, S-CH_{cy}), 1.69 (m, 4H, H_{cy}), 1.57 (m, 4H, H_{cy}), 1.43-1.29 (m, 12H, H_{cy}), 4.06–1.41 (br s, 18H, B-H). $^{13}C\{^{1}H\}$-NMR: δ = 68.42 (s, C_c-S), 64.24 (s, C_c-H), 50.53 (s, S-C), 34.98 (s, C_{ortho}), 26.28 (s, C_{metha}), 25.20 (s, C_{para}). ^{11}B-NMR: δ = 8.69 (d, $^{1}J(B,H)$ = 147 Hz, 2B), 1.12 (d, $^{1}J(B,H)$ = 140 Hz, 2B), -2.70 (d, $^{1}J(B,H)$ = 139 Hz, 6B), -7.31 (d, $^{1}J(B,H)$ = 141 Hz, 2B), -12.70 (d, $^{1}J(B,H)$ = 168 Hz, 2B), -14.96 (d, $^{1}J(B,H)$ = 170 Hz, 2B), -18.45 (d, $^{1}J(B,H)$ = 157 Hz, 2B). MALDI-TOF MS: m/z (%): 552.41 (M, 100%), 468.26 (M-C_6H_{11}, 18%), 438.29 (M-SC_6H_{11}, 35%), 354.19 (M-$SC_{12}H_{22}$, 22%), 323.22 (M-$S_2C_{12}H_{22}$, 11%).

Synthesis of $[N(CH_3)_4][1,1'\text{-}(SEt)_2\text{-}3,3'\text{-}Co(1,2\text{-}C_2B_9H_{10})_2]$ (4). This compound was prepared using the same procedure as for **2,** but using ethyl disulfide (0.27 mL, 2.19 mmol) instead of phenyl disulfide. Yield: 0.09 g (80%). Elemental analysis calcd (%) for $C_{12}H_{42}B_{18}CoNS_2$: C=27.82, H=8.17, N=2.70, S=12.38; found: C=27.38, H=7.98, N=2.99, S=10.11. ^{1}H-NMR: δ = 3.97 (br s, 2H, C_c-H), 3.44 (s, 12H, $N(CH_3)_4$), 2.91 (q, $^{3}J(H,H)$= 7, 4H, CH_2), 1.15 (t, $^{3}J(H,H)$= 7, 6H, CH_3), 3.10–1.64 (br s, 18H; B-H). $^{13}C\{^{1}H\}$-NMR: δ = 67.15 (s, C_c-S), 63.81 (s, C_c-H), 55.20 (s, $N(CH_3)_4$), 25.25 (s, CH_2), 12.71 (s, CH_3). ^{11}B-NMR: δ = 7.96 (d, $^{1}J(B,H)$ = 142 Hz, 2B), 0.66 (d, $^{1}J(B,H)$ = 140 Hz, 2B), -3.50 (d, $^{1}J(B,H)$ = 143 Hz, 6B), -7.90 (d, $^{1}J(B,H)$ = 142 Hz, 2B), -13.68 (d, $^{1}J(B,H)$ = 157 Hz, 2B), -15.96 (d, $^{1}J(B,H)$ = 171 Hz, 2B), -19.75 (d, $^{1}J(B,H)$ = 164 Hz, 2B). MALDI-TOF MS: m/z (%): 444.24 (M, 100%).

Synthesis of $[N(CH_3)_4][\mu\text{-}1,1'\text{-}S\text{-}3,3'\text{-}Co(1,2\text{-}C_2B_9H_{10})_2]$ (5). This compound was prepared using the same procedure as for **2,** but using elemental sulphur (0.45 g, 14 mmol) instead of phenyl disulfide and by using overnight reflux.

Yield: 0.16 g (79%). Elemental analysis calcd (%) for $C_8H_{32}B_{18}CoNS$: C=22.45, H=7.54, N=3.27, S=7.49; found: C=21.97, H=7.04, N=2.57, S=7.93. ^{1}H-NMR: δ = 5.94 (br s, 2H, C_c-H), 3.44 (s, 12H, $N(CH_3)_4$), 3.37–1.52 (br s, 18H; B-H). ^{11}B-NMR: δ = 6.58 (d, ^{1}J(B,H) = 145 Hz, 2B), 1.71 (d, ^{1}J(B,H) = 145 Hz, 4B), -1.51 (d, ^{1}J(B,H) = 160 Hz, 2B), -4.54 (d, ^{1}J(B,H) = 138 Hz, 2B), -5.93 (d, ^{1}J(B,H) = 138 Hz, 2B), -15.89 (d, ^{1}J(B,H) = 153 Hz, 2B), -17.45 (d, ^{1}J(B,H) = 152 Hz, 2B), -21.29 (d, ^{1}J(B,H) = 169 Hz, 2B). MALDI-TOF MS: m/z (%): 354.59 (M, 100%).

Synthesis of $[N(CH_3)_4][1$-$(1''$-S-$2''$-CH_3-$1'',2''$-$C_2B_{10}H_{10})$-$1'$-$(1'''$-S-$2'''$-CH_3-$1''',2'''$-$C_2B_9H_{10})$-$3,3'$-$Co(1,2$-$C_2B_9H_{10})_2]$ (6). This compound was prepared using the same procedure as for **2,** but using methyl thiocarborane (0.166 g, 0.44 mmol) instead of phenyl disulfide. ^{11}B-NMR: δ = 6.19, 1.23, -2.09, -5.07, -6.81, -7.58, -9.06, -10.13, -10.53, -11.96, -16.96, -16.40, -17.86, -21.83, -23.39 (38B).

Synthesis of $[N(CH_3)_4]_2[1$-$(1''$-S-$2''$-CH_3-$1'',2''$-$C_2B_9H_{10})$-$1'$-$(1''$-S-$2''$-CH_3-$1'',2''$-$C_2B_9H_{10})$-$3,3'$-$Co(1,2$-$C_2B_9H_{10})_2]$ (7). This compound was obtained after degradation of **6** in ethanol during the work-up procedure. Yield: 0.11 g (60%). ^{1}H-NMR: δ = 3.94 (br s, 2H, C_c-H), 3.45 (s, 24H, $N(CH_3)_4$), 2.30 (s, 3H, CH_3), 2.13 (s, 3H, CH_3), 3.38–1.44 (br s, 37H; B-H). ^{13}C{^{1}H}-NMR: δ = 85.89 (s, C_c-S-$\mathbf{C_c}$), 81.94 ($\mathbf{C_c}$-CH_3), 65.68 (s, $\mathbf{C_c}$-S), 55.23 (s, N($\mathbf{C}H_3)_4$), 51-03 (s, $\mathbf{C_c}$-H), 23.94 (s, CH_3), 22.57 (s, CH_3). ^{11}B-NMR: δ = 6.57 (d, ^{1}J(B,H) = 139 Hz, 3B), 1.68 (d, ^{1}J(B,H) = 150 Hz, 4B), -1.48 (d, ^{1}J(B,H) = 147 Hz, 2B), -4.51 (m, 2B), -6.02 (d, ^{1}J(B,H) = 138 Hz, 6B), -7.03 (m, 1B), -8.53 (d, 1B), -9.95 (d, ^{1}J(B,H) = 165 Hz, 4B), -14.70 (m, 1B), -15.93 (d, ^{1}J(B,H) = 147 Hz, 2B), -17.46 (d, ^{1}J(B,H) = 151 Hz, 4B), -21.29 (d, ^{1}J(B,H) = 172 Hz, 2B), -22.94 (d, ^{1}J(B,H) = 157 Hz, 2B), -33.32 (dd, ^{1}J(B,H) = 145 Hz, ^{1}J(B,H) = 33 Hz, 1B), -36.41 (d, ^{1}J(B,H) = 137 Hz, 1B).

Synthesis of $[N(CH_3)_4][1$-$(1''$-S-$2''$-C_6H_5-$1'',2''$-$C_2B_{10}H_{10})$-$1'$-$(1'''$-S-$2'''$-C_6H_5-$1''',2'''$-$C_2B_9H_{10})$-$3,3'$-$Co(1,2$-$C_2B_9H_{10})_2]$ (8). This compound was prepared using the same procedure as for **2,** but using phenyl thiocarborane (0.231 mg, 0.46 mmol) instead of phenyl disulfide. Yield: 0.16 g (81%). ^{1}H-NMR: δ = 7.72 (m, 4H, C_6H_5), 7.45 (m, 2H, C_6H_5), 7.32 (m, 4H, C_6H_5), 5.94 (br s, 2H, C_c-H), 3.41 (s, 12H, $N(CH_3)_4$), 3.25–1.51 (br s, 38H; B-H). ^{11}B-NMR: δ = 6.61 (d, ^{1}J(B,H) = 144 Hz, 2B), 1.68 (d, ^{1}J(B,H) = 145 Hz, 4B), -1.52 (d, ^{1}J(B,H) = 153 Hz, 2B), -4.55 (d, ^{1}J(B,H) = 136 Hz, 6B), -6.07 (d, ^{1}J(B,H) = 157 Hz, 8B), -10.16 (d, ^{1}J(B,H) = 163 Hz, 6B), -12.80 (d, ^{1}J(B,H) = 148 Hz, 4B), -15.91 (d, ^{1}J(B,H) = 157 Hz, 2B), -17.48 (d, ^{1}J(B,H) = 155 Hz, 2B), -21.33 (d, ^{1}J(B,H) = 165 Hz, 2B).

Chart 1.- C-substituted thioether derivatives **2-8**.

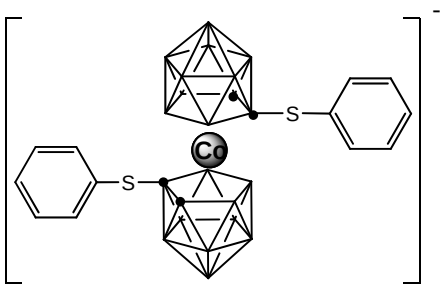

2

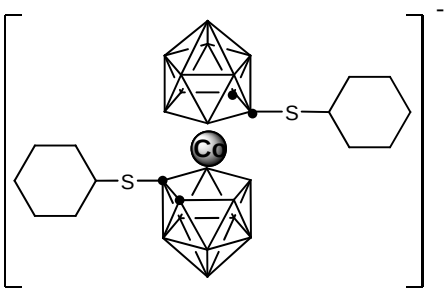

3

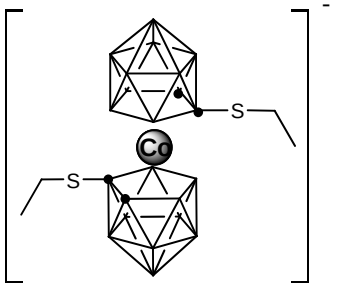

4

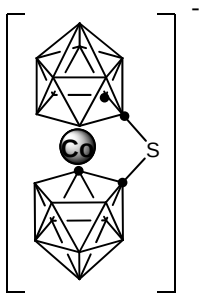

5

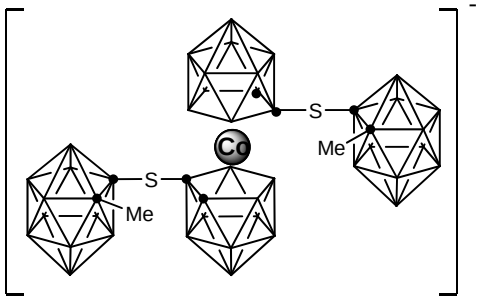

6

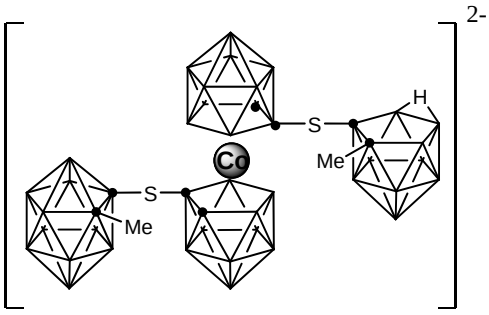

7

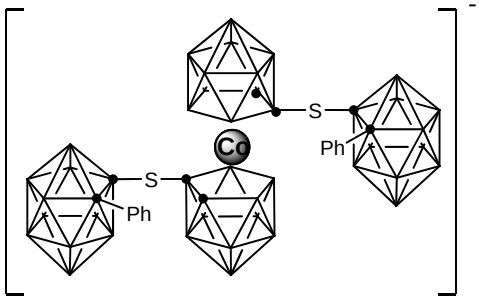

8

Scheme 1. Synthetic procedure for the preparation of thioether derivatives of **1**.

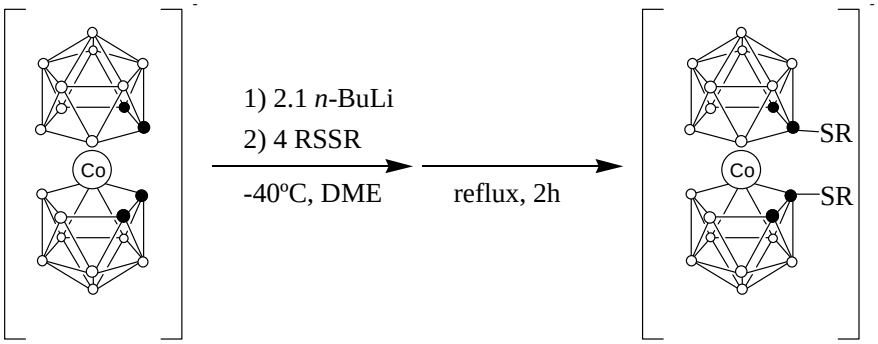

Figure 1. Schematic representation of the partial degradation in the presence of a nucleophile.

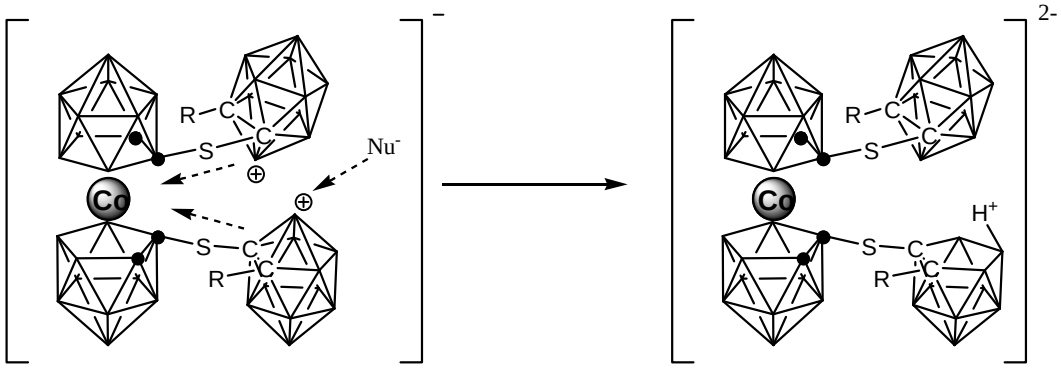

Figure 2. Comparison between the $^{11}B\{^{1}H\}$-NMR spectra of **6** and **7** corresponding to the non-degraded (up) and partially degraded (down) clusters.

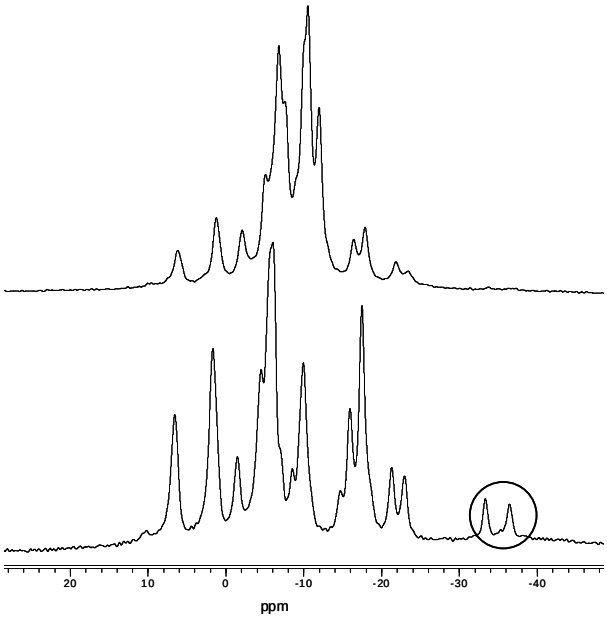

Figure 3. X-ray structure packing of anion **2**.

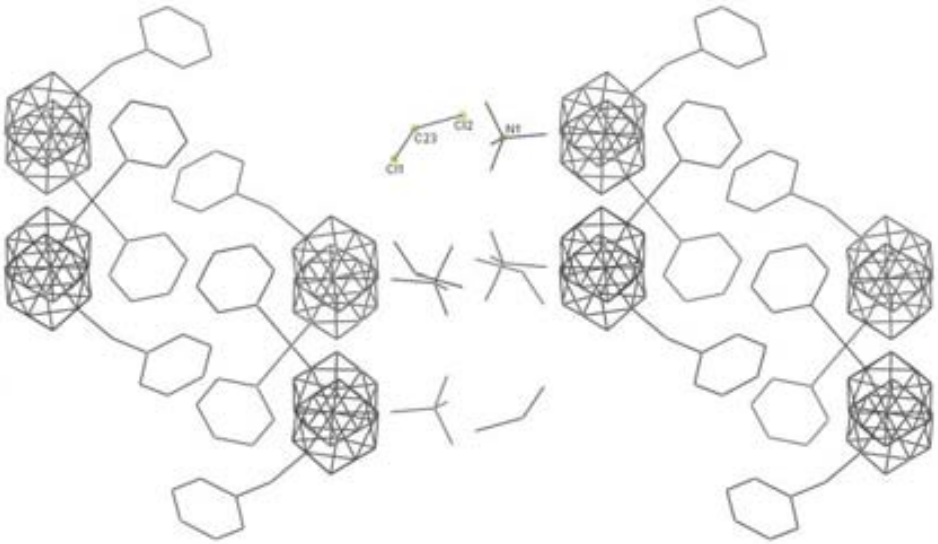

Figure 4. Electron density maps of **5** from the NBO analysis corresponding to : a) Co-S interaction; b) C_c-C_c antibond orbital-S interaction.

a)

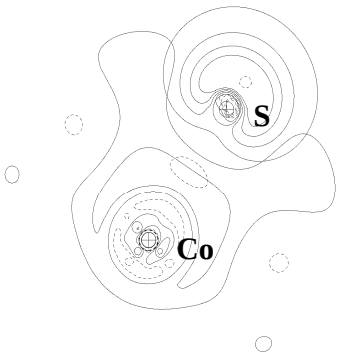

b)

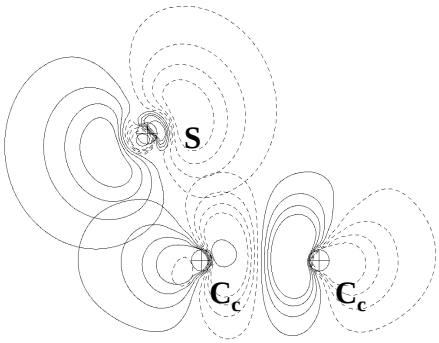

Figure 5. HOMO and LUMO orbitals of **5**.

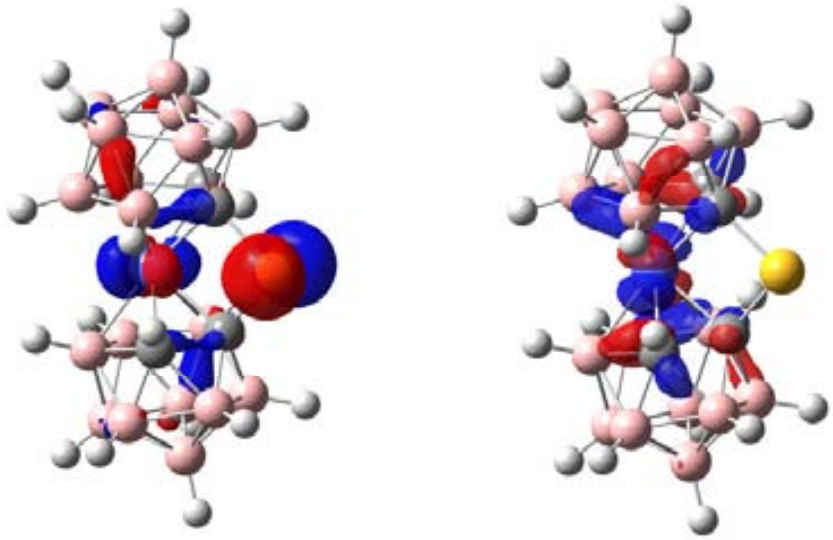

HOMO **LUMO**

Table 1. Redox potential, CTC charges and HOMO and LUMO orbitals for compounds **1** and **5**.

Compound	$E_{1/2}$ [V]	CTC	E_{HOMO} [eV]	E_{LUMO} [eV]	$\Delta E_{HOMO-LUMO}$
1	-1.83	-3.48	-3.96	0.55	-4.51
5	-1.51	-2.88	-4.04	0.27	-4.30

References

[1] Frisch, M. J.; Trucks, G. W.; Schlegel, H. B.; Scuseria, G. E.; Robb, M. A.; Cheeseman, J. R.; Montgomery, Jr., J. A.; Vreven, T.; Kudin, K. N.; Burant, J. C.; Millam, J. M.; Iyengar, S. S.; Tomasi, J.; Barone, V.; Mennucci, B.; Cossi, M.; Scalmani, G.; Rega, N.; Petersson, G. A.; Nakatsuji, H.; Hada, M.; Ehara, M.; Toyota, K.; Fukuda, R.; Hasegawa, J.; Ishida, M.; Nakajima, T.; Honda, Y.; Kitao, O.; Nakai, H.; Klene, M.; Li, X.; Knox, J. E.; Hratchian, H. P.; Cross, J. B.; Bakken, V.; Adamo, C.; Jaramillo, J.; Gomperts, R.; Stratmann, R. E.; Yazyev, O.; Austin, A. J.; Cammi, R.; Pomelli, C.; Ochterski, J. W.; Ayala, P. Y.; Morokuma, K.; Voth, G. A.; Salvador, P.; Dannenberg, J. J.; Zakrzewski, V. G.; Dapprich, S.; Daniels, A. D.; Strain, M. C.; Farkas, O.; Malick, D. K.; Rabuck, A. D.; Raghavachari, K.; Foresman, J. B.; Ortiz, J. V.; Cui, Q.; Baboul, A. G.; Clifford, S.; Cioslowski, J.; Stefanov, B. B.; Liu, G.; Liashenko, A.; Piskorz, P.; Komaromi, I.; Martin, R. L.; Fox, D. J.; Keith, T.; Al-Laham, M. A.; Peng, C. Y.; Nanayakkara, A.; Challacombe, M.; Gill, P. M. W.; Johnson, B.; Chen, W.; Wong, M. W.; Gonzalez, C.; Pople, J. A. *Gaussian 03*, Revision C.02,; Gaussian, Inc.: Wallingford CT, **2004**.

[2] a) Hariharan, P. C.; Pople, J. A. *Theor. Chim. Acta* **1973**, *28*, 213. b) Becke, A. D. *J. Chem. Phys.* **1993**, *98*, 5648.

[3] Glendening, E. D.; Badenhoop, J, K.; Reed, A. E.; Carpenter, J. E.; Bohmann, J. A.; Morales, C. M.; Weinhold, F., *NBO 5.0*, Theoretical Chemistry Institute, University of Wisconsin, Madison, **2001**.

[4] Smith, H. D.; Obenland, C. O.; Papetti, S., *Inorg. Chem.*, **1966**, *5*,1013.

[5] Llop, J.; Viñas, C.; Oliva, J. M.; Teixidor, F.; Flores, M. A.; Kivekäs, R.; Sillanpää, R., *J. Organomet. Chem.*, **2002**, *657*, 232.

[6] Teixidor, F.; Viñas, C.; Sillanpää, R.; Kivekäs, R. *Inorg. Chem.* **1994**, *33*, 2645.

[7] Smoes, S., *Boils. Soc. Chim. Belg.*, **1972**, *81*, 45. Also can calculate of approximate way doing the stocking of l?energy of the links Co-Co (30.4 kcal/mole) and S-S (101.65 kcal/mole), giving as a result 66 kcal/mole.

[8] Teixidor, F.; Benakki, R.; Viñas, C.; Kivekäs, R., Sillanpää, R. *Inorg. Chem.* **1999**, *38*, 5916.

DOI: 10.1002/anie.200((will be filled in by the editorial staff))

Chlorination of carborane anions. An experimental and theoretical study

*Pau Farràs,[±] Clara Viñas, Reijo Sillanpää, Milagros Rey and Francesc Teixidor**

closo-Carborane anions are finding applications as doping agents,[1] as radioactive waste remediation synergists,[2] in catalysis,[3] metathesis, oxidation chemistry as well as in stabilizing highly reactive cations,[4] and strong Brønsted acids.[5] Halogenated derivatives have attracted particular interest because of their robustness that make them suitable for applications. However, despite their relevance little is known about the halogenation process, how many halogen atoms can be introduced?, is the process dominated by thermodynamic or kinetic factors?, is it radical or ionic?. In this paper we will refer in particular to chlorine substituents as these have, excluding B-F, the largest B-X bond enthalpies,[6] and again with the exception of fluorine, are the least polarizable and reactive of the halogens providing the highest protection against degradation.[7] The most investigated monoanionic closo deltahedral clusters are $[CB_{11}H_{12}]^-$, $[CB_9H_{10}]^-$ and [3,3'-Co(1,2-$C_2B_9H_{11})_2]^-$, they are also the ones more readily available. For this initial work we decided to focus on $[CB_9H_{10}]^-$ because there are 6 crystal structures available on CSD of halogenated derivatives of [1-C_6H_5-1-$CB_9H_9]^-$ [**1**]$^-$,[8] and in particular [1-(4'-BrC_6H_4)-1-$CB_9Br_5H_4]^-$.[8a] This singular example results from the bromination of [**1**]$^-$, and had the aryl ring brominated before the cluster C adjacent boron atoms suffered bromination. Therefore a reliable theory that explained the halogenation had to account for this particular case.

In this study, we combine experimental work with calculations to come through the former questions. We will show here that all of the B-H positions can be substituted, that there are preferential sites, and that the latter are not the result of thermodynamics but kinetics. Also, our studies evidence the radical nature of the chlorination reaction. This contradicts earlier reports and is opposite to aromatic halogen substitution.[5c]

To learn on the preferential halogenation number and on the preferential halogenation sites we planned experiments each leading to the synthesis of a set of compounds that could easily be quantified. For the quantification we have used the MALDI-TOF-MS technique that is quantitative for mixtures of monoanionic boron clusters.[9] Recognizing that MALDI-TOF-MS determines only elemental composition, we refer to each peak in the MS corresponding to a halogenated derivative of [**1**]$^-$ as a 'compound' as it may consist of positional isomers. We have done the synthesis of mixtures of chlorinated derivatives of [**1**]$^-$ by reacting it with N-clorosuccinimide (NCS) in solid state at 194±6ºC. In Table 1 are summarized the experimental results for the reaction of NCS with [**1**]$^-$ (see Table S.1 for detailed data). The ratio of reagents utilized is shown in column r_y, so r_y=10 means a ratio of NCS/[**1**]$^-$=10 and r_y=19 a ratio of NCS/[**1**]$^-$=19. Column y indicates the compounds observed in each reaction and the dominant one is enlightened in bold. Each number indicates the number of Cl on [**1**]$^-$. So 7 means that 7 H in [1-C_6H_5-1-$CB_9H_9]^-$ have been substituted by 7 Cl. Alternatively it could be named [Cl_7-**1**]$^-$. It is to be seen in Table 1 that from r_1 to r_6 the dominant chlorinated product parallels r_y. e.g. at a ratio NCS/[**1**]$^-$=5 the major product is [Cl_5-**1**]$^-$. The observed discontinuity from [Cl_6-**1**]$^-$ to [Cl_7-**1**]$^-$, that breaks the parallel between r_y and the major compound in y, and that requires a reagents ratio NCS/[**1**]$^-$ equal to 9 to produce [Cl_7-**1**]$^-$ as the major product suggests that the 7th chlorination shall take place on a different plane in the framework of [**1**]$^-$ than the former substitutions. Conversely it implies that [Cl_6-**1**]$^-$ has completally filled a full set of equivalent positions in pristine [**1**]$^-$. Inspecting the structure of [**1**]$^-$ the only way to fill six positions having a 7th in another set of non-equivalent positions is by filling the platform as in the crystal structure of [Cl_6-**1**]$^-$ shown in Figure 1. The discontinuity from [Cl_7-**1**]$^-$ to [Cl_8-**1**]$^-$ is even more pronounced than this from [Cl_6-**1**]$^-$ to [Cl_7-**1**]$^-$. [Cl_8-**1**]$^-$ is produced as the major product for r_y=12, thereafter it is dominant. This implies that [Cl_6-**1**]$^-$ and [Cl_8-**1**]$^-$ are very stable compounds that very likely could be obtained almost pure directly from reaction. To prove this we conducted reactions at slightly different conditions that permitted to get [Cl_6-**1**]$^-$ pure enough to get crystals. Therefore albeit [Cl_{14}-**1**]$^-$, corresponding to perchlorination, has been achieved some preferential numbers of chlorination exist, [Cl_6-**1**]$^-$ and [Cl_8-**1**]$^-$, the latter shown in Figure 1b.

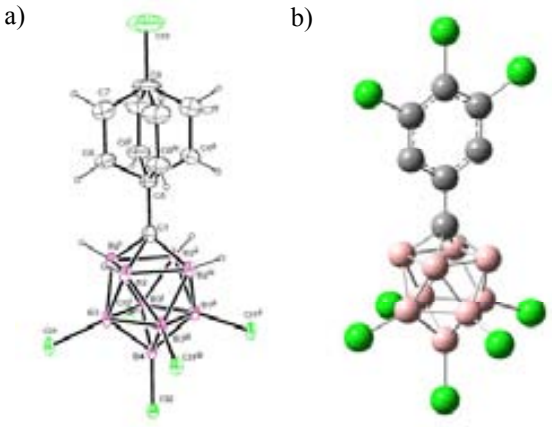

Figure 1. a) Crystallographically determined structure of the [1-(4'-ClC_6H_4)-6,7,8,9,10-Cl_5-1-$CB_9H_4]^-$ anion in its salt Cs^+(see Supporting information); b) Computed structure of [Cl_8-1]- anion at B3LYP/6-31G*.

[*] P. Farràs, M. Rey, Prof. Dr. C. Viñas, Prof. Dr. F. Teixidor
Institut de Ciència de Materials de Barcelona (CSIC)
Campus de la U.A.B., 08193 Bellaterra (Spain)
Fax: (+34) 935805729
E-mail: teixidor@icmab.es

Prof. Dr. R. Sillanpää
Department of Chemistry, University of Jyväskylä
FIN-40014, Finland

[±] P. Farràs is enrolled in the U.A.B. PhD program.

[**] We thank EU (FP6-508854), CICYT (Project MAT2006-05339 and CTQ2006-26257-E/PPQ), Generalitat de Catalunya (2001/SGR/00337), CSIC (I3P grant for P.F.), and MEyC (FPU grant for M.R.). We are grateful to Dra. Joyce Lockhart for her comments. Access to the computational facilities to the Centre de Supercomputació de Catalunya and the CSIC computing center is also gratefully acknowledged

Supporting information for this article is available on the WWW under http://www.angewandte.org or from the author.

Table 1. MALDI-TOF-MS compositions after the reaction of [**1**]$^-$ and NCS. r_y represents the initial molar ratio. In the column headed by y, the compounds observed by MALDI-TOF-MS are indicated. In bold it is indicated the major compound. The numbers are indicative of the number of inserted chlorine atoms.

r_y	y	r_y	y
1	0, **1**, 2	11	6, **7**, 8, 9, 10
2	0, 1, **2**, 3, 4	12	6, 7, **8**, 9, 10
3	2, **3**, 4, 5	13	6, 7, **8**, 9, 10
4	3, **4**, 5, 6	14	6, 7, **8**, 9, 10
5	3, 4, **5**, 6	15	6, 7, **8**, 9, 10, 11
6	**6**, 7	16	6, 7, **8**, 9, 10, 11, 12
7	**6**, 7	17	6, 7, **8**, 9, 10, 11, 12
8	5, **6**, 7, 8, 9	18	6, 7, **8**, 9, 10, 11, 12, 13
9	6, **7**, 8, 9	19	6, 7, **8**, 9, 10, 11, 12, 13, 14
10	6, **7**, 8, 9	20	7, **8**, 9, 10, 11, 12, 13, 14

The diatomic bond enthalpies for B-Cl, B-H, C-Cl and C-H are 128, 81, 95±7 and 81 kcal/mol, respectively.[6] Therefore total substitution of B-H by B-Cl and of C-H by C-Cl should produce a net enthalpy gain in [**1**]$^-$. If only thermodynamic considerations are contemplated it would be expected that the observed chlorination regioselectivity in [**1**]$^-$ would imply larger enthalpy gains in the more favoured cluster sites and the full chlorination of the boron cluster, in preference to the aromatic ring. The plot of ΔH_{add} computed at the DFT level (see Supporting information) *vs.* number of added Cl on B, according to equation 1, is a straight line with no singular points.

$$[Cl_yH_{14-y}\text{-}1\text{-}C_6\text{-}1\text{-}CB_9]^- + Cl_2 \xrightarrow{\Delta H} [Cl_{y+1}H_{13-y}\text{-}1\text{-}C_6\text{-}1\text{-}CB_9]^- + HCl$$

Equation 1

The slope is altered when substitution takes place on C. Thus there is no site related thermodynamic stabilization and, given suitable conditions, all B-H and C-H could be chlorinated. Indeed perchlorination of the simpler $[1\text{-}CB_9H_{10}]^-$ has been demonstrated by Xie et al,[10] and in the former experiments where $[Cl_{14}$-**1**$]^-$ has been obtained. Details of these calculations and the plot can be found in Table S.2 and Figure S.1.

Despite experimental evidence given above that *preferential chlorination* sites exist in [**1**]$^-$, it is unlikely that adequate protocols of synthesis for the highly chlorinated derivatives, except perhaps for $[Cl_{14}$-**1**$]^-$ can be found. This situation is not unique, and in a sense is reminiscent of electrophilic aromatic substitution where the mixtures are likewise generated for kinetic reasons. The proportions of *ortho*-, *meta*- and *para*- isomers in a substituted benzene reflect the relative rates at each of these sites and the determining step is related to the accumulation of negative charge on the aromatic ring induced by the substituent. To interpret the former experimental results we studied the charges on [**1**]$^-$. The NPA charges on B and C atoms shown in Figure 2a suggest that electrophilic substitution would take place first on *p*-C, then on *m*-C on the benzene ring. As shown by the NCS chlorination experiments, and by the crystal structures available, the NPA charges do not provide the correct order of halogenation. A precise correlation is obtained, however, by considering the two atoms Natural Population Analysis method (2a-NPA) charges on B-H or C-H (where 2a-NPA charges are defined as the sum of the NPA charges of the two bonded atoms). According to the 2a-NPA, the sequence of substitution would be first on B(10), next on B(6-9), then on *p*-C and then on *m*-C. Our experimental evidence ends at this point, but we could predict from the 2a-NPA that next step would be on *o*-C to finalize with chlorination at B(2-5). To show the consistency of the method, NPA and 2a-NPA charges have been calculated for $[Cl_6$-**1**$]^-$. The subsequent halogenations for the latter would, according to 2a-NPA charges, follow the same sequence as for [**1**]$^-$. Details for $[Cl_6$-**1**$]^-$ are given in Figure S.2.

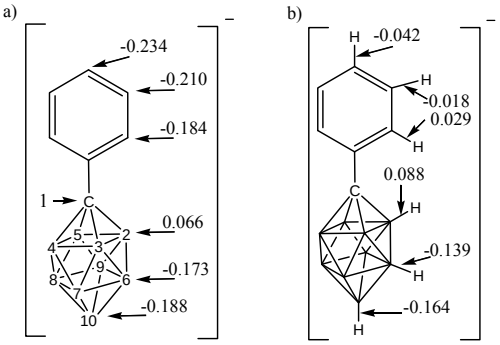

Figure 2. a) NPA charges on boron and carbon, displaying the numbering of the boron atoms. b) 2a-NPA charges on B-H and C-H bonds calculated in this work at the B3LYP/6-31+G* level of theory.

It is known experimentally that B(6) is the first position to be chlorinated in [**1**]$^-$ despite 2a-NPA calculations indicate that B(10) should be the first targeted boron. The energy difference between isomers $[6\text{-Cl-}1\text{-}C_6H_5\text{-}1\text{-}CB_9H_8]^-$ and $[10\text{-Cl-}1\text{-}C_6H_5\text{-}1\text{-}CB_9H_8]^-$ in the ground state, calculated at the B3LYP/6-31+G* level of theory is low: the 10-Cl isomer is 1.4 kcal/mol more stable than the 6-Cl isomer. The discrepancy between experiment and theory could be due to the simplicity of the computational method, as it only refers to the fundamental state of the molecule. To get a more precise view of the first step of chlorination it is required to learn on the transition state and to calculate activation energy barriers. Thus, following atom relaxation on a transition state calculation it is found that Cl^+ has preference for B(6), while former H(6) has moved closer to the aryl ring in an adjacent triangular face of the cluster. Detailed information can be found in the supplementary material. However, in the search for a transition state derived from the interaction of Cl^+ and $[1\text{-}C_6H_5\text{-}1\text{-}CB_9H_9]^-$ assuming that the attack takes place first on B(6)-H, unusual high energy barriers of 283.2 kcal/mol were calculated. In Figure S.3 the best calculated pathway for the monochlorination of [**1**]$^-$ is shown. These high energy barriers would prevent the reaction to happen, but experiments show that chlorination takes place, therefore the reaction is not electrophilic. Then what is it?. We considered the possibility that it could be a radical reaction as had been suggested earlier.[11]

Fukui indexes,[12] used to predict the susceptibility of a certain position to be attacked by a nucleophile, an eletrophile or a radical, were calculated for [**1**]$^-$. The results are found in Table S.3 but the most important point is that in B(6) we find that the radical index is 0.05 higher than the electrophilic one, suggesting that, actually, the reaction could be of a radical origin. The mechanism, shown in Figure 3, was then recalculated as a radical attack to the boron cluster. The simple anion $[1\text{-}CB_9H_{10}]^-$ was taken as a model to simplify the calculations. By replacing Cl^+ by Cl^- in the reaction mechanism, the activation energy of the reaction has become reasonable with a value of 6.21 kcal/mol. The transition state reminds very much this found for the electrophilic pathway so that the initial H in B(6)-H has moved to a triangular face nearest to the

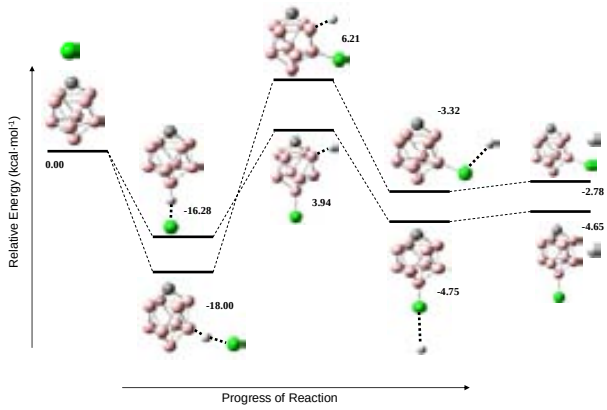

Figure 3. Reaction pathway for the chlorination of $[1\text{-}CB_9H_{10}]^-$ by a $Cl^\cdot$. Calculations performed at the B3LYP/3-21G* level of theory. Hydrogen atoms are not shown except for H(6) and H(10).

C of the boron cluster. We shall see that the position of the substituted hydrogen atom does not differ much either in the 6-Cl or 10-Cl activated complex. But, why does the substitution take place preferentially at B(6) and not at B(10)?. The answer can be found in the pre-reaction complexes. The pre-reaction 6-substituted adduct is 1.72 kcal/mol more stable than the pre-reaction 10-substituted adduct.

Therefore theory indicates that chlorination on [**1**]$^-$ occurs in a radical and not electrophilic mechanism. To support such a mechanism and following our experiment↔theory interdependence we sought for one experiment that validated the mechanism. For that purpose we chose a radical scavenger as TEMPO and a radical initiator as VAZO® catalyst 88. If the mechanism was ionic the addition of TEMPO or VAZO®-88 would not alter the reaction. On the contrary the reaction with VAZO®-88 would be more efficient than with TEMPO. Indeed the last situation is the one that occurred. For a specific experiment at the oven with a particular r_y we noticed that the chlorination degree on the dominant product varied 4 Cl depending on the addition of VAZO®-88 or TEMPO. The results are shown in Table S.4.

Summarizing, $[1\text{-}C_6H_5\text{-}1\text{-}CB_9H_9]^-$ has been taken as model compound to study chlorination in monoanionic boron clusters. It has been shown experimentally that there exists preferential chlorination sites in this cluster. Theoretical calculations have shown that these preferential sites are of a kinetic origin and that the attack is not ionic but by radicals. The substitution reaction rates have been rationalised by considering 2a-NPA on the starting material unperturbed by chlorine substituents. The 2a-NPA charges reproduce the chlorination order of attack much more accurately than simple NPA.

Received: ((will be filled in by the editorial staff))
Published online on ((will be filled in by the editorial staff))

Keywords: Radical substitution · Aromatic electrophilic substitution · Chlorination · NPA charges · kinetics · solid state reaction · carboranes

[1] a) C. Masalles, S. Borrós, C. Viñas, F. Teixidor, *Adv. Mater.* **2000**, *12*, 1199; b) C. Masalles, F. Teixidor, S. Borrós, C. Viñas, *J. Organomet. Chem.* **2002**, *657*, 239; c) C. Masalles, J. Llop, C. Viñas, F. Teixidor, *Adv. Mater.* **2002**, 14, 826; d) C. Masalles, S. Borrós, C. Viñas, F. Teixidor, *Adv. Mater.* **2002**, *14*, 449; e) S. Gentil, E. Crespo, I. Rojo, A. Friang, C. Viñas, F. Teixidor, B. Grüner, D. Gabel, *Polymer* **2005**, *46*, 12218.

[2] a) J. Rais, J. Plesek, P. Selucky, M. Kyrs, L. Daklecova, *J. Radioanal. Nucl. Chem.* **1991**, *148*, 349; b) J. Plesek, *Chem. Rev.* **1992**, *92*, 269; c) P. Selucky, N. V. Sistkova, J. Rais, *J. Radioanal. Nucl. Chem.***1997**, *224*, 89; d) B. Grüner, J. Plesek, J. Baca, I. Cisarova, J. F. Dozol, H. Rouquette, C. Viñas, P. Selucky, J. Rais, *New J. Chem.***2002**, *26*, 1519; e) C. Viñas, S. Gomez, J. Bertran, J. Barron, F. Teixidor, J. F. Dozol, H. Rouquette, R. Kivekäs, R. Sillanpää, *J. Organomet. Chem.* **1999**, *581*, 188; f) C. Viñas, S. Gomez, J. Bertran, J. Barron, F. Teixidor, J. F. Dozol, H. Rouquette, R. Kivekäs, R. Sillanpää, *Dalton Trans.* **1998**, *17*, 2849; g) C. Viñas, S. Gomez, J. Bertran, F. Teixidor, J. F. Dozol, H. Rouquette, *Inorg. Chem.* **1998**, *37*, 3640; h) C. Viñas, S. Gomez, J. Bertran, F. Teixidor, J. F. Dozol, H. Rouquette, *Chem. Commun.* **1998**, *2*, 191.

[3] a) P. E. Behnken, J. A. Belmont, D. C. Busby, M. S. Delaney, R. E. King III, C. W. Kreimendahl, T. B. Marder, J. J. Wilczynski, M. F. Hawthorne, *J. Am. Chem. Soc*., **1984**, *106*, 3011; b) P. E. Behnken, D. C. Busby, M. S. Delaney, R. E. King III, C. W. Kreimendahl, T. B. Marder, J. J. Wilczynski, M. F. Hawthorne, *J. Am. Chem. Soc*., **1984**, *106*, 7444; c) G. Zi, H. W. Li, Z. Xie, *Organometallics* **2002**, *21*, 3850; d) H. Wang, Y. Wang, H. W. Li, Z. Xie, *Organometallics* **2001**, *20*, 5110; e) F. Teixidor, M. A. Flores, C. Viñas, R. Kivekäs, R. Sillanpää, *Angew. Chem., Int. Ed. Engl.*, **1996**, *35*, 19; f) F. Teixidor, M. A. Flores, C. Viñas, R. Sillanpää, R. Kivekäs, *J. Am. Chem Soc*., **2000**, 122, 1963; f) O. Tutusaus, C. Viñas, R. Núñez, F. Teixidor, A. Demonceau, S. Delfosse, A. F. Noels, I. Mata, E. Molins, *J. Am. Chem Soc*., **2003**, *125*, 11830.

[4] a) C. A. Reed, *Acc. Chem. Res.* **1998**, *31*, 133; b) C. A. Reed, *Acc. Chem. Res.* **1998**, *31*, 325; c) S. H. Strauss, *Chem. Rev.* **1993**, *93*, 927.

[5] a) C. A. Reed, N. L. P. Fackler, K. C. Kim, D. Stasko, D. R. Evans, P. D. W. Boyd, C. E. F. Rickard, *J. Am. Chem. Soc.* **1999**, *121*, 6314; b) I. A. Koppel, P. Burk, I. Koppel, I. Leito, T. Sonoda, M. Mishima, *J. Am. Chem. Soc.* **2000**, *122*, 5114; c) S. Körbe, P. J. Schreiber, J. Michl, *Chem. Rev.* **2006**, *106*, 5208.

[6] http://www.webelements.com/

[7] I. B. Sivaev, V. I. Bredagze, *Collect. Czech. Chem. Commun.***1999**, *64*, 783.

[8] a) A. Franken, C. A. Kilner, M. Thornton-Pett, J. D. Kennedy, *Collect. Czech. Chem. Commun.* **2002**, *67*, 869; b) C. J. Sumby, M. J. Carr, A. Franken, J. D. Kennedy, C. A. Kilner, M. J. Hardie, *New J. Chem.* **2006**, *30*, 1390.

[9] a) F. Teixidor, P. Angles, C. Viñas, *Inorg. Chem.***1999**, *38*, 3605; b) J. Llop, C. Masalles, C. Viñas, F. Teixidor, R. Sillanpää, R. Kivekäs, *Dalton Trans.* **2003**, 556; c) B. Grüner, J. Plešek, J. Báča, I. Císařová, J. F. Dozol, H. Rouquette, C. Viñas, P. Selucký, J. Rais, *New J. Chem.* **2002**, *26*, 1519; d) G. Barbera, C. Viñas, F. Teixidor, A.J. Welch, G. M. Rosair, *J. Organomet. Chem.* **2002**, *657*, 217; e) F. Teixidor, J. Pedrajas, I. Rojo, C. Viñas, R. Kivekäs, R. Sillanpää, I. Sivaev, V. I. Bregadze, S. Sjöberg, *Organometallics* **2003**, *22*, 3414.

[10] C. W. Tsang, Q. Yang, E. T. Sze, T. C. Mak, D.T. Chan, Z. Xie, *Inorg. Chem.* **2000**, *39*, 3582.

[11] a) G. E. Ryschkewitsch, V. R. Miller, *J. Am. Chem. Soc.* **1973**, *95*, 2836; b) K. E. Stockman, D. L. Garrett, R. N. Grimes, *Organometallics* **1995**, *14*, 4661; c) J. Holub, M. Bakardjiev, B. Stibr, *Collect. Czech. Chem. Commun.* **2002**, *67*, 783.

[12] F. Mendez, J. L. Gazquez, *J. Am. Chem. Soc.* **1994**, *116*, 9298.

Additive tuning redox potential in metallacarboranes by sequential halogen substitution

Patricia González-Cardoso,[a]± Anca-Iulia Stoica,[a,b] Pau Farràs,[a]± Ariadna Pepiol,[a]± Clara Viñas[a] and Francesc Teixidor*[a]

[a] Institut de Ciència de Materials de Barcelona (CSIC), Campus de la U.A.B., 08193 Bellaterra (Spain). Fax: (+34) 935805729. E-mail: teixidor@icmab.es

[b] On leave from the Department of Analytical Chemistry. University of Bucharest (Romania).

± P. González-Cardoso, P. Farràs and A. Pepiol are enrolled in the Ph.D. program of the UAB.

Electron transfer (ET) is fundamental in many processes of life, including oxygen binding, photosynthesis and respiration.[1] All organisms obtain energy by transferring electrons from an electron donor to an electron acceptor.[2] Besides, ET attracts considerable attention because of the possible application in energy storage and photovoltaic energy conversion.[3-6]

Maximum efficiency in photosynthesis is obtained when electrons are passed from one carrier molecule to another in a downhill direction. Can a similar downhill sequence be obtained with artificially made molecules? Certainly taking a combination of different platforms this should be possible,[7] however it has not been made with a unitary electroactive framework such as ferrocene, C_{60}, or perylene diimide.[8-13]

In this work we describe the largest downhill sequence of individual electron donors and acceptors made from a common frame. Interest in modulating the redox properties of electroactive frameworks such as ferrocene, C_{60}, or perylene diimide has been manifested but the results have been very limited,[14-18] and certainly a cumulative effect has to date not been demonstrated.

Boron clusters approximate to deltahedra or to deltahedra with one or more vertices missing. In the early 1970s, it was realized that the geometry of boron clusters is related with the number of electron pairs available for bonding, therefore redox processes should be able to produce structural change.[19-22]

Although C_{60} and 1,2-, 1,7-, and 1,12-$C_2B_{10}H_{12}$ *closo*-carboranes are all neutral molecules characterized by a closed-cage structure, the first requires much less energy to incorporate $2e^-$ than the carboranes, -0.87 V vs. -2.5 V, respectively being both values referred to SCE.[23,24] The low lying LUMO in C_{60} and the structural rearrangement required for the carboranes may account for this large voltage difference. The low reduction potential of C_{60} has made it very valuable as an electron acceptor in devices,[14-18] and could have been an excellent platform to generate a large sequential set of electron acceptors. However, up to now, this has not been achieved,[25-27] and does not seem to be possible.

According to their reduction potentials, carboranes could not compete with C_{60} as electron acceptors; however, the B-X bond, (X = halogen), in boron clusters is much more stable to reduction than the C-X bond in sp^2 carbon atoms and this could make it valuable for the sought redox tuning.[28]

As borane clusters are not suited to be redox modulated due to the structural changes caused by addition or removal of electrons, we looked for a system that took advantage of the properties of boron clusters and skipped their problems so attention was set on the somehow less severe electron regulated metallacarboranes, and in particular to the well known Co^{III} species $[Co(C_2B_9H_{11})_2]^-$, $[\mathbf{1}]^-$.[29,30] This shows three quasi-reversible waves in cyclic voltammetry at +1.67, -1.31 and -2.26 V vs $Ag/AgCl/KCl_{sat}$ assigned to Co^{IV}/Co^{III}, Co^{III}/Co^{II} and Co^{II}/Co^{I}, respectively.[31,32]

The negative $E_{1/2}$ peaks indicate that introducing one and two electrons into the Co^{III} system is energy intensive. It was known that the redox potential of $[Co(C_2B_9H_{10}Cl)_2]^-$, was -0.99V for the couple Co^{III}/Co^{II},[33] about 0.3 V more positive than for $[\mathbf{1}]^-$. Should further B-Cl substitutions not cancel the redox shift of a previous one, adding Cl substituents into the cluster could be a way for fine redox modulation.

Results and Discussion

All this relied, however, in possessing a good set of consecutive halogenated derivatives of $[\mathbf{1}]^-$, and this was not the case. For the coming paragraphs the halogenated species are named as $[Cl_x\text{-}\mathbf{1}]^-$, x stating the number of chlorine atoms in the $[\mathbf{1}]^-$ anion. Before this work, only $[Cl_2\text{-}\mathbf{1}]^-$ and $[Cl_6\text{-}\mathbf{1}]^-$ were known and the latter is indeed a mixture of chlorinated species from $[Cl_2\text{-}\mathbf{1}]^-$ to $[Cl_6\text{-}\mathbf{1}]^-$, so its redox value was not reliable and produced an intractable cyclic voltammetry (CV) wave (see Fig. 1a).[30] The synthesis described in the literature is in solution and only allows the synthesis up to six chlorine atoms.

In order to have a full set of chlorinated species, we developed a new method solvent-free to obtain a higher degree of chlorination. We produced the $[Cl_x\text{-}\mathbf{1}]^-$ (x > 2) anions by reacting *N*-chlorosuccinimide with $[\mathbf{1}]^-$ in the oven in a vacuum sealed tube (see Supporting Information). By varying the ratio of reagents, a set of series of $[Cl_x\text{-}\mathbf{1}]^-$ was obtained, each series consisting of a limited number of x values in approximately a Gaussian distribution. Despite having a mixture of compounds, we were able to synthesize up to the $[Cl_{10}\text{-}\mathbf{1}]^-$. The molecular composition was obtained by MALDI-TOF-MS analysis by comparing the areas under each peak envelop (see Table S1 in Supporting Information). As the $[Cl_x\text{-}\mathbf{1}]^-$ mixtures are made of chemically and structurally very similar compounds, their MALDI-TOF-MS represent very well the chemical composition of the studied samples. With all these in mind, we prepared a set of mixtures named A to F (see Table S2 in Supporting Information) in order to study their electrochemistry, from both the experimental procedure described above and the one in the literature. Mixtures E and F were prepared specifically comprising a full set of chlorinated species to confirm the validity of the method. As these were mixtures, their CVs reminded very much the shape of Fig. 1a, but were consistently shifted to anodic potentials the higher was the average x value in the $[Cl_x\text{-}\mathbf{1}]^-$ mixture.

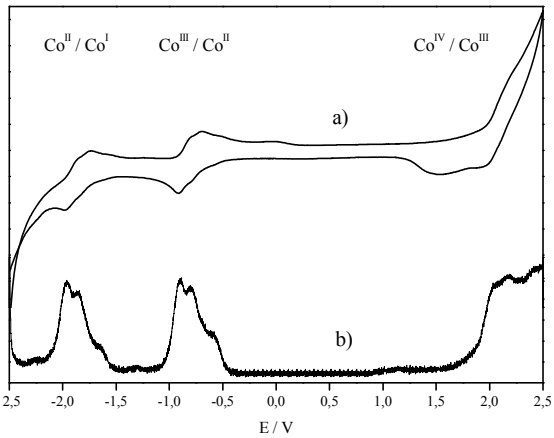

Figure 1. Cyclic voltammogram (a) and Square Wave voltammogram (b) responses recorded at glassy carbon electrode in MeCN of $5 \bullet 10^{-3}$M $[Cl_x\text{-}\mathbf{1}]^-$ (x = 2-6) using $[Bu_4N][PF_6]$ (0.1M) as supporting electrolyte. The electrochemical cell contained also $Ag/AgCl/KCl_{sat}$ as the reference electrode and a platinum wire as the auxiliary electrode. Scan rate: a) 0.2 $V \bullet s^{-1}$, b) 0.025 $V \bullet s^{-1}$.

Thus, the expected shift was found but no $E_{1/2}$ value for every x could be drawn from the CVs. However, Square Wave Voltammetry (SWV) provided sufficient fine structure to retrieve more information. In Fig. 1b the SWV for $[Cl_x\text{-}\mathbf{1}]^-$ (x = 2-6) is indicated. By combining chemical composition drawn from MALDI-TOF-MS and deconvolution by Gaussians of the SWV, a set of self-consistent $E_{1/2}$ values for every x could be obtained. In Figure 2 the MALDI-TOF-MS and the SWV of the Co^{III}/Co^{II} couple of $[Cl_x\text{-}\mathbf{1}]^-$ (x = 2-6) are displayed. Both are periodic, in terms of peak separation, and present the same intensity pattern.

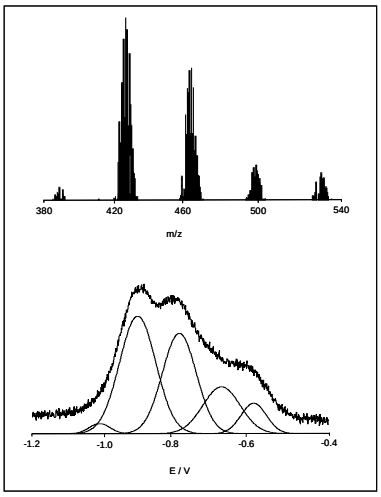

Figure 2. MALDI-TOF mass spectrum of $[Cl_x\text{-}\mathbf{1}]^-$ with x = 2-6 (up) and deconvolution into Gaussians of its Co^{III}/Co^{II} SWV (down).

The MALDI-TOF-MS is due to the mixture of species $[Cl_2\text{-}\mathbf{1}]^-$, $[Cl_3\text{-}\mathbf{1}]^-$, $[Cl_4\text{-}\mathbf{1}]^-$, $[Cl_5\text{-}\mathbf{1}]^-$ and $[Cl_6\text{-}\mathbf{1}]^-$, each peak showing the properly isotopic distribution centered at 391.51, 426.53, 461.53, 495.51 and 530.50, respectively, each step due to an extra Cl in the molecule and the periodic anodic shift in the SWV is also due to the influence of one extra chloride on $[Cl_{x\text{-}1}\text{-}\mathbf{1}]^-$. The periodicity in the consecutive $E_{1/2}$ values supports that additional dehydrochlorination does not cancel the previous redox shift. Thus, it could be hypothesized that a 0.9 V drop of the Co^{III}/Co^{II} couple from -1.31 V in $[\mathbf{1}]^-$ to near -0.41 V would require 9 Cl^- substitutions or $[Cl_9\text{-}\mathbf{1}]^-$. Indeed this is the case. In Table 1 the whole sequence of $E_{1/2}$ potentials are shown. For each x value, $E_{1/2}$ has been calculated as many times as $[Cl_x\text{-}\mathbf{1}]^-$ has been found in the different synthetic mixtures; the dispersion of $E_{1/2}(x)$ is very low, proving that the values are self-consistent (see Fig. S1 in Supporting Information).

The $E_{1/2}$ additivity hypothesis is satisfied very reasonably, and also applies to the Co^{II}/Co^{I} couple and most probably to the Co^{IV}/Co^{III}. Some values are slightly out of the rule, e.g. the $E_{1/2}$ value for $[Cl_9\text{-}\mathbf{1}]^-$, but this may be due to the always low yield of this particular anion in any sample produced, more than to a failure of the additivity. In Fig. 1b, the SWV for the Co^{III}/Co^{II} and Co^{II}/Co^{I} look very similar. This has allowed to double check the goodness of fit of the Gaussians deconvolution. Less data has been obtained for the Co^{IV}/Co^{III} couple due to the overall anodic shift upon higher chlorination that has led the $E_{1/2}$ value for this couple to the anodic edge of the solvent.
Preliminary results show that the $E_{1/2}$ additivity modulation also occurs with Br and I derivatives. For the same number of halogen substituents, the anodic shift is $E_{1/2}(Cl) < E_{1/2}(Br) < E_{1/2}(I)$, each one shifted near 0.10 V for Co^{III}/Co^{II} and 0.07 V for Co^{II}/Co^{I} when moving from Cl to Br and 0.10 V for both redox processes when moving from Br to I.

To find a theoretical basis on the redox tunability of $[Cl_x\text{-}\mathbf{1}]^-$ species, the $E_{1/2}$ values for Co^{III}/Co^{II} have been correlated with their HOMO and LUMO energies. Table 1 displays the HOMO and the LUMO energies along with the $E_{1/2}$ for the couple Co^{III}/Co^{II}. There is a good parallel between the plots of $E_{1/2}$ and $-E_{LUMO}$ vs the number of chlorine substituents. Similarly, there is a good correlation between $E_{1/2}$ and $-E_{HOMO}$ with the number of chlorine substituents. Although the $E_{1/2}$ for Co^{III}/Co^{II} correlation with both E_{LUMO} and E_{HOMO} may seem contradictory, it is not if the first relates to the reduction of Co^{III} to Co^{II} and the second relates to the oxidation of Co^{III} to Co^{IV}. The easiest $[Cl_x\text{-}\mathbf{1}]^-$ to be oxidized is the one with x = 0, which is the one with the more positive HOMO energy, in agreement with the Koopman's theorem. Conversely, the easiest $[Cl_x\text{-}\mathbf{1}]^-$ to be reduced is the one with x = 12 as it has the more stable LUMO.

Of notice is that these redox values are very comparable to the first two reduction waves of C_{60} at -0.48 for $[C_{60}]^{0/-I}$ and -0.87 V for $[C_{60}]^{-I/-II}$ vs SCE, which is remarkable considering that C_{60} is a neutral molecule whereas $[Co(C_2B_9H_{11})_2]^-$ is an anionic species. Moreover, if we were able to increase the degree of chlorination, we would be able to reach even positive values of $E_{1/2}$. In fact, we are developing a new

Table 1. Calculated energy values of the HOMO and the LUMO of $[Cl_x\text{-}\mathbf{1}]^-$ compared with the $E_{1/2}$ value for their corresponding Co^{III}/Co^{II} process (vs $Ag/AgCl/KCl_{sat}$).

Compound	$E_{1/2}$ / [V]	$-E_{HOMO}$ / [eV]	$-E_{LUMO}$ / [eV]
$[\mathbf{1}]^-$	-1.31	3.963	-0.546
$[Cl_1\text{-}\mathbf{1}]^-$	-	4.060	-0.379
$[Cl_2\text{-}\mathbf{1}]^-$	-1.01	4.163	-0.153
$[Cl_3\text{-}\mathbf{1}]^-$	-0.89	4.261	0.019
$[Cl_4\text{-}\mathbf{1}]^-$	-0.78	4.409	0.195
$[Cl_5\text{-}\mathbf{1}]^-$	-0.68	4.492	0.344
$[Cl_6\text{-}\mathbf{1}]^-$	-0.57	4.609	0.496
$[Cl_7\text{-}\mathbf{1}]^-$	-0.47	4.698	0.596
$[Cl_8\text{-}\mathbf{1}]^-$	-0.36	4.784	0.698
$[Cl_9\text{-}\mathbf{1}]^-$	-0.32	4.838	0.819
$[Cl_{10}\text{-}\mathbf{1}]^-$	-	4.984	0.925
$[Cl_{11}\text{-}\mathbf{1}]^-$	-	5.017	1.026
$[Cl_{12}\text{-}\mathbf{1}]^-$	-	5.149	1.130

method of synthesis, still under study, that allows us to synthesize species up to the $[Cl_{12}\text{-}\mathbf{1}]^-$. We can assure that their $E_{1/2}$ values follow the lineal tendency described in this paper, so that the $E_{1/2}$ for $[Cl_{12}\text{-}\mathbf{1}]^-$ is -0.11V.

Acknowledgements

This work was supported by MEC (MAT2006-05339, SAB2006-0127), Generalitat de Catalunya (2005/SGR/00709) and CESCA. P. G.-C., P. F. and A. P. thank CSIC for a pre-doctoral grant.

References

[1] Blankenship, R. E. *Molecular Mechanisms of Photosynthesis* Ch. 6 and 7 (Blackwell Science, Oxford, 2002).

[2] Cotterill, R. *Biophysics: An Introduction* Ch. 9 (Wiley-VCH, West Sussex, 2003).

[3] Eisenberg, R. & Gray, H.B. Preface on Making Oxygen. *Inorg. Chem.* **47**, 1697 (2008).

[4] Herrero, C., Lassalle-Kaiser, B., Leibl, W., Rutherford, A. W. & Aukauloo, A. Solar water-splitting into H_2 and O_2: design principles of photosystem II and hydrogenases. *Coord. Chem. Rev.* **252**, 456 (2008).

[5] Sanderson, K. *Nature News* Feature "The photon trap" *Nature* **452**, 400-402 (2008).

[6] Sala, X., Romero, I., Rodríguez, M., Escriche, L. & Llobet, A. Molecular Catalysts that Oxidize Water to Dioxygen. *Angew. Chem. Int. Ed.* **48**, 2842-2852 (2009).

[7] Liegghio, R., Potvin, P. G. & Lever, A. B. P. 2,6-dipyrazinylpyridines and their ruthenium(II) complexes: A new polynucleating ligand family. *Inorg. Chem.* **40**, 5485-5486 (2001).

[8] Araki, Y., Chitta, R., Sandanayaka, A. S. D., Langewalter, K., Gadde, S., Zandler, M. E., Ito, O. & D'Souza, F. Self-assembled supramolecular ferrocene−fullerene dyads and triad: Formation and photoinduced electron transfer. *J. Phys. Chem. C* **112**, 2222-2229 (2008).

[9] Morisue, M., Kalita, D., Haruta, N. & Kobuke, Y. Fine-tuning of a ferrocene|porphyrin|ITO redox cascade for efficient sequential electron transfer commenced by an S_2 photoexcited special-pair mimic. *Chem. Commun.* 2348-2350 (2007).

[10] Sautter, A., Kaletaş, B. K., Schmid, D. G., Dobrawa, R., Zimine, M., Jung, G., Van Stokkum, I. H. M., De Cola, L., Williams, R. M. & Würthner, F. Ultrafast energy-electron transfer cascade in a multichromophoric light-harvesting molecular square. *J. Am. Chem. Soc.* **127**, 6719 (2005).

[11] Konishi, T., Ikeda, A. & Shinkai, S. Supramolecular design of photocurrent-generating devices using fullerenes aimed at modelling artificial photosynthesis. *Tetrahedron* **61**, 4881-4899 (2005).

[12] Martin, N., Sanchez, L., Illescas, B., Perez, I. C_{-60}-based electroactive organofullerenes. *Chem. Rev.* **98**, 2527-2547 (1998).

[13] Segura, J.L., Martin, N., Guldi, D.M. Materials for organic solar cells: the C_{-60}/pi-conjugated oligomer approach. *Chem. Soc. Rev.* **34**, 31-47 (2005).

[14] Laiho, A., Ras, R. H. A., Valkama, S., Ruokolainen, J., Osterbacka, R. & Ikkala, O. Control of self-assembly by charge-transfer complexation between C_{60} fullerene and electron donating units of block copolymers. *Macromolecules* **39**, 7648-7653 (2006).

[15] Hong, Z. R., Huang, Z. H. & Zeng, X. T. Investigation into effects of electron transporting materials on organic solar cells with copper phthalocyanine/C_{60} heterojunctions. *Chem. Phys. Lett.* **425**, 62-65 (2006).

[16] Shrotriya, V., Ouyang, J., Tseng, R. J., Li, G. & Yang, Y. Absorption spectra modification in poly(3-hexylthiophene): methanofullerene blend thin films. *Chem. Phys. Lett.* **411**, 138-143 (2005).

[17] Xie, R. H., Bryant, G. W., Sun G. Y., Kar, T., Chem, Z. F., Smith, V. H., Araki,, Y., Tagmatarchis, N., Shinohara, H. & Ito, O. Tuning spectral properties of fullerenes by substitutional doping. *Phys. Rev. B: Condens. Matter. Mater Phys* **69**, 201403 (2004).

[18] Popov, A. A., Kareev, I. E., Shustova, N. B., Stukalin, E. B, Lebedkin, S. F., Seppelt, K., Strauss, S. H., Boltalina, O. V. & Dunsch, L. Electrochemical, spectroscopic, and DFT study of $C_{60}(CF_3)_n$ frontier orbitals (n = 2−18): the link between double bonds in pentagons and reduction potentials. *J. Am. Chem. Soc.* **129**, 11551-11568 (2007).

[19] Williams, R. E. Carboranes and boranes - polyhedra and polyhedral fragments. *Inorg. Chem.* **10**, 210-214 (1971).

[20] Wade, K. Structural significance of number of skeletal bonding electron-pairs in carboranes, higher boranes and borane anions, and various transition-metal carbonyl cluster compounds. *Chem. Comm.* 792-793 (1971).

[21] Mingos, D. M. P. General theory for cluster and ring compounds of main group and transition-elements. *Nature (Phy. Science)* **236**, 99-102 (1972).

[22] Jemmis, E. D., Balakrishnarajan, M. M. & Pancharatna, P. D. Electronic requirements for macropolyhedral boranes. *Chem. Rev.* **102**, 93-144 (2002).

[23] Echegoyen, L. & Echegoyen, L. E. Electrochemistry of fullerenes and their derivatives. *Acc. Chem. Res.* **31,** 593-601 (1998). According to this reference, the measured potential ($E_{1/2}$) for $C_{60}^{0/-I}$ was -0.98 V vs Fc^+/Fc. For comparison purposes, we have converted it to SCE by adding 0.5V.

[24] Morris, J. H., Gysling, H. J. & Reed, D. Electrochemistry of boron compounds. *Chem. Rev.* **85**, 51-76 (1985).

[25] Zheng, M., Li, F. F., Shi, Z. J., Gao, X. & Kadish, K. M. Electrosynthesis and characterization of 1,2-Dibenzyl C_{60}: A revisit. *J. Org. Chem.* **72**, 2538-2542 (2007).

[26] Carano, M., Marcaccio, M., Paolucci, F. & Birkett, P. Voltammetric characterization of $C_{60}(PhX)_2$ (X = H, Br) and digital

simulation of their electrochemically-induced reactivity. *Photochem. Photobiol. Sci.* **5**, 1132-1136 (2006).
[27] Zhou, F., Van Berkel, G. J. & Donovan, B. T. Electron-transfer reactions of fluorofullerene $C_{60}F_{48}$. *J. Am. Chem. Soc.* **116**, 5485-5486 (1994).
[28] Páramo-Garcío, U., Ávila-Rodríguez, M., García-Jiménez, M. G., Gutiérrez-Granados, S. & Ibáñez-Cornejo, J. G. Electrochemical reduction of hexachlorobenzene in organic and aquo-organic media with Co(II)Salen as catalyst. *Electroanalysis* **18**, 904-910 (2006).
[29] Sivaev, I. B. & Bregadze, V. I. Chemistry of cobalt bis(dicarbollides). A review. *Collect. Czech. Chem. Commun.* **64**, 783-805 (1999).
[30] Matel, L., Macasek, F. & Rajec, P. B-halogen derivatives of the bis(1,2-dicarbollyl)cobalt(III) anion. *Polyhedron* **6**, 511 (1982).
[31] Hawthorne, M. F., Young, D. C., Andrews, T. D., Howe, D. V., Pilling, R. L., Pitts, A. D., Reintjes, M., Warren Jr., L. F. & Wegner, P. A. π-Dicarbollyl derivatives of the transition metals. Metallocene analogs. *J. Am. Chem. Soc.* **90**, 879-896 (1968).
[32] Corsini, M., Fabrizi, de Biani, F. & Zanello, P. Mononuclear metallacarboranes of groups 6-10 metals: Analogues of metallocenes - Electrochemical and x-ray structural aspects. *Coord. Chem. Rev.* **250**, 1351-1372 (2006).
[33] Rudakov, D.A., Shirokii, V. L., Knizhnikov, V. A., Bazhanov, A. V., Vecher, E. I., Maier, N. A., Potkin, V. I., Ryabtsev, A. N., Petrovskii, P. V., Sivaev, I. B., Bregadze, V. I. & Eremenko, I. L. Electrochemical synthesis of halogen derivatives of bis(1,2-dicarbollyl)cobalt(III). *Russ. Chem. Bull., Int. Ed.* **53**, 2554 (2004).

Starting materials for π-conjugated systems in metallacarborane chemistry

(Preliminary version)

Pau Farràs,[±] Isabel Rojo, Francesc Teixidor, Clara Viñas,*

[a] Institut de Ciència de Materials de Barcelona (CSIC), Campus de la U.A.B., E-08193 Bellaterra, Spain. Telefax: Int. Code + 34 93 5805729. E-mail: clara@icmab.es.

[1] P.F. is enrolled in the PhD program of the UAB.

Introduction

To be written later.

Results and Discussion

Palladium-catalyzed B-C cross-coupling reactions on Cs[8-I-3,3'-Co(1,2-$C_2B_9H_{10}$)(1',2'-$C_2B_9H_{11}$)] with Grignard reagents: These investigations were the continuation of the cross-coupling methodology that successfully had been used in iodinated derivatives of *o*-carborane[1] and cobaltabisdicarbollide.[2] No Grignard reagents with terminal functional groups had been tested until now on cobaltabisdicarbollide. Successful B-C coupling reactions were achieved by using Cs[8-I-3,3'-Co(1,2-$C_2B_9H_{10}$)(1',2'-$C_2B_9H_{11}$)] Cs(**2**) as the starting compound. The B-I unit was transformed into B-R by using a Grignard reagent in the presence of a palladium catalyst and copper(I) iodide as a cocatalyst. In a typical experiment, the Cs(**2**) salt was dissolved in THF and treated with the appropriate Grignard reagent at low temperatures (Scheme 1). A brown precipitate formed; the mixture was then allowed to warm to room temperature, whereupon the palladium catalyst and CuI were added in a single portion. In the case of anions **3** and **6**, the catalyst and cocatalyst were added at once with Cs(**2**) and dried before use. A period of reflux, ranging from two to ten hours, followed by work-up and functional group deprotection if necessary, yielded the desired compounds. The reaction provided good to very good yields of all the compounds (between 70 and 92%), except for **6** that couldn't be isolated in pure form. The reaction seems to be quite general, once the optimal conditions in terms of temperature and reaction time have been found.

Nevertheless, the formation of the Grignard reagent has been done in two different ways, depending on the nature of the organic molecule. For anions **4** and **5**, the formation of the Grignard reagent has been done following the method described by Gilman and Kirby,[3] which consists on the activation of the magnesium surface by iodine. However, this method didn't give any good results for the preparation of Grignard reagent leading to anions **3** and **6**. In this case, where a vinyl group is present on the organohalide compound, the formation of the Grignard reagent was done following the procedure described by Pearson et al.[4] A solution of dibromoethane in THF is added dropwise for several hours to a solution containing the organohalide compound and the Mg, which is carefully dried in vacuo with a heat gun. The reaction mixture is kept overnight at 35ºC to mantain the reflux. Then, it is necessary to filter the white precipitate that is formed during the reaction. Once the Grignard reagent is generated, it is very important to titrate its concentration that has to be between 0.2 and 0.25 M in the coupling step with Cs(**2**). With a lower concentration, the reaction doesn't take place, while a higher concentration degrades the starting material leading to *nido*-carborane. The nature of **3**-**6** has been corroborated by elemental analysis, MS, IR, and ^{1}H, ^{1}H{^{11}B}, ^{13}C{^{1}H}, ^{11}B, and ^{11}B{^{1}H}-NMR spectroscopies, and for [Me_4N] (**3**), by x-ray crystal structure determination.

NMR spectral considerations: The ^{11}B{^{1}H}-NMR data of the monosubstituted compounds prepared in this work are shown in Table 1 along with the resonances of anions **1** and **2**. The spectra can be interpreted considering the ^{11}B{^{1}H}-NMR spectra of **1** and **2**, the latter also being a derivative of **1**. The ^{11}B{^{1}H}-NMR spectrum of **1** displays five resonances in the range -6.5 to -22.7 ppm with a 2:2:8:4:2 pattern, in agreement with an averaged C_{2v} symmetry. The ^{11}B-NMR chemical shifts of anion **1** were assigned with the aid of a 2D ^{11}B{^{1}H}-^{11}B{^{1}H}-NMR COSY experiment and correspond to B(8,8'), B(10,10'), B(4,4',7,7',9,9',12,12'), B(5,5',11,11'), and B(6,6') from low to high field.[5] Incorporation of one iodine atom at position B8 lowers the symmetry to C_s, maintaining only one symmetry plane and rendering the two dicarbollide moieties nonequivalent. Therefore, the ^{11}B{^{1}H}-NMR spectrum of **2** displays ten resonances in the range -6.5 to -23.1 ppm, with a 1:1:1:2:5:2:2:2:1:1 pattern. The resonance in italics integrating as five corresponds to the B-I signal, which overlaps with four B-H signals. Substitution of iodine by alkyl and aryl groups keeps the same C_s symmetry and therefore the observed pattern is almost the same. In Table 1, the B-C resonance is also shown in italics. The rather complex ^{11}B{^{1}H} spectra of [3,3'-Co(1,2-$C_2B_9H_{11}$)$_2$]$^-$ derivatives with a B8-C bond consist of one set of signals for each carborane ligand moiety, one perturbed by the B-C substitution and the second, almost unchanged, corresponding to that of the parent unsubstituted anion **1**. Only when no peak coincidence overlap was found could the positions be assigned on the basis of cross-peaks in the ^{11}B{^{1}H}-^{11}B{^{1}H}-NMR COSY experiments. The resonance at -13.2 ppm is not split into a doublet in the ^{11}B-NMR spectrum of **3**, indicating that this resonance corresponds to the B-C vertex (Figure 1).

In agreement with the C_s symmetry, the ^{1}H and ^{13}C{^{1}H}-NMR spectra exhibit two slightly

different C-H carborane signals due to the substituted and the unsubstituted cage for **2-6** (Table 2), and one C-H carborane signal for **1**. The difference in chemical shift can also be observed in figure 2 where it can be seen that for the substituted cage, the C-H groups are being affected by the R group. Meanwhile, the unsubstituted remains unchanged because the infuence of the R group doesn't reach this cage. Both ^{1}H and $^{13}C\{^{1}H\}$-NMR spectra also display resonances attributable to the R groups at the expected positions.

X-ray crystal structure of [Me_4N] (3): Suitable single crystals of **3** were obtained by slow evaporation of the solvent from a solution in dichloromethane. The structure of **3** is presented in figure 3. Crystallographic data for [Me_4N][**3**] is given in Table 3. Crystallographic analyses confirmed the expected B(8)-substituted cobaltabisdicarbollide structure for the compound.

Conclusions

To be written later.

Experimental Section

Instrumentation. Elemental analyses were performed using a Carlo Erba EA1108 microanalyzer. IR spectra were recorded from KBr pellets on a Shimadzu FTIR-8300 spectrophotometer. The ^{1}H NMR, $^{1}H\{^{11}B\}$ NMR (300.13 MHz), ^{11}B NMR (96.29 MHz), and $^{13}C\{^{1}H\}$ NMR (75.47 MHz) spectra were recorded with a Bruker ARX 300 instrument equipped with the appropriate decoupling accessories. Chemical shift values for ^{11}B NMR spectra were referenced to external $BF_3{\cdot}OEt_2$, and those for ^{1}H, $^{1}H\{^{11}B\}$, and $^{13}C\{^{1}H\}$ NMR spectra were referenced to $Si(CH_3)_4$. Chemical shifts are reported in units of parts per million downfield from the reference, and all coupling constants are reported in Hertz. The mass spectra were recorded in the negative ion mode using a Bruker Biflex MALDI-TOF-MS (N_2 laser; λ_{exc} 337 nm (0.5 ns pulses); voltage ion source 20.00 kV (Uis1) and 17.50 kV (Uis2)).

Materials. Experiments were carried out, except when noted, under a dry, oxygen-free dinitrogen atmosphere using standard Schlenk techniques, with some subsequent manipulation in the open laboratory. THF was distilled from sodium benzophenone before use. Other solvents were reagent grade. All organic and inorganic salts were Fluka or Aldrich analytical reagent grade and were used as received. Cs(**2**) was prepared according to the literature.[2]

Synthesis of [$N(CH_3)_4$] [8-*p*-$C_6H_4C_2H_3$-3,3'-Co(1,2-$C_2B_9H_{10}$)(1',2'-$C_2B_9H_{11}$)] (3): A round bottom flask with 3 necks (250 mL) with Mg (1.27 g, 52.39 mmol) is dried under vacumm with a heat gun for 10 minuts. Then, it is cooled to room temperature and 60 mL of anhydrous THF and 4-bromostyrene (2.95 mL, 22.58 mmol) are added. A solution of dibromoethane (1.95 mL, 22.59 mmol, 40 mL anhydrous THF) is added dropwise using an addition funnel and the reaction mixture is kept at 30ºC overnight. A white precipitate is formed and it is filtered under nitrogen. Cs[**2**] (2.0 g, 3.44 mmol), [$PdCl_2(PPh_3)_2$] (200 mg, 0.29 mmol) and CuI (60 mg, 0.30 mmol) are dried under vacumm for 30'. Then, a solution of the styrenemagnesium bromide (50 mL) generated before is added and the mixture is refluxed for 4h. Ten drops of water were then added to quench the excess Grignard reagent, the grey precipitate is filtered and the solvent is removed in vacuo. 50 mL of diethyl ether are added and this is extracted with HCl (0.5M) (3x30 mL) at low temperature, then the combined organic layers were dried over anhydrous magnesium sulfate. The residue was dissolved in the minimum volume of EtOH and an aqueous solution containing an excess of [Me_4N]Cl was added, resulting in the formation of a precipitate. This was filtered off, washed with water and petroleum ether, and dried in vacuo. Yield: 92%, 2.16 g. Elemental analysis calcd (%) for $C_{16}H_{40}B_{18}CoN$: C= 38.43, H= 8.06, N= 2.80; found: C= 38.26, H= 8.04, N= 2.85. IR: ν = 3038 (C_c-H), 2950, 2922, 2854 (C_{aryl}-H), 2542 (B-H), 1624 (C=C), 1479 δ(C_{alkyl}-H), 945 (C-N), 748, 721 (B-C). ^{1}H-RMN: δ = 7.29 (d, $^{3}J(H,H)$= 8, 2H, $C_6\mathbf{H_4}$), 7.20 (d, $^{3}J(H,H)$= 8, 2H, $C_6\mathbf{H_4}$), 6.64 (d, $^{3}J(H,H_a)$= 11, d, $^{3}J(H,H_b)$= 18, 1H, C**H**), 5.69 (dd, $^{3}J(H,H_b)$= 18, d, $^{2}J(H_b,H_a)$= 1, $1H_a$, C$\mathbf{H_aH_b}$), 5.07 (dd, $^{3}J(H,H_a)$= 11, d, $^{2}J(H_a,H_b)$= 1, $1H_b$, C$\mathbf{H_aH_b}$), 4.56 (br s, 2H, C_c-**H**), 3.79 (br s, 2H, C_c-**H**), 3.41 (s, 12H, N(C$\mathbf{H_3}$)$_4$), 3.11-1.48 (m, 17H, B-**H**). $^{1}H\{^{11}B\}$-RMN: δ = 7.29 (d, $^{3}J(H,H)$= 8, 2H, $C_6\mathbf{H_4}$), 7.20 (d, $^{3}J(H,H)$= 8, 2H, $C_6\mathbf{H_4}$), 6.64 (d, $^{3}J(H,H_a)$= 11, d, $^{3}J(H,H_b)$= 18, 1H, C**H**), 5.69 (dd, $^{3}J(H,H_b)$= 18, d, $^{2}J(H_b,H_a)$= 1, $1H_a$, C$\mathbf{H_aH_b}$), 5.07 (dd, $^{3}J(H,H_a)$= 11, d, $^{2}J(H_a,H_b)$= 1, $1H_b$, C$\mathbf{H_aH_b}$), 4.56 (br s, 2H, C_c-**H**), 3.79 (br s, 2H, C_c-**H**), 3.41 (s, 12H, N(C$\mathbf{H_3}$)$_4$), 3.11 (s, 2H, B-**H**), 2.77 (s, 2H, B-**H**), 2.55 (s, 2H, B-**H**), 1.93 (s, 2H, B-**H**), 1.75 (s, 4H, B-**H**), 1.71 (s, 2H, B-**H**), 1.48 (s, 3H, B-**H**). $^{13}C\{^{1}H\}$-RMN: δ = 137.11 (s, $\mathbf{C}_6H_4$), 135.93 (s, $\mathbf{C}_6H_4$), 131.85 (s, $\mathbf{C}_6H_4$), 126.21 (s, $\mathbf{C}_6H_4$), 123.99 (s, $\mathbf{C}_6H_4$), 112.90 (s, CH**C**H_2), 110.57 (s, **C**HCH_2), 54.62 (s, N(**C**H_3)$_4$), 53.55 (s, $\mathbf{C_c}$-H), 49.62 (s, $\mathbf{C_c}$-H). ^{11}B-RMN: δ = 13.19 (s, 1B, B(8)), 6.07 (d, $^{1}J(B,H)$= 137, 1B), 2.44 (d, $^{1}J(B,H)$= 136, 2B), -2.86 (d, $^{1}J(B,H)$= 154, 2B),

-4.50 (d, ^{1}J(B,H)= 146, 4B), -5.90 (d, ^{1}J(B,H)= 142, 2B), -16.46 (d, ^{1}J(B,H)= 138, 2B), -17.70 (d, ^{1}J(B,H)= 141, 2B), -21.10 (d, ^{1}J(B,H)= 145, 1B), -22.23 (d, ^{1}J(B,H)= 122, 1B). MALDI-TOF MS: m/z (%): 426.38 (M).

Synthesis of Cs [8-*p*-C_6H_4CHO-3,3'-Co(1,2-$C_2B_9H_{10}$)(1',2'-$C_2B_9H_{11}$)] (4): Cs[**2**] (200 mg, 0.34 mmol) in THF (5 mL) and a solution of 4-benzaldehyde dimethyl acetal bromide (5 mL, 1.38 mmol), prepared from magnesium turnings (0.134 g, 5.5 mmol) and 4-bromobenzaldehyde dimethyl acetal (0.46 mL, 2.75 mmol), were reacted at 0ºC. After 30 min at room temperature, [$PdCl_2(PPh_3)_2$] (20 mg, 0.03 mmol) and CuI (6 mg, 0.03 mmol) were added. The brown solution was heated under reflux for 10h. Work-up and purification as described above gave the desired cesium salt Cs(**4**). Yield: 82%, 0.16 g. IR: ν = 3045 (C_c-H), 2924, 2851 (C_{aryl}-H), 2538 (B-H), 1693 (C=O), 1597 δ(C_{alkyl}-H), 752, 723 (B-C). ^{1}H-RMN: δ = 10.13 (s, 1H, C**H**O), 8.07 (d, ^{3}J(H,H)= 8, 2H, C_6**H$_4$**), 8.00 (d, ^{3}J(H,H)= 8, C_6**H$_4$**), 4.44 (br s, 2H, C_c-**H**), 3.87 (br s, 2H, C_c-**H**), 3.07-1.48 (m, 17H, B-**H**). ^{1}H{^{11}B}-RMN: δ = 10.13 (s, 1H, C**H**O), 8.07 (d, ^{3}J(H,H)= 8, 2H, C_6**H$_4$**), 8.00 (d, ^{3}J(H,H)= 8, C_6**H$_4$**), 4.44 (br s, 2H, C_c-**H**), 3.87 (br s, 2H, C_c-**H**), 3.07 (s, 2H, B-**H**), 2.91 (s, 1H, B-**H**), 2.81 (s, 1H, B-**H**), 2.67 (s, 2H, B-**H**), 1.97 (s, 2H, B-**H**), 1.77 (s, 4H, B-**H**), 1.74 (s, 2H, B-**H**), 1.48 (s, 3H, B-**H**). ^{13}C{^{1}H}-RMN: δ = 191.68 (s, **C**HO), 133.02 (s, **C$_6$**H$_4$), 130.06 (s, **C$_6$**H$_4$), 127.99 (s, **C$_6$**H$_4$), 127.22 (s, **C$_6$**H$_4$), 53.25 (s, **C$_c$**-H), 50.33 (s, **C$_c$**-H). ^{11}B-RMN: δ = 14.55 (s, 1B, B(8)), 9.15 (d, ^{1}J(B,H)= 157, 1B), 3.96 (d, ^{1}J(B,H)= 135, 2B), -1.53 (d, ^{1}J(B,H)= 104, 2B), -2.59 (d, ^{1}J(B,H)= 129, 2B), -4.08 (d, ^{1}J(B,H)= 140, 4B), -14.73 (d, ^{1}J(B,H)= 140, 2B), -15.99 (d, ^{1}J(B,H)= 132, 2B), -19.92 (d, ^{1}J(B,H)= 142, 1B), -20.87 (d, ^{1}J(B,H)= 158, 1B). MALDI-TOF MS: m/z (%): 427.85 (M).

Synthesis of Cs [8-*m*-C_6H_4CHO-3,3'-Co(1,2-$C_2B_9H_{10}$)(1',2'-$C_2B_9H_{11}$)] (5): Similarly, Cs[**2**] (200 mg, 0.34 mmol) in THF (5 mL) and 5 mL of the Grignard reagent prepared from magnesium turnings (0.165 g, 6.8 mmol), 2-(3-bromophenyl)-1,3-dioxolane (0.52 mL, 3.43 mmol) and 10 mL of THF, were reacted at 0ºC. After 30 min at room temperature, [$PdCl_2(PPh_3)_2$] (10 mg, 0.01 mmol) and CuI (3 mg, 0.01 mmol) were added. The brown solution was heated under reflux for 10h. Work-up and purification as described above gave Cs(**5**). Yield: 70%, 0.073 g. IR: ν = 3047 (C_c-H), 2962, 2856 (C_{aryl}-H), 2545 (B-H), 1676 (C=O), 1585 δ(C_{alkyl}-H), 752 (B-C). ^{1}H-RMN: δ = 9.97 (s, 1H, C**H**O), 7.90 (s, 1H, C_6**H$_4$**), 7.67 (d, ^{3}J(H,H)= 7.5, C_6**H$_4$**), 7.55 (d, ^{3}J(H,H)= 7.5, C_6**H$_4$**), 7.28 (t, ^{3}J(H,H)= 7.5, C_6**H$_4$**), 4.42 (br s, 2H, C_c-**H**), 3.89 (br s, 2H, C_c-**H**), 3.06-1.46 (m, 17H, B-**H**). ^{1}H{^{11}B}-RMN: δ = 9.97 (s, 1H, C**H**O), 7.90 (s, 1H, C_6**H$_4$**), 7.67 (d, ^{3}J(H,H)= 7.5, C_6**H$_4$**), 7.55 (d, ^{3}J(H,H)= 7.5, C_6**H$_4$**), 7.28 (t, ^{3}J(H,H)= 7.5, C_6**H$_4$**), 4.42 (br s, 2H, C_c-**H**), 3.89 (br s, 2H, C_c-**H**), 3.06 (s, 2H, B-**H**), 2.91 (s, 1H, B-**H**), 2.82 (s, 1H, B-**H**), 2.63 (s, 2H, B-**H**), 1.98 (s, 2H, B-**H**), 1.74 (s, 4H, B-**H**), 1.70 (s, 2H, B-**H**), 1.46 (s, 3H, B-**H**). ^{13}C{^{1}H}-RMN: δ = 193.38 (s, **C**HO), 152.70 (s(a), **C$_6$**H$_4$), 138.80 (s, **C$_6$**H$_4$), 134.84 (s, **C$_6$**H$_4$), 126.68 (s, **C$_6$**H$_4$), 125.65 (s, **C$_6$**H$_4$), 53.16 (s, **C$_c$**-H), 50.38 (s, **C$_c$**-H). ^{11}B-RMN: δ = 13.39 (s, 1B, B(8)), 7.69 (d, ^{1}J(B,H)= 138, 1B), 2.26 (d, ^{1}J(B,H)= 139, 2B), -3.34 (d, ^{1}J(B,H)= 72, 2B), -3.99 (d, ^{1}J(B,H)= 151, 4B), -5.74 (d, ^{1}J(B,H)= 151, 2B), -16.41 (d, ^{1}J(B,H)= 134, 2B), -17.65 (d, ^{1}J(B,H)= 135, 2B), -21.65 (d, ^{1}J(B,H)= 138, 1B), -22.61 (d, ^{1}J(B,H)= 131, 1B). MALDI-TOF MS: m/z (%): 427.85 (M).

Synthesis of Cs [8-$(CH_2)_3$CH=CH_2)-3,3'-Co(1,2-$C_2B_9H_{10}$)(1',2'-$C_2B_9H_{11}$)] (6): This compound was prepared using the same procedure as for **3,** but using Mg (0.201 g, 8.3 mmol), bromopentane (0.48 mL, 4.1 mmol) and 10 mL of THF to prepare the Grignard reagent. Work-up and purification as describe above give Cs(6), although it is not isolated pure. ^{11}B-RMN: δ = 7.19 (d, 1B), 1.53 (d, 1B), 1.17 (d, 1B), -4.82 (d, 4B), -5.45 (d, 5B), -16.74 (d, 4B), -22.11 (d, 2B).

X-ray Structure Determination of [Me_4N] (3): Single-crystal X-ray data for [Me_4N] (**3**) were collected at 120ºK on a *Nonius KappaCCD* diffractometer using graphite-monochromated MoKa radiation. A total of 12263 unique reflections were collected. The structures were solved by direct methods and refined against F^2 using the SHELXL-97 program. For all structures, the hydrogen atoms were treated as riding atoms using the SHELXL-97 default parameters.

CCDC-?? contain the supplementary crystallographic data for this paper. These data can be obtained free of charge via www.ccdc.cam.ac.uk/conts/retrieving.html (or from the Cambridge Crystallographic Data Centre, 12 Union Road, Cambridge CB2 1EZ, U.K.; fax: (+44) 1223-336033; or e-mail: deposit@ccdc.cam.ac.uk).

Supporting material available:

Acknowledgement

This work was supported by MEC (Grant MAT2006-05339), CSIC (I3P grant to P.F.) and the Generalitat de Catalunya 2005/SGR/00709.

Chart 1. B-substituted derivatives of cobaltabisdicarbollide **3**-**6**.

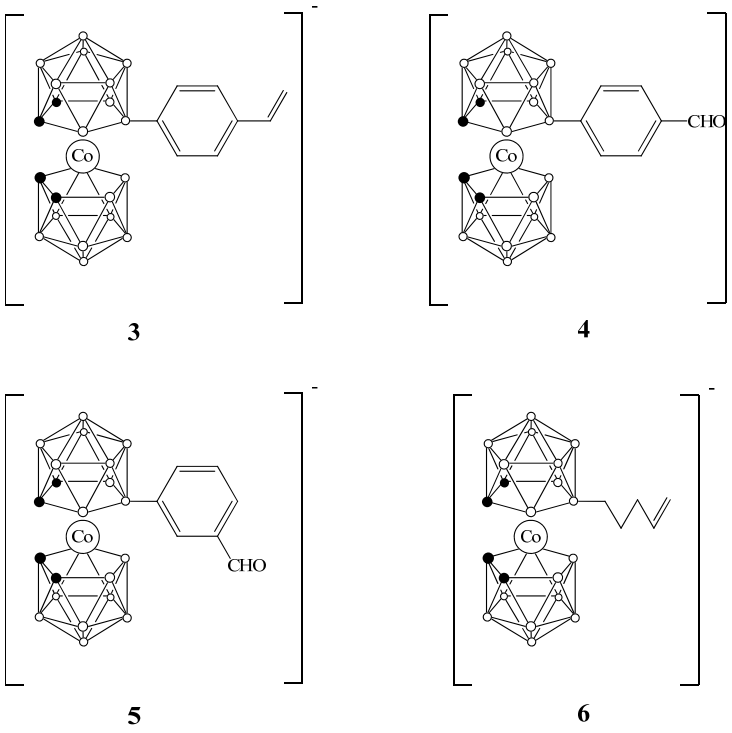

3 **4**

5 **6**

Scheme 1. Cross-coupling reaction between **2** and the corresponding organohalide compounds. For **4** and **5** the deprotection of the acetal group is done under acidic conditions.

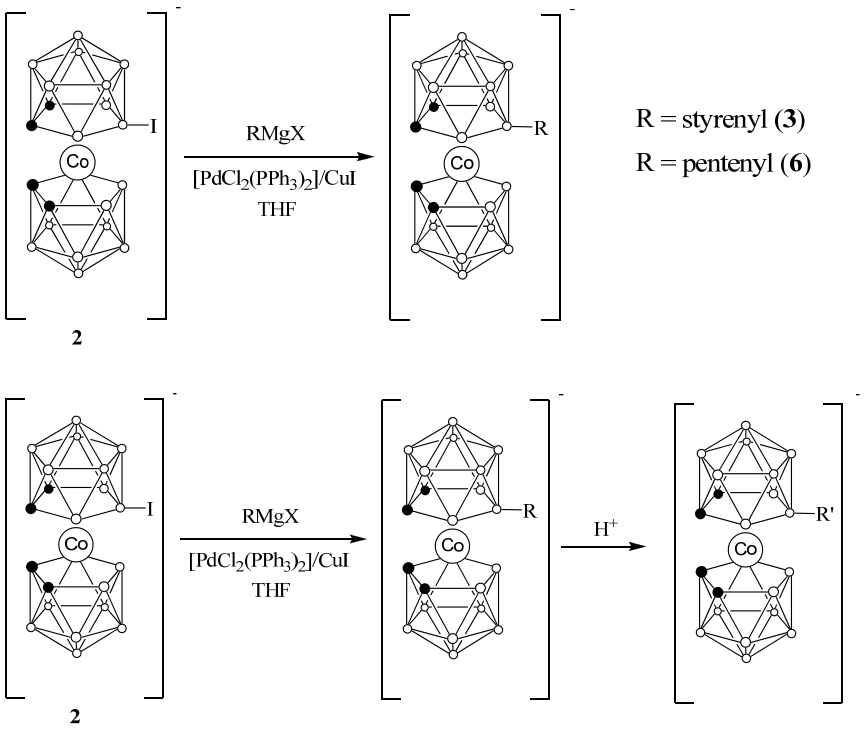

2

R = styrenyl (**3**)
R = pentenyl (**6**)

2

R' = 4-benzaldehyde (**4**)
R' = 3-benzaldehyde (**5**)

Figure 1. ^{11}B and $^{11}B\{^{1}H\}$-NMR spectra of $[Me_4N]$(**4**).

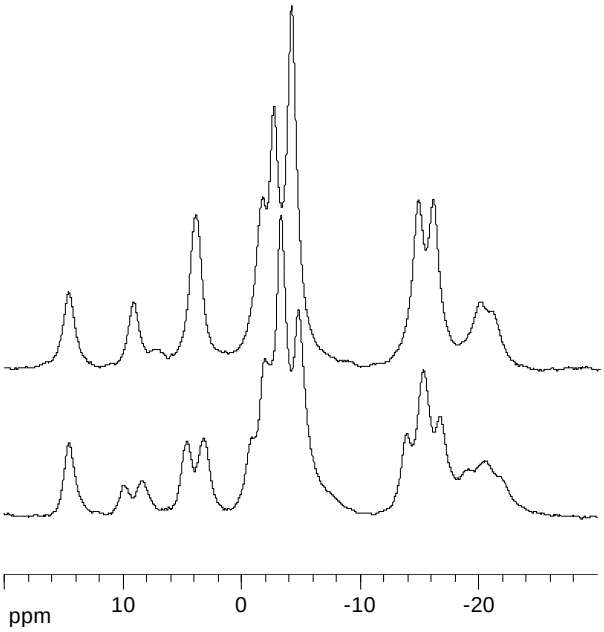

Figure 2. Schematic representation of the influence of the R group to the ^{1}H and ^{13}C-NMR chemical shift.

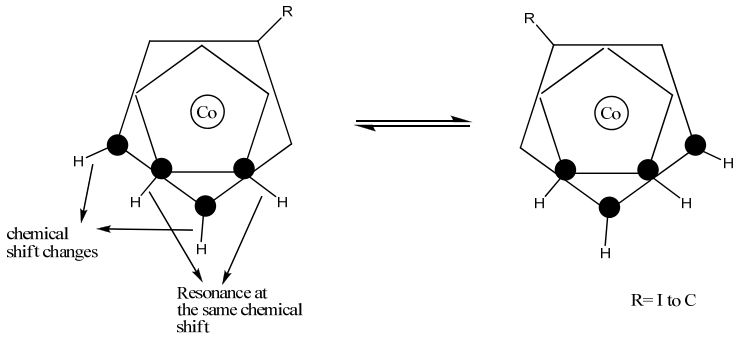

Figure 3. One of the 2 molecule pairs in the asymmetric unit of [Me_4N] (**3**). Thermal ellipsoids drawn at the 50% probability level.

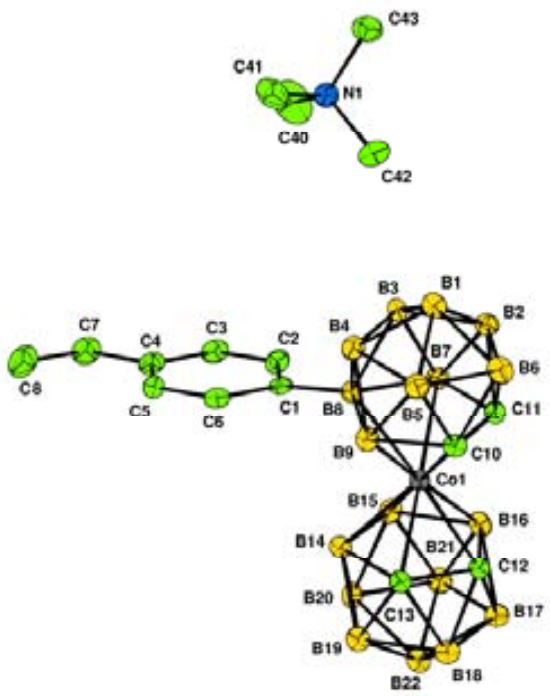

Table 1. $^{11}B\{^1H\}$ NMR spectra [ppm] of B8-monosubstituted derivatives of [3,3'-Co(1,2-$C_2B_9H_{11})_2]^-$. Numbers in italics relate to the resonances due to B-R (R≠H).

Compound	δ($^{11}B\{^1H\}$) Integration									
1	6.50 (2)		1.40 (2)		-6.00 (8)		-17.20 (4)		-22.70 (2)	
2	6.54 (1)	3.51 (1)	1.28 (1)	-1.73 (2)	*-4.78* (5)	-5.38 (2)	-16.02 (2)	-17.45 (2)	-20.92 (1)	-23.06 (1)
3	*13.19* (1)	6.07 (1)	2.44 (2)	-2.86 (2)	-4.50 (4)	-5.90 (2)	-16.46 (2)	-17.70 (2)	-21.10 (1)	-22.23 (1)
4	*14.55* (1)	9.15 (1)	3.96 (2)	-1.53 (2)	-2.59 (2)	-4.08 (4)	-14.73 (2)	-15.99 (2)	-19.92 (1)	-20.87 (1)
5	*13.39* (1)	7.69 (1)	2.26 (2)	-3.34 (2)	-3.99 (4)	-5.74 (2)	-16.41 (2)	-17.65 (2)	-21.65 (1)	-22.61 (1)
6		*7.19* (1)	1.53 (1)	1.17 (1)	-4.82 (4)	-5.45 (5)	-16.74 (4)		-22.11 (2)	

Table 2. Chemical shift values [ppm] of the hydrogen and carbon cluster atoms in the ^1H and $^{13}C\{^1H\}$-NMR spectra of B(8)-monosubstituted derivatives of [3,3'-Co(1,2-$C_2B_9H_{11})_2]^-$.

Compound	δ(^1H)-NMR	δ($^{13}C\{^1H\}$)-NMR
1	3.94	51.03
2	4.54, 4.29	59.34, 49.16
3	4.56, 3.79	53.55, 49.62
4	4.44, 3.87	53.25, 50.33
5	4.42, 3.89	53.16, 50.38

Table 3. Crystallographic data and structural refinement details for compound $[Me_4N]$(**3**).

	$[Me_4N]$ (**3**)
empirical formula	$C_{16}H_{40}B_{18}CoN$
formula weight	500.00
crystal system	Monoclinic
space group	*P*21/*n*
a [Å]	19.554(3)
b [Å]	13.533(2)
c [Å]	20.323(4)
β [º]	90.811(15)
V [Å^3]	5377.5(17)
Z	8
T [ºK]	120(2)
ρ [g cm^{-3}]	1.235
μ [cm^{-1}]	0.648
goodness-of-fit	1.041
$R1$[a] [$I>2\sigma(I)$]	0.0611
w$R2$[b] [$I>2\sigma(I)$]	0.1289

References

[1] a) C. Viñas, G. Barbera, J. Oliva, F. Texidor, A. J. Welch, G. M. Rosair, *Inorg. Chem.* **2001**, *40*, 6555. b) G. Barbera, A. Vaca, F. Texidor, R. Kivekäs, R. Sillanpää, C. Viñas, *Inorg. Chem.* **2008**, *47*, 7309.
[2] I. Rojo, F. Teixidor, C. Viñas, R. Kivekäs, R. Sillanpää, *Chem. Eur. J.* **2003**, *9*, 4311.
[3] H. Gilman, R. H. Kirby, *Recl. Trav. Chim. Pays-Bas.,* **1935**, 54, 577.
[4] D.E. Pearson, D. Cowan, J.D. Beckler, *J. Org. Chem.,* **1959**, 24, 504.
[5] Z. Janousek, J. Plesek, S. Hermanek, K. Base, L. J. Todd, W. F. Wright, *Collect. Czech. Chem. Commun.* **1981**, *46*, 281

Unprecedented B-H activation through Pd catalysed B-C bond coupling on borane systems.

(Preliminary version)

Pau Farràs,[±] David Olid,[±] Clara Viñas, Francesc Teixidor*

Institut de Ciència de Materials de Barcelona (CSIC), Campus de la U.A.B., E-08193 Bellaterra, Spain. Telefax: Int. Code + 34 93 5805729. E-mail: teixidor@icmab.es.

[±] Pau Farras and David Olid are enrolled in the PhD program of the UAB.

Transition-metal-catalyzed C-C bond coupling is a very useful reaction[1] that can be done using palladium, nickel, copper, cobalt or other metal complexes as catalysts.[1, 2, 3] In addition, the construction of carbon-carbon bonds via the palladium-catalyzed cross-coupling reactions has become a routine synthetic tool of organic synthesis by using both unactivated or organometallic reagents. Several reactions have become essential and received the names of their pioneers, namely, the Heck, Stille, Suzuki, Sonogashira, Tsuji-Trost, Negishi or Kumada reactions. More recently, a unique value inherent to Pd-catalyzed transformations has become the ability to couple them to other powerful carbon-carbon bond-formation events in one reaction vessel, also named tandem or cascade reactions.[4] This is possible due to a C-H bond activation assisted by directing groups, such as acetyl, acetamino, carboxylic acid, oxazolyl, pyridyl, and imino moieties.[5]

On the other hand, there are only few examples of substitution in boron clusters based on similar boron-carbon cross-coupling reactions. Reactions found in the literature are based mostly on Kumada C,C-couplings, and there exists only one example in which the B-C bond has been inspired by the Heck, Negishi or Suzuki-Miyaura reactions conditions. The methodology using Kumada reaction conditions was first applied to iodocarboranes by Zakharkin et al.[6] and further developed by Jones[7] and Hawthorne,[8] Beletskaya et al.[9] and our group.[10] Peymann et al. reported the reaction of the monoiodo derivative of dodecaborate $[B_{12}H_{11}I]^{2-}$ with alkyl and aryl reagents.[11] Kumada inspired boron-carbon bond formations have been also extended to monocarborane derivatives.[12] Eriksson et al.[13] were successful on the substitution of iodine in 2-I-1,12-$C_2B_{10}H_{11}$ by various aryl groups using either Heck or Suzuki-Miyaura reaction conditions.

We are interested in the application of this methodology to the monoiodo derivative of cobaltabisdicarbollide anion [8-I-3,3'-Co-(1,2-$C_2B_9H_{10}$)(1',2'-$C_2B_9H_{11}$)]$^-$ (**1**). In previous work,[10b] we demonstrated the feasibility to react this compound with Grignard reagents in a Pd-catalyzed reaction. However, no more studies on the application of Heck reaction conditions have been done on boron clusters. Herein, we report the synthesis of the first examples of a B-C=C moiety in metallacarboranes. Moreover, an unprecedented B-H activation has been found theoretically as an explanation of the unexpected formation of disubstituted species.

The reaction conditions were initially screened using the parent substrate **1** with styrene to investigate the effects of different palladium sources, equivalents of reagents, bases, solvents and temperatures as shown in Scheme 1. We found that 5% $PdCl_2(PPh_3)_2$/CuI in dry DMF with 3 equiv of dry 2,6-Lutidine as base at 140 °C (Table 1, entry 7) were optimal conditions. We noted that small amounts of water in either the base or the solvent lead to a significant decrease in the yields. Although the influence of the temperature is important, the existence of humidity and mostly the quality of the catalyst seemed the key features for the reaction. The use of triethylamine as base produced lower yields due, most probably, to its low boiling point, causing its evaporation. Instead, the use of $Ag_3(PO_4)$ gave good results as we could reduce significantly the amount of Pd. We also tried the reaction conditions described by Sjöberg et al[13b] but this lead to a large amount of side products. Finally, the use of a non-nucleophillic base as 2,6-Lutidine gave the best results for the studied case. It was possible to obtain compound [NMe_4]**2** pure enough to get crystals (see Suplementary Material for synthesis and characterization) from a dichloromethane/hexane mixture. The x-ray crystal structure is shown in figure 1.

With these optimized conditions in hand, we set out to investigate the scope of the domino process. We began by using substituted aryl rings (Table 2). It was found that metallacarboranes bearing a wide variety of functional groups could be synthesized. Halide (entries 3, 4, 5 and 6), electron donating and electron withdrawing (entries 2, 7 and 8) moieties were all well tolerated, except for entry 8 where under these conditions no reaction occurred. It was also possible to use substituted alkyl chain (entries 9, 10, 11 and 12) with the formation of the products in low to moderate yields. In the case of entry 12, the effect of an electron withdrawing group is dramatic as the yield is the lowest of this series. On the contrary, reagents in which no hydrogen atom is present in alpha position of the double bond (entries 13 and 14) or it is not on a terminal position (entry 15), it completely shuts down the reactivity.

The unexpected formation of the disubstituted molecules seen in Table 2 (entries 2 to 6) puzzled us because no explanation couldn't be found. Moreover, anions **2** and **8** (entries 1 and

7) showed a low conversion to the disubstituted species although they couldn't be separated. Characterization of the disubstituted molecules has been done by ^{1}H-NMR, ^{11}B-NMR and MALDI-TOF mass spectra. There is no doubt about the formation of these species. In ^{1}H-NMR spectra only one resonance corresponding to the four groups C_c-H is found instead of the 2:2 pattern in monosubstituted molecules. In addition, it can also be seen in ^{11}B-NMR spectra, where the pattern 1:1:2:2:4:2:2:2:1:1 found for monosubstituted species changes to a 2:2:8:4:2 pattern. This is due to the C_s symmetry of the fragment, not found on monoderivatives. Furthermore, mass spectrum MALDI-TOF technique gives relevant information on these compounds. Peaks corresponding to the molecular mass m/z are found and no fragmentation is observed for the purified anions **2**, **4**, **6** and the monoderivative **11**. Instead, MALDI-TOF-MS of unpurified fractions of anions **6** and **7**, with a bromine atom on *para* position, reveal the formation of hexasubstituted derivatives.

This unexpected experimental result encouraged us to study the mechanism of the reaction. Taking as a model the mechanism described by Surawatanawong et al. for the Heck reaction with palladium diphosphines,[14] we evaluated the relevant parts of the catalytic cycle. The results for the reaction pathway for $Pd(PR_3)_2$ catalyst with monoiodo derivative of cobaltabisdicarbollide **1** and propylene by density-functional theory are presented below beginning with an energy profile of the oxidative addition, and then the insertion of the propylene. Further steps, namely β-hydride transfer/olefin elimination of the product and the abstraction of proton by the base, are not considered.

Monoligated palladium species have been proposed to be important intermediates in the catalytic cycle.[14] Therefore, we considered to use PdL instead of PdL_2 as the catalyst for the oxidative addition step and to simplify the calculations we used PH_3 as the ligand. The most stable reaction pathway is shown in figure 2. Intermediate min_2 is energetically favourable by 40 kcal/mol. Interestingly, in the first complex min_1 an interaction between palladium and the two most reactive B-H vertices, B(9) and B(12), is found, with a B-H···Pd distance of 2.06 and 2.09Å. This kind of interaction is recursive in all the mechanism. The transition state ts_1 has the typical B(8)-Pd-I arrangement with angle of 59º as expected for an early transition state. Bond distances are 2.61 and 2.46Å for the Pd-B and Pd-I respectively. Following transition state the system rearranges to min_2 to the T-shaped structure with a 90.4º angle between B(8)-Pd-I and the Pd-B(8) bond is shorter than for ts_1, being 2.05Å. Again, close distance is found between palladium and the most reactive B-H vertex of the unsubstituted cage Pd-B(8') at 2.02Å. This B-H···Pd interaction can be explained by the position of the halogen atom in the structure. Our group reported some years ago that B-H vertices dissipate better the electron density out of the cluster than C_c-H vertices,[15] and this causes that the halogen atom prefer being *trans* to B(8')-H···Pd instead of B(8)-Pd.

For the migratory insertion of propylene we examined two possible pathways for the starting point. Propylene can insert to the palladium complex coming from the substituted (min'_3) or unsubstituted (min_3) cage plane. As expected, the energy of min_3 structure is lower and propylene binds to the vacant site of min_2. Then, the connection found in min_2 between B(8')-H···Pd is broken and causes a migration of the iodine due to a higher *trans* influence of the B(8)-Pd bond. Transition state ts_2 has the typical Pd-‖ arrangement with a Pd-C distance of 2.10 and 2.20Å and the C=C distance on propylene is about 0.04Å longer in respect to min_3. Of notice is the relatively short distance between B(8')-H···H-C causing an intramolecular reaction catalyzed by the palladium that lead to the formation of min_4. It is totally unexpected that the generated B-C bond is formed in the previous unsubstituted B(8')-H cage instead of the B(8)-I, as one could expect for a typical Heck reaction mechanism. The hydrogen atom bonded to B(8') or one of the atoms from the propylene carbon atom has migrated to the B(8) vertex making an agostic type B-H···Pd bond with a 109º angle, and a H···Pd distance of 1.78Å. The iodine has moved to a trans position in respect to the B-C··Pd structure telling us that the electronic connection between B(8)-H···Pd is lower than that for the B(8')-C···Pd. It is at this point that we suppose that a second propylene molecule can interact with the palladium complex forming the disubstituted species observed in our experiments. For the next steps, no calculation has been done as we have supposed that the same mechanism occurs as for the described Heck's catalytic cycle.

In conclusion, we have successfully developed a new efficient palladium-catalyzed synthesis of B-funcionalized cobaltabisdicarbollide derivatives. By using the optimal conditions found in this work we have been able to obtain several B-C bonds with different functional groups, leading to compounds with π-

conjugated systems. The generation of unexpected disubstituted species prompted us to calculate a theoretical reaction mechanism to explain this situation. This transformation involves an unprecedented B-H activation that strongly supports the experimental evidence.

Acknowledgement
This work was supported by MEC (Grant MAT2006-05339 and FPU grant to D.O.), CSIC (I3P grant to P.F.) and the Generalitat de Catalunya 2005/SGR/00709. Access to the computational facilities of Centre de Supercomputació de Catalunya and the CSIC computing center is also gratefully acknowledged.

Scheme 1. Cross-coupling between styrene and monoiodo compound **1**.

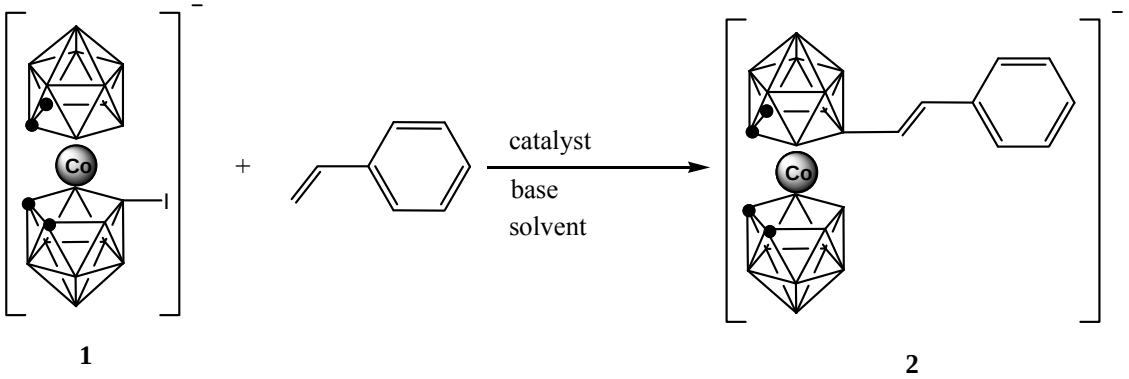

1 **2**

Figure 1. Molecular structure of $[NMe_4][8\text{-}C_8H_7\text{-}3,3'\text{-}(1,2\text{-}C_2B_9H_{10})(1',2'\text{-}C_2B_9H_{11})]$ (**2**). The displacement ellipsoids are drawn on the 30% probability level.

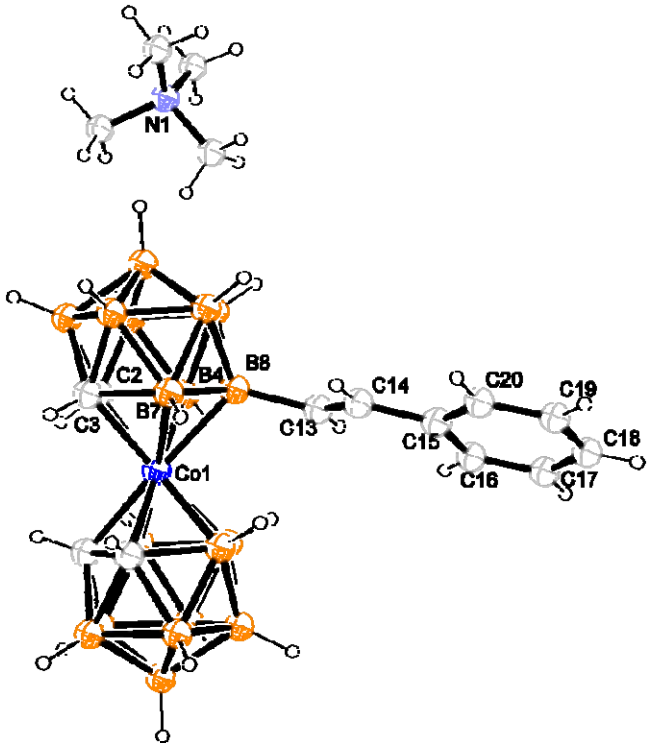

Figure 2. Energy profile for the oxidative addition to palladium phosphine complex. The relative energies are given in kcal/mol.

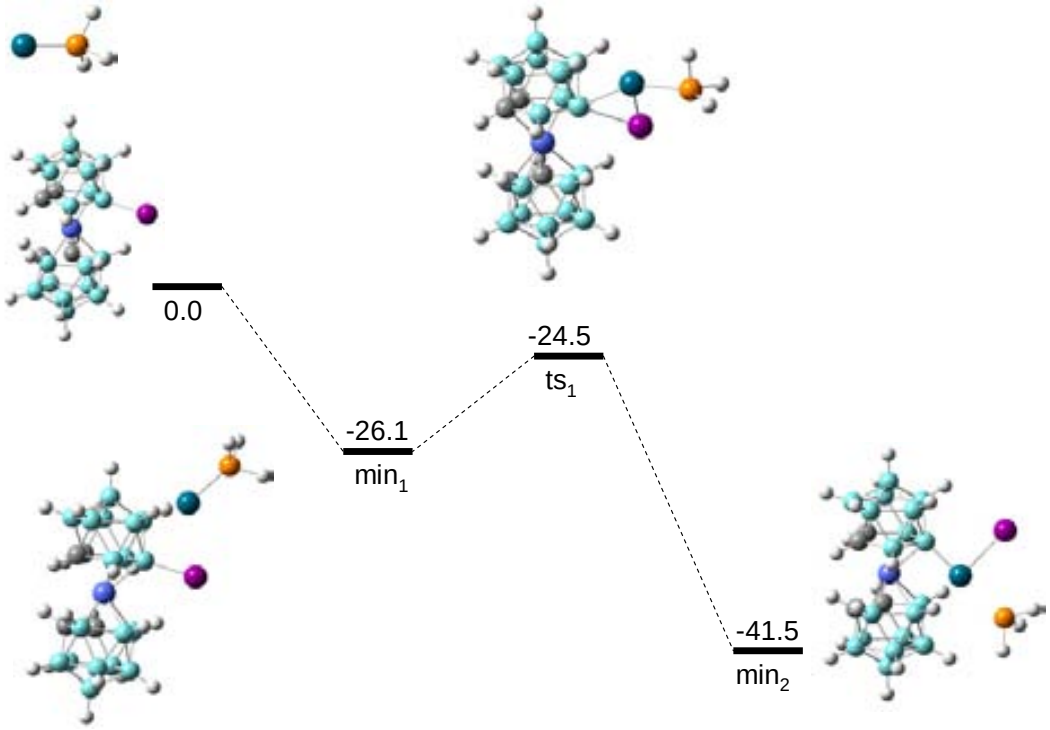

Figure 3. Energy profile for the migratory insertion of propylene. The relative energies are given in kcal/mol.

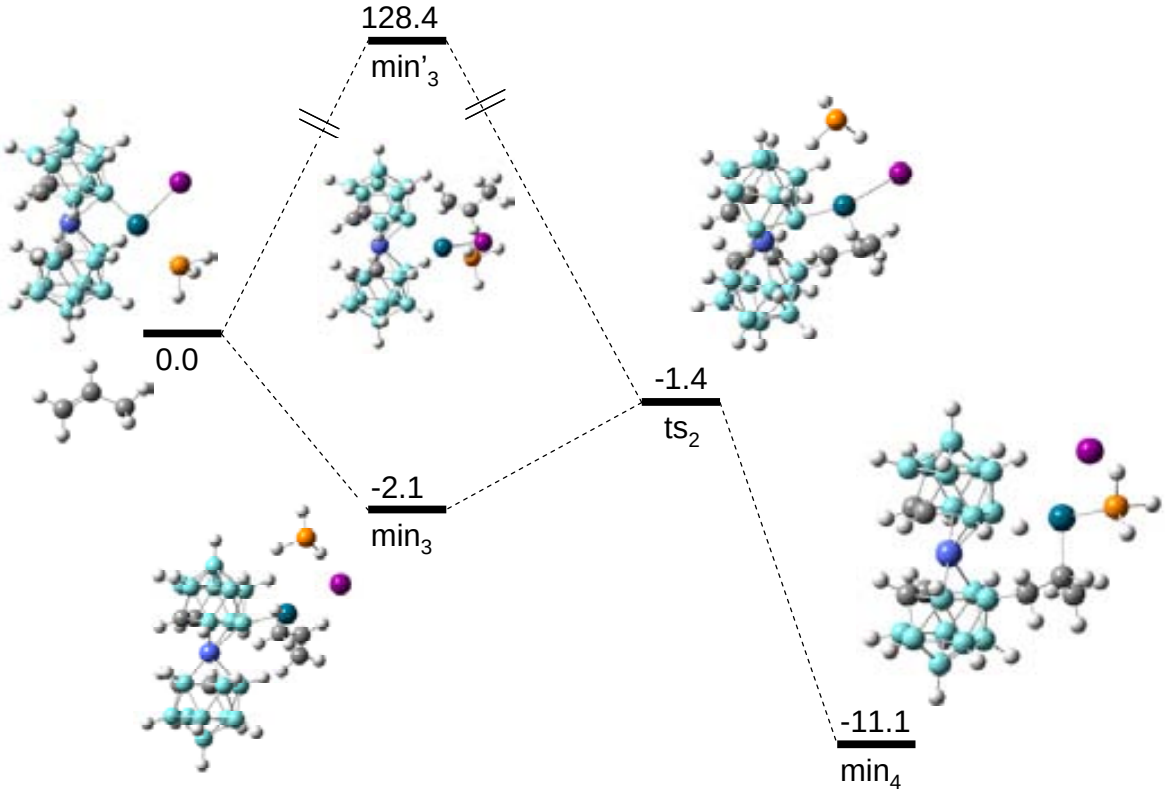

Table 1. Optimization studies of cross-coupling reaction.[16]

entry	equiv of styrene	catalyst	base (equiv)	solvent	reaction time (h)	yield (%)	T (ºC)
1[a]	2.5	8%$PdCl_2(PPh_3)_2$ 8%CuI	dry NEt_3 (2.5)	dry DMF	24	80	120
2	2.5	8%$PdCl_2(PPh_3)_2$ 8%CuI	NEt_3 (2.5)	THF	48	0	90
3	2.5	8%$PdCl_2(PPh_3)_2$ 8%CuI	$Ag_3(PO_4)$ (2.5)	DMF	24	60	120
4	1.5	8%$PdCl_2(PPh_3)_2$ 8%CuI	NEt_3 (2.5)	DMF	16	45	120
5[b]	1.2	1% Pd Hermman's	$Ag_3(PO_4)$ (1.5)	DMF	6	45	120
6	5	5%$PdCl_2(PPh_3)_2$ 5%CuI	2,6-Lutidine (3)	dry DMF	16	45	140
7	5	5%$PdCl_2(PPh_3)_2$ 5%CuI	dry 2,6-Lutidine (3)	dry DMF	24	90	140
8	2.5	5%$Pd(PPh_3)_4$	2,6-Lutidine (3)	dry DMF	16	45	130
9	5	5%$PdCl_2(PPh_3)_2$ 5%CuI	2,6-Lutidine (3)	dry DMF	24	55	130

Table 2. Pd-catalyzed cross-coupling reaction of **1** with vinyl groups.[16] Anions are numbered next to the graphical representation of the compound in column *product*.

entry	substrate	product	yield (%)	entry	substrate	product	yield (%)
1	R = Ph	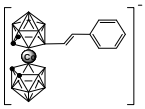	90	9	R = C_4H_9	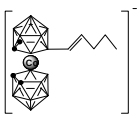	48
2	R = 4-Me-Ph		77	10	R = $C_{10}H_{17}$	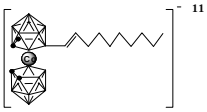	40
3	R = 4-F-Ph	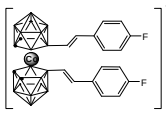	84	11	R = CN	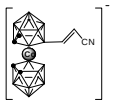	63
4	R = 4-Cl-Ph	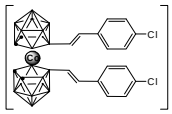	55	12	R = CH_2OH	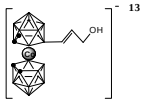	10
5	R = 4-Br-Ph	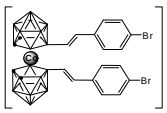	25	13		-	0
6	R = 3-Br-Ph	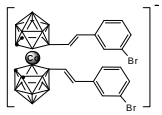	15	14	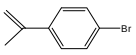	-	0
7	R = 4-OH-Ph	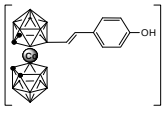	57	15		-	0
8	R = 4-NH_2-Ph	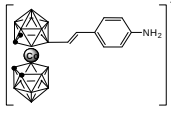	0				

References

[1] (a) For recent reviews on metal-catalyzed C-C bond coupling reactions, see: *Metal-Catalyzed Cross-Coupling Reactions, Vol. 1–2, 2nd ed.* (Eds.: A. de Meijere, F. Diederich), Wiley-VCH, Weinheim, **2006**. (b) For recent reviews on metal-catalyzed cross-coupling reactions with alkyl halides, see: A. C. Frisch, M. Beller, *Angew. Chem.* **2005**, *117*, 680; *Angew. Chem. Int. Ed.* **2005**, *44*, 674; and J. Terao, N. Kambe, *Bull. Chem. Soc. Jpn.* **2006**, *79*, 663. (c) For a recent review on metal-catalyzed C-C bond coupling reactions with Grignard reagents, see: H. Shinokubo, K. Oshima, *Eur. J. Org. Chem.* **2004**, 2081. d) H. Prokopcova, C. O. Kappe, *Angew. Chem. Int. Ed.* **2009**, *48*, 2276.

[2] B. H. Lipshutz, S. Sengupta, *Org. React.* **1992**, *41*, 135.

[3] (a) M. R. Netherton, G. C. Fu, *Adv. Synth. Catal.* **2004**, *346*, 1525. (b) M. Jeganmohan, C. H. Cheng, *Chem. Eur. J.* **2008**, *14*, 10876.

[4] (a) Metal Catalyzed Cascade Reactions. *Top. Organomet. Chem., Vol. 19, 1-91, 149-205* (Eds.: T. J. J. Müller), **2006**. (b) K. C. Nicolaou, P. G. Bulger, D. Sarlah, *Angew. Chem., Int. Ed.* **2005**, *44*, 4442. (c) G. Poli, G. Giambastiani, A. Heumann, *Tetrahedron* **2000**, *56*, 5959. (d) A. de Meijere, S. Bräse, *J. Organomet. Chem.* **1999**, *576*, 88.

[5] (a) A. Lazareva, O. Daugulis, *Org. Lett.* **2006**, *8*, 5211. (b) V. G. Zaitsev, O. Daugulis, *J. Am. Chem. Soc.* **2005**, *127*, 4156. (c) D. Kalyani, N. R. Deprez, L. V. Desai, M. S. Sanford, *J. Am. Chem. Soc.* **2005**, *127*, 7330. (d) A. R. Dick, K. L. Hull, M. S. Sanford, *J. Am. Chem. Soc.* **2004**, *126*, 2300. (e) R. Giri, X. Chen, J.-Q. Yu, *Angew. Chem.* **2005**, *117*, 2150; *Angew. Chem. Int. Ed.* **2005**, *44*, 2112. (f) S. Yanagisawa, T. Sudo, R. Noyori, K. Itami, *J. Am. Chem. Soc.* **2006**, *128*, 11748.

[6] L. I. Zakharkin, A. I. Kovredov, V. A. Ol'shevskaya, Zh. S. Shaugumbekova, *J. Organomet. Chem.* **1982**, *226*, 217.

[7] J. Li, C. F. Logan, M. Jr. Jones, *Inorg. Chem.* **1991**, *30*, 4866.

[8] (a) Z. Zheng, W. Jiang, A. Zinn, C. B. Knobler, M. F. Hawthorne, *Inorg. Chem.* **1995**, *34*, 2095. (b) W. Jiang, C. B. Knobler, C. E. Curtis, M. D. Mortimer, M. F. Hawthorne, *Inorg. Chem.* **1995**, *34*, 3491. (c) W. Jiang, D. E. Harwell, M. D. Mortimer, C. B. Knobler, M. F. Hawthorne, *Inorg. Chem.* **1996**, *35*, 4355. (d) G. Harakas, T. Vu, C. B. Knobler, M. F. Hawthorne, *J. Am. Chem. Soc.* **1998**, *120*, 6405.

[9] I. P. Beletskaya, V. I. Bregadze, V. A. Ivushkin, P. V. Petrovskii, I. B. Sivaev, G. G. Zhigareva, *J. Organomet. Chem.* **2004**, *689*, 2920.

[10] (a) C. Viñas, G. Barbera, J. Oliva, F. Texidor, A. J. Welch, G. M. Rosair, *Inorg. Chem.* **2001**, *40*, 6555. (b) I. Rojo, F. Teixidor, C. Viñas, R. Kivekäs, R. Sillanpää, *Chem. Eur. J.* **2003**, *9*, 4311. (c) G. Barbera, A. Vaca, F. Texidor, R. Kivekäs, R. Sillanpää, C. Viñas, *Inorg. Chem.* **2008**, *47*, 7309.

[11] T. Peynman, C. B. Knobler, M. F. Hawthorne, *Inorg. Chem.* **1998**, *37*, 1544.

[12] (a) J. H. Morris, K. W. Henderson, V. A. Ol'shevskaya, *J. Chem. Soc., Dalton Trans.* **1998**, 1951. (b) B. Grüner, Z. Janoušek, B. T. King, J. N. Woodford, C. H. Wang, V. Všetečka, J. Michl, *J. Am. Chem. Soc.* **1999**, *121*, 3122. (c) A. Franken, C. A. Kilner, M. Thornton-Pett, J. D. Kennedy, *J. Organomet. Chem.* **2002**, *657*, 176. (d) M. Finze, *Inorg. Chem.* **2008**, *47*, 11857.

[13] (a) L. Eriksson, I. P. Beletskaya, V. I. Bregadze, I. B. Sivaev, S. Sjöberg, *J. Organomet. Chem.* **2002**, *657*, 267. (b) L. Eriksson, K. J. Winberg, R. Tascon-Claro, S. Sjöberg, *J. Org. Chem.* **2003**, *68*, 3569.

[14] P. Surawatanawong, Y. Fan, M. B. Hall, *J. Organomet. Chem.* **2008**, *693*, 1552.

[15] F. Teixidor, J. Casabo, A. M. Romerosa, C. Viñas, J. Rius, C. Miravitlles, *J. Am. Chem. Soc.* **1991**, *113*, 9895.

[16] Yield determined by NMR spectroscopy.

Alternative cobaltabisdicarbollide reagents

(Preliminary version)

Pau Farràs,[a,±] Patricia González,[a,±] Raikko Kivekäs,[b] Reijo Sillanpää,[c] Francesc Teixidor,[a] Clara Viñas,[a,*]

[a] Institut de Ciència de Materials de Barcelona (CSIC), Campus de la U.A.B., E-08193 Bellaterra, Spain. Telefax: Int. Code + 34 93 5805729. E-mail: clara@icmab.es.

[b] Department of Chemistry, P.O. Box 55, University of Helsinki, FIN-00014, Finland.

[c] Department of Chemistry, University of Jyväskylä, FIN-40351, Finland.

[±] Pau Farràs and Patricia González are enrolled in the PhD program of the UAB.

Introduction

To be written later.

Results and Discussion

The dioxanato cobaltabisdicarbollide derivative has become one of the most favourite metallacarborane starting materials. Attack by a nucleophile provides a linker between the metallacarborane and a molecule or fragment of interest. We were interested in exploring the possibility of using new types of nucleophiles containing halogen or sulphur so that halogen or thiol terminated $[3,3'\text{-}Co(1,2\text{-}C_2B_9H_{10})_2]^-$ derivatives can be synthesized. This would allow further reaction such as cross-coupling reactions or surface functionalization. Although a large range of nucleophiles has already been investigated in boron clusters, the use of halogenated acids or a simple hydrogensulfide salt was not investigated for cobaltabisdicarbollide in the ring-opening reaction of cyclic oxonium $[3,3'\text{-}Co(8\text{-}C_4H_8O_2\text{-}1,2\text{-}C_2B_9H_{10})(1',2'\text{-}C_2B_9H_{11})]$, **2**. This would lead to the synthesis of derivatives incorporating the $(OCH_2CH_2)_2R$ chain. Albeit there has been a lot of research functionalizing the $[3,3'\text{-}Co(1,2\text{-}C_2B_9H_{10})_2]^-$ using $[3,3'\text{-}Co(8\text{-}C_4H_8O_2\text{-}1,2\text{-}C_2B_9H_{10})(1',2'\text{-}C_2B_9H_{11})]$, no derivatives incorporating halogen or thiol terminated chains had been reported. With no doubt these halogenated or thiol terminated compounds are of great interest either by the reaction in which they can participate or material's science for the modification of surfaces. Chart 1 shows the anionic species synthesized from the zwitterion **2**.

The reactions leading to these compounds are very simple and do not require controlled conditions of humidity. The use of aqueous hydracids directly for the comercial bottle allows us to use commercial grade THF instead of anhydrous THF or DME as usually used for ring-opening reactions. The addition shall be done dropwise and at 0ºC, even if very low quantity is added, to prevent side-product formation. After stirring overnight, compounds **3**-**6** are isolated by evaporation of the solvent and are obtained after cationic metathesis as Na^+, Cs^+ or NMe_4^+ salts. The same procedure has been applied to obtain **10** but the reaction has to be heated under reflux for 6h to get the desired molecule.

The formation of compounds **7**-**9** has been achieved in a different way (figure 1). As said before, one of the objectives of synthesizing molecules with terminal halogen atom in a polyether chain is their use as starting materials for further reactions. One of the foreseen reactions that can be done with $-CH_2X$ terminated reagents is cross-coupling but this bond has to be activated. Kumada cross-coupling reaction conditions use Grignard reagents as activated species. As we wanted to obtain the Grignard reagent of this compound, either starting from **5** or **6**, which are the most reactive halogen atoms (Br or I). The general procedure to obtain a Grignard reagent of an organic halide was followed. However, the reaction proceeded in an alternative way and compounds **7** and **8** were obtained. This was possible due to the presence of iodine in the media, used to activate the magnesium surface. The tendency of cobaltabisdicarbollide to generate B-I instead of B-H is demonstrated in this case. Moreover, **7** and **8** have also been prepared using the same reaction conditions as for the monoiodo derivative of cobaltabisdicarbollide described in the literature.[1] Finally, after having found that iodine was not the best choice to activate the magnesium surface to generate the Grignard reagent, dibromoethane which is also usually used on Grignard reagent formation was employed. Again, the sought Grignard compound could not be obtained, but instead the partial degradation of the polyether chain as seen in **9**. In figure 1 the reactions leading to **7**-**9** are indicated.

The nature of anions **3**-**10** with cations like $[NMe_4]^+$, Cs^+ and Na^+ has been corroborated by elemental analysis, MALDI-TOF-MS, IR, ^{1}H-, ^{1}H{^{11}B}-, ^{13}C{^{1}H}-, ^{11}B- and ^{11}B{^{1}H}-NMR spectroscopies. For $[NMe_4]$[**5**] and $[NMe_4]$[**6**] the solid state X-ray crystal structures were also determined. (see figures 2 and 3)

This work is being complemented by the PhD student Patricia González, who is synthesizing derivatives with larger polyether chains.

Conclusions

To be written later.

Experimental Section

Instrumentation. Elemental analyses were performed using a Carlo Erba EA1108 microanalyzer. IR spectra were recorded from KBr pellets on a Shimadzu FTIR-8300 spectrophotometer. The ^{1}H NMR, ^{1}H{^{11}B} NMR (300.13 MHz), ^{11}B NMR (96.29 MHz), ^{11}B{^{1}H} NMR (96.29 MHz) and ^{13}C{^{1}H} NMR (75.47 MHz) spectra were recorded with a Bruker AdvancedII instrument equipped with

the appropriate decoupling accessories. Chemical shift values for ^{11}B, $^{11}B\{^1H\}$ NMR spectra were referenced to external $BF_3{\cdot}OEt_2$, and those for ^1H, $^1H\{^{11}B\}$, and $^{13}C\{^1H\}$ NMR spectra were referenced to $Si(CH_3)_4$. Chemical shifts are reported in units of parts per million downfield from the reference, and all coupling constants are reported in Hertz. The mass spectra were recorded in the negative ion mode using a Bruker Biflex MALDI-TOF-MS (N_2 laser; λ_{exc} 337 nm (0.5 ns pulses); voltage ion source 20.00 kV (Uis1) and 17.50 kV (Uis2)).

Materials. Experiments were carried out, except when noted, under a dry, oxygen-free dinitrogen atmosphere using standard Schlenk techniques, with some subsequent manipulation in the open laboratory. 1,2-Dimethoxyethane was distilled from sodium benzophenone before use. Other solvents were reagent grade. All organic and inorganic salts were Fluka or Aldrich analytical reagent grade and were used as received. **2** was prepared according to the literature.[2]

Synthesis of [Na][3,3'-Co-8-{$(OCH_2CH_2)_2F$}-(1,2-$C_2B_9H_{10}$)(1',2'-$C_2B_9H_{11}$)] (3). Hydrofluoric acid (7.6 μL, 0.488 mmol) (48% in water) was added dropwise to a stirred solution of **2** (200 mg, 0.488 mmol) in 10 mL of THF at 0 ºC. The resulting solution was stirred overnight. The solvent was removed and acidic water (10 mL) (1 M HCl) was added to the orange residue. This was extracted with diethyl ether (3x10 mL).The organic phase was then extracted by $NaHCO_{3(aq)}$ (3x10mL) and $NaCl_{(aq)}$ (3x10mL). The solvent was removed and the resulting orange precipitate was washed with water and petroleum ether, and dried in vacuo. Yield: 0.162 g (73%). Anal. Calcd for $C_8H_{29}B_{18}CoFNaO_2$: C: 21.04, H: 6.41. Found: C: 21.89, H: 6.19. ^1H NMR: δ= 4.16 (br s, 2H, C_c-H), 4.13 (br s, 2H, C_c-H), 3.67 (m, 2H, OCH_2CH_2), 3.55 (t, $^3J(H,H)$= 5Hz, 2H, OCH_2CH_2), 3.27 (br s, 4H, OCH_2CH_2), 2.88-1.43 (m, 17H, B-H). $^1H\{^{11}B\}$ RMN: δ= 4.16 (br s, 2H, C_c-H), 4.13 (br s, 2H, C_c-H), 3.67 (m, 2H, OCH_2CH_2), 3.55 (t, $^3J(H,H)$= 5Hz, 2H, OCH_2CH_2), 3.27 (br s, 4H, OCH_2CH_2), 2.88 (s, 4H, B-H), 2.68 (s, 4H, B-H), 2.00 (s, 2H, B-H), 1.80 (s, 2H, B-H), 1.66 (s, 1H, B-H), 1.61 (s, 2H, B-H), 1.52 (s, 1H, B-H), 1.43 (s, 1H, B-H). $^{13}C\{^1H\}$ RMN: δ= 71.96 (s, OCH_2), 71.61 (s, OCH_2), 68.33 (s, OCH_2), 60.76 (s, CH_2F), 53.32 (s, C_c-H), 46.57 (s, C_c-H). ^{11}B RMN: δ= 24.54 (s, 1B, B(8)), 5.90 (d, $^1J(B,H)$= 134 Hz, 1B), 1.33 (d, $^1J(B,H)$= 140 Hz, 1B), -1.55 (d, $^1J(B,H)$= 170 Hz, 1B), -3.70 (d, $^1J(B,H)$= 160 Hz, 2B), -6.33 (d, $^1J(B,H)$= 132 Hz, 4B), -7.44 (d, $^1J(B,H)$= 133 Hz, 2B), -16.39 (d, $^1J(B,H)$= 154 Hz, 2B), -19.53 (d, $^1J(B,H)$= 155 Hz, 2B), -21.18 (d, $^1J(B,H)$= 158 Hz, 1B), -27.68 (d, $^1J(B,H)$= 156 Hz, 1B). MALDI-TOF-MS: (m/z)= 428.28 (M).

Synthesis of [Cs][3,3'-Co-8-{$(OCH_2CH_2)_2Cl$}-(1,2-$C_2B_9H_{10}$)(1',2'-$C_2B_9H_{11}$)] (4). This compound was prepared using the same procedure as for **3,** but using hydrochloric acid (0.101 mL, 1.22 mmol) instead of hydrofluoric acid. Yield: 0.57 g (88%). Anal. Calcd for $C_8H_{29}B_{18}CoCsO_2$: C: 16.49, H: 5.02. Found: C: 16.43, H: 5.08. ^1H NMR: δ= 4.24 (br s, 4H, C_c-H), 3.72 (m, 2H, OCH_2CH_2), 3.68 (m, 2H, OCH_2CH_2), 3.60 (m, 4H, OCH_2CH_2), 2.90-1.46 (m, 17H, B-H). $^1H\{^{11}B\}$ RMN: δ= 4.24 (br s, 4H, C_c-H), 3.72 (m, 2H, OCH_2CH_2), 3.68 (m, 2H, OCH_2CH_2), 3.60 (m, 4H, OCH_2CH_2), 2.90 (s, 3H, B-H), 2.74 (s, 2H, B-H), 2.68 (s, 1H, B-H), 2.47 (s, 1H, B-H), 1.98 (s, 2H, B-H), 1.78 (s, 2H, B-H), 1.68 (s, 1H, B-H), 1.64 (s, 2H, B-H), 1.55 (s, 2H, B-H), 1.46 (s, 1H, B-H). $^{13}C\{^1H\}$ RMN: δ= 71.87 (s, OCH_2), 70.99 (s, OCH_2), 68.38 (s, OCH_2), 54.00 (s, C_c-H), 46.47 (s, C_c-H), 43.08 (s, CH_2Cl). ^{11}B RMN: δ= 25.37 (s, 1B, B(8)), 6.58 (d, $^1J(B,H)$= 137 Hz, 1B), 2.71 (d, $^1J(B,H)$= 140 Hz, 1B), -0.21 (d, $^1J(B,H)$= 157 Hz, 1B), -2.00 (d, $^1J(B,H)$= 162 Hz, 2B), -5.00 (d, $^1J(B,H)$= 128 Hz, 2B), -5.87 (d, $^1J(B,H)$= 115 Hz, 4B), -14.98 (d, $^1J(B,H)$= 154 Hz, 2B), -18.09 (d, $^1J(B,H)$= 154 Hz, 2B), -19.70 (d, $^1J(B,H)$= 158 Hz, 1B), -26.24 (d, $^1J(B,H)$= 158 Hz, 1B). MALDI-TOF-MS: (m/z)= 446.18 (M).

Synthesis of [NMe_4][3,3'-Co-8-{$(OCH_2CH_2)_2Br$}-(1,2-$C_2B_9H_{10}$)(1',2'-$C_2B_9H_{11}$)] (5). This compound was prepared using the same procedure as for **3,** but using hydrobromic acid (0.17 mL, 1.22 mmol) instead of hydrofluoric acid. Yield: 0.412 (60%). Anal. Calcd for $C_{12}H_{41}B_{18}CoNO_2$: C: 25.51, H: 7.32, N: 2.48. Found: C: 25.83, H: 7.85, N: 2.52. ^1H NMR: δ= 4.25 (br s, 4H, C_c-H), 3.79 (t, $^3J(H,H)$= 5Hz, 2H, OCH_2CH_2), 3.56 (m, 4H, OCH_2CH_2), 3.53 (m, 2H, OCH_2CH_2), 3.44 (s, 12H, NMe_4), 2.89-1.45 (m, 17H, B-H). $^1H\{^{11}B\}$ RMN: δ= 4.25 (br s, 4H, C_c-H), 3.79 (t, $^3J(H,H)$= 5Hz, 2H, OCH_2CH_2), 3.56 (m, 4H, OCH_2CH_2), 3.53 (m, 2H, OCH_2CH_2), 3.44 (s, 12H, NMe_4), 2.89 (s, 3H, B-H), 2.75 (s, 2H, B-H), 2.68 (s, 1H, B-H), 2.43 (s, 1H, B-H), 1.97 (s, 2H, B-H), 1.77 (s, 2H, B-H), 1.70 (s, 1H, B-H), 1.65 (s, 2H, B-H), 1.55 (s, 2H, B-H), 1.45 (s, 1H, B-H). $^{13}C\{^1H\}$ RMN: δ= 71.62 (s, OCH_2), 70.87 (s, OCH_2), 68.48 (s, OCH_2), 55.28 (s, $N(CH_3)_4$), 54.33 (s, C_c-H), 46.42 (s, C_c-H), 30.98 (s, CH_2Br). ^{11}B RMN: δ= 23.72 (s, 1B, B(8)), 4.78 (d, $^1J(B,H)$= 136 Hz, 1B), 1.26 (d, $^1J(B,H)$= 141 Hz, 1B), -1.62 (d, $^1J(B,H)$=

155 Hz, 1B), -3.38 (d, $^{1}J(B,H)$= 160 Hz, 2B), -6.56 (d, $^{1}J(B,H)$= 96 Hz, 2B), -7.45 (d, $^{1}J(B,H)$= 126 Hz, 4B), -16.44 (d, $^{1}J(B,H)$= 153 Hz, 2B), -19.58 (d, $^{1}J(B,H)$= 192 Hz, 2B), -21.12 (d, $^{1}J(B,H)$= 155 Hz, 1B), -27.62 (d, $^{1}J(B,H)$= 162 Hz, 1B). MALDI-TOF-MS: (m/z)= 490.78 (M).

Synthesis of [NMe_4][3,3'-Co-8-{$(OCH_2CH_2)_2I$}-(1,2-$C_2B_9H_{10}$)(1',2'-$C_2B_9H_{11}$)] (6). This compound was prepared using the same procedure as for **3,** but using hydroiodic acid (0.07 mL, 0.49 mmol) instead of hydrofluoric acid. Yield: 0.24 g (80%). Anal. Calcd for $C_{12}H_{41}B_{18}CoNO_2$: C: 23.55, H: 6.75, N: 2.29. Found: C: 23.61, H: 6.77, N: 2.41. ^{1}H NMR: δ= 4.26 (br s, 4H, C_c-H), 3.71 (t, $^{3}J(H,H)$= 6Hz, 2H, OCH_2CH_2), 3.54 (m, 4H, OCH_2CH_2), 3.45 (s, 12H, NMe_4), 3.30 (t, $^{3}J(H,H)$= 6Hz, 2H, OCH_2CH_2I), 2.89-1.46 (m, 17H, B-H). $^{1}H\{^{11}B\}$ RMN: δ= 4.26 (br s, 4H, C_c-H), 3.71 (t, $^{3}J(H,H)$= 6Hz, 2H, OCH_2CH_2), 3.54 (m, 4H, OCH_2CH_2), 3.45 (s, 12H, NMe_4), 3.30 (t, $^{3}J(H,H)$= 6Hz, 2H, OCH_2CH_2I), 2.89 (s, 3H, B-H), 2.74 (s, 2H, B-H), 2.69 (s, 1H, B-H), 2.42 (s, 1H, B-H), 1.97 (s, 2H, B-H), 1.77 (s, 2H, B-H), 1.70 (s, 1H, B-H), 1.65 (s, 2H, B-H), 1.55 (s, 2H, B-H), 1.46 (s, 1H, B-H). ^{11}B RMN: δ= 23.70 (s, 1B, B(8)), 4.73 (d, $^{1}J(B,H)$= 135 Hz, 1B), 1.28 (d, $^{1}J(B,H)$= 139 Hz, 1B), -1.60 (d, $^{1}J(B,H)$= 157 Hz, 1B), -3.35 (d, $^{1}J(B,H)$= 158 Hz, 2B), -6.55 (d, $^{1}J(B,H)$= 100 Hz, 2B), -7.46 (d, $^{1}J(B,H)$= 122 Hz, 4B), -16.43 (d, $^{1}J(B,H)$= 153 Hz, 2B), -19.56 (d, $^{1}J(B,H)$= 154 Hz, 2B), -21.09 (d, $^{1}J(B,H)$= 152 Hz, 1B), -27.62 (d, $^{1}J(B,H)$= 166 Hz, 1B).

Synthesis of [NMe_4][3,3'-Co-8-{$(OCH_2CH_2)_2Br$}-8'-I-(1,2-$C_2B_9H_{10}$)(1',2'-$C_2B_9H_{11}$)] (7).
Iodine (26 mg, 0.103 mmol) was added to a stirred solution of **5** (29 mg, 0.05 mmol) in 5 mL of EtOH. The reaction mixture was left to stand overnight at room temperature and was then heated under reflux 1.5h. The excess iodine was decomposed by the additionof a solution of Na_2SO_3 in water and the resulting mixture was evaporated. This was washed with water and the product was redissolved in the minimum volume of ethanol and an aqueous solution containing an exces of [NMe_4]Cl was added, resulting in the formation of an orange precipitate. This was filtered off, washed with water and petroleum ether, and dried in vacuo. Yield: 0.028 g (81%). ^{1}H NMR: δ= 4.49 (br s, 2H, C_c-H), 4.19 (br s, 2H, C_c-H), 3.73 (t, $^{3}J(H,H)$= 8Hz, 2H, OCH_2CH_2), 3.56 (t, $^{3}J(H,H)$= 6Hz, 4H, OCH_2CH_2), 3.53 (m, 2H, OCH_2CH_2), 3.45 (s, 12H, NMe_4), 3.16-1.66 (m, 16H, B-H). $^{1}H\{^{11}B\}$ RMN: δ= 4.49 (br s, 2H, C_c-H), 4.19 (br s, 2H, C_c-H), 3.73 (t, $^{3}J(H,H)$= 8Hz, 2H, OCH_2CH_2), 3.56 (t, $^{3}J(H,H)$= 6Hz, 4H, OCH_2CH_2), 3.53 (m, 2H, OCH_2CH_2), 3.45 (s, 12H, NMe_4), 3.16 (s, 2H, B-H), 3.01 (s, 2H, B-H), 2.85 (s, 1H, B-H), 2.81 (s, 1H, B-H), 2.40 (s, 2H, B-H), 1.95 (s, 1H, B-H), 1.72 (s, 2H, B-H), 1.66 (s, 3H, B-H). $^{13}C\{^{1}H\}$ RMN: δ= 71.57 (s, OCH_2), 70.80 (s, OCH_2), 68.13 (s, OCH_2), 56.47 (s, C_c-H), 55.27 (s, $N(CH_3)_4$), 54.64 (s, C_c-H), 30.63 (s, CH_2Br). ^{11}B RMN: δ= 22.38 (s, 1B, B(8)), 0.31 (d, $^{1}J(B,H)$= 136 Hz, 2B), -3.84 (d, $^{1}J(B,H)$= 105 Hz, 2B), -4.87 (d, $^{1}J(B,H)$= 145 Hz, 4B), -6.45 (d, $^{1}J(B,H)$= 127 Hz, 3B), -17.10 (d, $^{1}J(B,H)$= 180 Hz, 2B), -19.19 (d, $^{1}J(B,H)$= 177 Hz, 2B), -22.36 (d, $^{1}J(B,H)$= 180 Hz, 1B), -26.55 (d, $^{1}J(B,H)$= 175 Hz, 1B). MALDI-TOF-MS: (m/z)= 616.3 (M).

Synthesis of [NMe_4][3,3'-Co-8-{$(OCH_2CH_2)_2I$}-(1,2-$C_2B_9H_{10}$)(1',2'-$C_2B_9H_{11}$)] (8). This compound was prepared using the same procedure as for **7,** but using **6** (29 mg, 0.047 mmol) instead of **5**. Yield: 0.029 g (83%). ^{1}H NMR: δ= 4.49 (br s, 2H, C_c-H), 4.19 (br s, 2H, C_c-H), 3.68 (t, $^{3}J(H,H)$= 6Hz, 2H, OCH_2CH_2), 3.60 (m, 4H, OCH_2CH_2), 3.45 (s, 12H, NMe_4), 3.30 (t, $^{3}J(H,H)$= 6Hz, 2H, OCH_2CH_2), 3.16-1.66 (m, 16H, B-H). $^{1}H\{^{11}B\}$ RMN: δ= 4.49 (br s, 2H, C_c-H), 4.19 (br s, 2H, C_c-H), 3.68 (t, $^{3}J(H,H)$= 6Hz, 2H, OCH_2CH_2), 3.60 (m, 4H, OCH_2CH_2), 3.45 (s, 12H, NMe_4), 3.30 (t, $^{3}J(H,H)$= 6Hz, 2H, OCH_2CH_2), 3.16 (s, 2H, B-H), 3.00 (s, 2H, B-H), 2.85 (s, 1H, B-H), 2.77 (s, 1H, B-H), 2.36 (s, 2H, B-H), 1.95 (s, 1H, B-H), 1.72 (s, 2H, B-H), 1.66 (s, 3H, B-H). $^{13}C\{^{1}H\}$ RMN: δ= 71.56 (s, OCH_2), 71.27 (s, OCH_2), 68.17 (s, OCH_2), 56.42 (s, C_c-H), 55.22 (s, $N(CH_3)_4$), 54.60 (s, C_c-H), 3.11 (s, CH_2I). ^{11}B RMN: δ= 22.36 (s, 1B, B(8)), 0.36 (d, $^{1}J(B,H)$= 147 Hz, 2B), -3.87 (d, $^{1}J(B,H)$= 109 Hz, 2B), -4.87 (d, $^{1}J(B,H)$= 140 Hz, 4B), -6.44 (d, $^{1}J(B,H)$= 127 Hz, 3B), -17.08 (d, $^{1}J(B,H)$= 180 Hz, 2B), -19.17 (d, $^{1}J(B,H)$= 177 Hz, 2B), -22.37 (d, $^{1}J(B,H)$= 177 Hz, 1B), -26.49 (d, $^{1}J(B,H)$= 165 Hz, 1B). MALDI-TOF-MS: (m/z)= 664.16 (M).

Synthesis of [NMe_4][3,3'-Co-8-{OCH_2CH_2OH}-(1,2-$C_2B_9H_{10}$)(1',2'-$C_2B_9H_{11}$)] (9). To a 25 mL round-bottom flask were added Mg metal (45 mg, 1.85 mmol) and 2mL of anhydrous THF. Then, a solution of **5** (50 mg, 0.09 mmol) in THF and dibromoethane (0.05 mL, 0.12 mmol) were added dropwise, at the same time, to the Mg suspension. Once addition was completed the reaction mixture was heated for 5' and left refluxing. When it reaches room temperature, water is added to destroy the excess of magnesium. The solution is evaporated. The resulting residue is dissolved in Et_2O and extracted 3x HCl (1M). The product

was redissolved in the minimum volume of ethanol and an aqueous solution containing an exces of $[NMe_4]Cl$ was added, resulting in the formation of an orange precipitate. This was filtered off, washed with water and petroleum ether, and dried in vacuo. Yield: 0.031 g (76%). IR: $\nu(cm^{-1})$= 3524 (O-H), 3038 $(C-H)_c$, 2956, 2925, 2857 $(C-H)_{aryl/alkyl}$, 2556 (B-H), 1482 $\delta(CH_3)$, 1167 δ(CH), 946 (C-N). ^1H NMR: δ= 4.18 (s(a), 4H, C_c-H), 3.55 (br s, 4H, OCH_2CH_2), 3.44 (s, 12H, $N(CH_3)_4$), 2.88-1.44 (m, 17H, B-H). $^1H\{^{11}B\}$ RMN: δ= 4.18 (s(a), 4H, C_c-H), 3.55 (br s, 4H, OCH_2CH_2), 3.44 (s, 12H, $N(CH_3)_4$), 2.88 (s, 3H, B-H), 2.71 (s, 2H, B-H), 2.69 (s, 1H, B-H), 2.67 (s, 1H, B-H), 2.00 (s, 2H, B-H), 1.78 (s, 2H, B-H), 1.68 (s, 1H, B-H), 1.61 (s, 2H, B-H), 1.54 (s, 2H, B-H), 1.44 (s, 1H, B-H). $^{13}C\{^1H\}$ RMN: δ= 70.36 (s, OCH_2), 62.66 (s, CH_2OH), 55.22 (s, $N(CH_3)_4$), 53.67 (s, C_c-H), 46.36 (s, C_c-H). ^{11}B RMN: δ= 24.31 (s, 1B, B(8)), 5.45 (d, $^1J(B,H)$= 137 Hz, 1B), 1.07 (d, $^1J(B,H)$= 142 Hz, 1B), -1.84 (d, $^1J(B,H)$= 162 Hz, 1B), -3.69 (d, $^1J(B,H)$= 164 Hz, 2B), -6.57 (d, $^1J(B,H)$= 125 Hz, 2B), -7.30 (d, $^1J(B,H)$= 123 Hz, 4B), -16.57 (d, $^1J(B,H)$= 155 Hz, 2B), -19.57 (d, $^1J(B,H)$= 159 Hz, 2B), -21.40 (d, $^1J(B,H)$= 179 Hz, 1B), -27.94 (d, $^1J(B,H)$= 166 Hz, 1B). MALDI-TOF-MS: (m/z)= 384.31 (M).

Synthesis of $[NMe_4][3,3'$-Co-8-$\{(OCH_2CH_2)_2SH\}$-$(1,2-C_2B_9H_{10})(1',2'$-$C_2B_9H_{11})]$ (10). This compound was prepared using the same procedure as for **3,** but using sodium hydrosulfide (15 mg, 0.244 mmol) instead of hydrofluoric acid, and the reaction mixture was heated under reflux for 6h after overnight stirring. Yield: 0.087 g (69%). ^1H NMR: δ= 4.27 (br s, 4H, C_c-H), 3.70 (t, $^3J(H,H)$= 6Hz, 2H, OCH_2CH_2), 3.58 (m, 2H, OCH_2CH_2), 3.50 (m, 2H, OCH_2CH_2), 3.44 (s, 12H, $N(CH_3)_4$), 2.91 (t, $^3J(H,H)$= 6Hz, 2H, CH_2SH), 2.92-1.46 (m, 17H, B-H). $^1H\{^{11}B\}$ RMN: δ= 4.27 (br s, 4H, C_c-H), 3.70 (t, $^3J(H,H)$= 6Hz, 2H, OCH_2CH_2), 3.58 (m, 2H, OCH_2CH_2), 3.50 (m, 2H, OCH_2CH_2), 3.44 (s, 12H, $N(CH_3)_4$), 2.91 (t, $^3J(H,H)$= 6Hz, 2H, CH_2SH), 2.90 (s, 3H, B-H), 2.76 (s, 2H, B-H), 2.69 (s, 1H, B-H), 2.39 (s, 1H, B-H), 1.97 (s, 2H, B-H), 1.77 (s, 2H, B-H), 1.71 (s, 1H, B-H), 1.65 (s, 2H, B-H), 1.55 (s, 2H, B-H), 1.46 (s, 1H, B-H). $^{13}C\{^1H\}$ RMN: δ= 72.62 (s, OCH_2), 69.22 (s, OCH_2), 68.28 (s, OCH_2), 55.25 (s, $N(CH_3)_4$), 54.65 (s, C_c-H), 46.37 (s, C_c-H), 38.65 (s, CH_2SH). ^{11}B RMN: δ= 22.84 (s, 1B, B(8)), 3.74 (d, $^1J(B,H)$= 135 Hz, 1B), 0.45 (d, $^1J(B,H)$= 143 Hz, 1B), -2.44 (d, $^1J(B,H)$= 147 Hz, 1B), -4.12 (d, $^1J(B,H)$= 159 Hz, 2B), -7.52 (d, $^1J(B,H)$= 89 Hz, 2B), -8.23 (d, $^1J(B,H)$= 121 Hz, 4B), -17.24 (d, $^1J(B,H)$= 153 Hz, 2B), -20.43 (d, $^1J(B,H)$= 149 Hz, 2B), -21.80 (d, 1B), -28.39 (d, $^1J(B,H)$= 149 Hz, 1B). MALDI-TOF-MS: (m/z)= 444.66 (M, 100%), 410.63 (M-SH), 382.58 ($M-SHC_2H_4$), 366.56 ($M-SHC_2H_4O$), 337.49 ($M-SHC_4H_8O$).

X-ray Structure Determinations of $[NMe_4]5$ and $[NMe_4]$:

CCDC-?? contain the supplementary crystallographic data for this paper. These data can be obtained free of charge via www.ccdc.cam.ac.uk/conts/retrieving.html (or from the Cambridge Crystallographic Data Centre, 12 Union Road, Cambridge CB2 1EZ, U.K.; fax: (+44) 1223-336033; or e-mail: deposit@ccdc.cam.ac.uk).

Supporting material available:

Acknowledgement

This work was supported by MEC (Grant MAT2006-05339), CSIC (I3P grant to P.F.) and the Generalitat de Catalunya 2005/SGR/00709.

Chart 1. Monosubstituted anions **3-10**.

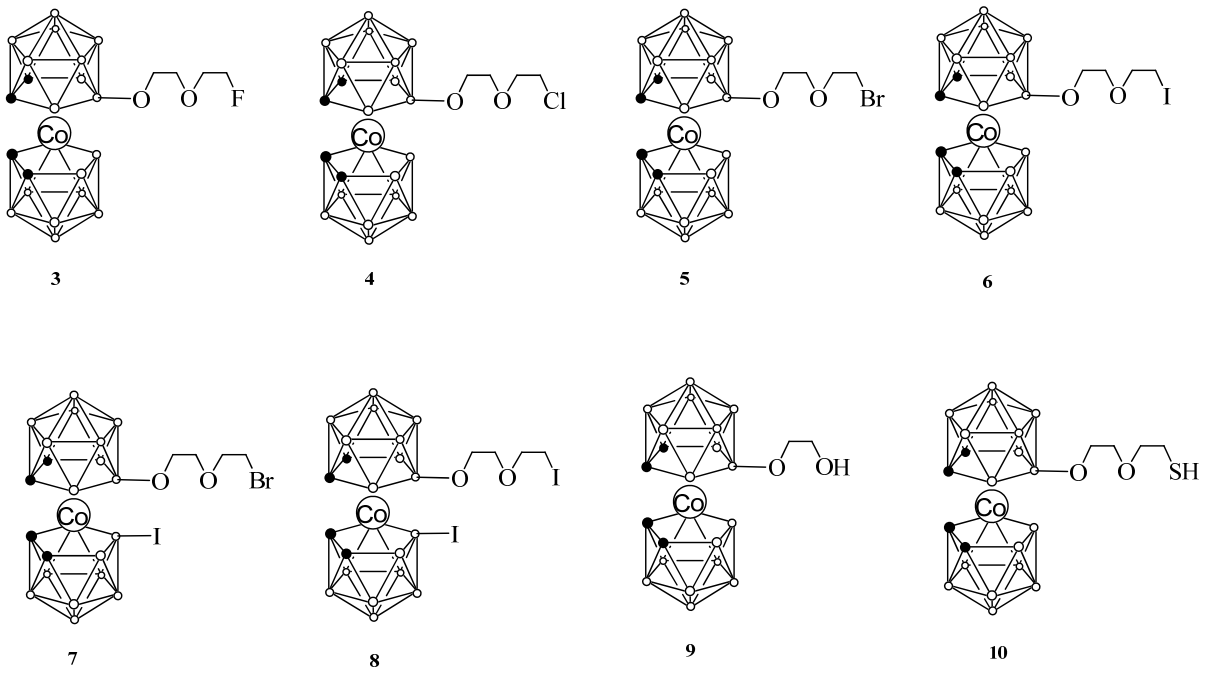

Figura 1. Schematic synthesis of compounds **7-9**.

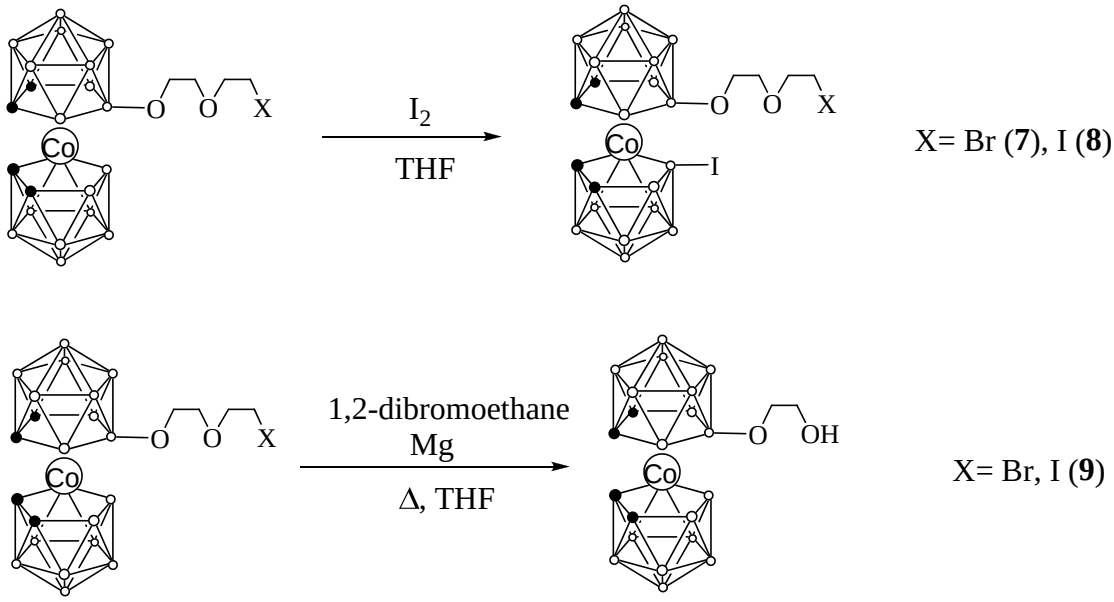

Figure 2. Molecular structure of [NMe_4]**5**. The thermal ellipsoids are set at 30% probability.

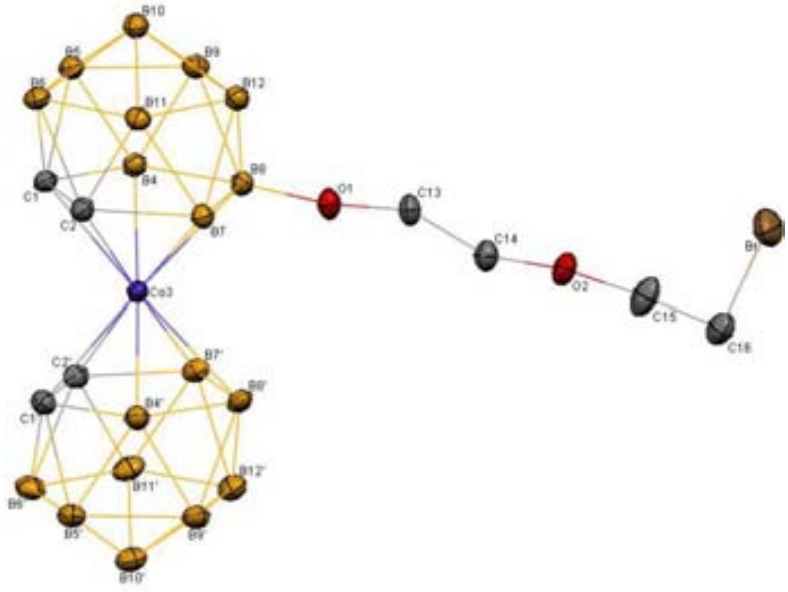

Figure 3. Molecular structure of [NMe_4]**6**. The thermal ellipsoids are set at 30% probability.

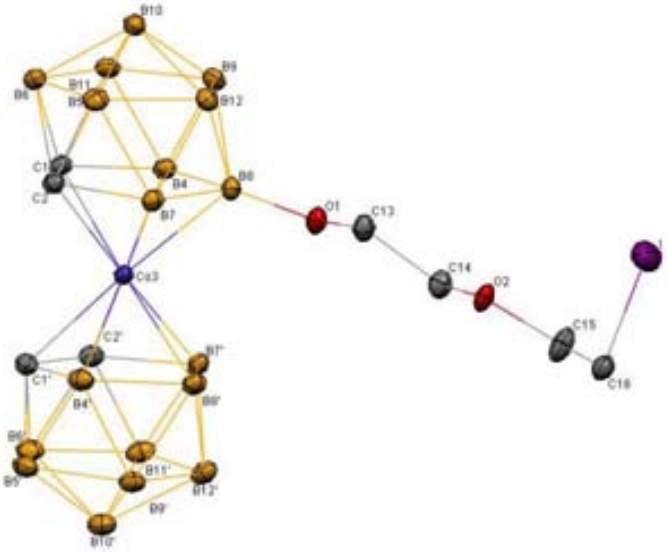

References

[1] I. Rojo, F. Teixidor, C. Viñas, R. Kivekäs, R. Sillanpää, *Chem. Eur. J.* **2003**, *9*, 4311.
[2] I. Rojo, J. Pedrajas, F. Teixidor, C. Viñas, R. Kivekas, R. Sillanpaä, I. Sivaev, V. Bregadze, S. Sjöberg. *Organometallics* **2003**, *22*, 3414.

Boron clusters' effect in rotaxane dynamics.

(Preliminary version)

P. Farràs,[a] P. McGonigal,[b] E. R. Kay,[b] C. Viñas,[a] D. A. Leigh,[b*] F. Teixidor [a*]

[a] Institut de Ciència de Materials de Barcelona (CSIC), Campus de la U.A.B., E-08193 Bellaterra, Spain. Telefax: Int. Code + 34 93 5805729. E-mail: teixidor@icmab.es.

[b] School of Chemistry, University of Edinburgh, The King's Buildings, West Mains Road, Edinburgh EH9 3JJ, UK. E-mail: david.leigh@ed.ac.uk

[±] Pau Farras is enrolled in the PhD program of the UAB.

Molecular machines are being deeply studied nowadays with a lot of publications in journals with the highest scientific level. As an example, more than 100 papers have been published only in 2009.[1] A molecular machine can be defined as a discrete number of molecular components that have been designed to perform mechanically-like movements in response to specific external stimuli. Moreover, we are interested on molecular motors which are based in a unidirectional movement of rotation. External stimuli can be of many different kinds: from temperature or pH changes to the modulation of redox properties of the molecule or even a light source.

Application of boron clusters in molecular machines is reduced to the papers published by Prof. Tour or Prof. Hawthorne. The first used *p*-carborane as wheels of nanocars or, later, nanoworms.[2] The second explored the possible use of metallacarborane nickelbisdicarbollide as a molecular rotor controlled by the redox properties of nickel.[3] This general interest on molecular motors prompted us to use for the first time cobaltabisdicarbollide as one of the components of a molecular rotor. The aim of this work was focused on the influence of boron clusters in chemical structures already used as molecular rotors. The boron compounds that have been used in this work, shown in figure 1, are $[3,3'\text{-Co-}(1,2\text{-}C_2B_9H_{11})_2]^-$ (**1**), $[8,8',9,9',12,12'\text{-}Br_6\text{-}3,3'\text{-Co-}(1,2\text{-}C_2B_9H_8)_2]^-$ (**2**) and $[8\text{-}(OCH_2CH_2)_2\text{-}3,3'\text{-Co-}(1,2\text{-}C_2B_9H_{10})(1,2\text{-}C_2B_9H_{11})]$ (**3**). These have been made part of organic structures called rotaxanes. These are mechanically interlocked molecular architectures consisting of a "dumbbell shaped molecule" which is called the thread and a macrocycle. Both components are kinetically trapped since the ends of the dumbbell are larger than the internal diameter of the macrocycle, preventing the dissociation of the components.

Therefore, molecular rotors is a new field to be explored by cobaltabisdicarbollide. Our study has been focused on the effect of a boron cluster on the dynamics of a rotaxane. We wanted to explore the influence of the intermolecular and intramolecular interactions between these anions and the organic part of the molecule. To measure the dynamics of the rotaxane, we have used the bidimensional nuclear magnetic resonance 2D-EXSY,[4] which allowed us to calculate the rate of pirouetting of the macrocycle. For the study of intermolecular interactions some rotaxanes have been synthesized with functional groups susceptible to be protonated to use cobaltabisdicarbollide as its anion. On the other hand, for the intramolecular interactions boron clusters had to be directly bonded to the rotaxane body and this has been achieved by using compound **3**. This compound is very susceptible to nucleophilic attack and we have used the ring-opening methodology to synthesize the rotaxane.[5]

Then, the synthesis of rotaxane **5** has been done as shown in figure 2. The first step is to obtain the thread **4** by the reaction between an amine and an acid chloride. The amine will have bulky substituents to avoid the dissociation of the macrocycle while the acid chloride will act as a template to help the formation of the rotaxane by hydrogen interactions. The second step is the formation of the rotaxane joining the pieces together, the thread and the two components of the macrocycle. The strong hydrogen interactions between the hydrogen atom of the N-H group in the macrocycle and the oxygen atom of the C=O group from the thread acts as templates and the units of the macrocyle close by themselves forming a dimer.[6] Therefore, the reaction has to be done in very low dilution to favour intramolecular and not intermolecular reactions. Another rotaxane was synthesized having aryl rings as stoppers but the solubility of the protonated compounds was very poor. Instead, alkyllic chains help to solubilize these rotaxanes in a mixture of chloroform:acetonitrile 50%, which would be used to perform 2D-NMR measurements. The protonation of the two pyridine groups on the macrocycle of rotaxane **5** with trifluoroacetic acid lead to **6**, with the cobaltabisdicarbollide acid **7** was obtained, while hexabromo derivative of cobaltabisdicarbollide lead to **8**.

As introduced before, to study intramolecular interactions we have synthesized rotaxane **15** which contains two units of cobaltabisdicarbollide in the thread that act as bulky groups. The synthesis has been done in three steps shown in figure 3. First, a thread with an NH group to be functionalized (**13**) was needed. The second step is the deprotonation of the hydrogen atom from the NH group with a base such as sodium hydride and its further reaction with **3**. This deprotonated nitrogen atom is nucleophile enough to attack the dioxane ring of **3** to produce thread **14**, which has the cobaltacarborane unit directly bonded. At last, the third step is the formation of rotaxane **15** using the same methodology as described before. Most probably, the presence of the boron clusters prevents the folding of the

alkyllic chains (isooctyl fragments) and this may be the reason for the higher yield of **15** in respect to **5**, 18% and 8% respectively. Both rotaxanes had to be separated by column chromatography, and this allowed the recovery of all unreacted threads. Remarkable is the formation of rotaxane **15** as its protonated form represents a unique example of zwitterionic rotaxane, in which a full charge separation has been achieved since the negative charges are located on the thread and the positive on the macrocycle.

The fumaramide group has been chosen as a station as it offers the possibility of changing the isomery of the final compounds. The application of light causes the isomerization of the fumaramide station from *trans* to *cis* leading to the maleamide group. The isomerization causes a radical change on the dynamics of the rotaxane so that the pirouetting rate can vary six orders of magnitude as published in the literature.[7] This is explained by the absence of half of the hydrogen interactions between the thread and the macrocycle as shown in figure 4. The photochemical reaction for rotaxane **5** is done at 312 nm during 15', and the photostationary state is found at 30% of conversion. The separation of the two isomers is done by column chromatography using a chloroform:methanol mixture. In the case of rotaxane **15** the same reaction conditions are used and the photostationay state is found at 50% of conversion. However, until now it has not been possible to separate both isomers, but more work is under way.

2D-EXSY experiments are based on the exchange rate between positions of two non-equivalent hydrogen atoms, that at enough speed become equivalent. In our synthesized molecules the hydrogen atoms of our interest are these in the $-CH_2-$ groups of the macrocycle, that are adjacent to the -NH- groups. A slow rotation speed causes that the axial and equatorial hydrogen atoms appear in different chemical shifts on ^{1}H-NMR spectrum. The change on the ^{1}H-NMR spectra between *trans* and *cis* isomers can be observed in figure 5. It is interesting to see that some hydrogen atoms shift their resonances from one isomer to the other but we are especifically interested on the resonance peaks corresponding to the $-CH_2-$ groups. For the *trans* isomer they appear at 3.8 and 5.1 ppm, but only one resonance at 4.5 ppm is found for *cis* isomer. All resonance peaks can be assigned in the ^{1}H-NMR spectra of compounds **5**-**12**. As an example figure 5(up) show the assignement for the non-protonated *trans* isomer **5**.

Once it is known which hydrogen atoms exchange, a 2D-EXSY experiment to measure the pirouetting rate of compounds **6**-**8** and **10**-**12** was carried on. This method is based on measuring the integral of the off-diagonal peaks of the exchanging hydrogen atoms, and compare the values with the integral of the diagonal peaks. Then, equation 1 is used to calculate the rotation frequency.

$$k = \frac{1}{t_m} \ln \frac{r+1}{r-1}$$ where:

t_m: mixing time

$r = (I_{AA}+I_{BB})/(I_{AB}+I_{BA})$ are the intensities of the diagonal and off-diagonal peaks

equation 1

Once we have calculated the frequency, equation 2 is used to obtain the energy barrier between the two states.

$$\Delta G = \left[R \cdot T \cdot \ln\left(\frac{k \cdot h}{k_B \cdot T}\right) \right] \Big/ 1000$$ where:

R: gas constant; T: temperature; k: rotation frequency; h: Planck constant; k_B: Boltzmann constant.

equation 2

The mixing time is changed in each experiment to get a constant value of k independent of the mixing time. For compounds **6**-**8** and **15** the values shown in table 1 have been obtained. For compounds **10**-**12**, that correspond to the *cis* isomers, it has been impossible to calculate the rotation frequency because it was too high and the necessary separation between the two peaks corresponding to the axial and equatorial hydrogen atoms couldn't be observed, even at 210ºK. If no separation is observed it was not possible to get the integral of each one. If the published value of pirouetting rate that is of 10^6 s^{-1} is considered,[7] it comes out that this value is out of the application range for the 2D-EXSY technique which cannot be above 10^3 s^{-1}.[8] The pirouetting rate of 10^3 s^{-1} found in the literature was calculated using the line shape analysis method.

Comparing the values for **6**-**8** it is possible to see that compounds containing the boron cluster (**7** and **8**) have a pirouetting rate slightly higher. This is the effect we were expecting from the beginning because boron clusters are poor coordinating anions; therefore, the interaction of the anion with the proton would be softer than that of the trifluoroacetate. Moreover, it can be observed that **15** has a similar rate to **6**, thus the intramolecular interactions between the boron cluster and the

protons on the macrocycle are quite important. However, these changes on the pirouetting rate depending on the anion are minimal compared with the changes observed on the photochemical reaction. Anyway, it is not possible to compare the effect of the isomerization with the effect of the counteranion as the change in the intramolecular interactions due to the photochemical reaction is more accentuated. Our hypothesis is that even though metallacarboranes are considered to be poor coordinating anions, they still can interact through the C_c-H groups. [9] This can be observed in the case of **7** where the ^{1}H-NMR spectrum show no equivalence on the 8 hydrogen atoms of the C_c-H groups. Instead there appears three resonances with intensities 1:1:6 (see figure 6). This could only mean that one hydrogen atom of each cobaltacarborane fragment interacts with some atom or atoms on the rotaxane, slowing down the rate of rotation. More studies are needed to confirm this hypothesis and a new rotaxane having as couteranion a boron cluster with no C_c-H groups need to be synthesized. If possible, the most reactive B-H groups need to be protected to minimize the possible interactions.

In conclusion, with the results we have in hand the effect of the counteranion on the dynamics of rotaxanes has not been significant. The change on the rate of pirouetting follows the expected trend of **6**<**7**<**8** being the latter the fastest to rotate since hexabromo derivative of cobaltabisdicarbollide is the weakest coordinating anion. However, the difference on rotation frequency is less than one order of magnitude and therefore, very small in comparison to the six orders of magnitude obtained when the photochemical reaction isomerize the compound from *trans* to *cis*. We suspect that the problem has been either the choice of boron clusters, because it seemed not to be weakly coordinating anions, or most probably due to the limited motion of the *trans* isomers. A possible solution would be to change the polarity of the solvent, as increasing the polarity would break the NH···OC interactions found between the thread and the macrocycle, causing an increase of the pirouetting rate. Then, the effect of the counteranion may be bigger and thus, observable on the 2D-EXSY measurements. On the other hand, compound **15** had an intermidiate rate of rotation between compounds **6** and **7**, indicating that the intramolecular interaction between cobaltabisdicarbollide anions and the protonated pyridine rings is significant. Besides, this compound is a unique example of zwitterion with full charge separation. We think that it would be important to study its properties, especially the electrochemical ones, that would allow to use the redox properties of the studied anion as an additional stimulus to control the dynamics of the rotaxane.

Experimental Section

Instrumentation and Materials. Unless stated otherwise, all reagents and solvents were purchased from Aldrich Chemicals and used without further purification, dichloromethane, chloroform and N,N-dimethylformamide were dried using a solvent purification system manufactured by Innovative Technology, Newburyport, MA, USA. Unless stated otherwise, all reactions were carried out under an atmosphere of nitrogen. Column chromatography was carried out using Silica 60A (particle size 35-70 μm, Fisher, UK) as the stationary phase, and TLC was performed on precoated silica gel plates (0.25 mm thick, 60 F254, Merck, Germany) and observed under UV light. ^{1}H spectra were recorded on Bruker AV 400 instruments. Chemical shifts are reported in parts per million (ppm) from low to high frequency and referenced to the residual solvent resonance. Coupling constants (J) are reported in hertz (Hz). Standard abbreviations indicating multiplicity were used as follows: s = singlet, d = doublet, t = triplet, dd = double doublet, q = quartet, m = multiplet, b = broad, ddd = doublet of double doublets. FAB mass spectrometry was carried out by the services at the University of Edinburgh. Cs[3,3'-Co(1,2-$C_2B_9H_{11})_2$] **(1)** was obtained from Katchem and protonated using 3xHCl (1M). Cs[8,8',9,9',12,12'-Br_6-3,3'-Co(1,2-$C_2B_9H_8)_2$] **(2)** was synthesized according to the literature [10] and protonated using 3xHCl (1M). [8-$(OCH_2CH_2)_2$-3,3'-Co(1,2-$C_2B_9H_{10})$(1',2'-$C_2B_9H_{11})$] (**3**) was prepared according to the literature. [11]

Synthesis of *N,N,N,N*-tetraisooctylfumaramide [4]: Fumaryl chloride (0.52 mL, 4.85 mmol in $CHCl_3$, 5 mL) was added dropwise to a stirred solution of diisooctylamine (3.2 mL, 10.6 mmol) and Et_3N (1.48 mL, 10.6 mmol) in $CHCl_3$ (50 mL) at 0˚C under an atmosphere of nitrogen. The reaction was stirred at 0˚C for a further 2 h. The solution was then washed with 1M aqueous HCl solution (2 x 10 mL), saturated aqueous $NaHCO_3$ solution (2 x 10 mL) and saturated aqueous NaCl solution (2 x 10 mL), dried ($MgSO_4$) and concentrated under reduced pressure. This material was purified by flash

chromatography (SiO_2: methanol/chloroform, 0:100 to 3:97) to provide thread [**4**] as a yellowish oil. Yield: 2.05 g (75%). ^{1}H NMR (400 MHz, $CDCl_3$): δ = 7.42 (s, 2H, CH=CH), 3.35 (m, 8H, CH_2N), 1.28 (m, 32H, CH_2), 0.89 (m, 24H, CH_3).

Synthesis of the rotaxane of *N,N,N,N*-tetraisooctylfumaramide [5]: Thread [**4**] (281 mg, 0.50 mmol) was dissolved in anhydrous $CHCl_3$ (50 mL) and stirred vigorously whilst solutions of p-xylylene diamine (539 mg, 3.96 mmol) and Et_3N (1.2 mL, 3.96 mmol) in anhydrous $CHCl_3$ (20 mL) and pyridine-3,5-dicarbonyl dichloride (810 mg, 3.96 mmol) in anhydrous $CHCl_3$ (20 mL) were simultaneously added over a period of 4 h using a motor-driven syringe pumps. After a further 16 h the resulting suspension was filtered and concentrated under reduced pressure. This material was purified by flash chromatography (SiO_2: methanol/dichloromethane, 4:96) to provide rotanaxe [**5**] as a colourless solid. Yield: 43 mg, 8%. ^{1}H NMR (400 MHz, $CDCl_3$): δ = 9.41 (s, 4H, py), 9.04 (s, 2H, py), 7.46 (m, 4H, NH), 7.00 (s, 8H, Ph), 5.94 (s, 2H, CH=CH), 5.09 (m, 4H, CH_2), 3.81 (m, 4H, CH_2), 3.14 (m, 4H, CH_2N), 2.91 (m, 4H, CH_2N), 1.10 (m, 32H, CH_2), 0.86 (m, 24H, CH_3).

Protonation of rotaxane [5] with CF_3COOH [6]: Rotaxane [5] (10 mg, 9.1 μmol) was dissolved in dichloromethane (2 mL) and trifluoroacetic acid (3 μL, 30 μmol) was added. After stirring for 10' it was concentrated under reduced pressure. ^{1}H NMR (400 MHz, CD_3CN): δ = 9.23 (s, 4H, py), 9.08 (s, 2H, py), 7.47 (m, 4H, NH), 7.06 (s, 8H, Ph), 5.91 (s, 2H, CH=CH), 4.92 (m, 4H, CH_2), 3.86 (m, 4H, CH_2), 3.23-2.82 (m, 8H, CH_2N), 1.10 (m, 32H, CH_2), 0.75 (m, 24H, CH_3).

Protonation of rotaxane [5] with H[1] [7]. Rotaxane [5] (10 mg, 9.9 μmol) was dissolved in dichloromethane (2 mL) and a solution H[**1**] (9.6 mg, 30 μmol) in dichloromethane (2 mL) was added slowly. The orange solution is concentrated under reduced pressure. The remaining solid was washed with Et_2O the remove the excess of H[**1**]. ^{1}H NMR (400 MHz, CD_3CN): δ = 9.73 (s, 2H, py), 9.17 (s, 4H, py), 7.55 (m, 4H, NH), 7.00 (s, 8H, Ph), 5.82 (s, 2H, CH=CH), 4.74 (m, 4H, CH_2), 4.03, 4.00 (br s, 2H, C_c-H), 3.90 (m, 4H, CH_2), 3.66 (br s, 6H, C_c-H), 2.09 (m, 8H, CH_2N), 1.21-1.01 (m, 32H, CH_2), 0.63-0.48 (m, 24H, CH_3).

Protonation of rotaxane [5] with H[2] [8]: Rotaxane [**5**] (10 mg, 9.9 μmol) was dissolved in dichloromethane (2 mL) and an excess of a H[2] solution in dichloromethane was added. The orange solution is concentrated under reduced pressure. The remaining solid was washed with Et_2O the remove the excess of H[2]. ^{1}H NMR (400 MHz, CD_3CN): δ = 9.76 (s, 2H, py), 9.20 (s, 4H, py), 7.58 (m, 4H, NH), 7.03 (s, 8H, Ph), 5.85 (s, 2H, CH=CH), 4.77 (m, 4H, CH_2), 4.49 (br s, 8H, C_c-H), 3.93 (m, 4H, CH_2), 3.15-2.82 (m, 8H, CH_2N), 1.04-0.98 (m, 32H, CH_2), 0.66-0.51 (m, 24H, CH_3).

Synthesis of the rotaxane of *N,N,N,N*-tetraisooctylmaleamide [9]: Rotaxane [**5**] (80 mg, 0.07 mmol) was dissolved in dichloromethane and irradiated for 15' in a 312nm photoreactor. The solution was concentrated under reduced pressure. This material was purified by flash chromatography (SiO_2: methanol/dichloromethane, 5:95) to provide rotanaxe [**9**] as a colourless solid. The remaining *trans* isomer was irradiated again for 15' and the material was purified with the same column. Yield: 44.9 mg, 56%. ^{1}H NMR (400 MHz, $CDCl_3$): δ = 9.18 (s, 4H, py), 8.19 (s, 2H, py), 7.50 (m, 4H, NH), 7.18 (s, 8H, Ph), 4.82 (s, 2H, CH=CH), 4.47 (m, 8H, CH_2), 2.82-2.56 (m, 8H, CH_2N), 1.04 (m, 32H, CH_2), 0.78-0.68 (m, 24H, CH_3).

Protonation of rotaxane [9] with CF_3COOH [10]: Rotaxane [**9**] (11 mg, 10 μmol) was dissolved in dichloromethane (2 mL) and trifluoroacetic acid (3 μL, 30 μmol) was added. After stirring for 10' it was concentrated under reduced pressure. ^{1}H NMR (400 MHz, $CDCl_3$): δ = 9.30 (s, 4H, py), 8.73 (s, 2H, py), 8.19 (m, 4H, NH), 7.22 (s, 8H, Ph), 4.85 (s, 2H, CH=CH), 4.46 (m, 8H, CH_2), 2.91-2.76 (m, 8H, CH_2N), 1.06 (m, 32H, CH_2), 0.84-0.67 (m, 24H, CH_3).

Protonation of rotaxane [9] with H[1] [11]: Rotaxane [**9**] (11 mg, 10 μmol) was dissolved in dichloromethane (2 mL) and an excess of a H[**1**] solution in dichloromethane was added. The orange solution is concentrated under reduced pressure. The remaining solid was washed with Et_2O to remove the excess of H[**1**]. ^{1}H NMR (400 MHz, CD_3CN): δ = 9.12 (s, 4H, py), 8.13 (s, 2H, py), 7.90 (m, 4H, NH), 7.44 (s, 8H, Ph), 5.31 (s, 2H, CH=CH), 4.51 (m, 8H, CH_2), 4.45, 4.35 (br s, 2H, Cc-H), 4.25, 4.22 (br s, 6H, C_c-H), 3.10 (m, 8H, CH_2N), 1.24 (m, 32H, CH_2), 0.95-0.69 (m, 24H, CH_3).

Protonation of rotaxane [9] with H[2] [12]: Rotaxane [**9**] (11 mg, 10 μmol) was dissolved in dichloromethane (2 mL) and an excess of a

H[**2**] solution in dichloromethane was added. The orange solution is concentrated under reduced pressure. The remaining solid was washed with Et_2O the remove the excess of H[**2**]. ^{1}H NMR (400 MHz, CD_3CN): δ = 9.20 (s, 2H, py), 9.06 (s, 4H, py), 8.54 (m, 4H, NH), 7.28 (s, 8H, Ph), 4.86 (s, 2H, CH=CH), 4.98, 4.72 (br s, 2H, Cc-H), 4.58 (br s, 6H, C_c-H), 4.38 (m, 8H, CH_2), 3.10 (m, 8H, CH_2N), 1.30-1.10 (m, 32H, CH_2), 0.80-0.60 (m, 24H, CH_3).

Synthesis of *N,N*-diisooctylfumaramide [13]: Fumaryl chloride (0.52 mL, 4.85 mmol in $CHCl_3$, 5 mL) was added dropwise to a stirred solution of 2-ethylhexylamine (1.8 mL, 10.6 mmol) and Et_3N (1.48 mL, 10.6 mmol) in $CHCl_3$ (50 mL) at 0˚C under an atmosphere of nitrogen. The reaction was stirred at 0˚C for a further 2 h. The solution was then washed with 1M aqueous HCl solution (2 x 10 mL), saturated aqueous $NaHCO_3$ solution (2 x 10 mL) and saturated aqueous NaCl solution (2 x 10 mL), dried ($MgSO_4$) and concentrated under reduced pressure. This material was purified by flash chromatography (SiO_2: methanol/chloroform, 3:97) to provide thread [**13**] as a yellowish oil. Yield: 0.69 g (42%). ^{1}H NMR (400 MHz, $CDCl_3$): δ = 6.90 (s, 2H, CH=CH), 6.16 (br s, 2H, NH), 3.23 (m, 4H, CH_2N), 1.44 (m, 2H, CH), 1.21 (m, 16H, CH_2), 0.83 (m, 12H, CH_3).

Synthesis of *N,N*-{8-(1,3-dioxohexane)-3,3'-Co-(1,2-$C_2B_9H_{10}$)(1',2'-$C_2B_9H_{11}$)}-*N,N*-diisooctylfumaramide [14]: A solution of thread [**13**] (0.31 g, 0.90 mmol) in toluene (10 mL) was added at 0˚C to a stirred solution of sodium hydride (0.15 g, 3.6 mmol) in tetrahydrofuran (20 mL). The reaction was stirred at 0˚C for a further 2 h. Then, a solution of [3,3'-Co(8-$C_4H_8O_2$-1,2-$C_2B_9H_{10}$)(1',2'-$C_2B_9H_{11}$)] [**3**] (0.73 g, 1.8 mmol) was slowly added at 0˚C and left overnight. The solution was concentrated under reduced pressure. The residue was then washed with 1M aqueous HCl solution (3 x 20 mL) and saturated aqueous $KHCO_3$ solution (3 x 20 mL), dried ($MgSO_4$) and concentrated under reduced pressure. This material was purified by flash chromatography (SiO_2: acetonitrile/dichloromethane, 30:70) to provide thread [**14**] as an orange solid. Yield: 1.00 g (90%). ^{1}H NMR (400 MHz, $CDCl_3$): δ = 7.04 (s, 2H, CH=CH), 3.90 (m, 4H, CH_2O), 3.67-3.20 (20H, C_c-H, CH_2O), 2.78 (m, 4H, CH_2N), 2.68 (m, 4H, CH_2N), 1.40 (m, 2H, CH), 1.04 (m, 16H, CH_2), 0.67 (m, 12H, CH_3). FAB-MS: m/z (%): 578.9 (M).

Synthesis of rotaxane of thread 14 [15]: Thread [**14**] (612 mg, 0.50 mmol) was dissolved in anhydrous $CHCl_3$ (50 mL) and stirred vigorously whilst solutions of p-xylylene diamine (540 mg, 3.96 mmol) and Et_3N (1.1 mL, 3.96 mmol) in anhydrous $CHCl_3$ (20 mL) and pyridine-3,5-dicarbonyl dichloride (810 mg, 3.96 mmol) in anhydrous $CHCl_3$ (20 mL) were simultaneously added over a period of 4 h using a motor-driven syringe pumps. After a further 16 h the resulting suspension was filtered and concentrated under reduced pressure. The residue was then washed with 1M aqueous HCl solution (3 x 20 mL), dried ($MgSO_4$) and concentrated under reduced pressure. This material was purified by flash chromatography (SiO_2: ethyl acetate/acetonitrile, 90:10 to 70:30) to provide rotanaxe [**15**] as an orange solid. Yield: 148 mg, 18%. ^{1}H NMR (400 MHz, $CDCl_3$): δ = 9.29 (s, 4H, py), 9.20 (s, 2H, py), 7.65 (m, 4H, NH), 7.16 (s, 8H, Ph), 6.03, 5.97 (s, 2H, CH=CH), 5.10 (m, 4H, CH_2), 4.21 (br s, 8H, C_c-H), 4.13, 4.10 (8H, CH_2O), 3.90 (m, 4H, CH_2), 3.65-3.50 (4H, CH_2O), 3.30-3.10 (m, 8H, CH_2N), 1.40-0.80 (m, 30H, CH-CH_2-CH_3). FAB-MS: m/z (%): 846.6 (M, 100%), 578.9 (M-macrocyle, 25%).

Chart 1. Synthesized rotaxanes.

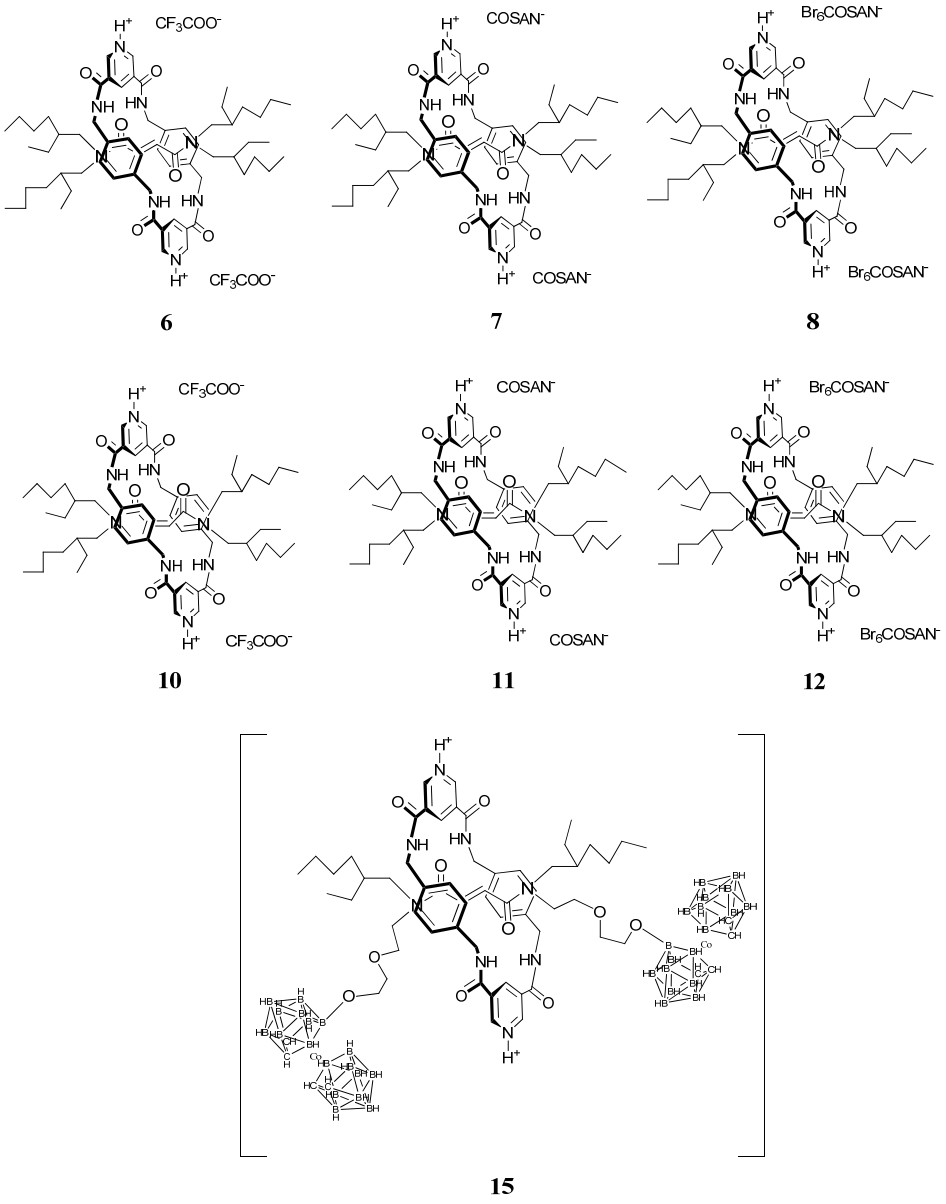

Figure 1. Boron clusters used in this work.

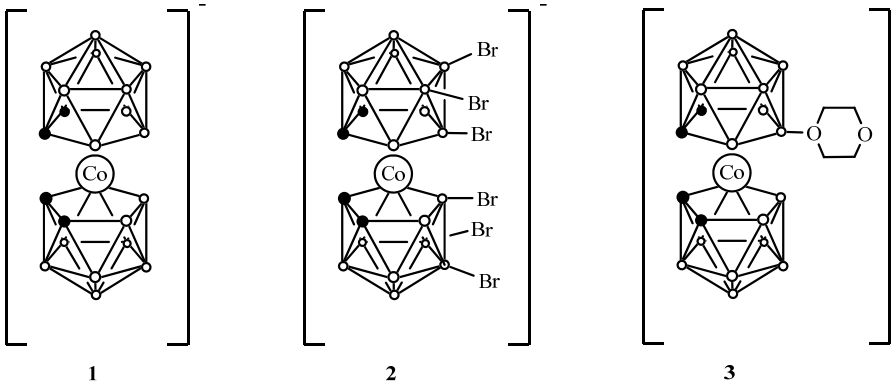

Figure 2. Synthetic procedure to obtain rotaxane **5**.

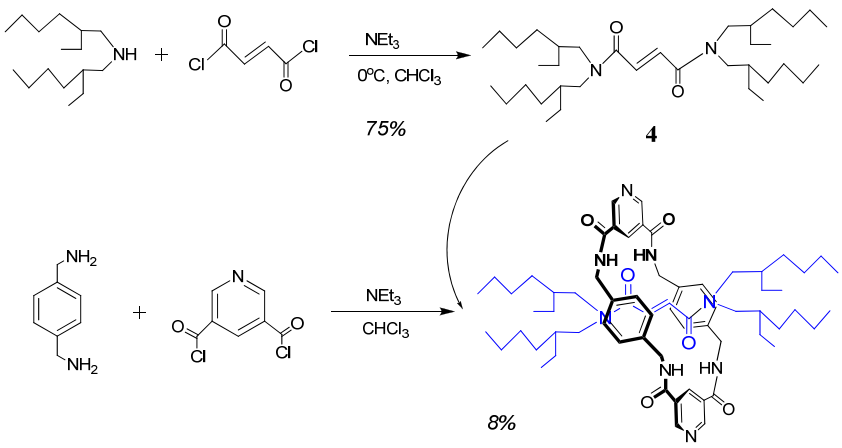

Figure 3. Synthetic procedure to obtain rotaxane 1**5**.

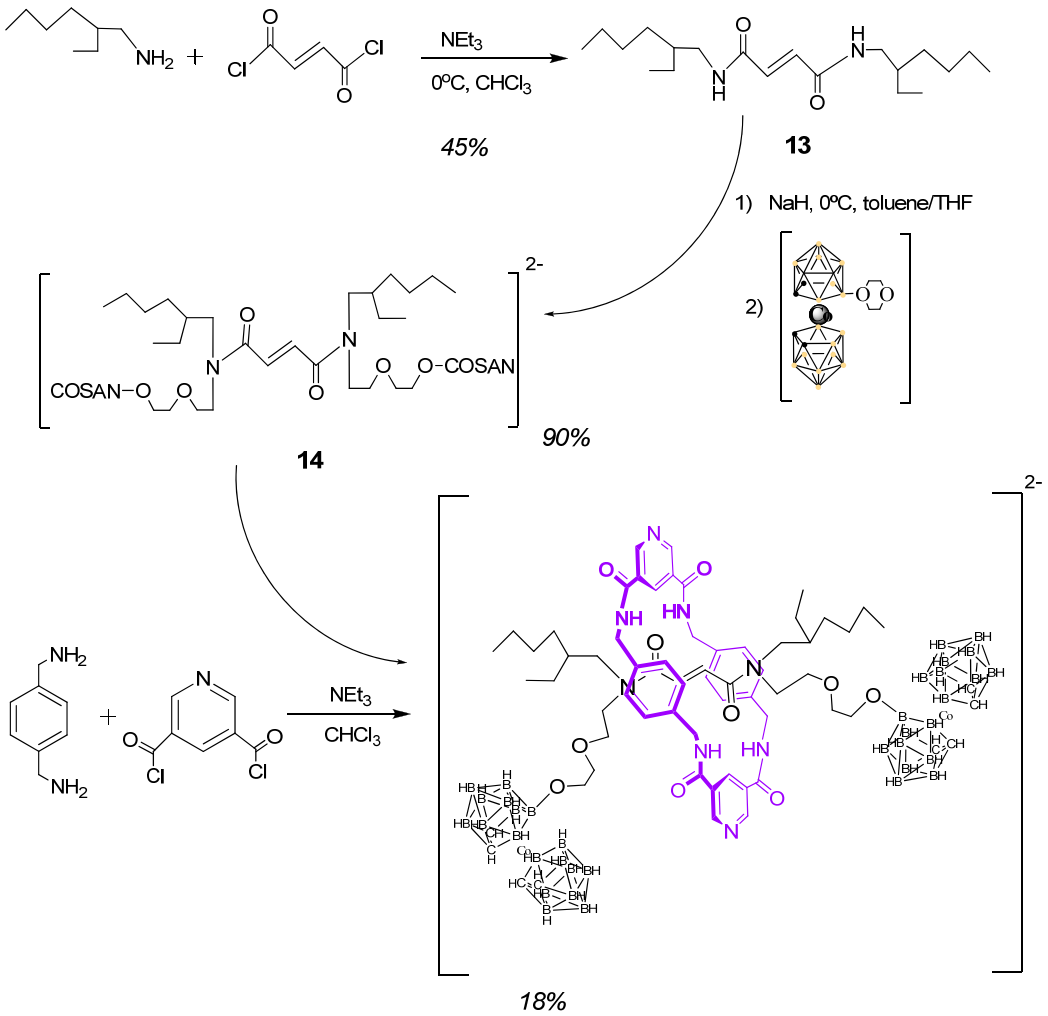

Figure 4. Photochemical reaction to isomerize rotaxane **5** to rotaxane **9**. In dashed lines are shown the hydrogen interactions between NH···OC groups.

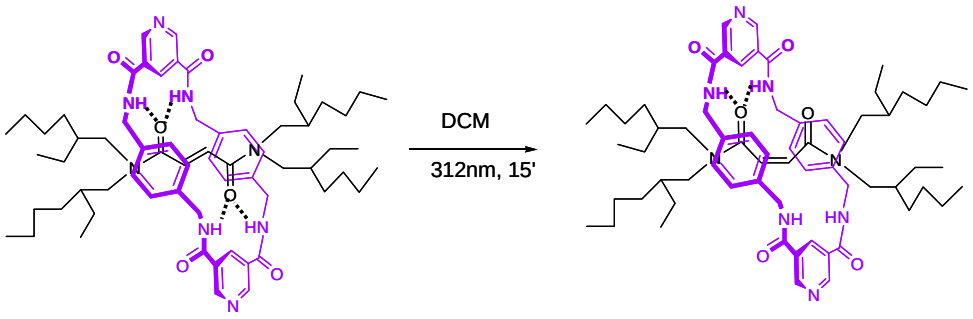

Figure 5. Comparison between ^{1}H-NMR spectra of the unprotonated rotaxanes **5** *trans* (up) and **9** *cis* (down) isomers. Shown also the assignement of the hydrogen atoms of **5**.

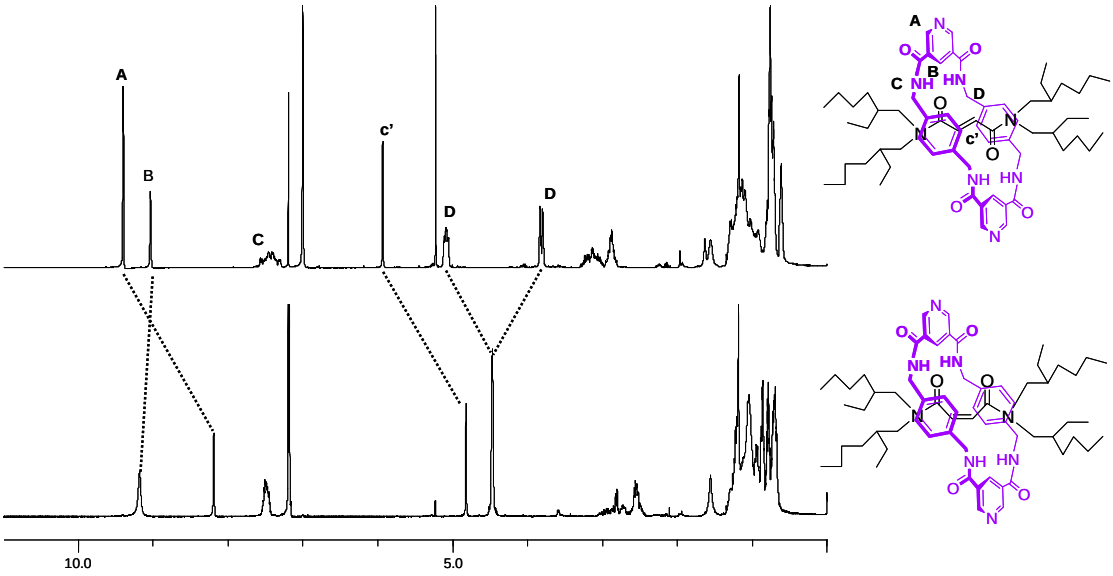

Figure 6. ^{1}H-NMR spectrum of compound **7** on the area between 3-5 ppm.

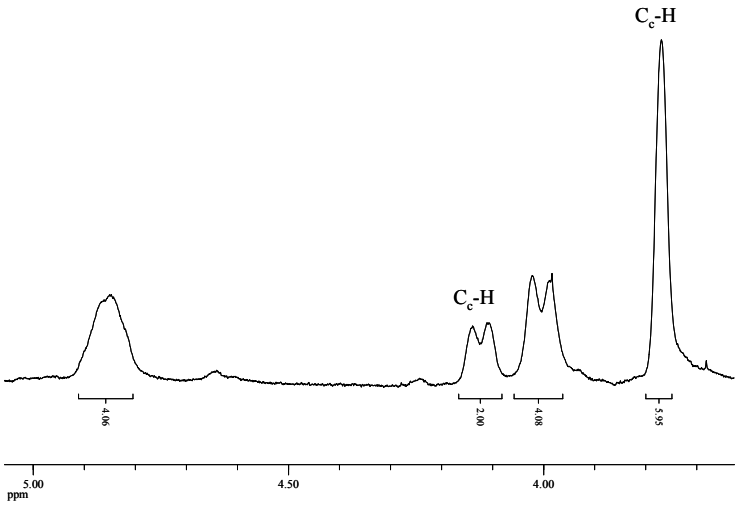

Table 1. *k* and ΔG values for compounds **6-8** and **15** calculated by the 2D-EXSY technique.

Compound	k (s^{-1})	ΔG (kJ/mol)
6	19.75	65.59
7	40.33	63.82
8	45.59	63.52
15	24.25	65.08

References

[1] a) T. Omabegho, R. Sha, N. C. Seeman, *Science*, **2009**, *324*, 67; b) C. F. Lee, D. To. Leigh, R. G. Pritchard, D. Schultz, S. J. Teat, G. To. Timco, R. E. P. Winpenny, *Nature*, **2009**, *458*, 314; c) Z. Okten, M. Schliwa, *Nature*, **2007**, *450*, 625; d) V. Serreli, C. F. Lee, E. R. Kay, D. To. Leigh, *Nature*, **2009**, *445*, 523.

[2] a) J. F. Die, T. Sasaki, Y. Shirai, J. M. Guerrero, J. M. Tour, *J. Org. Chem.*, **2007**, *72*, 9481; b) Y. Shirai, A. J. Osgood, Y. Zhao, Y. Yao, L. Saudan, H. Yang, C. Yu-Hung, T. Sasaki, J. F. Die, J. M. Guerrero, K. F. Kelly, J. M. Tour, *J. Am. Chem. Soc.*, **2006**, *128*, 4854; c) Y. Shirai, A. J. Osgood, Y. Zhao, K. F. Kelly, J. M. Tour, *Nano Lett.*, **2005**, *5*, 2330.

[3] a) M. F. Hawthorne, B. M. Ramachandran, R. D. Kennedy, *Pure Appl. Chem.*, **2006**, *78*, 1299; b) M. F. Hawthorne, J. And. Zink, J. M. Skelton, M. J. Bayer, C. Liu, E. Livshits, R. Baer, D. Neuhauser, *Science*, **2004**, *303*, 1849.

[4] C. Wynants, G. Go Binst, C. Miigge, K. Jurkschat, A. Tzschach, H. Pepermans, M. Gielen, R. Willem, *Organometallics*, **1985**, *4*, 1906.

[5] J. Plešek, S. Hermánek, A. Franken, *Collect. Czech. Chem. Commun.* **1997**, *62*, 47.

[6] A. G. Johnston, D. A. Leigh, L. Nezhat, J. P. Smart, M. D. Deegan, *Angew. Chem. Int. Ed. Eng.*, **1995**, *34*, 1212.

[7] F. G. Gatti, S. Leon, J. K. Y. Wong, G. Bottari, A. Altieri, M. A. Farran-Morales, S. J. Teat, C. Frochot, D. A. Leigh, A. M. Brouwer, F. Zerbetto, *Proc. Natl. Acad. Sci.*, **2003**, *100*, 10.

[8] C. L. Perrin, T. J. Dwyer, *Chem. Rev.*, **1990**, *90*, 935.

[9] J. G. Planas, C. Viñas, F. Teixidor, A. Comas-Alive, G. Ujaque, A. Lledós, M. E. Light, M. B. Hursthouse, *J. Am. Chem. Soc.*, **2005**, *127*, 15976.

[10] L. Matel, F. Macásek, P. Rajec, S. Hermánek, J. Plešek, *Polyhedron* **1982**, *1*, 511.

[11] I. Rojo, J. Pedrajas, F. Teixidor, C. Viñas, R. Kivekas, R. Sillanpaä, I. Sivaev, V. Bregadze, S. Sjöberg. *Organometallics* **2003**, *22*, 3414.

Investigations on antimicrobial effect of metallacarboranes and their influence on viability and proliferation of cultured tumor and nontumor cells

(Preliminary version)

R. Alexandrova,[a] P. Farràs,[b,±] C. Viñas,[b] R. Toshkova,[a] T. Popova,[c] F. Teixidor,[b] G. Miloshev,[d] R. Kalfin[e]

[a] Institute of Experimental Pathology and Parasitology, Bulgarian Academy of Sciences, Acad. Georgi Bonchev Str., Block 25, Sofia 1113, Bulgaria; rialexandrova@hotmail.com

[b] Institut de Ciència de Materials de Barcelona (CSIC), Campus de la U.A.B., E-08193 Bellaterra, Spain. Telefax: Int. Code + 34 93 5805729. E-mail: clara@icmab.es

[c] Faculty of Veterinary Medicine, Forest Technical University, 10 Kliment Ohridski Blvd, 1756 Sofia, Bulgaria

[d] Institute of Molecular Biology, Bulgarian Academy of Sciences, Acad. Georgi Bonchev Str., Block 21, Sofia 1113, Bulgaria

[e] Institute of Neurobiology, Bulgarian Academy of Sciences, Acad. Georgi Bonchev Str., Block 23, Sofia 1113, Bulgaria

± P.F is enrolled in the Ph.D. program of the UAB.

Introduction

Recently, there is an increasing interest in biological activity and medicinal application of boron and boron compounds.[1,2] Boronated compounds have been shown to be potent anti-osteoporotic, anti-inflammatory, hypolipemic, anti-coagulant and anti-neoplastic agents both *in vitro* and *in vivo* in animals.[3] Boron compounds (boronic acids, boron heterocycles, etc.) are reported to be potent antibacterials and antiestrogens.[4,5,6] There are data that some curcumin boron complexes,[7] boronic acid compounds,[8] boron-modified polypeptides[9] and metallocarboranes[10] are specific and potent inhibitors of HIV protease. Boron may also play a role in improving arthritis, plasma lipid profiles, and brain function.[11] There are evidence confirming the potential antineoplastic activity of boron and boron compounds: Bortezomib (PS-341, Velcade), a modified dipeptidyl boronic acid, is a proteasome inhibitor approved by the USA Food and Drug Administration (FDA) and European Medicines Agency (EMEA) for use in patients with refractory or relapsed multiple myeloma.[12,13,14] The anionic *closo* icosahedral cobaltabisdicarbollide [3,3'-Co(1,2-$C_2B_9H_{11}$)$_2$], [**1**]$^-$, has been the object of many studies[15] since its discovery in 1965.[16] Their derivatives are highly air-stable, very robust, withstanding strong acid, moderate base, high temperatures and intense radiation.[15a] The cobaltabisdicarbollide [**1**]$^-$ has been proposed in a wide range of applications such as extraction of radionuclides,[17] conducting organic polymers[18] or use in medicine.[19] The use of polyhedral boron hydrides for cancer treatment is traditionally connected with boron neutron capture therapy.[20] Boron neutron capture therapy (BNCT) is a binary approach for cancer treatment that provides a way to selectively destroy malignant cells and spare normal tissue.[21,22] Boroxifen is a *nido*-carborane analogue of tamoxifen, a widely employed drug for the treatment of hormone dependent breast cancer.[23] In addition, boron compounds were proved to express promising antitumour properties (Gielen et al., 1995; Nakamura et al., 2006; Barranco et al., 2007).

More recently, polyhedral borate anions were proposed as carriers of radionuclide label for targeted radionuclide therapy and diagnostics of cancer.[24] Some metal derivatives of carboranes were found to demonstrate significant antitumor activity themselves.[25] There is a significant global need for new antibacterials and alternative mechanisms of action given the rise in resistance among bacteria.[26] The chemical and biological stability, low toxicity, and the possibility to introduce various modifications make boron clusters and specially [**1**]$^-$ attractive pharmacophores for potent and specific enzyme inhibition.

The aim of this study is to expand the biomedical applications by evaluating the putative antimicrobial properties of anionic weakly coordinating cobaltallacarboranes [**1**]$^-$, [**3**]$^-$ to [**8**]$^-$ as well as their influence on cultured tumor and nontumor cells.

Experimental section

1. Materials Metallacarborane compounds: Following our studies on metallacarboranes' direct substitution, we recently reported on the high yield synthesis of polyanionic species as novel high-boron content molecules with enhanced water solubility.[27] The synthetic ways were based on the use of carboxylic acid and alcoxides as nucleophiles in the ring-opening reaction of cyclic oxonium [3,3'-Co(8-$C_4H_8O_2$-1,2-$C_2B_9H_{10}$)(1',2'-$C_2B_9H_{11}$)], (**2**). We synthesized ligands incorporating the $(OCH_2CH_2)_2OR$ chain and the [3,3'-Co(1,2-$C_2B_9H_{11}$)$_2$]$^-$ moiety. Chart 1 shows the anionic species Na(H_2O)[3,3'-Co(8-O(CH_2CH_2O)$_2$C(O)CH_3-1,2-$C_2B_9H_{10}$)(1',2'-$C_2B_9H_{11}$)], [**3**]$^-$; Na[1''-{3,3'-Co(8-O(CH_2CH_2O)$_2$C(O)-1,2-$C_2B_9H_{10}$)(1',2'-$C_2B_9H_{11}$)}-2''-OH-C_6H_4}], [**4**]$^-$; Na_3[1'',3'',5''-{3,3'-Co(8-O(CH_2CH_2O)$_2$-1,2-$C_2B_9H_{10}$)(1',2'-$C_2B_9H_{11}$)}$_3$-C_6H_3], [**5**]$^-$; Na[3,3'-Co(8-O(CH_2CH_2O)$_2$$CH_3$-1,2-$C_2B_9H_{10}$)(1',2'-$C_2B_9H_{11}$)], [**6**]$^-$; Na[3,3'-Co(8-O($CH_2CH_2O$)$_2$$CH_2CH_3$-1,2-$C_2B_9H_{10}$)(1',2'-$C_2B_9H_{11}$)], [**7**]$^-$ that were synthesized from the zwitterionic (**2**) according to Scheme 1. The quelating ligand derivative [1,1'-(PPh_2)$_2$-3,3'-Co(1,2-$C_2B_9H_{10}$)$_2$]$^-$, [**8**]$^-$, was synthesized (see Scheme 2) in one pot reaction in very good yield and with an easy working up process according to the method reported at the literature.[28]

The compounds were dissolved in dimethylsulfoxide (DMSO, Serva) and diluted in culture medium (for antitumor investigations) or sterile phosphate buffered saline (PBS, for antibacterial tests). The final concentration of DMSO in the stock solutions (where the concentration of the tested compound was 1 mg/ml) was 2%. The metallacarboranes were stored at 4^{o}C. The commercially available broad spectrum antibiotic thiamphenicol was used in the experiments as a positive control. The dilutions of the antibiotic were prepared in sterile PBS.

Microorganisms: The antimicrobial activity of the compounds was tested on broad range of Gram-positive and Gram-negative pathogenic bacterial strains (isolated from animals and humans and control strains) as well as on *Candida spp.* In our experiments we used 4 strains of *Staphylococcus aureus (S. aureus* TSA MRSA*, S. aureus* Kowan*, S. aureus* 131*, S. aureus* 230*)*, 4 of *Streptococcus pyogenes (S. pyogenes* 1*, S. pyogenes* 2, *S. pyogenes* 184*, S. pyogenes* 383*),* 4 of *Escherichia coli* (*E. coli* 045, *E. coli* 075-20, *E. coli* 16 – B, *E.*

coli 0621 – C) and 4 of *Pseudomonas aeruginosa (P. aeruginosa* 1*, P. aeruginosa* 177*, P. aeruginosa* 318*, P. aeruginosa* 357*)*. Pure cultures of 3 pathogenic strains of *Candida albicans* (*C. albicans* 1, C. albicans 332*, C. albicans* 398*)* and 1 of *Candida tropicalis (C. tropicalis* 324*)* were also used. The bacterial strains were isolated from patients with infections of different location (skin, ears, conjunctiva, respiratory and urogenital tracts) that were subject to continuous treatment with different antibacterial means. The strains we used showed *in vitro* a high drug resistance mainly to streptomycin, penicillin, oxacillin, ampicillin, and some of them also to amoxicillin but are sensitive to amphenicols.

Cell cultures and experimental tumors: The cell cultures that were used as model systems in the experiments are presented in Table 1.
The cell lines LSCC-SF(Mc29) (Alexandrova et al., 2002) and LSR-SF(SR) (Alexandrov, 1996) were established, characterized and maintained in the Institute of Experimental Pathology and parasitology, Bulgarian Academy of Sciences. The cell line 8MG BA (Perjelova et al.,etc.) was kindly provided by Dr Perjelova and Prof. C. Altaner from the Institute of Cancer Research, Bratislava, Slovakia. The other cell lines (MCF-7, K562, Hep-2) are from Laboratory of Cell Cultures, National Centre of Infectious and Parasitic Diseases, Sofia, Bulgaria.
Transplantable Graffi myeloid tumor was induced in newborn hamsters by murine leukemia Graffi virus and was maintained as solid tumor by monthly s.c. injection of 1 – 2 x 10^6 viable trypan blue dye excluded tumor cells in the interscapular area of hamsters. [29]

Experimental animals: Golden Syrian Hamsters (weighed 80-100g, 2 months old) and C57 BL mice (18-20 g, 2-4 months old) from both sexes were purchased from Laboratory Animal Center (National Oncology Center – Sofia). Animals were given standard pellet diet and tab water ad libitum.
All experiments with laboratory animals, included in the present study were performed in accordance to the Veterinary Medical Office in Bulgaria and the rules of the Ethics Committee of the Institute of Experimental Pathology and Parasitology, which follows the European Committee Standards concerning the care and use of laboratory animals (Registrations 197/27.07.2006 by the Regional Veterinary Medical Office, Sofia, and 11130006 by the National Veterinary Medical Office in Bulgaria).

Chemicals
Dimethyl sulfoxide (DMSO), trypsin, Romanovski-Giemsa stain, trypan blue were purchased from AppliChem (Darmstadt, Germany); thiazolyl blue tetrazolium bromide (MTT) and RPMI-1640 culture media were obtained from Sigma-Aldrich Chemie GmbH (Germany), Dulbecco's modified Eagle's medium (D-MEM) cell culture medium and fetal bovine serum were purchased from Gibco (UK), poly-L-lysine hydrobromide and Mueller-Hinton's agar were from Scharlau Chemie S.A. (Barcelona, Spain). All other chemicals of the highest purity commercially available were purchased from local agents and distributors.

2. Methods

2.1. Cell culturing

For the preparation of primary cell cultures, the experimental animals were euthanized by carbon dioxide according to the institutional guidelines.

Isolation of peritoneal macrophages
Healthy mice were killed under deep CO_2 anesthesia, and the resident peritoneal cells were aseptically collected by peritoneal lavage with 10 ml sterile ice cold PBS (pH=7.2-7.4). Differential cell counts were determined by cytospin preparations stained with Romanovski-Giemsa. This procedure yielded peritoneal cells with more than 98% being macrophages; we used only suspensions with 98% or more viability determining by trypan blue exclusion test.

Spleen lymphocytes isolation
Spleens from healthy mice were harvested immediately in an aseptic way, cooled in ice-cold PBS supplemented with 5.0% FCS and suspended by passing through a stainless steel seeve to prepare a single cell lymphocyte suspension. The spleen cells were diluted in PBS, layered on 3 ml Ficoll-Paque (Pharmacia, Uppsala, Sweden) in ratio 2:1. The gradient was centrifuged at 1850 rpm for 40 min at 20 ^oC. The lymphocytes were collected from the inter-phase and washed three times with RPMI-1640 medium. The viability of lymphocytes tested by trypan blue exclusion test was about 98 %.

Isolation of bone marrow cells
Femurs from healthy mice and Graffi tumour-bearing hamsters were dissected out, freed of connective tissue and muscle with gauze. Each bone was cut in half with scissors and the marrow was flushed out with RPMI-1640 (Sigma) media using a syringe and a 26G needle. The cell suspension (pooled from both femur bones of each animal) was washed three times by centrifugation at 200 x *g* for 10 min.

Primary cultures from experimental tumors
For the present study primary cultures from Graffi tumor were generated by mechanical disaggregating of tumour tissue.[30]
The cell cultures were grown in plastic ware (Orange Scientific, Belgium), RPMI-1640 (primary cell cultures, K562) or DMEM (the rest of cell cultures) supplemented with 5-10% fetal bovine serum, 100 U/ml penicillin and 100 μg/ml streptomycin. The number and viability of cells

were determined by trypan blue dye exclusion test. The cultures were kept in a humidified incubator (Thermo Scientific) at 37°C under 5% CO_2 in air. For routine passages adherent cells were detached using a mixture of 0.05% trypsin and 0.02% ethylendiaminotetraacetic acid (EDTA). The cell lines were passaged 2-3 times per week (1 : 2 to 1: 3 split). The experiments were performed during the exponential phase of cell growth.

2.2. Antimicrobial tests

Studies were carried out by the classic agar-diffusion method of Bauer-Kirby[31]. Bacterial suspensions were inoculated at a concentration of 2.10^6 cells/ml on Mueller-Hinton's agar with pH 7.2 – 7.4 and 4 mm layer thickness in Petri dishes with diameter 9 cm. The compounds and controls were applied as phosphate-saline solutions by dropping of 0.1 ml in 9-mm holes in the agar at concentrations of 50 μg/well for the compounds and 30 μg/well for the antibiotic. Results were recorded after 24 h incubation period by measuring the diameters of inhibitory zones in mm, including the hole diameter. Inhibitory effect of the metallacarboranes was established at zones > 12 mm.

The determination of the minimum inhibitory concentrations (MICs) was performed by the method of twofold serial dilutions on Mueller-Hinton's agar as per Ericsson and Sherris.[32] MIC_{50} were calculated mathematically depending on the number of inhibited colonies of the medium with the respective compound or antibiotic dilution compared to the control medium colonies without drugs.

2.3. Methods for evaluation of cell viability and proliferation

MTT test

The cells were seeded in 96-well flat-botommed microplates (Orange scientific) at a concentration of 2×10^4 cells/well for permanent lines and 1×10^5 in the case of primary cultures. Microplates coated with poly-L-lysine as described by Montefori et al. (1988) were used for suspension of cell cultures.

At the 24th h cells from monolayers were washed and covered with media modified with different concentrations of the compound tested (each concentration in 6 to 8 repetitions). Samples of cells grown in non-modified medium served as control. After 24 and 48 h of incubation, the solutions were removed from the plates and MTT colorimetric assay of cell survival was performed as described by Mossman.[33] This consisted of three hours incubation with MTT solution (5 mg MTT in 10 ml DMEM) at 37°C under 5% CO_2 and 95% air; then extracted with a mixture of ethanol and DMSO (1 : 1, vol/vol). The absorbance of each well at 540 nm was read by an automatic microplate reader (Absorbance Reader Tecan). Relative cell viability, expressed as a percentage of the untreated control (100% viability), was calculated for each concentration. Concentration-response curves were constructed manually for each experiment. The effective concentrations of metallacarboranes causing a 50% reduction of cell viability (Effective concentration 50, EC_{50}) were estimated from these curves. All data points represent an average of at least four independent assays.

Colony-forming assay

Tumor cells (approximately 10^3 cells/well) suspended in 0.45% purified agar (Difco) in medium containing different concentrations of metal complexes (ranging from 1 to 200 μg/ml) were layered in 24 well microplates (Cellstar). The presence/absence of colonies was registered using an inverted microscope during 16-day period.

Single cell gel electrophoresis (Comet Assay).

The single cell gel electrophoresis was performed in neutral conditions at which the method detects only DNA double-strand breaks. The cells were mixed with 1.4 % of low-gelling agarose (Sigma, Type II) and immediately spread onto microscopic slides. After 20 min of incubation of the gels in a lysis solution (146 mM NaCl, 30 mM EDTA, pH 8; 10 mM Tris-HCl, pH 8, 0.1% N-lauroylsarcozine; pH 9), an electrophoresis was conducted for 20 min in 1 x TBE buffer at 0,4 V/cm. After electrophoresis the slides were subsequently dehydrated for 5 min in 75% and in 96% of ethanol. After drying at room temperature, the slides were stained with SYBR green (Molecular Probes) and the results visualized under a fluorescent microscope (450nm/490nm). Images were acquired by a CCD video camera SONY.

2.4. Statistical analysis

The data are presented as mean ± standard error of the mean. Statistical differences between control and treated groups were assessed using one-way analysis of variance (ANOVA) followed by Dunnett post-hoc test.

Results

Antimicrobial properties

The results obtained by the agar-gel diffusion method are presented in Figure 1. They revealed that [**7**]$^-$ possess significant antibacterial activity both against Gram-positive (Fig. 1A) and Gram-negative (Fig 1B) bacteria as compared to the wide-spectrum potent antibiotic thiamphenicol, used as a positive control.

According to their antimicrobial and antifungal activity (the diameter of the inhibitory zones) the most effective metallacarboranes are [**7**]$^-$, [**4**]$^-$ and [**5**]$^-$. The same compounds manifested also significant antifungal activity *in vitro* (Fig. 1 C). From a practical point of view it is important that the meticillin-resistant strain of *S. aureus* (TSA

MRSA), the poliresistant strains of *P. aeruginosa*, as well as of *Candida spp.,* show sensitivity to this three compounds.

The less active among the examined compounds was [**1**]$^-$. Weakest effect the investigated compounds showed against the strains of *P. aeruginosa*.

The establishment of the minimum inhibitory concentrations (MICs) of tested compounds is more precise method for determination of their effect. MICs of the most active compounds are presented in Table 2. The antimicrobial effect of the compounds according to the minimum inhibitory concentration is as follows:

S. aureus: [**4**]$^-$ > [**7**]$^-$ > Thiam > [**8**]$^-$ > [**5**]$^-$
S. pyogenes: [**4**]$^-$ > [**7**]$^-$ > Thiam > [**8**]$^-$ > [**5**]$^-$
E. coli: [**4**]$^-$ > [**7**]$^-$ > Thiam > [**5**]$^-$ > [**8**]$^-$
P. aeruginosa: [**4**]$^-$ > [**5**]$^-$ > [**7**]$^-$ >Thiam > [**8**]$^-$

The antifungal effects against *Candida spp*: [**7**]$^-$ > [**4**]$^-$ > Thiam > [**8**]$^-$ > [**5**]$^-$

Effect of the compounds on cell viability and proliferation

MTT assay

Three groups of experiments were performed using MTT assay in order to:

I. Evaluate the effects of metallacarboranes on viability and proliferation of cultured tumor permanent cell lines. The results as EC_{50} values (μg/ml) derived from concentration-response curves are given in Table 3. Examples of these concentration-response curves are shown in Fig. 2.

II. Compare the influence of the tested compounds on tumor (Primary cultures from Graffi myeloid tumor in hamster) and nontumor (bone marrow cells from Graffi tumor bearing hamsters) (Fig. 3).

III. Examine the ability of the compounds to affect viability and proliferation of effector immune cells – peritoneal macrophages, spleen lymphocytes and bone marrow cells from healthy mice (Table 4). This study was carried out with metallacarboranes ([**4**]$^-$, [**1**]$^-$, [**5**]$^-$) and concentrations (10, 20 and 50 μg/ml) that were found to show comparatively lower cytotoxicity in the previous experiments (I).

Independently tested DMSO (applied at the same concentrations as in the solutions of investigated metallacarboranes) had no significant cytotoxic effect as compared to the control – the cell viability was > 94% ($P > 0.05$).

DNA damages. Applied at a concentration of 50 μg/ml for 48 h the metallacarboranes [**7**]$^-$, [**3**]$^-$ and [**6**]$^-$ were found to induce DNA damages (double stranded DNA breaks) in respectively 70%, 60% and 44% of the treated K562 human erythroleukemia cells.

Colony-forming ability of tumor cells. The influence of tested compounds in effective concentrations on tumor cell growth inhibition is presented in Table 5.

Discussion

Antimicrobial activity

Nowadays more strains of pathogenic microorganisms, including *Staphylococci, Streptococci* and *Enterobacteria*, become resistant to many of the available antibiotics and chemotherapeutic agents, creating a serious problem in the treatment of infectious diseases. Antimicrobial resistance has produced alarming situation worldwide. There is a serious risk that a growing proportion of infections, especially in hospitals, will become effectively untreatable.[34, 35, 36] For that reason the trials to request for new antimicrobial means are very indispensable. Our investigations presented in this study showed that the tested metallacarboranes express promising antimicrobial properties *in vitro* – comparable or even better than tose of the broad spectrum antibiotic thiamphenicol (positive control). The most active among the compounds examined were found to be [**4**]$^-$ and **[7]**$^-$. Particularly important from a practical point of view is the fact that meticillin-resistant strain of *S. aureus* (TSA MRSA) and the strains of *P. aeruginosa* were found to be sensitive to the tested substances. Methicillin-resistant *Staphylococcus aureus* (MRSA) bacteria are a common cause of hospital- and community- acquired infections which are difficult to treat and are associated with significant morbidity and mortality. There is great interest in preventing the transmission of MRSA and decolonizing persons who harbor these bacteria (McConeghy et al., 2009; Hanson, Chung, 2009). *Pseudomonas aeruginosa* (primarily a nosocomial organism that most commonly colonizes respiratory secretions and urine) resistance to antimicrobials is also an important therapeutic consideration (Cunha, 2002). Whereas several laboratories have reported that boron status affects the response to injury or infection and some boron compounds are proved to exhibit antimicrobial properties (Baker et al., 2006; Alencar et al., 2006; Luan et al., 2008, Nielsen, 2008), in the literature available there are no data about antimicrobial activity of metallacarboranes. In addition, it has to be mentioned also that of the various known antibacterial agent classes, amphiphilic compounds act through perturbation and disruption of the prokaryotic membrane.[37] Cobaltabisdicarbollide is considered a weakly coordinating anion that although lacking the amphiphilic topology, behave as anionic surfactant.[38] There are many reports of linear polycationic agents but only a few descriptions of polyanionic antibacterial agents (e.g., sulfonated polystyrene).[39]

In the light of interesting antimicrobial properties of the metallacarboranes investigated, some more details have to be mentioned: 1) One of the most promising antibacterial agents [**4**]$^-$, was also found to possess comparatively low cytotoxicity in cultured tumor and nontumor cells; 2) The metallacarborane **[7]**$^-$ was found to express highest cytototoxic and antiproliferative as well as antimicrobial properties. It has to be remained that the biological activity of cis-platin - the world's leading anti-tumour drug for the modern chemotherapy of human cancer, was accidentally discovered in 1965 by Barnet Rosenberg and his coworkers who reported first the inhibitory activity of this compound on *E. coli* division.[40,41]; 3) The metallacarborane [**1**]$^-$ was found to express comparatively lower antibacterial and antifungal properties as compared to its derivatives; 4) There are data that boron affects the synthesis of the extracellular matrix and is beneficial in wound healing. This fact as well as the antimicrobial activity of the metallacarboranes investigated (for example [**4**]$^-$) and their ability to stimulate the proliferation of normal murine cells ([**4**]$^-$), suggest that these compounds could be tested in experimental wound healing.

Influence on cell viability and proliferation

Our experiments revealed that metallacarboranes investigated decreased in a time- and concentration-dependent manner the viability and proliferation of various cultured human and animal tumor cell lines. The cell specific response was observed - the cell cultures differ in their susceptibility to the cytotoxic and antiproliferative effects of metallacarboranes. It has to be emphasized that in all cell cultures used as model systems in our investigations and in all assays performed, the highest cytotoxic and antiproliferative potential was shown by **[7]**$^-$ followd by **[6]**$^-$ and [**3**]$^-$, whereas **[8]**$^-$ and [**5**]$^-$ were found to be the less effective. Among the cell cultures tested, the virus-transformed chicken hepatoma cells were found to be the most sensitive to the cytotoxic and antiproliferative effects of metallacarboranes. These data are in accordance with our previous investigations.[42,43,44]

On the basis of their ability to affect proliferation and viability of cultured tumor and nontumor cells, the metallacarboranes investigated could be divided into two groups: i) compounds that express higher cytotoxic and antiproliferative properties ([**7**]$^-$, [**6**]$^-$ and [**3**]$^-$) and, ii) less cytotoxic compounds (such as [**4**]$^-$, [**5**]$^-$, [**1**]$^-$ and [**8**]$^-$). We found that metallacarboranes [**5**]$^-$, [**4**]$^-$ and [**1**]$^-$ affected viability and/or proliferation of peritoneal macrophages, spleen lymphocytes, and bone marrow cells isolated from healthy mice. Macrophages are known to play an essential role in host defense against microbial agents and neoplasia.[45] Since phagocytes acts as a regulatory and effector cells in the immune system, the enhancement of phagocyte function has potential therapeutic efficacy against infections and cancer. It is well known that the phagocytosis action of macrophages is a key process in nonspecific immune function.[46]

Undoubtedly, the most intriguing question is whether the metallacarboranes investigated could be considered as potential antitumor/boron delivery agents. The answer of this question is not an easy task and requires a complex and multistep approach.

It is widely accepted that tumor cell lines have played an important part in our understanding of cancer and have been used extensively in the discovery and characterization of new chemotherapeutic drugs. Potential weaknesses of such cell lines are that: i) they may have lost important properties originally possessed *in vivo*, including potential targets for therapy (Baguley, Marshall, 2004); ii) common 2D cell cultures do not adequately represent the functions of 3D tissues that have extensive cell-cell and cell-matrix interactions, as well as markedly different diffusion/transport conditions (Smalley et al., 2006; Lee et al., 2009); iii) each permanent cell line was established from a neoplastic formation in only one human or animal. At the same time, because of so called tumor heterogeneity phenomenon, each tumor/tumor cell line can differ in biological characteristics and behavior from the other tumors/tumor cell lines of the same type and as a result can not fully represent this type of cancer (Alexandrova, 2001). Possible differences between tumor cells in cancer patients and cell lines might be avoided by the use of short-term cultures of human tumor cells taken directly from cancer tissue, termed primary cell cultures. In addition, it is very important to evaluate comparatively the cytotoxic effect of the compounds investigated on tumor and non-tumor cells (controls). Theoretically, the best choice will be to use as controls primary cultures of healthy human tissues of the same type as tumor is (for example brain tumor and normal brain tissue) as well as bone marrow cells. Obviously, it is not so easy to be achieved. All these obstacles as well as the phenomenon of cell-specific response, prompted us to: i) use as experimental models variety of cell cultures that differ in many biological characteristics such as: origin (chicken, mouse, rat, hamster, human); histologic type of the tumor (hepatoma, sarcoma, carcinoma, glioblastoma, myeloma, erytroleukemia); etiology (spontaneous and virus-induced); perform investigations not only in monolayer cell cultures, but also in 3D colonies of tumor cells in a semi-solid medium; ii) evaluate comparatively the effect of metallacarboranes on primary cultures from experimental tumor (Graffi myeloid tumor in hamster) and bone marrow cells from the same tumor-bearing animals. Such model

system represents the situation of cancer patients receiving chemotherapy.

The results obtained revealed that in all cell cultures investigated the metallacarboranes [**7**]$^-$ and [**6**]$^-$, followed by [**3**]$^-$, express highest cytotoxic and antiproliferative activities. We observed a good correlation between the data obtained for the short term cytotoxicity of the compounds (assess by MTT test after 24h and 48h treatment) and prolonged effect on viability and proliferation of tumor cells (evaluated by colony-firming assay, 16 day incubation period). In our investigations Graffi myeloid tumor cells were found to be less sensitive to the toxic effects of metallacarboranes than bone-marrow cells isolated from the same tumor bearing hamsters. This fact could be explained by the nature of the cells – normal haemopoietic progenitor cells and malignant cells respectively, as well as the type of the proliferation – normal and malignant. These are different by nature processes, which could be affected in a completely different way by externally applied compounds. It is well known that the bone marrow cells are very sensitive and each change in their chemical surrounding could be fatal to their development. On the contrary tumor cells are supposed to fight in different biochemical surrounding and are more fit to survive chemical changes in their environment. It is well known that myelosuppression is one of the main side effects of current cancer chemotherapy.[47] This fact is not surprising because the anticancer agents used in current oncology practice recognize and attack tumor cells because of their high proliferative potential. Bone-marrow cells also have high proliferative potential that makes them "visible" for the antitumor drugs. In addition, the so called P-glycoprotein (PGP) that is responsible for the multidrug resistance of the cells is not expressed or expressed at a very low level in the cytoplasmic membranes of bone-marrow cells (Alexandrova, 1998).

The currently used in oncology practice antitumor agents were proved to induce their antineoplastic properties via one or more of the following mechanisms: microtubule interference; topoisomerase poisoning or topoisomerase catalytic inhibition; DNA alkylation; inhibition of DNA synthesis; protein synthesis inhibition; lipoxygenase inhibition; immune mechanisms. It is completely possible that some of these mechanisms could be responsible for the cytotoxic and antiproliferative activities of the metallacarboranes examined in the present study. Though our data are not sufficient to make firm conclusions at this stage of the investigations, there are details that have to be discussed. Doublestranded breaks are highly deleterious DNA lesions as they lead to chromosome aberrations and/or apoptosis (Smart et al., 2008). The results obtained using neutral variant of Comet assay revealed that metallacarboranes tested (especially [**7**]$^-$, [**6**]$^-$ and [**3**]$^-$) induce double stranded DNA damages in the treated cells. These findings raise at least 3 questions: i) are these compounds genotoxic and mutagenic?; ii) are they able to induce apoptosis; iii) do metallacarboranes investigated work as topoisomerase II inhibitors? Series of additional experiments are needed to answer to these questions. It has to be reminded; however, that many currently used in oncology practice anticancer agents can express genotoxic and mutagenic effects (Celicler et al., 2006; Tiburi et al., 2002; Yarema et al., 1994).

The metallacarboranes examined are not water-soluble and were dissolved in dimethylsulfoxide (DMSO), which raises the question are such compounds perspective for medicinal applications? On one hand, DMSO is not a normal ingredient of human's body and several systemic side effects from the use of this compound have been reported. On the other hand, DMSO was proved to be a cell-differentiation agent, hydroxyl radical scavenger, antidote to the extravasation of vesicant anticancer drugs, topical analgetic, etc. DMSO is one of the most common solvents for the *in vivo* administration of several water-insoluble substances (Santos et al., 2003). In relation to our study, two more facts have to be mentioned: 1) the concentrations of DMSO in the working solutions of the metallacarboranes investigated were proved to be non-toxic. The simple calculations reveal that when the concentration of metallacarborane is 100 μg/ml, the amount of DMSO inside is only 0.2%; 2) water-insoluble compounds could be suitable for liposome drug delivery systems, that are one of the most promising new technologies for increasing the efficacy of Boron neutron capture therapy (Yanagie et al., 2008).

The data presented in this study confirm the antineoplastic properties of boron and boron compounds. Indeed, boron intake was shown to be inversely associated with incidence and mortality of malignant neoplasms of the lung (Mahabir et al., 2008), prostate (Cui et al. 2004; Barranco et al., 2007), cervix (Koekmaz et al., 2007) and breast (Touillaud et al., 2005).

Some of the metallacarboranes investigated have very similar chemical structure, but more or less different biological (antimicrobial, cytotoxic, antiproliferative) properties. This result is not surprising. For example, we found in previous investigations that bisbensykisoquinoline alkaloids – hernandesine and thalfoetidine, differed significantly in their cytotoxic and antiproliferative properties. Both alkaloids have one and the same chemical structure, the only difference between them is observed at position C-12 – methoxyl group in the structure of thalidasine and hydroxyl group in the structute of thalfoetidine (Alexandrova et al).

In summary, the metallacarboranes examined in the present study demonstrate cytotoxic and

antiproliferative properties ([**7**]$^-$, [**6**]$^-$, [**3**]$^-$), antimicrobial efficacy ([**7**]$^-$, [**4**]$^-$) and merit further investigations to clarify better the cellular targets, mechanism(s) of action and biological safety of these compounds. The knowledge concerning the relationship between the physical and chemical structure of such metallacarboranes and their biological activities will facilitate the design of drugs with improved anticancer or antimicrobial properties.

Acknowledgement

This work was supported by MEC (MAT2006-05339), CSIC (I3P grant to P.F.), the Generalitat de Catalunya 2005/SGR/00709, a bilateral project (2007BG0017) between Institute of Experimental Pathology and Parasitology (Bulgarian Academy of Sciences) and Institute of Material Science (C.S.I.C.).

References

[1] Yang W., Gao X., Wang B., Med. Res. Rev., 2003, 23, 346-368.

[2] Valliant J.F., Guenther K.J., King A.S., Morel P., Schaffer P., Sogbein O.O., Stephenson K.A., Coord. Chem. Rev., 2002, 232, 173-230.

[3] Benderdour M., Bui-Van T., Dicko A., Belleville, F., J. Trace Elem. Med. Biol., 1998, 12, 2-7.

[4] Groziak, M.P., Am. J. Ther., 2001, 8, 321-328.

[5] Alencar de Queroz A.A., Abraham G.A., Pires Camillo M.A., Higa O.Z., Silva G.S., del Mar Fernandez M., San Roman J., J. Biomater. Sci. Polym. Ed., 2006, **17**, 689-707.

[6] Baker S.J., Akama T., Zhang Y.K., Sauro V., Pandit C., Singh R., Kully M., Khan J. et al., Bioorg. Med. Chem. Lett., 2006, **16**, 5963-5967.

[7] Sui Z., Salto R., Li J., Craik C., Ortiz de Montellano P.R., Bioorg. Med. Chem., 1993, 1, 415-422.

[8] Chen X., Bastow K., Goz B., Kucera L., Moeeis-Natschke S.L., Ishag K.S., Antivir. Chem. Chemother., 1996, **7**, 108, 114.

[9] Pivazyan A.D., Matteson D.S., Fabry-Asztalos, L., Singh R.P., Lin P.F., Blair W., Guo K., Robinson B., Prusoff W.H., Biochem. Pharmacol., 2000, 60, 927-936.

[10] Cigler P., Kozisek M., Rezacova P., Brynda J., Otwinowski Z.et al., PNAS, 2005, **102**, 15394-15399.

[11] Devirian T.A. Volpe, S.L. Crit. Rev. Food Sci. Nutr., 2003, 43, 219-231.

[12] Richardson PG, Mitsiades C., Schlossman R., Ghobrial I., Hideshima T., Munshi N., Anderson K.C., Anticancer Ther., 2008, 8, 1053-72.

[13] Utecht KN, J. Kolesar J. Am J Health Syst Pharm. 2008 Jul 1;65(13):1221-31.

[14] van Rij C.M., Wilhelm A.J., Sauerwein W.A.G., van Loenen A.C., Pharm. World. Sci., 2005, 27, 92-95.

[15] a) Plesek, J. Potential applications of the boron cluster compounds. *Chem. Rev* **1992**, *92*, 269. b) Hawthorne, M. F.; Maderna, A. Applications of Radiolabeled Boron Clusters to the Diagnosis and Treatment of Cancer. *Chem. Rev.* **1999**, *99*, 12, 3421. c) Sivaev, B.; Bregadze, V. I. *Collect. Czech. Chem. Commun.* **1999**, *64*, 783.

[16] Hawthorne, M. F.; Young, D. C.; Wegner, P. A. Carbametallic Boron Hydride Derivatives. I. Apparent Analogs of Ferrocene and Ferricinium Ion. *J. Am. Chem. Soc.* **1965**, *87*, 1818.

[17] b) Viñas, C.; Gomez, S.; Bertran, J.; Teixidor, F.; Dozol, J. F.; Rouquette, H. Cobaltabis(dicarbollide) derivatives as extractants for europium from nuclear wastes. *Chem. Commun.* **1998**, 191. c) Viñas, C.; Gomez, S.; Bertran, J.; Teixidor, F.; Dozol, J. F.; Rouquette, H. New Polyether-Substituted Metallacarboranes as Extractants for ^{137}Cs and ^{90}Sr from Nuclear Wastes. *Inorg. Chem.* **1998**, *37*, 3640. d) Viñas, C.; Bertran, J.; Gomez, S; Teixidor, F.; Dozol, J. F.; Rouquette, H.; Kivekäs, R.; Sillanpää, R. Aromatic substituted metallacarboranes as extractants of ^{137}Cs and ^{90}Sr from nuclear wastes. *J. Chem. Soc., Dalton Trans.* 1998, 2849. c) Grüner, B.; Plešek, J.; Báča, J.; Císařová, I.; Dozol, J.-F.; Rouquette, H.; Viñas, C.; Selucký, P.; Rais, J. Cobalt bis(dicarbollide) ions with covalently bonded CMPO groups as selective extraction agents for lanthanide and actinide cations from highly acidic nuclear waste solutions. *New J. Chem.* 2002, *26*, 1519. d) Rais, J.; Grüner, B. in *Ion Exchange and Solvent Extraction*, eds. Y. Marcus and A. K. Sengupra, CRC Press, Boston, **2004**, vol. *17*, 243.

[18] a) Masalles, C.; Borros, S.; Viñas, C.; Teixidor, F. Are low coordinating anions of interest as doping agents in organic conducting polymers?. *Adv. Mater.* **2000**, *12*, 1199. b) Masalles, C.; Llop, J.; Viñas, C.; Teixidor, F. Extraordinary overoxidation resistance increase in self-doped PPy's by using non-conventional low charge-density anions *Adv. Mater.* **2002**, *14*, 826. c) Masalles, C.; Borrós, S.; Viñas, C.; Teixidor, F. Surface Layer Formation on Polypyrrole Films. *Adv. Mater.* **2002**, *14*, 449.

[19] a) Hao, E.; Vicente, M. G. H. A facile and versatile preparation of bilindiones and biladienones from tetraarylporphyrins. *Chem. Commun.* **2005**, 1306. b) Barth, R. F.; Coderre, J. A.; Vicente, M. G. H.; Blue, T. E. *Clin. Cancer Res.* **2005**, *11*, 3987. c) Gottumukkala, V., Ongayi, O.; Baker, D. G.; Lomax, L. G.; Vicente, M. G. H. *Bioorg. Med. Chem.* **2006**, *14*, 1871. c) Bregadze, V. I.; Sivaev, I. B.; Glazun, S. A. Polyhedral boron compounds as potential diagnostic and therapeutic antitumor agents *AntiCancer Agents Med. Chem.*, **2006**, *6*, 75. d) Cigler, P.; Kožišek, M.; Řezačova, P.; Brynda, J.; Otwinowski, Z.; Pokorna, J.; Plešek, J.; Gruner, B.; Dolečkova-Marešova, L.; Maša, M.; Sedlaček, J.; Bodem, J.; Kräusslich, H.; Kral, V.; Konvalinka. From nonpeptide toward noncarbon protease inhibitors: metallacarboranes as specific and potent inhibitors of HIV protease. J. *Proc. Natl. Acad. Sci. USA* **2005**, *102*, 15394.

[20] a) Paxton, R. J.; Beatty, B. G.; Hawthorne, M. F.; Varadarajan, A.; Williams, L.; Curtis, F. L.; Knobler; C. B.; Beatty, J. David; Shively, J. E. A Transition Metal Complex (Venus Flytrap Cluster) for Radioimmunodetection and Radioimmunotherapy. *Proc. Natl. Acad. Sci.* **1991** *88*, 3387. b) Guan, L.; Wims, L. A.; Kane, R. R.; Smuckler, M.; Morrison, S. L.; Hawthorne, M. F. Homogeneous Immunoconjugates for Boron Neutron Capture Therapy: Design, Synthesis and Preliminary Characterization. *Proc. Natl. Acad. Sci. USA* **1998**, *95*, 13206. c) Watson-Clark, R. A. ; Banquerigo, M. L. ; Shelly, K.; Hawthorne, M. F.; Brahn, E. L. Model Studies Directed Toward the Application of Boron Neutron Capture Therapy to Rheumatoid Arthritis: Boron Delivery by Liposomes to Rat Collagen-Induced Arthritis. *Proc. Natl. Acad. Sci. USA* **1998**, *95*, 2531. d) Nakanishi, A.; Guan, L.; Kane, R. R.; Kasamatsu H.; Hawthorne, M. F. Toward a Cancer Therapy with Boron-rich Oligomeric Phosphate Diesters that Target the Cell Nucleus. *Proc. Natl. Acad. Sci. USA* **1999**, *96*, 238.

[21] Barth R.F. J. Neuro-Oncol., 2003, 62, 1-5.

[22] Barth, R.F., Coderre J.A., Vicente M.G.H., Blue T.E., Clin. Cancer. Res., 2005, **11**, 3987-4002.

[23] Valliant, J.F.; Schaffer, P.; Stephenson, K.A.; Britten, J.F. *J. Org. Chem*. **2002**, *67*, 383.

[24] a) Cherry, S. R. In vivo molecular and genomic imaging: new challenges for imaging physics. *Phys. Med. Biol*. **2004**, *49***,** R13. b) Sogbein, O. O.; Merdy, P.; Morel, P.; Valliant, J. F**.** Preparation of Re(I)− and ^{99m}Tc(I)−Metallocarboranes in Water under Weakly Basic Reaction Conditions. *Inorg. Chem.* **2004**, *43*, 3032. c) Green, A. E. C.; Causey, P. W.; Louie, A. S.; Armstrong, A. F.; Harrington, L. E.; Valliant, J. F. Microwave-Assisted Synthesis of 3,1,2- and 2,1,8-Re(I) and ^{99m}Tc(I)−Metallocarborane Complexes. *Inorg. Chem.* **2006**, *45*, 5727.

[25] a) Bregadze, V. I.; Glazun, S. A. Metal_containing carboranes with antitumor activity. *Russ.Chem.Bull., Int.Ed.* **2007**, *56*, 643. b) Bregadze, V. I.; Sivaev, I. B.; Glazun, S. A. Polyhedral Boron Compounds as Potential Diagnostic and Therapeutic Antitumor Agents. *Anti-Cancer Agents in Medicinal Chemistry* **2006**, *6,* 75.
[26] a) MacDougall, C.; Polo, R. E. *Clin. Microbiol. Rev.* **2005**, *18*, 638. b) Mah, T. F.; O'Toole, G. A. *Trends Microbiol.* **2001**, *9*, 34.
[27] a) Teixidor, F.; Pedrajas, J.; Rojo, I.; Viñas, C.; Kivekäs, R.; Sillanpää, R.; Sivaev, I.; Bregadze, V.; Sjöberg, S. The chameleonic capacity of $[3,3'\text{-}Co(1,2\text{-}C_2B_9H_{11})_2]^-$ in coordination. Generation of the highly uncommon S(thioether)-Na bond. *Organometallics* **2003,** *22,* 3414. b) Farras, P.; Teixidor, F.; Kivekäs, R.; Sillanpää, R.; Viñas, C.; Grüner, B.; Cisarova, I. Metallacarboranes as Building Blocks for Polyanionic Polyarmed Aryl-ether Materials. *Inorg. Chem.* **2008**, *47*, 9497.
[28] Rojo, I.; Teixidor, F.; Viñas, C.; Kivekäs, R.; Sillanpää, R. Synthesis and Coordinating Ability of an Anionic Cobaltabisdicarbollide Ligand Geometrically Analogous to BINAP.
Chem. Eur. J. **2004**, 10, 5376.
[29] Toshkova, R., E. Ivanova, V. Ivanova, M. Kolarova. Effect of Ulva lactuca heteropolysaccharide on the immune response of hamsters of progressing Graffi tumour. Compt. Rend. Acad. Bulg. Sci., 48(N 5), 1995, 95-98.
[30] Freshney, R.I. Culture of Animal Cells: A manual of basic technique. 2nd Edn. Alan R. Liss, New York,
[31] Bauer A. W., Kirby W. M., Cherris J. C., Truck M. Antibiotic susceptibility testing by a standardized single disk method. The Am. J. of Clin. Pathol.. 45 (1966) 493 – 496.
[32] Ericsson H. M., Sherris J. S. Antibiotic sensitivity testing. Acta Path. Microb. Scand. Suppl., 217 (1971) 3 – 86.
[33] Mosmann, T. Rapid colorimetric assays for cellular growth and survival: application to proliferation and cytotoxicity assays. J. Immunol. Methods., 65, 1983, pp. 55-59.
[34] Stojiljkovic I., Kumar V., Srinivasan, N., Mol. Microbiol., 1999, 31/32,429-442.
[35] Conly J., CMAJ, 2002, 167, 885-891.
[36] Livermore D.M., Clin. Microbiol. Infect., 2004, 10, Suppl. 4, 1-9.
[37] Denyer, S. P. *Int. Biodeterior. Biodegrad.* **1995**, *36*, 227.
[38] Chevrot, G.; Schurhammer, R.; Wipff, G. Surfactant behavior of "ellipsoidal" dicarbollide anions: a molecular dynamics study. *J. Phys. Chem. B* **2006**, *110*, 9488.
[39] a) Anderson, R. A.; Feathergill, K. A.; Diao, X. H.; Cooper, M. D.; Kirkpatrick, R.; Herold, B. C.; Doncel, G. F.; Chany, C. J.; Waller, D. P., Rencher, W. F.; Zaneveld, L. J. Preclinical evaluation of sodium cellulose sulfate (Ushercell) as a contraceptive antimicrobial agent. *J. Androl.* **2002**, *23*, 426. b) Herold, B. C.; Bourne, N.; Marcellino, D.; Kirkpatrick, R.; Strauss, D. M.; Zaneveld, L. J.; Waller, D. P.; Anderson, R. A.; Chany, C. J.; Barham, B. J.; Stanberry, L. R.; Cooper, M. D. Poly(sodium 4-styrene sulfonate): an effective candidate topical antimicrobial for the prevention of sexually transmitted diseases. *J. Infect. Dis*. **2000**, *181*, 770.
[40] Rosenberg, B., L. Van Camp, T. Krigas. Inhibition of cell division in Escherichia coli by electrolysis products from platinum electrode. Nature, 205, 1965, 698-699.
[41] Lippert, B. Cisplatin. Chemistry and biochemistry of a leading anticancer drug. Lipperd, B. (ed). Verlag Helvetica Chimica Acta, Zurich, 1999.
[42] Alexandrova, R., G. Rashkova, M. Kirilova, G. Miloshev, S. Slavov, R. Kalfin, D. Culita, L. Patron. Investigations on cytotoxic and antiproliferative activities of Zn(II), Cu(II) and La(III) complexes with cholic acid on tumor cell line.
[43] Stoykova, R., R. Alexandrova, K. Nedkova, E. Ivanova, O. Sabotinov, K. Zdravkov, G. Minchev. Comparison of the photodynamic effect in human and animal tumor and animal tumor cell lines. Proceedings of SPIE, 5830, 2005, 468-472.
[44] Alexandrova, R., O. Sabotinov, E. Stoykova, R.-M. Ion, S. Shurulinkov, G. Minchev. In vitro cytotoxicity assessment of [5,10, 15, 20-tetra (4-sulfophenyl) porphyrin] on tumor and nontumour cells. Proc. S.P.I.E., 2003, 5449, 227-234.
[45] Verstovsek, S., Maccubin, D., Mihich, E. Tumorocidal activation of murine resident peritoneal macrophages by interleukin-2 and tumor-necrosis factor. Cancer Res., 52, 1992, 3880-3885.
[46] Sugiura, H, Sugiura, H., Ueya, E., Ueya, S., Mirbod, S.M. Enhanced macrophage functions and cytokine production of lymphocytes after ingection of born narine in female BALB/c mice. Life Sci., 2000, 68, 505-515.
[47] Repetto, L. Greater risks of chemotherapy toxicity in elderly patients with cancer. - J. Support. Oncol., 4 Suppl. 2, 2003, 18-24.

Montefori, D.C., Robinson Jr, W.E., Schuffman, S.S., Mitchel, W.M. Evaluation of antiviral drugs and neutralizing antibodies by a rapid and sensitive microtiter infection assay. J. Clin. Microbiol., 1988, 26, 231-235.

Hanson M.R., Chung C.L. Antibiotic selection for MRSA: case presentations and review of the literature. *J Drugs Dermatol.* **2009**, 8, 281.

Chart 1.- Monosubstituted cobaltabisdicarbollide anions

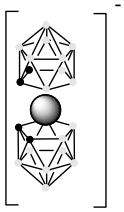

[1]$^-$

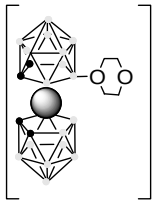

[2]

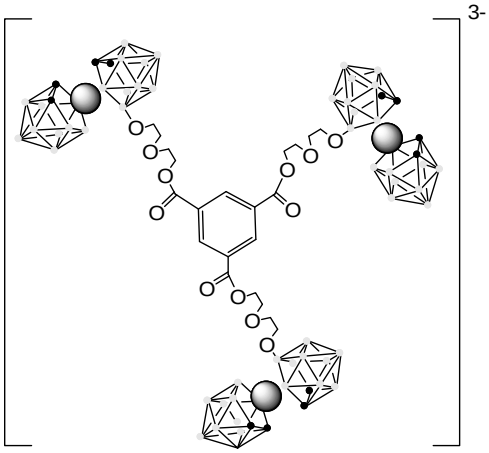

[5]$^{3-}$

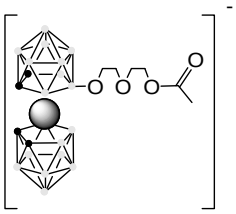

[3]$^-$

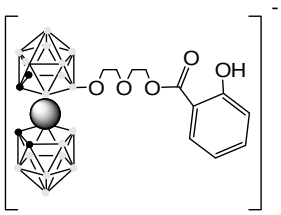

[4]$^-$

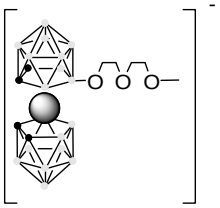

[6]$^-$

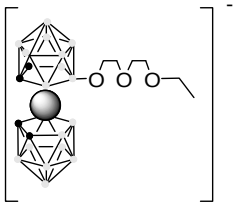

[7]$^-$

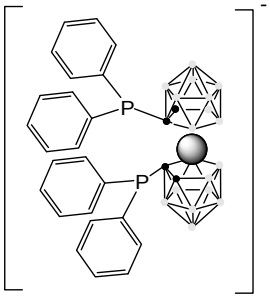

[8]$^-$

Scheme 1.- Opening of the *exo*-cluster dioxanate ring reaction by nucleophilic attack. Atoms in black are CH vertexes, the rest of the vertices in the clusters are BH

a) Alcoxides: compounds [6]- and [7]-

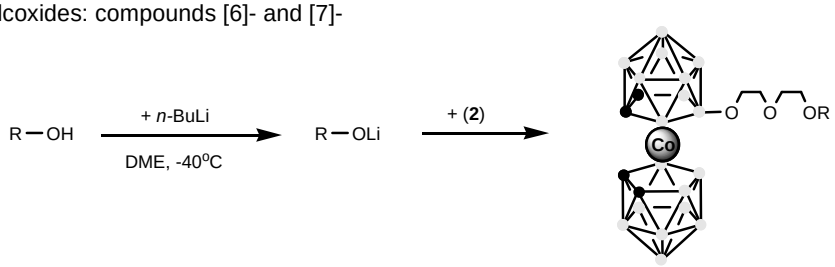

b) Carboxilic acids: compounds

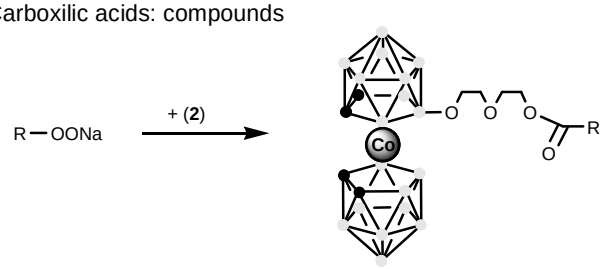

Scheme 2.- Synthesis of compound $[8]^-$.

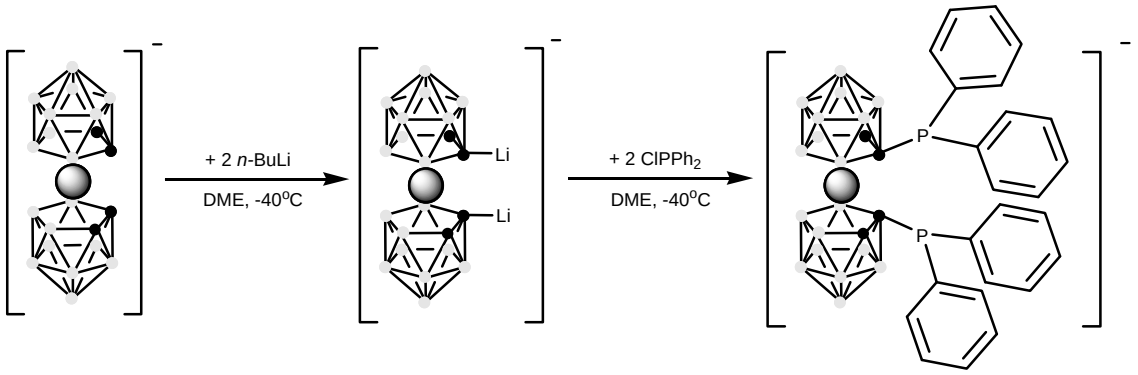

Figure 1.- Results of the agar-gel diffusion method for the Gram-positive (A), Gram-negative B) and antifungal activity (C).

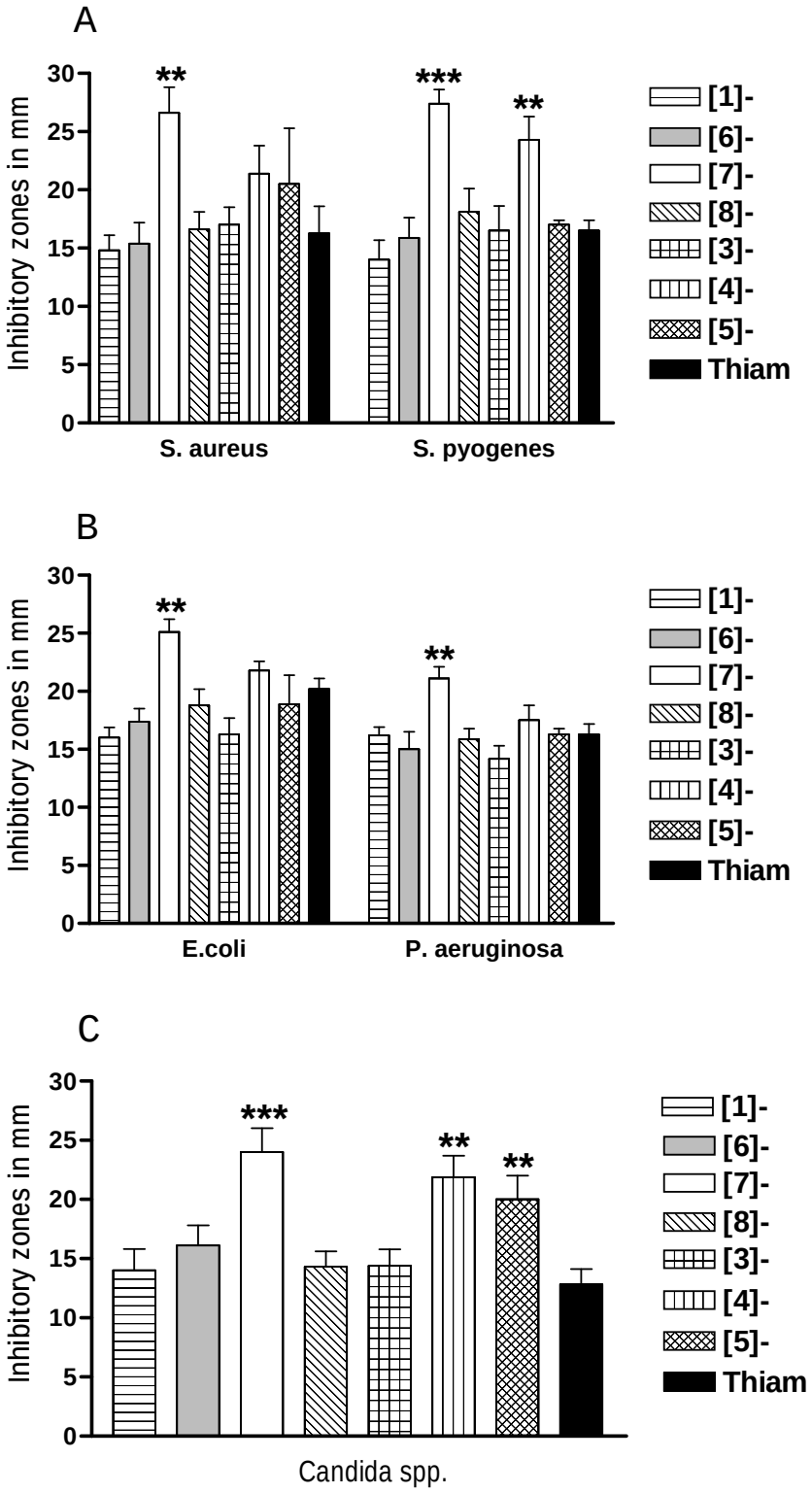

Figure 2.- Concentration-response curves from the MTT assay.

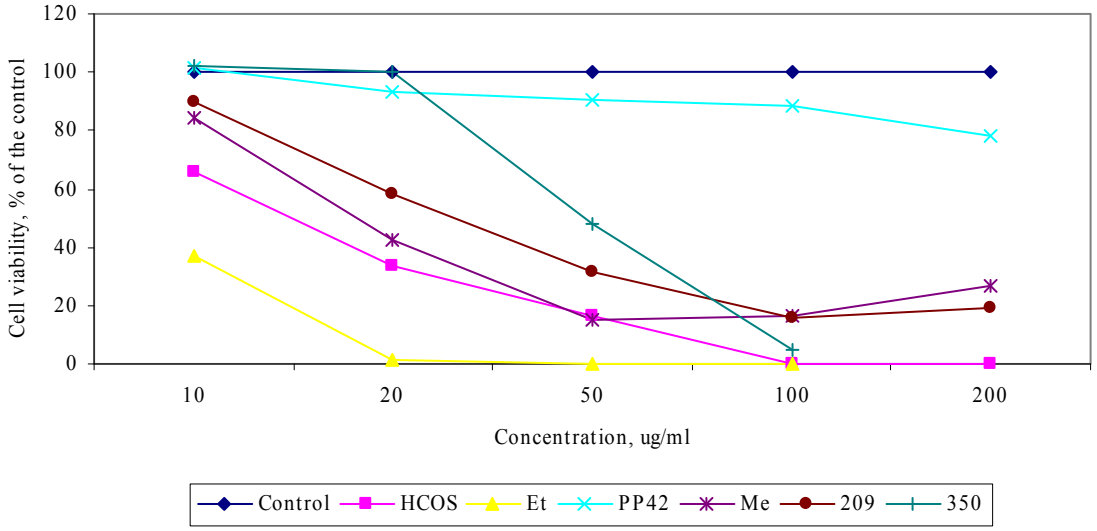

Figure 3.- Primary cultures from Graffi myeloid tumor in hamsters.

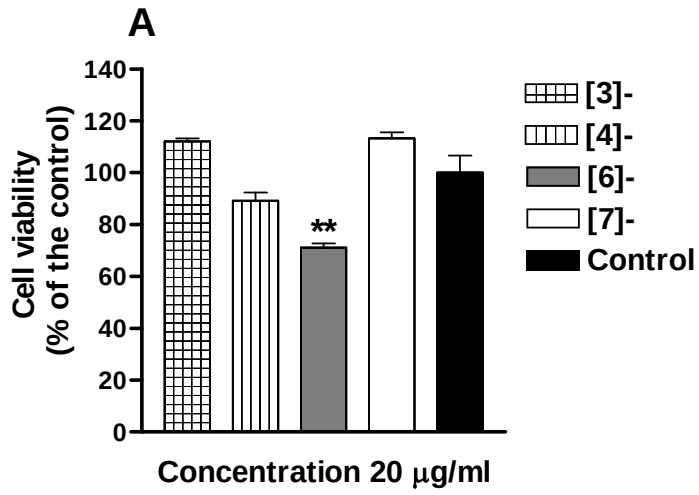

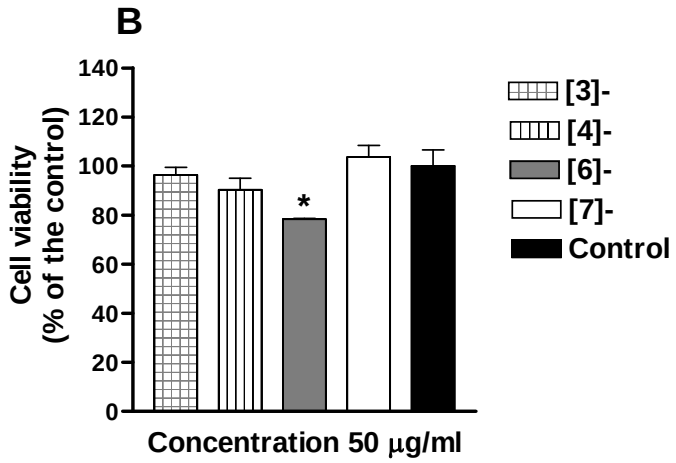

Figure 4.- Bone marrow cells from Graffi tumor bearing hamsters.

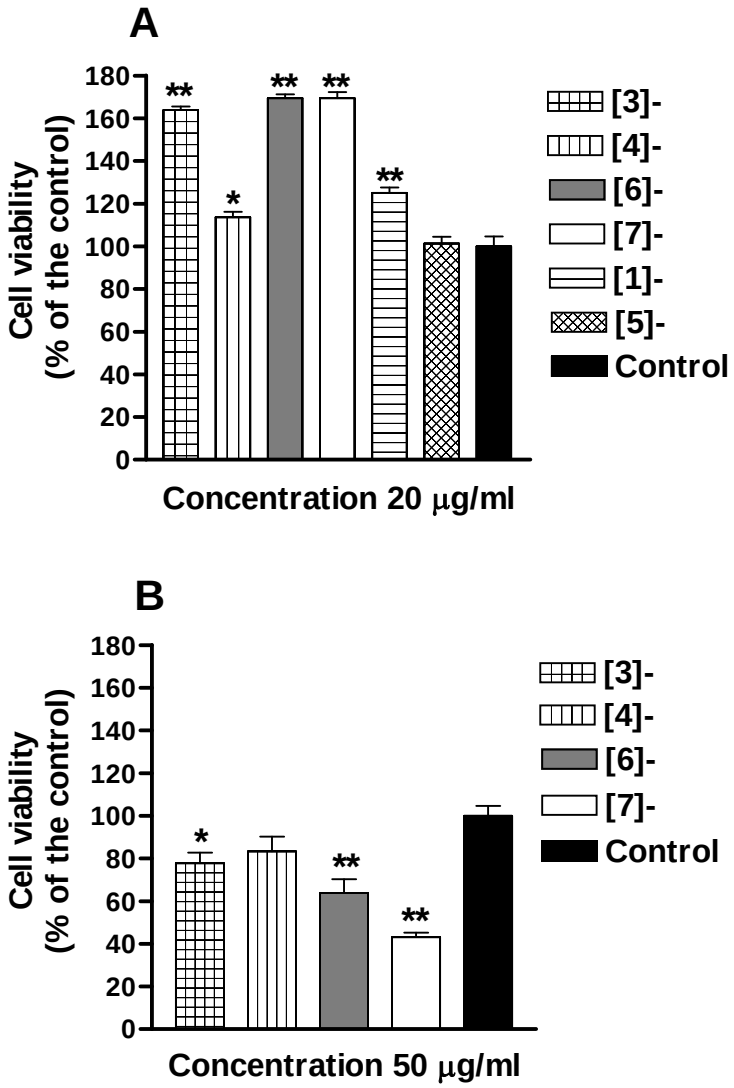

Table 1.- Cell cultures used as model systems in the experiments

Origin	**Tumor**	**Nontumor**
Human	**8 MG BA –** Glioblastoma multiforme **MCF-7** – Adenocarcinoma of the breast **HEp-2** – Carcinoma of the larynx; **K 562** – Erythroleukaemia	-
Rat	**LSR-SF(SR)** – Transplantable sarcoma in rat induced by *Rous sarcoma virus*, strain *Schmidt-Ruppin*	-
Hamster	Transplantable myeloid tumor induced by murine leukaemia virus of *Graffi*	**Bone-marrow cells** from Graffi tumor-bearing animals
Mouse	**P3U1 –** myeloma	**Spleen lymphocytes,** **Peritoneal macrophages** **Bone-marrow cells**
Chicken	**LSCC-SF(Mc29)** – Transplantable hepatoma induced by the myelocytomatosis virus Mc29	

Table 2. Minimum inhibitory concentration (MIC) of newly synthesized metallacarboranes on pathogenic microorganisms

MICRO-ORGANISMS	Num-ber of strains	MIC_{50}				
		$[7]^-$	$[8]^-$	$[4]^-$	$[5]^-$	THIAM-PHENICOL
S. aureus	4	12.8 ±7.3	36.0 ±10.1	10.1 ±7.3	48.0 ±9.2	21.3 ±6.2
S. pyogenes	4	3.1 ±1.6 *	26.0 ±6.0	2.5 ±0.6 **	48.0 ±9.2	20.0 ±9.9
E. coli	4	7.0 ±1.0 *	26.0 ±6.0	4.0 ±0.1 **	22.0 ±6.0	12.0 ±2.3
P. aeruginosa	4	18.0 ±5.0	22.0 ± 6.0	8.0 ±2.8 *	17.0 ±5.7	20.5 ±3.8
Candida spp	4	1.4 ±0.2 ***	28.0 ±4.0	2.3 ±0.4 ***	32.0 ±0.1	14.0 ±2.0

Significantly lower MICs versus wide-spectrum antibiotic thiamphenicol (used as positive control) are presented as follows: *$P < 0.05$; **$P < 0.01$; ***$P < 0.001$ vs. thiamphenicol

Table 3. Cytotoxic effect (CC_{50}) of metallacarboranes on tumor and nontumor cells

Cell culture	**[3]$^-$**	**[4]$^-$**	**[5]$^-$**	**[7]$^-$**	**[6]$^-$**	**[1]$^-$**	**[8]$^-$**	
	24 h 48 h	24 h 48 h	24 h 48 h	24 h 48 h	24 h 48 h	24 h 48 h	24 h	48 h
LSCC-SF(Mc29)	62 29	65 15	- 48.5	11 6	26 15	41 19	- -	- -
LSR-SF-SR	42 23	45 28.2	- -	24 16	30 20	54 27	n.d.	n.d.
P3U1	40.5 28.3	54.1 47.9	- -	37.4 26.1	45.8 30.4	58.6 40.8	n.d.	n.d.
HEP-2	40	30	- -	28 19	63 19		n.d.	n.d.
MCF-7	71.5 42	93.6 71.5	n.d. n.d.	62.5 35	48 17.5	84.5 74	n.d.	n.d.
8 MG BA	76 25	86 47.2	n.d. n.d.	60 28.5	66.5 43	n.d. n.d.	n.d.	n.d.

n.d. = not done
(-) means that CC_{50} was not determined because cell viability was more than 50 %

Table 4. Effect of metallacarboranes on viability and proliferation of murine cells.

Compound/ concentration, μg/ml		Spleen lymphocytes	Peritonesl macrophages	Bone marrow cells
[1]$^-$	10	144.83 ± 2.60**	161.7 ± 1.61**	130.43 ± 0.52**
	20	134.48 ± 1.59**	136.17 ± 2.58**	110.43 ± 0.82*
	50	113.79 ± 3.28**	102.130 ± 2.82	70.87 ± 2.75**
[4]$^-$	10	165.52 ± 5.05**	197.87 ± 3.77**	118.26 ± 0.42**
	20	165.520 ± 2.02**	191.49 ± 2.60**	100.00 ± 2.05
	50	131.03 ± 4.26**	131.91 ± 1.62**	63.47 ± 0.05**
[5]$^-$	10	110.34 ± 6.04	151.06 ± 2.06**	92.17 ± 1.28
	20	96.55 ± 3.84	108.51 ± 1.61*	99.13 ± 2.28
	50	137.93 ±5.79**	100.00 ± 1.96	94.78 ± 2.98

Table 5. Effect of metallacarboranes on colony-forming ability of tumor cells

	LSCC-SF(Mc29)	LSR-SF(SR)	P3U1	Hep-2	K562	8 MG BA	MCF-7
[3]$^-$	≥ 50*	≥ 50	≥ 75	≥ 75	≥ 75	≥ 50	≥ 75
[4]$^-$	≥ 75	≥ 75	≥ 100	≥ 100	≥ 100	≥ 200	≥ 200
[5]$^-$	≥ 100	n.i.	≥ 200	n.i.	n.i.	≥ 200	≥ 150
[6]$^-$	≥ 25	≥ 50	≥ 50	≥ 50	≥ 50	≥ 50	≥ 50
[7]$^-$	≥ 10	≥ 25	≥ 50	≥ 50	≥ 50	≥ 50	≥ 50
[1]$^-$	≥ 50	≥ 75	≥ 100	≥ 100	≥ 75	n.i.	≥ 150

***** Concentration (μg/ml) at which the compound inhibits the colony-forming ability of tumor cells; n.i. – no inhibition was observed at all concentrations tested; n.d. – not done